Hunting for Rare-Earth-Element (REE)-Bearing Minerals in Northern Labrador: MLA-SEM Analysis of Surficial Sediments within the Glacial Dispersion Zone from the Strange Lake Main Zone Deposit

© Mikayla Miller

A Thesis submitted to the School of Graduate Studies

in partial fulfillment of the requirements for the degree of Master of Science

Department of Earth Sciences, Memorial University

Spring 2021

TABLE OF CONTENTS

LIST OF FIGURES

LIST OF TABLES

ACKNOWLEDGMENTS

I would like to thank Dr. Andrew Kerr for accepting me as his graduate student and for his continuous guidance and support throughout the course of this project. Thanks also to Dr. Graham Layne, my committee member, for his assistance with the editing process. Thanks to Dr. Derek Wilton for securing the funding for this research and initiating and assisting with the early stages of this project. Thanks to the Nunatsiavut Government for their collaboration and to InnovateNL for funding this research. Thanks to Michelle Miskell and Dr. Greg Dunning for their support and encouragement. I would also like to thank Lori Wickert for her collaboration with this research. Thanks to Dr. David Grant and Dylan Goudie of Memorial's CREAIT SEM Facility, for their support in obtaining and interpreting MLA-SEM data. Thanks to Dr. Stephen Amor for advice and assistance with statistical methods and for his help with many of the maps in this thesis. Thanks to Dr. Alex Peace for his assistance creating maps used for data presentation. Thanks to Jeanne Percival for sharing her REE-bearing mineral spectra. Thanks to Dr. Steve Piercey for allowing the use of his TerraSpec instrument. Thanks to Philip Lypaczewski and David Coulter for their assistance analyzing the TerraSpec data and to Lypczewski for allowing the use of his own personal program for analyzing spectral data. Finally, sincere thanks to my family and friends, especially my husband, Stephen Ryan, and my mom and dad, Airdrie and Wayne Miller, for their continuous encouragement and support.

ABSTRACT

The Strange Lake area hosts important Zr-Nb-Y-REE deposits, associated with a small peralkaline granite intrusion. The deposits and the host rocks contain unusual minerals, some of which are essentially unique to this site. Geochemical data from glacial sediments or “tills” define dispersion from the deposits for at least 35 km, and the Strange Lake area is regarded as a “type example” of linear glacial dispersion from a point source. This thesis study uses Mineral Liberation Analysis – Scanning Electron Microscopy (MLA-SEM) methods to investigate the mineralogy of glacial sediments and document the dispersion of unusual (indicator) minerals. It is in part an assessment of the MLA-SEM technique for use in indicator-mineral studies, which are increasingly important in mineral exploration.

Seventy-six samples of till were collected from an area extending for 35 km ENE of the Strange Lake Main Zone deposit, aligned with the inferred direction of ice movement. Samples were processed to separate the 0.125 - 0.18 mm size fraction for direct analysis, without any preferential separation of denser minerals. MLA-SEM results thus directly document the abundances of 55 minerals, ranging from common silicates to rare accessory minerals diagnostic of the Strange Lake deposits. This large database was then evaluated using statistical and geographical analysis methods. Common silicates (e.g., quartz, feldspars, garnet and amphiboles) collectively make up > 90% of typical till samples, but the rarest indicator minerals occur at levels < 10 ppm. The reliability of data degrades at such low abundances (in part due to probability effects) but systematic geographic variation patterns can still be discerned for many such rare minerals. Numerous diagnostic minerals from Strange Lake were detected, although their abundance was lower than expected from previous MLA-SEM analyses of drill core samples.

Many minerals show linked abundance variation (correlation or anti-correlation) and such variation commonly has a geographic component. Systematic geographic variations for major minerals and many minor minerals seem to correspond with regional contrasts in bedrock geology from west to east, suggesting that patterns mostly record local provenance. Accessory minerals that are diagnostic of Strange Lake also show systematic geographic abundance variations, which are superimposed on these regional trends, but in some cases the patterns appear superficially similar. The most abundant and persistent indicator minerals are the Ca-Zr silicate gittinsite and the Y-Ca-REE silicate gerenite, which are also the most abundant in the Strange Lake source rocks. However, geographic variation patterns for these minerals are rather different. Gerenite abundance diminishes in a down-ice direction, as expected, but gittinsite seems to increase in abundance, which is unexpected. Other indicator minerals mostly diminish in abundance in a down-ice direction but even some of the rarest (e.g., stetindite, gadolinite and bastnaesite) remain sporadically detectable at 35 km from the source. The controls on dispersion patterns are not fully understood, but likely involve mineralogical factors as well as aspects of the glacial environment. MLA-SEM data suggest that many indicator minerals from Strange Lake typically form small domains within larger particles of common minerals, and these host minerals may thus influence dispersion patterns. In this context, it is interesting that the most persistent indicator minerals seem to be preferentially associated with quartz, which is the most durable of common rock-forming minerals.

Like most research studies, this project did not answer all questions posed at the outset, and it did not always follow the intended plan. However, the results indicate that the MLA-SEM method has considerable potential for use in indicator-mineral studies, and point to interesting future research directions connected to development of the method and its application to other geological problems.

CHAPTER 1: INTRODUCTION

PROJECT DESCRIPTION AND CONTEXT

This project is focused on a remote area located along the Québec-Labrador border, approximately 140 km west of Nain, Labrador, and 250 km northeast of Schefferville, Québec (Figure 1.1). The project area forms part of Labrador Inuit Lands administered by the Nunatsiavut Government, and has been a focus for mineral exploration and related geological studies for over 40 years. This interest is largely because the area holds at least two large mineral deposits enriched in Rare Earth Elements (REE) and associated commodities (yttrium, zirconium, niobium and beryllium). The research project is focused around the regional dispersion of material from these deposits by glacial processes during the last Ice Age, and seeks to define and understand patterns shown by dispersion of distinctive Zr-, Nb- and REE-bearing 'indicator minerals'. It is also intended to further investigate and evaluate the application of a new quantitative approach to such mineralogical studies, which uses the Mineral Liberation Analysis – Scanning Electron Microscope (MLA-SEM) technology. This is an alternative to conventional methods that emphasize the separation of heavy (dense) minerals from large samples, and use their optical and physical properties for identification. The project is in many respects a proving ground for this approach, which was pioneered at Memorial University (e.g., Wilton and Winter, 2012; Wilton et al., 2017), but it is also a geological study, with application to processes of glacial transport. It represents the first systematic investigation of indicator minerals in this area, which is now thought to represent the location of an ice-stream (a zone of fast-moving ice) within the Laurentide Ice Sheet (e.g., Margold et al., 2015, Paulen et al., 2017). Like most research projects, it did not always follow the planned course and did not always yield the expected results, but it leads to useful insights in all of these aspects, and will hopefully be of value to future research efforts.

RARE EARTH ELEMENTS (REE): TERMINOLOGY AND CONCEPTS

The Rare Earth Elements (REE) are a group of unusual chemical elements representing atomic numbers 58 to 71 in the periodic table. They are also referred to as the 'Lanthanide Series' in the periodic table, and the element yttrium (Y; atomic number 39) is commonly included within the grouping because it has very similar chemical properties. In the 1980s, the main interest around Strange

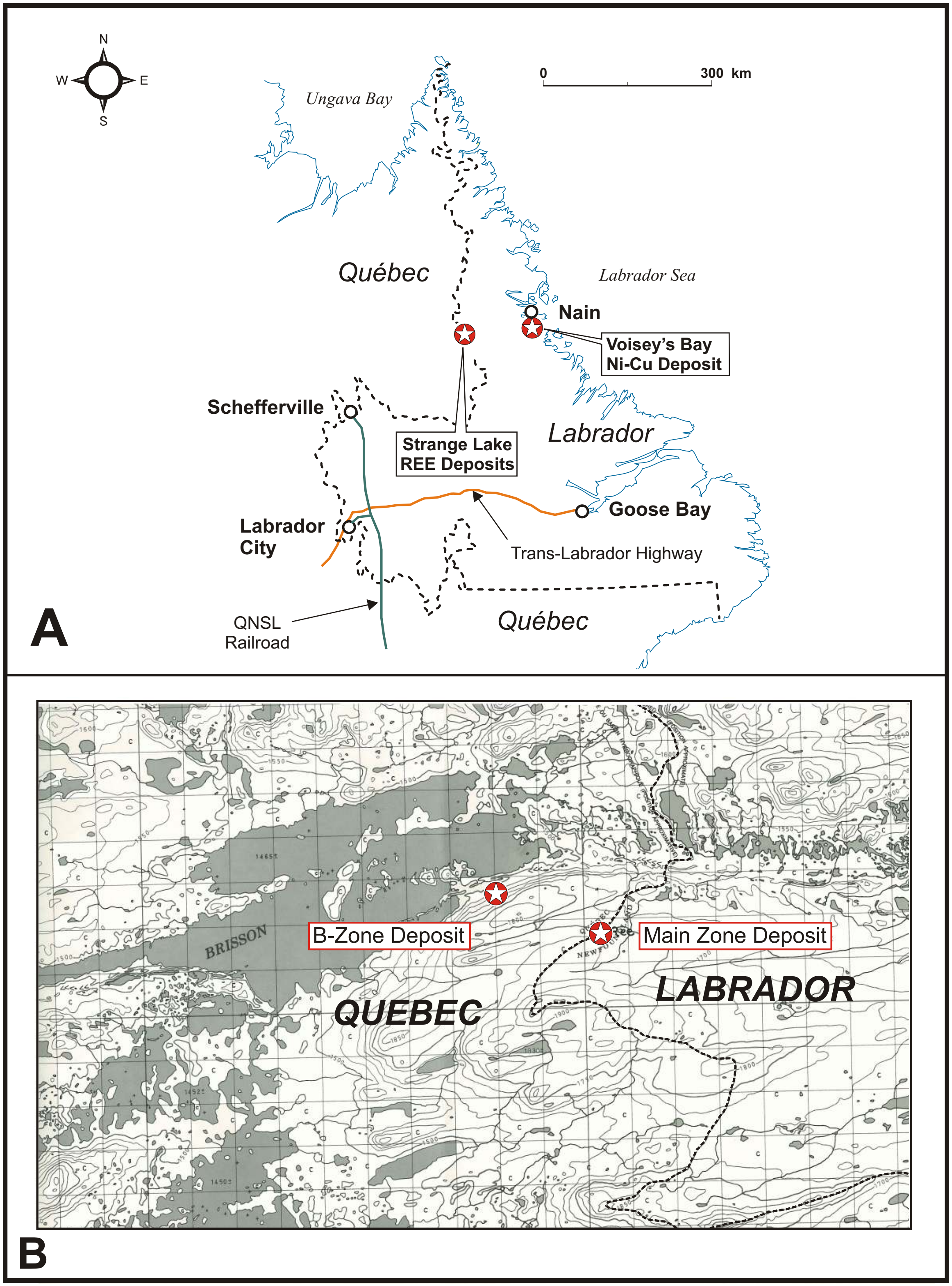

Figure 1.1 (A) Location of the Strange Lake deposits and the Project Area in Labrador and Québec. (B) Detailed topographic map of the local area of the deposit, extracted from NTS sheet 24A/08 (Lac Dihourse). Grid squares are 1 km.

Lake was for Y and Zr, because there was little interest in the REE. However, Rare Earth Elements have now become key technology components, essential in countless appliances, cell phones, rechargeable batteries, hybrid vehicles, and laptop computers. Demand for these “critical” metals will grow, as will interest in exploration techniques (e.g., Verplanck and Hitzman, 2016; Gysi et al., 2016). The REE are commonly divided into two groups, which are called ‘light REE’ (Lằ to Eu; or LREE) and ‘heavy REE’ (Gd to Lu, or HREE) on the basis of their atomic numbers. The light REE are generally more abundant in nature, but some of the heavy REE have attained high value due to their applications. In some cases, abundances of the REE are expressed as oxides (e.g., Ce2O3) or as total REE oxides (TREO), rather than as elemental measurements.

THE STRANGE LAKE DEPOSITS AND THEIR SETTING

This geology of this remote area was almost unknown until the late 1970s, when prospecting aimed mostly at uranium potential discovered unusual radioactive boulders close to the Québec-Labrador border. Follow-up exploration discovered similar material in bedrock, concealed beneath extensive glacial deposits. There was little uranium to be found, but the mineralization proved to be rich in a variety of unusual chemical elements, of the type collectively called ‘rare metals’, including zirconium (Zr), niobium (Nb), yttrium (Y) and Rare Earth Elements (REE) (e.g., Zajac et al., 1984; Zajac, 2015). The Strange Lake deposits are known to be enriched in the so-called ‘heavy REE’ (HREE), i.e., elements that have atomic numbers greater than 63 (Europium), which are the more valuable members of the group

Despite much effort, the original Strange Lake Deposit was not developed in the 1980s. However, it became well known to geologists as one of the largest potential REE deposits in Canada. Mineralization consists of mixed pegmatite and aplite zones within a small (< 6 km in diameter), circular peralkaline granite body known as the Strange Lake Intrusion (e.g., Miller, 1986; Zajac, 2015). The deposit is also well known for its uncommon minerals, including some Zr- and REE-bearing minerals that occur only in a handful of localities around the world, and at least one mineral that was until recently unique. It seems as if every research study connected to Strange Lake finds at least one previously unreported mineral. The original Strange Lake Deposit, discovered in 1979, is known as the ‘Main Zone’, but it is not the only such concentration in the area. Exploration from 2009 to 2013 defined a very similar deposit, known as the ‘B-Zone’, within a part of the Strange Lake Intrusion located in adjacent Québec. This is also known to contain large potential resources, with mineralization extending to considerable depth, but efforts at commercial development since 2015 also faltered.

The usage of the name ‘Strange Lake’ requires some clarification. It was originally coined during exploration as a name for the project, and was never applied to any geographic locality (Zajac, 2015). However, it subsequently became applied to a large lake in Labrador, within the present study area. The Strange Lake deposits are closer to Lac Brisson in Québec than to ‘Strange Lake’ in Labrador.

Geological research around Strange Lake has focused on the unusual rocks and minerals, but several studies using surficial geochemistry (e.g., the analyses of glacial sediments, stream sediments and even waters) showed that material from the deposits and host rocks was dispersed over long distances to the east by glacial transport and other processes (e.g., McConnell and Batterson, 1987; Batterson, 1989). This geochemical ‘footprint’ is enormous compared to the dimensions of the mineral deposits themselves, and detection of such dispersed signatures in surficial materials has long been an important method in exploring for many commodities in northern Canada. Investigations of glacial sediments (tills) in the area of the Voisey’s Bay Deposit, using the new MLA-SEM method, discovered small particles containing the rare Ca-Zr-silicate gittinsite as smaller grains (Wilton et al., 2017), suggesting that material from Strange Lake was transported for at least 100 km to the east. A recent reconnaissance indicator mineral study in the Strange Lake area (McClenaghan et al., 2017; 2019) using traditional methods detected some uncommon minerals in till samples, but was unable to document widespread dispersion. In 2016, a research project to use the capabilities of the MLA-SEM to investigate till mineralogy in the area was initiated, and was linked with similar studies of material from drill cores archived by the Newfoundland and Labrador Department of Natural Resources. The project was funded in part by the Nunatsiavut Government and in part by the Research Development Corporation of Newfoundland and Labrador.

COMPONENTS OF THE RESEARCH PROJECT

The purpose of this research is to evaluate the glacial dispersion of uncommon and characteristic Zr-, Nb and REE-bearing minerals in surficial sediments (tills) along a 30 km long corridor east-northeast of the Strange Lake Main Zone Deposit by using Mineral Liberation Analysis - Scanning Electron Microscope (MLA-SEM) methods. The study area is oriented parallel to the direction of transport and erosion inferred for the Laurentide Ice Sheet during the Pleistocene, and is known to include areas of geochemical dispersion from Strange Lake. The basis for the research work is a collection of 76 till samples collected in 2016, in collaboration with the Nunatsiavut Government. The research is also integrated with other MLA-SEM studies completed on archived (crushed) drill core from the deposit, including previous thesis projects by Baird (2018) and Currie (2019). In addition to the MLA-SEM work, the till samples were also analyzed using Visible/Infrared Reflectance Spectroscopy (VIRS) to ascertain if unusual minerals could be detected using this non-destructive, low-cost technique. However, the VIRS investigation did not prove successful.

The MLA-SEM analysis program resulted in a very large amount of numerical data including abundance determinations for over 50 individual minerals, and information about the physical characteristics of mineral grains and mineral associations in the samples. The organization and integration of these data were at times challenging, as was their interpretation. Evaluation relies extensively upon univariate and multivariate statistical analysis, which helps to illustrate patterns of correlation among minerals and groups of minerals. In addition to common rock-forming minerals such as quartz, feldspars, hornblende and garnet, many accessory and trace minerals were detected in the samples, including a suite of uncommon minerals derived from the Strange Lake deposits. The geographic variations in mineralogy were also investigated, and proved to be complex in detail, including patterns that are likely related to inferred bedrock geological units, and patterns that are related to the transport of detritus from the mineralized zones. Many of the uncommon minerals are present in very small quantities in the samples, so it also proved important to assess the precision and reliability of such data, but the ability of the MLA-SEM method to detect and define such patterns is demonstrated well by results.

The final component of the research involved some comparisons between results from the MLA-SEM study and information from other research efforts, including the reconnaissance indicator mineral study of McClenaghan et al. (2017; 2019) and an extensive till geochemistry program completed by Midland Exploration Ltd about 10 years ago. The results suggest that the MLA-SEM method could have many advantages over traditional indicator mineral methods, but they also point to possible modifications in methodology that might improve and extend results from MLA-SEM research in this and other applications.

It is important that new methods such as MLA-SEM analysis be deployed in practical applications or ‘case studies’ in order to understand the full extent and potential of the technology, but also to define any limitations and possible enhancements. The method appears to have considerable potential in the search for unusual deposits such as those of the Strange Lake area, and perhaps for other mineral deposit types. The key objective of this research is to aid in the creation of a tool used for regional resource assessment. The immediate results should benefit the Nunatsiavut Government with respect to decision-making in the Strange Lake region, and in wider assessment of mineral potential. The techniques and workflow processes developed should aid in mineral exploration for REE and other commodities in Nunatsiavut and elsewhere in the Canadian north.

HISTORY AND DEVELOPMENT OF THE RESEARCH PROJECT

This research project commenced in 2016, with the collection of till samples in the Strange Lake area by Dr. D. Wilton, but laboratory work and MLA-SEM analysis did not commence until 2017, and extended through 2019. As with all such projects, there were delays and some aspects did not work as well as had been hoped. In particular, the VIRS analysis of till samples proved to be time-consuming but ultimately did not produce useful results. The MLA-SEM analysis was more successful, but the abundances of unusual minerals characteristic of the Strange Lake deposits proved to be considerably lower than expected on the basis of previous analyses of crushed drill core from the deposit (Baird, 2018). The very large amount of information represented by data from 76 samples for > 50 minerals, combined with the abundant visual information from SEM imagery and the extensive numerical information on particle sizes and associations, proved very challenging to work with. As with many projects involving large amounts of data, organization and maintenance of databases can become an overwhelming task that impedes interpretation of results.

An initial first version of the thesis, developed in 2019, focused mostly on the distribution of the REE-bearing minerals, but following its completion it became apparent that some aspects of the project might need to be reconsidered, and that a more quantitative approach using statistics could perhaps help to unravel the rather tangled web of data. There was also some concern that additional MLA-SEM analysis might be required to address potential issues related to precision and reliability for some of the rarer minerals. A new set of complications arose in early 2020 with the global Covid-19 pandemic, which prevented access to laboratory facilities to complete additional work that would have aided project completion.

The project was essentially dormant for much of 2020, but it resumed later in that year as health restrictions were relaxed. Following the retirement of Dr. D. Wilton, a new supervisory committee was established, and work on a revised and extended version of the thesis was initiated. Unfortunately, it was not possible to complete additional analytical work due to Covid-19 restrictions, but the existing (and abundant) data were viewed from a broader perspective including assessment of regional patterns, and statistical methods were introduced to aid in interpretation. Like many projects of this type, the final content is not exactly what was intended at the outset, but it represents the most practical approach to the scientific problems posed at the outset.

ORGANIZATIONAL STRUCTURE OF THE THESIS

The thesis is divided into 8 Chapters, including this brief introduction. Each is briefly outlined below, and each commences with a short summary.

Chapter 2 provides background information on the study area, including regional bedrock and surficial geology, and discusses the local geology around the Strange Lake Main Zone Deposit. It also summarizes the mineral exploration history of the area, and describes the deposit and its mineralization, with emphasis on aspects connected to petrology, mineralogy, and glacial history. Chapter 3 provides a review of some previous surficial geochemical exploration projects, including work by exploration companies and later investigations completed by the Geological Surveys of Newfoundland-Labrador and Canada and Newfoundland-Labrador. These results are important for comparison with the MLA-SEM data, and are revisited in the discussions of Chapter 8.

Chapter 4 provides information on research methods, including field work at Strange Lake, the processing of samples for MLA-SEM and VIRS analysis, and analytical techniques. It includes an outline of scientific principles involved in the methods, and also a discussion of possible issues surrounding precision and accuracy of analyses. Chapter 5 presents the results of VIRS analysis of the samples. This did not prove successful, so there are few definitive conclusions to report. These findings are largely independent of the later discussion of MLA-SEM data and geographic variation patterns, so the the presentation of VIRS results is provided first, in order to preserve continuity of presentation and discussion of MLA-SEM data.

Chapter 6 is the longest chapter in the thesis and presents the most important component of the research, i.e., the results of MLA-SEM analysis. It provides information on minerals identified in the samples, statistical analysis of the mineral abundance data, and the patterns of variation. It also presents images of particles and grains of unusual minerals, and assesses quantitative data on particle and grain sizes and mineral associations that are important in the context of data reliability. Chapter 7 adopts a different perspective on mineralogical variations by assessing them in a geographic context. It examines patterns that appear to be of regional origin, likely linked to bedrock units, patterns that likely record dispersion from the Strange Lake deposits, and patterns that are more enigmatic, and difficult to interpret.

Chapter 8 focuses on discussion of the information presented largely in Chapters 4, 6 and 7, and seeks to interpret results in a variety of contexts. These include some comparisons with other research completed within the area, and also discussions of the influences of mineralogical, geological and surficial processes on dispersion. The Chapter concludes with a review of the main findings and conclusions from the research and makes some suggestions for future research connected to the MLA-SEM technique and the project area.

CHAPTER 2: BEDROCK AND SURFICIAL GEOLOGY

GENERAL SUMMARY

The Strange Lake deposit and the study area are located near the Québec-Labrador border, approximately 140 km from Nain, Labrador, and 250 km from Schefferville, Québec. The area forms part of the Canadian Shield, and is underlain by Precambrian metamorphic and igneous rocks. The deposit is hosted by a small (< 10 km diameter) peralkaline granite known as the Strange Lake Intrusion and constitutes a “point-source” for dispersal of mineralized material within surficial glacial sediments. The mineralization at Strange Lake contains potentially economic quantities of Zr, Y, Nb, Be and REE. These elements occur in a diverse assemblage of unusual minerals that are also enriched in other rare elements. These unusual “exotic” minerals were initially interpreted as late-stage products of the peralkaline magmatism (e.g., Miller, 1986; Birkett and Miller, 1991). However, other researchers suggested that mineralization was largely of hydrothermal origin, and superimposed upon igneous host rocks (e.g, Salvi and Williams-Jones, 1990; Gysi et al., 2016). The area around Strange Lake is part of an elevated plateau and is widely covered by surficial glacial deposits and traversed by prominent esker systems (Batterson, 1989). The alignment of glacial landforms and other directional indicators show that the direction of glacial transport was to the east-northeast (ENE). The area may be part of a fast-flowing ice stream within the Laurentide ice sheet (Paulen et al., 2017). The area of sampling for the MLA-SEM study described in the thesis is largely unexposed, but regional geological mapping suggests that it is mostly underlain by metamorphic rocks derived from various igneous rocks.

REGIONAL GEOLOGY

General Geology of Labrador

The bedrock geology of Labrador spans times from the earliest Archean (before ca. 3.6 Ga) to the Cenozoic. Most of Labrador forms part of the eastern Canadian Precambrian Shield, which is composed mainly of igneous and high-grade metamorphic rocks, with smaller areas of lower-grade sedimentary and volcanic rocks. The Labrador region contains parts of five major structural provinces that are defined across the Canadian Shield (Figure 2.1; Wilton, 1996; Wardle et al., 1997). These are:

1. The Archean Nain Province in the northeast, exposed largely in coastal regions.

2. The Archean Superior Province in southwestern Labrador, and adjacent regions of Québec.

3. The Paleoproterozoic Churchill Province (ca. 2.1 - 1.8 Ga) in north-central to central Labrador, sandwiched between the two Archean provinces noted above, and containing a central core of reworked Archean rocks.

4. The Paleoproterozoic Makkovik Province (ca. 2.0 - 1.8 Ga), a small triangular area located along the southern margin of the Nain Province.

5. The Paleoproterozoic to Mesoproterozoic Grenville Province (ca. 1.7 - 1.0 Ga), located all across the southern part of Labrador.

These five regions of Labrador all extend beyond its border with Québec and into other areas. The Superior Province and the Nain Province are parts of larger Archean cratons within central Canada and in Greenland, respectively. The Churchill Province extends into Nunavut, and the Makkovik Province was originally continuous with parts of southern Greenland, prior to the Cenozoic opening of the Labrador Sea. The Grenville Province extends throughout eastern Canada, and southward into the United States. Each of these regions has a distinct and complex geological history. The Churchill Province was developed through Paleoproterozoic oblique collision of the Nain and Superior Provinces (Corrigan et al., 2018), and the Makkovik and Grenville provinces form part of a long-lived accretionary orogenic belt developed along the southern margin of the Canadian Shield (Kerr et al., 1996; Gower, 1996).

In addition to the structural provinces outlined above, Labrador and adjacent Québec also include an extensive region of Mesoproterozoic (1.6 to 1.2 Ga) igneous rocks (Wardle et al., 1997; Ryan, 1998; Figure 2.1). These intruded into the Nain and Churchill provinces and transgress their mutual boundary, but their emplacement was not associated with regional deformation or metamorphism. For this reason, they are commonly termed “anorogenic”, and thought to be related to attempted continental rifting (Emslie et al., 1994; Ryan, 1998). The

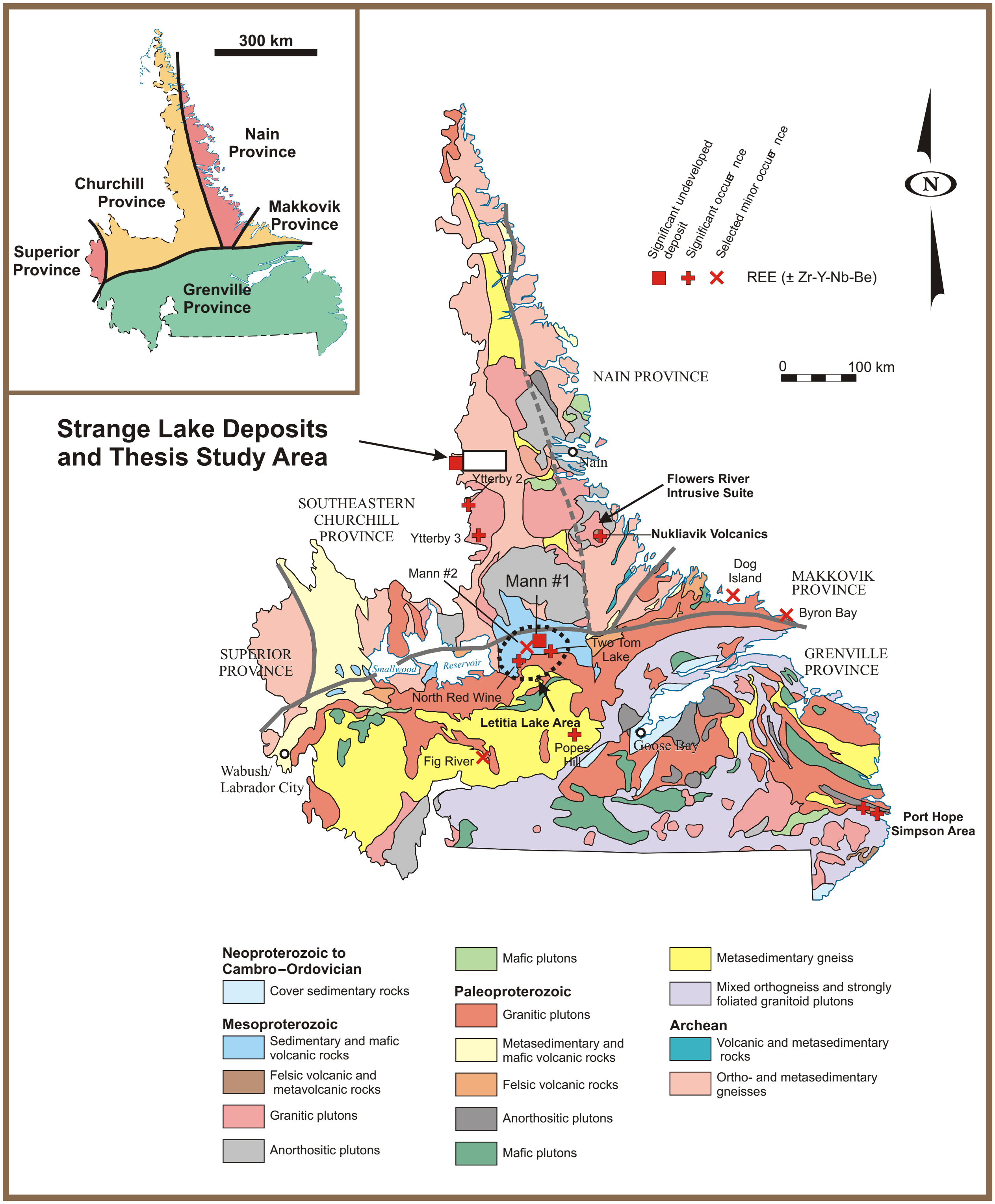

Figure 2.1. Regional geology of Labrador and locations of major REE and Rare-Metal deposits and prospects, modified after Rafuse and Kerr (2009). Inset map shows the five major structural provinces defined for the Canadian Shield in Labrador. Geology simplified after Wardle et al. (1997).

Strange Lake Intrusion, which is an important part of this project, is a small granitic body spatially associated with this much larger magmatic province.

For more information on the regional geology and tectonic history of Labrador and adjacent regions, readers are referred to the 1:1 million scale map (Wardle et al., 1997). There are no recent review articles about Labrador geology, but a report by Swinden et al. (1991) provides a useful general summary.

Geology of the Strange Lake Area

Archean and Paleoproterozoic metamorphic rocks

The Strange Lake area lies within the Churchill Province, and the local geology is shown in simplified form in Figure 2.2 (adapted from Miller et al., 1997). Geological mapping in this area is most detailed in Québec, where several units of metamorphic rocks are defined, trending generally north-south. These are termed the Mistinibi-Raude and Mistastin domains, and include both orthogneisses (of igneous origin) and paragneisses (of sedimentary origin). These domains are both interpreted to include rocks of both Archean and Paleoproterozoic age, but their age relationships are not well defined. In the vicinity of the Strange Lake Intrusion, metamorphic rocks are depicted to have mafic to granitic compositions, but field examination (Ryan et al., 2003; Kerr, 2015) suggests that they vary in composition on an outcrop scale. In the area of sampling for this project, there are few outcrops, but extrapolation from the map of Ryan et al. (2003) suggests that concealed bedrock is dominated by metamorphic rocks of mostly igneous origin, including mafic to intermediate compositions in the west, and largely granitic compositions in the east.

Mesoproterozoic Intrusive Rocks

In the south of the area (Figure 2.2), the metamorphic rocks are in contact with undeformed igneous rocks of the Mistastin Batholith, which are mostly coarse-grained granite, with lesser anorthosite and diorite. Two granites located along the Québec-Labrador border south of the study area were dated at 1439 Ma and 1423 Ma (Kerr and Hamilton, 2014). A large,

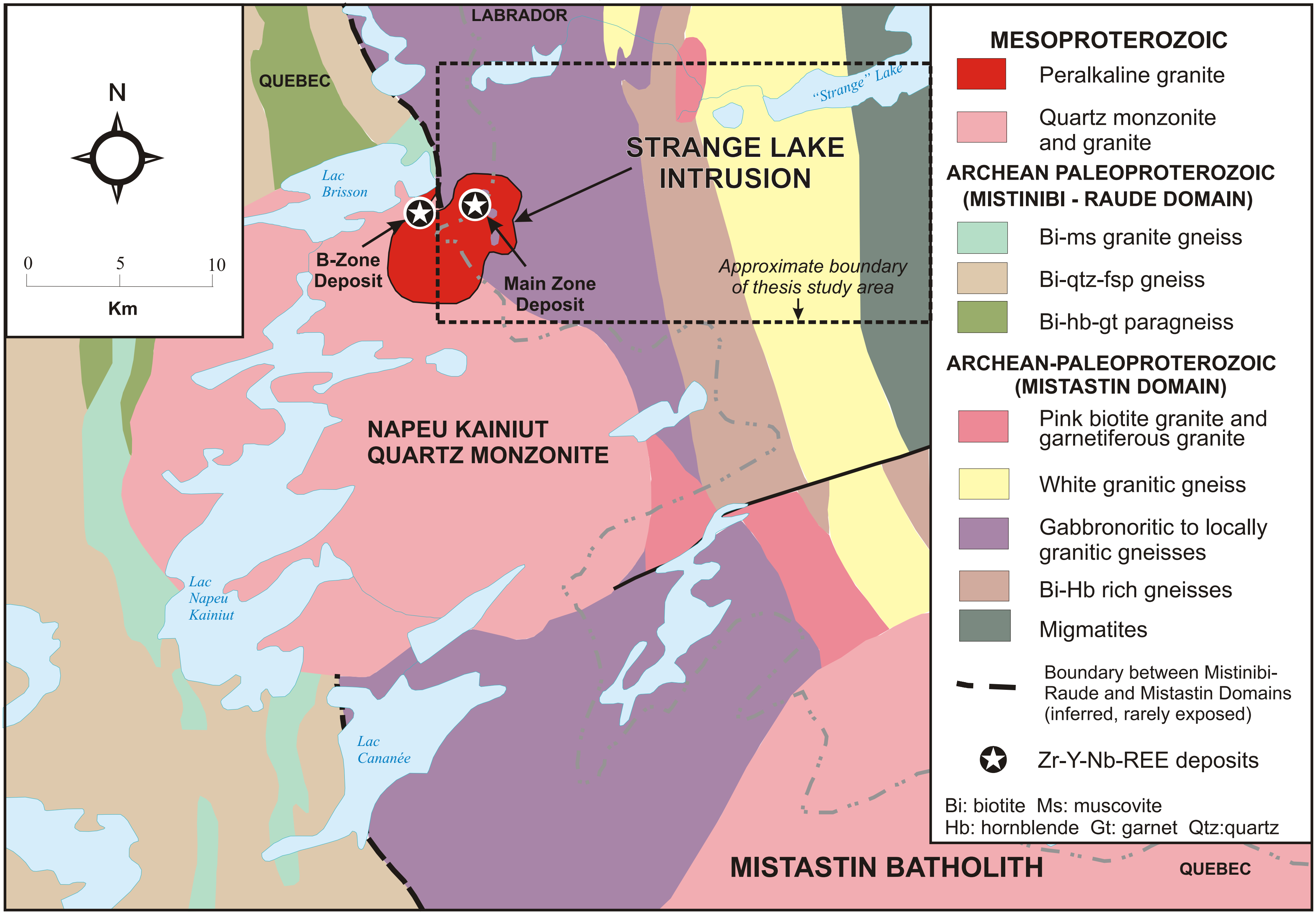

Figure 2.2 Regional geology the area in Quebec and Labrador around the Strange Lake deposits. Adapted from Miller et al., 1997. Geology simplified from regional maps produced by the Newfoundland and Labrador Deoartment of Natural Resources and the Québec Ministere des Ressources et de la Faune. Bi - biotite; Hb - hornblende; qtz - quartz; Fsp - feldspar; Gt - garnet; Ms - muscovite.

almost circular body of quartz monzonite and granite largely located in adjacent Québec is termed the Napeu Kainuit pluton. This is undated, but is generally considered to be part of the Mistastin Batholith, which it resembles (Ryan et al., 2003).

The youngest rocks in the area (aside from minor cross-cutting diabase dykes) are those of the Strange Lake Intrusion, located on the Québec-Labrador border (Figure 2.2). The intrusion is also known as the "Strange Lake Alkalic Complex" in many earlier publications. It is a small, roughly circular body of granite less than 10 km in diameter, that has an unusual Na-rich and Al-poor composition. It is an example of a 'peralkaline granite', defined by igneous petrologists as having molecular $(Na_2O + K_2O)/Al_2O_3 > 1.0$. Peralkaline granites are well known for unusual geochemical traits and many are enriched in rare chemical elements such as zirconium (Zr), niobium (Nb), yttrium (Y) and rare-earth elements (REE). The Strange Lake Intrusion has a U-. b zircon age of 1240 +/- 3 Ma (Miller et al., 1997). The geology and field relationships of the intrusion are mostly inferred from diamond drilling, because it forms few natural outcrops.

GEOLOGY AND PETROLOGY OF THE STRANGE LAKE INTRUSION

Geological Units and their Distribution

The Strange Lake Intrusion is roughly circular in shape, and is interpreted as a "ring complex" because its outer contact is marked by an arcuate system of faults. Figure 2.3 provides a simplified map of the Strange Lake Intrusion, after Miller (1986) and Miller et al. (1997). Outcrops are found mostly on a few hilltops along the border and in some stream valleys in Québec. Miller (1986, 1990) subdivided the intrusion into three distinct geological units, based upon the abundance of uncommon ("exotic") minerals containing Zr, Y, Nb and REE. This field classification was intended for visual identification, but the three units defined in this manner are also petrologically distinct. Minor units within the Strange Lake Intrusion include small areas of pegmatite and aplite (commonly containing high-grade Zr-Y-Nb-REE mineralization) and areas of older metamorphic rocks that probably represent parts of its roof zone. The map patterns (Figure 2.3) and the presence of aplite and pegmatite suggest that the present erosion surface lies close to the original upper boundary (roof) of the intrusion (Miller, 1986; 1990). Figure 2.4 illustrates some rock types and relationships from the Strange Lake Intrusion.

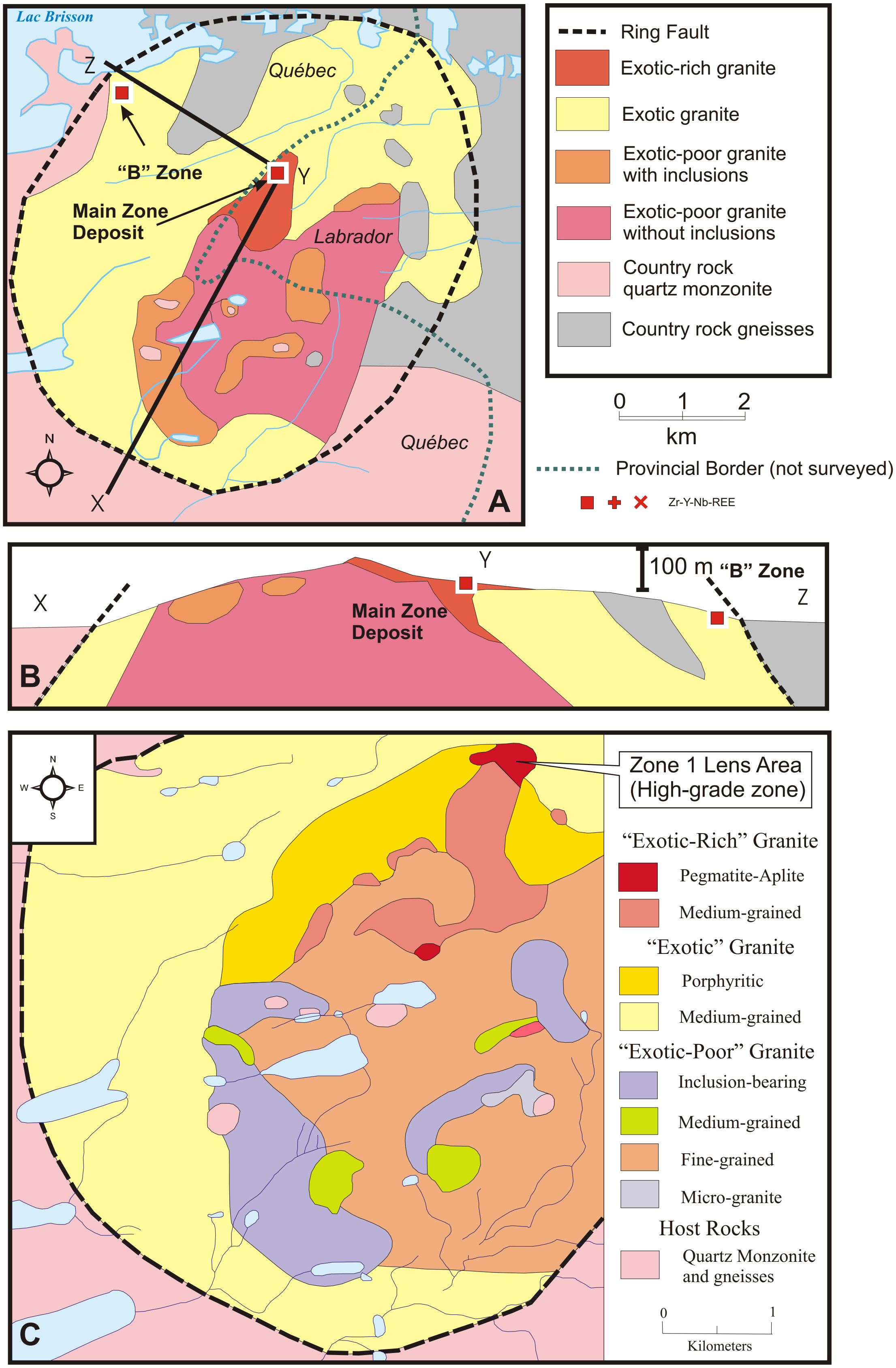

Figure 2.3 (A) General geology of the Strange Lake Intrusion. (B) Schematic cross section with locations of Main Zone and B-Zone deposits. Both after Miller (1986). (C) Detailed geology of the Strange Lake Intrusion and Main Zone Deposit, after Miller et al. (1997).

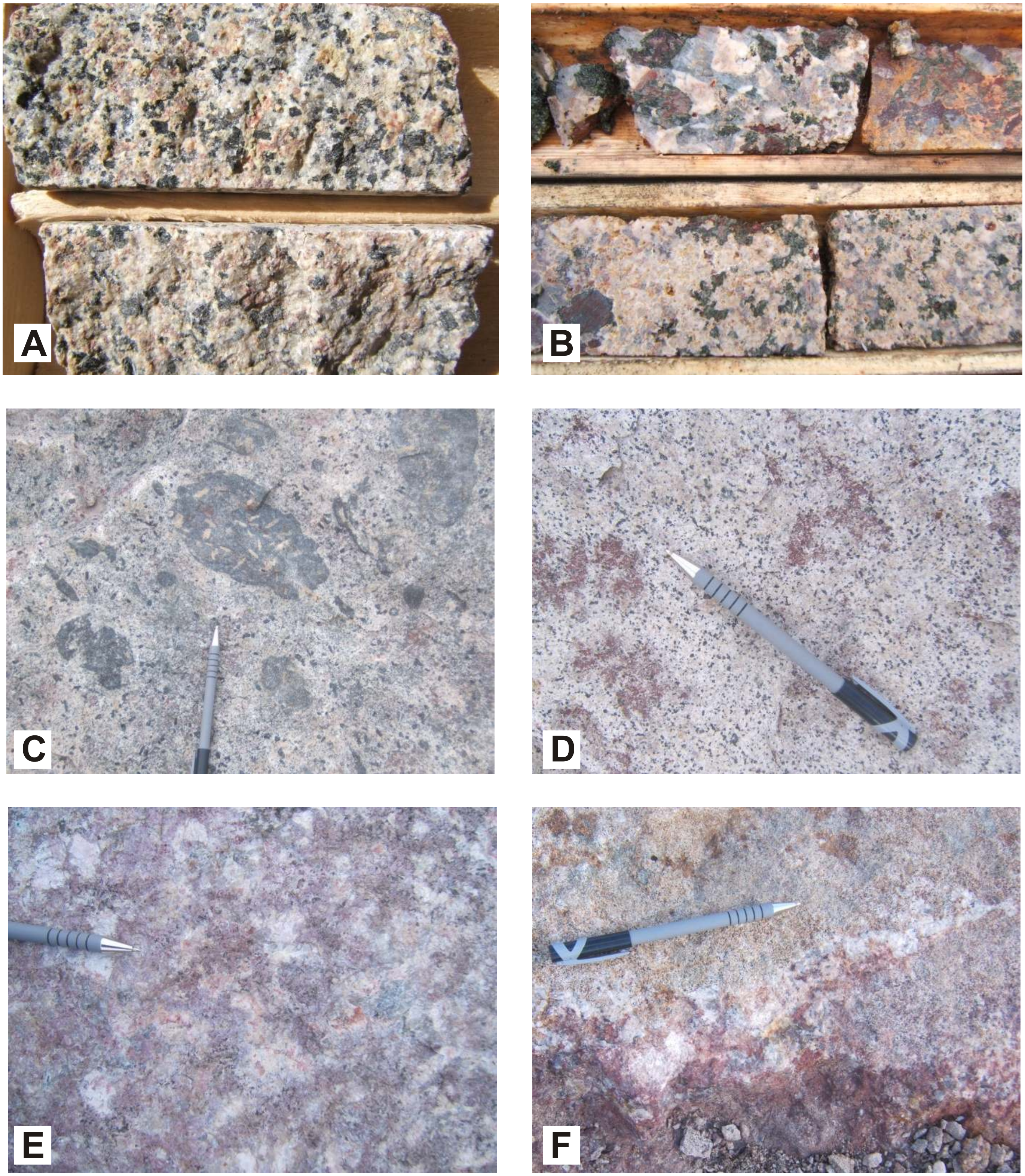

Figure 2.4. Examples of rock types from the Strange Lake area. (A) Typical drill cores from the exotic-rich granite unit, cores abut 2 cm wide. (B) Typical drill cores of heterogeneous mineralized pegmatite.(C) Mafic inclusions (probably not xenoliths, but globules of mixed magma) in the exotic granite unit. (D) Mineralized aplite with clots of Zr- and REE-bearing minerals, largely gittinsite. (E) Coarse-grained mineralized pegmatite with REE minerals. (F) Vein of pegmatite intruding fine-grained granite. Field photos from Main Zone excavation. Photos from A. Kerr (Geological Survey of NL).

"Exotic-poor" Granite (also termed Hypersolvus Granite)

The interior part of the Strange Lake Intrusion (Figure 2.3) is occupied by its oldest unit, termed the “exotic-poor” granite by Miller (1986). This is a homogeneous medium-grained granite that contains small quantities of "exotic" minerals (< 5%), and it is a hypersolvus granite, i.e., it contains K-feldspar crystals that include exsolution bands (perthitic texture) composed of albite (Na-feldspar). This texture indicates that the magma solidified at relatively high temperatures, and originally contained only one K-Na-bearing alkali feldspar. Other prominent minerals include quartz, Na-Fe-rich amphibole (arfvedsonite) and Na-Fe-rich pyroxene (aegirine). Dark-coloured inclusions occur locally, but are not as common as in the younger phases of the intrusion (Miller, 1986; Kerr and Rafuse, 2012)

"Exotic" Granite (also termed Subsolvus Granite)

The outer part of the Strange Lake Intrusion (Figure 2.3) consists of the “exotic” granite defined by Miller (1986), which typically contains 5-10% exotic minerals, and is more radioactive than the exotic-poor granite. The most abundant of the "exotic" minerals is gittinsite ($CaZrSi_2O_7$), which has a reddish colour, and is usually obvious as small interstitial grains. Gittinsite is one member of an extensive group of minerals called ‘zirconosilicates’, which are common at Strange Lake (Birkett et al., 1992). The "exotic" granite is petrologically distinct from the "exotic-poor" granite because it is a subsolvus granite, in which discrete crystals of K-feldspar and albite occur, without perthitic textures. This indicates that the magma solidified at a lower temperature than the hypersolvus granite and originally contained two discrete varieties of feldspar. The "exotic" granite commonly contains rounded dark inclusions that contain lath-like crystals which superficially resemble feldspar phenocrysts. These inclusions were initially described as xenoliths (Miller, 1986), but may instead be frozen ‘globules’ of a coexisting magma, based on microtextural relationships (Kerr, 2015; pers. comm., 2020).

"Exotic-rich" Granite (also termed Altered Subsolvus Granite)

The least extensive unit in the Strange Lake Intrusion is the “exotic-rich” granite of Miller (1986), which contains most of the Zr-Nb-Y-REE mineralization in Labrador. This occupies about 1 km^2 in the centre of the intrusion, along the boundary between the "exotic-poor" and "exotic" granites (Figure 2.3). As its name suggests, unusual minerals, including gittinsite, are most abundant in this unit (> 10%). It is a subsolvus granite with a fine to medium-grained, equigranular texture (Miller, 1986; Kerr and Rafuse, 2012). In many respects, it is similar to the other subsolvus granite unit (see above), but it is inclusion-free, and typically more enriched in Zr, Y, Nb and REE.

Some researchers (e.g., Salvi and Williams-Jones, 1990; 1992) interpreted the "exotic-rich" granite as a hydrothermally altered variant of the more extensive “exotic” subsolvus granite, which adjoins it (Figure 2.3). However, Kerr and Rafuse (2012) and Kerr (2015) view it as a discrete intrusive unit, following the original view of Miller (1986).

Mineralized Pegmatite and Aplite

The richest accumulations of unusual Zr, Nb, Y and REE-bearing minerals at Strange Lake are within restricted zones that have pegmatitic (i.e., very coarse-grained) or aplitic (i.e., very fine-grained) textures. These zones cross-cut the "exotic-rich" granite, indicating a younger relative age, and are mostly confined to this unit in Labrador (Miller, 1986; Kerr and Rafuse, 2012). However, similar pegmatite-aplite zones cut the inclusion-rich "exotic" granite in Québec, and also occur widely at the B-Zone deposit (see below). Aplites are homogeneous pale-coloured rocks, which typically contain coarser-grained patches including "exotic" minerals. Pegmatites are heterogeneous and coarse-grained rocks, which are spectacular in excavations, but are poorly preserved in drill cores. Pegmatites contain a wide variety of uncommon minerals. Potentially economic mineralization at Strange Lake largely consists of granite containing abundant pegmatite and aplite, although the "exotic-rich" granite itself represents a lower-grade resource. Due to their small size, only the most important pegmatite and aplite units are shown in Figure 2.3, which excludes the area of the B-Zone deposit.

Fluorite-rich Breccia

This unusual rock type outcrops near Lac Brisson in Québec, and was also encountered in some drill holes completed near the edges of the Strange Lake Intrusion. It consists of angular to locally rounded fragments of granite contained within a matrix consisting largely of purple fluorite. The fluorite mineralization is not of economic interest, and there is no associated Zr, Y or REE mineralization (Iron Ore Company of Canada, 1985).

MINERALIZATION

History of Mineral Exploration

The Iron Ore Company of Canada (IOC) first discovered the Strange Lake deposit in 1979 during investigations into regional geochemical anomalies revealed by the nationwide Uranium Reconnaissance Program (Zajac et al., 1984; Zajac, 2015). Airborne radiometric surveys assisted in definition of a larger boulder field, although the radioactivity is mostly related to Th rather than U. Exploration programs that followed the discovery, and efforts towards economic development, are detailed in the IOC Feasibility Study (Iron Ore Company of Canada, 1985; 1986) and summarized in a later report by Kerr and Rafuse (2010). The following account is drawn largely from these sources.

Between 1979 and 1983, IOC explored extensively on both sides of the border, using scintillometer prospecting and geochemical analysis of near-surface glacial material (till). IOC completed 118 diamond drill holes in 1981 and an additional 126 holes in 1982 on the Labrador side of the border, which defined the Main Zone Deposit. IOC also completed some drilling in Québec near Lac Brisson (Venkatswaran, 1983). About 30 years later, the Lac Brisson area became the focus of exploration by Quest Rare Minerals, who defined the “B-Zone” deposit (see below). IOC focused most attention on a flat hilltop area near the original discovery site, where pegmatite and aplite zones containing "exotic" minerals were most abundant and extensive. The IOC drilling program defined a 56 million tonne resource grading 2.99% ZrO_2, 0.38% Y_2O_3, 0.29% Nb_2O_3 and 0.076% BeO, A smaller higher grade resource included within this (called the Zone 1 Lens) was targeted for initial mining. Note that these resource estimates do not conform to present-day (NI-43-101) industry standards. IOC excavated a large (~ 1000 m^2) bulk sample trench within the Zone 1 Lens, on the Labrador-Québec border. This is the only area within the Main Zone Deposit where geological relationships can be investigated directly, rather than through drill core.

IOC aimed to recover zirconium (Zr), yttrium (Y) and niobium (Nb) from the deposit, with most emphasis on Y, which was then the most valuable commodity. The REE were recognized as possible by-products, but their economic significance was minor. Detailed work on material from the bulk sample identified many unusual and rare minerals, including gittinsite, which carries much of the Zr. An unnamed Ca-Na-Y-Silicate [$(Ca, Na)_2Y_3Si_6O_{18}.2(H_2O)$] was recognized as in important carrier of Y and REE. This mineral was later named gerenite (Jambor et al., 1998) and is essentially unique to Strange Lake.

The challenge of economically recovering Y, Nb, and Be (and some REE) through a single process proved daunting, and the high capital costs involved in establishing even a small seasonal mine at such a remote site were discouraging. At the time, the markets for the commodities in the deposit were very limited. The Mining Lease for the deposit site expired, and the area was designated as Exempt Mineral Lands (EML), meaning that new exploration licences could not be issued. Several other companies evaluated the deposits through the 1990s and early 2000s, but there were no proposals for further work. The Strange Lake area was selected as Labrador Inuit Lands (LIL) during negotiations, and the EML status of the area is unchanged.

In 2006, Freewest Ltd. staked claims adjacent to the Strange Lake Main Zone Deposit in both Québec and Labrador. The exploration interest was sparked by high uranium prices. Quest Uranium Ltd (later Quest Rare Metals) completed drill holes close to the border in 2009, but the uranium assays were low. Their attention then shifted to Lac Brisson in Québec, where drilling defined a larger region of Zr-Y-Nb-REE mineralization, which became known as the B-Zone Deposit. A preliminary report completed by Quest in 2014 was based on 345 drill holes. This defined an Indicated Mineral Resource of 278 million tonnes grading 0.93% Total Rare Earth Oxides (TREO) including 0.36% HREO+Y (Heavy Rare Earth Elements and Y), 1.92% ZrO_2 and 0.18% Nb_2O_5. There was also an Inferred Mineral Resource of 214 million tonnes grading 0.85% TREO (Gowans et al., 2014). Note that Quest (and many other companies) elected to quote grades as Total REE oxides, and include yttrium (Y) within that measure, even though it is not actually part of the lanthanide series in the periodic table. The grades reported for the B-Zone mineralization are broadly similar to those reported from the Main Zone Deposit (Kerr and

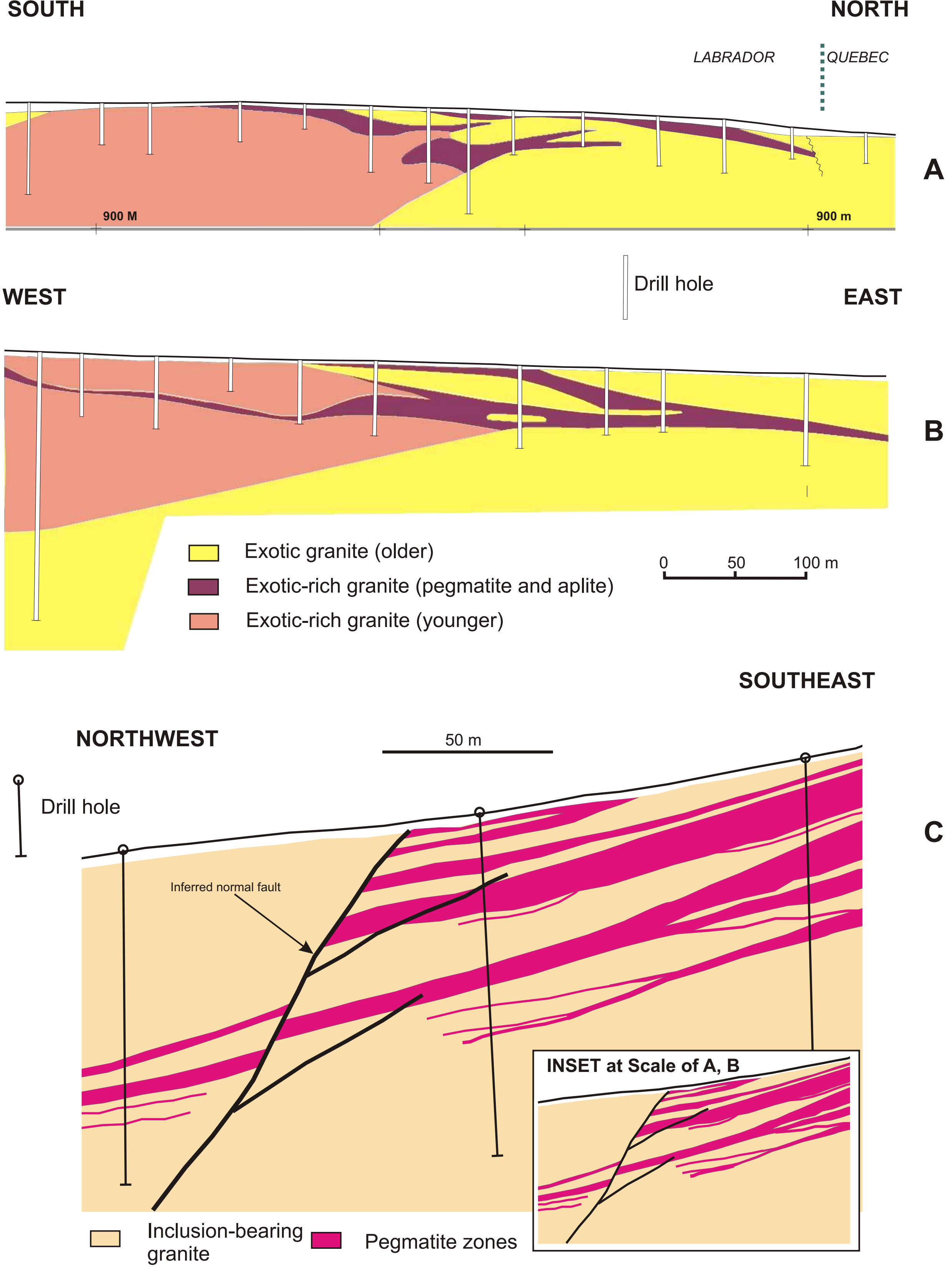

Figure 2.5 (A) North-South cross-section through the Strange Lake Main Zone deposit. (B) East-West cross-section through the Strange Lake Main Zone deposit. Redrawn from Iron Ore Company of Canada (1985) and Miller (1986). (C) Cross-section of part of the B-Zone deposit, showing stacked pegmatite sheets. Redrawn from Quest Rare Minerals website, 2010, by Kerr (2011). Inset in part (C) shows it at the same scale as parts A and B. Note that pegmatite zones shown in A and B are actually mixtures of pegmatite and host granite.

Rafuse, 2012; Kerr, 2013). However, the large resources identified at the B-Zone Deposit include mineralization at considerable depths, whereas the Main Zone Deposit is defined only to a depth of about 50 m.

Development proposals formulated by Quest were focused on a smaller near-surface zone containing the highest-grade material. Quest also continued research on mineralogy and mineral processing, using previous work by IOC as a starting point (Daigle et al., 2011; Gowans et al., 2014). The project progressed to preliminary assessment of commercial development options, but high capital costs and changes in the markets and demands for the REE again created obstacles. Quest Rare Minerals is no longer actively exploring in the area.

Work completed by IOC involved few direct analyses for the REE, because these elements were not then of economic interest. The REE geochemistry of the Strange Lake Main Zone was assessed by reanalysis of archived materials (Kerr and Rafuse, 2012; Kerr, 2013). Quest Rare Minerals analyzed thousands of samples for REE and many other trace elements. Overall, the compositions of mineralized material from the Main Zone and B-Zone deposits are similar (Kerr and Rafuse, 2012; Kerr, 2013).

Main Zone Deposit

The Main Zone Deposit is largely hosted within the the so-called “exotic-rich” granite but some mineralization on its northwestern side is associated with the adjoining “exotic” granite. The mineralization is defined largely by the abundance of smaller pegmatite-aplite veins and pods, which appear to intrude the host granites in sample trench exposures and in drill core. The mineralization is described by Miller (1986; 1990) and by Kerr (2013; 2015), and in IOC reports from the 1980s. The high-grade Zone 1 Lens) is a thin sheet-like, near-surface zone in the northwest, which merges with a thicker subsurface zone to the southeast (Figure 2.5). The area beneath the high-grade zone is mostly granite, but represents low-grade mineralization. The full depth extent of mineralization remains unknown, but the deepest drillhole terminated in such material at 270 m.

B-Zone Deposit

The B-zone Deposit is hosted by the inclusion-bearing ‘exotic’ granite of Miller (1986) rather than the younger "exotic-rich" granite associated with the Main Zone deposit. It resembles the Main Zone Deposit in that it consists of granite and pegmatite-aplite pods, and the latter define the highest-grade areas (Gowans et al., 2014; Kerr, 2015; Figure 2.5). The bulk grade of the B-Zone Deposit is similar to or slightly higher than that of the Main Zone deposit (Kerr and Rafuse, 2012; Kerr, 2013). However, the host granite is poorer in "exotic" minerals, and the proportion of near-surface pegmatite and aplite is greater.

Mineralogy

Mineralogical information from the Main Zone deposit was largely acquired in the 1980s and 1990s, and is documented in the IOC Feasibility Study (Iron Ore Company of Canada, 1985; 1986) and several research studies (Miller, 1986; 1990; 11111Birkett et al., 1992; 1996; Jambor et al., 1998). It is summarized by Kerr and Rafuse (2010; 2012) and Zajac (2015).

The rocks of the Strange Lake Intrusion consist largely of the common rock-forming minerals quartz, orthoclase (K-feldspar) and albite (Na-feldspar), with smaller amounts of Na-Fe-rich pyroxene (aegirine) and amphibole (arfvedsonite and reibeckite). These are accompanied by a wide range of uncommon minerals, which contain Zr, Nb, Y, Be, REE and other uncommon elements. Table 2.1 (adapted from Kerr and Rafuse, 2010) lists these minerals, which are most abundant in the pegmatites and aplites. The best known are gittinsite and gerenite, and these are of economic importance. Gittinsite is not unique to Strange Lake, but is found only in a few other localities worldwide. The Na-Ca-Y-REE silicate now known as gerenite (Jambor et al., 1998; Zajac, 2015) is essentially unique, as it is reported from only one other locality in Mongolia (see www.mindat.org). Kainosite [$Ca_2(Y,REE)_2Si_4O_{12}CO_3H_2O$] is a similar mineral, but not as unique as gerenite. Gadolinite [$Be_2(Ca, REE, Fe)_3Si_2O_{10}$] is another important host mineral for Y, Be and REE. Niobium is largely hosted by pyrochlore [$(Na,Ca)_2Nb_2O_6(OH, F)$] but may also occur in fergusonite [$(Y,Nb)O_4$]. Many other uncommon minerals were reported in subsequent scientific investigations (Table 2.1)

IOC determined bulk chemical and mineralogical compositions of the high-grade mineralization represented by the bulk sample (Iron Ore Company of Canada, 1985; 1986). Table 2.2 lists this information and Figure 2.6 summarizes mineralogy in the form of a pie chart.

Mineral name	**Formula**
Silicates:	
Allanite-(Ce)	$(Ce,Ca)_2(Al, Fe^{3+})_3(SiO_4)_3(OH)$
Aenigmatite	$Na_2Fe^{2+}{}_5TiSi_6O_{20}$
Armstrongite	$CaZrSi_6O_{15}\cdot 3H_2O$
Astrophyllite	$(K,Na)_3Fe^{2+}{}_7Ti(Si_8O_{24})(O,OH,F)_7$
Bafertisite	$Ba(Fe,Mn)_2TiSi_2O_7(O,OH)_2$
Barylite	$BaBe_2Si_2O_7$
Britholite	$(Ca,Th,REE)_5((Si,P)O_4)_3(OH,F)$
Catapleiite	$CaZrSi_30_9\cdot 2H_2O$
Chevkinite	$(Ca,Th,REE)_4(FeMg)_2(Ti,Fe)_3Si_4O_{22}$
Dalyite	$K_2ZrSi_6O_{15}$
Elpidite	$Na_2ZrSi_6O_{15}\cdot 3H_2O$
Eucolite	$(Ca,Na,Ce)_5(Fe^{2+}, Mn,Y)ZrSi_8O_{22}(OH,Cl)_2$
Eudialyte	$Na_4(Ca,Ce)_2(Fe^{2+}, Mn,Y)ZrSi_8O_{22}(OH,Cl)_2$
Eudidymite	$NaBeSi_3O_7(OH)$
Gadolinite	$Be_2(Ca,REE,Fe)_3Si_2O_{10}$
Gerenite	$(Ca,Na)_2(Y,REE)_3Si_6O_{10}\ 2(H_2O)$
Gittinsite	$CaZrSi_2O_7$
Kainosite	$Ca_2(Y,Ce)_2Si_4O_{12}(CO_3)\cdot H_2O$
Leifite	$Na_2(Si,Al,Be)_7(O,OH,F)_{14}$
Milarite	$K_2Ca_4Al_2Be_4Si_{24}O_{60}\cdot H_2O$
Mosandrite (Rinkite)	$(Na,Ca,Ce)_3Ti(SiO_4)_2F$
Narsarsukite	$Na_2(TiFe^{3+})Si_4(O,F)_{11}$
Niobophyllite	$(K,Na)_3(Fe^{2+}, Mn)_6(NbTi)_2Si_8(O,OH,F)_{31}$
Perclevite	$Ce\ (Ce,La,Nd)_2Si_2O_7$
Stetindite	$(Ce,LREE)SiO_4$
Thorite	$(Th,Fe,Y,P,Ca)SiO_4$
Titanite	$CaTiSiO_5$
Vlasovite	$Na_2ZrSi_4O_{11}$
Zircon	$ZrSiO_4$

Table 2.1. Listing of minerals known at Strange Lake (red) and others that are known in peralkaline granites and related rocks.

Oxides:	
Baddelyite	ZrO_2
Euxenite	$(Y,Ca,Ce)\ (Nb,Ta,Ti)_2O_6$
Fergusonite	$YNbO_4$
Perovskite	$(Ca,Na,Fe^{2+},Ce,Sr)(Ti,Nb)O_3$
Pyrochlore	$(Na,Ca)_2Nb_2O_6(OH,F)$
Uraninite	UO_2
Thorianite	ThO_2
Carbonates/fluorides:	
Bastnaesite-(Ce)	$(Ca,La)(CO_3)F$
Gagarinite-(Y)	$NaCaY(F,Cl)_6$
Parisite	$Ca(Ce,La)_2(CO_3)_3F_2$
Phosphates:	
Apatite	$Ca_5(PO_4)_3(OH,F,Cl)$
Monazite-(Ce)	$(La,Ce,Nd,Th)PO_4$
Rhabdophane	$(Ce,La)PO_4\ (H_2O)$
Xenotime	YPO_4

Table 2.1 (continued). Listing of minerals known at Strange Lake (red) and others that are known in peralkaline granites and related rocks.

Table 2.2. Chemical analyses and mineral proportions of the bulk sample from the Zone 1 Lens. Information from the IOC Strange Lake Feasibility Study (IOC, 1985; 1986)

Bulk Sample Analysis (1)		Mineralogy (2)		Mineralogy (3)
Element or Oxide	% (weight)	Mineral Name	% (weight)	% (weight)
SiO_2	63.40	Quartz	33.00	34.00
TiO_2	0.90	Albite	14.00	11.40
Al_2O_3	5.80	K-feldspar	17.50	13.00
Fe_2O_3	4.80	Pyroxene	5.00	5.70
MnO	0.23	Amphibole	8.00	5.20
MgO	1.00	Bastnaesite	0.25	0.25
CaO	6.30	Gadolinite	1.00	1.10
Na_2O	2.70	Gerenite	0.75	2.20
K_2O	2.70	Kainosite	0.25	n.d.
P_2O_5	0.10	Allanite	0.25	0.25
		Titanite	2.20	1.60
CO_2	0.20	Monazite	0.40	0.40
F	2.50	Gittinsite	7.50	5.20
H_2O	2.65	Fluorite	5.10	5.20
S	0.10	Pyrochlore	1.60	1.40
		Zircon	0.50	1.70
Y_2O_3	1.00	Thorite	0.25	0.20
ZrO_2	3.20	Hematite	0.50	0.40
Nb_2O_5	0.80	Galena	0.15	n.d.
BeO	0.17	Clays	1.00	8.80
SnO_2	0.07	Carbonates	0.20	0.20
REE oxide	1.30			
U_3O_8	0.02	Sulphides	n.d	0.40
ThO_2	0.18	Milarite	n.d	1.10
Ta_2O_5	0.04			
TOTAL	100.16	TOTAL	99.40	99.70

1 - Analysis of bulk sample listed in Feasibility Study.
2 - Mineral proportions of bulk sample provided by internal analysis.
3 - Mineral proportions of bulk sample provided to IOC by Hanna Research.

n.d. - Not determined.

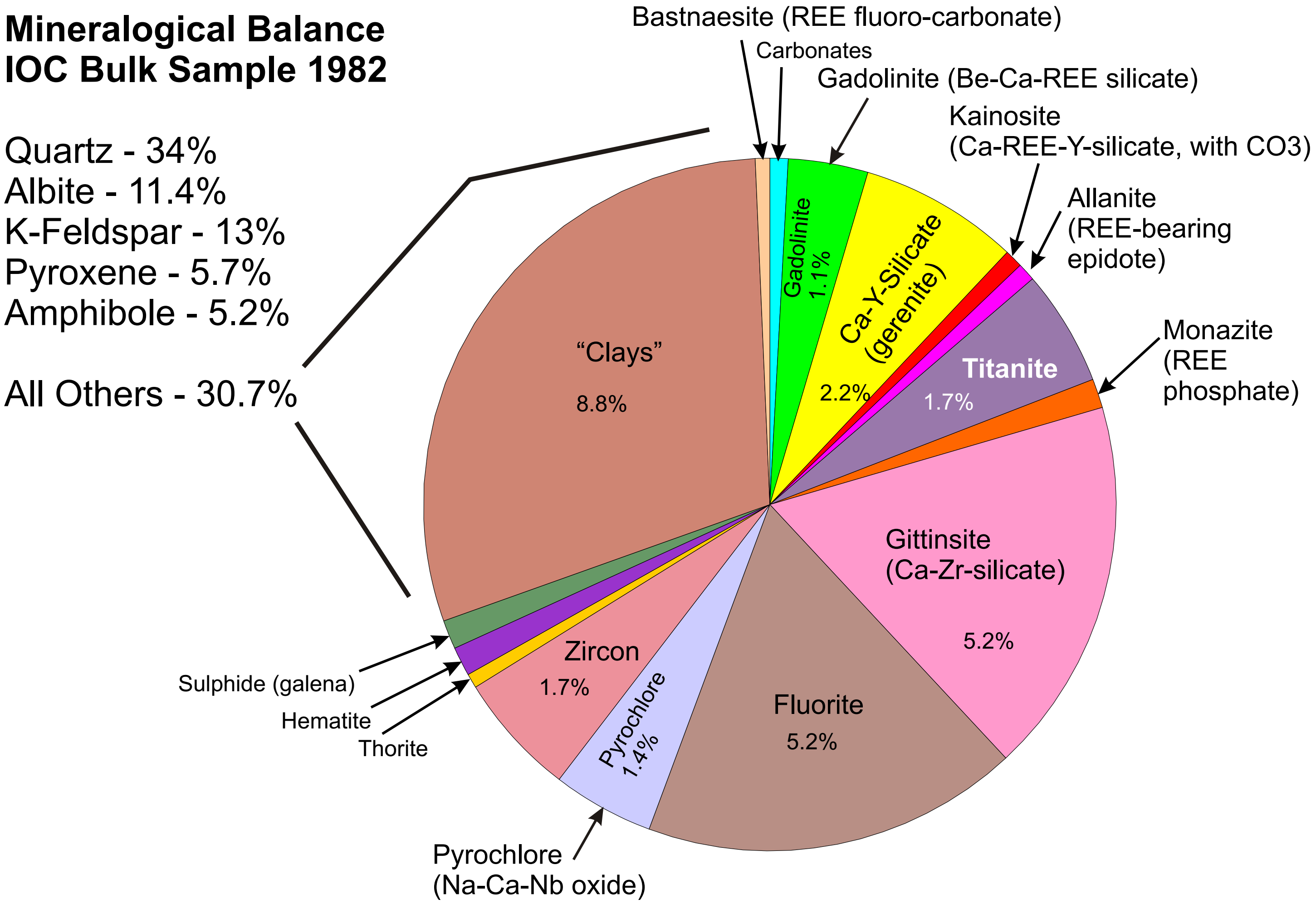

Figure 2.6. Chart summarizing mineralogical information from the bulk sample collected in 1982 from the Strange Lake Main Zone deposit, based on data presented by Iron Ore Company of Canada (1985) in their feasibility study. See also Table 2.1 for a listing of minerals and bulk chemical analysis. Note that mineral percentages are expressed here as weight measures.

Note that the chart only shows percentages for minerals other than the common silicates quartz, orthoclase, albite, amphibole and pyroxene, which collectively account for nearly 70% of the material. Note also that the material taken for the bulk sample represents a mixture of rock types including the exotic and exotic-rich granites of Miller (1986) and discrete pegmatite and aplite zones. Chart constructed by A. Kerr for a presentation at a GAC-MAC Meeting.

Excluding common rock-forming silicates (about 80% by weight), the most abundant minerals are gittinsite (5-7%), fluorite (~5%), titanite (1.6 – 2.2%), pyrochlore (~1.5%), gadolinite (~1%), gerenite (0.75 – 2.2%) and zircon (0.5 – 1.7%). Results from IOC work and an independent analysis from Hanna Mining (Table 2.2) differ slightly but are generally consistent. This work presumably used conventional density and magnetic separation techniques, followed by microprobe and/or wet chemical analysis. Note that mineral proportions are in weight % rather than volume%.

Similar investigations of the B-Zone deposit are summarized by Daigle et al. (2011) and by Gowans et al. (2014) but full data remain unavailable. Daigle et al. (2011) provide information in Table 2.3, representing high-grade, low-grade and 'altered' material from bulk samples. The work identified gittinsite and 'Ca-Y-REE silicate' (presumably gerenite and kainosite) as important carriers for Zr and REE, and other uncommon minerals listed in Table 2.1, notably pyrochlore, fluorite, zircon, thorite, and monazite. The work was completed using the QEMSCAN technique, a commercial application that is closely similar to the MLA-SEM method used in this study.

More recently, Baird (2018) completed MLA-SEM analyses on samples of crushed drill core material from the Main Zone Deposit. The purpose of this study was partly to obtain reference spectra from uncommon Zr- and REE-bearing minerals. This work identified a wide variety of zirconosilicate and REE-bearing minerals, including many of those listed in Table 2.1 and 2.2 and some which had not previously been reported. The results of Baird (2018) are important for this study because they provide a baseline for the primary abundance ranges in the probable source for uncommon minerals detected in this investigation of glacial materials (tills). The results of this study, and a related investigation of gittinsite (Currie, 2019) are discussed in more detail in Chapter 6.

Geochemistry of Mineralization

The bulk chemical analysis presented in Table 2.1 provides an estimate of the overall composition of the Main Zone Mineralization, but excludes individual REE. Total REE oxides (not including Y) were estimated at 1.3% by IOC. The Y, Nb, Be and REE values are higher than the mineral resource estimates, although the Zr content is broadly similar. The mineralization also contains elevated uranium (0.019% U_3O_8; 162 ppm U) and Thorium (0.18% ThO_2; 1584 ppm Th) and anomalous concentrations of tin (Sn) and tantalum (Ta).

Kerr and Rafuse (2012) and Kerr (2013; 2015) summarize analyses from archived drill core material and systematic sampling, and assessed the correlations between the REE and other elements. The limited correlation between Zr and the REE suggests that they are hosted by different minerals, but good correlation between Y and the REE suggests common mineralogical controls. The REE profiles of different geological units show that overall REE abundances are lowest in the "exotic-poor" hypersolvus granite and highest in the "exotic-rich" subsolvus granite, as predicted from observations (Kerr, 2015). The REE pattern (i.e., the relative abundance of the individual lanthanide elements) is consistent among the granite units, but pegmatite-aplite units have more varied profiles and tend to be more enriched in the heavy REE (i.e., those elements with atomic numbers higher than that of europium (63)). The REE patterns of the Main Zone and B-Zone deposits are similar (Kerr and Rafuse, 2012), which is consistent with mineralogical similarities.

Models for Mineralization Processes

The origins of mineralization at Strange Lake have limited relevance to economic aspects, or to mineralogical studies of glacial sediments, but are discussed extensively by researchers. All studies of the Main Zone agree that there is a spatial and likely a genetic link between mineralization and the "exotic-rich" granite unit of the Strange Lake Intrusion. Miller (1986; 1990) suggested a magmatic-hydrothermal model where Zr, Y, Nb, Be and REE were progressively concentrated during magmatic crystallization and then solidified in fluid-rich magmas that became trapped near the roof of the intrusion. The late-stage crystallization of these residual materials formed the high-grade pegmatite and aplite units containing highest-grade material. Salvi and Williams-Jones (1990) proposed an alternative model in which mixing of magmatic fluids and groundwater led to metasomatism, alteration and late-stage hydrothermal deposition of Zr, Y, Nb and REE. This model was disputed by Birkett and Miller (1991), and the debate has continued ever since. Kerr and Rafuse (2012) and Kerr (2013; 2015) support models that envisage largely magmatic processes with a limited hydrothermal overprint. However, Vayusukova and Williams-Jones (2014) and Gysi et al. (2016) recently argued the case for dominantly hydrothermal origins. Wider reviews of rare-metal and REE deposits associated with

Table 2.3. Mineralogical data reported from the B-Zone Deposit by Daigle et al. (2011)

Mineral	**High-Grade (weight %)**	**Low-Grade (weight %)**	**"Altered" (weight %)**
Quartz	40.4	32.7	31.4
Feldspar (unseparated)	22.3	34.7	38.6
Silicate Gangue (not separated)	16.2	18.3	17.2
Fluorite	1.67	0.75	1
Calcite	0.14	0.11	0.07
Apatite	0.13	0.09	0.07
Fe-oxyhydroxide	2.7	1.03	1.77
Zircon	5.02	3.71	2.24
Gittinsite	3.63	2.6	2.74
Fe-Ca-Zr-Ti Silicate (Titanite?)	1.12	0.75	0.64
Pyrochlore	0.88	0.63	0.28
Bastnaesite	0.06	0.003	0.003
Thorite	0.51	0.33	0.26
Monazite	0.26	0.06	0.16
Ca-Y-REE Silicate (Gerenite)	2.63	0.92	0.82
Epidote (REE+Y) (Allanite?)	1.11	1.69	1.95
Other Minerals (not specified)	0.21	0.18	0.2
Other Unidentified Minerals	1.06	0.65	0.67
Total	**100.00**	**100.00**	**100.00**

Note: Analyses are in weight percent rather than volume percent.
Note: Ca-Y-REE silicate may include both gerenite and kainosite.
Note: It is assumed that the REE-bearing epidote is allanite and that Fe-Ca-Ti silicate is titanite.

peralkaline granites rocks (e.g., Richardson and Birkett, 1995; Dostal, 2016) suggest that *all* involve local hydrothermal remobilization, but conclude that mineralization generally has a strong link to magmatism and related magmatic fluids.

SURFICIAL GEOLOGY

Glacial Dispersion and Glacial Deposits

Northern Labrador was extensively affected by Pleistocene glaciations. The most recent continental ice sheets of the Wisconsin Glaciation had several ice centres from which glacial flow was outward, towards and across present-day coastlines. The surficial geology of the Strange Lake area and adjacent regions is described by McConnell and Batterson (1987), Batterson (1989) and Batterson and Taylor (2009). The following summary is adapted from these sources. Figure 2.7 illustrates the surficial geology of the area around Strange Lake, modified after Batterson and Taylor (2009).

In northern Labrador and adjacent Québec, there was an ice centre located east of Hudson's Bay, and the general direction of ice flow was towards the east, towards the Labrador Sea. The Strange Lake area sits east of this ice centre, and forms a high dissected plateau, with elevations from 500 to 700 m above sea level. It was entirely covered by ice until deglaciation about 11,000 to 9000 years ago. The glacial record in the area is limited to the latest Wisconsin period, and the glacial flow history appears to be relatively simple. Glacial landforms and other indicators (including dispersion from the Strange Lake deposit) all point to a transport direction of around 70° (ENE). Bedrock is mantled by thick glacigenic deposits (up to 16 m) representing basal till from ice sheets, overlain by more varied glaciofluvial deposits and large expanses of organic accumulation (marshes and string bogs). The glaciofluvial deposits include veneers of well-sorted sand and gravel, and also numerous esker ridges that represent subglacial melt channels. An esker system that extends eastward from Lac Brisson is sufficiently large to appear in satellite images, and was included in a map of esker systems for all of northern Canada by Storrer et al. (2013). It can be traced to the Labrador coast, some 120 km to the east. Natural outcrops are rare, and there are extensive boulder fields, within which much material appears to be locally derived. McConnell and Batterson (1987) and Batterson (1989) describe two regional till units, interpreted as a lodgement till and an overlying subglacial melt-out till. The

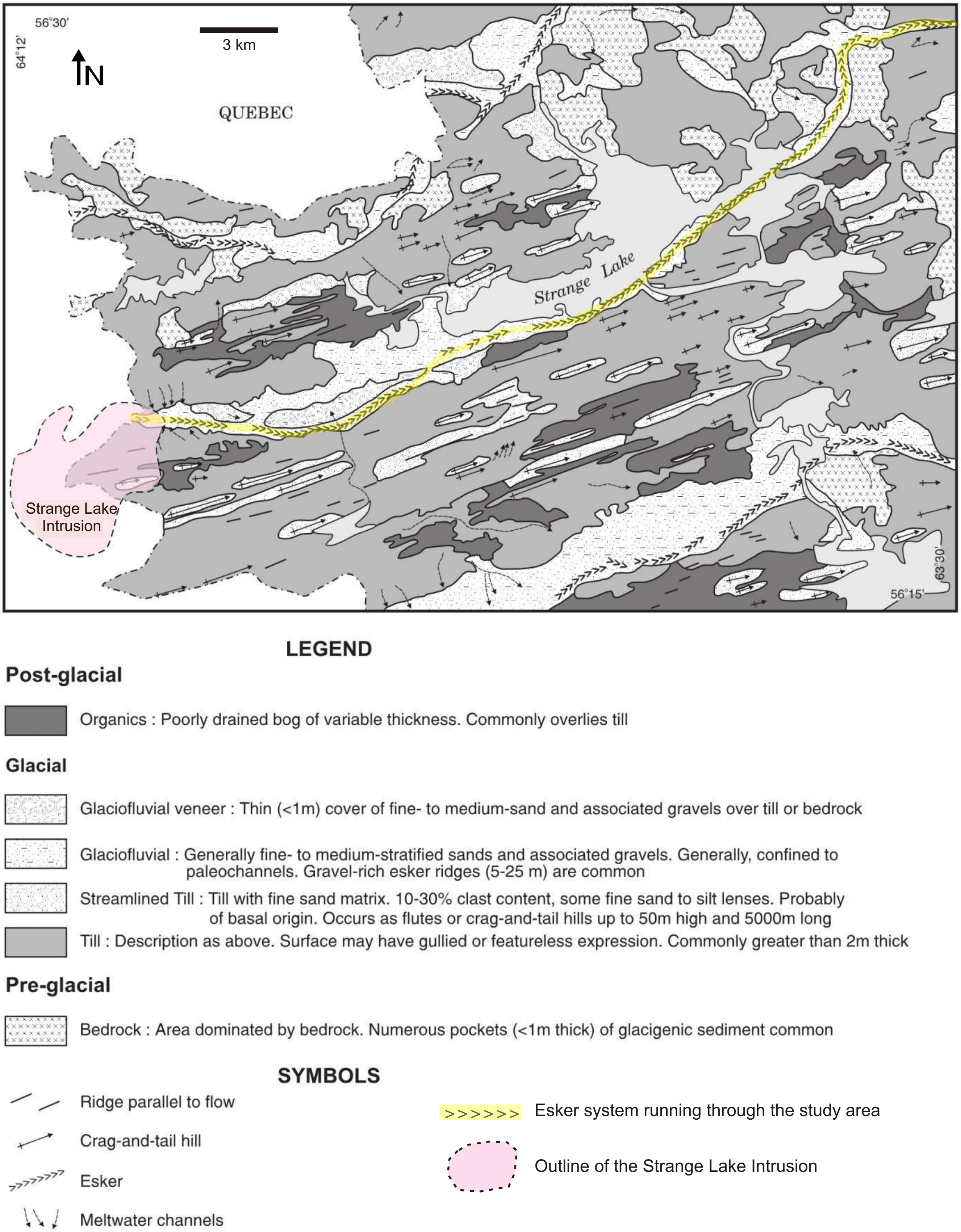

Figure 2.7. Quaternary geology of the area to the east of the Strange Lake Intrusion, showing the linear pattern of surficial units and the course of a prominent esker system that runs through the zone of glacial dispersion. Modified after Batterson and Taylor (2009). Note that "Strange Lake" is not an official name for the lake, but the name has become widely used.

lower unit contains material of very local origin, whereas the upper unit contains some clasts (fragments) of more distant origin, suggesting greater transport. The upper unit is widespread across the area, and represents the source material for most previous geochemical exploration programs involving glacial sediments. The present-day climate of the area is harsh, and surficial materials at depth have discontinuous permafrost. Periglacial surface features are present, including contraction cracking (frost polygons) and also ‘mudboils’ or ‘frostboils’ where fresher unweathered till is pushed upward through vegetation. These features provide a useful method of easily sampling the uppermost layers of the subsurface till.

The direction of glacial transport (to the ENE) is essentially at right angles to the trends of older metamorphic rock types within the area (Figure 2.2; see also Figure 2.7). Glacial sediments derived from bedrock sources would be expected to contain detritus from all of these rock types, and also from Mesoproterozoic igneous rocks. The Strange Lake Intrusion represents a point source of very unusual composition within this large and diverse source area.

Evidence for Ice Streams in the Strange Lake Area

The physical evidence for uniform ENE-directed glacial transport in the area of Strange suggests that the area formed part of an “Ice Stream” within the northeastern part of the Laurentide Ice Sheet (Paulen et al., 2017). Ice Streams are now recognized as an important aspect of present-day continental glaciation, and represent ‘corridors’ or ‘channels’ where ice flows more rapidly than in surrounding areas (e.g. Evans et al., 2008; Stokes et al., 2016). They represent the main routes by which ice-sheets discharge material to their margins. Recent regional analyses of the now-vanished Laurentide Ice Sheet, based on glacial landforms and other data, suggest that it also contained numerous ice streams (Margold et al., 2015). One of these proposed ice streams is located through the study area, and Paulen et al. (2017) suggest that it affected the glacial transport history and dispersion pattern. Evidence in favour of this idea comes largely from glacial landforms, which display remarkable linearity and continuity through this area (e.g., Figure 2.7). The nearly linear dispersion track revealed by previous geochemical exploration surveys in the Strange Lake area (see Chapter 3) is also an argument for the existence of a corridor of fast-flowing ice.

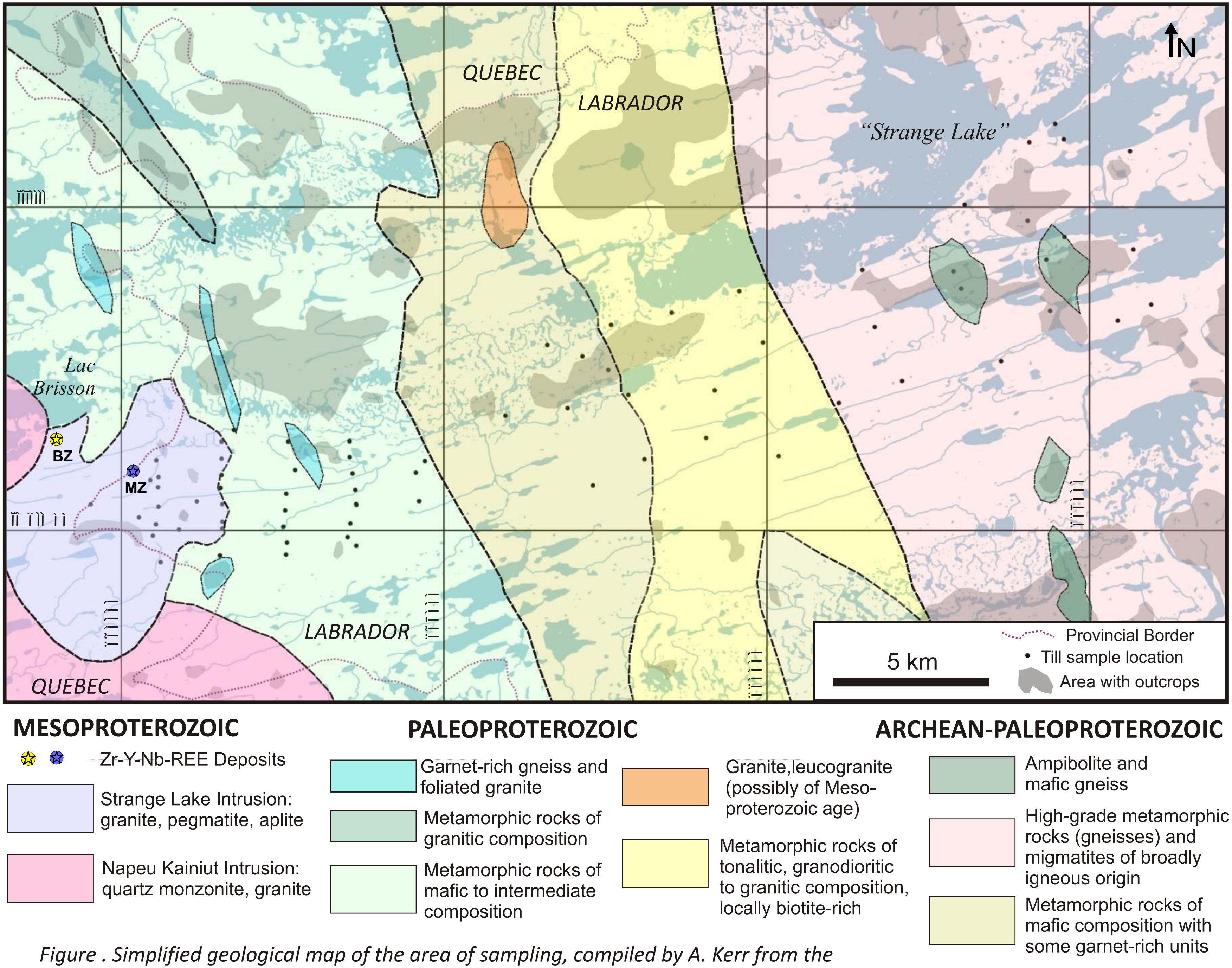

Figure . Simplified geological map of the area of sampling, compiled by A. Kerr from the regional maps of Ryan et al., 2003. MZ - Main Zone Deposit; BZ - B-Zone Deposit.

Paulen et al. (2017) and McLenaghan and Paulen (2017) discuss the implications of ice streams for glacial dispersion and suggest that such environments should lead to distinctive dispersion patterns for different indicator minerals from mineralized sources. The Strange Lake area thus offers a location in which to test some of these ideas, and also the impact and potential of different indicator mineral exploration techniques. These aspects are further discussed in Chapter 3, and in the discussions presented in Chapter 8.

INTERPRETED GEOLOGY OF THE STUDY SAMPLING AREA

This project is focused on a rectangular area of approximately 35 km by 15 km, which extends eastward from the Strange Lake Main Deposit (Figure 2.2). This represents the area of glacial dispersion recognized by previous work, and includes the locations of the 76 glacial sediment (till) samples that were analyzed by MLA-SEM methods. This area contains virtually no natural bedrock outcrop, so the exact details of geology remain unknown. However, the wider area was mapped by Ryan et al. (2003), and outcrops to the north and south consist mostly of metamorphic rocks derived from plutonic igneous rocks, aside from the southeast corner, where Mesoproterozoic igneous rocks (Napeu Kainuit and Strange Lake intrusions) form scattered outcrops. Thus, it is possible to extrapolate the strong north-south geological trends noted by Ryan et al. (2003) to construct a geological map for the sampling area (Figure 2.8).

Figure 2.8 shows that the area of study includes five main geological components, but some of these can be subdivided. In the southeast, it is underlain mostly by granitic rocks of the Strange Lake Intrusion, and this is confirmed by the extensive drilling completed by IOC in the 1980s. The remainder of the area consists of metamorphic rocks of Paleoproterozoic and possibly Archean age. Two broad units in the west, including the area immediately north of the Strange Lake Intrusion, consist of rocks that have mafic to intermediate compositions. These contain feldspars, hornblende, pyroxenes and some garnet, but are generally not quartz-rich, aside from one area in Quebec. This area also includes some metamorphic rocks of sedimentary origin that are rich in garnet. In contrast, the broad geological units in the east of the study area are of broadly granitic (tonalite to granodiorite) composition, and are more quartz-rich, and likely richer in K-feldspar compared to the bedrock in the west. Smaller areas of hornblende-rich mafic gneiss also occur in the east. A small region in the centre of the study area is underlain by granitic rocks of uncertain age. Due to the near-absence of outcrops, the boundaries between these broad geological units cannot be positioned accurately.

CHAPTER 3: PREVIOUS SURFICIAL GEOCHEMICAL STUDIES

GENERAL SUMMARY

Geochemistry is essential in understanding processes that result in potentially economic mineral concentrations or ore deposits. The Strange Lake area was the subject of several types of geochemical research focused on its unusual rocks and minerals, and it has also long provided a “type example” for geochemical dispersion patterns linked to glacial and postglacial processes (McConnell and Batterson, 198 ; Batterson, 1989; Batterson and Taylor, 2009; McLenaghan et al., 2017; 2019). This chapter summarizes previous investigations to provide a framework for subsequent discussion of the MLA-SEM data.

The Strange Lake deposit was originally discovered by following up the results of a surficial geochemical survey that analyzed lake sediments, and subsequent local surveys using tills and stream waters were used widely in exploration. A regional survey using a variety of media (lake sediment, stream sediment, glacial till and waters) indicated a well-defined geochemical dispersion from the deposit (McConnell and Batterson, 1987; Batterson, 1989), which was later refined by analysis for additional chemical elements (Batterson and Taylor, 2009). There are also indications that more subtle geochemical dispersion extends for > 100 km, from statistical treatment of regional lake sediment geochemical data (Amor, 2014) and reconnaissance MLA-SEM research (Wilton et al., 2017). A more recent indicator mineral investigation, using conventional heavy mineral concentration followed by petrographic and mineralogical analysis, confirmed that unusual zirconosilicate and REE-bearing minerals can be identified in tills, but did not provide results that closely match the known bedrock sources (McClenaghan et al., 2017; 2019). Investigations using MLA-SEM methods may provide a method to resolve some of these inconsistencies and better understand dispersion processes. Previous investigations, including till geochemistry, indicate that coarser material from Strange Lake is abundant for at least 35 km down-ice, but also that tills may be heterogeneous in composition, even in finer size fractions. These data provide important points of comparison for results from MLA-SEM analysis presented in Chapters 6 and 7.

SURFICIAL GEOCHEMISTRY AND DISCOVERY OF THE STRANGE LAKE DEPOSIT

Potentially economic Zr-Nb-Y-REE mineralization was first discovered at Strange Lake through surficial geochemical exploration. In the 1970s, nationwide programs were initiated to assess the potential for uranium mineralization in Canada. These consisted of regional sampling of lake-bottom sediments and also lake waters, followed by trace-element analyses of these materials. The element suite was limited by 21st century standards, comprising common base metals and precious metals, along with U, Th and F. There were no systematic analyses for REE and any related elements such as Zr, Y or Nb (Geological Survey of Canada, 1979). In the Strange Lake area, lake sediment data showed anomalous lead (Pb) concentrations for some 25 km east-north-east of what would later be identified as the Main Zone Deposit site, and showed wider dispersion of F in lake waters. There were also weaker anomalies for U and some other elements. The simp.est explanation of the pattern is that it indicates a point source at the up-ice end of the anomaly, and this reasoning led to the discovery of radioactive boulders near the Main Zone deposit. Subsequent investigations showed that the radioactivity came largely from Th, rather than U, and that the mineralized boulders were rich in Zr, Nb, Be, Y and REE (e.g., Zajac et al., 1984; Zajac, 2015). The Strange Lake Intrusion was subsequently recognized as the host to mineralization, although the first descriptions were not published until a few years later (Currie, 1985)

Exploration in the Strange Lake area from 1980 onwards also used surficial geochemical methods to seek unexposed areas of high-grade mineralization (Hlava and Krishnan, 1980; Venkateswaran, 1983). These were simple surveys, in which near-surface till was sampled in a grid pattern, largely through collecting material from the abundant “frost boils” caused by seasonal permafrost. Soil sampling programs were also completed, on densely-spaced sampling grids. The analysis program was limited to Cu, Zn, Be, Th, U, F, Y, Nb and Sn. The data from soils proved variable and was difficult to interpret (Hlava and Krishnan, 1980) but analysis of tills from frost boils proved effective. Samples close to known mineralization were anomalous in key indicator elements, and investigation of other anomalies led to the discovery of mineralized pegmatites and aplites. These geochemical data were used to map the extent of the "exotic-rich" granite that hosts most of the mineralization (Venkatswaran, 1983). From a regional perspective, analysis of stream waters showed strong enrichment in fluorine immediately eastward from the deposit, but also showed that the fluorine signature became weaker when small streams joined larger watercourses draining adjacent areas. No indicator-mineral surveys were attempted during exploration work, but the recognition of distinctive clasts and also boulders containing mineralization helped to define areas of interest and also the dispersion pattern from the deposits (Venkatswaran, 1983).

GOVERNMENT GEOSCIENCE SURVEYS – 1983 to 2009

Regional Multimedia Surveys

Following the discovery of the Strange Lake Main Zone deposit, regional bedrock and surficial mapping programs were initiated by the Geological Survey of Newfoundland and Labrador. These investigations were accompanied by systematic sampling of lake sediments, stream sediments, tills and stream waters, and analysis for a wider range of major and trace elements. The results provided excellent definition of a multi-element dispersion train from the deposit, which still figures prominently in most reviews of exploration geochemistry methods. The initial work by McConnell and Batterson (1987) and Batterson (1989) has now become a “textbook example” of geochemical dispersion from a point source.

McConnell and Batterson (1987) collected samples over an 800 km² area in the vicinity of the Strange Lake Intrusion, and towards the ENE, parallel to inferred glacial transport directions. Samples consisted of till material, stream sediment and stream water, and also lake sediment and waters. The analysis included key elements associated with the mineralization, such as Be, Ce, F, Ga, La, Nb, Pb, Sn, Th, Y, Zn and Zr. The results defined a linear to fan-shaped dispersion zone extending for more than 40 km to the ENE of the Main Zone Deposit, but different methods revealed different patterns. The geochemistry of the till samples revealed a long and narrow multi-element anomaly with a strikingly linear geometry. The data from stream sediments and stream waters showed a wider spatial anomaly, and data from lake sediments and waters defined an even wider and more extensive regional anomaly. The dispersion patterns were best defined using the data for Nb, Be, Pb and Y, all of which occur in the deposit. McConnell and Batterson (1987) also used multivariate “Factor Analysis” (also known as Principal Components Analysis) to group elements and understand their mutual relationships. McConnell and Batterson (1987) concluded that exploration for deposits similar to Strange Lake was best conducted using regional studies of lake sediments, followed by more detailed sampling of tills within anomalous regions to define dispersion and likely source areas. These studies did not investigate till mineralogy.

Detailed Surveys of Geochemical Dispersion near the Main Zone Deposit

Bell (1984) investigated the mineralogy and geochemistry of till samples collected from an area representing about the first 6 km of the regional dispersion train from the Strange Lake Main Zone deposit. Her investigation involved identification of mineral grains in sand-size material, description of clasts in the tills, geochemical analysis, and also investigation of particle size distributions and their impact on compositions.

Bell (1984) also showed that till materials in this area may be heterogeneous with respect to the amount of debris derived from the Strange Lake Deposit. Geochemical analysis of the finest particle size fraction (< 0.063 mm) showed higher values of Y and Nb than the sand-sized material (0.125 to 0.25 mm) used for mineralogical analysis. Size fractions with coarser-grained material (> 1 mm) showed even stronger enrichment, but gave less consistent results. This finding is important in the context of results from more systematic exploration till sampling in 2011 and 2012 and has implications for the long-distance dispersal of such material (see below, and Chapter 8).

Regional Studies of Geochemical Dispersion in Till

Batterson (1989) investigated the surficial geology of the area around and east of Strange Lake and analyzed 1081 glacial sediment (till) samples collected from 550 sites. He noted that dispersion from Strange Lake could be geochemically identified using Be, La, Pb, Nb, and Y analyses. The data for Ce, Rb, Th, U, and Zr contents provided some definition, although not as clearly. The data from geochemical analysis of tills was supplemented by regional geophysical data from airborne gamma-ray spectrometry that defines Th and U enrichment, and also by mapping the distribution of clasts of distinctive rock types from Strange Lake in the till samples. The results provided better definition of dispersion than the earlier study of McConnell and Batterson (1987) and also the first recognition of the possibility for long-distance detection through indicator-mineral studies:

"In all the cases documented above, there is evidence of considerable transport distances. Within the study area, maximum transport is at least 40 km, with expectation that a clearly defined dispersal train extends for at least 55 km and probably farther". Airborne geophysical surveys support this observation,

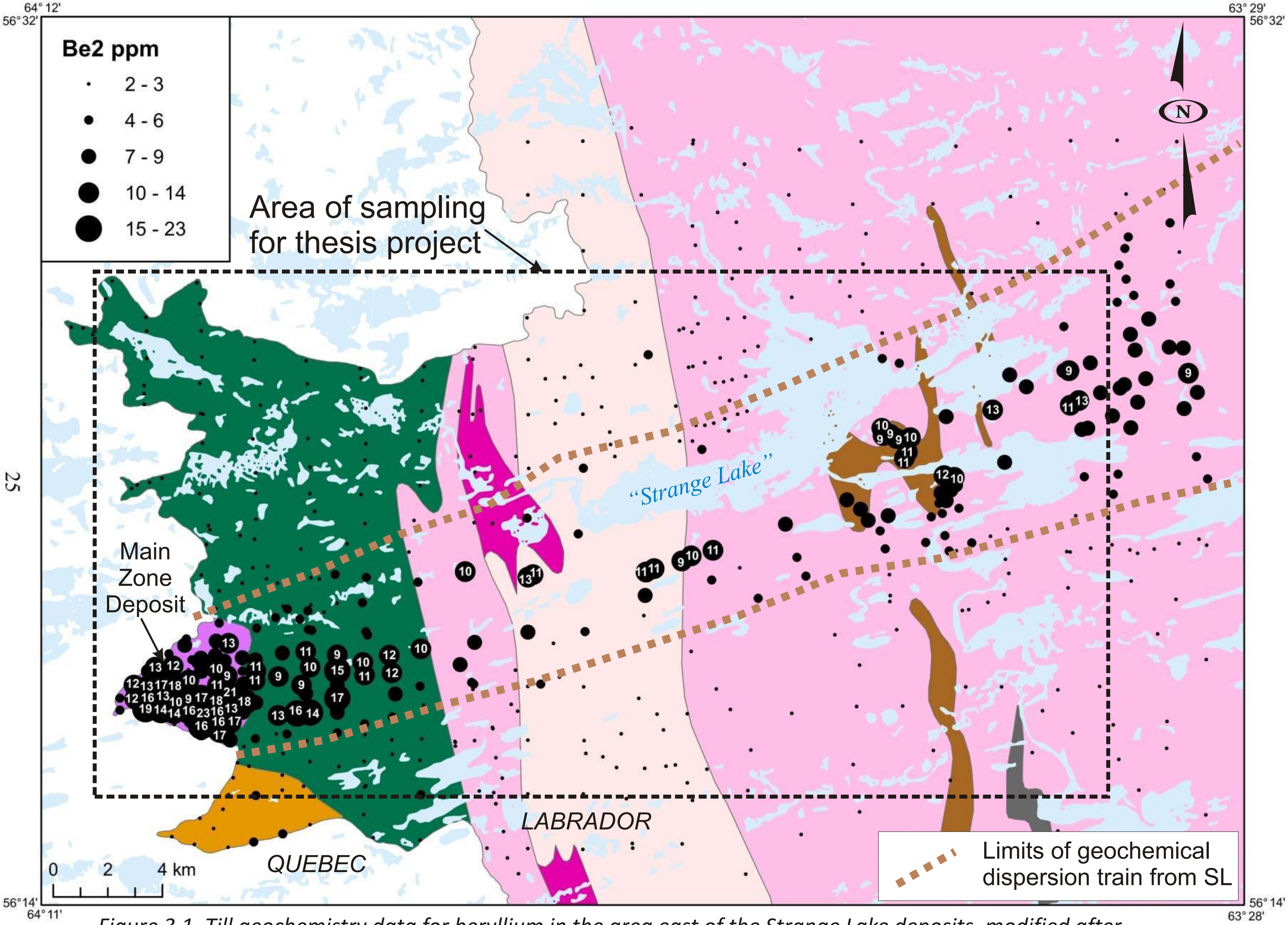

Figure 3.1. Till geochemistry data for beryllium in the area east of the Strange Lake deposits, modified after Batterson and Taylor (2009), showing the pattern of geochemical dispersion and the locations of till samples in relation to the thesis sampling area.

particularly airborne spectrometry. Distribution maps derived for uranium, total count and especially thorium, match the identified pattern of clast dispersal. The well-defined geophysical pattern extends outside of the study area to the vicinity of Anaktalik Brook, beyond which the pattern becomes more diffuse. It is not apparent what the specific tracer mineral content of the surface sediment must be to affect airborne data, but it is likely that remnants of the train (i.e., less than 0.01 percent of the surface clasts) should be observable for many more kilometres, out to Nain Bay 110 km down-ice of the complex" (Batterson, 1989, p. 29).

The trace elements analyzed by McConnell and Batterson (1987) and Batterson (1989) did not include the REE, or other elements of potential interest from Strange Lake. The samples were subsequently re-analyzed for a much wider element suite, and aspects of the glacial geology were re-evaluated in the light of newer ideas and data. The results of this work were presented by Batterson and Taylor (2009), which provides the most recent evaluation of dispersion patterns. The light REE lanthanum (La) provided good definition of glacial dispersion patterns, but the more abundant light REE Ce was less effective. Beryllium, Nb and Y remained the most effective tracers of dispersion from the deposit. Batterson and Taylor (2009) also noted that localized anomalies *within* the dispersion train appeared to be related to unusual concentrations of mineralized clasts, and were thus probably of 'englacial' origin, i.e., related to the disaggregation of larger mineralized boulders and fragments that were contained within moving ice. Figure 3.1 shows the regional distribution of Be in till from Batterson and Taylor (2009), and the distribution of their till samples compared to the area investigated in this study. Figure 3.2 shows the dispersion of Y from Strange Lake in three dimensions by superimposing geochemical data from Batterson and Taylor (2009) on satellite imagery. The image was prepared by Steven Amor of the Geological Survey of Newfoundland and Labrador using the Google Earth software.

Long-Distance Geochemical Dispersion from Strange Lake

Batterson (1989) suggested that the geochemical signature from Strange Lake likely extended beyond the well-defined dispersion train illustrated in Figures 3.1 and 3.2, and perhaps as far as coastal Labrador. At such distances, geochemical signatures would be subtle, and harder to distinguish from other regional patterns related to bedrock geology. Amor et al. (2019) recently presented integrated lake sediment geochemical data from Labrador and Québec, including analyses of previously unreported elements. They suggested that subtle enrichment in Zr, Hf and Sn over 80 km from Strange Lake defined

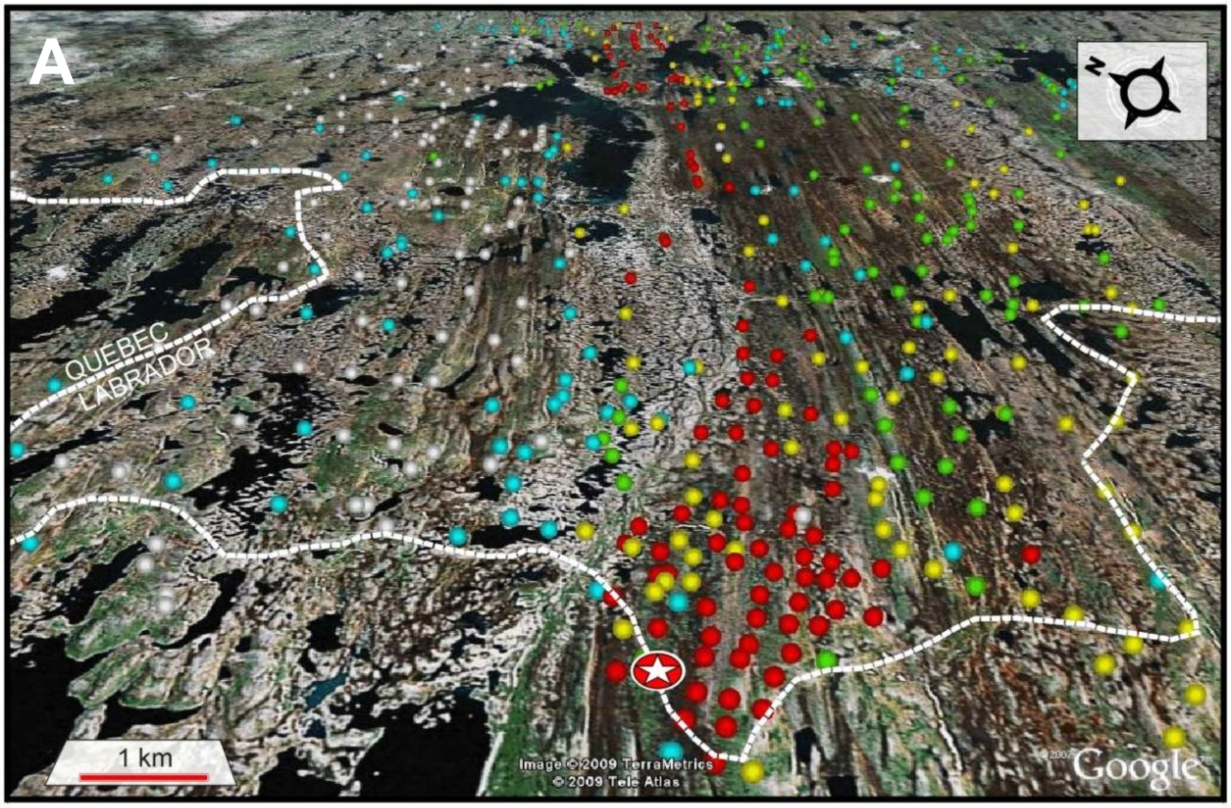

Figure 3.2. (A) Oblique view of geochemical dispersion from Strange Lake showing Y in till samples (warmer colours are higher values) draped on topography from Google Earth; image from S. Amor, Geological Survey of NL. (B) aerial photograph of barren, fluted terrain in the region down-ice of the Strange Lake deposits; photo by D. Wilton.

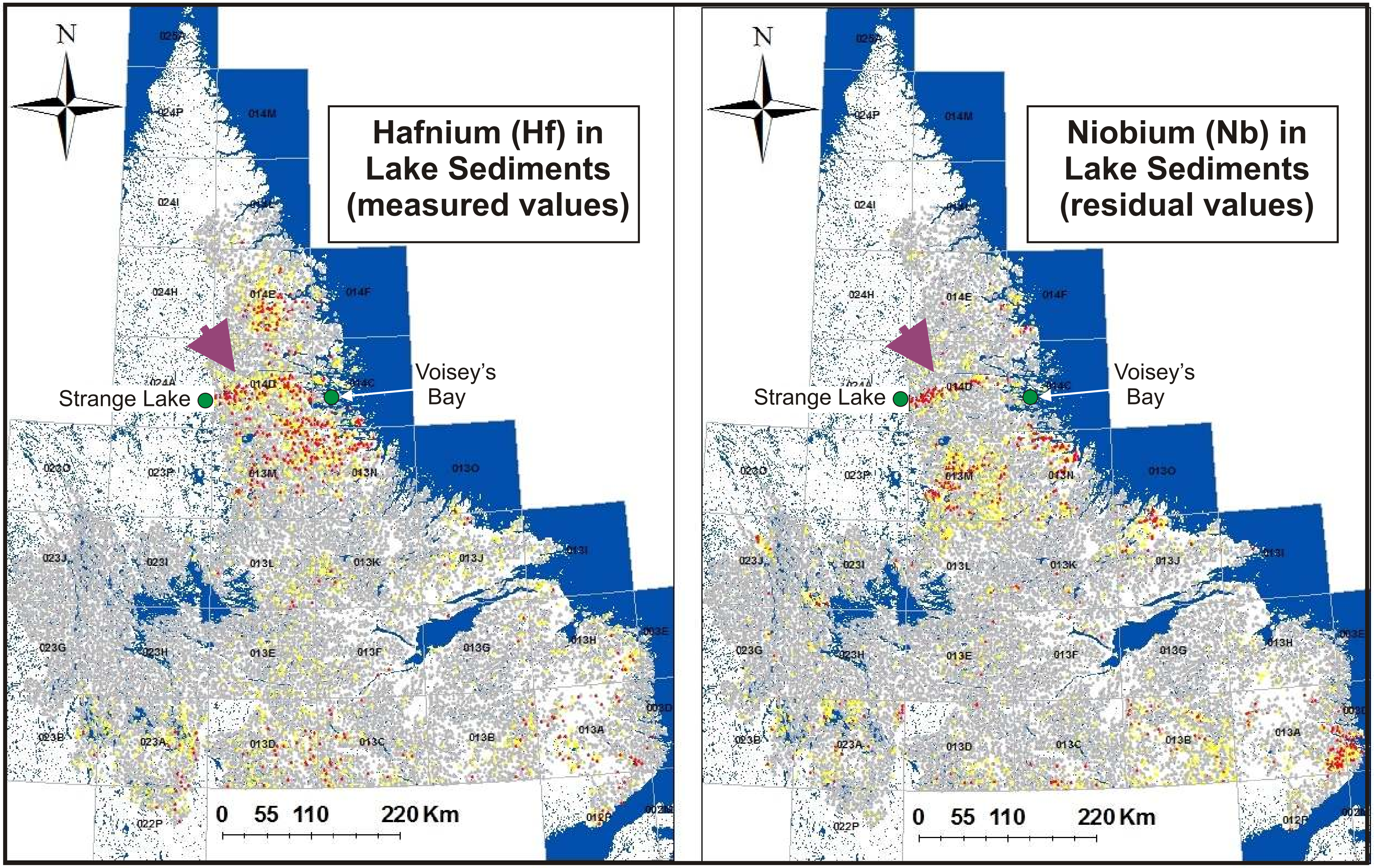

Figure 3.3. Geochemical evidence for long-distance transport of material from Strange Lake to the Labrador coast. LEFT: Hafnium (Hf) in lake sediments, measured data, warm colours indicate higher values. RIGHT: Niobium (Nb) in lake sediments, residual data with background patterns removed, warm colours indicate higher values. Dispersion train indicated by large arrowhead. Maps modified after Amor (2014).

a distal section of the dispersion train. The recognition of such patterns was aided by the use of statistical filtering methods that accentuate anomalous results by removing variation attributed to regional patterns, as described by Amor (2014). Figure 3.3 illustrates long-distance dispersion from Strange Lake indicated by results for Hf (uncorrected) and Nb (corrected for regional trends) from this study.

The geochemical expression of the Strange Lake Deposit at a distance of almost 100 km is very subtle, but it indicates that there must be physical materials from the site contained within glacial materials. This was recently confirmed in a survey of till materials from the area of the Voisey's Bay Ni-Cu-Co deposit (Wilton et al., 2017) intended for other purposes. MLA-SEM analysis of till samples, using identical methods to the present study, identified a few grains of the zirconosilicate mineral gittinsite (Wilton et al., 2017; see Figure 3.4). These were not discrete particles, but complex intergrowths of quartz and gittinsite, a texture also observed in this study. As gittinsite is known only in one other location in Canada (Kipawa, Québec), these grains almost certainly originated from Strange Lake. The findings of Wilton et al. (2017) formed the starting point for studies by Baird (2018) and Currie (2019) using the MLA-SEM technique. This work is discussed in more detail in Chapter 6.

INDICATOR MINERAL STUDIES BY THE GEOLOGICAL SURVEY OF CANADA

Increased exploration for REE deposits since 2010 has led to renewed interest in indicator-mineral analysis as an exploration technique. Strange Lake is a classic example of glacial dispersion from such a deposit, so it was a natural choice for initial investigation. A Geological Survey of Canada project, based largely on archived sample materials, is presented and discussed by McClenaghan et al. (2017; 2019). This work is directly relevant to the research discussed in this thesis and is reviewed in detail below.

McClenaghan et al. (2017) used long-established techniques developed largely for diamond exploration in glaciated terrains. They used samples of mineralized material from around the Main Zone Deposit (originally collected by D. Lentz of UNB in 2008) and till samples collected close to the deposit in the early 1980s. The relationship between till samples and those examined by Bell (1984) is not clear, but the latter were also provided through GSC. Several archived till samples from a confined area were amalgamated to provide sufficient material, so they may have the same origins. Six additional till samples were collected in 2015 from locations within the known dispersion train, using a hand-held

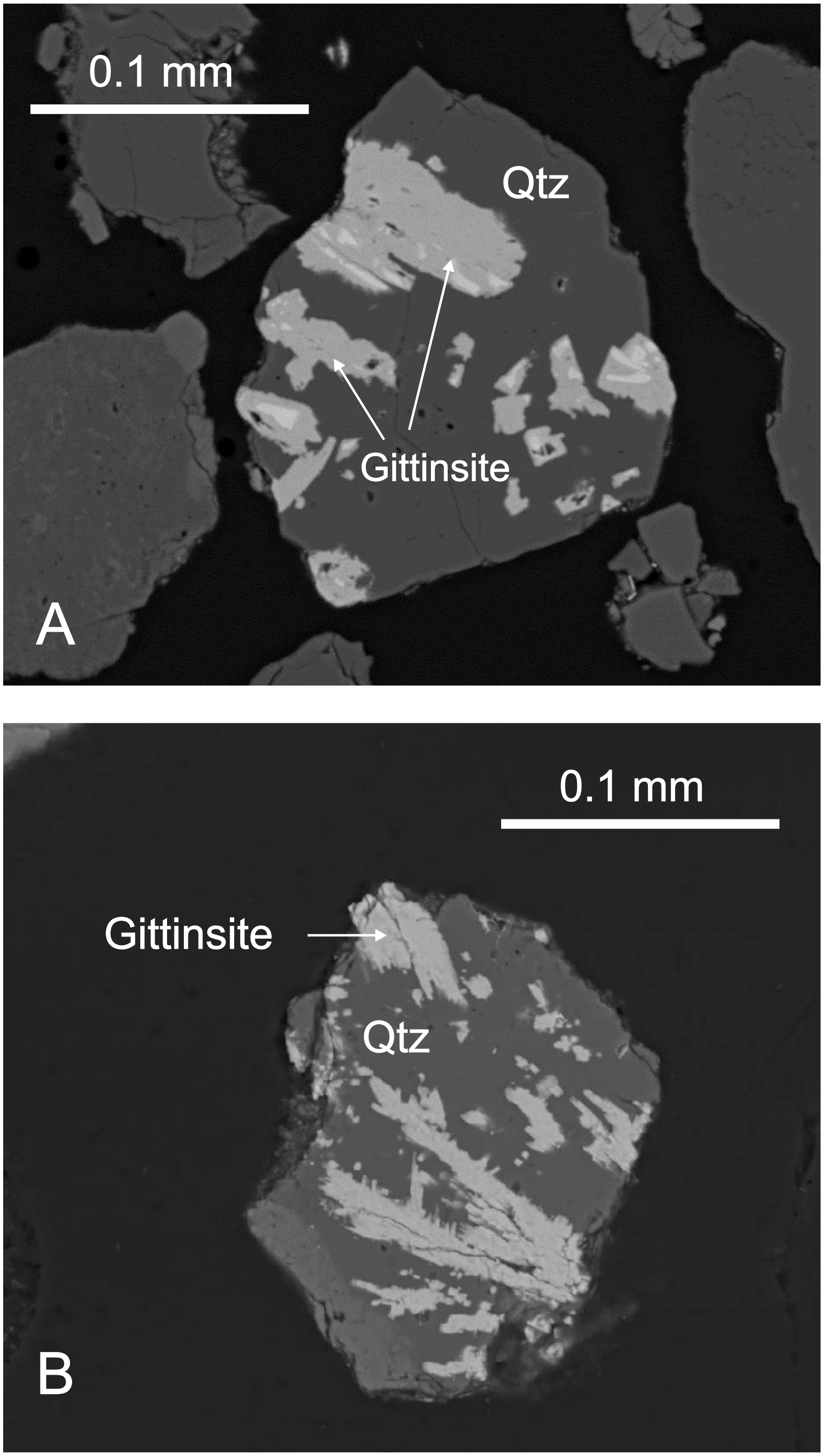

Figure 3.4. (A) Composite quartz-gittinsite particle detected in a till sample collected near Voisey's Bay, over 100 km from Strange Lake. From D. Wilton, discussed in Wilton et al., 2017. (B) Closely similar particle in sample G1-9 from this thesis study, located about 3 km from Strange Lake These are Back-scattered Electron (BSE) images. Please see Chapter 4 for more information.

gamma-ray spectrometer to identify materials that should contain mineralized debris. This observation suggests that the till samples were located in the vicinity of coarser debris from Strange Lake, which is more likely to show anomalous radioactivity (largely from thorium). A control sample was also collected in Québec, about 2 km to the WSW of the Main Zone deposit, in an 'up-ice' direction. The locations of till samples, relative to the sample locations used in this study and those of Batterson (1989) are indicated in Figure 3.5.

Sample processing followed the conventional protocol for indicator-mineral surveys. Particles that have high densities (> 3.0) are first separated from more abundant low-density materials using physical methods, and then separated from common Fe-oxides and Fe-Ti-oxides using magnetic methods. These processes preferentially concentrate uncommon minerals of potential interest, and reject more abundant materials such as quartz and feldspars. Heavy Mineral Concentrates (HMC) are identified using optical and physical methods, and also by selective use of scanning electron microscope (SEM) and electron microprobe (EMP) analysis. The mineralogical analyses were completed on sand-sized material ranging from 0.25 mm (250 microns) to 1 mm in size.

The results from the investigation successfully identified silicate minerals of high density, such as arfvedsonite (Na-rich amphihole) and aegirine (Na-rich pyroxene), both of which are characteristic of peralkaline granites. Minor minerals known at Strange Lake were also identified in bedrock and till samples, including pyrochlore, fluorite, zircon, gittinsite, titanite, apatite, allanite, monazite, and xenotime. Among the known REE-bearing minerals, only bastnaesite (Ce-La-fluorocarbonate; Table 2.1) was identified. Gerenite (Y-Ca-silicate; Table 2.1), which is known to host REE at Strange Lake, was not identified, but the similar Ca-Y silicate mineral kainosite was found in one till sample. McClenaghan et al. (2017; 2019) identified several previously unreported minerals, including cerianite, chevkinite, uraninite, rhabdophane, thorianite, danburite and aeschynite (see Table 2.1 and reference sources for formulae and details of these). Only monazite, apatite and allanite (which are common accessory minerals in many igneous and metamorphic rocks) were detected in the up-ice control sample, implying that uncommon minerals in other till samples came from Strange Lake. However, many till samples, including those located closest to the Main Zone Deposit, did not contain any uncommon Zr-, Nb- or REE-bearing minerals.

The results of McClenaghan et al. (2017; 2019) are best described as encouraging but inconclusive. They demonstrate that some uncommon minerals from Strange Lake can survive glacial transport and could therefore serve as valuable indicators for such mineralization. However, the correspondence between the minerals found in till samples and those known to exist in the bedrock

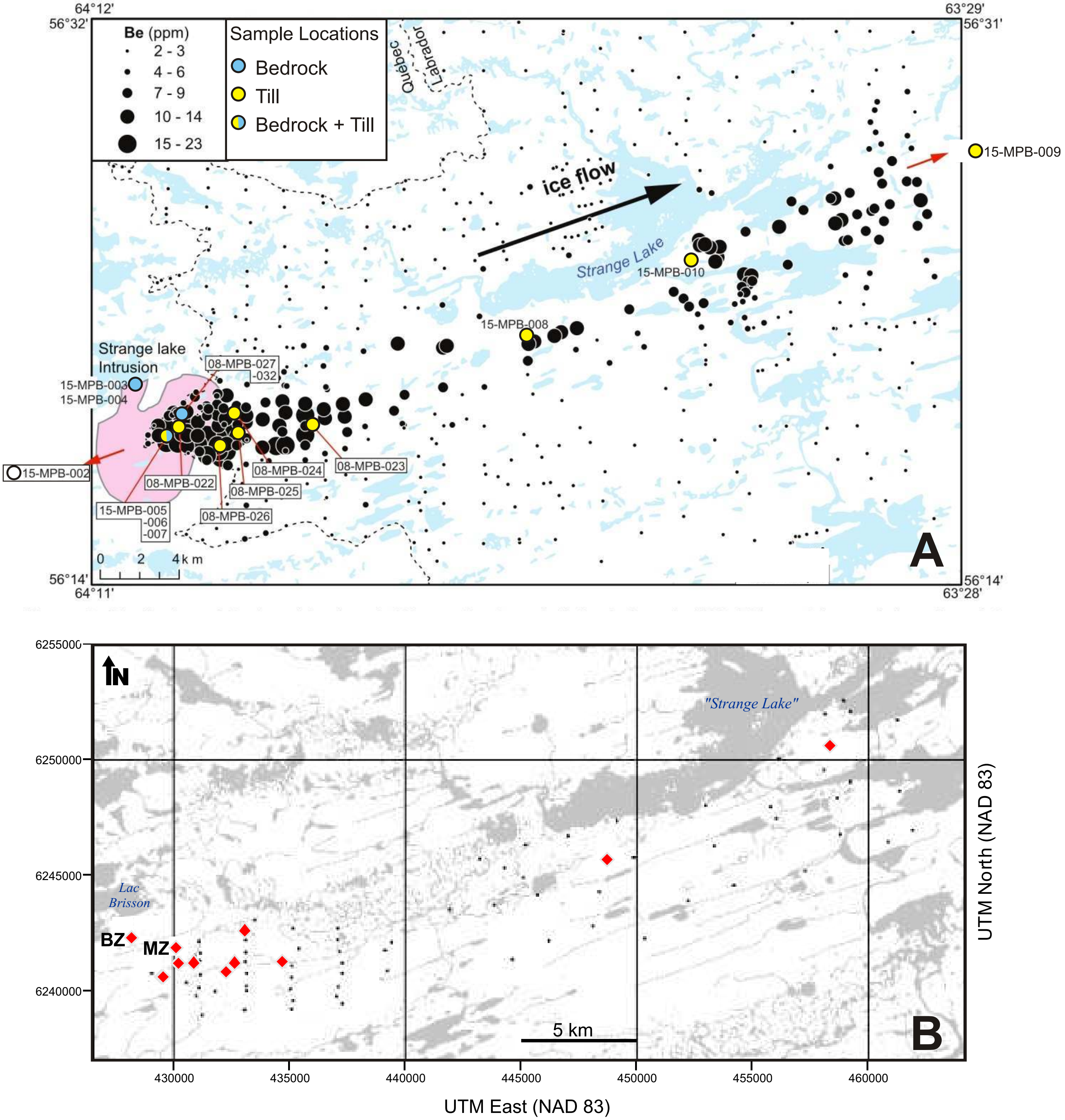

Figure 3.5. Sample locations for the GSC Indicator Mineral Study of McClenaghan et al. (2017; 2019). (A) Selected sample locations superimposed on pattern shown by Be concentrations in till (after Batterson and Taylor, 2009). (B) Sample locations superimposed on the till sampling locations from this thesis study. Note that the map scales differ slightly and that McClenaghan et al. (2019) omitted some locations on their map.

sources is not strong. Interestingly, many minerals known to be present in the Strange Lake Main Zone deposit (see Chapter 2; Table 2.1) were absent in materials derived from bedrock samples. McClenaghan et al. (2019) suggested that some minerals of possible interest were missed because they were too fine-grained and/or intergrown with other species in bedrock samples. Some, such as gerenite and kainosite, are known to be intergrown with low-density quartz, and to have fibrous crystal habits (Jambor et al., 1998; Zajac, 2015). McClenaghan et al. (2019) suggested that these might not persist in the surficial environment, which would limit potential transport distances. In closing, McClenaghan et al. (2019) state:

"Future research should include analysis of the < 0.25 mm HMC and mid-density fractions of bedrock and till from Strange Lake to determine the rare metals minerals present, how the indicator mineral population correlates with the grain size, and why gerenite and gadolinite were not visually observed in the > 0.25 mm HMC".

In part, the research described in this thesis attempts to answer some of the questions raised by McClenaghan et al. (2019).

RECENT TILL GEOCHEMISTRY SURVEYS BY MIDLAND EXPLORATION

Increased exploration for REE since 2010 has focused much attention on areas near Strange Lake in both Québec and Labrador. Midland Exploration acquired mineral rights licenses in Labrador that included the known glacial dispersion train from the Strange Lake deposits (see Figures 3.1; 3.2). They were interested by the potential for other mineralized peralkaline granites hidden beneath widespread surficial deposits. Although geophysical surveys did not yield suitable targets, field work suggested that surficial materials derived from Strange Lake locally had high concentrations of REE. Midland's program included high-density till sampling and analysis in an area 3 to 10 km ENE of the Main Zone Deposit, and reconnaissance sampling at greater distances (Bourassa and Banville, 2012; 2013). These data include complete trace element and REE analyses of glacial materials from different size fractions. The samples do not represent the same locations as those examined in the thesis study, but several are closely adjacent, and can be compared with MLA-SEM results. The brief summary below is drawn from Bourassa and Banville (2012; 2013), but aspects of these data are discussed in more detail in Chapter 8. The areas investigated by Midland Exploration are indicated in Figure 3.6.

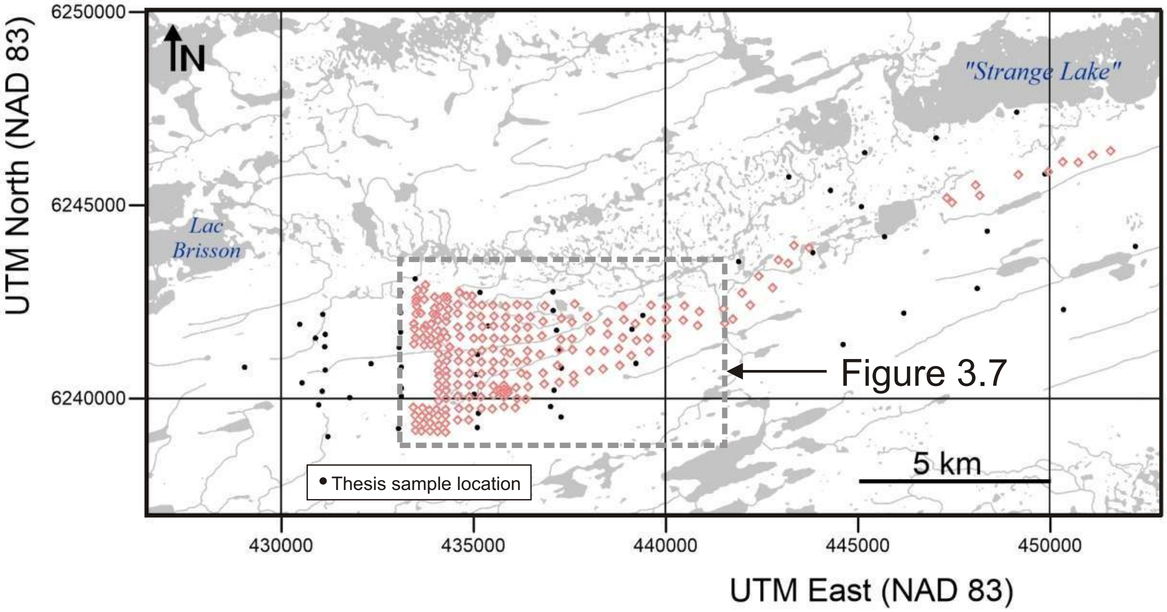

Figure 3.6. Sample locations for the Midland Exploration Till Geochemistry Survey (red diamonds) superimposed on the sample locations for the thesis study. From Bourassa and Banville, 2012; 2013. Area of Figure 3.7 (below) is indicated.

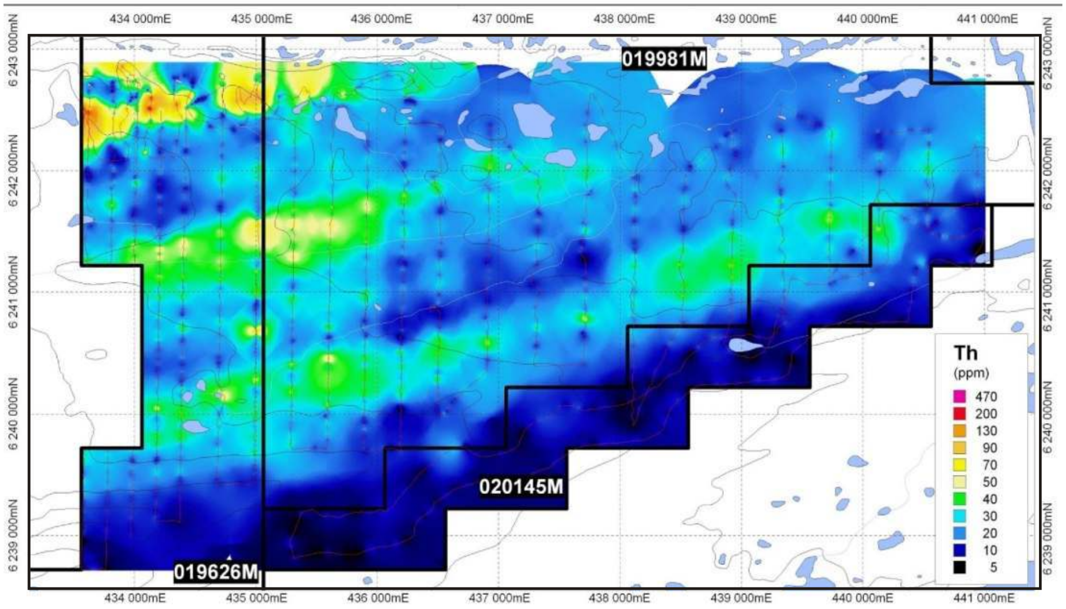

Figure 3.7. Map showing airborne radiometric data for part of the area investigated by Midland Exploration. The scale for equivalent Th contents is semi-quantitative. Areas of radioactivity are shown by warm colours. From Bourassa and Banville (2012).

The till sampling program was guided by the results of initial airborne aeromagnetic and radiometric geophysical surveys, which showed extensive thorium (Th) anomalies attributed to radioactive boulders and other material derived from Strange Lake. Figure 3.7 illustrates the radiometric anomalies, which lie immediately east of the Strange Lake EML area, and extend for up to 6 km. Note that these results define two subparallel zones of enhanced radioactivity. The results indicate that material from Strange Lake must be abundant, and present at the surface, likely as large boulders.

In total, Midland analyzed over 200 sites within 10 km of the Strange Lake Main Zone Deposit, and subdivided each sample into five size fractions. Strong Zr, Nb and REE enrichment was observed in the coarsest-grained fractions that included pebble- and cobble-sized material (19 – 63 mm and 64 mm – 128 mm), but such results were variable. The enrichment of these elements in finer-grained material, including the finest fraction (< 0.25 mm) was much less, although these data still defined anomalous regions. The Zr-Nb-REE enrichment remained detectable for up to 30 km to the east as a narrow zone associated with the prominent esker system noted by other studies (e.g., Batterson, 1989; Storrer et al., 2013). However, in more distant regions, only the coarser-grained fractions (> 19 mm) were analyzed. Sampling in these areas confirmed that mineralized pebbles, cobbles and boulders identical to the Strange Lake Main Zone Deposit were abundant.

Midland Exploration attempted to calculate potential resources, but acknowledged high levels of uncertainty from possible sampling bias in coarser material. They derived a general estimate of 95 million tonnes at 0.22% combined REE oxides and Y_2O_3, including a higher-grade ‘resource’ of 47 million tonnes at 0.37% combined REE oxides and Y_2O_3. Note that these are not compliant with NI-43-101 protocols, and that no proposal to actually extract till materials was developed. From the perspective of the thesis project, the large database provided by Bourassa and Banville (2012; 2013) confirms the widespread presence of mineralized material as clasts, and provides a basis for general comparisons of mineralogical data and bulk chemical analyses in Chapter 8.

CHAPTER 4: ANALYTICAL AND OTHER RESEARCH METHODS

GENERAL SUMMARY

This Chapter describes analytical and research methods, and also provides some discussion of the precision and reliability of MLA-SEM data, which is important in the context of interpretation. The field work in a large area located east of the Strange Lake deposits was completed by Dr. D. Wilton, with assistance from the Nunatsiavut Government. A total of 76 till samples were collected, using a generalized grid system, extending about 35 km east of the Strange Lake Main Zone Deposit. These samples were processed using sieves to retrieve three size fractions, of which the middle fraction (0.125 mm to 0.18 mm) was prepared for MLA-SEM analysis. This analytical method combines the capabilities of a scanning electron microscope (SEM) with the image analysis capability of the mineral liberation analyzer (MLA) to generate quantitative mineralogical data, and also information on particle sizes, grain sizes and mineral associations. The scientific background to the MLA-SEM method is discussed, and issues related to precision and reliability of data are explored and assessed. Some of the remaining sample material was also prepared for Visible/Infrared Reflectance Spectroscopy (VIRS) to investigate the potential of this method for detecting REE-bearing and other unusual minerals in till samples. The scientific background and analysis procedures for VIRS are briefly reviewed. Geographic data for the samples are summarized and the calculation procedures used to derive sample distances and azimuth directions from possible sources are summarized.

SAMPLING AND PREPARATION

Field Work and Sample Acquisition

The Strange Lake area is isolated, with access only by air. Small fixed-wing aircraft can land on an esker landing strip close to Lac Brisson, Québec, near the B-Zone deposit and about 2 km from the Main Zone deposit. Lac Brisson served as the logistical base for exploration in the 1980s by IOC and was also used by Quest Rare Metals during exploration of the B-Zone. The only facilities nearby are those established by Quest Rare Minerals, which are no longer in use. The Main Zone deposit can be accessed on foot from Lac Brisson, but a helicopter is required for access to the area where till samples were collected. Field work in the area was facilitated by support from the Nunatsiavut Government to Dr. D. Wilton at Memorial.University.

The topography of the Strange Lake region is dominated by a dissected peneplain surface that has a maximum elevation of about 700 m above sea level (Batterson, 1989). The Main Zone deposit has an elevation of approximately 500 m above sea level and is located in a flat marshy area to the southeast of the Québec-Labrador border (see Figures 1.1 and 2.1). The local climate is severe, with long and cold winters and summers that are short, cool, and damp. Luckily, the area tends to be windy, which affords limited relief from voracious summer blackflies and mosquitoes, and there are only a few stunted trees. This is part of a subarctic tundra biome that occupies all of the northern section of the Labrador peninsula. There is little natural outcrop exposure in the Strange Lake region and the area is swampy and boulder-strewn. The Main Zone deposit is artificially exposed in a trench excavated by IOC (Figure 4.1), but most of the geological information summarized in Chapter 2 comes from studies of drill cores. The B-Zone deposit is also exposed in some small excavations, and the fluorite-rich breccia zone at the margin of the Strange Lake Intrusion forms some outcrops near Lac Brisson. The host granitic rocks are exposed in outcrops on a high ridge southwest of the Main Zone deposit, and also in some streams that drain into Québec; most of these outcrops belong to the inner hypersolvus ("exotic-poor") granite unit (Figure 2.3). Figures 4.1 and 4.2 provide general illustrations of the topography and landscapes around Strange Lake.

Field work for this project was completed in September 2016. Seventy-six samples of surficial glacial sediment (till) were collected through an area extending east-northeast (ENE) from site of the Main Zone Deposit for approximately 35 km. Sampling was conducted by Dr. Derek Wilton with the assistance of Ernie Ford and Mary Denniston from the Nunatsiavut Government. The area covered by the sampling ranges from about 2 km wide close to the Main Zone Deposit to about 10 km wide at its eastern end. It lies within the larger area of systematic till sampling by the Geological Survey of Newfoundland and Labrador (Batterson, 1989; Batterson and Taylor, 2009; see Figure 3.1). A helicopter was used for transport between sites during sampling and a small shovel was used as the sampling instrument. The samples were

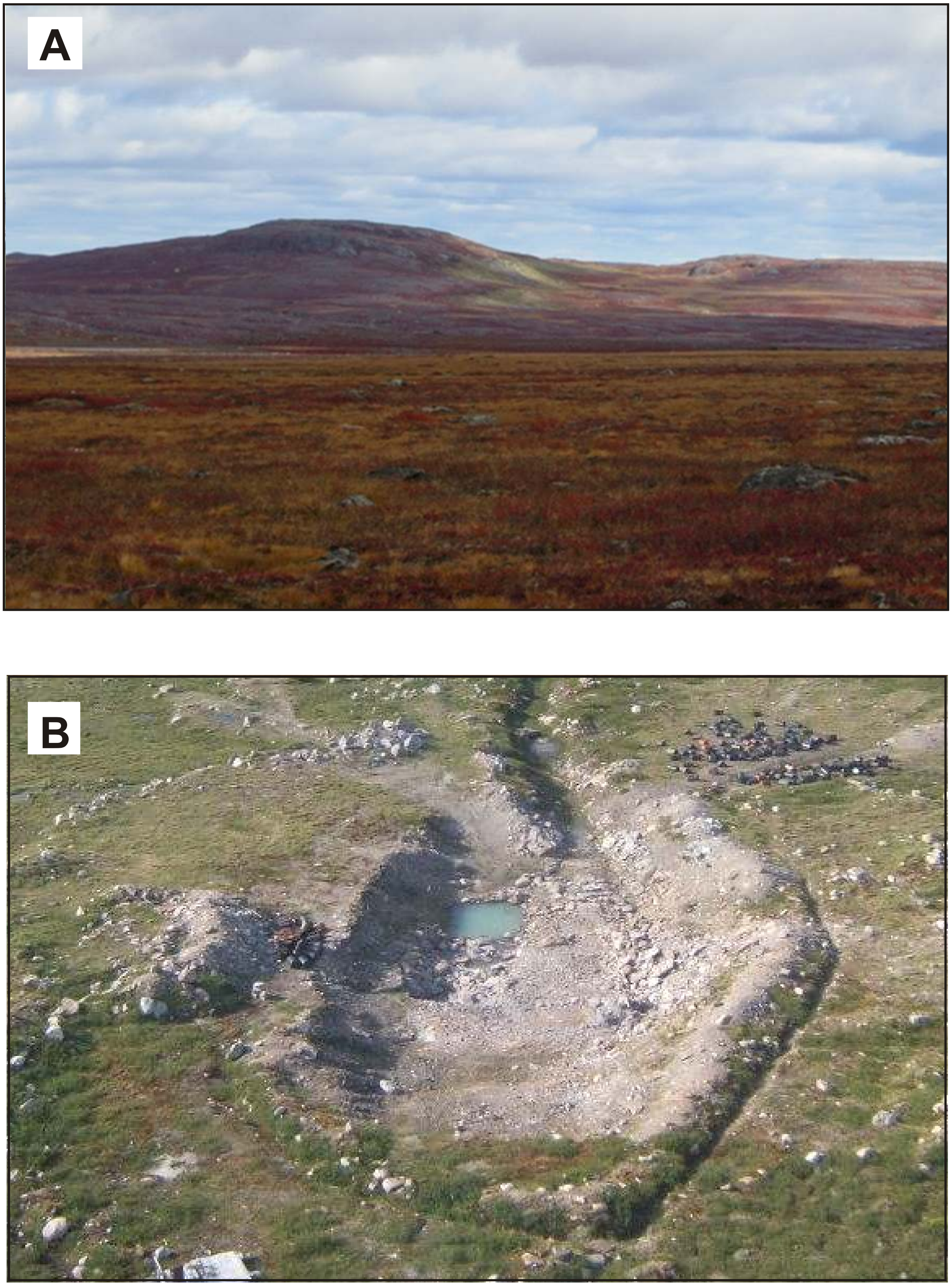

Figure 4.1. Typical landscapes in the area of the Strange Lake deposits, northern Labrador. (A) Barren high-elevation tundra in the area near the Main Zone Deposit. Photo by D. Wilton. (B) Aerial photograph of excavation trench at the site of the Main Zone Deposit, Labrador; the only extensive area of outcrop that is available for study. Note 45 gallon drums in photo for scale. Photo by A. Kerr.

Figure 4.2. Old and modern exploration camps near the Strange Lake deposits. (A) Wooden shacks constructed by IOC in the 1980s, providing rather primitive accommodations typical of those times. (B) The large and modern exploration camp of Quest Rare Minerals at lac Brisson, Québec, in 2011. Photos by A. Kerr, then with Geological Survey of NL.

collected by digging down to a depth of several tens of centimeters within “frost boils” produced by seasonal permafrost effects. These provide an ideal medium for easy sampling of unweathered till originally located at greater depths.

In detail, the sampling was guided by three generalized grid patterns that have slightly different sample densities. Figure 4.3 shows the distribution of sample sites, which form a fan-shaped array aligned with the inferred ENE direction of ice movement. At the southwestern end (closest to the Main Zone Deposit), samples were collected along 5 transverse grid lines about 2 km apart, and sample locations were spaced at about 0.5 km, or as close as possible to this spacing apart. The 40 samples collected from this region (Grid 1) are labelled G1-1 to G1-40. In the central portion of the area, samples were collected as close as possible to transverse grid lines at 2 km intervals, but the average sample spacing was increased to about 1.8 km. The samples collected from this region (Grid 2) were labelled G2-1 to G2-19. A similar spaced grid pattern was used at the eastern end of the area (Grid 3), where samples are labelled G3-2 to G3-13. The actual locations for samples were determined by topography, drainage and other constraints, but an effort was made to maintain a regular spatial distribution.

In addition to grid-based sampling, five samples (labelled E1, E3, E4, E7 and E8 in Figure 4.3), were collected from the prominent esker within the grid area. Esker are prominent sinuou ridges of stratified sand and gravel that are common in Canadian glaciated landscapes, and are records of subglacial water channels that deposited sediments derived from wider areas (Benn and Evans, 2010; Storrer et al., 2013) The purpose of these samples was to ascertain if patterns affected by glaciofluvial transport matched those produced by largely glacial transport of till material. A control sample (G2-15) was collected about 7.5 km north of the main sampling grids. The purpose of this sample was to check for the presence of indicator minerals outside the expected area of dispersion, which might indicate another source area, and/or establish background values. This control sample is not shown on the Figure 4.3 map but is located at 3E9N (UTM coordinate, NAD. The five esker samples are spaced at approximately 5km intervals along the course of the esker, which passes just north of the Main Zone deposit and close to the B-Zone deposit (Figure 2.7; Figure 4.3).

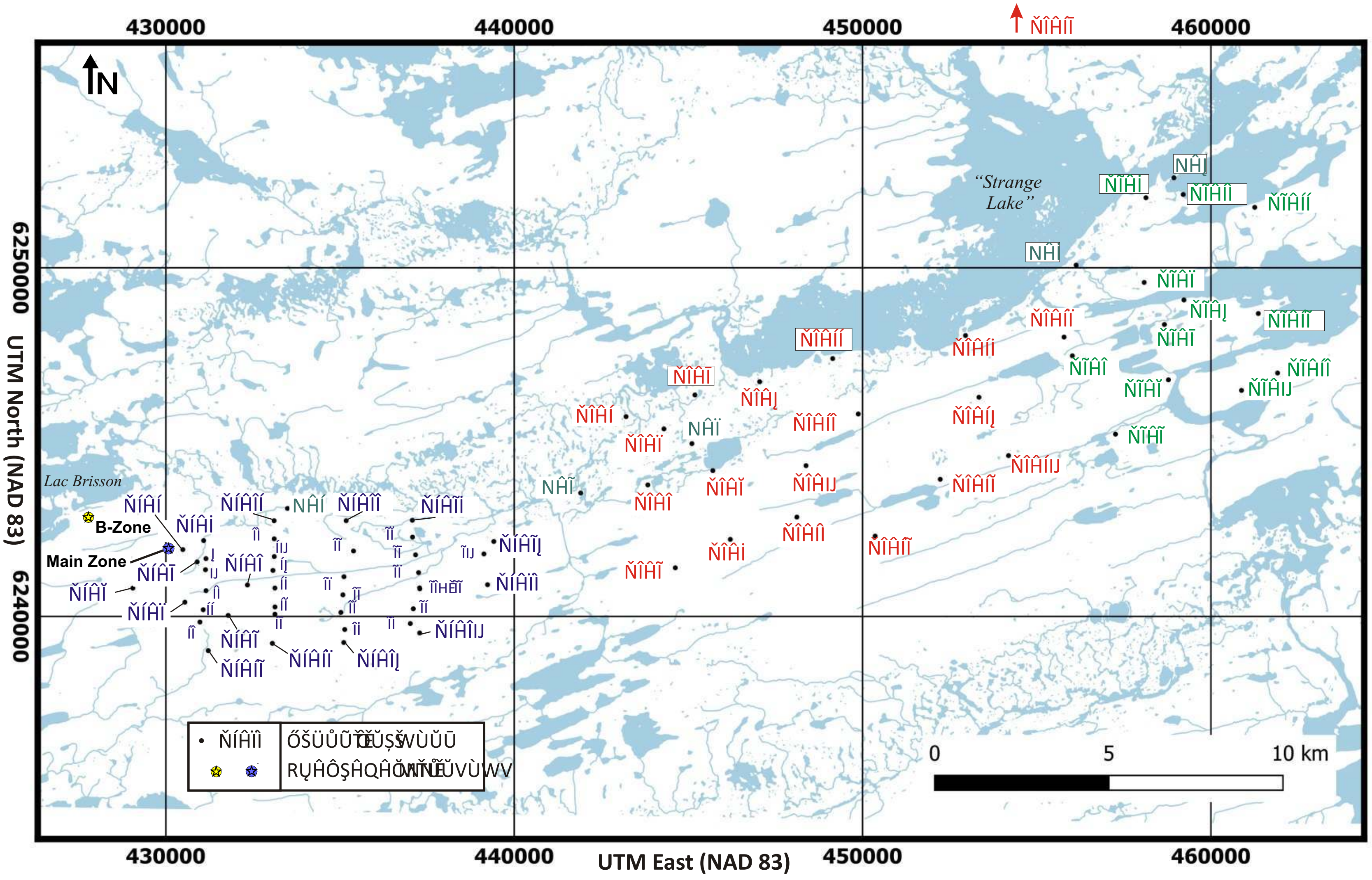

Figure 4.3. Location map for till samples in the study area. Base map kindly prepared by Stephen Amor, Geological Survey of NL.

All samples were collected at sites free of vegetation so that the sample material would be largely free of organic debris. The samples were simply collected using a stainless steel trowel, and the trowels were cleaned between each sample using a steel brush and disposable wipes. The individual samples were placed in standard kraft paper soil-sample bags. A duplicate sample was collected with every 20th sample. The intended purpose of these duplicate samples was to check analytical reproducibility for the MLA-SEM data, especially for minerals present at low abundances (see later discussion).

The sample locations were recorded using a Garmin Rino 650 GPS device, and digital photographs were taken of each sample site using a Canon Powershot SX280 HS camera. Field notes were recorded to note positions, sediment composition, grain size, texture and other information of possible relevance. The bagged samples were transported by helicopter to Nain and thence to Happy Valley-Goose Bay. At Happy Valley-Goose Bay the kraft sample bags were packaged in larger plastic sample bags which were then transported by air to St. John's and taken by private vehicle to the CREAIT labs at Memorial University. At the CREAIT labs the samples were air-dried in the bags and then laid out on paper to dry completely. Any obvious pieces of organic matter were removed and discarded. Figure 4.4 illustrates field sampling near Strange Lake.

Sample Processing and Preparation for MLA-SEM

There were several steps in sample preparation prior to the MLA-SEM analysis. The original samples weighed between 100 and 225 g. The samples were first weighed and sieved to produce three grain size fractions. All samples were sieved by hand using two stacked stainless-steel sieve pans with different-sized screens that pass size fractions of < 0.125 mm (125 µm), 0.125 to 0.18 mm (125-180 µm) and > 0.18 mm (180 µm). All size fractions were retained, including material of coarser grain size (granules and pebbles). In order to reduce cross-contamination between samples, all parts of the stainless-steel sieves were cleaned using an ultrasonic bath following the sieving of each sample (method of Grenier et al., 2015). Although this cleaning process is time-consuming, it is the best way to reduce the risk of cross-contamination when using reusable sieves (Lougheed et al., 2019). Wilton and Winter (2012)

Figure 4.4. Field work in the Strange Lake area, September 2016. (A) Typical flat, barren, unexposed area from the project area east-northeast of the Strange Lake Main Zone Deposit. (B) Ernie Ford and Mary Denniston sampling till from a frost boil, where fresh material was forced upward by seasonal permafrost. Photos by D. Wilton.

and Wilton et al. (2017) found that the 0.125 to 0.18 mm (125-180 μm) size fraction is the best size fraction for analysis by the MLA-SEM as it provides the optimum number of particles for efficient analysis. The other size fractions (< 0.125 mm and > 0.18 mm) were retained for possible use in future research.

After the sample material was sieved, the 125-180 μm size fraction of each sample (typically 30 to 70 g weight) was divided into eight equal portions using a Quantachrome Rotary Micro Riffler^{TM} Subsets of these aliquots were repeatedly riffled until an aliquot weighing approximately 0.3 g was produced. The mass of the final aliquot was estimated from the height of material in a small test tube, and was not weighed directly. The purpose of repeated riffling was to ensure that the final aliquot was as representative as possible of the bulk starting material. Test tubes used in this procedure were thoroughly cleaned using rubbing alcohol following the riffling of each sample, to avoid cross-contamination.

The next step involved mounting the final 0.3 g aliquot of sample material into epoxy pucks. The epoxy pucks were made by first placing approximately 0.3 g of riffled sample material into 30 mm diameter monolayer plastic moulds fitted with 25 mm inner ring moulds. The sample material was dispersed to form a single layer of particles (a monolayer) so that settling effects created by density contrasts among mineral grains could be avoided. Cold mounting epoxy Struers ExoFixTM; Resin: Hardener ratio was then poured into the mould and a small label with the sample identification number was gently placed on top. The pucks were then cured overnight. Figure 4.5 illustrates this part of the sample preparation routine, and the appearance of typical sample moulds.

Once manufactured, the lower grain-bearing surface of each epoxy puck was subsequently polished using an automated Struers Tegramin-30 polishing machine. The single specimen “fine sulphides option” was chosen for polishing. After each puck was polished, they were dried and then carbon coated by thermal graphite evaporation. Carbon coating is used to increase the electrical conductivity of the sample, which is essential in scanning electron microscopy (Goldstein et al., 1992).

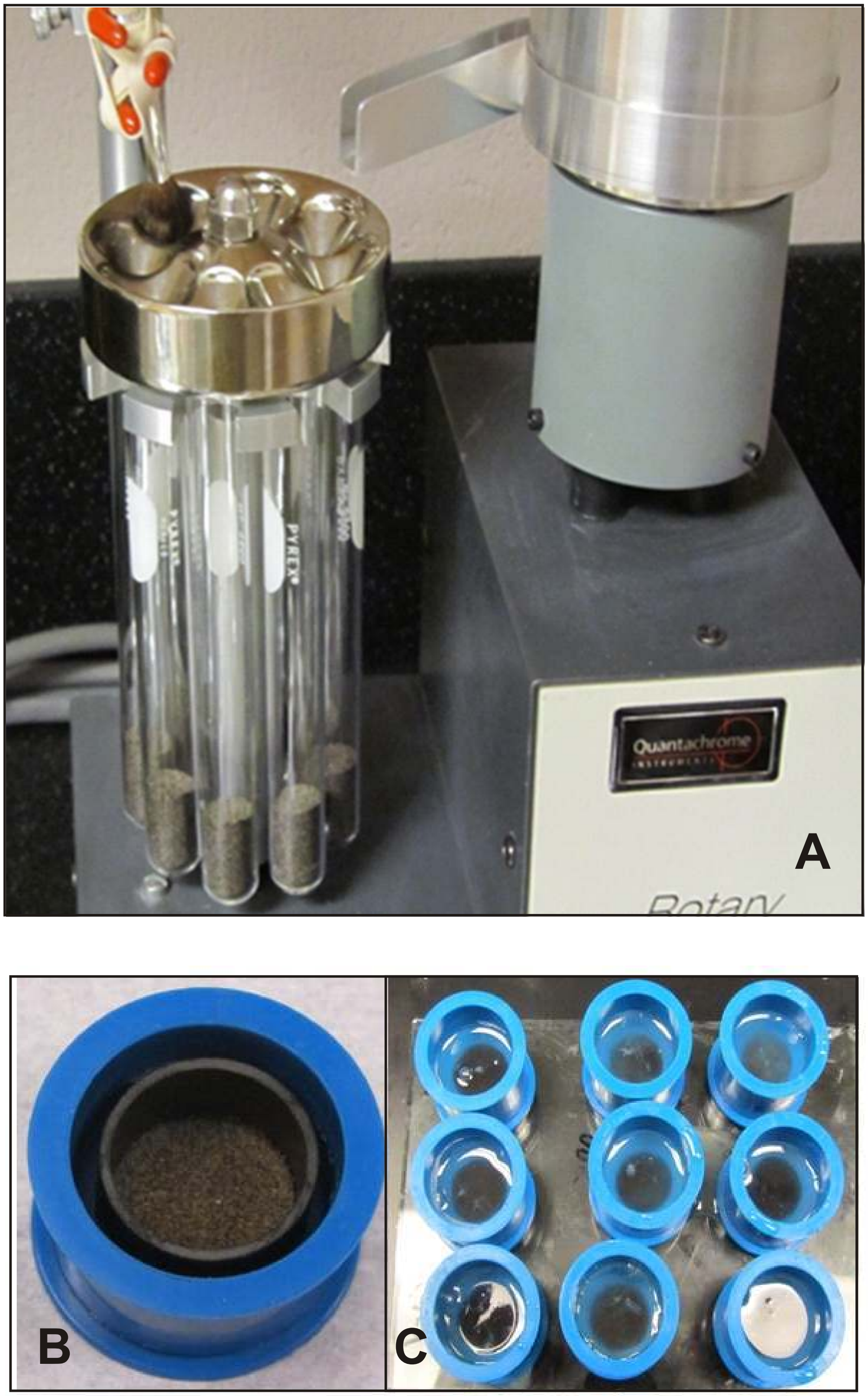

Figure 4.5. Sample preparation for MLA-SEM analysis. (A). Using the sample riffler to divide the original sieved till sample into smaller aliquots for analysis. (B) At left, monolayer of sample placed in cylindrical mould; (C) At right, several moulds now filled with clear epoxy resin.

The completed epoxy pucks were then used for the MLA-SEM analysis to identify mineral grains, derive physical parameters, and estimate the relative abundance of minerals. Analysis was completed in automated overnight runs over several weeks. In total, five batches containing 14 epoxy pucks each were analyzed over several weeks. The typical run-time for a single sample was about three hours. Details of the principles and analytical procedures involved in MLA-SEM methods are provided in a subsequent section.

Sample Processing and Preparation for Visible/Infrared Reflectance Spectroscopy (VIRS).

Visible/Infrared Reflectance Spectroscopy (VIRS) measurements were completed using an ASD TerraSpec portable spectrometer. Details of the principles and analytical procedures are provided in a subsequent section. The preparation of samples for VIRS analysis is very simple. The starting material was the same 0.125 mm to 0.18 mm (125-180 µm) size fraction that had been prepared by sieving for MLA-SEM analysis. This provided sufficient material to create a thick layer for analysis, and the small grain size allowed the spectrometer to collect spectra from as many grains as possible. The finer size fraction (< 0.125 mm) for most samples was too small in mass to create a suitably thick sample layer. In order to remove excessive clay in the sample material prior to final analysis, the material was washed and then dried. To undertake this preparation, the plastic sample containers containing each sample were filled with water, swirled, carefully drained, with the sample material then emptied into clean aluminum pans lined with aluminum foil, which were placed in an oven on a low temperature to dry overnight. Once the sample material was completely dry, it was placed back into the cleaned containers. The reason for this additional step is that clay minerals will absorb infrared radiation at certain wavelengths, and this might obscure any signatures from other primary silicate minerals. Washing was initiated after initial test analyses with the TerraSpec produced rather featureless spectra. However, there was little or no difference between spectra from washed and unwashed samples, suggesting that clay contamination was not the governing problem.

ANALYTICAL METHODS

Overview of MLA-SEM Method

MLA-SEM analysis was used to identify mineral grains and determine the modal mineralogy of the surficial sediment samples collected for this study. The technique is based on the methodology of Wilton and Winter (2012) and Wilton et al. (2017) for quantitative analysis of the mineralogy of various surficial media including stream sediments, soils, till, and unconsolidated materials. The original samples were processed in the manner described above, to produce a sample puck containing a very large number of particles. The number of particles depends on the particle size and the sample weight, but typically is between 10,000 and 20,000. The average number of particles contained in samples from this project was about 14,000, and the range was from about 5,000 to over 22,000. Note that the terms ‘particle’ and ‘grain’ have specific meanings in the context of MLA-SEM analysis. A ‘particle’ is a physically discrete object, which may consist only of one mineral, but might also contain two or more minerals. On the other hand, a ‘grain’ is a contiguous area that consists of a specific mineral. In a monomineralic particle (as commonly seen for quartz) the ‘particle’ and the ‘grain’ are one and the same, but other particles may contain two or more grains, e.g., several small grains of zircon might be intergrown with quartz within a larger particle. This distinction becomes important in the assessment of precision, and in the interpretation of some data.

Each individual grain in a sample puck is automatically examined and identified by comparing its compositional signature (EDX spectrum) to an electronic library of mineral spectra. The number of grains analyzed will always be greater than the number of particles, because some of the latter will be poymineralic in nature. The particle/grain distinction and its importance are further discussed by Wilton et al. (2017). New mineral spectra can be added to the electronic library by the user to expand the library database. Mineral identifications are based on the SEM capability of the system, whereas the MLA component evaluates the abundances of the minerals and also provides information about particle sizes, grain sizes and mineral associations.

The MLA-SEM instrument is illustrated in Figure 4.6. The instrument used for this research is the FEI MLA 650 - FEG SEM in MUN’s CREAIT labratory. The FEI MLA 650 - FEG SEM

Figure 4.6. The FEI MLA-SEM analysis system at the CREAIT facility, Memorial University.   For more information on the instrument and analytical methods, see text.

is described as “a laboratory-based, automated petrography analyzer”. Its key feature is its ability to retrieve quantitative data regarding modal mineralogy, grain sizes, mineral associations and mineral liberation and analyse the data using one coherent dataset (FEI Company, 2011). The MLA-SEM approach has some important advantages over other methods for investigating mineralogy in a quantitative manner.

Modern mining and mineral processing operations require detailed characterisation of ore compositions and many other parameters, and these are important in economic assessment (e.g., Hunt and Berry, 2017). Similarly, indicator mineral studies in exploration require numerical analysis of large populations of detrital particles. Traditionally, such information is acquired using optical microscopy and physical property determination, assisted by semi-automated scanning electron microscope (SEM) or electron microprobe (EMP) analysis for quantitative confirmation of results. These methods are time-consuming and expensive, and they may not deliver databases that can fully characterize ore deposits and their variability (Gu, 2003; Sylvester, 2012). In the last ten years, however, automated analysis using tools such as MLA-SEM has dramatically changed how research on ore deposits and their characterization is conducted (Haldar, 2013). The amount of data that can be acquired has increased by orders of magnitude, but this also brings challenges in data management and interpretation.

The modern MLA-SEM was developed in the mid-1990s by JKTech Pty Ltd., a technology transfer company, for the Julius Kruttschnitt Mineral Research Centre at the University of Queensland in Brisbane, Australia. The product became commercially available in 2000 and was marketed by FEI Company, which is now part of ThermoFisher Corporation. Essentially, the MLA-SEM method combines the analytical capability of Scanning Electron Microscope (SEM) methods for mineral identification and semi-quantitative analysis with the image analysis techniques of the Mineral Liberation Analyzer (MLA) software. Collectively, these allow accurate determination of mineral abundances in the sample and provide important textural and physical information (Sylvester, 2012). The QEMSCAN (Quantitative Evaluation of Minerals by Scanning Electron Microscopy) technology is based around very similar concepts, but was developed independently. The two methods converged following the acquisition of the QEMSCAN technology by FEI in 2009.

MLA-SEM Analysis Procedures

A Scanning Electron Microscope (SEM) is an electron microbeam instrument. It uses the kinetic energy of accelerated electrons and their dissipation to produce several types of signals from the target material (Haldar, 2013; Swapp, 2017). These signals include secondary electrons, backscattered electrons (BSE), diffracted backscattered electrons, photons, visible light, and heat (Layton-Matthews et al., 2014). The nature and intensity of these secondary signals are related to the chemical composition of the target, which provides valuable information for identification. For example, backscatter electron images display target materials in grey-scale shades, as the intensity of the signal is related to their composition as expressed as the average atomic number (Z) of the material. Minerals that contain heavier elements (with higher atomic weights) will appear brighter than those dominated by elements with lower atomic weights. Thus, quartz (SiO_2) and uraninite (UO_2) will appear very different, because of the enormous atomic weight difference between silicon and uranium (e.g., Swapp, 2017). An example relevant to this study is the zirconosilicate mineral gittinsite, which contains Zr (and also some REE), and is an important carrier of Zr at Strange Lake. Gittinsite appears very bright compared to common silicates when viewed in backscattered electron (BSE) images (Figure 4.7). The same general rule holds for many minerals of possible interest at Strange Lake, as they contain elements that have higher atomic weights than the most common elements in natural minerals. The SEM can also image objects << 1 micron in size with this method and can easily reveal small features and tiny inclusions in samples (Swapp, 2017). The BSE images are thus valuable in understanding fine-scale textural relationships between minerals, which are of particular importance in assessing metallurgical issues related to ore deposits. These are also important in understanding the nature of detrital particles.

The other important aspect of SEM analysis is Energy-Dispersive X-Ray Spectroscopy (EDS or EDX) which evaluates the X-ray emissions from the bombarded target. This provides a 'spectrum' in which peaks record the abundances of specific chemical elements in the target. This provides a means of mineral identification, or at least characterization, and is the basis of the spectral libraries used in MLA-SEM investigations. The EDX method is not as precise as Electron Microprobe (EMP) analysis, even though both use the same general principles of physics, but it can provide semi-quantitative data that aid in mineral identification. Figure 4.8

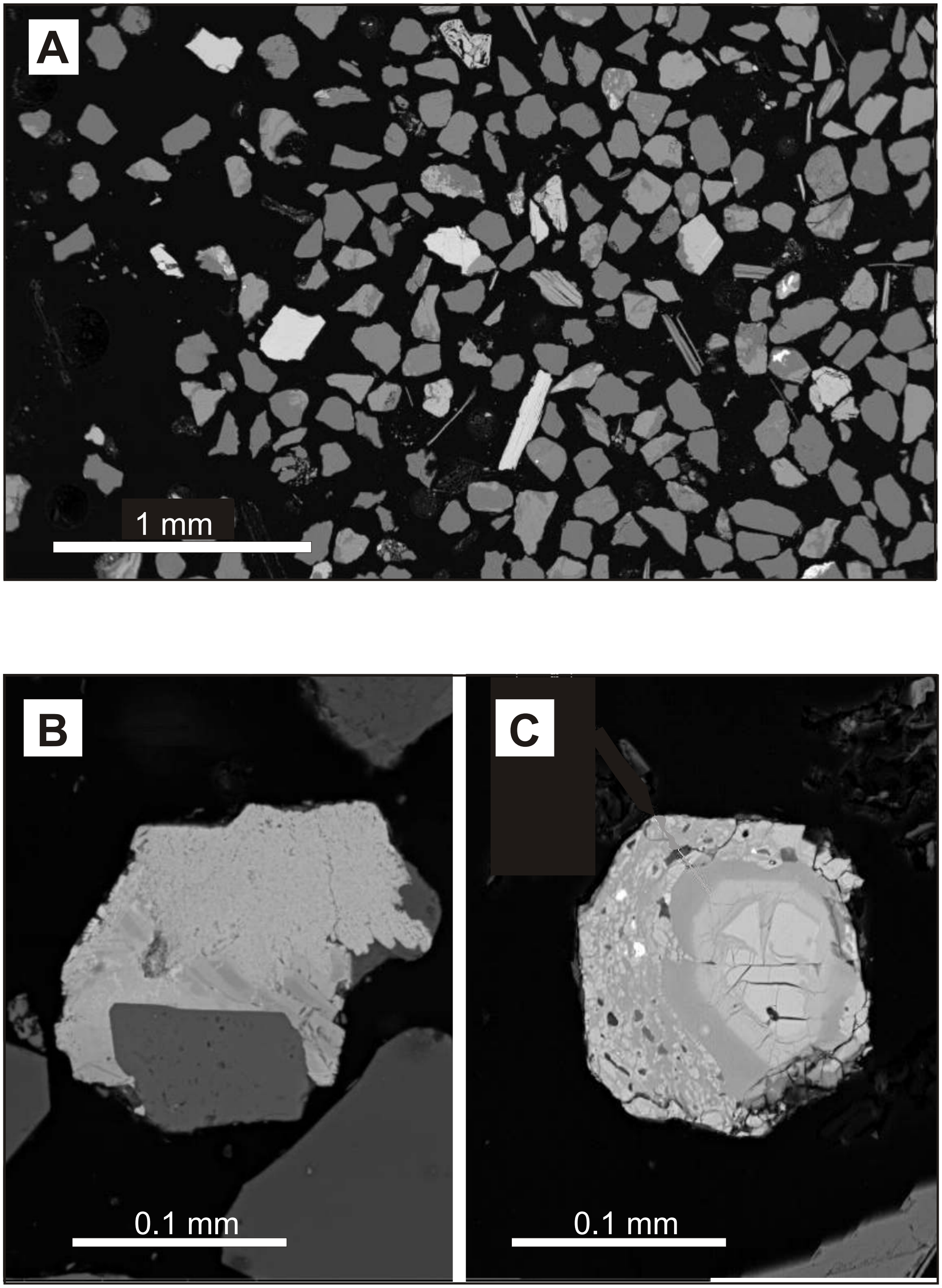

Figure 4.7. Examples of Back-Scattered Electron (BSE) images from till samples. (A) Image of hundreds of particles, showing variations in brightness; the bright particles include several that are gittinsite (Ca-Zr-Silicate). Sample G1-9. (B) Individual particle including gittinsite (bright) and quartz (dark grey). Sample G2-11. (C) Gittinsite particle showing a massive (zoned) core and an outer inclusion-rich zone. Bright specks in outer region are tiny grains of uraninite.

shows the EDX spectrum for the mineral gerenite, a hydrated Y-Ca-silicate that also contains significant REE, notably the heavy REE (Gd to Yb). This is one of the more important 'indicator minerals' from the Strange Lake Deposit. The EDX reference spectrum for another mineral, initially identified by the MLA as the rare Ba-Mn silicate *ericssonite* is also shown. "Ericssonite" is known mostly from mines in southern Sweden, although it has also been reported from Japan (see www.mindat.org). It is one of many Mn-bearing silicates. In this particular case, other information (G. Layne, pers. comm., 2020) (see Chapter 8, and also a paper by Birkett et al,,1996) suggests that a closely related (but less rare) mineral named bafertiasite might be a better diagnosis, in view of the high iron content. This question is discussed later in the thesis. It illustrates that for unusual minerals, other information may lead to correction of the labels applied by the MLA system. The label 'ericssonite' is retained in Chapter 6 and 7, because the recognition of this misidentification came at a late stage in preparation of the thesis.

Key advantages of the SEM method are its ease of use and minimal sample preparation (Haldar, 2013; Swapp, 2017). Limitations of SEM analysis include the overall sample size, which is limited. Solid samples are usually restricted to dimensions of 4 x 10 cm or less, and only the surface material is analyzed. The small sample size is advantageous in some contexts, but introduces uncertainties for minerals that may be present only in small amounts; they may not be present in the surface of the target. In the context of this project, the presence or absence of particles of rare minerals in a small analyzed sample is an issue (see later discussion).

The MLA component of the system performs the automated mineralogy determinations, based on the compositional information provided by the SEM. Essentially, the MLA is sophisticated software that works with the data from the SEM's Energy Dispersive X-ray Spectroscopy (EDX) capabilities and BSE images, to allow individual mineral grains to be recognized and described quantitatively (Sylvester, 2012). The MLA works by integrating multiple visual frames created by the SEM to identify the minerals and map their abundances, distribution and relationships (Gu, 2003). Figure 4.9 shows an image from a entire puck analyzed by MLA-SEM, and also the individual stitched 'frames' that are used in image analysis. This is a false-colour image in which individual minerals are coded to specific colours; this approach is valuable in revealing textural information. Although it is impossible to assess the details of images like Figure 4.9 visually, they illustrate how the method collects data from many thousands of individual particles. The MLA is able to discriminate minerals from their BSE

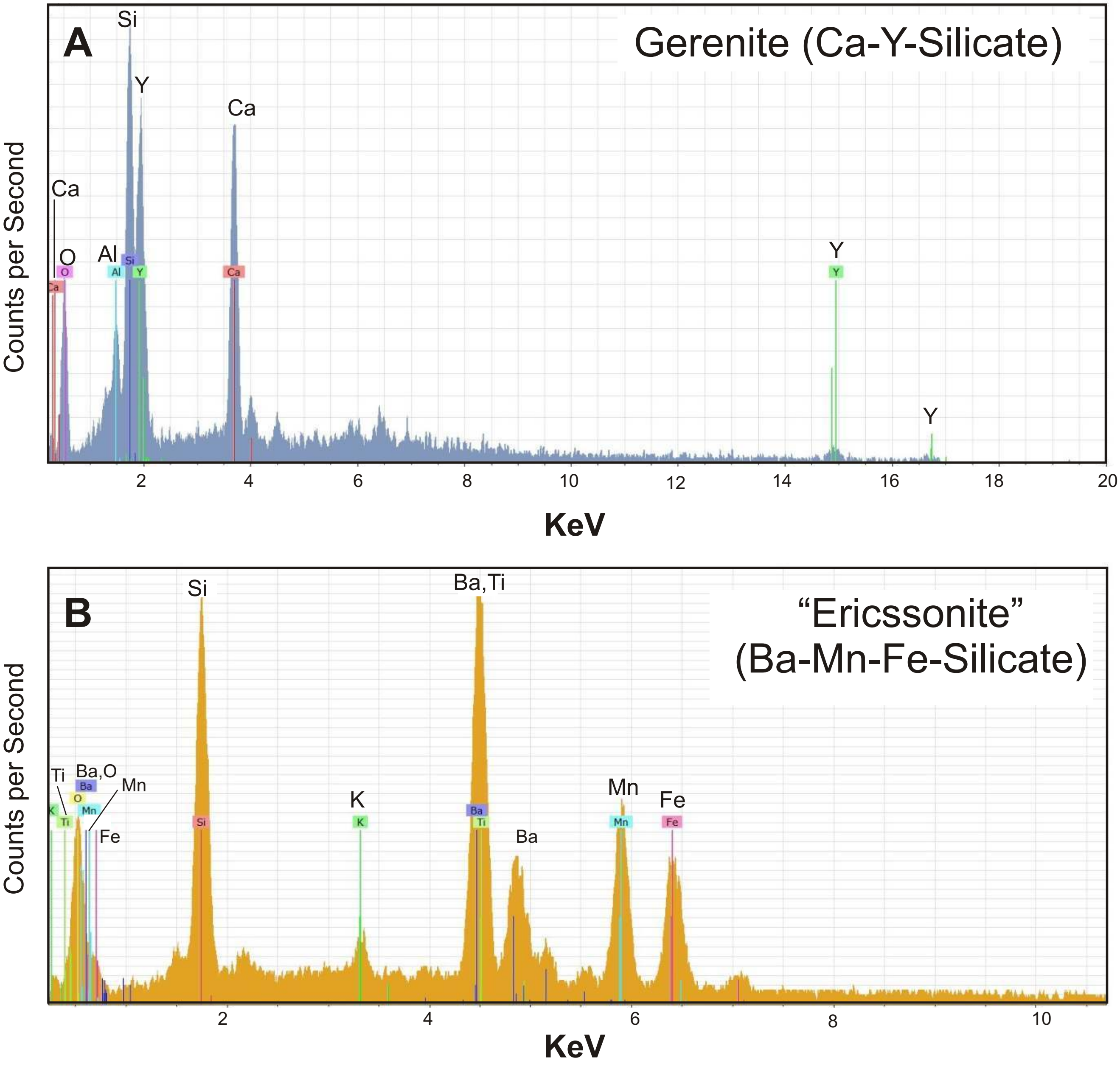

Figure 4.8. Examples of Energy-Dispersive X-Ray (EDX) Spectra for minerals obtained from the MLA-SEM System. (A). Spectrum for the Y-Ca-(REE)-Silicate mineral identified as gerenite, described and named by Jambor et al. (1998). (B) Spectrum for an unusual mineral identified by the MLA system as ericssonite, which is a rare Ba-Mn-silicate known only in Sweden. Only the more prominent 'peaks' in the spectra are labelled, for reasons of clarity.

Note that in the case of spectrum B ("ericssonite"), further examination and research suggested that the identification should be revised in light of the significant Fe and Ti revealed by the analysis. This is discussed in a later chapter.

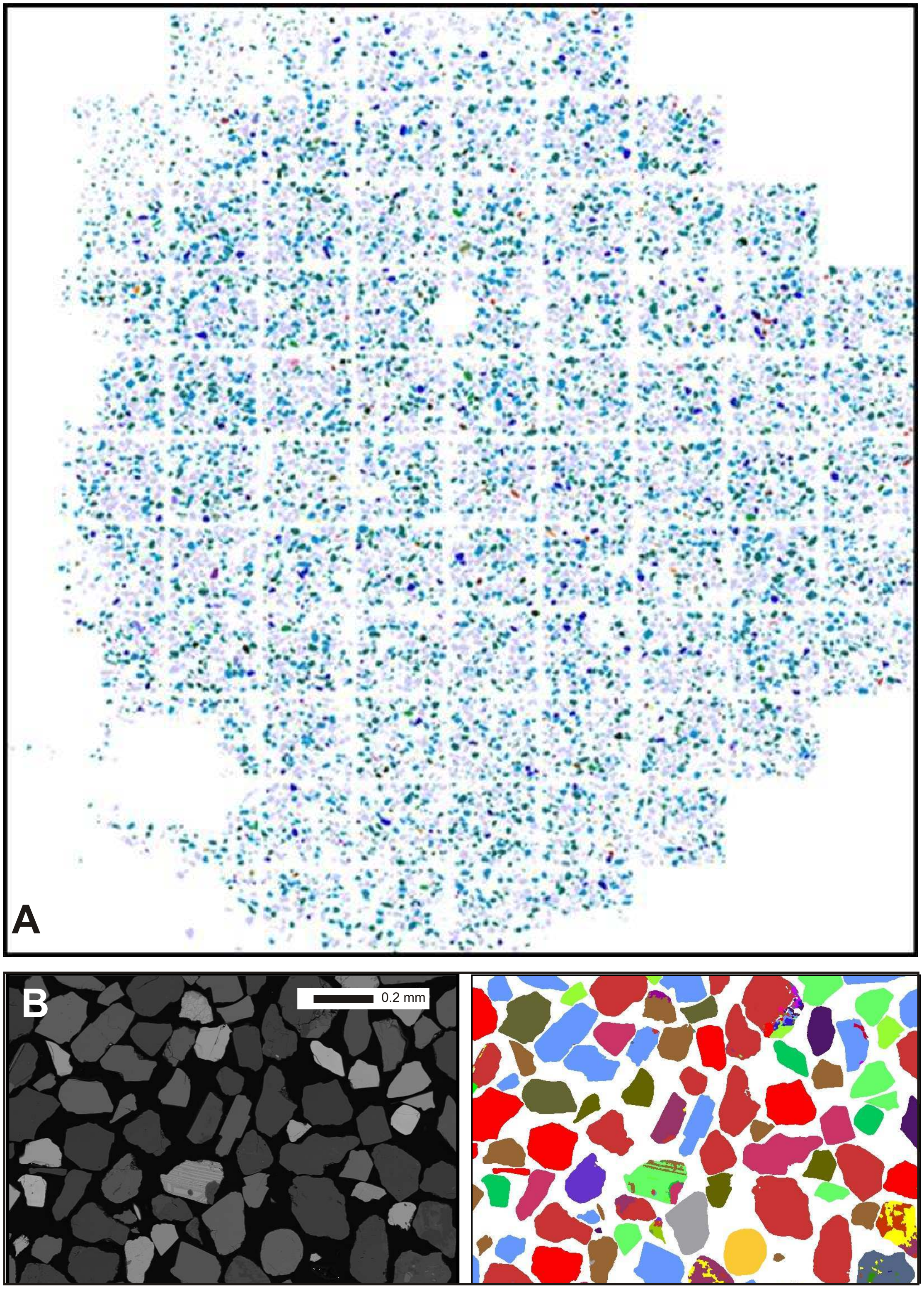

Figure 4.9. (A) False-colour image of an entire sample puck containing 20,325 particles (Sample G1-18); the square outlines show the individual frames analysed by the MLA. (B) BSE image and false-colour image of a till sample from near Voiseys Ba, showing how different minerals can be coded to accentuate textures, etc. Bright Red = calcic plagioclase; Bright Green = magnetite. Modified after Wilton et al., 2017).

intensity and EDX spectra, and derive quantitative data, most importantly the abundance of minerals, expressed as area %. Other information of importance includes the areas of all particles and of mineral grains that may exist within them, and also the frequency of mineral associations, i.e., which minerals are most commonly in contact with one another. The operating parameters for the FEI 650FEG MLA-SEM instrument, as employed in this project, correspond generally to those listed by Wilton et al. (2017), and are as follows. The operating voltage was 25 kV, with a horizontal field width of 2 mm, and a frame resolution of 800 pixels per frame. The X-ray collection time (for EDX spectra) was 12 ms per X-ray (information from D. Goudie, pers. comm., 2021. The analysis time for a typical sample with 20,000 particles was 1 to 2 hours.

The MLA-SEM data can be analysed using Dataview, a program specifically designed for the analysis and statistical interpretation of MLA data (Pietersen et al., 2009; Mateo, 2010). Some of the functions in this program apply to both solid materials and particle mounts, but not all can be applied to surficial materials such as till samples. The main emphasis in the current study is the nature of the mineral population and the relative abundance of minerals, although image analysis may reveal other features such as composite grains or mineral associations. One disadvantage of the Dataview program is that it is largely focused on individual samples, and less able to complete wider numerical and statistical analysis of a database containing many samples, as in this project. Such work requires that the sample-level data be collated and then exported for use in other programs such as Microsoft Excel or the statistics program MYSTAT (see later discussion and Chapter 6). The manipulation of MLA-SEM data to develop the large integrated database for this project, and the extraction of important information from multiple samples, proved to be time-consuming and at times frustrating.

Advantages and Disadvantages of the MLA-SEM Method

The MLA-SEM method has many advantages over more traditional optical microscopy methods. These include faster processing time, automation, the ability to derive thousands of measurements from a single sample mount, ease of use and lesser requirements for training (e.g., Layton-Matthews et al., 2014; Wilton et al., 2017). The ability to recognize mineral intergrowths at a sub-particle level effectively allows the user to see *inside* mineral particles, which cannot be accomplished through traditional microscopy. The methods used for mineral identification are semi-quantitative rather than qualitative, which leads to greater consistency, and provide the ability to discriminate compositional variants of minerals that may have similar optical and physical properties. The ability to automatically record mineral associations as a quantitative measure is also an important asset. Traditional methods for the investigation of indicator minerals in exploration start with a much larger sample and use physical, density and magnetic methods to derive a much smaller amount of material that is enriched in minerals of interest, which are commonly more dense than common rock-forming silicates. This processing of samples partly removes their connection to the original sources, because the relative abundances of minerals are altered, and some may be excluded from identification or analysis. Similar pre-concentration methods can be applied in the MLA-SEM investigations of till samples (e.g., Wilton et al., 2017), but they are not strictly necessary. The mineral abundance data derived from unprocessed till samples provide true compositional representation of the bulk materials, which are in turn representative of the source(s). For a complete review of possible advantages of MLA-SEM methods in the investigation of till mineralogy, see Wilton et al. (2017).

However, MLA-SEM methods have some limitations, as discussed by Sylvester (2012). The first is the difficulty in differentiating between minerals with near-identical chemical compositions such as gypsum and anhydrite, which have different physical properties but near-identical formulae. Minerals that have closely similar varied compositions but non-identical idealized formulae, such as the Y-Ca- REE silicates gerenite and kainosite, may also present problems as they could be recorded as a single mineral. The system cannot provide information about mineral structures when minerals have the same composition. An example of relevance to this project would be the common polymorphs of K-feldspar known as orthoclase and microcline, which are most common in igneous and metamorphic rocks, respectively. Both have the formula $KAlSi_3O_8$, so they will be recorded as a single mineral. Similarly, the three polymorphs of Al_2SiO_5 (andalusite, kyanite and sillimanite) would be indistinguishable, although their physical properties vary.

The final limitation, and perhaps the most significant, is that rapid and effective identification depends on the availability and accuracy of spectral libraries. This aspect is less problematic for common rock-forming minerals, but is of more concern with uncommon minerals such as zirconosilicates or REE-bearing species. For example, very few localities contain gittinsite, and Strange Lake is one of only two localities where the Ca-Y-REE silicate gerenite is known to occur. There are few publicly available reference spectra for many of the minerals anticipated in such unusual mineral deposits. This makes identifying unusual minerals like the ones found at Strange Lake challenging. Limits on publicly available reference spectral information mean that there is a greater risk for minerals to be misidentified and labelled incorrectly. The spectral libraries used in this project were derived from unpublished data collected by D. Wilton, supplemented by an earlier study that examined crushed material from archived drill-core samples from Strange Lake (Baird, 2018). This important database is reviewed in Chapter 6. However, the issue of mineral identification is to a large extent an issue of which name is attached to a mineral that has a specific set of properties. The combination of BSE intensity and EDX spectrum is in many cases highly restrictive, even if it may not always be diagnostic. The original identification data based on these parameters are retained by the MLA system, so identifications can easily be updated or revised in the light of new information or other evidence. This is not always the case for traditional optical or physical methods, which may require extensive re-examination of the original materials. However, it is important that mineral identifications, especially for rare minerals, be assessed by inspection of SEM data, and in some cases they may need to be verified using other methods such as the Electron Microprobe (EMP) or X-Ray diffraction (XRD).

Precision of MLA-SEM Analysis

It is important to assess the precision of the MLA-SEM analyses if they are to be compared with other results from the same database or with results from other methods. In most previous investigations of indicator minerals using MLA-SEM (e.g., Wilton and Winter, 2012; Wilton et al., 2017; Currie, 2019) emphasis was placed on the identification of unusual minerals rather than measurement of their abundance. Consequently, there is limited information available about the precision of MLA-SEM analyses, especially at relatively low abundances below 0.1 area % (1000 area ppm).

The MLA-SEM method reports the abundance of individual minerals as area %, and derives these data from the total area of all grains of the mineral mapped in the sample compared to the total area of all particles in the sample (expressed in square microns, or μm^2).

Note again that the definitions of ‘particles’ and ‘grains’ here are specific; particles are physical objects that may contain more than one mineral, whereas grains are contiguous areas composed of one mineral, which may be included within a particle. The weight % of minerals can be calculated from the area % data, by using idealized molecular weights, but there are uncertainties for minerals that vary in density according to composition. The area % measurement is preferred, and this is assumed to be equivalent to volume %. Although area % is a two-dimensional measurement from three-dimensional objects, this assumption is reasonable because there are many thousands of particles in the sample, and an even larger number of grains.

In the original plan for this project, duplicate samples were collected in the field, and duplicate aliquots (splits) of selected samples were prepared for analysis. The objective was to obtain empirical measurements of analytical precision that also included uncertainties related to natural geological factors. However, the duplicate and replicate samples were not analyzed in the first phase of the project, and restrictions from the 2020-21 Covid-19 pandemic prevented laboratory access for delayed analysis of these samples in the second phase. Empirical evaluation of analytical precision is instead based on other data acquired from crushed drill core from the Strange Lake Deposit and is summarized below.

Wilton (unpublished data) analyzed six replicate samples from a single sample of crushed drill core from the Main Zone Deposit (hole SL-147; 135.6 -145.4 m). These samples were sieved and prepared in the same manner as the till samples from this study, and MLA-SEM analysis followed the same procedures. Uncertainty is estimated using the standard deviations of the replicate analyses, and the absolute and relative uncertainties are inversely proportional to the average abundance of a given mineral. K-feldspar had an average abundance of 27.5 area % with a standard deviation of 0.4 area % indicating relative uncertainty of ± 1.5% at the 95% confidence level. The zirconosilicate mineral gittinsite had an average abundance of 1.39 area % with a standard deviation of 0.14 area % indicating relative uncertainty of ± 10.2% at the 95% confidence level. Apatite had an average abundance of 280 area ppm with a Standard Deviation of 79 area ppm indicating relative uncertainty of ± 28% at the 95% confidence level. Figure 4.10 illustrates the relationship between the mean abundance of these minerals (log-transformed) and relative uncertainties, which is approximately linear. Extrapolation to much lower

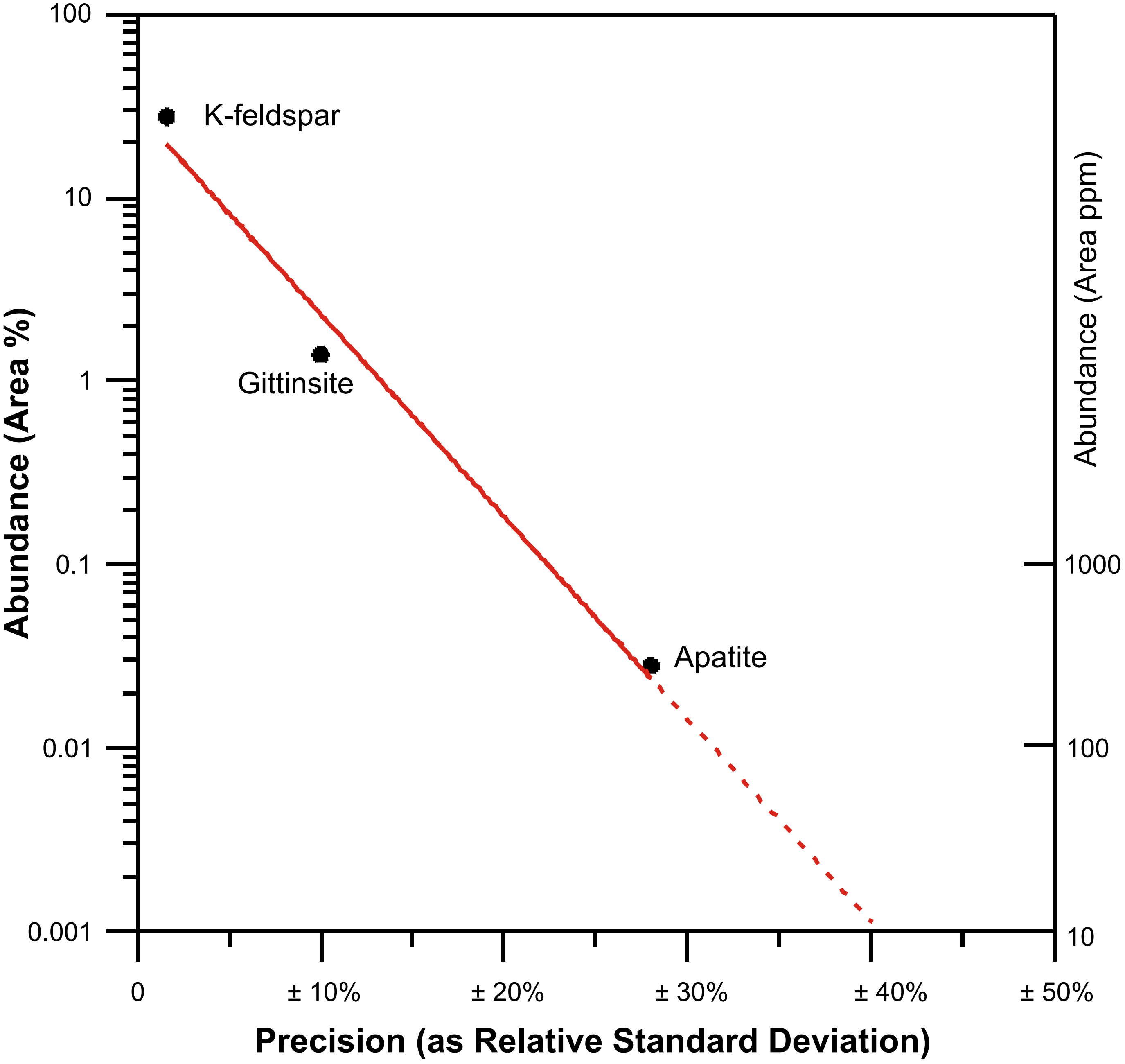

Figure 4.10. Estimates of analytical precision for MLA-SEM analysis based on six replicate analyses of splits from a sample of crushed drill core from Strange Lake (Hole SL-147) completed by D. Wilton (unpublished data). The analytical precision at low abundances (< 0.02 area % or 200 area ppm) is estimated from the regression line. See text for additional discussion.

abundances of around 100 and 10 area ppm suggests relative uncertainties of about ± 33% and ± 41%, respectively. This empirical approach suggests that data from rarer minerals (abundances below 0.01 area % or 100 area ppm) should be assessed with some caution, because scatter from analytical uncertainties will become more significant. A more detailed assessment using site duplicates and sample splits would provide more precise constraints, and should ideally be conducted in the future.

Note that the average abundances noted above are for crushed drill core, rather than glacial tills, and are not representative of these minerals in samples from this project. In till samples, quartz is commonly more abundant than K-feldspar, and the abundance of gittinsite is typically less than 0.1 area % (1000 area ppm). However, apatite abundances in drill cores and till samples are broadly similar (see Chapter 6).

The "Nugget Effect": Potential Influence of Probability on Analytical Precision

MLA-SEM analyses are derived from granular particulate material, rather than the finely-powdered material used for most types of geochemical analysis. This means that the division of an original sample into smaller amounts (aliquots) carries an additional source of uncertainty, because small aliquots may not be fully representative of the original sample. This has little impact for abundant minerals because particles of these minerals are so numerous, but it can be important for rarer minerals because there is no guarantee that their particles are included in smaller aliquots. Furthermore, if such particles *are* present, there is no guarantee that their measured abundance truly represents their abundance in the originally larger sample mass. These problems are examples of so-called 'probability effects' (e.g., Davis, 2003), which can be very difficult to assess and resolve. The best-known example of a 'probability effect' in geology is known as the 'nugget effect', as it is a common problem in exploration for gold. The most severe impact of the nugget effect is on the reliable assessment of mineral reserves in some gold deposits, and it is discussed in this context by Dominy et al. (2002; 2003). Simmonds (2009) provides some theoretical and statistical perspectives, but the summary below is given in very general terms.

Many natural gold deposits contain gold as dispersed specks of metal, which are generally small but locally large (so-called ‘visible gold’). When such material is sampled, the probability that a grain of gold will actually be present in *all* sample fractions is low, and most sample fractions will contain no gold. Gold will be detected intermittently, when it happens to be present in a given sample fraction, but its measured abundance in such samples will generally not represent its *true* average abundance. The nugget effect becomes most problematic when the sample fraction size is small, because the probability that a grain of gold will be included is then even smaller. The only way to mitigate or eliminate this problem is to collect larger samples and analyze larger fractions from them, which is not always practical. The nugget effect is very difficult to quantify, but it should be considered in the interpretation of MLA-SEM data for rare minerals, because these data are derived from a small aliquot removed from a larger sample of particulate matter. Simmonds (2009) suggests that the nugget effect can be recognized by its tendency to produce extreme positively-skewed frequency distributions, dominated by many analyses below detection limits, with some scattered highly anomalous values. As discussed later in Chapter 6, this type of pattern is seen for many of the least abundant minerals in the till samples.

The possible consequences of this problem are illustrated by a worked example that is specific to MLA-SEM analysis. If a sample puck is assumed to contain 20,000 particles of equal size, the numbers of particles that represent specific volumetric abundances are easily calculated. A mineral with an abundance of 10% equates to 2000 particles, and a mineral with an abundance of 1% equates to 200 particles, but a mineral with an abundance of 0.1% (1000 ppm) equates to only 20 particles. At lower abundances the particle count becomes very small, with 2 particles representing 100 ppm and only a single particle representing 50 ppm. Clearly, the probability that just a few particles from the larger sample would be included in the smaller aliquot that is analyzed is much less than the probability that they would not be included. However, there remains a small probability that particles of a rare mineral could be over-represented, especially if there are larger grains. If such effects apply, they would adversely impact the reliability and consistency of data for rare minerals from MLA-SEM analysis, and the estimates of precision derived by empirical methods (see above) might be too optimistic.

However, the simple example above makes some assumptions. Firstly, the particles in a given sample will actually vary in size, so rarer minerals that form smaller particles would be affected less than those that form larger particles. Secondly, and more importantly, it assumes that all minerals in a sample occur as single monomineralic particles, which is almost certainly not so. If a rare mineral instead occurs as smaller-scale intergrowths within larger particles of (a) more common mineral(s) then there is a greater probability that it will be included in a smaller aliquot and a greater probability that its measured abundance will approximate the correct value. This is easier to understand through pictorial methods, as shown in the cartoon of Figure 4.11. This shows that the probability of randomly selecting discrete particles of a rare mineral is much lower than the probability of selecting particles of a more abundant mineral that contain smaller 'grains' of the rare mineral. This example indicates that the textural relationships of minerals will have an important impact on the precision and reliability of data at low abundances.

Fortunately, MLA-SEM analysis allows visual examination of particles and grains, and it also measures the average particle size in a given sample and the average 'grain size' for each mineral (note again that 'grains' can be subareas within individual 'particles'). This allows calculation of the "Grain/Particle Size Ratio" (GPS Ratio; the average 'grain' size for a mineral divided by the average 'particle' size for the entire sample) for each mineral in a sample. Statistical measures of the GPS Ratio values for minerals across the wider database of MLA-SEM results can then be derived following compilation of these data. Chapter 6 of the thesis presents direct observations of particles and grains from BSE images, and evaluates important numerical data relevant to grain and particle sizes. Collectively, such observations suggest that many (but not all) rare minerals in the samples do typically form small-scale intergrowths with more common minerals. This indicates that probability effects would be mitigated at low abundances, but probably not eliminated. They will have an impact for the rarest minerals, some of which have abundances below 10 area ppm, and are also missing from many of the samples.

This conclusion is generally consistent with the limited empirical data from replicate analyses of drill core samples (D. Wilton, unpublished data; Figure 4.10). The possibility of probability effects on specific accessory and trace mineral data is discussed further in Chapters 6,

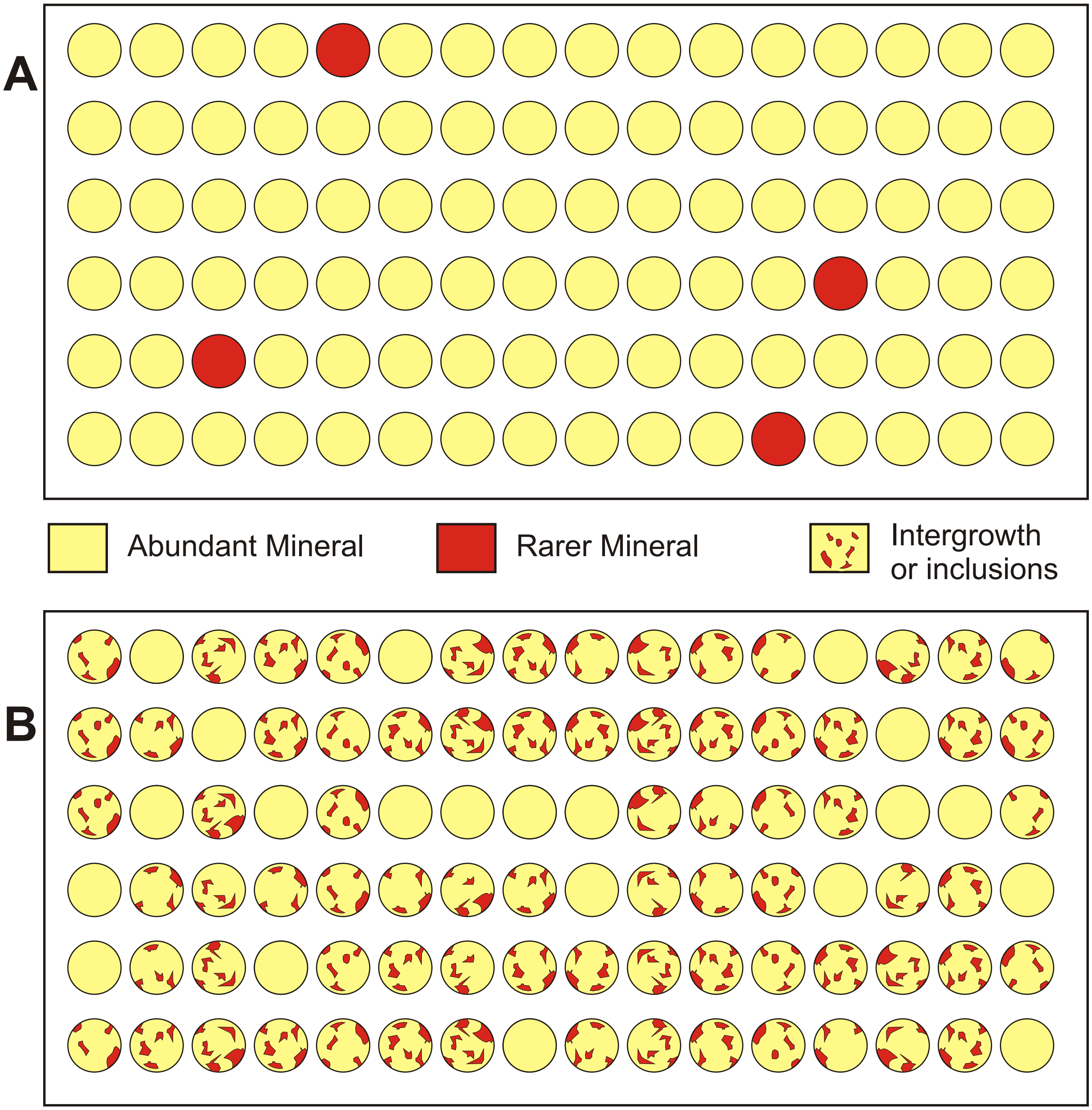

Figure 4.11. A cartoon illustration of how mineral textures could influence the uncertainties associated with the measurement of the abundance of rarer minerals by MLA-SEM methods. (A) In this panel, 4 of 112 particles are the rarer mineral. If 28 particles are extracted for analysis, that aliquot could contain between 0 and 4 particles of the rarer mineral, rather than just 1, which is the actual measure of abundance. The most likely outcome is that the rarer mineral is absent. (B) This panel shows about the same abundance of the rarer mineral but dispersed as smaller grains within particles. In this case, most sample aliquots would contain the rarer mineral and analysis would provide a more accurate representation of the true abundance of the rarer mineral in the material. See text for further discussion.

7 and 8 of the thesis. It also represents an interesting area for continued theoretical, observational and even experimental research.

Overview of Visible/Infrared Reflectance Spectroscopy (VIRS) Methods

Visible/Infrared Reflectance Spectroscopy (VIRS) measures absorption by materials in the visible to near infrared (VNIR) region (390 to 750 nm wavelength), the near infrared (NIR) region (750 to 1300 nm wavelength) and the short-wave infrared (SWIR) region (1300 to 2500 nm wavelength) of the electromagnetic spectrum. It utilizes absorption features at specific wavelengths to identify and analyze materials. The technique is well established for the identification of minerals, many of which have characteristic absorption spectra, but there is limited information on the characteristics of REE-bearing minerals (e.g., Kerr et al., 2011; Turner et al., 2015a, b; 2018).

For this research project, the ASD “TerraSpec” instrument was used. The TerraSpec is a compact, field-portable precision instrument developed by CSIRO in Australia. The machine itself is small (12.7 x 36.8 x 29.2 cm) and weighs less than 6 kg, so it is easy to move. A powerful handheld light probe, or stationary light probe (also referred to as a ‘mug light’), is attached to the processing machine by fiber optic cables. The light probe is positioned against the material of interest, which can be solid rock, silt, sand, or soil. The light probe projects a powerful beam of light and detectors relay reflected radiation to the spectrometers, which analyze component wavelengths. The principles of the method and the Terraspec instrument are illustrated in Figure 4.12. The components and usage of the instrument are shown in Figure 4.13, from Kerr et al. (2011), who also provide an explanation of the method and examples of applications in Newfoundland and Labrador, including some materials from Strange Lake.

The TerraSpec has a spectral range of 350-2500 nm at a spectral resolution of 6 to 7 nm. It has the capability to detect and identify a variety of minerals, and can also provide semiquantitative data on mineral compositions. Some of the benefits of the TerraSpec include non-destructive testing capabilities, little to no sample preparation, relatively low cost, and provision of a wider spectral coverage than earlier instruments such as the portable infrared mineral analyzer (PIMA). In Earth Sciences, the method is most widely used to evaluate the

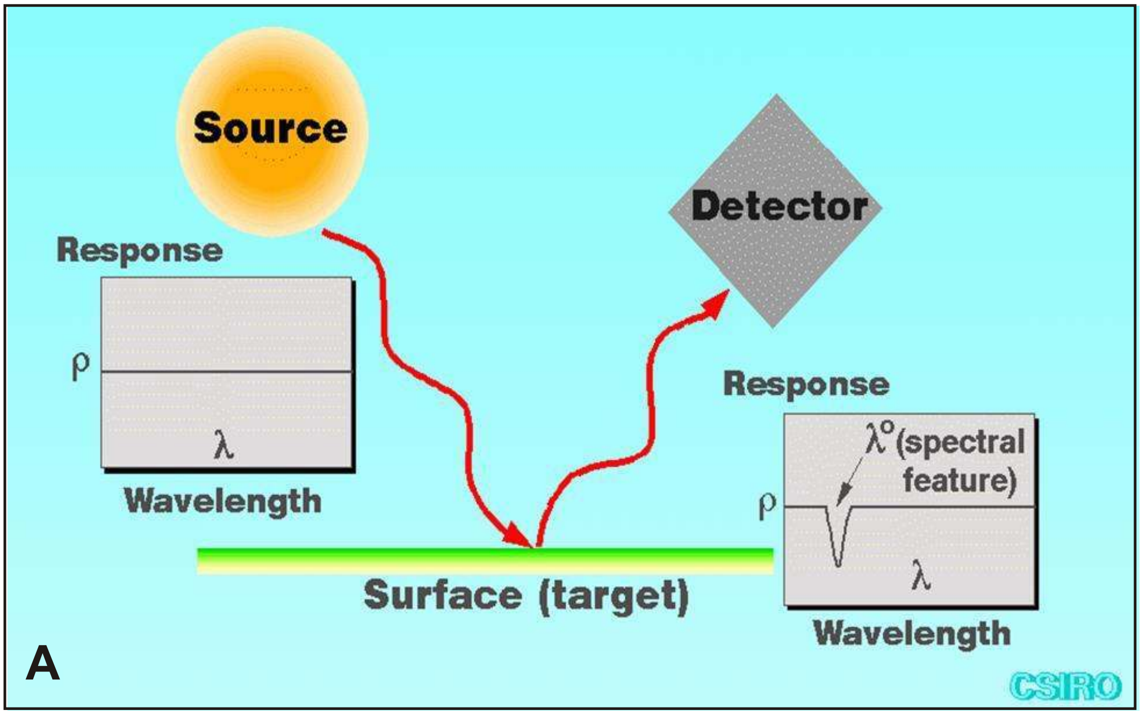

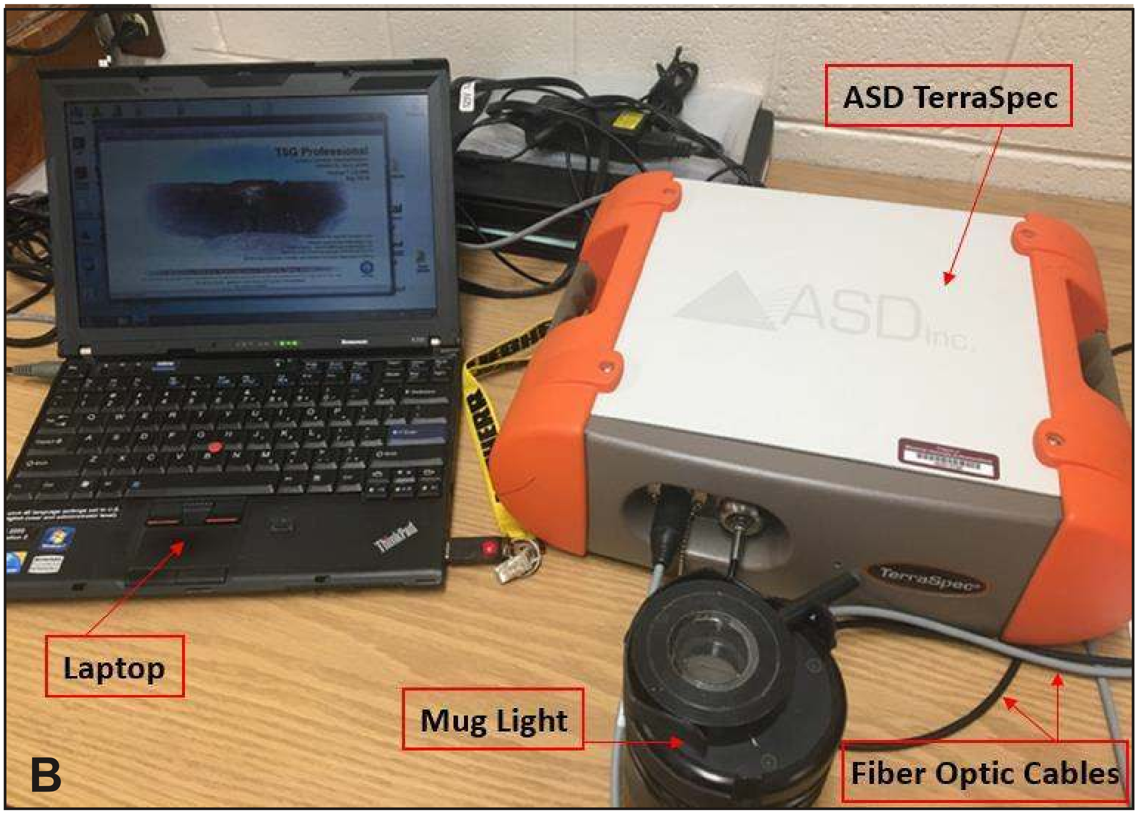

Figure 4.12. (A) Principle of Visual/Infrared Reflectance Spectroscopy (VIRS): Natural materials will absorb specific wavelengths and these patterns can be diagnostic. From CSIRO, Australia (B) Photo of the ASD TerraSpec with Mug Light attachment and linked laptop control computer.

secondary alteration minerals (typically water-bearing) that are associated with mineral deposits and can guide exploration. However, it can be applied in many other contexts in natural sciences, and in historical sciences such as archaeology. There is much interest in the use of VIRS methods to evaluate REE mineral deposits, in part due to the minimal sample preparation required and the potential to rapidly measure and map the distribution of REE minerals (e.g., Rowan et al., 1986). REE-bearing minerals are known to have distinctive absorption spectra, especially in the VNIR and SWIR regions (e.g., Turner et al., 2015a, b; 2018)., Kerr et al. (2011) examined materials from Labrador, including Strange Lake, and recognized some of these absorption patterns from high-grade samples containing visible mineralization, including the rare mineral eudialyte, known in central Labrador. However, absorption patterns diagnostic of the REE could not be discerned in lower-grade sample materials.

Visible/Infrared Reflectance Spectroscopy Procedures

The 125-180 µm size fraction of the surficial sediment samples was used due to its suitable grain size. The material from each sample was poured into an aluminum weighing dish. These disposable dishes were used because aluminum is not detected by the TerraSpec, which ensures that the dish does not interfere with the data. The TerraSpec light probe was then used to collect spectra from the sample. Spectra were collected from each sample in two different areas to obtain an average signature.

To eliminate instrumental drift, blank measurements were collected after every four samples, enabling the TerraSpec to recalibrate. A standard was also employed to monitor accuracy; for this study, crushed pyrite was used as a standard. The spectra from the standard were compared visually to ensure that they were consistent. The settings on the TerraSpec can be adjusted to adapt the instrument to various factors including material, grain size, and external light. The instrument settings used for data acquisition were a spectrum average of 20, a White Reference of 400, and a Dark Current of 100. These same settings were retained throughout the analyses.

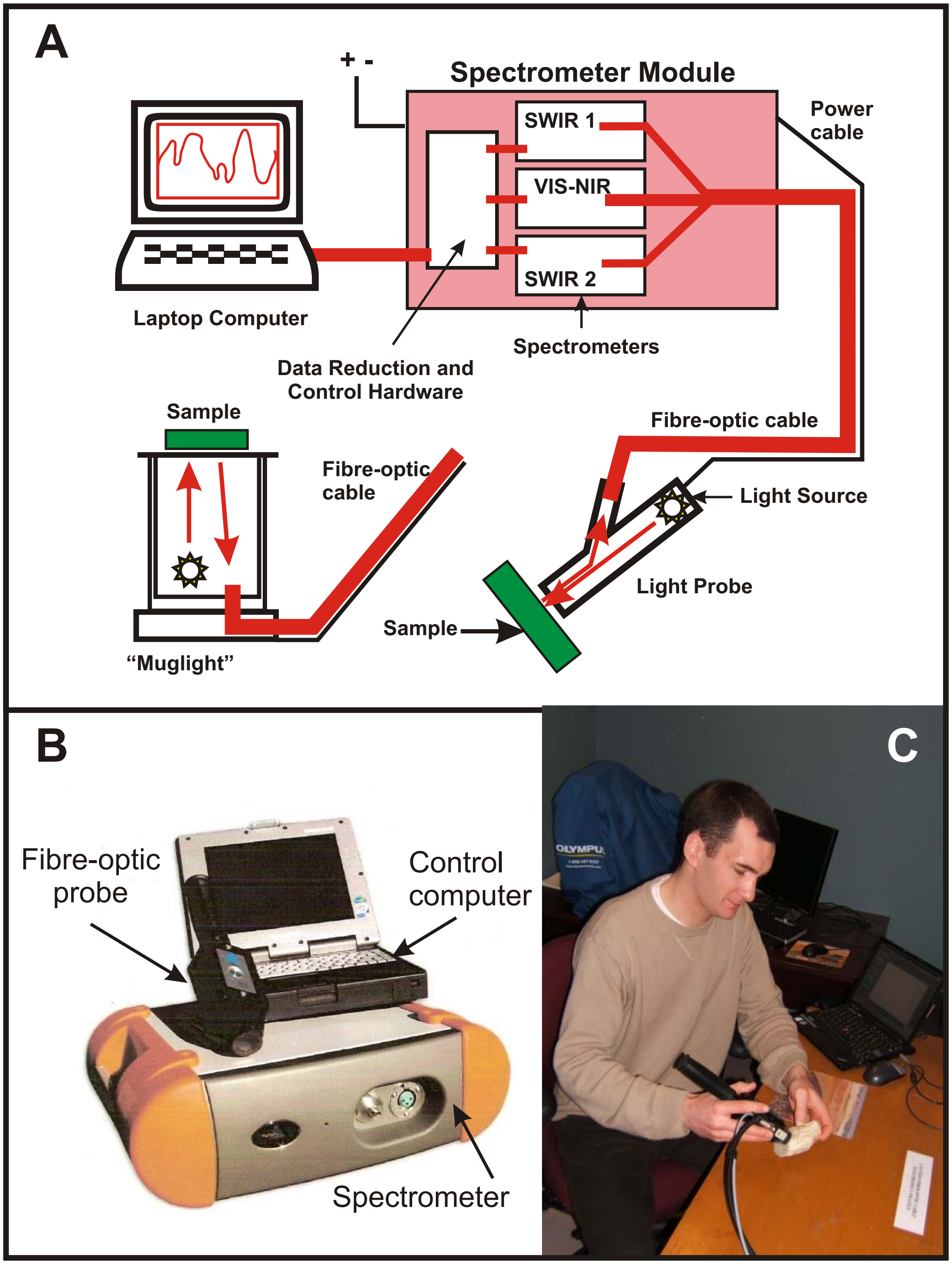

Figure 4.13. (A) Schematic diagram of the ASD TerraSpec showing the components and links. (B) Image of the spectrometer, computer and fibre-optic cable and probe. (C) Use of the spectrometer, with Greg Sparkes (Geological Survey of NL) acquiring data from a sample of gold mineralization. Images from Kerr et al. (2011) and ASD Reference Materials.

The data collected from the samples were exported onto a laptop computer attached to the TerraSpec. The unique signature created by the TerraSpec can, in some cases, be analyzed manually. Absorption features which appear at certain wavelengths are characteristic of specific minerals or mineral groups, as are unique combinations of such features. There are also several programs that automatically analyze spectral data from this method, and simplify the process of mineral identification. One of the best known and most used programs is The Spectral Geologist (TSG); TSG version 7 was used for this project. The program uses a reference library of spectra from different minerals, in the same way as the MLA-SEM software. However, REE-bearing minerals are not currently part of the database library, so these cannot be identified automatically. The reference spectra library mostly emphasizes secondary (generally low-temperature) minerals associated with fluid alteration processes. TSG does not allow users to create their own libraries, so automatic analysis is restricted to the pre-existing library and spectra from other sources cannot be added to it. The data from VIRS analyses, and comparisons with existing results from REE-bearing minerals and other minerals from Strange Lake (Kerr et al., 2011; Turner et al., 2015a, b; 2018; J. Percival, unpublished data) are presented and discussed in Chapter 5.

GEOGRAPHIC DATA PROCESSING AND RELATED CALCULATIONS

Coordinate Systems and Conversions

An important aspect of this project is the examination of geographic variation patterns in mineralogy related to dispersion from Strange Lake, or to other regional geological factors. Summary information on coordinate data and other geographic parameters is provided below, and listed in Table 4.1.

During field work, geographic locations were recorded as latitudes and longitudes from GPS readings taken at every sample site. All sample locations were converted to Universal Transverse Mercator (UTM) coordinates, which adhere to a regular grid with equal unit measures (metres) in north-south and east-west directions. This is more convenient for general use and for calculations. Coordinates were converted using a Microsoft Excel spreadsheet utility created and distributed by Steven Dutch of the University of Wisconsin in Green Bay (Wisconsin, USA).

Table 4.1. Sample location information as latitude, longitude and UTM coordinates (NAD 83).

Sample Number	Latitude (dd.dddd) (North)	Longitude (dd.dddd) (West)	NTS Map (1:50K Sheet)	UTM EAST (NAD 83) (metres)	UTM NORTH (NAD 83) (metres)	Distance from Strange Lake (Main Zone, km)	Distance from Strange Lake (B- Zone, km)	Azimuth (degrees) (Main Zone)	Azimuth (degrees) (B- Zone)	Distance Average (km)	Azimuth Average (degrees)
G1-1	56.3168	-64.1247	24A/08	430487	6241919	0.13	2.74	83.2	113.2	1.44	98.2
G1-2	56.3079	-64.0944	24A/08	432341	6240902	2.22	4.85	116.4	115.4	3.54	115.9
G1-3	56.3000	-64.1031	24A/08	431788	6240028	2.36	4.85	142.3	127.7	3.60	135.0
G1-4	56.3032	-64.1233	24A/08	430547	6240408	1.51	3.67	172.5	135.0	2.59	153.7
G1-5	56.3137	-64.1179	24A/08	430898	6241562	0.64	3.27	122.1	116.1	1.95	119.1
G1-6	56.3066	-64.1476	24A/08	429052	6240811	1.71	2.46	229.5	205.5	2.08	217.5
G1-7	56.3192	-64.1151	24A/08	431084	6242175	0.77	3.22	69.2	104.7	2.00	87.0
G1-8	56.3146	-64.1139	24A/08	431150	6241658	0.83	3.46	107.0	112.8	2.14	109.9
G1-9	56.3117	-64.1140	24A/08	431137	6241339	0.96	3.58	125.7	117.5	2.27	121.6
G1-10	56.3063	-64.1136	24A/08	431151	6240738	1.41	3.91	145.5	125.3	2.66	135.4
G1-11	56.3014	-64.1148	24A/08	431072	6240192	1.86	4.19	157.0	132.0	3.02	144.5
G1-12	56.2982	-64.1162	24A/08	430979	6239839	2.16	4.37	162.9	136.2	3.27	149.6
G1-13	56.2909	-64.1121	24A/08	431218	6239018	3.01	5.15	163.1	140.5	4.08	151.8
G1-14	56.2930	-64.0824	24A/08	433058	6239227	3.80	6.34	134.4	126.3	5.07	130.3
G1-15	56.3005	-64.0815	24A/08	433131	6240064	3.33	5.94	123.2	119.4	4.63	121.3
G1-16	56.3024	-64.0815	24A/08	433132	6240272	3.22	5.84	120.1	117.6	4.53	118.9
G1-17	56.3073	-64.0817	24A/08	433129	6240814	2.98	5.61	111.1	112.7	4.29	111.9
G1-18	56.3118	-64.0827	24A/08	433074	6241319	2.78	5.38	101.8	108.0	4.08	104.9
G1-19	56.3154	-64.0822	24A/08	433110	6241719	2.76	5.30	93.5	103.8	4.03	98.6
G1-20	56.3199	-64.0823	24A/08	433110	6242226	2.77	5.20	82.9	98.4	3.98	90.6
G1-21	56.3246	-64.0825	24A/08	433107	6242744	2.87	5.14	72.6	92.6	4.01	82.6
G1-22	56.3249	-64.0491	24A/08	435175	6242745	4.89	7.21	79.7	91.8	6.05	85.7
G1-23	56.3171	-64.0455	24A/08	435386	6241875	5.03	7.50	89.9	98.4	6.26	94.1
G1-24	56.3105	-64.0497	24A/08	435113	6241139	4.81	7.38	98.8	104.3	6.10	101.5
G1-25	56.3058	-64.0501	24A/08	435081	6240620	4.89	7.50	104.8	108.2	6.20	106.5
G1-26	56.3012	-64.0509	24A/08	435024	6240115	5.00	7.63	110.6	112.0	6.31	111.3
G1-27	56.2969	-64.0490	24A/08	435135	6239625	5.29	7.92	115.1	114.9	6.61	115.0
G1-28	56.2935	-64.0493	24A/08	435107	6239251	5.44	8.07	118.8	117.4	6.75	118.1
G1-29	56.2963	-64.0142	24A/08	437286	6239526	7.32	9.95	108.6	110.1	8.63	109.4
G1-30	56.2986	-64.0186	24A/08	437016	6239795	6.98	9.60	107.2	109.2	8.29	108.2
G1-31	56.3025	-64.0173	24A/08	437103	6240219	6.95	9.55	103.6	106.6	8.25	105.1
G1-32	56.3079	-64.0146	24A/08	437282	6240819	7.01	9.56	98.5	102.9	8.29	100.7
G1-33	56.3076	-64.0144	24A/08	437290	6240791	7.02	9.58	98.7	103.0	8.30	100.9
G1-34	56.3118	-64.0151	24A/08	437254	6241257	6.92	9.45	95.0	100.3	8.19	97.7
G1-35	56.3165	-64.0158	24A/08	437168	6241766	6.81	9.28	90.8	97.3	8.04	94.1
G1-36	56.3209	-64.0182	24A/08	437081	6242275	6.73	9.14	86.4	94.3	7.94	90.4
G1-37	56.3253	-64.0184	24A/08	437076	6242757	6.77	9.11	82.4	91.2	7.94	86.8
G1-38	56.3201	-63.9804	14D/05	439413	6242150	9.06	11.47	88.0	93.9	10.26	91.0
G1-39	56.3169	-63.9849	14D/05	439130	6241792	8.77	11.22	90.3	95.9	10.00	93.1
G1-40	56.3089	-63.9830	14D/05	439234	6240910	8.93	11.46	96.0	100.2	10.19	98.1

Table 4.1 (continued). Sample location information as latitude, longitude and UTM coordinates (NAD 83).

Sample Number	Latitude (dd.dddd) (North)	Longitude (dd.dddd) (West)	NTS Map (1:50K Sheet)	UTM EAST (NAD 83) (metres)	UTM NORTH (NAD 83) (metres)	Distance from Strange Lake (Main Zone, km)	Distance from Strange Lake (B- Zone, km)	Azimuth (degrees) (Main Zone)	Azimuth (degrees) (B- Zone)	Distance Average (km)	Azimuth Average (degrees)
G2-1	56.3527	-63.9198	14D/05	443210	6245730	13.41	15.48	73.0	79.5	14.44	76.3
G2-2	56.3352	-63.9093	14D/05	443836	6243772	13.60	15.88	81.7	86.9	14.74	84.3
G2-3	56.3140	-63.8960	14D/05	444624	6241395	14.27	16.73	91.6	95.2	15.50	93.4
G2-4	56.3497	-63.9022	14D/05	444298	6245378	14.36	16.49	75.6	81.4	15.43	78.5
G2-5	56.3586	-63.8880	14D/05	445186	6246352	15.48	17.53	72.9	78.6	16.51	75.8
G2-6	56.3391	-63.8792	14D/05	445702	6244182	15.51	17.77	81.2	85.8	16.64	83.5
G2-7	56.3215	-63.8707	14D/05	446203	6242209	15.85	18.25	88.5	92.1	17.05	90.3
G2-8	56.3622	-63.8580	14D/05	447045	6246733	17.37	19.43	73.5	78.6	18.40	76.0
G2-9	56.3407	-63.8360	14D/05	448376	6244325	18.18	20.44	81.9	85.9	19.31	83.9
G2-10	56.3274	-63.8399	14D/05	448113	6242848	17.78	20.14	86.6	90.1	18.96	88.3
G2-11	56.3684	-63.8242	14D/05	449142	6247397	19.57	21.62	73.3	77.9	20.59	75.6
G2-12	56.3542	-63.8120	14D/05	449876	6245806	19.90	22.08	78.3	82.3	20.99	80.3
G2-13	56.3228	-63.8035	14D/05	450361	6242303	20.00	22.40	88.5	91.4	21.20	89.9
G2-14	56.3746	-63.7168	14D/05	455782	6248011	26.15	28.25	76.1	79.4	27.20	77.8
G2-15	56.4631	-63.7876	14D/05	451523	6257909	26.53	27.86	52.9	57.3	27.20	55.1
G2-16	56.3376	-63.7736	14D/05	452229	6243933	21.96	24.27	84.3	87.4	23.12	85.9
G2-17	56.3747	-63.7626	14D/05	452954	6248057	23.42	25.48	74.4	78.2	24.45	76.3
G2-18	56.3588	-63.7560	14D/05	453341	6246286	23.39	25.58	78.8	82.3	24.49	80.5
G2-19	56.3439	-63.7420	14D/05	454189	6244613	23.98	26.26	83.1	86.1	25.12	84.6
G3-2	56.3698	-63.7128	14D/05	456022	6247475	26.26	28.40	77.8	80.6	27.33	79.2
G3-3	56.3497	-63.6924	14D/05	457260	6245228	27.10	29.37	83.0	85.3	28.24	84.1
G3-4	56.3889	-63.6798	14D/05	458083	6249580	28.77	30.82	74.5	77.3	29.79	75.9
G3-5	56.3781	-63.6702	14D/05	458664	6248374	29.03	31.15	77.1	79.7	30.09	78.4
G3-6	56.3638	-63.6681	14D/05	458779	6246786	28.84	31.04	80.3	82.6	29.94	81.4
G3-7	56.4107	-63.6794	14D/05	458134	6252010	29.55	31.47	70.0	73.0	30.51	71.5
G3-8	56.3845	-63.6612	14D/05	459224	6249077	29.74	31.83	76.0	78.6	30.79	77.3
G3-9	56.3613	-63.6341	14D/05	460876	6246483	30.86	33.09	81.5	83.6	31.97	82.5
G3-10	56.4116	-63.6620	14D/05	459204	6252103	30.59	32.53	70.5	73.4	31.56	72.0
G3-11	56.4085	-63.6287	14D/05	461257	6251733	32.42	34.41	72.4	74.9	33.41	73.6
G3-12	56.3811	-63.6266	14D/05	461359	6248688	31.73	33.86	77.7	80.0	32.80	78.8
G3-13	56.3659	-63.6174	14D/05	461912	6246982	31.96	34.17	80.9	82.9	33.06	81.9
E-1	56.3278	-64.0764	24A/08	433491	6243096	3.35	5.52	69.2	88.8	4.43	79.0
E-3	56.3329	-63.9404	14D/05	441907	6243540	11.66	13.94	81.9	87.4	12.80	84.7
E-4	56.3460	-63.8891	14D/05	445100	6244956	15.05	17.24	78.3	83.1	16.14	80.7
E-7	56.3932	-63.7115	14D/05	456131	6250076	27.04	29.03	72.4	75.5	28.03	74.0
E-8	56.4159	-63.6665	14D/05	458936	6252581	30.51	32.41	69.5	72.4	31.46	71.0

NOTES

For information on coordinate conversion and methods for calculation of distances and azimuth directions, see text discussions.

Table 4.1 lists the coordinates for all samples with reference to the North American Datum 1983 (NAD 83), which is the current standard for topographic maps in Canada. Some older maps use a different datum (NAD 27); the NAD 83 coordinates table 4.1 can be converted simply into NAD 27 by subtracting 55 metres from the Easting coordinate, and subtracting 225 m from the Northing coordinate. Note that this simplified arithmetic conversion is precise only within NTS topographic map sheets Lac Dihourse (24A/08) and the adjacent unnamed map sheet in Labrador (14D/05). Other data from the area are mostly reported with reference to NAD 83 (e.g., Midland Exploration; Bourassa and Banville, 2012; 2013; GSC; McClenaghan et al., 2017; 2019). Some older data in this area (e.g., Batterson and Taylor, 2009) use the older NAD 27 datum, and this is also used presently by the “Geoscience Online” GIS system operated by the Geological Survey of Newfoundland and Labrador.

Geographic Calculations: Distance and Azimuth from Strange Lake

As one of the objectives of this project is to assess mineral dispersion from the Strange Lake deposits, it is important to have formal geographic measures. Calculations are easy using UTM coordinates because they are expressed in metres. The distance of sample locations from possible sources is calculated using simple trigonometry (the famous theorem of Pythagoras). It corresponds to the hypotenuse (A) of a right-angle triangle for which the other sides are the displacement from the source in an east-west direction (B), and the displacement from the source in a north-south direction (C). The distance from the source is then calculated from the famous expression $A^2 = B^2 + C^2$. Distances were calculated twice for each sample, using the Strange Lake Main Zone and B-Zone deposits as possible sources. The assumed coordinate for the Main Zone Deposit is 430305E / 6241680N, and the assumed coordinate for the B-Zone is 427918E / 6242782N. These coordinates come from field notes by A. Kerr, and McClenaghan et al. (2019). These calculated data are listed in Table 4.1.

The azimuth (bearing) from possible sources to each sample site was also calculated. This is derived from the tangent of the angle at the corner of the same right-angled triangle that corresponds to the source. This angle is either added to or subtracted from 90°, according to the direction of the sample north-south displacement. A trivial correction ($< 1^{\circ}$) is also required because the UTM grid is not exactly aligned with true north in this area. Only one sample (G1-4) lies west of the Main Zone Deposit, and this requires a different calculation with respect to 270°

rather than 90°. As for the absolute distance from sources, azimuth calculations were completed for all samples with respect to both the Main Zone Deposit and the B-Zone Deposit. These calculated data are listed in Table 4.1.

Although the thesis project is confined to Labrador and mostly involves information from the Strange Lake Main Zone Deposit, the B-Zone deposit could also be a source for dispersed material in Labrador. Assuming the direction of glacial transport to be about 070° (ENE), as indicated by glacial landforms and striae (Batterson, 1989), the apparent separation of the Main Zone and B-Zone deposits viewed from this direction is only about 1 km, but the B-Zone deposit is located about 2.4 km in an up-ice direction (see Figure 4.3). To account for the possibility that there are two possible sources for detritus, the calculated distances and azimuths for with respect to the Main Zone and B-Zone were averaged, and these values (see Table 4.1) are used subsequently in statistical analysis (Chapter 6) and evaluation of geographic variation patterns (Chapter 7). Effectively, this method arbitrarily locates the potential source for detritus at the hypothetical mid-point between the Main Zone and B-Zone deposits.

Data Processing and Statistical Analysis Methods

This project uses statistical analysis methods to understand and interpret the large volume of data generated by MLA-SEM analysis of the 76 till samples. Further information on the steps taken to organize and subdivide the database, and discussion of the statistical methods used, is given in the introduction to Chapter 6. Statistical analysis was largely accomplished using the *MYSTAT* software, which is a free educational version of a comprehensive statistics and data analysis package known as *SYSTAT*. Although MYSTAT does not contain the multiple techniques included as part of SYSTAT, and is limited to databases with less than 100 variables, it is more than adequate for this project and is very easy to use. Inbuilt tutorials also provide extensive factual information and advice about the use and misuse of statistics. It also produces a wide range of graphs and charts that can be used to illustrate data. Some simpler calculations (such as averages, standard deviations, etc.) were produced using the features available in Microsoft Excel. Graphs and charts were produced using MYSTAT and the *Grapher* program of Golden Software, and maps used in geographic analysis were produced largely using the *Surfer* program, developed by the same company. The Surfer program contains features that resemble those included in more sophisticated Geographic Information Systems (GIS) such as ArcInfo or Q-GIS. The Golden Software products are well known in the Earth Science community, and include features designed specifically for geological research projects.

CHAPTER 5: DATA FROM VISIBLE/INFRARED REFLECTANCE SPECTROSCOPY (VIRS) ANALYSIS

GENERAL SUMMARY

Prior to the acquisition of the MLA-SEM data discussed in the next chapter, the till samples collected from the project area were analyzed using Visible-Infrared Reflectance Spectroscopy (VIRS) methods outlined in Chapter 4, with the ASD Terraspec instrument . The objective was to test for responses that might indicate potential for the possible use of satellite-based spectrometry data to map dispersal from Strange Lake. This was connected to a wider objective to investigate the application of “Remote Predictive Mapping” techniques developed by the Geological Survey of Canada (Harris et al., 2011). Initial results were not encouraging, as the only absorption features visible were those associated with clay minerals. The samples were then treated to remove any clay coatings on mineral grains, and reanalyzed, but this did not improve results. Comparisons between spectra from till samples and reference spectra for REE-bearing minerals did not reveal any absorption features in common. MLA-SEM data later indicated that REE-bearing minerals were actually present in small amounts, but it appears that the VIRS method is not sensitive enough to detect them. It is concluded that remote spectroscopic data would not be useful in investigating dispersion from the Strange Lake deposit.

SUMMARY OF ANALYTICAL DATA

Procedures

The methods employed in sample preparation and data acquisition were described in Chapter 4. All samples from the study area were analyzed using the TerraSpec™ instrument to derive absorption spectra. An examples of a typical absorption spectrum for a till sample is provided in Figure 5.1, where it is compared to absorption spectra from hand samples of granite and pegmatite from Strange Lake, and spectra from selected REE oxides (data from Kerr et al., 2011). These charts show the relative amounts of reflected visible and infrared radiation (Y-Axis) with respect to the wavelength (X-axis). The instrument measures wavelengths from 390 nm (within the visible light range) to 2500 nm (in the region referred to as short-wave infrared, or SWIR). Reflectance spectra commonly display "absorption features" at specific wavelengths, which are indicated by prominent minima or 'dips' in the absorption patterns**,** as shown by these examples. Combinations of absorption features, and changes in the wavelength associated with specific absorption features, provide information that can identify minerals or provide compositional inferences about them (Hauff, 2008; Kerr et al., 2011).

Each region of the spectrum measured is relevant to specific minerals or mineral groups, and also to other materials such as vegetation. The visible and "near infrared" region (390 nm to 750 nm; VNIR) is useful for characterization of iron-bearing minerals such as hematite, goethite and jarosite, and also for many REE-bearing minerals. The adjoining "near infrared" (NIR) region is useful for characterization of many common water or (OH)-bearing minerals, including amphiboles, micas, sulphates and diverse types of clay minerals. Absorption features in this region are especially useful for the recognition and definition of secondary minerals associated with alteration processes. The "short-wave infrared" (SWIR) region provides some information on silicate minerals such as quartz, feldspar, garnet and pyroxene, and also carbonates, halides and other mineral groups. Some REE-bearing minerals also may exhibit distinctive absorption features in the SWIR spectral region. However, not all minerals have unique or diagnostic absorption spectra.

Initial examination of absorption spectra from till samples indicated obvious absorption features at around 1400 nm, 1930 nm and 2200-2300 nm (e.g., Figure 5.1). These features are characteristic of water (H_20), the hydroxyl molecule (OH^-) and aluminum hydroxide (AlOH) and collectively indicate the presence of phyllosilicate minerals and/or clay minerals. No absorption features were observed in the VNIR region, and responses in the SWIR region were subtle and not diagnostic. Given the possible abundance of clays in material from Strange Lake mineralization, and the more general presence of clays in glacial sediments, it was decided that samples should be treated to remove any clay that might coat the surfaces of mineral grains and inhibit their analysis. The samples were rinsed vigorously (see Chapter 4) and reanalyzed, but this did not noticeably change results.

The spectra from the samples were examined manually for comparison with available reference spectra for minerals of interest. To do this, a process known as "continuum removal" was employed to accentuate possible features of interest (P. Lypaczewski, pers. comm., 2018). This is essentially a normalization method in which the reflectance is recalculated as a proportion of the total reflectance variation shown by the sample, rather than in absolute units. Automated methods, from the software

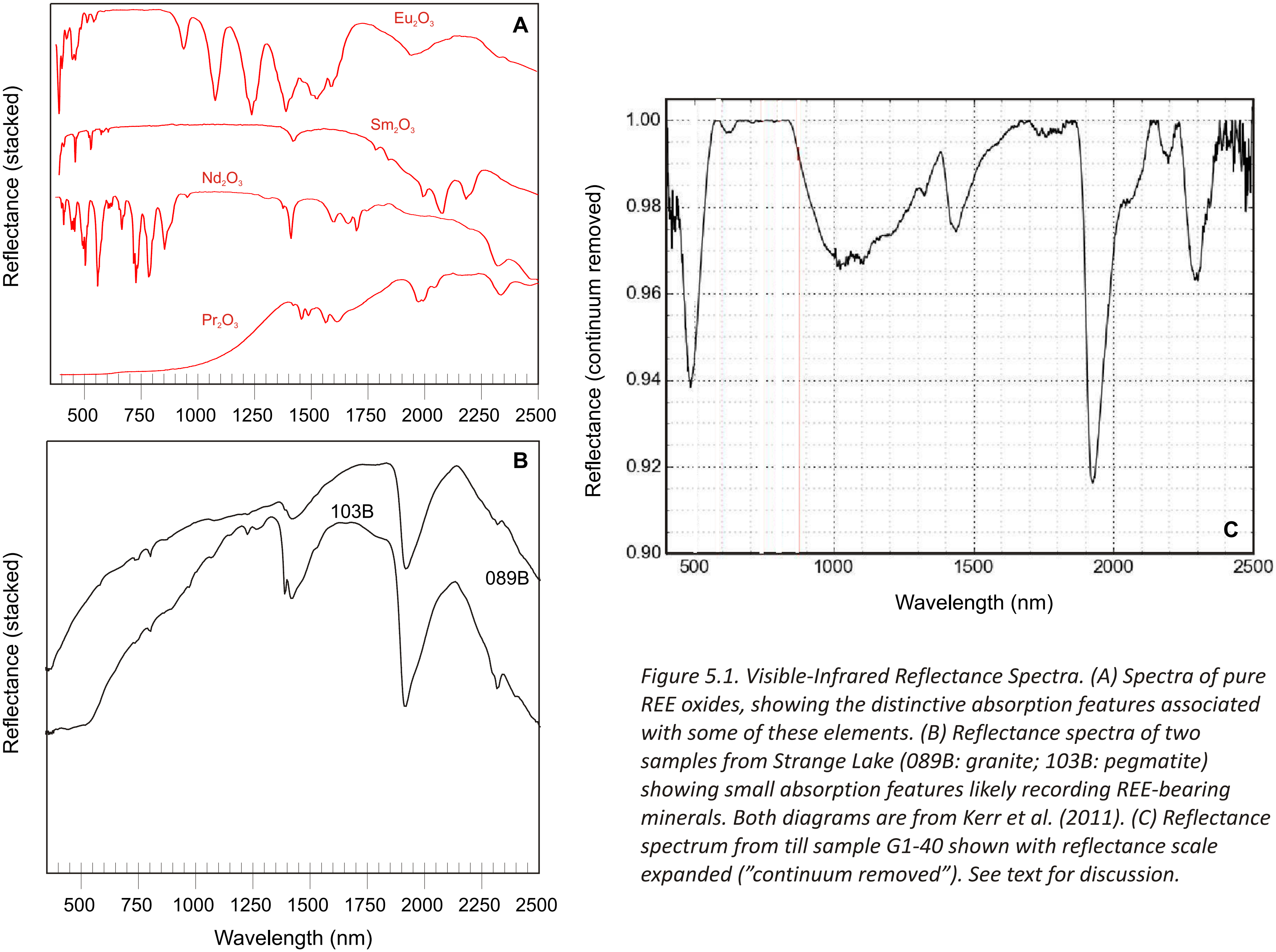

Figure 5.1. Visible-Infrared Reflectance Spectra. (A) Spectra of pure REE oxides, showing the distinctive absorption features associated with some of these elements. (B) Reflectance spectra of two samples from Strange Lake (089B: granite; 103B: pegmatite) showing small absorption features likely recording REE-bearing minerals. Both diagrams are from Kerr et al. (2011). (C) Reflectance spectrum from till sample G1-40 shown with reflectance scale expanded ("continuum removed"). See text for discussion.

program “The Spectral Geologist” (TSG) were also used to characterize minerals and estimate their abundances; however, the TSG program does not contain reference spectra for REE-bearing minerals, so these cannot be detected automatically.

Consistency and Variability of VIRS Results

The measured spectra were compared with one another by “stacking” multiple results in one chart, using the TSG program. This method makes individual absorption features weaker than they would appear in a single chart but allows easy visual assessment and comparison. Examining multiple spectra in one view makes it easier to identify repeating patterns, blocks of similar spectra, or changing trends throughout the dataset. The actual (absolute) reflectance for each region of the spectrum is indicated by colour-coding of the results. Figure 5.2 shows “stacked” spectra for numerous analyzed till samples, and indicates that they are all closely similar, with absorption features at around 1400 nm, 1930 nm and 2200 – 2300 nm. The VNIR region of the spectra, of most interest in the context of REE-bearing minerals, is generally featureless, at least when displayed in this fashion.

Mineral Identifications

The TSG program identified several minerals including muscovite, paragonite, Fe-rich chlorite, siderite, goethite, dolomite and reibeckite. The abundance estimates from the program are semi-quantitative and not necessarily inclusive, as not all minerals can be identified by the VIRS methods. None of the identified minerals are fully characteristic of the Strange Lake Intrusion, although the presence of reibeckite may be significant, as this Na-rich amphibole is common in granitic rocks of peralkaline composition. As noted above, the TSG program prioritizes minerals that are commonly associated with hydrothermal alteration processes, so these mineral identifications were of limited value for this study. Although the compilation of spectra shown in Figure 5.2 suggests that the VNIR region is generally featureless for all samples, examination of individual spectra at an expanded scale, with the aid of “continuum removal” did reveal some diffuse low-magnitude absorption features. These were investigated by visual comparisons with available reference spectra for minerals of interest.

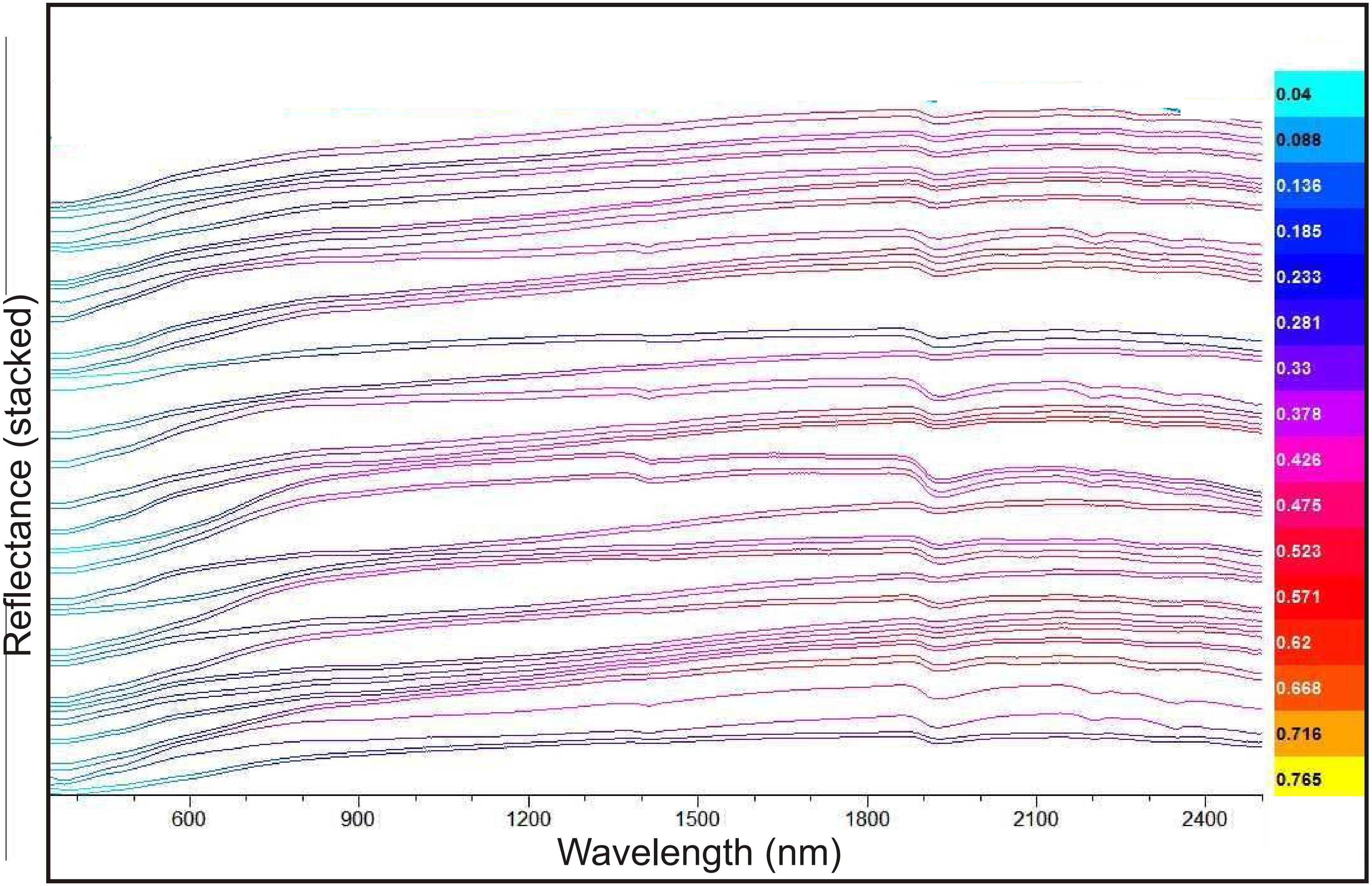

Figure 5.2. Visible-Infrared Reflectance Spectra for selected till samples analyzed using the Terraspec instrument. Note that these are stacked, so the vertical scale is arbitrary, and contrasts within a spectrum are 'flattened' by processing. The absolute reflectance values are shown by colour coding, as in the scale bar at the right. The important conclusion from such a comparison is that all the samples show closely similar patterns.

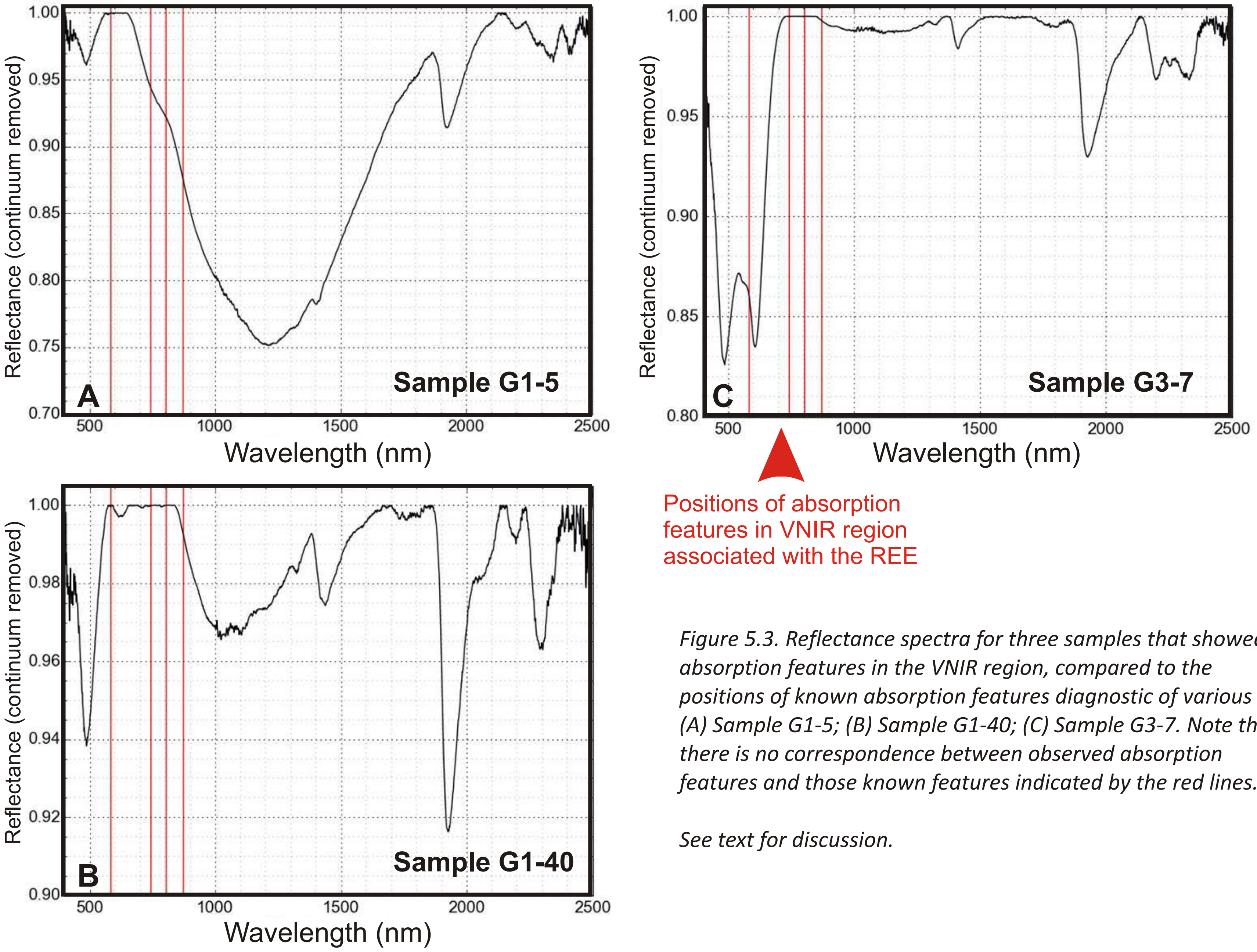

Positions of absorption features in VNIR region associated with the REE

Figure 5.3. Reflectance spectra for three samples that showed absorption features in the VNIR region, compared to the positions of known absorption features diagnostic of various REE. (A) Sample G1-5; (B) Sample G1-40; (C) Sample G3-7. Note that there is no correspondence between observed absorption features and those known features indicated by the red lines.

See text for discussion.

Evidence for the Presence of Rare Earth Element Minerals

The VNIR is the wavelength region in which most REE-bearing minerals absorb radiation (e.g., Hauff, 2008; Amhed et al., 2012; Turner et al., 2015a, b; 2018). Two methods were used in an attempt to identify possible signatures from REE-bearing minerals in the samples. These methods both involve visual comparison of spectra with reference materials, aided by the TSG software.

Spectra were examined carefully following "continuum removal" to accentuate absorption features. This revealed that some samples do indeed have subtle features within the VNIR wavelength region, including samples G1-05, G1-40 and G3-7 (Figure 5.3). One of these absorption features is close to 500 nm, which is known from several REE-bearing minerals but the others could not be linked to features documented in other studies (e.g., Turner et al., 2018). As shown in Figure 5.3, there is no correspondence between subtle absorption features in these spectra and the known wavelength locations of absorption features linked to the REE.

The measured spectra were also compared to spectra previously obtained from known REE-bearing minerals and other unusual minerals known from Strange Lake. Absorption spectra for a variety of minerals including, zircon, allanite, gittinsite, and bastnaesite were provided by Dr. Jeanne Percival of the Geological Survey of Canada. Spectra are also provided by Turner et al. (2018) provide for a variety of REE-bearing silicate minerals, including kainosite, but not for gerenite. Samples known to contain relatively high concentrations of unusual minerals on the basis of the later MLA-SEM analyses were chosen for comparisons. Figure 5.4 compares sample G3-4, which had the highest abundance of allanite (0.15 area %; 1500 ppm) to allanite spectra (J. Percival, unpublished data) using the TSG 'stacked' viewing option. The VNIR region of the G3-4 spectrum does not show any characteristic absorption features, and the only features common to sample G3-4 and the reference spectra are those related to water, hydroxide, and aluminum hydroxide. The sample spectrum contains no features to indicate the presence of allanite, although the mineral is known to be present on the basis of later analysis.

Sample G1-18 had the highest abundance of zircon (1.75 area %). Figure 5.5 compares the measured spectrum from this sample with reference zircon spectra provided by Percival (unpublished data) using the TSG 'stacked' viewing option. The only absorption feature common to measured and reference spectra is at about 1930 nm, known to be associated with the hydroxyl (OH-) molecule. The sample spectrum contains no features to indicate the presence of zircon, although the mineral is known to be present on the basis of later analysis.

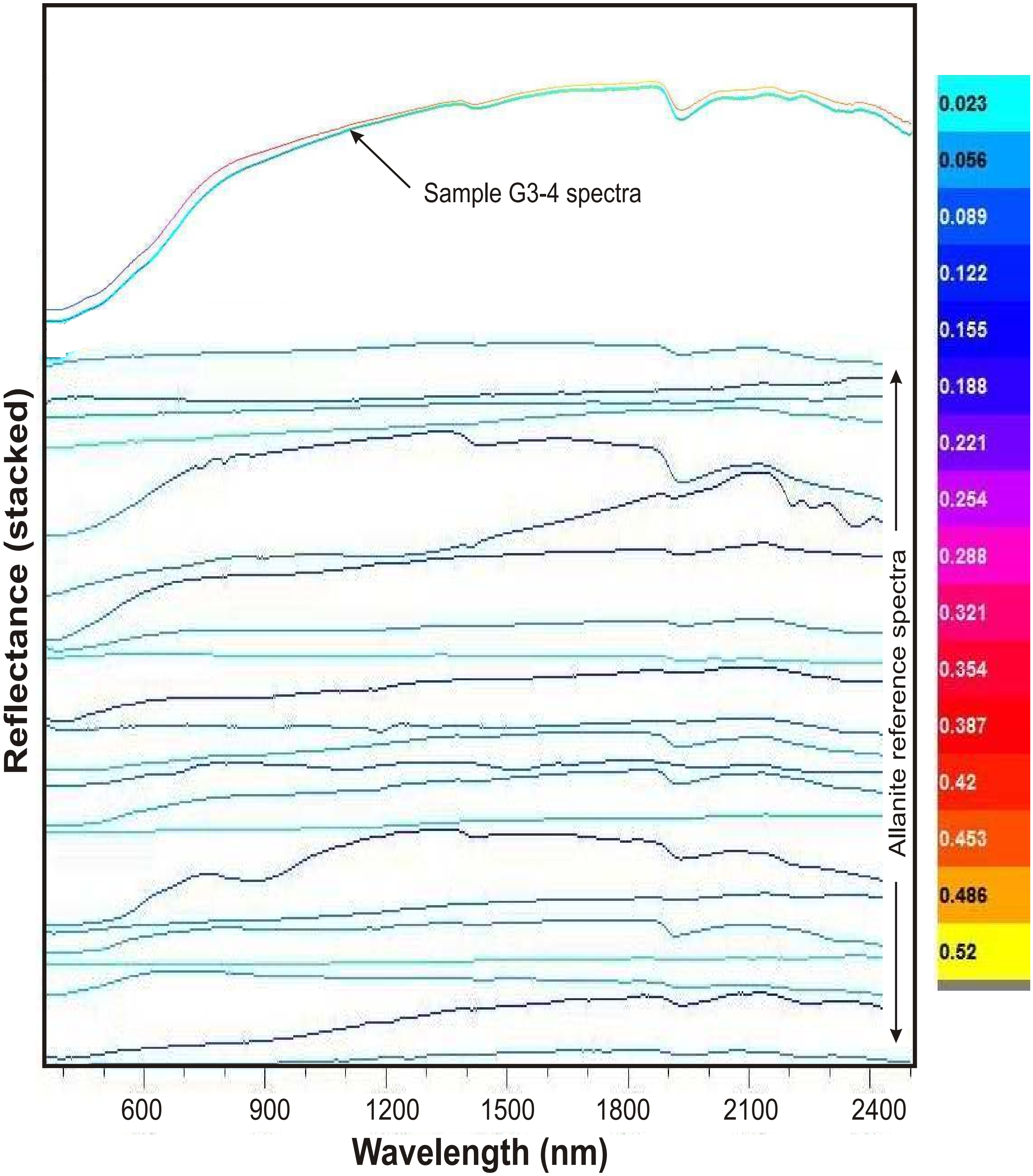

Figure 5.4. Comparison between spectra from sample G3-4 (upper lines) and spectra from the mineral allanite provided by J. Percival (unpublished data) shown by multiple lower lines. See text for discussion.

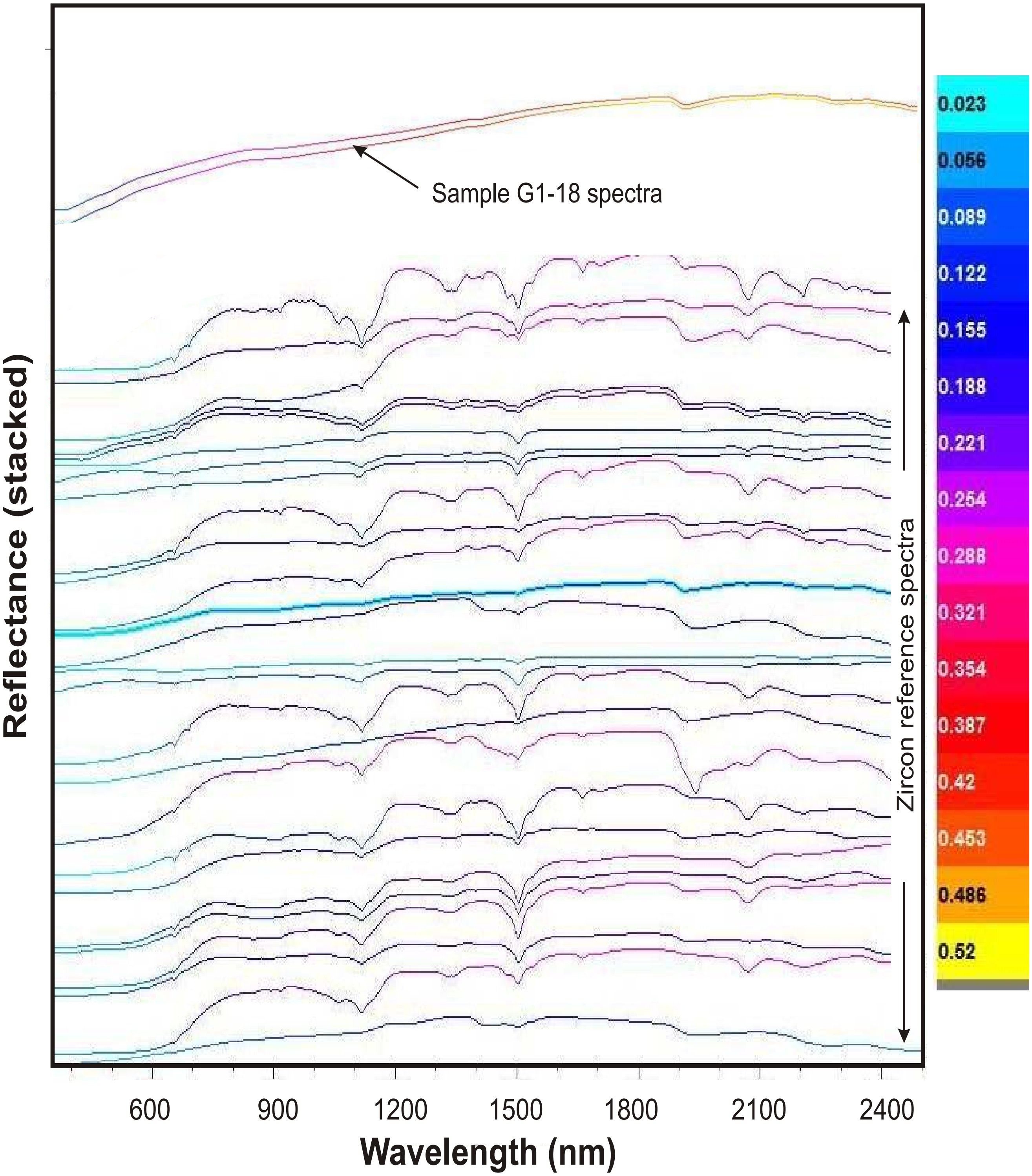

Figure 5.5. Comparison between spectra from sample G1-18 (upper lines) and spectra from the mineral zircon provided by J. Percival (unpublished data) shown by multiple lower lines. See text for discussion.

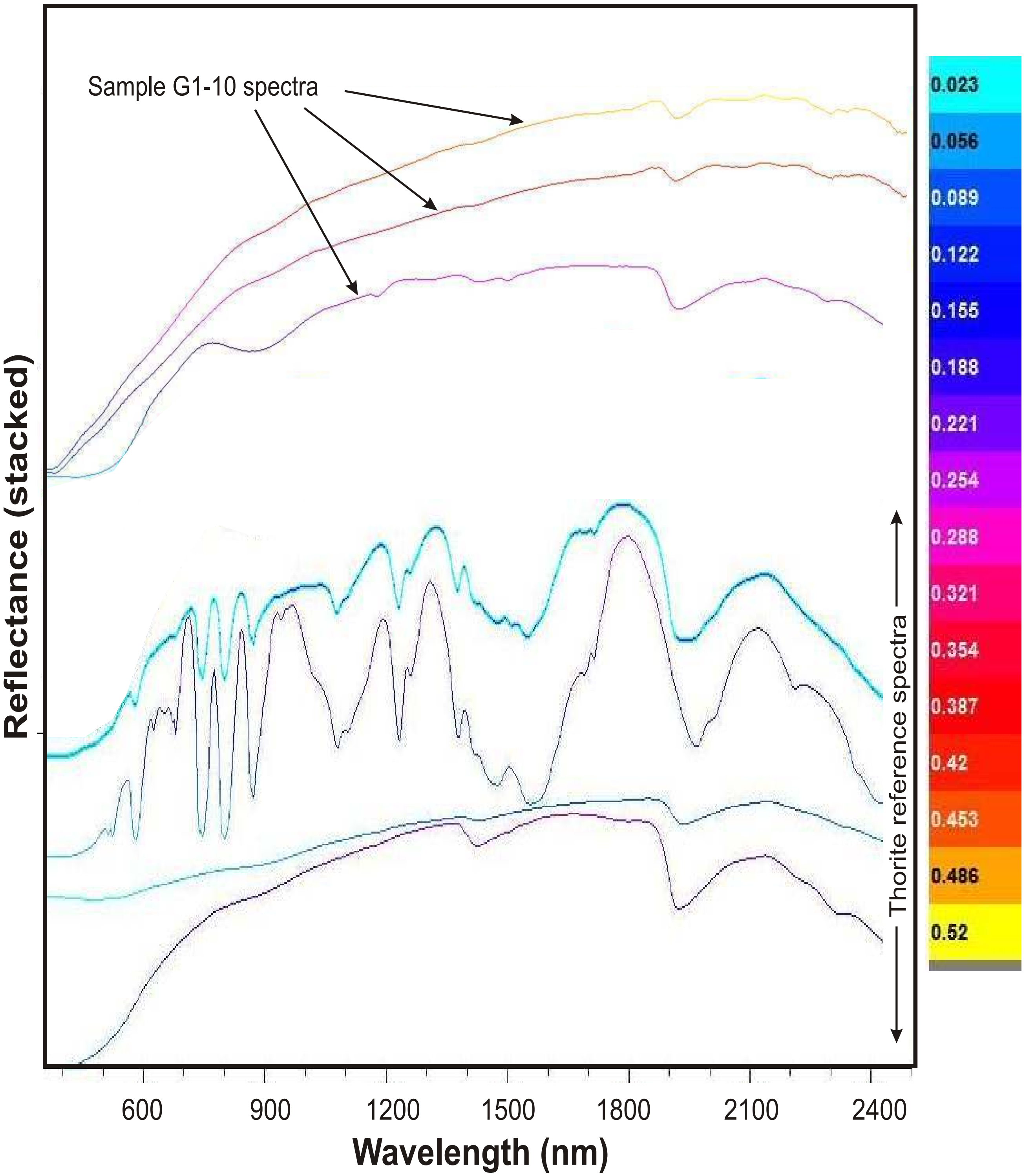

Figure 5.6. Comparison between spectra from sample G1-10 (upper lines) and spectra from the mineral thorite provided by J. Percival (unpublished data) shown by multiple lower lines. See text for discussion.

Sample G1-10 has the highest abundance of thorite (0.14 area %; 1400 ppm). Thorite is not a REE-bearing mineral but it is present at Strange Lake and in many other REE deposits, and it has a distinctive absorption spectrum. Figure 5.6 compares measured spectra from G1-10 with reference thorite spectra provided by Percival (unpublished data) using the TSG 'stacked' viewing option. The spectra are quite different in appearance, and those from sample G1-10 are relatively featureless. As in the case of G3-4, the only feature shared by measured and reference spectra is at 1930 nm, associated with hydroxyl (OH-). Although thorite was confirmed in the sample by later MLA-SEM analysis, there is no sign of it in the reflectance spectrum.

EVALUATION OF THE VIRS METHOD IN REE EXPLORATION

The VIRS method is certainly capable of detecting REE-bearing minerals and other unusual minerals by virtue of their distinctive spectra, but this investigation indicates that it cannot detect such minerals at low abundances. With the exception of zircon and titanite, which are locally present at > 1% and > 0.3%, respectively, the areal abundances of Zr- and REE-bearing accessory minerals in the till samples only rarely approaches 0.05 area %. The rarity of such accessory minerals is better appreciated if the data are converted to ppm; the most abundant of them amount to less than 500 ppm, and most of the REE-bearing minerals are present at levels below 100 ppm (see Chapter 6).

All of the spectra obtained were examined using the "continuum removal" software provided by P. Lypaczewski (pers. comm., 2018) which allows examination at a greatly expanded vertical scale. This showed clearly that there were no subtle absorption features in the spectral regions of most interest.

Kerr et al. (2011) experimented with VIRS analyses of mineralized hand samples from Labrador, including material from Strange Lake (see Figure 5.1). Although absorption features indicative of REE-bearing minerals were found in some samples, these represented high-grade mineralization in which such minerals were generally visible with the unaided eye. In more typical lower-grade hand samples from Strange Lake and other sites in Labrador, no discernable absorption responses were found in the spectra. Although Kerr et al. (2011) suggested that VIRS methods might be useful for screening samples for REE mineralization, it is clear that this does not apply to low-grade materials. The results obtained in this study suggest that VIRS methods have limited application in early-stage exploration for the REE. They may have merit for identifying REE-bearing minerals that are abundant in samples, but there are presently very few reference spectra that can be used for reliable identification. It seems unlikely that satellite-based spectrometry data could detect dispersion from REE deposits in areas of northern Canada that resemble Strange Lake, although they might have application in other settings or for other commodities (e.g., Harris et al., 2012; Turner et al., 2015a, b).

CHAPTER 6: MLA-SEM DATA AND QUANTITATIVE MINERALOGY

GENERAL SUMMARY

MLA-SEM analysis is exceptional at extracting large amounts of data from samples, but the analysis and interpretation of such data can be complex. It is crucial that such data is organized and interpreted in a systematic way. This chapter presents the data that forms the foundation of this thesis study, and uses univariate and multivariate statistical methods to analyze them. The following chapter provides a more detailed analysis of spatial and geographic variations defined by quantitative mineralogical data.

T ` ... ĀĀĀĀĀĀĀĀĀ ĀĀ ĀĀĀĀĀĀĀĀĀĀĀĀĀĀĀĀĀĀ ĀĀĀ ĀĀĀĀĀĀ ĀĀĀĀĀĀĀĀĀĀThe till samples are dominated by 20 minerals (mostly common rock-forming silicates) that have average abundances greater than 0.1 area % (1000 area ppm). These major and minor minerals typically make up 99% or more of each sample. The major minerals show systematic variations in abundance, which allow division of the database into two groups of samples, which show a systematic geographic distribution. These patterns are most likely linked to variations in the relative contributions of different regional bedrock sources to the samples. Thirty-five other minerals, including silicates, oxides, phosphates and other types, are present at much lower abundances (< 1000 area ppm). Some of these minerals show variation patterns that appear to be linked to the major mineral patterns.

Uncommon Nb-, Zr- and REE-bearing minerals that are characteristic of the Strange Lake deposits were also identified, but the rarer examples (those with average abundances below about 50 area ppm) are missing from many samples. These uncommon minerals have more complex variation patterns that are not as easily linked to major mineral patterns. These minerals must have been derived from the Strange Lake area, but some individual minerals show inconsistent and/or contradictory patterns, suggesting that controls on their dispersion are complex. The abundances of these diagnostic minerals in till samples are much lower than those recorded from analyses of drill cores from Strange Lake, and dilution factors for the till samples compared to the core samples cover three orders of magnitude (< 10 to over 600). These observations underline the complexity of glacial dispersion processes in the area. Not all minerals derived from Strange Lake show the same patterns of variation, or the expected patterns of variation.

In addition to the data on mineral abundances, MLA-SEM data on grain and particle size distributions are assessed. These show that major minerals (> 1 area %) consistently form larger monomineralic particles, as do some minor minerals (0.1 to 1 area %). However, most of the accessory and trace minerals (< 0.1 area % or < 1000 area ppm) are present as smaller 'grains' within composite 'particles', and the relative size of these 'grains' generally diminishes with the average abundance of the minerals. This has implications for the precision and reliability of abundance data for these rare minerals, but it also has implications for the behaviour of these minerals in natural systems, which will be governed by the more abundant minerals in these composite particles.

PREVIOUS MLA-SEM RESEARCH AND OTHER MINERALOGICAL STUDIES

General Information

This project is the first large-scale MLA-SEM investigation of glacial dispersion from the Strange Lake deposit, but it builds upon previous work from mineral exploration and government mapping, and upon previous MLA-SEM investigations. Early work was summarized in Chapter 3, and MLA-SEM research completed by Baird (2018) and Currie (2019) is discussed in more detail below.

Mineralogical Studies from Exploration Programs and Government Surveys

As discussed in Chapter 2, assessment of the Main Zone deposit in the 1980s by the Iron Ore Company of Canada (IOC, 1985; 1986) and more recent work on the B-Zone deposit by Quest Rare Minerals (Daigle et al., 2011; Gowans et al., 2014) included mineralogical studies of bulk samples. The early IOC work first identified many of the rare minerals contained in the deposit, including gittinsite (the main carrier of Zr), bastnaesite, gadolinite, gerenite and kainosite (important carriers of the REE) and pyrochlore (the main carrier of Nb). Other accessory minerals were also identified in smaller amounts. The public-domain data from the B-Zone deposit are less complete, but generally match these earlier results (Daigle et al., 2011). The results of the IOC and Quest mineralogical studies were previously listed in Tables 2.2 and 2.3.

Other research studies in the 1980s and 1990s were directed towards the host granites as well as the mineral deposits. Birkett et al. (1992) identified several rare zirconosilicate minerals, including elpidite, armstrongite and vlasovite, and Birkett et al. (1996) reported on titanosilicate minerals in granites. More recent research at the B-Zone deposit (e.g., Gysi et al, 2016) identified several additional REE-bearing minerals. The long history of mineralogical research in the Strange Lake area was summarized by Zajac (2015). It seems that every research study at Strange Lake finds some previously unreported minerals, although generally only in trivial amounts.

The most recent example comes from the indicator mineral study of McClenaghan et al. (2017; 2019), which was summarized in Chapter 3. This identified previously unreported REE-bearing minerals cerianite, rhabdophane and chevkinite, and also thorianite (see Table 2.1 for details). McClenaghan et al. (2019) provide the most up-to-date listing of all Strange Lake mineral species in their Table 1, although this still has some omissions. This information, included as a compilation table in the Appendix, also lists important physical properties.

MLA-SEM Investigations of Drill Cores from the Main Zone Deposit

MLA-SEM investigations of drill core samples from the Strange Lake Main Zone Deposit (Baird, 2018) provide important background and comparative information for this thesis project. Baird (2018) analyzed 21 samples of core from four drill holes that define a north-south cross-section through the Main Zone Deposit. These were previously crushed samples from the IOC drilling program that were archived by the Newfoundland and Labrador Department of Natural Resources. The samples were assigned by IOC into three rock types, namely granite, pegmatite and aplite (Venkatswaran, 1983). Research by Baird (2018) was intended to identify and characterize uncommon minerals in the Main Zone deposit and evaluate their relationships to these rock types. Sample preparation and all subsequent analysis procedures correspond to those described in Chapter 4, aside from the processing of samples by IOC in the 1980s. The SEM analyses completed by Baird (2018) were added to an existing spectral database of Strange Lake minerals compiled by D. Wilton from other archived drill core and rock samples. These data are very important, because they provide direct information on the abundance ranges of rarer minerals in the possible source rocks, which can be compared to data from till materials investigated in this thesis.

Baird (2018) confirmed that the most important minerals in the Strange Lake deposit are quartz, K-feldspar, albite, aegirine (Na-Fe-rich pyroxene) and amphibole (grunerite and ‘hornblende’, although the latter is probably a Na-rich amphibole variety named arfvedsonite). This is not unexpected given the broadly granitic composition of the materials, but there were some differences between rock types, largely shown by variations in the proportions of albite and the mafic minerals (aegirine and amphibole) versus quartz and K-feldpspar. Calcium-rich feldspar (plagioclase) was only present in minor amounts. Minor and accessory minerals detected by Baird (2018) include titanite, thorite, fluorite, zircon and allanite, and three key minerals of economic interest were detected, i.e., gittinsite, gerenite and pyrochlore. These carriers of Zr, REE and Nb were relatively abundant with average abundances of 3.4 area % gittinsite, 0.56 area % gerenite and 0.22 area % pyrochlore. The zirconosilicate mineral elpidite was also important, averaging 0.24 area % (Baird, 2018). The Zr-, Nb- and REE-bearing minerals were most abundant in aplites and pegmatites, and least abundant in granites. These findings were broadly consistent with those reported from the earlier studies completed by IOC and Quest Rare Minerals, although the average abundances of minerals do not match exactly.

Baird (2018) identified several other Zr- Nb- and REE-bearing minerals at lower abundances (< 1000 area ppm or 0.1 area %). In alphabetical order, these include bastnaesite, britholite, euxenite, fergusonite, gadolinite (both Y- and Ce-rich varieties), monazite, parisite, perclevite and stetindite. She also identified other accessory minerals of which many (but not all) were also encountered in the till samples analyzed for this thesis. The uncommon minerals identified by Baird (2018) closely matched the spectra obtained by D. Wilton from earlier MLA-SEM studies of high-grade samples from Strange Lake, and spectra from other known sources. The REE-bearing mineral kainosite, identified by IOC, was not detected by Baird (2018) and some other uncommon trace minerals reported from Strange Lake by others were also not found. She suggested that they might be included with “unknowns” (i.e., minerals for which no matching spectra were found), or that some less robust minerals might have been preferentially reduced to a size below 0.125 mm by crushing. In the case of kainosite, which is a Y-Ca-REE silicate chemically similar to gerenite, it is also possible that the SEM method could not easily discriminate it as a discrete mineral.

Baird (2018) found differences in the abundance of some minerals between the three rock types. For example, bastnaesite was most abundant in granite samples, whereas gittinsite and gerenite were most abundant in pegmatites. In cases where MLA-SEM analysis differentiated between chemical variants of rare minerals, light-REE-enriched varieties were most abundant in granites, and heavy-REE-enriched varieties were most abundant in pegmatites and aplites. This suggests that variations in the compositions of some unusual minerals at Strange Lake are at least in part a function of their host rock type.

MLA-SEM Investigations of Rock Samples and Glacial Sediments, Voisey's Bay and Strange Lake Areas

Currie (2019) used MLA-SEM analysis and Laser Ablation Inductively-Coupled Plasma Spectroscopy (LA-ICPMS) to investigate hercynite (Mg-Fe spinel) and gittinsite from the Voisey's Bay and Strange Lake areas. The objective of her study was to compare the mineralogy of tills and stream sediments with data from whole-rock samples in both areas. The study also attempted to link gittinsite particles and grains in tills near Voisey's Bay (previously noted by Wilton et al., 2017) to their suspected source at Strange Lake via trace-element geochemistry.

Currie (2019) prepared till samples for MLA-SEM analysis using the same methods as this study and analyzed the same size fraction (0.125 to 0.18 mm). However, till samples were processed prior to analysis to concentrate heavy minerals by gravitational separation, because gittinsite and hercynite were expected to occur only in very small quantities. The Strange Lake core samples came from archived crushed material leftover from IOC exploration, but were from different drill holes than those examined by Baird (2018).

Observations of gittinsite in Strange Lake core samples by Currie (2019) are important in the context of the current project. Gittinsite was mostly fine-grained and commonly intergrown with other minerals, notably quartz, K-feldspar, calcite, zircon and the zirconosilicate mineral elpidite. Several other Zr- and REE-bearing minerals were identified in association with gittinsite and elpidite, but these were not investigated in detail. Gittinsite-bearing particles in the stream sediment and till samples from the Voisey's Bay area were rare and very small, even following concentration of the heavy minerals. Most examples of gittinsite in till samples were enclosed by or intergrown with quartz, i.e., the mineral formed 'grains' within composite 'particles', to use the specific definitions for the MLA (see Chapter 4). Composite particles containing gittinsite were well-rounded, suggesting long transport distances, consistent with their derivation from Strange Lake.

Currie (2019) showed that MLA-SEM analysis can identify minerals at very low abundances, within composite particles containing two or more minerals. She suggested that such particles would have likely been missed by traditional indicator mineral methods, because they would have been rejected due to their low bulk density or misclassified as quartz. Currie (2019) analyzed some gittinsite grains for trace elements using LA-ICPMS methods, and showed that REE patterns for gittinsite in tills near Voisey's Bay were closely similar to those of gittinsite from Strange Lake drill cores. This strongly supports (but does not prove) a connection between the two locations. The REE abundances in gittinsite are similar to those of whole-rock samples from the pegmatite and aplite units of the Strange Lake Main Zone deposit (Kerr and Rafuse, 2012; Kerr, 2015), but gittinsite is only a minor constituent of such rocks (< 5%; Baird, 2018). Thus, despite some REE enrichment, gittinsite makes only a small contribution to the REE budget of the mineralization at Strange Lake.

Development of MLA-SEM database for REE-bearing and Zirconosilicate Minerals

The research projects by Baird (2018) and Currie (2019) are part of a longer-term effort at Memorial University to develop MLA-SEM analysis methods as tools in petrology and mineral exploration, directed by Dr. D. Wilton. In the context of Strange Lake, this involved initial analysis of rock samples and core samples provided by A. Kerr (then at the Geological Survey of Newfoundland and Labrador) and material collected by other workers during exploration and survey work in the area over the years. Through this initial work and subsequent MLA-SEM research performed on samples from Strange Lake and elsewhere, a broad database has been assembled from EDX spectra. As new minerals are identified they are added to this database allowing for their automatic identification by the MLA. This now provides a reliable basis for identification and quantitative estimation of most minerals known to occur at Strange Lake. Given the complexity and diversity of Strange Lake mineralogy, especially for those minerals that occur only in trivial amounts, the development of a *truly* comprehensive database would be a never-ending task. Many minerals from Strange Lake vary naturally in composition, and it is not always easy to reliably separate closely related species, as may be the case of gerenite and kainosite. However, the reference database is adequate for investigation of surficial sediments, and contains spectra from other sources that characterize common and rare accessory minerals not specifically associated with Strange Lake. Given sufficient time and effort, additional minerals could probably be characterized, and the existing reference spectra could be refined with new information from this thesis project, but this was not a primary focus for the thesis research.

SUMMARY OF DATABASE AND OVERVIEW OF STATISTICAL ANALYSIS METHODS

Contents of MLA-SEM Numerical Database

General Information

The MLA-SEM analysis produced an initial large database consisting of 94 variables (i.e., mineral identifications) and 76 records (i.e., analyzed samples) that characterize the relative proportions (by area) of all minerals that were identified in each sample. A small fraction of mineral grains were not identified, but these 'unknowns' average only 0.24 area % (2400 area ppm) across the entire database. A database of such size and complexity presents challenges to description and interpretation, so several sequential steps were taken to simplify it. These procedures, and the methods used in the analysis of numerical data, are explained in this section.

Criteria for the Subdivision of Records

Two of the 76 samples were collected at least in part for 'control' purposes, as outlined in Chapter 4. Sample G2-15, located about 27 km northeast of the Strange Lake deposits (azimuth of 55°) is outside the glacial dispersal from the deposit identified by regional till geochemistry (Batterson, 1989). Information from this sample provides an indication of background levels for various minerals, and it should not contain any detritus from the Strange Lake Intrusion or its mineral deposits. G2-15 is retained for general statistical analysis, but is excluded from maps used to illustrate patterns of spatial distribution in Chapter 7. Sample G1-6 was collected close to the Main Zone deposit (about 1.7 km) but is located to its southwest (azimuth of about 230°), close to the Québec border. It is located about 2.4 km south-southwest from the B-Zone deposit (azimuth of about 206°). The displacement of this sample from the two deposits is in the opposite direction to inferred glacial transport towards the east-northeast, and it should not contain detritus from them. However, granites of the Strange Lake Intrusion lie to the southwest ("up-ice") from sample G1-6, in Québec, so it would be expected to contain material from these sources. McClenaghan et al. (2017, 2019) collected a control sample outside the area of the Strange Lake Intrusion in Québec, which provides additional constraints. G1-6 is retained as part of the database for statistical analysis and interpretation of spatial patterns.

As outlined in Chapter 4, samples were collected over three grids (Grid 1, Grid 2 and Grid 3) that are progressively further from the Main Zone Deposit (see Figure 4.3). Summary statistical data (e.g., means, medians, standard deviations, etc.) were calculated and grouped according to grid in order to crudely assess geographic variations in mineral abundances. The five samples (E-1, E-3, E-4, E-7 and E-8) that were collected from the prominent esker that runs through the area were also treated separately for comparative purposes, across all three grids. These esker samples are included with the other data for statistical analysis, but are represented separately in most maps and diagrams.

Criteria for Reducing the Number of Variables (Minerals) in the Database

The initial database was reduced in size by selectively combining individual variables (minerals), and this list of minerals was then subdivided into five groups on the basis of average abundance, to provide a simple framework for description and discussion.

SEM analysis can distinguish some compositional variants of minerals on the basis of their EDX spectra. This applies to common silicates such as garnet (which has Fe-rich, Mg-rich and Mn-rich subtypes) and also to many less abundant minerals such as monazite, titanite, allanite and thorite. The uncommon Zr- and REE-bearing minerals at Strange Lake also vary in composition, especially in the relative proportions of light and heavy REE (e.g., La, Ce) and heavy REE (e.g., Y, Er, Dy). Baird (2018) showed that compositional variants of some REE-bearing minerals were preferentially associated with different host rock units at Strange Lake. Understanding such variation and its causes may be important in petrology, where the context(s) of minerals can be constrained, but is less critical in glacial sediments, which have diverse sources. For this reason, most compositional variants of single mineral species were added together. For example, varieties of garnet labelled ‘almandine’ and ‘spessartine’ were summed and labelled simply as ‘garnet’. The same premise was applied to less abundant minerals, in order to group the compositional variants of titanite, zircon, apatite, thorite and some rarer REE-bearing minerals. This consolidation process reduced the original 94 variables (minerals) to a more manageable 22 variables (minerals), as listed in Table 6.1.

Criteria for Grouping of Variables (Minerals)

The 52 variables (minerals) listed in Table 6.1 have an enormous range in abundance from over 50 area % for quartz in some samples, to less than 10 area ppm for the rarest minerals. Some of the rarer minerals are absent from some or most of the samples, despite the large total number of particles in each sample.

Table 6.1. Univariate statistical data for all variables (minerals) defined in the final database for the project area.

Mineral	**Unit (area)**	**N (> 0)**	**Mean**	**Median**	**Standard Deviation**	**Minimum**	**Maximum**
Major Minerals (Mean Abundance > 1%)							
Quartz	%	76	34.40	38.81	13.28	11.07	51.54
Albite	%	76	22.26	22.15	3.43	15.24	33.18
K-Feldspar	%	76	14.66	14.66	2.53	9.08	19.56
Hornblende (total)	%	76	10.49	5.66	9.38	1.31	30.31
Garnet (total)	%	76	7.94	2.15	8.78	0.24	29.51
Plagioclase	%	76	4.19	3.43	2.68	0.68	13.57
Ilmenite	%	76	1.13	0.63	1.08	0.04	3.69
Minor Minerals (Mean Abundance from 0.1% to 1%)							
Biotite (total)	%	76	0.80	0.52	0.70	0.08	2.59
Chlorite	%	76	0.70	0.39	0.89	0.00	4.08
Epidote	%	76	0.47	0.44	0.39	0.00	1.43
Grunerite (total)	%	76	0.53	0.43	0.35	0.07	1.42
Nepheline	%	76	0.34	0.20	0.29	0.01	1.08
Zircon (total)	%	76	0.41	0.20	0.41	0.01	1.75
Augite	%	75	0.23	0.06	0.34	0.00	1.54
Aegirine	%	76	0.21	0.19	0.13	0.02	0.60
Limonite	%	76	0.18	0.08	0.22	0.01	0.93
Magnetite (total)	%	76	0.22	0.18	0.20	0.03	1.24
Hypersthene	%	73	0.13	0.08	0.16	0.00	0.75
Titanite (total)	%	76	0.12	0.12	0.08	0.00	0.34
Apatite (total)	%	76	0.13	0.09	0.13	0.00	0.53
Common Accessory Minerals (Mean Abundance from 100 ppm to 1000 ppm)							
Staurolite	ppm	76	396.9	226.3	500.7	0.4	2303.4
Zoisite	ppm	75	343.4	227.5	392.4	0.0	1873.4
Goethite	ppm	76	324.1	198.7	444.0	19.0	3406.8
Al Silicate	ppm	73	312.0	234.0	298.5	0.0	1208.3
Rutile	ppm	73	187.0	93.2	223.9	0.0	963.1
Gittinsite	ppm	70	174.7	41.1	264.6	0.0	1400.8
Allanite (total)	ppm	75	135.7	105.3	114.6	0.0	496.6
Aenigmatite	ppm	76	107.8	38.2	140.2	2.1	710.4

Table 6.1 (continued). Univariate statistical data for all variables (minerals) defined in the final database for the project area.

Mineral	Unit (area)	N (> 0)	Mean	Median	Standard Deviation	Minimum	Maximum
Rare Accessory Minerals (Mean Abundance from 10 ppm to 100 ppm)							
Gerenite	ppm	73	92.4	51.1	111.0	0.0	523.1
Ericssonite	ppm	62	57.8	16.5	92.3	0.0	458.9
Serpentine	ppm	31	54.7	0.0	143.1	0.0	1042.4
Monazite (total)	ppm	58	38.2	4.3	81.2	0.0	454.9
Calcite	ppm	62	25.6	9.2	59.5	0.0	451.1
Wollastonite	ppm	65	20.6	9.6	40.7	0.0	280.3
Percleveite	ppm	60	19.7	4.4	43.8	0.0	264.9
Elpidite	ppm	64	17.9	6.8	37.9	0.0	281.0
Astrophyllite	ppm	59	16.5	4.8	43.2	0.0	332.4
Thorite	ppm	47	14.0	2.3	32.9	0.0	193.0
Parisite	ppm	26	12.8	0.0	34.3	0.0	178.8
Britholite (total)	ppm	37	11.2	0.0	25.0	0.0	153.8
Trace Minerals (Mean Abundance < 10 ppm)							
Benitoite	ppm	32	9.9	0.0	32.6	0.0	163.2
Pyrite	ppm	48	9.8	1.8	21.6	0.0	93.4
Barite	ppm	50	9.8	1.8	18.3	0.0	92.2
Gadolinite (total)	ppm	31	9.9	0.0	41.3	0.0	329.8
Bastnaesite	ppm	36	6.6	0.0	19.8	0.0	156.5
Uraninite	ppm	22	5.8	0.0	30.4	0.0	259.0
Rhodonite	ppm	17	5.6	0.0	22.0	0.0	129.5
Scheelite	ppm	3	5.0	0.0	40.7	0.0	354.1
Stetindite	ppm	35	4.8	0.0	12.9	0.0	83.0
Pyrochlore	ppm	31	4.4	0.0	10.4	0.0	56.4
Fergusonite	ppm	42	4.1	0.7	9.4	0.0	63.6
Euxenite	ppm	18	4.1	0.0	15.5	0.0	91.9
Pectolite	ppm	28	2.8	0.0	10.6	0.0	89.0
Fluorite	ppm	23	1.4	0.0	4.7	0.0	31.3
Changbaiite	ppm	20	1.2	0.0	3.6	0.0	26.1
Other							
Unknown Minerals	%	76	0.24		0.10	0.05	0.43

The minerals in the database are grouped by their mean area abundance, as listed in Table 6.1, which also summarizes univariate statistics (mean, median, standard deviation, minimum and maximum) for each of them. This provides 5 mineral groupings to serve as a simple and objective discussion framework. The wide range in abundance makes a single measurement unit (area %) inconvenient, so data for minerals that have mean abundances less than 0.1 area % are all converted to area ppm (1% = 10,000 ppm, and 0.1% = 1000 ppm). This resembles the conventional system used for representation of geochemical analyses as weight % for major elements and weight ppm for trace elements. It is intended to make visualization of relative abundances convenient and easier for the reader. Note that unless otherwise specified the terms % and ppm in this thesis, as applied to minerals, refer to the proportion of total area of minerals mapped by the MLA. Proportions estimated by weight would differ, although the absolute differences would be small for minerals that have densities close to those of most major minerals (2.5 to 3.0 g/cc). Compositional variations for some minerals cause their densities to vary, which further complicates conversion from area % to weight %. As discussed in Chapter 4, area % data are assumed to closely approximate volumetric proportions.

Major Minerals are those that have mean abundances greater than 1 area %. These include common silicates (e.g., quartz, albite, K-feldspar, plagioclase and hornblende) and the Fe-Ti-oxide ilmenite. Among them, quartz is the most abundant and ilmenite is the least abundant (Table 6.1). Major minerals occur in all samples, and could be derived from a wide variety of source rock types. All of these major minerals are also present in the Strange Lake drill core samples (Baird, 2018) with the important exception of garnet. *Minor Minerals* are those that have mean abundances between 0.1 area % and 1 area %. This includes some common silicates, e.g., biotite, chlorite, epidote, pyroxenes (augite, aegirine, hypersthene), titanite and nepheline, oxides (e.g., limonite, magnetite) and one phosphate (apatite) (Table 6.1). These minor minerals also occur in every till sample, and most also have many possible sources. With the exception of chlorite and hypersthene, all were also reported from Strange Lake drill core samples by Baird (2018).

Common Accessory Minerals are defined as those that have mean abundances between 0.01 area % and 0.1 area % (i.e., from 100 to 1000 area ppm). This small group includes one mineral that is characteristic of Strange Lake, i.e., the zirconosilicate mineral gittinsite. It also includes REE- and Th-rich varieties of the epidote group (known as allanite), the titanosilicate aenigmatite ($Na_2Fe_5TiO_2Si_6O_{18}$) and two Al-rich silicate minerals, staurolite and undivided Al-silicate (Table 6.1).

The latter two are most common in metamorphic rocks derived from sedimentary precursors (Deer et al., 1992), and were not reported by Baird (2018) from Strange Lake drill core samples. Allanite is widespread in many igneous and metamorphic rocks. Common accessory minerals are generally present in more than 70 of the 76 samples.

Rare Accessory Minerals are defined as those that have mean abundances between 0.001 area % and 0.01 area % (i.e., from 10 to 100 area ppm). This group includes some normally common minerals (e.g., serpentine and calcite) and several Zr- Y- and REE-bearing minerals known to occur at Strange Lake (e.g., gerenite, elpidite, britholite, perclevite and astrophyllite). The mineral identified as “ericssonite” (a rare Ba-Mn-silicate) also appears in this list, as does thorite (Table 6.1). Rare accessory minerals are more sporadic in their occurrence, ranging from only 31 of 76 samples (serpentine) to 73 of 76 samples (gerenite). No members of this group occur in all 76 samples (Table 6.1)

Trace Minerals are defined as having mean abundances less than 0.001 area % (i.e., < 10 area ppm). This group includes some other uncommon minerals known from Strange Lake (e.g., pyrochlore, gadolinite. pectolite and euxenite), some assorted silicates, sulphides, oxides, phosphates and also fluorite (Table 6.1). Trace minerals generally occur in less than half of the samples, and some are found only in handful of them. For example, scheelite (a calcium tungstate mineral) occurs in only 3 samples, but in one of these it accounts for 354 area ppm. This is likely an example of the ‘nugget effect’ (see Chapter 4) and the average abundance of 5 ppm for scheelite for the database is not representative. Changbaiite (a rare Pb-Nb oxide) was identified in 20 samples, but its mean abundance of 1.2 ppm is unlikely to be representative. With the exception of scheelite, all trace minerals were detected by Baird (2018) in drill cores, although some are present only in small amounts.

The MLA-SEM analysis identified several other minerals that have average abundances below 1 area ppm (0.0001%) but these all occur very sporadically. Constraints on precision, and potential complications from probability effects (see Chapter 4), restrict the usefulness of these data for these minerals, so they are excluded from discussion. Thus, data for baddeleyite (Zr-oxide), galena, chalcopyrite and sphalerite (sulphides), brockite and xenotime (REE-bearing phosphates), and rynersonite (a Ca-Nb-oxide) were discarded on this basis. Aside from baddeleyite and xenotime, all these minerals were also recorded by Baird (2018) from drill-core samples, but only in small amounts.

Statistical Analysis Methods

Summary of Univariate Statistical Data for the Complete Database

Statistical analysis was conducted using MYSTAT (a freely available student version of the professional SYSTAT system) and Microsoft Excel. Descriptive statistics (frequency of occurrence, mean, median, standard deviation, minimum and maximum) for all minerals are listed in Table 6.1. These data convey important information about the five mineral groupings defined above. For example, comparisons of the mean (arithmetic midpoint) and median (geometric midpoint) illustrate the frequency distributions of variables. Variables that have symmetrical or 'normal' distributions will have similar mean and median values, and would show a bell-shaped histogram (a plot of the abundances of various values or ranges) whereas divergence of mean and median indicates asymmetric frequency distributions and/or the presence of discrete subpopulations. Asymmetric frequency distributions are termed "skewed" and can be positively skewed (mean >> median) or negatively skewed (mean << median). Standard deviations and ranges give an indication of data variability for all minerals.

Major minerals (> 1% mean abundance) have similar means and medians, suggesting broadly normal distributions, although this may not apply to quartz (see later discussion). They have standard deviations that are relatively small compared to their mean values, indicating limited variability. The relative standard deviation (RSD; standard deviation expressed as a proportion of the mean) increases with decreasing abundance (Table 6.1), which is typical for major element geochemical data (e.g. Davis, 2003). In contrast, most minor and accessory minerals have standard deviations that exceed the mean and median values, and the medians are consistently less than mean values (Table 6.1). Most or all of these minerals thus have positively-skewed frequency distributions (i.e., a large number of low values and a few anomalously high values). This is more typical of trace element geochemical data, and is often called 'log-normal', because it can be transformed into a more symmetrical pattern by converting values to base-10 logarithms (e.g., Davis, 2003). Some rare accessory and trace minerals have medians of 0 because these minerals are absent from many or most of the samples. Note that zero values are included as valid data points, because they record the absence of the mineral in question, and so cannot be treated as 'missing values' (i.e., a variable for which no analysis was available). In this respect, treatment of data from the MLA-SEM analysis differs from the system more commonly used in geochemistry, where detection limits are instead substituted if an element is not detected (Davis, 2003). Complications from probability effects (e.g., the 'nugget effect') are most obvious for extreme cases such as scheelite (see earlier example), but similar considerations likely also apply to some of the less abundant rare accessory and trace minerals (see Chapter 4).

Multivariate Statistical Analysis Methods: A Simple Example

Multivariate statistical methods such as Principal Components Analysis and Cluster Analysis are used in geochemistry and Earth Sciences to unravel large databases (e.g., Davis, 2003). A simpler multivariate technique, termed “Correlation Analysis” proved very useful in this project, and is explained and illustrated below.

Correlation analysis examines the relationships between pairs of variables, to identify those that show linked variation, and to distinguish them from those that have no apparent relationship. This resembles the use of a scatter plot showing X and Y values to derive a linear regression equation. The ‘fit’ of a regression line (a measure of the divergence of measured data from it) provides an indication of the strength of correlation or inverse correlation (Davis, 2003). Correlation analysis of a large database involves calculations for many pairs of variables, but not all variable combinations will show significant correlation. For this project, it proved useful to conduct correlation analysis on the smaller subsets of minerals provided by the mineral groupings discussed above, and to also include geographic parameters such as the distance of the sample from possible sources at Strange Lake. Correlations between minor, accessory and trace minerals were also assessed against two ‘composite variables’ derived from major mineral abundance data, which appear to break the data into two distinct sample populations.

The most common methods for correlation analysis are termed Pearson Correlations and Spearman Correlations. The Spearman method was used for this project, as it is less influenced by any data that lie well outside the main data array (S. Amor, pers. comm., 2020). However, in most of the cases discussed subsequently, the two correlation analysis methods gave broadly similar results. High positive values for correlation coefficients for a mineral pair (> 0.7) indicate a strong correlation, whereas larger negative values (e.g., < -0.7) indicate strong inverse correlation. The terms ‘moderate’ and ‘weak’ are used here for absolute values of correlation coefficients between 0.5 and 0.7, and 0.3 and 0.5, respectively. Correlation coefficients between 0.3 and -0.3 are considered to indicate little or no correlation. To aid in the depiction of correlations, tables of correlation coefficients are colour-coded using this hierarchy.

A simple example is provided by relationships between three minerals (quartz, gittinsite and gerenite) and the distance between the sample locations and the probable Strange Lake source (defined as the midpoint between the Main Zone and B-Zone; see Chapter 4). Gittinsite (mean abundance of 175 area ppm) is an important Zr-bearing mineral at Strange Lake, and gerenite (mean abundance of 92 area ppm) carries a significant proportion of the REE. Gittinsite occurs only in one other location in Canada, and gerenite is essentially unique to Strange Lake, so the source for both of these minerals is known. Results are portrayed by a correlation matrix (Table 6.2) showing that quartz and gittinsite have moderate and weak positive correlations with distance (0.50 and 0.43 respectively), but that gerenite has a strong inverse correlation against distance (-0.71) and weak inverse correlation against quartz (-0.44). The correlations can also be seen in simple scatter plots of the data for distance and these three minerals (Figure 6.1). The correlation between the abundance of gerenite and gittinsite is not significant (-0.16), even though both minerals must have been derived and transported from the Strange Lake deposit. This is just one of several interesting (and at times puzzling) observations from the MLA-SEM data, which are discussed in subsequent sections of this Chapter and in Chapters 7 and 8.

Although correlation analysis is a useful tool, it is important to understand that analytical precision may limit its effectiveness. For rare accessory and trace minerals, analytical uncertainties are relatively large (as much as +/- 25% to +/- 40%), which will increase scatter, and may obscure correlations. The probability effects discussed in Chapter 4 could add significantly to this uncertainty. It is also important to understand that correlations between variables are not in themselves evidence for a common causal process, although they may favour such an explanation (e.g., Davis, 2003). In the example above, it is not clear if the abundance of gittinsite and gerenite is linked to the abundance of quartz, or if all three minerals are linked in different ways to the distance of the sample locations from Strange Lake.

QUANTITATIVE MINERALOGY OF CONTROL SAMPLES

General Information

This section summarizes MLA-SEM results from control samples G2-15 (from outside the area of dispersion from Strange Lake) and G1-6 (southwest of the Main Zone deposit), and compares results to those from a third sample (G1-1) which is located closest to the Main Zone deposit, only about 130 m from it in a down-ice direction (azimuth of 83^{o}). The expected result would be that G2-15 should lack detritus from Strange Lake, but G1-1 should contain abundant material from the Main

Table 6.2. Spearman Correlation Matrix for Quartz, Gittinsite, Gerenite and Distance from Strange Lake

	Distance from Strange Lake	Quartz	Gittinsite	Gerenite
Distance from Strange Lake	1	.	.	.
Quartz	0.50	1.00	.	.
Gittinsite	0.43	0.50	1.00	.
Gerenite	-0.71	-0.44	-0.16	1.00

Colour Code
> 0.7
0.5 to 0.7
0.3 to 0.5
-0.3 to 0.3
-0.3 to -0.5
-0.5 to -0.7
< -0.7

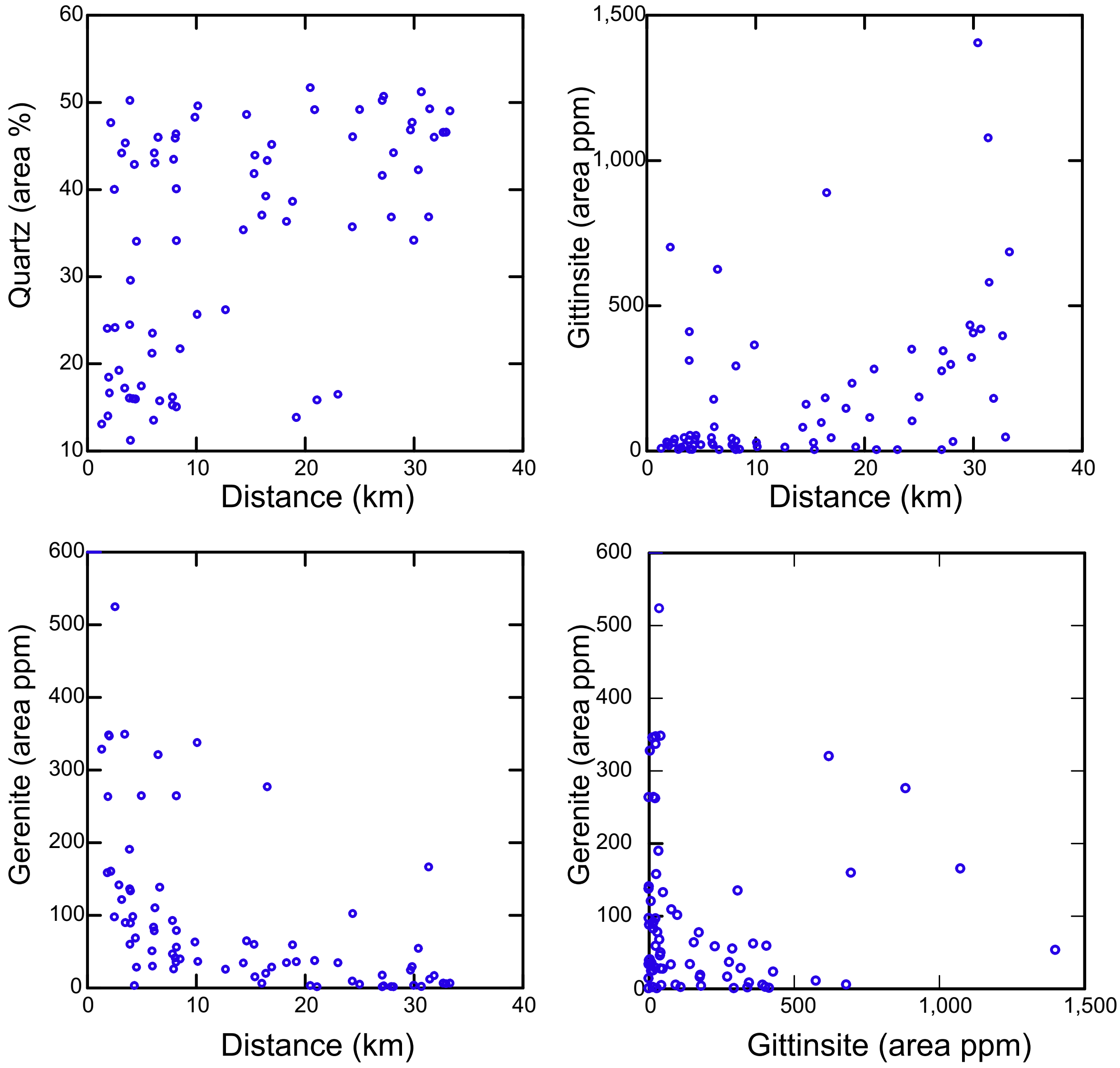

Figure 6.1. (A) Scatter plot of quartz against distance from Strange Lake. (B) Scatter plot of gittinsite against distance from Strange Lake. (C) Scatter plot of gerenite against distance from Strange Lake. (D) Scatter plot of gerenite against gittinsite. See text for discussion.

Zone Deposit. Sample G1-6 would be expected to contain some material from the associated granites, because it is within the area of the Strange Lake Intrusion. The results are compared in Table 6.3, which also lists the mean, maximum and minimum values for the entire database (also included in Table 6.1). In addition to assessing results from the control samples, some specific comparisons are made in this section between till samples and the MLA-SEM results from Strange Lake drill cores analyzed by Baird (2018).

Summary of Numerical Data

Major and Minor Minerals

There are obvious contrasts in the abundances of major and minor minerals between the three samples (Table 6.3). These are most obvious between the off-grid control sample (G2-15) and the two samples closer to the Main Zone deposit (G1-6 and G1-1). Given that the distance between G2-15 and the other two samples is about 26 km, identical compositions would not be expected. None of the major minerals have any unique association with Strange Lake, but garnet has never been reported in the Strange Lake Intrusion, and was not detected in any drill core samples by Baird (2018). The zircon contents of the two samples located close to the Main Zone are not the highest recorded in the database, although they are significantly above the mean zircon abundance value of 0.41 area % (Table 6.3). Enrichment in zircon at the Main Zone is documented by previous bulk-sample analyses (IOC, 1985; 1986) and also by the data of Baird (2018).

Common Accessory Minerals

Common accessory minerals have very different abundances in the off-grid control sample G2-15 and the two samples collected closer to the Main Zone, but most of these minerals have no unique association with Strange Lake. The exception is gittinsite, which is characteristic of Strange Lake. Gittinsite is absent from G2-15, but is present in both G1-6 and G1-1. However, gittinsite abundance in these two samples is significantly below the mean for the entire database (175 area ppm), and well below the maximum of 1401 area ppm (Table 6.3). It is also much lower than the abundance of 2.5% to 5.3 area % reported by Baird (2018) from Strange Lake drill cores. Sample G1-1, located closest to the Main Zone, contains only traces of gittinsite (4.4 area ppm), whereas G1-6 has a modest abundance of only 24.5 area ppm. This is certainly not the simple pattern that would be expected on the basis of their locations, and the close proximity of G1-1 to the Main Zone deposit.

Table 6.3. Mineralogical analyses of samples G2-15, G1-6 and G1-1, compared to the mean, minimum and maximum values for the database

		Analyses of Specific Samples			**Parameters for Entire Database**		
Mineral	**UNIT (area)**	**G2-15**	**G1-6**	**G1-1**	**Mean**	**Minimum**	**Maximum**
Quartz	**%**	41.48	18.31	12.94	34.40	11.07	51.54
Albite	**%**	25.55	19.37	24.51	22.26	15.24	33.18
K-Feldspar	**%**	13.49	11.01	10.36	14.66	9.08	19.56
Hornblende (total)	**%**	2.56	24.46	28.28	10.49	1.31	30.31
Garnet (total)	**%**	0.77	19.77	13.53	7.94	0.24	29.51
Ilmenite	**%**	0.25	2.19	3.52	1.13	0.04	3.69
Plagioclase	**%**	10.15	1.06	2.73	4.19	0.68	13.57
Biotite (total)	**%**	1.15	0.10	0.19	0.80	0.08	2.59
Chlorite	**%**	0.71	0.02	0.03	0.70	0.00	4.08
Epidote	**%**	0.38	0.00	0.01	0.47	0.00	1.43
Grunerite (total)	**%**	0.91	0.91	1.21	0.53	0.07	1.42
Nepheline	**%**	0.10	0.07	0.13	0.34	0.01	1.08
Zircon (total)	**%**	0.03	0.97	0.84	0.41	0.01	1.75
Augite	**%**	0.71	0.00	0.00	0.23	0.00	1.54
Aegirine	**%**	0.09	0.19	0.17	0.21	0.02	0.60
Limonite	**%**	0.02	0.38	0.73	0.18	0.01	0.93
Magnetite (total)	**%**	0.19	0.17	0.37	0.22	0.03	1.24
Hypersthene	**%**	0.69	0.00	0.00	0.13	0.00	0.75
Titanite (total)	**%**	0.19	0.01	0.01	0.12	0.00	0.34
Apatite (total)	**%**	0.19	0.53	0.01	0.13	0.00	0.53
Total (Major and Minor Minerals)	**%**	**99.61**	**99.53**	**99.57**	**99.55**	**n/a**	**n/a**
Staurolite	**ppm**	469.1	9.1	55.3	396.9	0.4	2303.4
Zoisite	**ppm**	1279.4	42.9	13.3	343.4	0.0	1873.4
Goethite	**ppm**	281.4	189.8	193.0	324.1	19.0	3406.8
Al Silicate	**ppm**	1208.3	45.7	24.9	312.0	0.0	1208.3
Rutile	**ppm**	211.6	34.8	62.7	187.0	0.0	963.1
Gittinsite	**ppm**	0.0	24.5	4.4	174.7	0.0	1400.8
Allanite (total)	**ppm**	98.7	186.8	81.2	135.7	0.0	496.6
Aenigmatite	**ppm**	3.6	337.2	412.4	107.8	2.1	710.4

Table 6.3 (continued) Mineralogical analyses of samples G2-15, G1-6 and G1-1, compared to mean, minimum and maximum values for the database

		Analyses of Specific Samples			Parameters for Entire Database		
Mineral	**UNIT (area)**	**G2-15**	**G1-6**	**G1-1**	**Mean**	**Minimum**	**Maximum**
Gerenite	**ppm**	0.0	346.7	327.0	92.4	0.0	523.1
Ericssonite	**ppm**	0.0	189.9	444.0	57.8	0.0	458.9
Serpentine	**ppm**	66.8	0.0	0.0	54.7	0.0	1042.4
Monazite (total)	**ppm**	0.0	0.0	0.0	38.2	0.0	454.9
Calcite	**ppm**	18.2	33.8	13.6	25.6	0.0	451.1
Wollastonite	**ppm**	39.7	32.1	132.6	20.6	0.0	280.3
Percleveite	**ppm**	0.0	6.8	3.2	19.7	0.0	264.9
Elpidite	**ppm**	21.0	13.1	28.1	17.9	0.0	281.0
Astrophyllite	**ppm**	0.0	32.3	19.6	16.5	0.0	332.4
Thorite	**ppm**	0.0	110.0	0.0	14.0	0.0	193.0
Parisite	**ppm**	0.0	0.0	0.0	12.8	0.0	178.8
Britholite (total)	**ppm**	0.0	153.8	13.7	11.2	0.0	153.8
Benitoite	**ppm**	0.0	10.3	0.0	9.9	0.0	163.2
Pyrite	**ppm**	84.1	1.8	0.0	9.8	0.0	93.4
Barite	**ppm**	1.8	0.0	0.0	9.8	0.0	92.2
Gadolinite (total)	**ppm**	0.0	0.0	0.0	9.9	0.0	329.8
Bastnaesite	**ppm**	0.0	26.4	0.0	6.6	0.0	156.5
Uraninite	**ppm**	0.0	0.0	7.7	5.8	0.0	259.0
Rhodonite	**ppm**	0.7	14.1	0.0	5.6	0.0	129.5
Scheelite	**ppm**	0.0	0.0	0.0	5.0	0.0	354.1
Stetindite	**ppm**	0.0	0.6	0.0	4.8	0.0	83.0
Pyrochlore	**ppm**	0.0	0.0	0.0	4.4	0.0	56.4
Fergusonite	**ppm**	30.3	0.0	3.1	4.1	0.0	63.6
Euxenite	**ppm**	0.0	0.0	16.0	4.1	0.0	91.9
Pectolite	**ppm**	0.0	0.0	0.0	2.8	0.0	89.0
Fluorite	**ppm**	0.0	0.0	0.0	1.4	0.0	31.3
Changbaiite	**ppm**	0.0	0.0	0.0	1.2	0.0	26.1
Unknown Minerals	**%**	0.01	0.40	0.36	0.24		

Rare Accessory Minerals and Trace Minerals

The known REE-bearing indicator minerals from Strange Lake (gerenite, perclevite, parasite, britholite, gadolinite, bastnaesite, stetindite and euxenite) are all absent from control sample G2-15 (Table 6.3). However, of these key minerals only two (gerenite and britholite) occur in both G1-6 and G1-1, and some others (e.g., gadolinite) are absent from both samples, despite their locations close to the Main Zone deposit. Gerenite is strongly enriched in both G1-6 and G1-1 (> 400 area ppm) compared to the overall mean for the database (92 area ppm). Aenigmatite and astrophyllite are enriched in samples located close to the Main Zone deposit, but traces of aenigmatite are also present in control sample G2-15 (Table 6.3). Elpidite (a Na-zirconosilicate with a similar structure to gittinsite) is present in G2-15 and in samples G1-6 and G1-1 at broadly similar abundances, and the elpidite content of G2-15 (21 ppm) is slightly higher than the mean for the entire database (Table 6.3). On this basis, it would appear that Strange Lake is not the only potential source for aenigmatite and elpidite.

The main niobium-bearing mineral at Strange Lake (pyrochlore) is absent from all three of these samples (Table 6.3) and its abundance in the wider database is also very low. Fergusonite (a Y-Nb-oxide) is present in G2-15 (30 area ppm), but is absent from G1-6, and amounts to only 3 area ppm in G1-1. The fergusonite content of control sample G2-15 is actually several times greater than the average fergusonite content of the entire database (4.1 area ppm, with a maximum of 64 area ppm). Finally, the unusual mineral identified by the MLA as “ericssonite” (a Ba-Mn silicate) is absent from G2-15, but relatively abundant in both of the samples close to the Main Zone. The abundance of “ericssonite” in samples G1-6 and G1-1 is well above its average abundance in the wider database, and in sample G1-1, it is close to the maximum value for the entire database (Table 6.3). As discussed later, “ericssonite” may not be the best identification label for this mineral.

The MLA-SEM analysis of drill core samples (Baird, 2018) detected all of the minerals noted above with the exception of astrophyllite, so Strange Lake does represent a possible source for them. “Ericssonite” was also detected by Baird (2018) but only at very low abundances (< 10 area ppm) compared to the average of 58 area ppm reported for the till samples in this project.

Summary of Results

Results from these three control samples and the analysis of drill cores by Baird (2018) demonstrate that patterns of mineral abundance are complex. Nevertheless, results from the off-grid control sample G2-15 show that characteristic accessory and trace minerals known from the Strange Lake deposit are indeed absent, with the exception of elpidite. These minerals were also unrepresented in the Québec control sample examined by McClenaghan et al. (2019). This suggests that the presence of these unusual accessory minerals in other samples, even if intermittent, indicates the presence of some material derived from Strange Lake. The presence of elpidite in G2-15 does not invalidate this conclusion, because this mineral is more common than either gittinsite or gerenite (based on data from mindat.org) and could come from other sources (see also Currie and Zaleski, 1985). It does have a strong association with Strange Lake, but this association is not as restrictive as for the other accessory and trace minerals.

The results from samples G1-6 and G1-1, located close to the Main Zone deposit but in opposing directions with respect to local glacial transport, are puzzling. Only some of the characteristic minerals known at Strange Lake are present in both samples, and those that do occur are not always preferentially enriched in G1-1, which is located closest to the Main Zone deposit. Contrasts in the abundance of thorite and uncommon silicate minerals aenigmatite and astrophyllite between G2-15 and samples close to the Main Zone suggest that these minerals could also have sources at Strange Lake, although they are by no means exclusive. Contrary to expectations, there is no sign that Nb-rich minerals such as pyrochlore and fergusonite are enriched in samples close to the Main Zone deposit, and they seem to have very low abundances throughout the till-sample database compared to the results of Baird (2018) from drill core samples.

Patterns in these control samples argue against any simple relationship between relative mineral abundances in till samples and location with respect to the Strange Lake deposits, but they do not rule out systematic patterns on a larger scale within the database. There may be different patterns for different minerals, as suggested by the example of gittinsite and gerenite summarized in the preceding section. Secondly, the MLA-SEM analyses measure the abundances of minerals in a specific size fraction (0.125 mm to 0.18 mm) and do not provide information on coarser-grained material or very fine silt-size material. It is possible, for example, that gittinsite remains largely in the form of larger particles or in rock fragments very close to the Main Zone deposit, and so was not detected to any extent in the sand-sized material analyzed by MLA-SEM methods. Geographic variations between samples may also be influenced by factors other than transport distance from Strange Lake, For example, there could be regional variations in mineralogy that are linked to varied contributions from regional geological units. The presence of garnet in till materials, even those closest to the Strange Lake deposits, suggests that local metamorphic rocks must contribute some of the mineral particles. The following sections within this chapter evaluate numerical data for the five mineral groups through statistical analysis and other methods. These discussions also provide some general indications of geographic variations in mineralogy, which are then described and evaluated in more detail in Chapter 7.

QUANTITATIVE MINERALOGY OF TILL SAMPLES

Sample Groups, Variable Groups and Data Representation

The MLA-SEM database was subdivided according to the criteria outlined in the first section of this Chapter. The discussion of mineralogy is organized according to the five groupings outlined in the first section (i.e., major minerals, minor minerals, common accessory minerals, rare accessory minerals and trace minerals).

The data are assessed in several ways. Univariate statistical summaries provide first-order information about variation, and allow comparisons between grid areas that may illustrate geographic trends. Multivariate correlation analysis provides insight into relationships between variables (minerals) that show linked variation. Histograms are used to illustrate frequency patterns and identify any subpopulations. Scatter diagrams are used to illustrate specific trends of possible importance, and to further examine inferences based on correlation analysis.

Major Minerals

Mineral Types and Summary of Numerical Data

The major minerals in the till samples are mostly the same as those identified by previous mineralogical studies of the Strange Lake deposits (IOC, 1985; 1986; Daigle et al., 2011; Baird, 2018). In general order of abundance, these are quartz, albite, K-feldspar, hornblende, garnet, plagioclase and ilmenite. Garnet is not present in rock or core samples from Strange Lake, but is abundant across the till database, with a mean abundance of nearly 8 area % (Table 6.1). Table 6.4 lists univariate statistics for major and minor minerals, subdivided according to grid. The exact order of

Table 6.4. Summary statistical information for major and minor minerals, subdivided by area.

GRID 1 STATISTICS (N=40)

MINERAL	Mean	Median	SD	Min	Max
Quartz	28.56	23.95	13.42	11.07	50.08
Albite	21.01	20.29	2.93	15.24	27.45
K-Feldspar	14.22	13.77	2.81	9.30	19.56
Hornblende (total)	14.78	18.00	9.41	2.35	30.31
Garnet (total)	12.02	13.85	8.85	0.51	27.73
Ilmenite	1.63	1.87	1.18	0.09	3.69
Plagioclase	3.34	2.65	1.88	0.68	6.95
Biotite (total)	0.67	0.40	0.66	0.09	2.40
Chlorite	0.32	0.09	0.40	0.00	1.52
Epidote	0.30	0.16	0.32	0.00	0.94
Grunerite (total)	0.64	0.60	0.38	0.07	1.42
Nepheline	0.35	0.25	0.30	0.01	1.08
Zircon (total)	0.65	0.67	0.43	0.03	1.75
Augite	0.04	0.03	0.04	0.00	0.19
Aegirine	0.19	0.18	0.12	0.03	0.55
Limonite	0.26	0.20	0.25	0.01	0.93
Magnetite (total)	0.19	0.17	0.12	0.04	0.58
Hypersthene	0.04	0.01	0.06	0.00	0.25
Titanite (total)	0.08	0.04	0.08	0.00	0.23
Apatite (total)	0.17	0.11	0.16	0.00	0.53

GRID 2 STATISTICS (N=19)

MINERAL	Mean	Median	SD	Min	Max
Quartz	38.79	42.44	11.96	13.71	51.54
Albite	21.79	21.20	2.58	16.67	27.23
K-Feldspar	14.80	15.73	2.61	9.08	17.83
Hornblende (total)	8.04	5.35	8.73	1.31	29.96
Garnet (total)	5.06	1.64	7.91	0.24	29.51
Ilmenite	0.77	0.63	0.74	0.04	2.60
Plagioclase	5.59	5.71	3.09	0.74	11.02
Biotite (total)	1.05	0.92	0.82	0.08	2.49
Chlorite	0.96	0.43	1.04	0.00	3.37
Epidote	0.65	0.64	0.42	0.01	1.35
Grunerite (total)	0.42	0.41	0.26	0.09	1.19
Nepheline	0.45	0.53	0.31	0.04	1.04
Zircon (total)	0.21	0.15	0.20	0.01	0.69
Augite	0.18	0.09	0.24	0.00	0.79
Aegirine	0.16	0.15	0.09	0.02	0.33
Limonite	0.11	0.05	0.17	0.01	0.73
Magnetite (total)	0.26	0.17	0.24	0.05	0.93
Hypersthene	0.17	0.18	0.11	0.00	0.37
Titanite (total)	0.13	0.12	0.08	0.00	0.32
Apatite (total)	0.09	0.07	0.07	0.00	0.29

Table 6.4 (continued). Summary statistical information for major and minor minerals.

GRID 3 STATISTICS (N=12)

MINERAL	Mean	Median	SD	Min	Max
Quartz	46.07	46.57	4.57	34.04	51.07
Albite	25.75	25.07	1.98	23.17	29.01
K-Feldspar	15.89	16.40	1.26	12.95	17.05
Hornblende (total)	2.49	2.41	0.74	1.52	4.31
Garnet (total)	0.87	0.73	0.58	0.27	2.45
Ilmenite	0.35	0.28	0.37	0.14	1.50
Plagioclase	3.55	3.04	1.43	1.94	6.20
Biotite (total)	0.56	0.50	0.34	0.20	1.33
Chlorite	1.04	0.66	1.05	0.21	4.08
Epidote	0.64	0.57	0.25	0.42	1.24
Grunerite (total)	0.32	0.25	0.22	0.09	0.78
Nepheline	0.16	0.16	0.04	0.09	0.23
Zircon (total)	0.09	0.07	0.04	0.04	0.19
Augite	0.68	0.63	0.27	0.23	1.31
Aegirine	0.36	0.37	0.16	0.10	0.60
Limonite	0.06	0.04	0.05	0.01	0.20
Magnetite (total)	0.23	0.15	0.33	0.03	1.24
Hypersthene	0.26	0.19	0.20	0.06	0.75
Titanite (total)	0.18	0.17	0.07	0.08	0.34
Apatite (total)	0.08	0.07	0.06	0.02	0.23

ESKER SAMPLE STATISTICS (N=5)

MINERAL	Mean	Median	SD	Min	Max
Quartz	35.83	36.72	6.04	26.07	42.75
Albite	24.96	25.88	5.77	19.30	33.18
K-Feldspar	14.95	15.68	1.66	12.52	16.70
Hornblende (total)	5.80	4.38	3.95	3.01	12.53
Garnet (total)	4.05	1.89	5.28	1.12	13.44
Ilmenite	0.49	0.54	0.23	0.20	0.81
Plagioclase	6.24	4.84	4.79	1.00	13.57
Biotite (total)	1.45	1.67	0.83	0.54	2.59
Chlorite	2.00	2.00	1.10	0.48	3.55
Epidote	0.84	0.82	0.43	0.23	1.43
Grunerite (total)	0.44	0.35	0.33	0.11	0.99
Nepheline	0.35	0.29	0.33	0.03	0.90
Zircon (total)	0.12	0.09	0.11	0.03	0.31
Augite	0.76	0.93	0.58	0.14	1.54
Aegirine	0.22	0.24	0.04	0.16	0.26
Limonite	0.10	0.07	0.10	0.04	0.27
Magnetite (total)	0.37	0.33	0.15	0.23	0.62
Hypersthene	0.29	0.18	0.22	0.05	0.60
Titanite (total)	0.16	0.16	0.11	0.02	0.27
Apatite (total)	0.09	0.10	0.04	0.03	0.13

relative abundance differs between the three grids, but quartz, albite and K-feldspar dominate in total throughout, ranging from 51 area % (mean for Esker samples) to over 78 area % (mean for Grid 2). Note that garnet includes both almandine (Fe-rich) and spessartine (Mn-rich) subtypes, although the latter are generally minor. Similarly, hornblende includes two compositional variants. The MLA-SEM method cannot discriminate between polymorphs, so the label K-feldspar is used here instead of 'orthoclase', as used in previous studies (e.g., Baird, 2018; Currie, 2019). Although the K-feldspar in rock samples from Strange Lake is variably perthitic orthoclase, K-feldspar in till samples would likely be a mixture of orthoclase and microcline, as the latter is common in metamorphic rocks (Deer et al., 1992).

Inspection of the data for the three Grids suggests significant geographic variations in major mineralogy. For example, quartz content is lowest in Grid 1 (mean of 28.6 area %), but much higher in Grid 3 (mean of 46.1 area %). Garnet is most abundant in Grid 1 samples (mean of 12 area %) but far less abundant in Grid 3 (mean of 0.9 area %), and hornblende shows a similar pattern. There are some differences in the relative abundance of albite and K-feldspar between grids, but these are less extreme, and overlap within their respective standard deviations. Overall, summary data suggest that samples from Grids 2 and 3, and the Esker samples, more closely resemble one another than they resemble the samples from Grid 1, which have more distinct mineralogical compositions.

Major minerals are mostly non-diagnostic for possible source rock types. Quartz and feldspars are widespread in many rocks, as are hornblende (in the broad sense) and ilmenite, at least in small amounts. However, garnet is notably absent from the granites of the Strange Lake Intrusion and other Mesoproterozoic granitoid rocks (Ryan et al., 2003), and is more commonly found in metamorphic rocks of either mafic igneous or sedimentary origin (e.g., Deer et al., 1992). Garnet is also a hard and durable mineral (it is used as an industrial abrasive) and will persist well in the surficial environment. Variation in garnet content should be generally proportional to the contribution of material from regional metamorphic rocks, and it cannot be linked to Strange Lake. The higher garnet content in Grid 1 samples is likely linked to regional provenance, despite an apparent relationship to their proximity to the Strange Lake deposits. Quartz and feldspars could come from many different rock types, but they are the dominant constituents of granites. The increased abundance of these minerals in Grids 2 and 3 could reflect greater contributions from igneous (granitic) sources, including the Strange Lake Intrusion, but metamorphic rocks in the east of the study area are gneisses of granitoid composition, containing quartz and K-feldspar (see Chapter 2), so these might also play a role.

Correlation Patterns

Table 6.5 illustrates a correlation coefficient matrix for the major minerals, which also includes the distance of samples from the Strange Lake area. There are strong correlations among the major minerals, most notably between garnet, hornblende, and ilmenite, for which correlation coefficients are all > 0.85. These three minerals display similarly strong negative correlations against quartz, and slightly weaker negative correlations against K-feldspar. The correlation between quartz and K-feldspar is also strong (0.73). Plagioclase and albite have weak to moderate correlations with quartz and feldspar, and moderate negative correlations with garnet, hornblende and ilmenite.

Correlations among abundant variables in ‘closed-sum data’ (i.e, data that is required to add up to a fixed value, such as 100%) are not always indications of strong causal relationships. For example, increased proportions of quartz must inevitably decrease the relative proportion of garnet. However, the correlations between minerals highlighted in Table 6.5 do correspond to known geological associations. Hornblende and ilmenite are generally more abundant in mafic to intermediate igneous rocks or their metamorphic derivatives, whereas quartz and K-feldspar are more abundant in granites or metamorphic rocks of similar composition. The Strange Lake Intrusion also contains amphibole, which is included in the general classification of ‘hornblende’, but it amounts to less than 5% (IOC, 1985; Baird, 2018). Garnet is uncommon in igneous rocks, but occurs in metamorphic rocks of both igneous (mafic) and sedimentary origin (Deer at al., 1992). Thus, these correlations are consistent with an influence from regional bedrock source regions on major mineralogy of the till samples.

Table 6.5 also indicates weak to moderate positive correlations between the distance of samples from Strange Lake and the abundance of quartz, albite and K-feldspar (0.3 to 0.5), and similar negative correlations between distance and the abundance of garnet, hornblende and ilmenite (-0.44 to -0.58). These correlations confirm geographic variations in major mineral abundances implied by univariate statistics for the three grids (Table 6.4). Figure 6.2 illustrates some of the correlations among major minerals using scatter diagrams, which also subdivide the data according to grid location and sample type. The samples collected from eskers lie within the overall trends indicated by the wider database. An effective separation of the data into two groups is possible using two composite variables representing [quartz + K-feldspar] and [garnet + hornblende + ilmenite]. The results are shown in Figure 6.3. These two composite variables are used in subsequent assessment of trends shown by other less abundant minerals, because they are

Table 6.5. Spearman Correlation Matrix for major minerals and distance from Strange Lake.

	Distance from Strange Lake	Quartz	Albite	K-Feldspar	Garnet	Hornblende	Ilmenite
Quartz	0.50	.	.	.	.	.	.
Albite	0.40	0.34	.	.	.	.	.
K-feldspar	0.30	0.73	0.43	.	.	.	.
Garnet	-0.58	-0.93	-0.51	-0.78	.	.	.
Hornblende	-0.53	-0.89	-0.53	-0.81	0.90	.	.
Ilmenite	-0.44	-0.85	-0.48	-0.78	0.89	0.86	.
Plagioclase	0.26	0.53	0.15	0.47	-0.52	-0.58	-0.55

Classification	Colour Code	
"Strong" +	> 0.7	POSITIVE
"Moderate" +	0.5 to 0.7	CORRELATION
"Weak" +	0.3 to 0.5	
Not Significant	-0.3 to 0.3	
"Weak" -	-0.3 to -0.5	
"Moderate" -	-0.5 to -0.7	NEGATIVE (INVERSE)
"Strong" -	< -0.7	CORRELATION

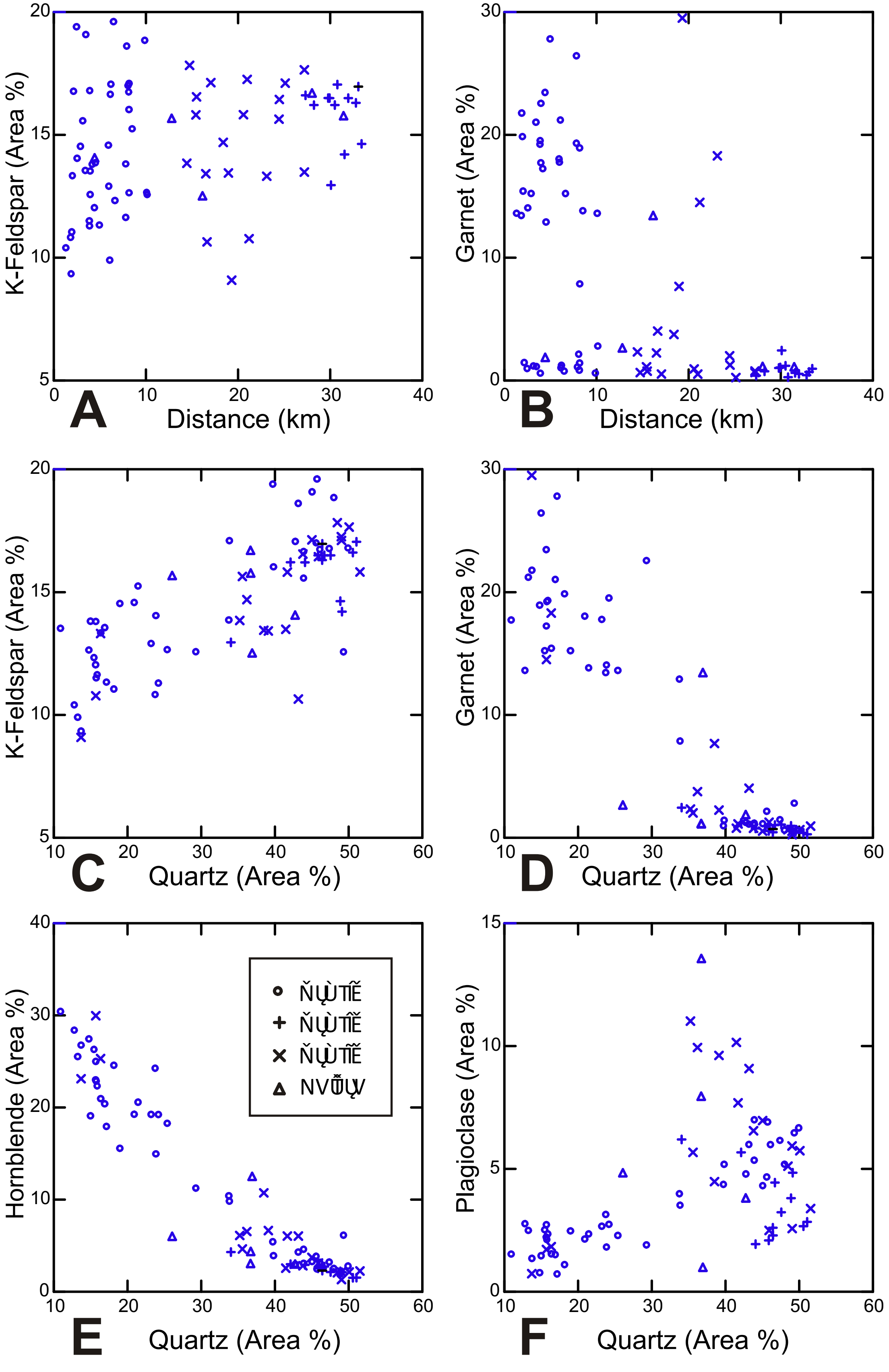

Figure 6.2. Scatter diagrams illustrating major mineral correlations. (A) K-feldspar against distance from Strange Lake. (B) Garnet against distance from Strange Lake. (C) K-feldspar against quartz. (D) Garnet against quartz. (E) Hornblende against quartz. (F) Plagioclase against quartz.

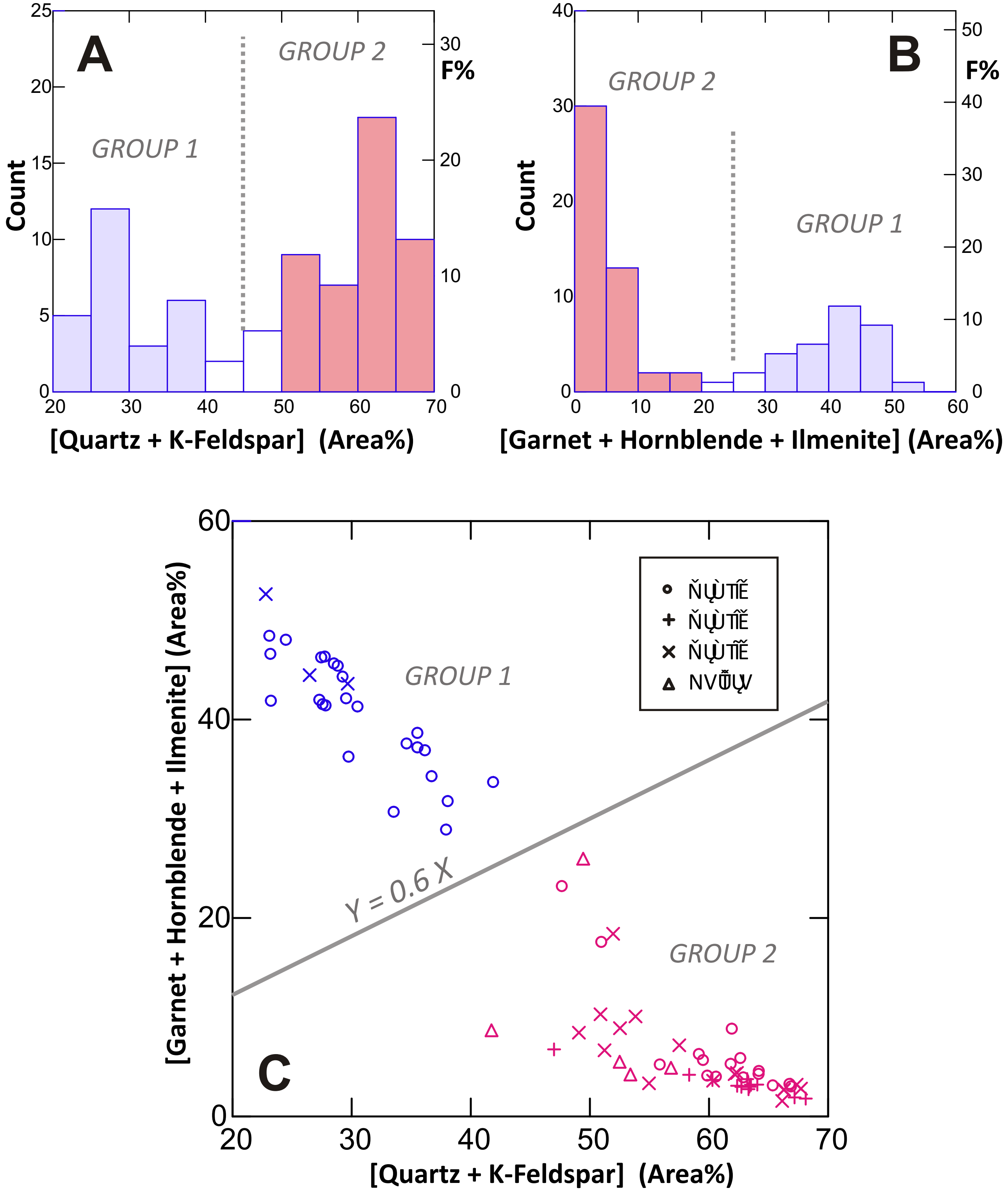

Figure 6.3. The separation of samples into two groups using composite variables. (A) Histogram for [quartz + K-feldspar]. (B) Histogram for [garnet + hornblende + ilmenite]. (C) Scatter plot of [garnet + hornblende + ilmenite] against [quartz + K-feldspar]. GROUP 1 samples are thought to be dominated by metamorphic sources of mafic to intermediate composition or metasedimentary origin, whereas GROUP 2 samples are thought to be dominated by granitic igneous sources or their metamorphic derivatives. See text for discussion.

considered to general indicators of contrasting regional bedrock sources for the tills, and less influenced by material derived from the Strange Lake area.

Frequency Distributions

Frequency patterns for selected major minerals are shown in Figure 6.4. Comparisons of mean and median values (Table 6.4) suggest that not all of these have simple 'normal' (i.e., symmetrical) distributions, and the histograms confirm this. Albite has the simplest pattern, and both plagioclase and K-feldspar are only slightly asymmetrical, but the histograms for quartz, garnet, hornblende and ilmenite are visibly bimodal (i.e., with two discrete frequency peaks). Such patterns suggest that two or more subpopulations exist within the data, which is consistent with the inferences from correlation patterns and the presence of two partly discrete sample groupings in some scatter diagrams (Figures 6.2 and 6.3).

Minor Minerals

Mineral Types and Summary of Numerical Data

MLA-SEM analysis identified 13 minor minerals, defined by mean abundances of 0.1 to 1.0 area % (1000 to 10,000 area ppm). These are listed in Table 6.4, for comparison with the major minerals. In order of mean abundance, the minor minerals are biotite, chlorite, epidote, grunerite, zircon, nepheline, augite, aegirine, limonite, magnetite, hypersthene, titanite, and apatite. Most are silicates, with the exception of limonite and magnetite (oxides) and apatite (a phosphate). Augite, aegirine and hypersthene all belong to the pyroxene group, whereas grunerite is an amphibole, and epidote is the most common member of a group of complex Ca-Fe-silicates. These minor minerals are not significant carriers of the REE, although zircon, titanite and apatite can show variable REE enrichment, and zircon contains more than 50 weight % Zr on a formula basis. With the exception of nepheline, all these minerals are common in a wide variety of rock types (Deer et al., 1992), and none are diagnostic of the Strange Lake Intrusion or its mineral deposits. Nepheline is a Na-K-Al silicate mineral ($Na_3KAl_4Si_4O_{16}$) that is similar to feldspars, but poorer in silica (SiO_2). It mostly occurs in Na- and/or K-rich igneous rocks that lack quartz, but can also occur in metamorphic rocks of sedimentary (calcareous) origin that are quartz-poor (Deer et al., 1992). Nepheline is not specifically reported in other studies of the Strange Lake Intrusion granites, but it was detected in very small amounts (average 150 area ppm) in the drill core analyses of Baird (2018).

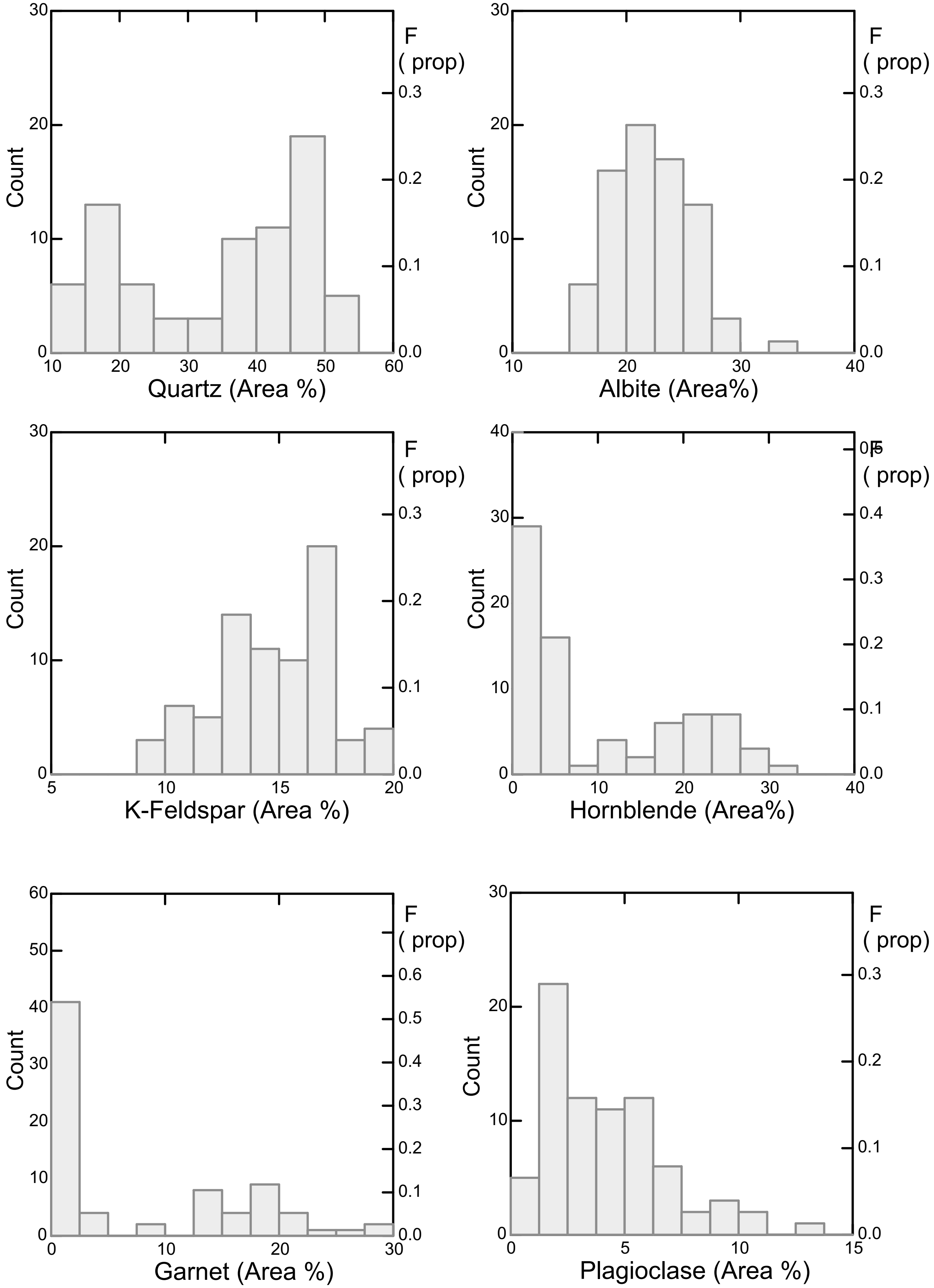

Figure 6.4. Frequency distributions (histograms) for selected major minerals. The pattern for ilmenite (not shown) resembles the patterns illustrated for garnet and hornblende..

Table 6.4 shows that for the minor minerals, mean values commonly exceed median values, and data ranges are large, so mean values are in many cases not fully representative of populations, and frequency distributions are probably asymmetric and positively skewed.

Biotite, chlorite, epidote and grunerite (a Mg-rich amphibole) show broadly similar mean abundances within the three grid areas, although chlorite is notably less abundant in Grid 1 and most abundant in the esker samples. Zircon shows the most obvious geographic variation, being most abundant in Grid 1 (a mean of 0.65 area % versus an overall mean of 0.42 area %), falling to 0.21 area % in Grid 2 and only 0.09 area % in Grid 3. Augite shows the opposite pattern, with mean abundances rising from only 0.04 area % in Grid 1 to 0.68 area % in Grid 3, Aegirine (a Na-Fe-rich pyroxene similar to augite in structure) shows a smaller increased abundance in Grid 3 relative to other areas. Other minerals present in smaller amounts (limonite, magnetite, titanite and apatite) do not show any obvious patterns, but hypersthene (Fe-Mg pyroxene) increases in mean abundance from Grid 1 to Grid 3, in a manner similar to augite. Apatite appears to be more abundant in Grid 1 (mean of 0.17 area %) compared to all other areas. Of the minor minerals, only aegirine (Na-Fe pyroxene) and zircon are known to be enriched at Strange Lake, but aegirine also occurs in other Mesoproterozoic plutonic rocks (e.g, Ryan et al., 2003) and zircon is present in a wide variety of other rock types. Consequently, neither mineral is diagnostic of the Strange Lake deposits.

Correlation Patterns

Table 6.6 displays a matrix of correlation coefficients for the minor minerals, and also shows correlations with the average distance of samples from Strange Lake, and the two composite major mineral variables that separate samples into two distinct groups (see earlier discussion). The composite variables are [quartz + K-feldspar] and [garnet + hornblende + ilmenite], which are abbreviated below to [Qz+Kf] and [Gt+Hb+Ilm]. The observed correlations of minor minerals with [Qz+Kf] and [Gt+Hb+Ilm] imply that the abundances of some of these minor minerals are also influenced by regional provenance, rather than by derivation from Strange Lake.

Moderate positive correlations against [Qz+Kf] are shown by epidote (0.57), chlorite (0.59), zircon (0.64), hypersthene (0.64) and titanite (0.62), suggesting that these minerals are preferentially associated with regional sources of broadly granitic composition. As expected, these same minerals have moderate to strong negative correlations with [Gt+Hb+Ilm]. Moderate to strong positive correlations with [Gt+Hb+Ilm] are shown by grunerite (0.68) and limonite (0.80), which show complementary negative correlations with [Qz+Kf]. Individual mineral pairs within these two groups

Table 6.6. Spearman Correlation Matrix for minor minerals, composite variables [quartz + K-feldspar] and [garnet + hornblende + Ilmenite], and distance from Strange Lake.

	Distance from Strange Lake	[Quartz + K-Feldspar]	[Garnet + Hornblende + Ilmenite]	Biotite	Epidote	Chlorite	Grunerite	Nepheline	Zircon	Augite	Aegirine	Limonite	Magnetite	Hypersthene	Titanite
[Quartz + K-Feldspar]	0.47	.	.	.	.	.	.	.	.	.	.	.	.	.	.
[Garnet _+ Hornblende + Ilmenite	-0.56	-0.95	.	.	.	.	.	.	.	.	.	.	.	.	.
Biotite	0.16	0.45	-0.42	.	.	.	.	.	.	.	.	.	.	.	.
Epidote	0.46	0.57	-0.61	0.83	.	.	.	.	.	.	.	.	.	.	.
Chlorite	0.41	0.59	-0.61	0.85	0.86	.	.	.	.	.	.	.	.	.	.
Grunerite	-0.36	-0.71	0.68	-0.47	-0.48	-0.60	.	.	.	.	.	.	.	.	.
Nepheline	0.04	0.44	-0.39	0.72	0.56	0.67	-0.43	.	.	.	.	.	.	.	.
Zircon	-0.66	-0.74	0.80	-0.57	-0.73	-0.74	0.72	-0.35	.	.	.	.	.	.	.
Augite	0.68	0.64	-0.71	0.63	0.84	0.78	-0.53	0.26	-0.82	.	.	.	.	.	.
Aegirine	0.12	0.11	-0.15	-0.11	0.10	-0.02	0.16	-0.12	0.07	0.19	.	.	.	.	.
Limonite	-0.46	-0.81	0.80	-0.41	-0.52	-0.59	0.60	-0.44	0.71	-0.59	0.02	.	.	.	.
Magnetite	-0.06	-0.34	0.30	0.13	0.06	0.11	0.39	-0.04	0.19	0.02	0.03	0.23	.	.	.
Hypersthene	0.65	0.64	-0.66	0.67	0.79	0.77	-0.40	0.48	-0.74	0.81	0.16	-0.61	0.17	.	.
Titanite	0.40	0.62	-0.67	0.71	0.72	0.81	-0.66	0.54	-0.75	0.70	-0.04	-0.58	-0.16	0.66	.
Apatite	-0.29	-0.36	0.33	-0.22	-0.26	-0.31	0.25	-0.25	0.26	-0.32	0.01	0.34	0.02	-0.25	-0.08

Classification	Colour Code	
"Strong" +	> 0.7	POSITIVE
"Moderate" +	0.5 to 0.7	CORRELATION
"Weak" +	0.3 to 0.5	
Not Significant	-0.3 to 0.3	
"Weak" -	-0.3 to -0.5	
"Moderate" -	-0.5 to -0.7	NEGATIVE (INVERSE)
"Strong" -	< -0.7	CORRELATION

also show moderate to strong positive correlations, as would be expected. A connection between limonite (an iron oxi-hydroxide) and the iron-rich minerals (e.g., hornblende, ilmenite) is not surprising as limonite is a common weathering product, especially of oxides .ike ilmenite (Deer et al., 1992).

There are significant correlations between some minor minerals and the average distance of samples from the Strange Lake source region. The most obvious is for zircon, which is negatively correlated with distance (-0.66), and the pyroxenes augite and hypersthene, which show similar positive correlations against distance (0.68 and 0.65), Moderate positive correlations against distance are also shown by other minerals that are correlated with [Qz+Kf], such as epidote, chlorite and titanite. Some of the correlations revealed by Table 6.6 are illustrated by scatter diagrams in Figure 6.5.

Frequency Distributions

Frequency distributions for selected minor minerals are illustrated in Figure 6.6. In contrast to the major minerals, the histograms for minor minerals are all notably asymmetric, and positively-skewed, with mean values that exceed median values. Many of these minor minerals have 'log-normal' patterns characterized by many low values and a few anomalously high values. The most extreme example of such a pattern is for augite, but magnetite, apatite, hypersthene, biotite and chlorite also show such tendencies. Nepheline and zircon also show this general pattern, but show a less obvious frequency maximum at higher values, perhaps indicating the presence of subpopulations. Aegirine and grunerite, and also epidote, show slightly broader frequency distributions of more symmetrical appearance, but remain positively skewed.

Common Accessory Minerals

Mineral Types and Summary of Numerical Data

Common accessory minerals, defined by mean abundances between 100 and 1000 area ppm (0.01% to 0.1 area %) form a group of 8 minerals. In order of mean abundance, these are staurolite, zoisite, goethite, Al-silicate, rutile, gittinsite, allanite, and aenigmatite. These are all silicates, aside from rutile (Ti-oxide) and goethite (Fe-hydroxide). Zoisite and allanite are both part of the epidote group of complex Ca-Fe-silicates. Zoisite is a Fe-poor and Ca-rich variety, and allanite is enriched in Th and REE (Deer et al., 1992). Zoisite is found mostly in metamorphic rocks of Ca-rich composition, but allanite is a common accessory mineral in many igneous and metamorphic rocks

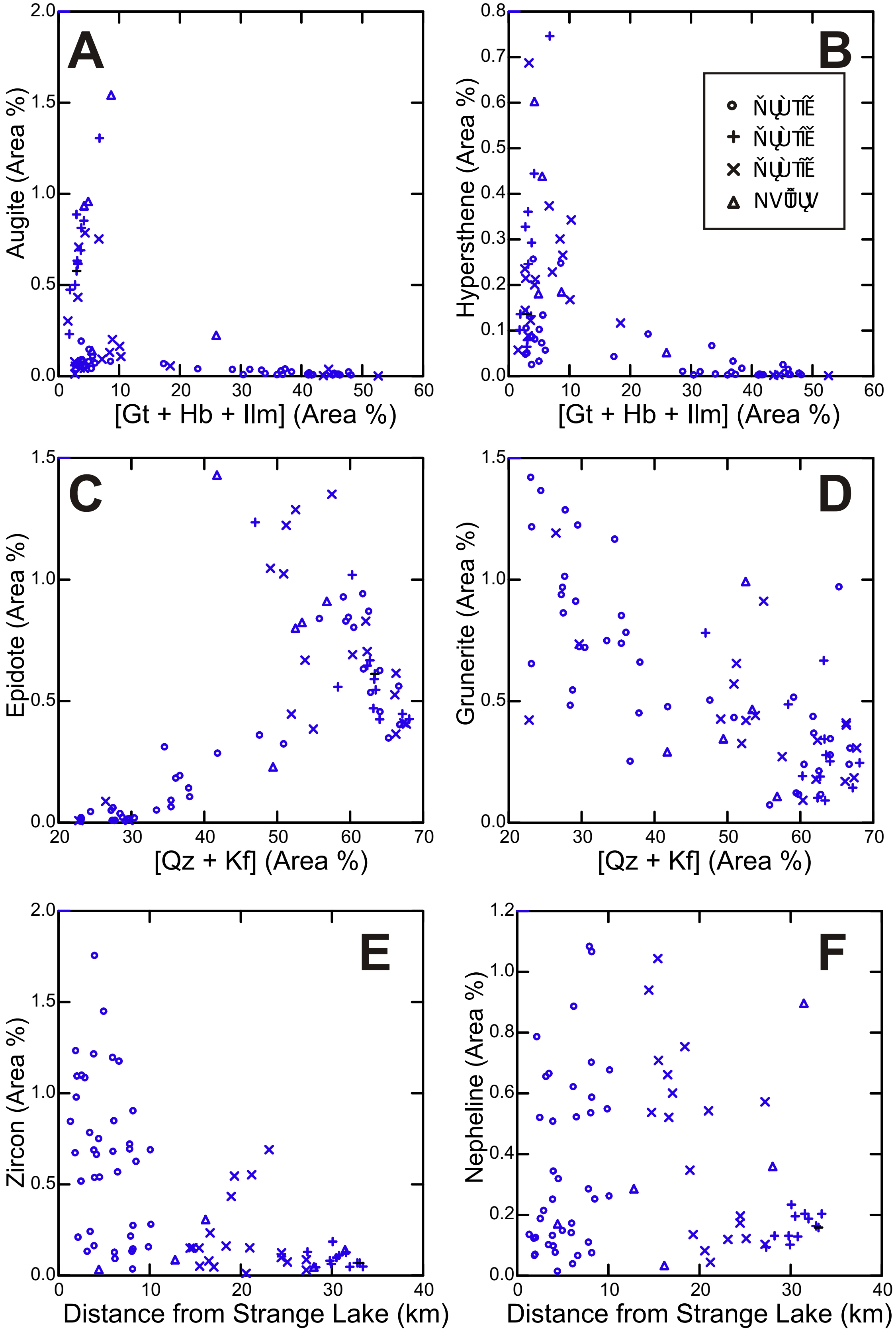

Figure 6.5. Scatter diagrams illustrating minor mineral correlations. (A) Augite against [Gt+Hb+Ilm]. (B) Hypersthene against [Gt+Hb+Ilm]. (C) Epidote against [Qz+Kf}. (D) Grunerite against [Qz+Kf]. (E) Zircon against distance from Strange Lake. (F) Nepheline against distance from Strange Lake.

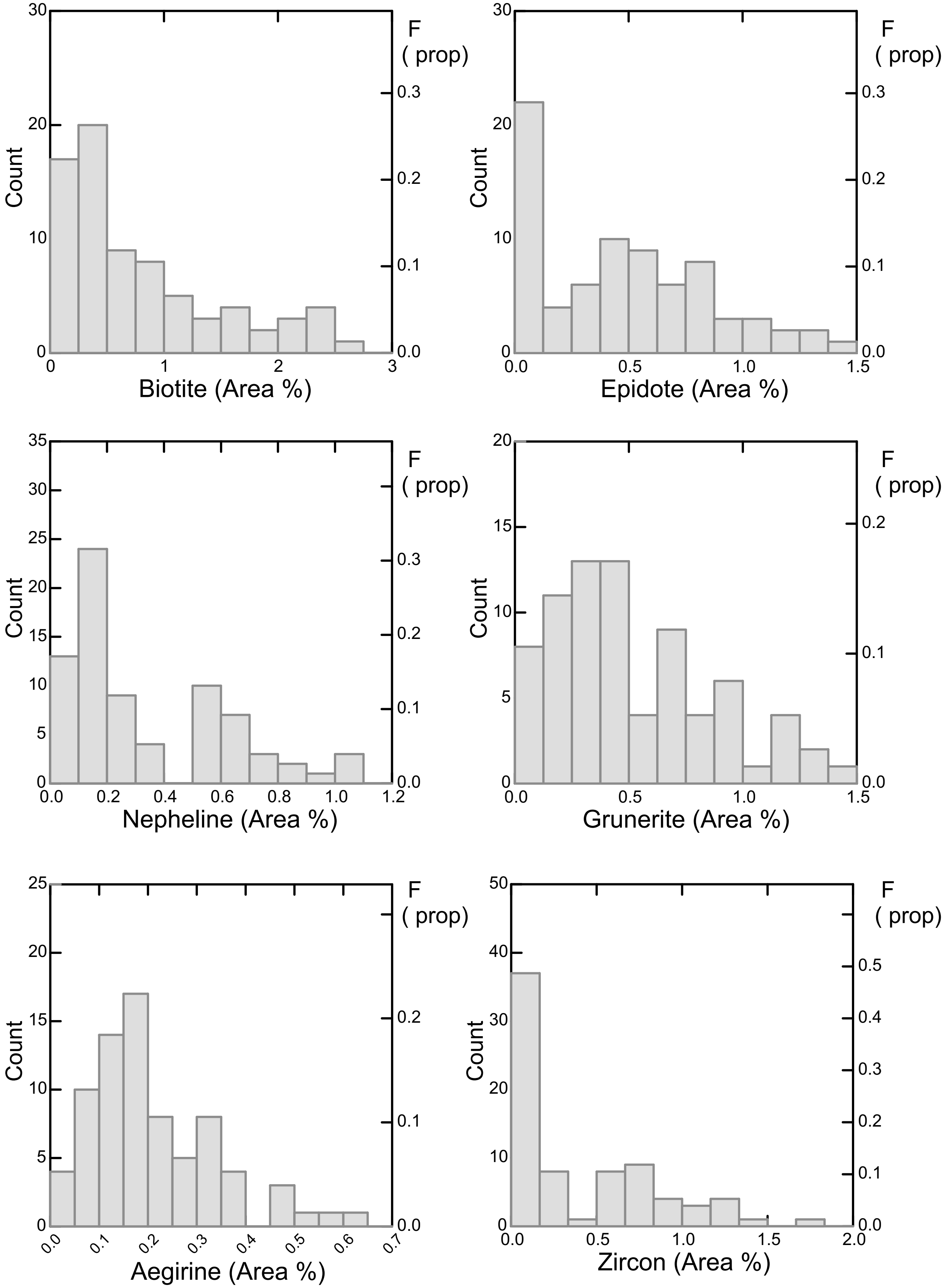

Figure 6.6. Frequency distributions (histograms) for selected minor minerals. The patterns for other minerals in this group are asymmetric, and broadly resemble the histogram shown for biotite.

(Deer et al., 1992). Al-silicate is used here as a general name for three polymorphs of Al_2SiO_5 (andalusite, kyanite and sillimanite) that cannot be distinguished by SEM analysis. These minerals are found mostly in metamorphic rocks of sedimentary origin, in which each polymorph defines specific pressure-temperature conditions. Staurolite is a similar (but complex) Fe-Al-silicate mineral that is found in a similar geological setting (Deer et al., 1992). Rutile is a common accessory mineral in igneous and metamorphic rocks, and goethite, like limonite, is a weathering product of many Fe-rich minerals.

A crucial member of this group is the zirconosilicate gittinsite, which is an important carrier of Zr in the Strange Lake deposits. Gittinsite is not unique to Strange Lake, but is presently known from only one other location in Canada (Kipawa, Québec). Gittinsite is thus an important indicator of detritus from Strange Lake. Aenigmatite also occurs at Strange Lake, but is not as diagnostic as gittinsite. Aenigmatite is an uncommon Na-Fe-Ti-silicate known also from many other peralkaline igneous suites. Allanite is reported from Strange Lake, but it also occurs in many igneous and metamorphic rock types.

These common accessory minerals occur in nearly all the analyzed till samples, but gittinsite is absent from 6 samples in Grids 1 and 2. A summary of statistical data is provided in Table 6.7, which also lists data for rare accessory and trace minerals (discussed in the next sections). Aenigmatite shows highest mean values in Grid 1 (163 area ppm), but values for grids 2 and 3 are similar at around 52 area ppm. Staurolite, zoisite and gittinsite show increasing mean values from Grid 1 to Grid 3, as do goethite and (to a lesser extent) Al-silicate. The mean abundance of allanite is similar for all three grids. The data for the esker samples most closely resemble those from Grid 2, aside from higher mean values for zoisite and goethite.

Correlation Patterns

Table 6.8 provides correlation coefficients for common accessory minerals, and includes their correlations with the average distance from Strange Lake, and the composite variables [quartz + K-feldspar] and [garnet + hornblende + ilmenite]. The strongest correlations are for aenigmatite, which is negatively correlated with distance from Strange Lake and positively correlated with [garnet + hornblende + ilmenite]. Staurolite, zoisite and Al-silicate show moderate positive correlations with [quartz + K-feldspar], as do gittinsite and zoisite. Patterns for goethite, rutile and allanite show little correlation with the other minerals in the group, although there is a weak association between allanite and gittinsite.

Table 6.7. Summary of statistical data for accessory and trace minerals, subdivided according to grid location and sample types.

GRID 1 STATISTICS (Maximum number of samples = 40)								**GRID 2 STATISTICS (Maximum number of samples = 19)**					
Mineral	**UNIT**	**N (> 0)**	**Mean**	**Median**	**SD**	**Min**	**Max**	**N (> 0)**	**Mean**	**Median**	**SD**	**Min**	**Max**
Staurolite	ppm	40	259.0	92.3	487.5	0.4	2303.4	19	384.5	92.3	367.8	3.1	1011.5
Zoisite	ppm	39	113.0	45.8	130.6	0.0	511.4	19	515.4	45.8	412.0	0.7	1279.4
Goethite	ppm	40	189.9	158.1	127.1	22.1	525.9	19	274.7	158.1	232.9	19.0	1065.4
Al Silicate	ppm	37	207.5	144.6	220.5	0.0	864.4	19	428.8	144.6	370.1	3.0	1208.3
Rutile	ppm	38	135.2	60.3	170.7	0.0	621.5	18	239.7	60.3	279.5	0.0	963.1
Gittinsite	ppm	38	89.1	24.2	166.5	0.0	696.8	15	159.3	24.2	205.9	0.0	885.0
Allanite	ppm	40	131.1	124.4	96.9	18.5	480.9	19	137.0	124.4	121.1	6.9	386.8
Aenigmatite	ppm	40	162.5	107.9	152.7	3.7	710.4	19	52.8	107.9	68.6	3.6	244.5
Gerenite	ppm	40	146.7	96.4	121.4	24.5	523.1	17	42.8	96.4	62.1	0.0	275.4
Ericssonite	ppm	40	93.5	52.4	113.5	4.7	458.9	15	32.8	52.4	33.7	0.0	104.3
Serpentine	ppm	6	4.7	0.0	21.3	0.0	124.5	11	62.3	0.0	88.4	0.0	264.0
Monazite (total)	ppm	27	28.4	2.0	63.0	0.0	251.8	16	59.7	2.0	118.8	0.0	454.9
Calcite	ppm	37	27.1	11.9	41.2	0.0	191.5	17	35.7	11.9	101.6	0.0	451.1
Wollastonite	ppm	34	27.5	10.0	53.8	0.0	280.3	15	10.6	10.0	10.9	0.0	39.7
Percleveite	ppm	31	28.0	4.1	57.1	0.0	264.9	15	13.2	4.1	22.8	0.0	95.0
Elpidite	ppm	33	23.4	7.2	49.4	0.0	281.0	17	6.4	7.2	7.2	0.0	21.0
Astrophyllite	ppm	36	16.5	8.9	26.9	0.0	157.0	12	29.4	8.9	76.3	0.0	332.4
Thorite	ppm	29	14.7	3.5	35.6	0.0	193.0	11	15.2	2.3	32.7	0.0	111.3
Parisite	ppm	21	22.3	1.6	44.8	0.0	178.8	4	3.9	1.6	11.2	0.0	45.1
Britholite (total)	ppm	29	19.6	7.1	31.8	0.0	153.8	6	3.3	7.1	8.3	0.0	30.2
Benitoite	ppm	17	5.1	0.0	18.1	0.0	114.7	9	3.2	0.0	6.6	0.0	24.3
Pyrite	ppm	19	2.4	0.0	5.7	0.0	33.3	17	20.9	0.0	30.4	0.0	93.4
Barite	ppm	27	12.0	2.5	20.3	0.0	92.2	17	10.1	2.5	18.3	0.0	80.2
Gadolinite (total)	ppm	11	6.0	0.0	22.5	0.0	127.8	10	20.8	0.0	75.3	0.0	329.8
Bastnaesite	ppm	20	5.6	0.3	10.9	0.0	55.0	8	2.3	0.3	3.5	0.0	10.3
Uraninite	ppm	17	10.2	0.0	41.5	0.0	259.0	4	1.6	0.0	5.3	0.0	23.2
Rhodonite	ppm	8	10.0	0.0	29.8	0.0	129.5	7	1.1	0.0	2.6	0.0	10.8
Scheelite	ppm	2	8.9	0.0	56.0	0.0	354.1	1	1.3	0.0	5.7	0.0	24.8
Stetindite	ppm	12	1.2	0.0	2.9	0.0	13.4	10	5.0	0.0	10.9	0.0	44.4
Pyrochlore	ppm	9	2.4	0.0	8.1	0.0	38.9	10	3.9	0.0	8.7	0.0	29.7
Fergusonite	ppm	27	5.9	1.6	11.7	0.0	63.6	9	3.1	1.6	7.0	0.0	30.3
Euxenite	ppm	14	7.6	0.0	20.8	0.0	91.9	3	0.3	0.0	0.7	0.0	2.7
Pectolite	ppm	17	1.9	0.0	3.2	0.0	11.4	9	7.1	0.0	20.5	0.0	89.0
Fluorite	ppm	14	1.4	0.0	4.1	0.0	23.8	7	1.0	0.0	2.0	0.0	8.1
Changbaiite	ppm	8	1.5	0.0	4.7	0.0	26.1	2	0.3	0.0	1.0	0.0	4.0

Table 6.7 (continued). Summary of statistical data for accessory and trace minerals, subdivided according to grid location and sample types.

GRID 3 STATISTICS (Maximum number of samples = 12)								**ESKER SAMPLE STATISTICS (Maximum number of samples = 5)**					
Mineral	**UNIT**	**N (> 0)**	**Mean**	**Median**	**SD**	**Min**	**Max**	**N (> 0)**	**Mean**	**Median**	**SD**	**Min**	**Max**
Staurolite	ppm	12	793.4	721.4	549.9	152.6	2105.7	5	595.4	375.7	481.8	318.2	1449.1
Zoisite	ppm	12	550.5	521.7	263.8	264.0	946.4	5	1035.8	984.3	604.8	391.7	1873.4
Goethite	ppm	12	621.6	320.9	895.9	151.9	3406.8	5	871.0	750.5	506.5	240.7	1549.7
Al Silicate	ppm	12	456.8	441.3	331.3	48.8	1111.6	5	356.1	287.3	198.9	177.8	661.7
Rutile	ppm	12	172.6	100.3	138.9	48.4	471.4	5	435.6	461.0	364.6	7.7	813.7
Gittinsite	ppm	12	433.4	397.1	359.9	28.2	1400.8	5	296.7	93.2	449.4	8.5	1073.7
Allanite (total)	ppm	11	138.2	99.5	132.2	0.0	411.2	5	162.2	54.0	198.9	25.0	496.6
Aenigmatite	ppm	12	52.1	8.5	141.7	2.1	500.9	5	12.7	15.1	7.5	3.2	21.1
Gerenite	ppm	11	12.3	5.0	15.7	0.0	52.9	5	39.1	4.7	71.0	0.2	164.9
Ericssonite	ppm	5	0.6	0.0	1.5	0.0	5.1	2	5.3	0.0	11.6	0.0	26.1
Serpentine	ppm	9	189.0	65.1	303.4	0.0	1042.4	5	103.1	74.2	94.4	17.4	211.8
Monazite (total)	ppm	10	33.7	13.9	64.7	0.0	228.6	5	45.7	11.5	80.8	1.1	189.6
Calcite	ppm	6	10.0	0.1	21.1	0.0	66.0	2	12.9	0.0	27.3	0.0	61.6
Wollastonite	ppm	11	14.2	2.9	18.3	0.0	46.2	5	18.4	21.6	17.2	0.9	39.5
Percleveite	ppm	10	7.3	5.6	9.9	0.0	36.6	4	7.6	1.7	9.5	0.0	19.6
Elpidite	ppm	11	17.5	9.7	15.3	0.0	52.6	3	17.4	0.5	37.4	0.0	84.3
Astrophyllite	ppm	7	2.4	0.7	4.8	0.0	17.0	4	1.1	0.8	1.3	0.0	3.4
Thorite	ppm	4	6.4	0.2	15.4	0.0	52.9	2	21.6	0.0	47.7	0.0	106.9
Parisite	ppm	0	0.0	0.0	0.0	0.0	0.0	1	1.1	0.0	2.5	0.0	5.5
Britholite (total)	ppm	1	0.1	0.0	0.2	0.0	0.7	1	0.2	0.0	0.5	0.0	1.0
Benitoite	ppm	3	26.4	0.0	59.9	0.0	163.2	3	33.5	0.5	68.4	0.0	155.5
Pyrite	ppm	9	17.2	2.7	30.7	0.0	91.3	3	9.1	0.7	18.6	0.0	42.4
Barite	ppm	3	2.2	0.0	6.6	0.0	23.2	3	9.2	0.6	19.8	0.0	44.6
Gadolinite (total)	ppm	7	5.8	2.0	13.7	0.0	48.7	3	9.0	1.1	15.3	0.0	35.7
Bastnaesite	ppm	5	3.2	0.0	7.0	0.0	22.2	3	40.1	8.5	66.7	0.0	156.5
Uraninite	ppm	0	0.0	0.0	0.0	0.0	0.0	1	0.2	0.0	0.4	0.0	1.0
Rhodonite	ppm	1	0.1	0.0	0.3	0.0	1.1	1	0.2	0.0	0.4	0.0	0.9
Scheelite	ppm	0	0.0	0.0	0.0	0.0	0.0	0	0.0	0.0	0.0	0.0	0.0
Stetindite	ppm	9	16.3	1.9	26.3	0.0	83.0	4	4.6	1.7	8.1	0.0	19.0
Pyrochlore	ppm	10	10.9	3.9	16.1	0.0	56.4	2	6.2	0.0	12.2	0.0	27.9
Fergusonite	ppm	4	1.0	0.0	2.1	0.0	5.5	2	1.1	0.0	2.0	0.0	4.6
Euxenite	ppm	0	0.0	0.0	0.0	0.0	0.0	1	0.5	0.0	1.1	0.0	2.6
Pectolite	ppm	1	0.1	0.0	0.2	0.0	0.6	1	1.1	0.0	2.6	0.0	5.7
Fluorite	ppm	2	2.7	0.0	9.0	0.0	31.3	0	0.0	0.0	0.0	0.0	0.0
Changbaiite	ppm	8	1.8	0.9	2.7	0.0	7.9	2	0.7	0.0	0.9	0.0	2.0

Table 6.8. Spearman Correlation Matrix for common accessory minerals, composite variables [quartz + K-feldspar] and [garnet + hornblende + Ilmenite], and distance from Strange Lake.

	Distance from Strange Lake	[Quartz + K-Feldspar]	[Garnet + Hornblende + Ilmenite]	Staurolite	Zoisite	Al-Silicate	Goethite	Rutile	Gittinsite	Allanite
[Quartz + K-Feldspar]	0.47	.	.	.	.	.	.	.	.	.
[Garnet + Hornblende + Ilmenite	-0.56	-0.95	.	.	.	.	.	.	.	.
Staurolite	0.39	0.51	-0.54	.	.	.	.	.	.	.
Zoisite	0.60	0.59	-0.67	0.66	.	.	.	.	.	.
Al-Silicate	0.32	0.50	-0.52	0.58	0.62	.	.	.	.	.
Goethite	0.29	-0.09	0.02	0.31	0.31	0.19	.	.	.	.
Rutile	0.20	0.31	-0.35	0.30	0.52	0.36	-0.03	.	.	.
Gittinsite	0.43	0.49	-0.50	0.42	0.45	0.34	0.09	0.11	.	.
Allanite	-0.03	0.03	-0.02	0.12	0.16	0.05	-0.02	0.10	0.44	.
Aenigmatite	-0.61	-0.66	0.73	-0.53	-0.72	-0.52	-0.07	-0.37	-0.39	-0.05

Classification	Colour Code	
"Strong" +	> 0.7	POSITIVE
"Moderate" +	0.5 to 0.7	CORRELATION
"Weak" +	0.3 to 0.5	
Not Significant	-0.3 to 0.3	
"Weak" -	-0.3 to -0.5	
"Moderate" -	-0.5 to -0.7	NEGATIVE (INVERSE)
"Strong" -	< -0.7	CORRELATION

Most of the common accessory minerals, including gittinsite, show only weak to moderate correlations with distance from Strange Lake. If aenigmatite is derived at least in part from Strange Lake, it behaves differently from gittinsite, because its abundance diminishes with increasing distance, As noted earlier, a similar contrast was also observed between gittinsite and the Y-Ca-silicate gerenite, but both of these minerals *must* be derived from Strange Lake, because they are so rare. Some of the correlations between common accessory minerals are illustrated in the scatter diagrams included in Figure 6.7.

Frequency Patterns

Frequency distributions for selected common accessory minerals are illustrated in Figure 6.8. All are positively-skewed (log-normal) patterns in which most samples show very low abundances, and a few samples have high abundances. The wide divergence of mean and median values, and very low median values compared to means (Table 6.7) also indicates this pattern. Frequency patterns for the common accessory minerals are in general less varied than those previously presented for major and minor minerals (Figures 6.4, 6.6).

Rare Accessory Minerals

Mineral Types and Summary of Numerical Data

Rare accessory minerals, defined as those that have mean abundances between 10 and 100 area ppm, are an extremely diverse group. Summary statistical data for these minerals are listed in Table 6.7, with the equivalent data for common accessory and trace minerals. This group includes several Zr- and REE-rich minerals that are of particular interest in the context of Strange Lake. The most abundant mineral in the group is the Y-Ca-REE silicate gerenite, which is unique to Strange Lake. Baird (2018) reported gerenite abundances above 1 area % (i.e., > 10,000 area ppm) in many of her core samples, but its mean abundance in the till samples is only 92 area ppm, with a maximum value of only 523 area ppm. Other REE-bearing minerals in this group are perclevite, parisite and britholite, all of which were reported previously from Strange Lake (e.g., McClenaghan et al., 2017) and confirmed by MLA-SEM methods (Baird, 2018). Perclevite is a rare REE silicate mineral described from southern Sweden (Holtstam et al., 2003) and in its type locality is mostly enriched in the light REE Ce, La, and Nd. The type locality for perclevite is at the Bastnaes Fe-Cu-REE deposit, for which the more common REE-F-carbonate mineral bastnaesite is also named. Parisite is another LREE-rich

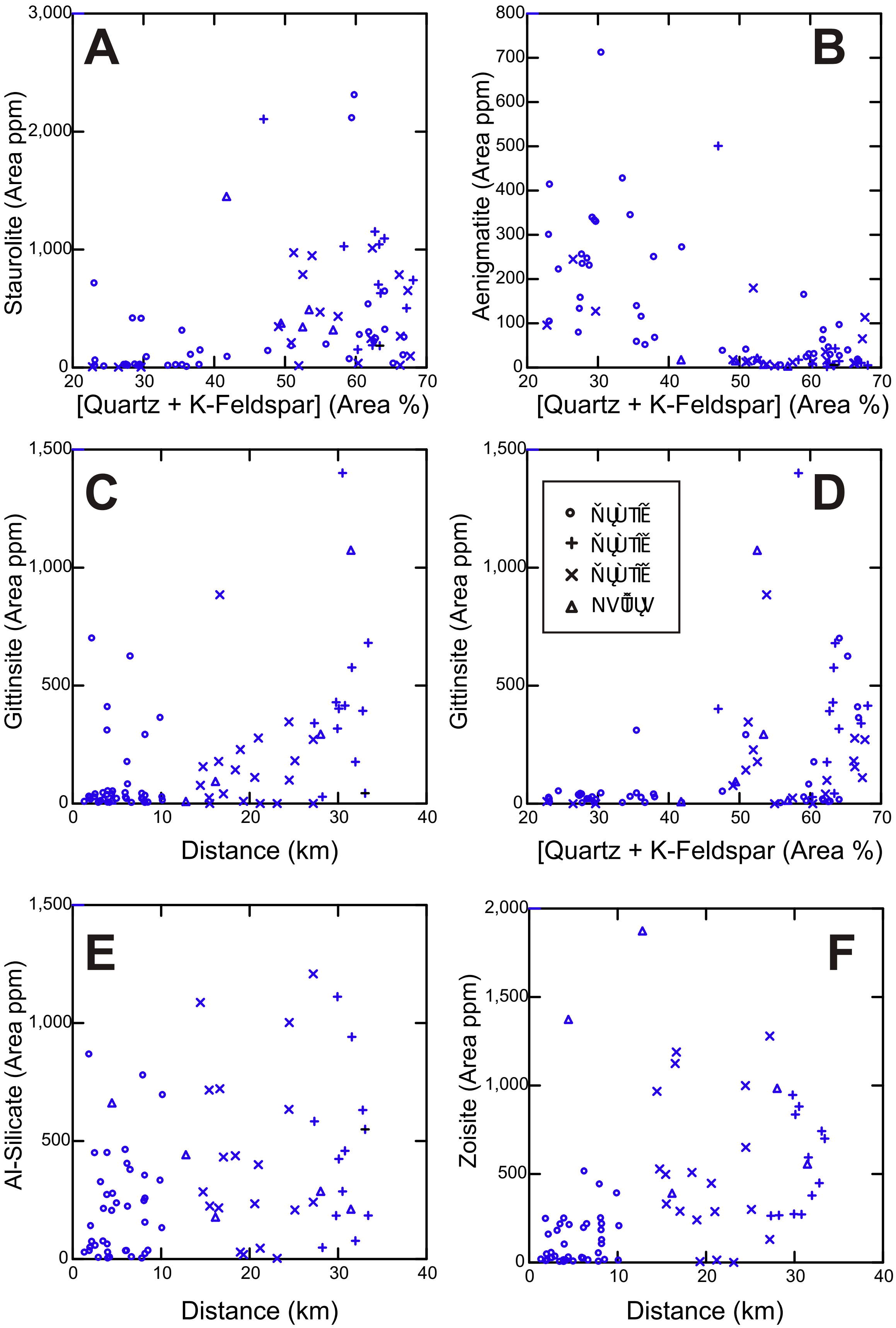

Figure 6.7. Scatter diagrams illustrating common accessory mineral correlations. (A) Staurolite against [Qz + Kf]. (B) Aenigmatite against [Qz + Kf]. (C) Gittinsite against distance from Strange Lake. (D) Gittinsite against [Qz + Kf]. (E) Al-silicate against distance from Strange Lake. (F) Zoisite against distance from Strange Lake.

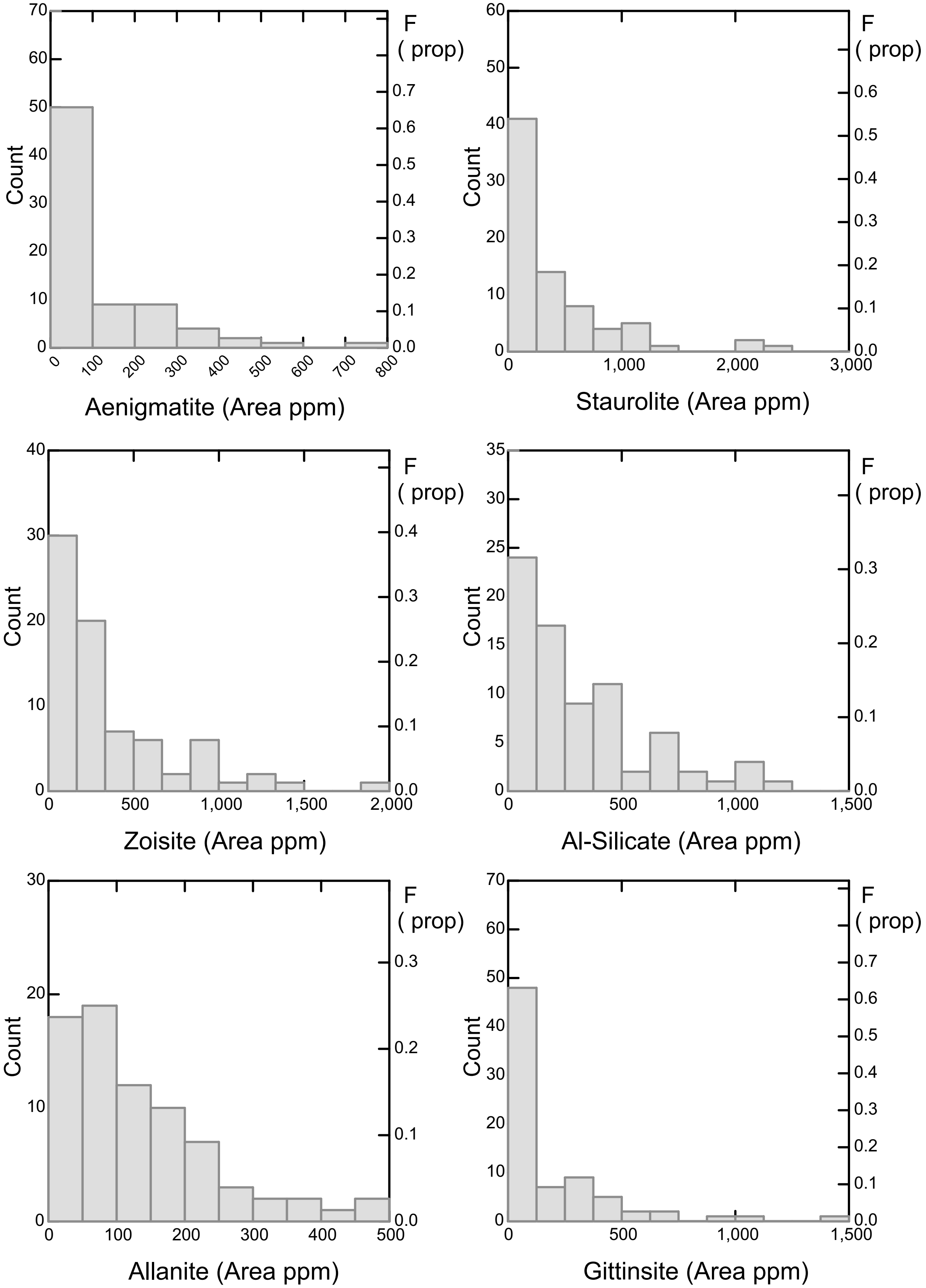

Figure 6.8. Frequency distributions (histograms) for selected common accessory minerals. The patterns for other minerals in this group are similar to these examples.

fluorocarbonate, similar in structure to bastnaesite, and britholite is a hydrated Ca-REE-silicate that can be enriched in LREE or in HREE. The Na-Zr-silicate mineral elpidite is known from Strange Lake, but is more widespread than its Ca-rich analogue gittinsite. The gittinsite in the Strange Lake granites is believed to have developed from elpidite by late-stage alteration processes (Birkett et al., 1992). These important indicator minerals are present at low mean abundances (< 20 area ppm area) but their maximum abundances locally exceed 100 area ppm. The least abundant members of this group are absent from at least half of the samples, but gerenite and elpidite are present in more than 90% of the samples.

Rare accessory minerals also include some better-known minerals that have diverse sources, such as calcite, monazite, wollastonite (Ca-silicate) and serpentine. The mineral identified as “ericssonite” was also detected, with a mean abundance of 58 area ppm, second only to gerenite. “Ericssonite” is one of several unusual Ba-Mn silicates, so its identification from the reference spectra is tentative, and other information suggests that a different name should be applied (see later discussion). “Ericssonite” was also detected in Strange Lake drill cores (Baird, 2018) but only in a few samples and only in trivial amounts. Astrophyllite is an uncommon K-Fe-Ti silicate mineral that is found in alkaline and peralkaline igneous rocks, and is previously reported from Strange Lake (Birkett et al., 1992; 1996). Thorite ($ThSiO_4$) is among the rarer accessory minerals, but is known to be important at Strange Lake from work by IOC and from the analyses of Baird (2018). The total thorite content of some pegmatites exceeds 10,000 area ppm (1 area %) and many granite drill cores contain > 1000 area ppm thorite (Baird, 2018). The very low thorite abundances in till samples are surprising in the light of these data, especially in samples located close to the Main Zone deposit. It is also interesting to note that thorite abundances are low in till samples from areas where anomalous radioactivity (attributed to thorium) is documented by airborne and ground surveys (Batterson, 1989; Bourassa and Banville, 2012; see Figure 3.7).

Summary statistical data (Table 6.7) are more difficult to interpret than data for more abundant minerals. At levels below 100 area ppm, uncertainties in MLA-SEM analysis likely approach or exceed +/- 25%, and this introduces considerable scatter in the data. The least abundant minerals are also missing from many samples, and these data are possibly subject to complications from probability effects. In other words, the absence of the mineral in the analyzed sample does not necessarily mean that is absent in the till, but a single anomalously large grain of such a mineral in the analyzed sample could generate anomalously high abundances.

Despite these complications, some geographic contrasts are evident in the summary data listed in Table 6.7. Gerenite and “ericssonite” are most abundant in Grid 1 samples, and least abundant in Grid 3 samples. Similar patterns are seen for the rare REE-bearing minerals perclevite, parisite and britholite, and elpidite is also more abundant in Grid 1 compared to other areas. Serpentine shows the reverse of this pattern, being most abundant in Grid 3 samples, but there is no obvious pattern for monazite, calcite, wollastonite or astrophyllite. The low mean abundance of monazite in the till samples (overall average of 38 area ppm) is also puzzling, because this mineral is reported from Strange Lake, and was detected at much higher abundances (300 to 500 area ppm) in drill core samples (Baird, 2018). Thorite abundances, although low, also appear to diminish from Grid 1 to Grid 3.

Correlation Patterns

Table 6.9 lists correlation coefficients for rare accessory minerals and also indicates their correlation with the average distance of samples from Strange Lake, and the composite variables [quartz + K-feldspar] and [garnet + hornblende + ilmenite] considered as general indicators of provenance for the till samples. Note that higher analytical uncertainties for rare accessory minerals, and potential complications from probability effects, may obscure some correlations. In general, there is a lack of strong correlation among the rare accessory minerals, which may reflect these complications. The strongest positive correlations are between “ericssonite”, gerenite and [Gt + Hb + Ilm] (0.71 and 0.49) and (not surprisingly) between “ericssonite” and gerenite (0.69). There is limited systematic correlation among other members of this group, but the Zr- and REE-bearing minerals associated with Strange Lake do show weak to moderate correlations with one another.

Both gerenite and “ericssonite” show strong to moderate negative correlations with the average distance of samples from Strange Lake (-0.71 and -0.66, respectively), and britholite also shows this pattern (-0.65), but the other REE- and Zr-bearing minerals associated with Strange Lake show little or no correlation, despite the apparent trends noted from summary statistical data in Table 6.7. In contrast, astrophyllite shows a moderate negative correlation with distance from Strange Lake, although this was not evident from summary data in Table 6.7. Some of the correlations among rare accessory minerals are illustrated by scatter plots in Figure 6.9.

Table 6.9. Spearman Correlation Matrix for rare accessory minerals, composite variables [quartz + K-feldspar] and [garnet + hornblende + Ilmenite], and distance from Strange Lake.

	Distance from Strange Lake	[Quartz + K-Feldspar]	[Garnet + Hornblende + Ilmenite]	Gerenite	Ericssonite	Serpentine	Monazite	Calcite	Wollastonite	Perclevite	Elpidite	Astrophyllite	Thorite	Parisite
[Quartz + K-Feldspar]	0.47	.	.	.	.	.	.	.	.	.	.	.		.
[Garnet + Hornblende + Ilmenite	-0.56	-0.95	.	.	.	.	.	.	.	.	.	.		.
Gerenite	-0.71	-0.41	0.49	.	.	.	.	.	.	.	.	.		.
Ericssonite	-0.66	-0.64	0.71	0.69	.	.	.	.	.	.	.	.		.
Serpentine	0.51	0.38	-0.44	-0.41	-0.48	.	.	.	.	.	.	.		.
Monazite	0.25	0.45	-0.40	-0.29	-0.30	0.34	.	.	.	.	.	.		.
Calcite	-0.26	-0.19	0.23	0.44	0.44	-0.27	-0.18	.	.	.	.	.		.
Wollastonite	-0.11	0.04	-0.06	0.04	-0.01	0.03	0.09	0.20	.	.	.	.		.
Perclevite	0.02	0.25	-0.18	0.14	-0.02	0.03	0.23	0.20	0.09	.	.	.		.
Elpidite	0.07	0.27	-0.26	0.03	-0.11	-0.08	0.09	0.16	0.16	0.41	.	.		.
Astrophyllite	-0.45	-0.40	0.42	0.44	0.57	-0.52	-0.22	0.43	0.18	0.14	0.09	.		.
Thorite	-0.12	-0.06	0.13	0.34	0.18	-0.22	-0.26	0.32	0.09	0.26	0.14	0.20		
Parisite	-0.39	-0.32	0.37	0.47	0.47	-0.27	-0.26	0.35	-0.02	-0.05	-0.10	0.09	0.30	.
Britholite	-0.65	-0.36	0.42	0.58	0.48	-0.33	-0.14	0.29	0.21	0.15	0.05	0.41	0.22	0.38

Classification	Colour Code	
"Strong" +	> 0.7	POSITIVE
"Moderate" +	0.5 to 0.7	CORRELATION
"Weak" +	0.3 to 0.5	
Not Significant	-0.3 to 0.3	
"Weak" -	-0.3 to -0.5	
"Moderate" -	-0.5 to -0.7	NEGATIVE (INVERSE)
"Strong" -	< -0.7	CORRELATION

Frequency Patterns

Frequency patterns for selected rare accessory minerals are illustrated in Figure 6.10. These histograms for show strongly asymmetrical, positively-skewed patterns in which most samples have very low abundances (including zero values) and a few samples have anomalously high abundance. These resemble patterns previously illustrated for common accessory minerals in Figure 6.8, but are more extreme. The frequency of occurrence is highest for gerenite and elpidite (73 and 62 of 76 samples, respectively) but most other minerals in this group are missing from many samples. The zero values add to the strong asymmetry of the frequency patterns.

Trace Minerals

Trace minerals are present only in trivial amounts (< 10 area ppm) and are absent from some or most of the till samples. The very low abundances, a high proportion of zero values, and potential complications from probability effects, coupled with greater analytical uncertainties in analysis (see Chapter 4), make it difficult to assess patterns for these minerals from numerical data. Summary statistical data for trace minerals are listed in Table 6.7, with data from more abundant accessory minerals. Multivariate correlation analysis was not attempted for trace minerals due to the small number of valid cases for many of them.

Based on mean abundances for the entire database (Table 6.1) the trace minerals are “benitoite”, pyrite, barite, gadolinite, bastnaesite, uranininite, rhodonite, scheelite, stetindite, pyrochlore, fergusonite, euxenite, pectolite, fluorite, and changbaiite. This is a truly diverse group that includes both common and obscure species. Pyrite, fluorite, barite and uraninite are found in many different rock types and environments. Pectolite is a hydrated Na-Ca silicate that is similar in general composition to plagioclase; it is known to occur in association with nepheline (Deer et al., 1992); it was detected by Baird (2018) in drill core samples. Rhodonite is a Mn-rich pyroxene mineral that is usually associated with metamorphic rocks or metasomatism (Deer et al., 1992), and was detected in small amounts by Baird (2018) from Strange Lake drill cores. Scheelite, present only in 3 samples, is associated with tungsten (W) mineralization in granites or metasomatic settings (Deer et al., 1992). It was not detected in Strange Lake drill cores by Baird (2018)

Several trace minerals are rich in REE (gadolinite, bastnaesite, stetindite, fergusonite, and euxenite) and three of them are rich in Nb (pyrochlore, fergusonite and changbaite). All of these minerals were previously reported from Strange Lake (Baird, 2018), so it is likely that they represent detritus from the Strange Lake area. Gadolinite and euxenite are complex silicate minerals, and

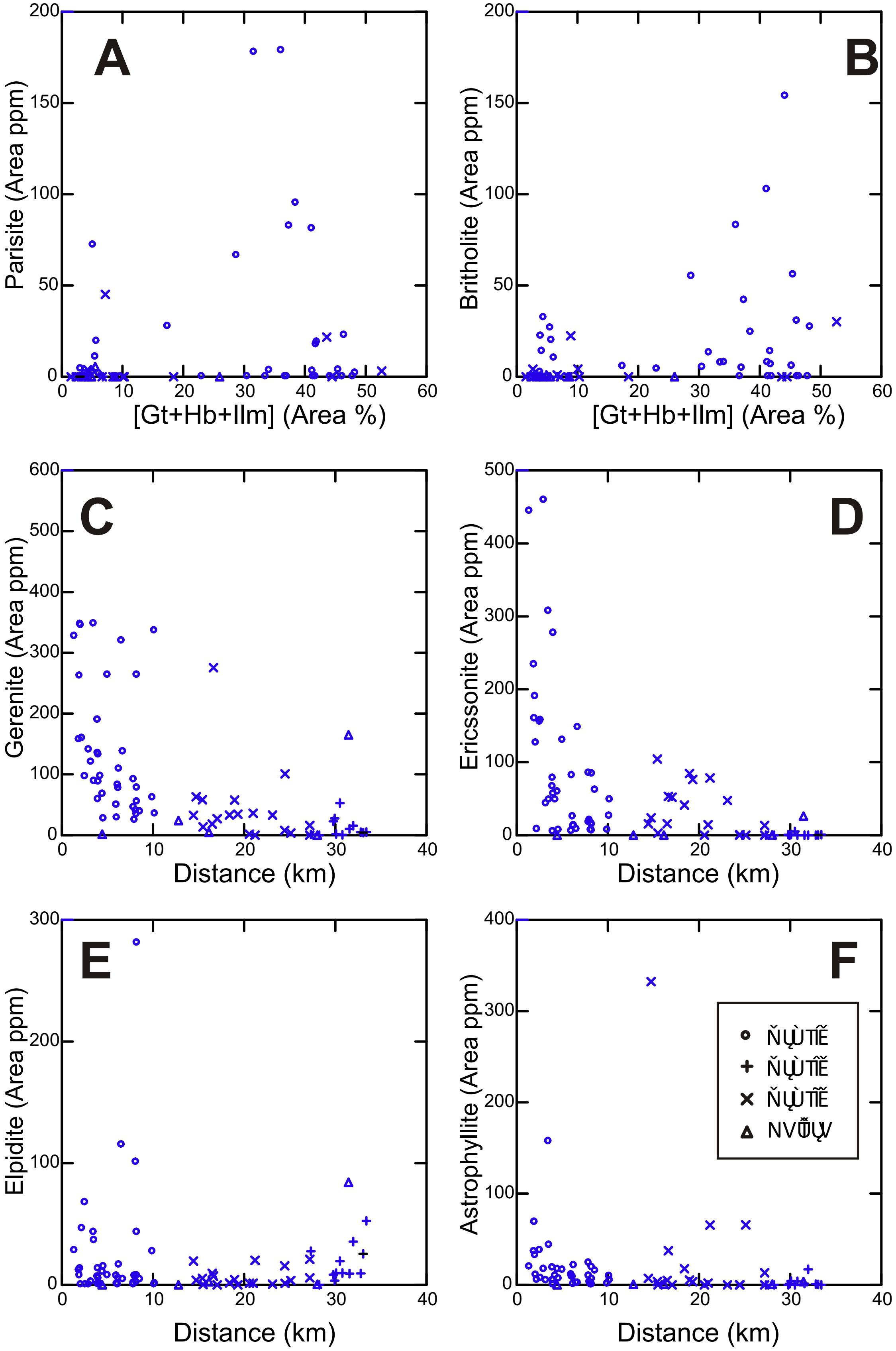

Figure 6.9. Scatter diagrams illustrating some rare accessory mineral correlations. (A) Parisite against [Gt+Hb+Ilm]. (B) Britholite against [Gt+Hb+Ilm]. (C) Gerenite against distance from Strange Lake. (D) Ericssonite against distance from Strange Lake. (E) Elpidite against distance from Strange Lake. (F) Astrophyllite against distance from Strange Lake.

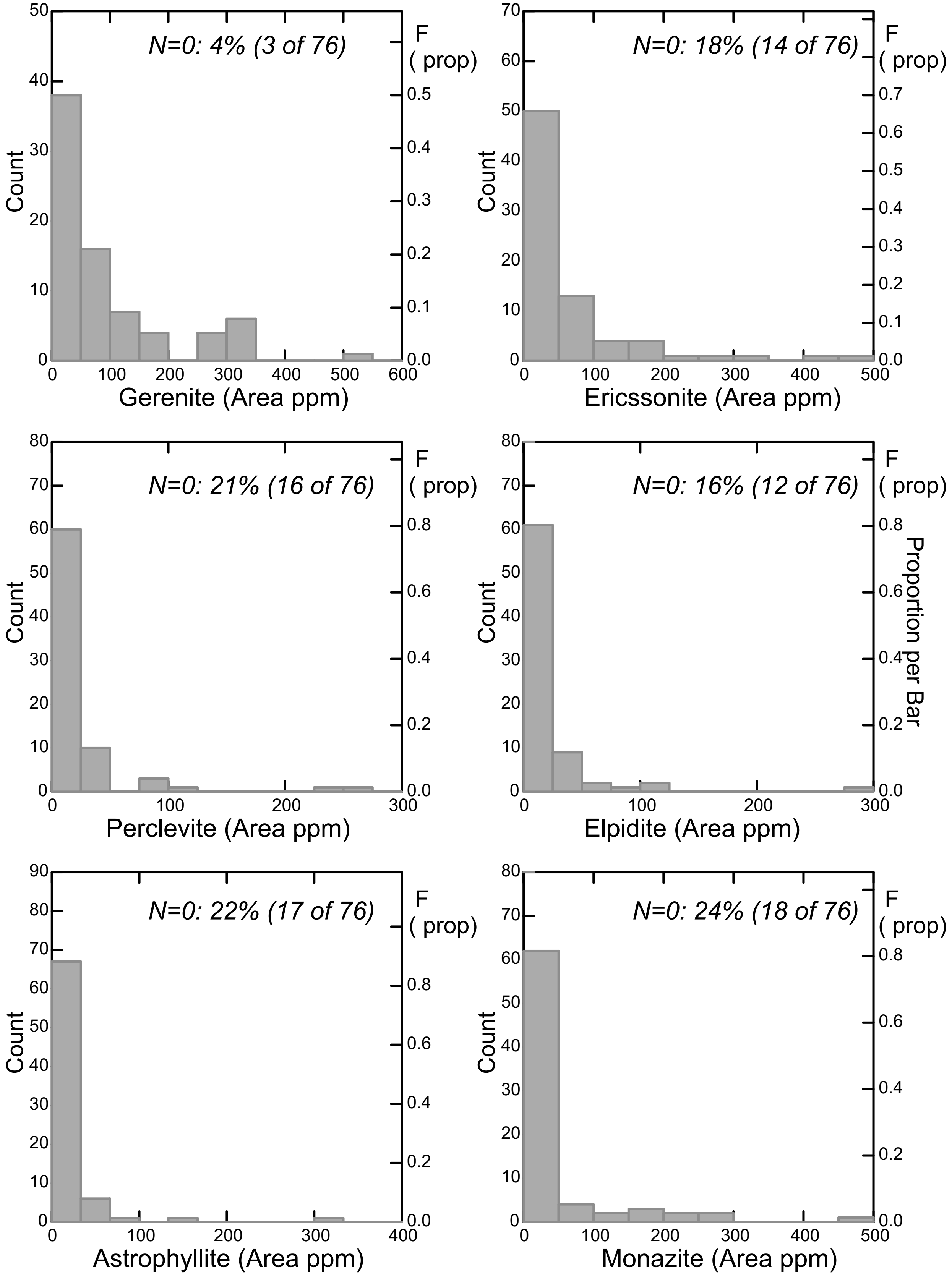

Figure 6.10. Frequency distributions (histograms) for selected rare accessory minerals. The patterns for other rare minerals are similar to these examples. These indicate the number of samples in which the mineral was not detected, e.g., 'N=0: 22% (17 of 76)' indicates absence in 22% of samples, or 17 out of 76.

stetindite is a Ce-rich analogue of zircon (Schluter et al., 2009). Pyrochlore is known to be an important carrier of Nb at Strange Lake, but its abundance in tills is pitifully low at 4 area ppm. The scarcity of pyrochlore is puzzling because it is present in drill cores analyzed by Baird (2018), which contain up to 4200 area ppm pyrochlore (0.41 area %). Less than half the analyzed till samples actually contain pyrochlore. Changbaiite is a rare Pb-Nb oxide mineral known mostly from southern China, and occurs only in 20 samples, with an average abundance of slightly more than 1 area ppm. It was detected by Baird (2018) in drill core samples, with an average abundance of 228 area ppm.

One of the least-known trace minerals identified by the MLA deserves special mention. "Benitoite" is a rare Ba-Ti silicate known only from the area of San Benito, California, and is in fact the official mineral of the State of California. Furthermore, it is a recognized gemstone, valued for its intense blue colour and high refractive index. In California, the mineral is associated with skarn zones (regions of metasomatism) in high-pressure metamorphic rocks ('blueschists') associated with serpentinites (www.mindat.org; Laurs et al., 1997). Carat-for-carat, high quality gem benitoites are extremely valuable. Among the trace minerals, it has fairly high mean abundance (almost 10 area ppm) and one sample contains 163 area ppm, but the latter is an anomaly.

However, as in the case of "ericssonite", the identification of this mineral requires more examination and assessment. The geological setting of known benitoite deposits (Laurs et al., 1997) does not correspond well with any aspect of the Strange Lake area. Although "benitoite" was categorized as a discrete mineral by the MLA-SEM analysis, its EDX reference spectrum is actually very similar to that of the rare Ba-Mn-silicate identified as "ericssonite" (D. Grant, pers. comm., 2021; see Chapter 4). Thus, it is possible that the two minerals should actually be combined under one name. "Benitoite" was also detected sporadically in drill core samples from Strange Lake by Baird (2018), although she did not specifically discuss it. Its average abundance in the drill core samples is about 8 area ppm, compared to nearly 10 area ppm in the till samples from this project. Thus, both "ericssonite" and "benitoite" are more abundant in till samples than in drill core samples.

The question of the true identities for "ericssonite" and "benitoite" is an interesting (albeit minor) aspect of this thesis project, but the possible relationship of these minerals to Strange Lake is of more importance. Further discussion of both minerals is deferred to a later Chapter in the thesis (Chapter 8). For present purposes, the names assigned by the MLA are retained, but with the addition of quotation marks. The identities of other minerals in the trace group are much better established, through previous work by D. Wilton and the investigation of Baird (2018). Nevertheless "ericssonite" and "benitoite" illustrate the need to assess results from MLA analyses in the context of other geological and mineralogical data.

PHYSICAL PROPERTIES AND ANATOMY OF MINERAL PARTICLES

General Information

The very large amount of data on mineral abundances provided by MLA-SEM analysis of the till samples presents a challenge for discussion and interpretation. However, the method provides an even larger amount of information about the individual particles that are examined during analysis. The total number of particles involved in this project exceeds 1 million, and for each of these there is information on the particle size, its shape, the number of 'grains' (i.e., individual areas of a single mineral) within it, and the contact relationships between individual mineral grains (i.e., mineral associations). This quantitative information is accompanied by back-scattered electron (BSE) imagery that visually documents some of these aspects. This section provides some analysis of information on particle statistics (notably relationships between average particle sizes and grain sizes for individual minerals) and also some preliminary information on mineral associations. Both aspects are important in assessing the reliability of abundance data at low levels and the potential impact of probability effects (see discussion in Chapter 4). They are also important in comparing the results of MLA-SEM based indicator mineral studies with those that use more traditional methods including density separations. The section concludes with BSE images of selected grains that support and illustrate some of the conclusions from quantitative MLA data.

Grain/Particle Size Relationships

For every sample analyzed by MLA-SEM methods, there is a record of the total number of individual 'particles' and the total area that is represented by all particles in the sample. From this information, the average size (i.e., the area) of particles (measured in square microns) is easily calculated for each sample. The MLA also records the number of 'grains' for each mineral that it identifies in a sample, and the area of each, and calculates the total area represented by a particular mineral. This is the basis of the area % calculation that provides the abundance data for individual minerals. Thus, for every mineral in a given sample, the average 'grain size' (i.e., area) can be calculated, and this can then be expressed as a percentage of the average particle size (area) for that same sample. This parameter is here termed the Grain/Particle Size Ratio, or the GPS ratio (for convenience), and it can be treated as a variable across the entire database for every mineral identified in analysis.

In an effort to understand the size relationships of mineral grains and particles, the GPS ratio was calculated for each mineral in every sample, and these data were then amalgamated. Univariate statistics (mean, median, standard deviation, minimum and maximum) were calculated for each mineral, and the results are shown in Table 6.10, and depicted in the graph of Figure 6.11, which shows average GPS ratio against average abundance (see also Table 6.1) for all minerals. Note that for cases where a mineral variable is derived by summing two or more compositional variants, the average values were weighted according to the abundance of each. In most cases, one compositional variant dominates and others have only minor influence.

The information in Table 6.10 is ordered according to mineral category (major, minor, common accessory, rare accessory and trace) as used in presentation of numerical data and statistical results. There is a general inverse relationship between GPS ratio averages and the average abundance of minerals (Figure 6.11) although there are some exceptions to this pattern. However, the mineral groupings based on average abundances are at least partially distinct. Major minerals (mean abundance > 1 area %) all have high average GPS ratios ranging from about 39% (garnet) to 115% (quartz). If the GPS ratio exceeds 100%, it indicates that the average grain size for the mineral is greater than the average particle size for samples, which means that the mineral in question tends to form larger-than-average monomineralic particles. The fact that most major minerals have such high average GPS ratios (locally > 100%) indicates that they tend to occur as discrete monomineralic particles or at least occupy most of the area of typical particles. Garnet, on the basis of maximum values (Table 6.10), probably occurs as smaller particles than the other major minerals. Minor minerals (mean abundance of 0.1 to 1 area %) show a wide range of GPS ratio values from about 12% (limonite) to 61% (nepheline). This indicates that some of these minerals will also occur as larger particles that are essentially monomineralic (e.g., nepheline and hypersthene) whereas other minerals will form composite particles with grains of other minerals, or form smaller monomineralic particles. These two latter options cannot be fully distinguished, but maximum GPS ratio values (approaching or exceeding 200%) suggest that large monomineralic particles are common for some of these minerals (e.g., nepheline, hypersthene and titanite).

Table 6.10. Summary of information for grain and particle size distributions for Strange Lake till samples, with average abundances for minerals.

			Grain / Particle Size (GPS) Ratios					Average Abundances	
Mineral	**N**	**Average Grain Size** (square microns)	**Average** %	**Median** %	**Std. Deviation** %	**Minimum** %	**Maximum** %	Area %	Area ppm
Quartz	76	5400	115.1	109.1	27.3	74.4	196.9	34.40	n/a
Albite	76	3787	77.7	73.0	15.9	48.1	137.3	22.26	n/a
K-Feldspar	76	2916	65.2	61.4	18.6	36.7	111.9	14.66	n/a
Hornblende	76	3873	88.5	83.0	37.2	24.8	226.5	10.49	n/a
Garnet	76	1709	38.8	37.2	14.1	12.8	73.7	7.94	n/a
Plagioclase	76	4144	84.9	82.6	18.0	36.2	164.4	4.19	n/a
Ilmenite	76	3323	87.9	62.3	60.0	9.6	227.4	1.13	n/a
Biotite	76	1024	19.3	16.5	11.3	7.8	77.6	0.803	8031.9
Chlorite	76	1566	28.4	26.3	13.7	4.5	76.8	0.700	6997.0
Epidote	76	1389	28.0	26.7	13.2	3.9	71.5	0.471	4711.6
Grunerite	76	1837	38.2	36.1	15.5	10.1	94.0	0.527	5268.4
Nepheline	76	3119	61.4	54.9	30.6	1.7	193.6	0.341	3412.6
Zircon	76	1224	33.8	24.5	26.1	1.7	123.3	0.414	4144.8
Augite	75	1788	29.1	26.4	18.4	3.2	64.8	0.229	2291.4
Aegirine	76	1147	20.7	18.5	10.2	4.4	58.9	0.211	2113.9
Limonite	76	493	12.3	10.0	8.7	1.3	43.6	0.181	1813.9
Magnetite	76	1238	29.9	25.2	18.8	6.1	99.0	0.225	2245.7
Hypersthene	73	2869	57.1	51.2	48.7	0.7	247.8	0.131	1310.2
Titanite	75	971	21.8	16.0	29.8	2.7	247.6	0.116	1162.4
Apatite	74	1123	24.8	20.8	15.0	3.7	87.9	0.133	1330.9
Staurolite	76	1755	41.0	17.6	154.6	0.8	1350.5	0.0397	396.9
Zoisite	75	916	16.0	14.0	12.6	0.9	56.1	0.0343	343.4
Goethite	76	276	7.3	5.8	5.4	1.2	24.6	0.0324	324.1
Al-Silicate	73	3077	50.8	41.4	40.2	2.8	149.7	0.0312	312.0
Rutile	73	1033	24.7	13.0	29.0	0.8	143.7	0.0187	187.0
Gittinsite	70	541	12.8	9.7	14.1	0.9	101.3	0.0175	174.7
Allanite	75	553	11.8	8.7	8.5	2.0	40.0	0.0136	135.7
Aenigmatite	76	357	9.9	8.0	9.8	0.5	56.2	0.0108	107.8

Notes: The Grain/Particle Size Ratio is the average grain size for a mineral, divided by the average particle size for the sample. Particles are physical grains that may include two or more 'grains' of individual minerals. The abundance data for minerals is drawn from Table 6.1.

Table 6.10 (continued). Summary of information for grain and particle size distributions for Strange Lake till samples, with average abundances.

			Grain / Particle Size (GPS) Ratios					Average Abundances	
Mineral	**N**	**Average Grain Size** (square microns)	**Average** %	**Median** %	**Std. Deviation** %	**Minimum** %	**Maximum** %	Area %	Area ppm
Gerenite	73	303	8.2	6.1	11.6	0.2	89.7	0.0092	92.4
Ericssonite	62	265	8.4	6.7	9.1	0.3	60.4	0.0058	57.8
Serpentine	31	4409	75.6	47.4	89.3	0.9	369.4	0.0055	54.7
Monazite	58	706	13.3	4.6	30.8	0.6	213.2	0.0038	38.2
Calcite	62	761	18.5	6.4	52.4	0.2	388.1	0.0026	25.6
Wollastonite	65	711	16.0	6.2	46.8	0.2	360.3	0.0021	20.6
Percleveite	60	280	7.5	3.5	12.2	0.5	63.0	0.0020	19.7
Elpidite	64	193	4.9	2.8	4.8	0.5	21.2	0.0018	17.9
Astrophyllite	59	425	10.0	5.3	19.4	0.6	135.6	0.0016	16.5
Thorite	75	411	10.3	9.5	7.0	0.3	41.0	0.0014	14.0
Parisite	26	302	10.4	7.8	7.9	1.9	30.1	0.0013	12.8
Britholite	37	239	6.9	6.5	4.7	0.5	18.9	0.0011	11.2
Benitoite	32	1252	16.9	5.7	31.9	0.4	144.0	0.0010	9.9
Pyrite	48	270	5.4	3.7	6.1	0.4	33.4	0.0010	9.8
Barite	50	192	4.9	3.7	4.5	0.5	18.4	0.0010	9.8
Gadolinite	31	266	5.3	1.5	7.8	0.5	32.5	0.0010	9.9
Bastnaesite	36	385	7.4	4.0	11.8	0.3	68.7	0.0007	6.6
Uraninite	22	896	33.1	7.2	113.7	0.8	541.1	0.0006	5.8
Rhodonite	17	283	9.1	5.2	11.8	0.7	44.7	0.0006	5.6
Scheelite	3	6500	260.2	39.4	415.9	1.4	739.9	0.0005	5.0
Stetindite	36	325	5.6	1.3	8.5	0.3	31.2	0.0005	4.8
Pyrochlore	31	402	6.1	3.3	11.2	0.6	62.5	0.0004	4.4
Fergusonite	42	225	5.1	4.0	5.6	0.4	31.8	0.0004	4.1
Euxenite	18	301	9.1	5.5	10.4	0.7	36.3	0.0004	4.1
Pectolite	28	447	10.9	3.7	33.6	0.5	181.1	0.0003	2.8
Fluorite	23	220	4.5	2.0	5.5	0.6	19.8	0.0001	1.4
Changbaiite	20	248	4.6	2.1	5.6	0.4	20.2	0.0001	1.2

Notes: The Grain/Particle Size Ratio is the average grain size for a mineral, divided by the average particle size for the sample. Particles are physical grains that may include two or more 'grains' of individual minerals. The abundance data for minerals is drawn from Table 6.1.

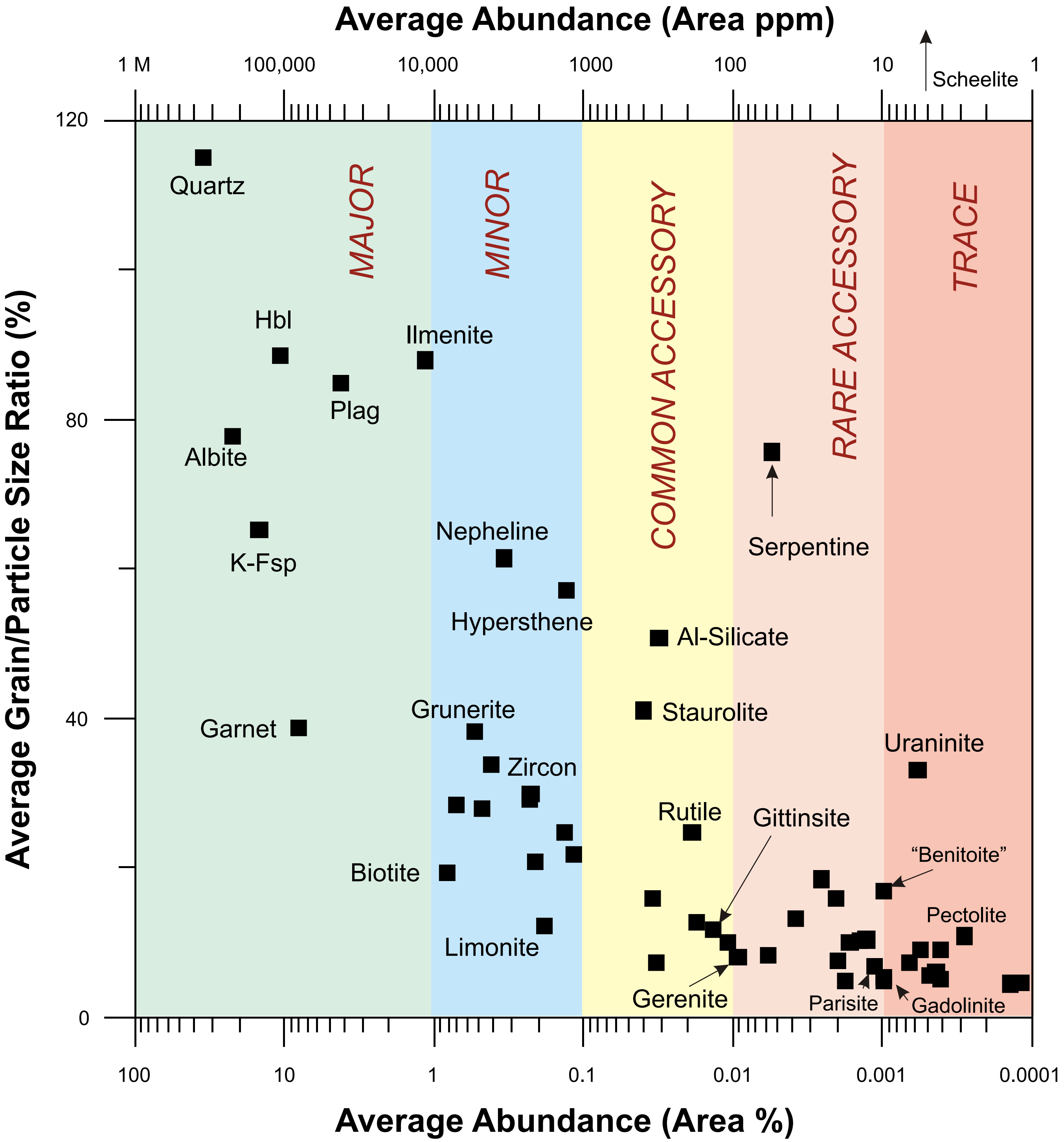

Figure 6.11. An illustration of the variation in the size of mineral grains relative to the average particle size in samples. The X-axis shows the mean abundance of a mineral in the database, and the Y-axis shows the average Grain/Particle Size (GPS) Ratio, derived for each sample by dividing average grain size for the mineral by the average particle size in the sample. Notable minerals and exceptions to the general pattern are labelled, and the anomalous GPS ratio for scheelite (260) is omitted for clarity. See text for discussion.

Average GPS ratios for accessory and trace minerals are also variable, especially for the common accessory minerals, but in general most of these minerals have much lower average GPS values. This is especially clear for the rare accessory minerals (average abundance 10 to 100 area ppm) and trace minerals (average abundance < 10 area ppm). Most minerals in these groupings have average grain sizes that are less than 10% of the average particle sizes for samples, indicating that they occur as intergrowths or inclusions in composite particles. There are some exceptions, such as serpentine (76%) and scheelite (260%). The latter is an unusual case as the mineral only occurs in three samples, and one of these contains an unusually large grain.

Zr-, Nb- and REE-bearing minerals that are characteristic of the Strange Lake Deposit and host rocks mostly have average GPS ratios below 10%, and the highest average GPS ratio is shown by gittinsite (about 13%). These minerals will thus mostly be present as small grains within larger composite particles. Note that this inference does not mean that larger discrete monomineralic particles of such minerals are *absent* from the samples, but it does suggest that they are uncommon; in most cases, these characteristic minerals will form smaller grains within larger composite particles. In the case of gittinsite, some larger particles were imaged, but these are uncommon.

As discussed in Chapter 4, the mode of occurrence of these minerals is probably an important influence on the reliability and precision of abundance data from MLA-SEM analysis. Because these unusual minerals are widely distributed as grains among particles, they are more likely to be transferred into smaller aliquots in amounts that approximate their overall abundance in the larger sample mass. Secondly, the behaviour of particles containing grains of these characteristic minerals will be determined largely by the properties of the more abundant ‘host’ minerals within those particles. For example, the bulk density of a quartz-dominated particle containing 10-20% gittinsite (density of ~ 3.5 g/cc) will only be slightly higher than the density of quartz (~ 2.7 g/cc). This will influence the behaviour of the particle in natural processes, and also in artificial processing of samples through density separation. The effective hardness of such a composite particle will be determined by the high hardness of quartz (7 on Moh’s scale) rather than the lesser hardness of gittinsite (3.5 to 4 on Moh’s scale), which would influence the durability of particles, and their ability to survive long-distance transport. These aspects are discussed further in Chapter 8.

The most abundant minerals in the till samples are almost invariably quartz and feldspars, which are relatively low in density and hard (although quartz is harder and less susceptible to weathering than feldspar). These are also the dominant minerals in granites, aplites and pegmatites.

It is logical to suppose that the rarer minerals derived from Strange Lake are mostly associated with these more common silicates, but they could also be associated with other uncommon minerals, or with Na-rich amphiboles (included with 'hornblende' or aegirine. The GPS ratio data cannot convey this information, but MLA data on mineral associations, and direct observations of particles, can supply partial answers.

Mineral Associations derived from MLA-SEM Data

The way in which MLA-SEM approaches mineral associations requires some explanation, because it is designed for integral materials (e.g., rock slices) as well as for particulate material such as till samples. The information is provided on a sample basis, so large amounts of data must be amalgamated manually to gain insight that applies to a large database of samples. This limits application of the method in this thesis study.

The MLA approaches mineral associations by assessing contact relationships and enumerating2the length of all shared boundaries between pairs of minerals. For example, it may indicate that contacts of Mineral A with Mineral B account for 50% of all contacts for Mineral A, but this does not mean that contacts for Mineral B are described by the same value. If Mineral B is vastly more abundant than Mineral A, the percentage of shared contacts viewed from its perspective may be trivial. In the case of particulate materials such as the till samples, many 'contacts' will actually be the external surfaces of particles, and these are classified as "free surfaces", because they do not define any association. For major minerals, free surfaces will outnumber other contacts, whereas they will be less important for less abundant minerals that occur as 'grains' in composite particles. To complicate things even more, the significance of information on mineral associations will depend on the abundance of the mineral in question. For example, if a mineral is present in a sample in very small amounts (say, < 10 area ppm) its mineral contact associations may be less representative of its natural habitat than for a sample in which that mineral is more abundant (say, 500 area ppm). This means that any attempt to amalgamate information from multiple samples should ideally incorporate some sort of 'weighting' procedure, but this would need to be mineral-specific, in addition than sample-specific. These complications need further assessment, and the short summary that follows should be viewed as preliminary.

A complete assessment of all mineral associations for the entire database was deemed impossible at this time. However, an attempt was made to assess mineral associations for some of the rarer minerals that characterize dispersion from Strange Lake, because this aspect may be important in controlling their behaviour. This was completed using a subset of nine samples chosen to cover a range of abundances for each mineral, and no attempt was made to weight results. The information is presented in Table 6.11, which shows only the most important mineral associations for each (including free surfaces, as described above, and grouping 'all others' as a separate category). Each mineral is summarized in a separate sub-table for clarity, and the 'free surface' category can be ignored (although it does convey some information about grain sizes versus particle sizes).

Table 6.11 shows the principal mineral associations for eight minerals that are diagnostic of the Strange Lake deposit. Although based only on nine selected samples, there are some differences among the patterns. Some minerals (e.g., gittinsite and pyrochlore) have a strong association with quartz, whereas others (e.g., gerenite, perclevite and bastnaesite) have much more diverse mineral associations in which quartz is less prominent. There are also associations between individual Strange Lake minerals, such as gittinsite and elpidite, or gerenite and gadolinite. Changbaiite (Nb-Pb-oxide) and another Nb-bearing oxide mineral named rynersonite appear in the associations for pyrochlore and fergusonite. Note that rynersonite is not discussed elsewhere in this thesis because of its low mean abundance (< 1 area ppm) and sporadic occurrence (only 20 samples).

The results of this preliminary assessment are further discussed in Chapter 8, in conjunction with evaluations of controls on dispersion patterns. The information in Table 6.11 shows that mineral associations are not random, but they are not uniform. It suggests that a more extensive compilation of mineral associations for indicator minerals across the entire database would be a useful step if it could be performed more easily. The differences in mineral associations for specific indicator minerals are interesting because in some cases these minerals show contrasting geographic variation patterns.

Table 6.11. Mineral Associations for selected indicator minerals associated with the Strange Lake Deposits

Gerenite Associations (%)		**Gittinsite Associations (%)**		**Elpidite Associations (%)**		**Perclevite Associations (%)**	
Free Surface	42.8	Free Surface	26.2	Free Surface	26.9	Free Surface	44.9
Zircon	16.1	Zircon	31.9	Gittinsite	26.8	K-Feldspar	12.8
Hornblende	8.1	Quartz	25.6	Quartz	20.5	Parisite	11.1
Gadolinite	7.6	Allanite	4.7	Allanite	7.1	Stetindite	6.0
Gittinsite	4.8	Albite	3.0	Zircon	5.5	Albite	4.9
Quartz	4.1	Elpidite	2.7	Albite	4.7	Al-Silicate	4.5
Allanite	4.0	K-Feldspar	1.6	Hornblende	3.8	Quartz	4.3
Albite	3.0	Gerenite	1.5	Apatite	1.3	Allanite	2.9
K-Feldspar	2.8	Apatite	1.4	K-Feldspar	1.0	Bastnaesite	2.6
All Others	6.8	All Others	1.5	All Others	2.4	All Others	6.1

Stetindite Associations (%)		**Bastnaesite Associations (%)**		**Pyrochlore Associations (%)**		**Fergusonite Associations (%)**	
Free Surface	37.6	Free Surface	39.5	Quartz	37.9	Zircon	21.4
Quartz	22.0	K-Feldspar	20.7	Free Surface	30.0	Free Surface	19.2
K-Feldspar	14.6	Stetindite	8.0	K-Feldspar	10.6	Quartz	17.5
Garnet	6.3	Albite	6.9	Aegirine	6.2	Albite	13.4
Bastnaesite	5.0	Perclevite	6.2	Rynersonite	4.1	Allanite	7.6
Perclevite	3.8	Quartz	4.7	Changbaiite	4.1	K-Feldspar	5.3
Albite	1.7	Garnet	2.5	Albite	3.9	Gittinsite	2.9
Monazite	1.1	Grunerite	2.4	Chlorite	3.0	Rynersonite	2.8
Allanite	0.9	Thorite	1.6			Hornblende	2.7
All Others	6.9	All Others	7.5	All Others	0.0	All Others	7.2

NOTES:

Average values based on a subset of 9 samples (G1-6; G1-10; G1-33; G1-40; G2-6; G3-7; G3-9; G3-12: E-8).

The values listed in the table represent the percentage of grain contact lengths associated with specific minerals; The term "Free Surface" refers to grain contacts that are on the external surfaces of particles (i.e., not in contact with other minerals). "Rynersonite" is a Nb-bearing mineral with average abundance < 1 area ppm, not discussed elsewhere in the thesis.

See text for additional discussion of this information and how it is interpreted.

Direct Observations of Monomineralic and Composite Particles

Direct observations of particles and grains are time-consuming and, given the number of particles, it is impossible for them to be fully comprehensive. Numerous images were retrieved in the first phase of this research project, but these were dominated by gittinsite, which is the most abundant of the uncommon minerals. The initial objective of this work was to see if there were any differences in the sizes and textural habits of the unusual minerals that might be related to the distance of samples from Strange Lake. However, no consistent differences were observed. Unfortunately, very few images of any other minerals were obtained, and it was not possible to acquire additional images for minerals other than gittinsite in the second phase of the project in 2020-21, due to Covid-19 restrictions on laboratory access. However, some visual information that corroborates inferences from the MLA-SEM data is available.

Figures 6.12 to 6.14 provide examples of BSE images showing monomineralic particles and composite particles that include smaller smaller grains of uncommon Zr-, Nb- and REE-bearing minerals. The captions to the figure contain additional information on each image. The composite nature of particles containing gittinsite and pyrochlore is evident from these images, although two other images included in Chapter 4 do show that larger, near-monomineralic particles do occur. Figure 6.15 is an image reproduced from Baird (2018) that shows a selection of gittinsite grains from drill core samples, which show very similar textures to grains illustrated from the till samples.

SUMMARY OF OBSERVATIONS

In view of the length of this chapter and its numerous tables and illustrations, key observations are summarized in this final section.

MLA-SEM analysis of till samples from the Strange Lake area provides quantitative data that measure the abundance (by area) of 94 minerals for 76 samples, although these include several compositional variants of some minerals (e.g. garnet, titanite, allanite). The size of this database was reduced by combining most compositional variants into single mineral variables, and minerals with abundances below 1 area ppm (0.0001%) were removed from consideration. The simplified database contains 55 variables (minerals) that vary in abundance across the database by several orders of magnitude, from greater than 50 area % to less than 10 area ppm (0.001 area %). The average abundances of minerals provide an objective subdivision for presentation and discussion of results. Minerals are divided into major (> 1% area), minor (0.1% to 1%; 1000 area ppm to 10,000 area ppm), common accessory (100 area ppm to 1000 area ppm), rare accessory (10 area ppm to 100 area ppm) and trace (< 10 area ppm) categories.

Evaluation of data from control samples located outside the dispersion area from Strange Lake, and close to the site of the Main Zone deposit, demonstrates that patterns of variation are not simple. A control sample from outside the dispersion area lacks most of the uncommon minerals that are characteristic of Strange Lake, with the exception of the zirconosilicate mineral elpidite. Contrary to expectations, till samples located closest to the Main Zone deposit do not show the highest abundances of the uncommon minerals known from the deposit. Some of the diagnostic minerals show contrasting patterns of behaviour. For example, gittinsite is actually more abundant in distant samples within Grid 3, whereas gerenite is most abundant in samples within Grid 1, closer to Strange Lake, and diminishes in abundance with distance. As both minerals are very rare and both *must* come from Strange Lake, it is clear that the controls on their dispersion are complex.

Major and minor minerals, mostly silicates, make up 99 area % of most till samples and 7 of these (quartz, albite, K-feldspar, hornblende, plagioclase, garnet and ilmenite) typical make up 95 area % or more. Summary data show apparent variations in the abundance of some major minerals with distance from Strange Lake. In particular, hornblende, garnet and ilmenite are more abundant in Grid 1 (close to the deposit) whereas quartz and K-feldspar are more abundant in Grids 2 and 3 (further from the deposit). As the Strange Lake Intrusion does not contain garnet, and contains little ilmenite, such patterns cannot be explained by the dispersion of material from Strange Lake. It is more likely that such patterns must be related (in a general sense) to the regional geological units that represent sources for till materials. Higher abundances of garnet and hornblende suggest influences from metamorphic rocks derived from mafic and intermediate igneous rocks, or from metamorphosed sedimentary rocks. Higher abundances of quartz and K-feldspar suggest influences from granitic igneous rocks or their metamorphic derivatives. The presence of these regional compositional variations must be taken into account in evaluating and explaining the variation patterns of other minerals, including those that are associated with Strange Lake. Major mineral abundances allow division of the till samples into two partially discrete groups based on the relative proportions of [garnet + hornblende + ilmenite] and [quartz + K-feldspar]. These groupings proved to be useful measures in the assessment of data variation patterns for less abundant minerals.

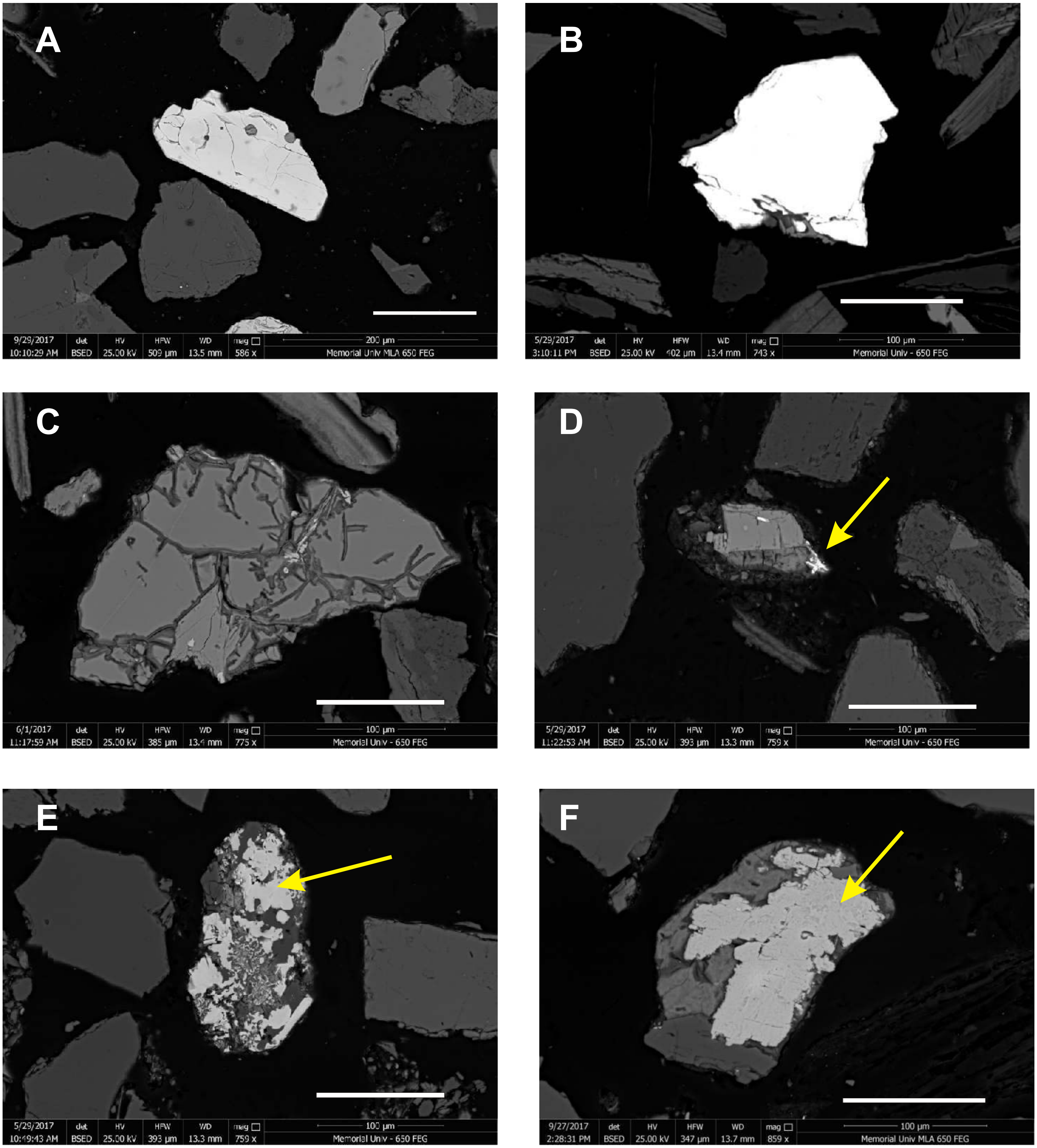

Figure 6.12. Selected back-scattered electron (BSE) images illustrating particles and grains in till samples from the Strange Lake area. (A) monomineralic particle of zircon. (B) large monomineralic particle of scheelite. (C) particle of grunerite (Mg-amphibole). (D) Tiny grain of fergusonite (bright material) within a small grain dominated by quartz. (E) gittinsite grains associated with intergrown quartz and zircon. (F) larger gittinsite grain (bright) associated with quartz and feldspar in a larger particle. Scale bars in all images are 0.1 mm (100 microns).

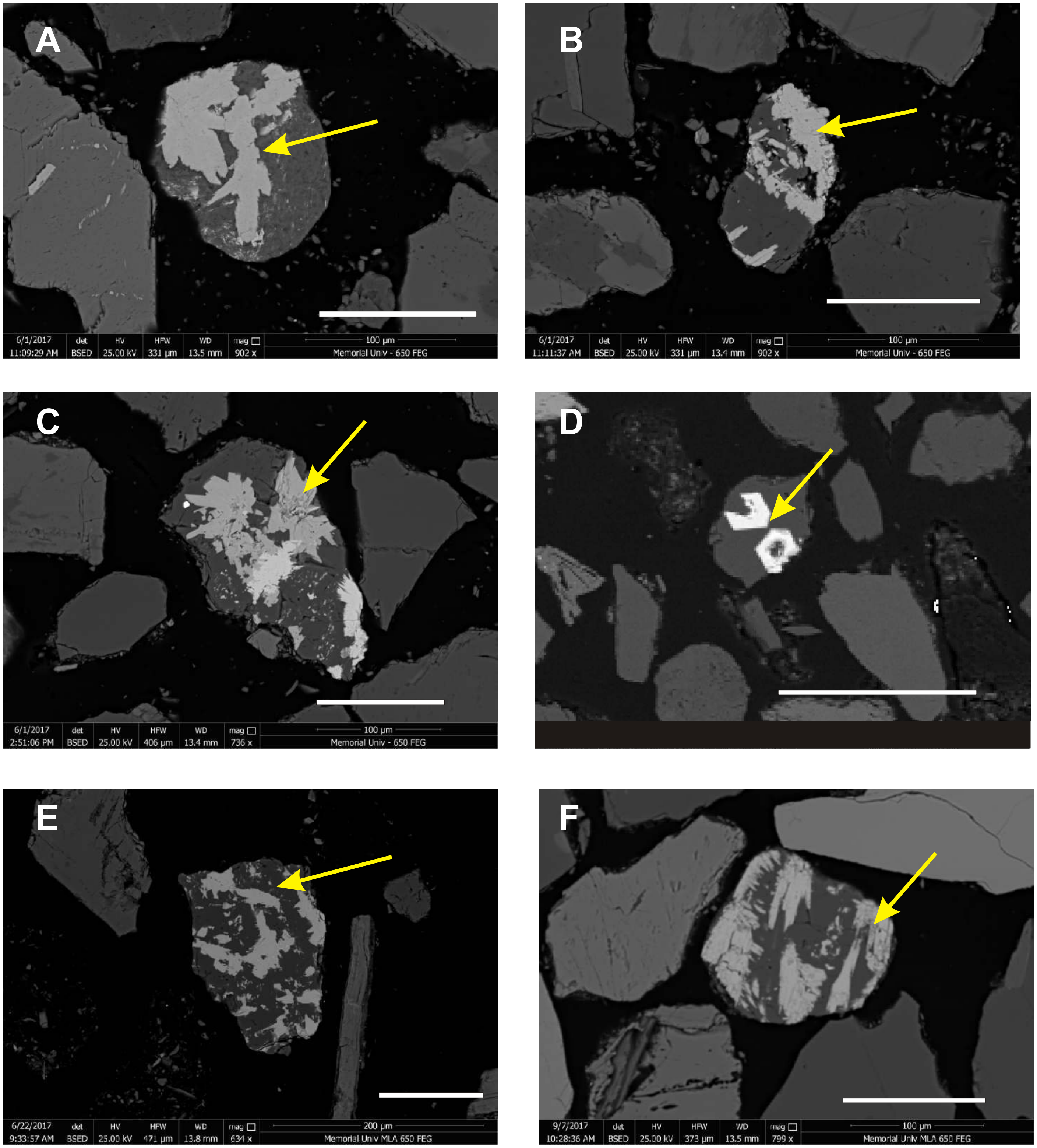

Figure 6.13. Selected back-scattered electron (BSE) images illustrating particles and grains in till samples from the Strange Lake area. (A) composite particle including quartz and gittinsite (brighter material). (B) similar composite particle of gittinsite and quartz. (C) composite particle including gittinsite and another brighter mineral (unidentified). (D) grains of pyrochlore within quartz. (E), (F) composite particles including gittinsite and quartz. Scale bars in all images are 0.1 mm (100 microns).

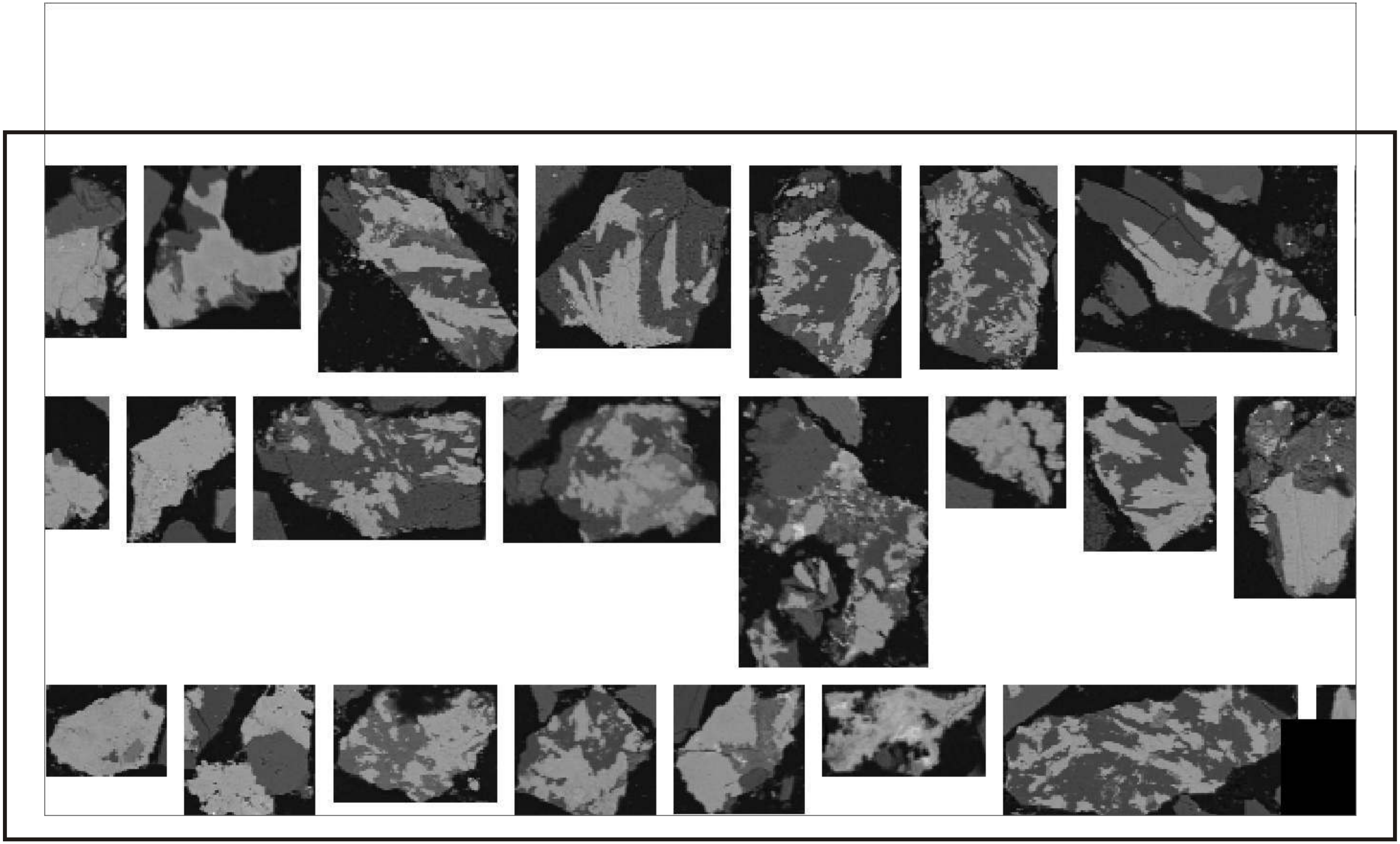

Figure 6.14. A collage of BSE images showing composite particles that include the zirconosilicate mineral gittinsite and other silicate minerals, mostly quartz and feldspars. These particles are from crushed samples of Strange Lake drill core, rather than the till samples examined in this project, and show closely similar textures. From Baird (2018). Note that the original figure did not include scale bars, so the absolute sizes of particles cannot be indicated.

Minor minerals, most of which are also silicates, show variations that are broadly linked to the regional patterns defined above. Some (e.g., grunerite, a Mg-amphibole) are strongly correlated with [garnet + hornblende + ilmenite] whereas others (e.g., biotite and epidote) show correlation with [quartz + K-feldspar]. Some minor minerals show patterns that do not fit with expectations; for example zircon is more abundant in the garnet-rich tills that are close to Strange Lake, and depleted in quartz- and K-feldspar-rich tills located at greater distances. Given that zircon is abundant in granites (and especially so in the Mesoproterozoic granites of this region), this is a contradiction. The most likely explanation is that much (but not all) zircon in samples originated from Strange Lake.

Variation patterns for common accessory minerals, rare accessory minerals and trace minerals are more complex and less easily resolved by statistical methods. Some minerals (e.g, staurolite, zoisite and serpentine) correlate well with major and minor minerals that follow these regional trends but others lack clear correlations. This is especially so for unusual Zr-, Th- and REE-bearing minerals known to be abundant at Strange Lake, such as gittinsite, gerenite, aenigmatite, perclevite, elpidite, parisite, thorite, britholite, gadolinite, bastnaesite and euxenite. However, correlations between such minerals are not always consistent, or even evident, as in the case of gerenite and gittinsite noted above. Statistical analysis of data for these rarer minerals is complicated by increased analytical uncertainties at low abundances, and also because some of these minerals are absent from many till samples. Other unusual accessory minerals that are not clearly linked to Strange Lake (such as the Ba-Mn silicate "ericssonite" and a similar Ba-Ti silicate named "benitoite") were also recorded, but these results are discussed in Chapter 8.

The abundances of known indicator minerals from Strange Lake, even in till samples where they are most common, are orders of magnitude less than the primary abundances recorded from MLA-SEM investigations of Strange Lake drill cores by Baird (2018). Table 6.12 lists these data, and Figure 6.15 summarizes comparisons of the two sets of measurements. Even in locations that are close to the Main Zone deposit, the abundances of these minerals in the till samples remain very low, and their mean abundances relative to the source rocks vary considerably. The contrast is greatest for Nb-bearing minerals such as pyrochlore and fergusonite, and for thorite, which are found only in trivial amounts in the till samples. These dilution factors apply in the strict sense only to minerals that can only be derived from the Strange Lake deposits. For zircon, apatite, monazite and some other minerals, there are other sources available. Note that dilution factors for some minerals are close to or less than 1, which is likely an indication of derivation from elsewhere. The wide variation in 'dilution factors' among the minerals known from Strange Lake (< 10 to > 600) indicates that influences on their dispersion patterns are multiple and complicated, but this variation must have some significance.

Table 6.12. Comparison of abundance data for diagnostic minerals in till samples and core samples of Baird (2018)

Part A: Analytical Data

		Strange Lake Till Samples (this project)		**Strange Lake Drill Core Samples (Baird, 2018)**			
Mineral	**Unit (area)**	**Mean (all data)**	**Mean (converted)**	**Mean (all data)**	**Mean (granites)**	**Mean (pegmatites)**	**Mean (aplites)**
Zircon (total)	%	0.414	(4140 ppm)	0.790	0.319	0.159	2.457
Titanite (total)	%	0.116	(1160 ppm)	1.531	0.980	2.282	1.990
Apatite (total)	%	0.133	(1330 ppm)	0.031	0.023	0.050	0.032
Gittinsite	%	0.017	(175 ppm)	3.419	2.966	5.289	2.546
Gerenite	%	0.009	(93 ppm)	0.560	0.474	0.980	0.329
Allanite (total)	%	0.014	(136 ppm)	0.228	0.226	0.271	0.191
Aenigmatite	ppm	107.8	(0.011%)	554.5	372.9	498.3	1010.5
Monazite (total)	ppm	38.2	(0.004%)	420.0	445.7	369.5	414.0
Percleveite	ppm	19.7	(0.002%)	391.7	439.1	347.6	331.7
Elpidite	ppm	17.9	(0.002%)	2419.7	2380.7	3188.2	1736.9
Thorite	ppm	14.0	(0.001%)	2524.0	1668.0	4644.0	1691.0
Parisite	ppm	12.8	(0.001%)	127.5	89.9	169.9	168.0
Britholite (total)	ppm	11.2	(0.001%)	1015.8	893.0	1870.4	431.5
Gadolinite (total)	ppm	9.9	(<0.001%)	596.6	708.9	721.2	224.7
Bastnaesite	ppm	6.6	(<0.001%)	49.3	73.7	20.9	24.3
Stetindite	ppm	4.8	(<0.001%)	588.4	718.4	728.7	162.2
Pyrochlore	ppm	4.4	(<0.001%)	2248.5	1281.2	2957.4	3667.8
Fergusonite	ppm	4.1	(<0.001%)	199.2	135.4	318.7	220.1
Euxenite	ppm	4.1	(<0.001%)	5.4	2.3	4.4	13.4
Pectolite	ppm	2.8	(<0.001%)	518.0	435.0	772.8	445.7

Part B: Dilution Factors

Mineral	**Unit (area)**	**Mean (all data)**	**Dilution** (from granite)	**Dilution** (from pegmatite)	**Dilution** (from aplite)	**Dilution** (average)
Zircon (total)	%	0.414	0.8	0.4	5.9	2.4
Titanite (total)	%	0.116	8.4	19.6	17.1	15.1
Apatite (total)	%	0.133	0.2	0.4	0.2	0.3
Gittinsite	%	0.017	174.5	311.1	149.8	211.8
Gerenite	%	0.009	52.7	108.9	36.6	66.0
Allanite (total)	%	0.014	16.2	19.3	13.6	16.4
Aenigmatite	ppm	107.8	3.5	4.6	9.4	5.8
Monazite (total)	ppm	38.2	11.7	9.7	10.8	10.7
Percleveite	ppm	19.7	22.3	17.6	16.8	18.9
Elpidite	ppm	17.9	133.3	178.5	97.3	136.4
Thorite	ppm		119.1	331.0	120.8	180.3
Parisite	ppm	12.8	7.0	13.3	13.1	11.1
Britholite (total)	ppm	11.2	80.0	167.5	38.6	95.3
Gadolinite (total)	ppm	9.9	71.6	72.9	22.7	55.7
Bastnaesite	ppm	6.6	11.1	3.1	3.6	6.0
Stetindite	ppm	4.8	149.8	152.0	33.8	111.9
Pyrochlore	ppm	4.4	291.9	673.7	835.5	600.4
Fergusonite	ppm	4.1	32.9	77.3	53.4	54.5
Euxenite	ppm	4.1	0.6	1.1	3.3	1.6
Pectolite	ppm	2.8	153.6	272.9	157.4	194.6

Note: Dilution is calculated by dividing the abundance in drill core data by the average abundance in the till sample data.

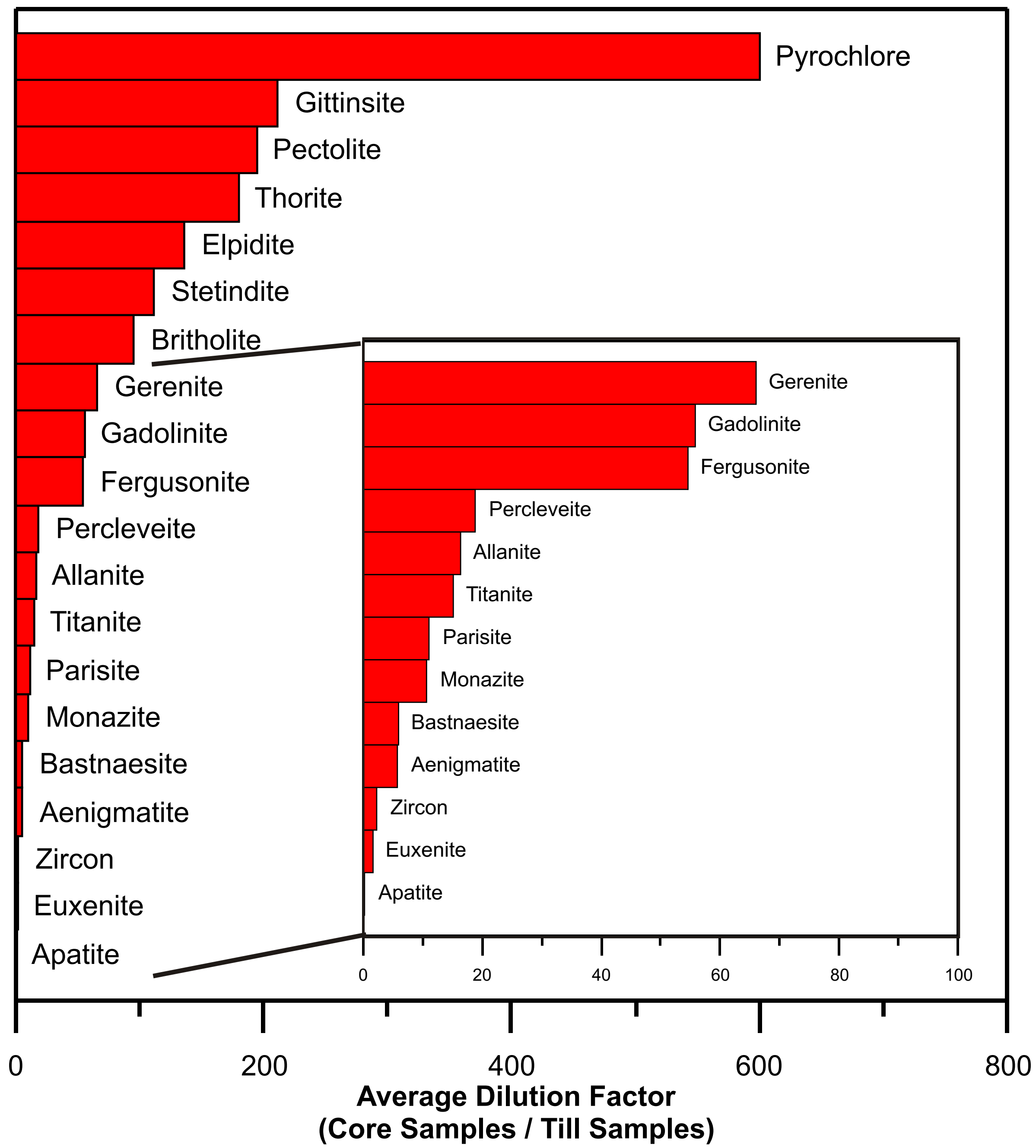

Figure 6.15. Chart illustrating the "dilution factors" for minerals known to be at least partially diagnostic of the Strange Lake deposits. The dilution factor is calculated by dividing the average abundance in drill-core samples from Baird (2018) by the average abundance in till samples from this project. Note that dilution factors would change if more specific averages of rock types analyzed by Baird (2018) were used instead of the overall abundance in all data. See text for discussion.

An evaluation of particle and grain size information for minerals identified by MLA analysis reveals systematic differences between minerals present at various abundance levels. Major minerals and some minor minerals dominantly occur as larger monomineralic particles, but less abundant accessory and trace minerals occur mostly as smaller ‘grains’ within larger composite particles, suggesting that they form intergrowths with or inclusions in more common minerals. Observations from BSE images of grains and particles support these inferences. This mode of occurrence will influence their behaviour in natural settings, and it also has implications for reliability and precision of data for some of the rarer minerals associated with Strange Lake. Some preliminary information on mineral associations derived from the MLA-SEM data suggest that these vary among potential indicator minerals.

In summary, the MLA-SEM data provide important information about systematic mineralogical variations in till samples from the Strange Lake area. Data reveal patterns that likely have a geographic component of probable regional origin, and also geographic patterns that record dispersion from Strange Lake. To gain more insight into these aspects, an additional step is required, i.e., the preparation of maps that display such geographic variation patterns in more detail. This material is presented in the next chapter.

CHAPTER 7: SPATIAL AND GEOGRAPHIC VARIATION PATTERNS IN MINERALOGY

GENERAL SUMMARY

Evaluation of numerical and statistical data in Chapter 6 suggested that many minerals detected by MLA-SEM analysis exhibit systematic geographic abundance variations. This chapter evaluates such patterns in more detail. The most obvious trends are shown by major silicate minerals such as quartz, the feldspars, garnet and hornblende. These patterns are considered to have regional causes linked to the relative contributions from different igneous and metamorphic rock types in the area. Some minor and accessory minerals mimic these regional patterns, suggesting that their abundance is controlled by similar factors. A suite of distinctive minor, accessory, and trace minerals, some of which are characteristic of Strange Lake, show more diverse individual patterns that suggest derivation and dispersion from this specific source. For the rarest minerals associated with Strange Lake, the clarity of patterns is partly obscured by seemingly random variation that is likely linked to the influence of ‘probability effects’ connected to sampling and preparation. Nevertheless, geographic patterns reveal contrasts where specific indicator minerals decline in abundance with increasing distance, but others increase in abundance with distance or retain near-constant abundance. The most effective and widespread indicator minerals are gittinsite and gerenite, which are the most abundant of the diagnostic Strange Lake minerals, but several other minerals remain detectable over distances of some 35 km. The persistence of at least some indicator minerals at the eastern end of the sample grid implies that they could remain detectable over greater distances in a down-ice direction.

METHODS AND DATA PREPARATION

Introduction

This Chapter presents and assesses spatial and geographic patterns revealed by the MLA-SEM data from the till samples. It builds the upon observations from numerical data and statistical analyses presented in Chapter 6, which suggest that many minerals show systematic geographic variation patterns in abundance or occurrence. Such patterns probably have more than one cause, and analysis of numerical data suggests that some, especially for major minerals, are regional in nature, caused by variable contributions from different regional bedrock sources. The separation of the samples into two groups based upon composite variables [garnet + hornblende + ilmenite] and [quartz + K-feldspar] supports this view. However, other geographic variation patterns may result from the dispersion of uncommon Zr-, Nb- and REE-bearing minerals from the mineral deposits and granites of the Strange Lake area. Numerical or statistical methods cannot easily distinguish between regional and local patterns, and broad measures such as correlation coefficients and average compositions may miss subtler patterns or trends. The first part of this chapter summarizes the methods used to display and assess geographic variations in mineralogy, and the second part assesses patterns for groups of minerals, based again on mean abundance. The chapter presents numerous maps at different scales, and its final section summarizes the key observations, and integrates these with observations from Chapter 6.

Regional Mineral Abundance Maps

The simplest way to assess geographic variations is to make a map, which explains why maps outnumber text pages in this chapter. All maps were prepared using the software program “Surfer”, which is a simple GIS application marketed by Golden Software, Inc.

An example is provided in Figure 7.1, which illustrates patterns for an important minor mineral (apatite). This shows all till samples, aside from control sample G2-15, and indicates the relative abundance of apatite by symbol size, with larger symbols representing higher values. The variation in symbol size is continuous, and five index values representing specific abundances are provided in the legend. The five samples collected from eskers are distinguished by symbol colour. These ‘bubble maps’ are semi-quantitative, but illustrate broad trends well, and highlight samples that have unusually high or low abundances. For apatite, the map shows that most of the higher values (> 0.4 area %) are located at the west end of the sample grid, nearest to Strange Lake, and that apatite abundance generally diminishes with distance from Strange Lake. The samples from eskers also have low apatite abundances. However, the pattern is more complex in detail, because *some* samples in Grid 1 (close to Strange Lake) actually have low apatite abundances similar to those of the most distant samples in Grid 3. Details such as this are generally not evident from simple inspection of statistical data.

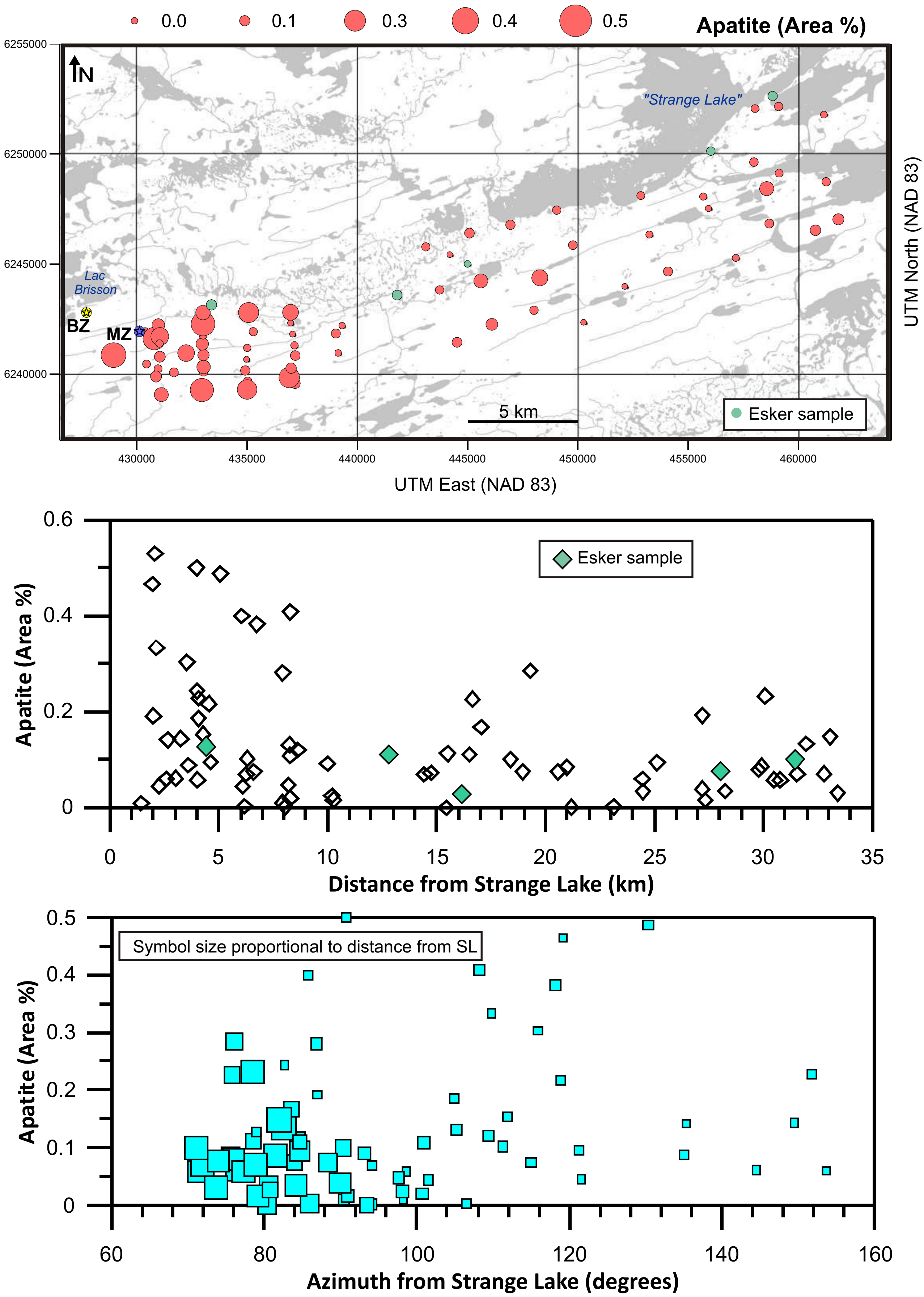

Figure 7.1. Geographic variation patterns for apatite (area %). Upper Panel is a map view with proportional symbols. Lower panels show apatite abundances against distance and azimuth from Strange Lake. See text for discussion of these examples.

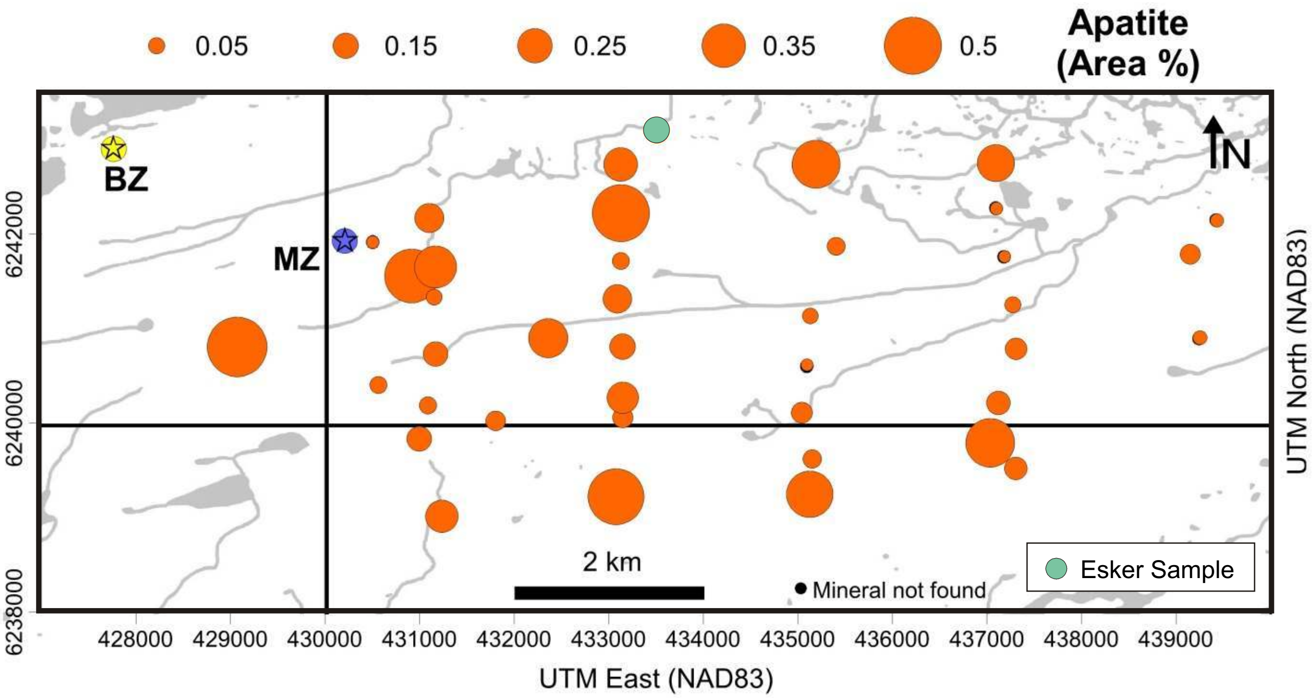

Figure 7.2. Example of a more detailed mineral abundance map for the western part of the area (Grid 1) showing the distribution of apatite (area %) in till samples. See text for discussion.

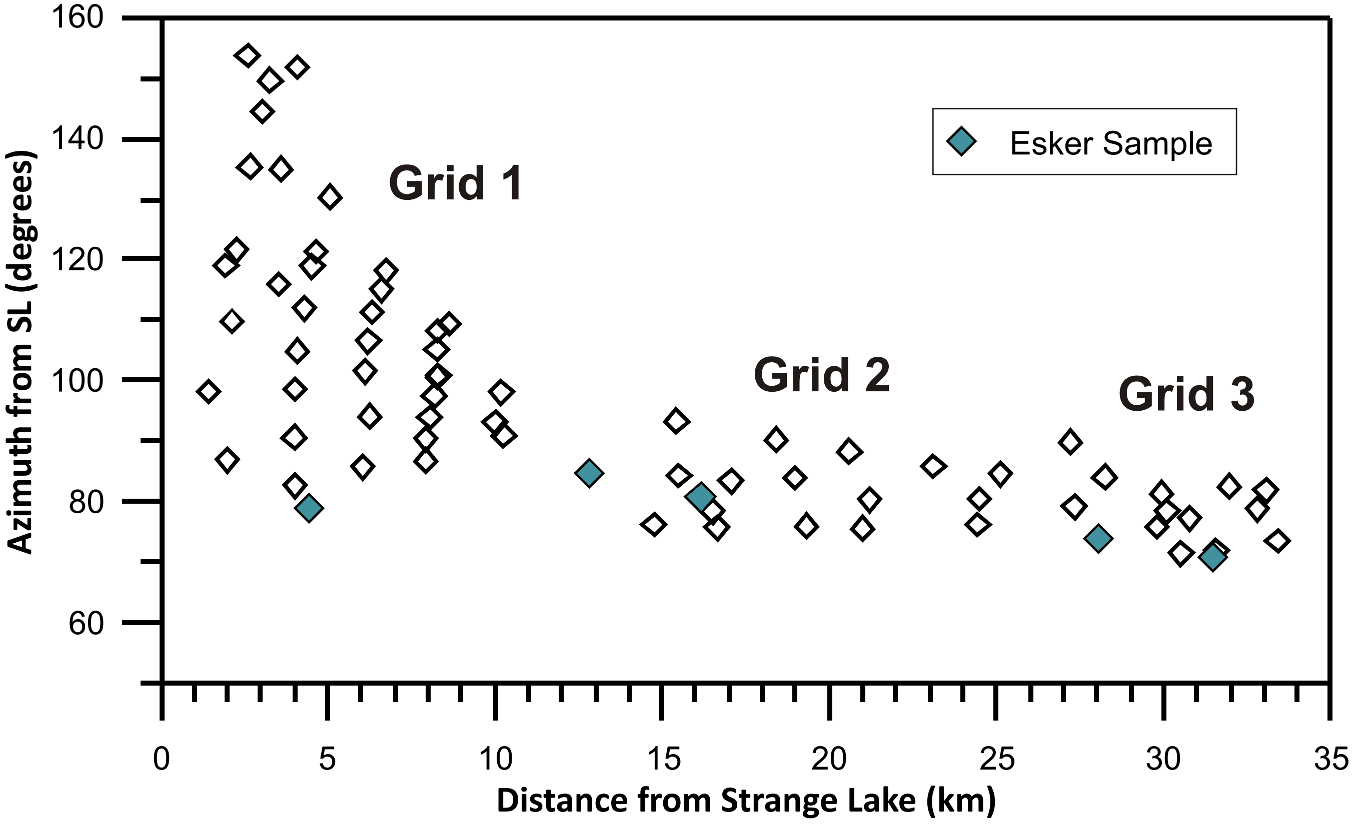

Figure 7.3. The relationship between the distance of till samples from Strange Lake and their azimuth direction from Strange Lake, showing the greater range in azimuth for Grid 1 samples and the convergence of azimuth values with increasing distance.

Detailed Mineral Abundance Maps for Grid 1

Some minerals are found mostly or only within Grid 1, closest to Strange Lake, where the closer sample spacing in this area makes it more difficult to see patterns. Detailed mineral abundance maps for Grid 1 are thus used to complement regional maps for selected minerals, and allow closer comparison. Figure 7.2 provides a detailed map for apatite in Grid 1. The format is identical to regional mineral abundance maps, but the symbol sizes and index values may differ. Detailed maps allow easier recognition of more local features, such as a group of apatite-rich samples extending eastward from the Main Zone deposit, and a possible subparallel trend of apatite enrichment on the southern edge of Grid 1. Figures 7.1 and 7.2 also illustrate some of the challenges in interpreting results. At first sight, these patterns could be taken to indicate derivation of apatite from Strange Lake, but a comparison of data from till samples with the drill core data of Baird (2018) from the Main Zone shows that till samples (on average) contain more apatite than the drill core samples. In fact, apatite is the only potential indicator mineral from Strange Lake that has a core/till dilution factor that is consistently less than 1 (see Table 6.12; Figure 6.15), implying that it must mostly be derived from other rock units. This suggests that other regional factors dominate geographic variation in apatite abundance, even if material from Strange Lake plays some part.

Mineral Abundance Profiles

Regional mineral abundance maps are accompanied by profiles that relate mineralogy to the distance of the samples from Strange Lake, and their azimuth directions from Strange Lake. Figure 7.1 (lower panels) illustrates both types of profiles for apatite. The distance profile shows that apatite generally decreases in abundance eastward through the grid, but also shows many apatite-poor samples even within a few kilometres of Strange Lake. The azimuth profile shows that apatite abundance has little relationship to geographic direction, and that higher values are mostly (but not exclusively) shown by samples that are closer to Strange Lake. The distance from Strange Lake is indicated by the relative symbol size, with larger symbols representing greater distances.

As summarized in Chapter 4, the distance and azimuth values are averages of the respective calculations with reference to locations of the Main Zone and B-Zone deposits. Azimuth is defined as the compass bearing leading from the potential source to the sample location. Due to the elongated geometry of the sampling area (Figures 4.3 and 7.1), azimuth directions naturally converge to 70°-90°

with increasing distance, so the larger (distant) symbols will always cluster in these profiles. In order to avoid excessive compression of the scales, samples G2-15 (off-grid control sample) and G1-6 (located southwest of Strange Lake Main Zone deposit) are omitted from azimuth profiles. The relationship between azimuth and distance is illustrated for reference purposes in Figure 7.3; note that Grid 1 samples will always display greater variation in azimuth direction from Strange Lake compared to samples from Grids 2 and 3.

EXAMPLES OF GEOGRAPHIC VARIATION PATTERNS

Major Minerals

Examination of numerical data (see Chapter 6) suggested that quartz, K-feldspar, garnet, hornblende and ilmenite all show systematic geographic patterns, but no patterns were evident for albite and plagioclase. Patterns for some selected major minerals are indicated via maps, and profiles described in the following text. Additional maps for other minerals not discussed in detail are placed in the Appendices.

Regional abundance maps and profiles for quartz (Figure 7.4) show that its pattern is not as simple as the averages of data from the three grids might suggest. Samples in the east (Grids 2 and 3) do indeed contain more quartz (30-50 area %) on average compared to those from Grid 1, but the Grid 1 area also includes some local high values. The geographic variation in quartz is largely defined by lower quartz abundances (< 15 area %) confined mostly in Grid 1, closest to Strange Lake. This pattern is also illustrated well by distance and azimuth profiles, which also show that high quartz abundances are not restricted to the most distant samples. A similar pattern is shown by the geographic distribution of K-feldspar (Figure 7.5). For both minerals, there is a diffuse ‘transition’ in abundance patterns located slightly west of the mid-point of the sample array, roughly 15 km from the Strange Lake Main Zone deposit (Figures 7.4; 7.5).

Hornblende, garnet and ilmenite show marked geographic variation that has the *opposite* sense, in that they are typically most abundant in the area of Grid 1, closest to Strange Lake. The pattern for garnet (Figure 7.6) is especially striking. Aside from 3 samples, till samples in Grids 2 and 3 contain less than 5 area % garnet, and almost all garnet-rich samples are located in Grid 1. However, the distance and azimuth profiles show that Grid 1 also contains some samples that have low garnet abundances, which correspond with samples that have higher quartz contents in this area. The patterns for hornblende and ilmenite are almost identical to the pattern shown by garnet. For all three minerals, there seems to be a west-east ‘transition’, located in the same general position as the transition noted above for quartz and K-feldspar.

Analysis of numerical data (see Chapter 6) suggested that the composite variables [quartz + K-feldspar] and [garnet + hornblende + ilmenite] allow subdivision of the samples into two groups. The geographic variation of these composite variables (Figures 7.7; 7.8) amplifies this conclusion, and the pattern for [garnet + hornblende + ilmenite] is especially striking (Figure 7.8). Aside from three samples within Grid 2, high values of [gt + hbl + ilm] are clearly restricted to Grid 1. Regional mineral abundance maps for the other feldspars (albite and plagioclase) show little systematic geographic variation, although plagioclase abundances do seem to increase slightly with distance from Strange Lake (Figure 7.9).

The major minerals are not diagnostic of the Strange Lake Intrusion or its mineral deposits, and some of them (garnet, ilmenite and plagioclase) are absent or of trivial importance in these potential source rocks. It is highly unlikely that material derived from Strange Lake is responsible for these geographic patterns. These geographic patterns more likely reflect the relative contributions of various igneous and metamorphic rocks in the wider area, as discussed in Chapter 6. The relationships between till mineralogy and regional geological units are further discussed in the next chapter, but the ‘transition’ noted in the centre of the area roughly corresponds with the boundary between metamorphic rocks derived from mafic and intermediate igneous rocks (west) and those derived from more quartz-rich granitic rocks (east), as outlined in Figure 2.8 and by Ryan et al. (2003).

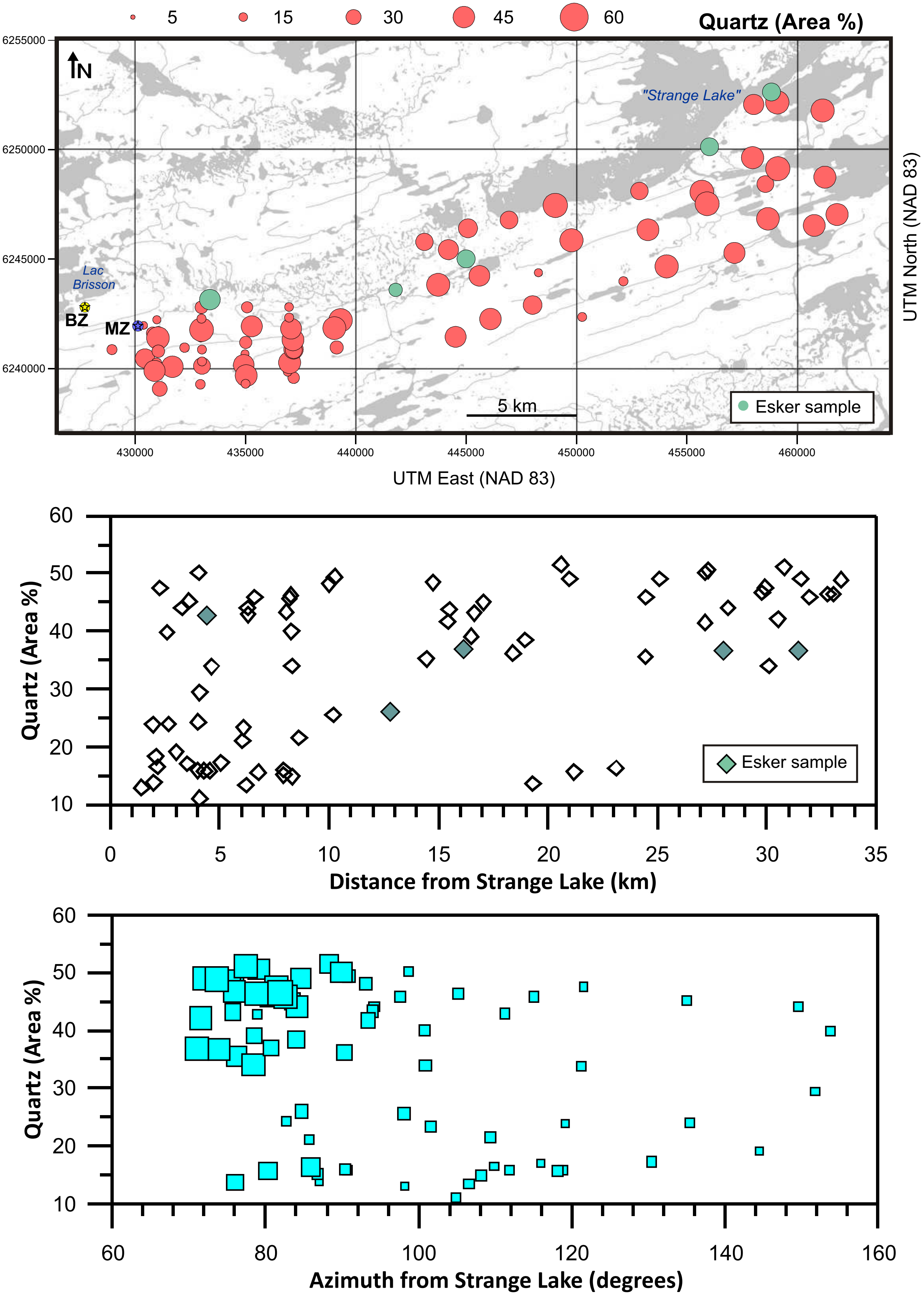

Figure 7.4. Geographic variation patterns for quartz (area %). Upper Panel is a map view with proportional symbols. Lower panels show quartz abundances against distance and azimuth from Strange Lake. See text for discussion.

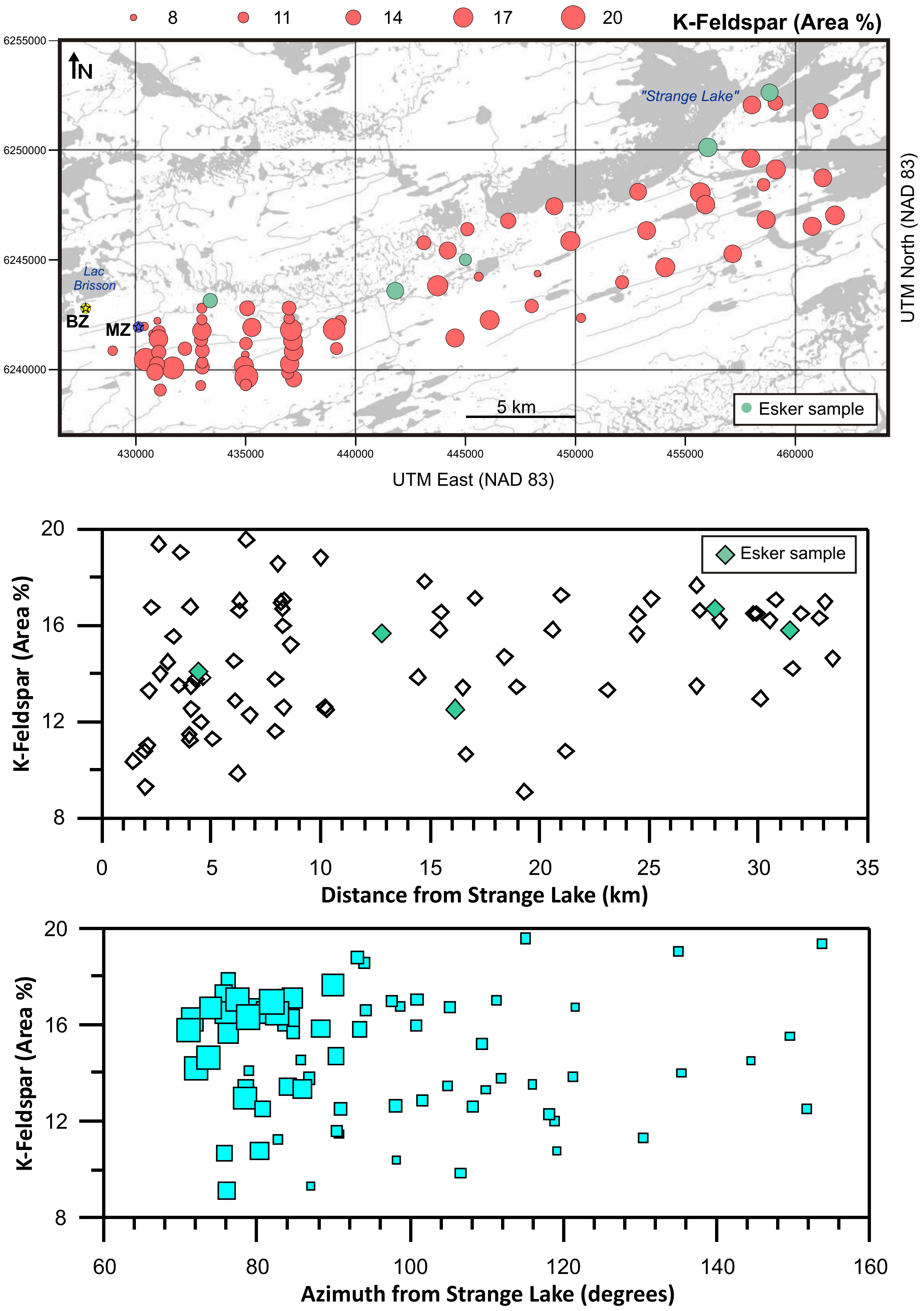

Figure 7.5. Geographic variation patterns for K-Feldspar (area %). Upper Panel is a map view with proportional symbols. Lower panels show albite abundances against distance and azimuth from Strange Lake. See text for discussion.

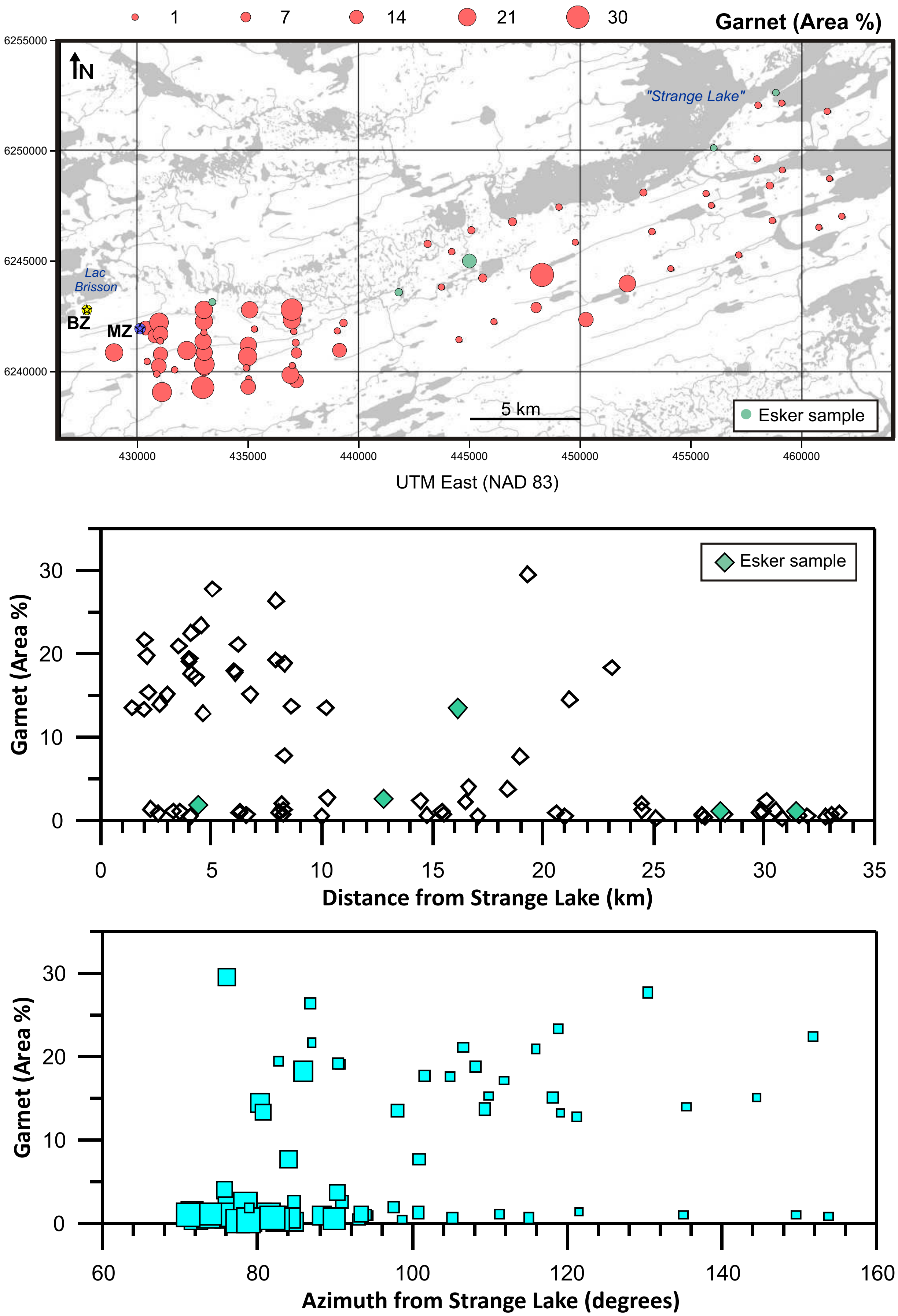

Figure 7.6. Geographic variation patterns for garnet (area %). Upper Panel is a map view with proportional symbols. Lower panels show garnet abundances against distance and azimuth from Strange Lake. See text for discussion.

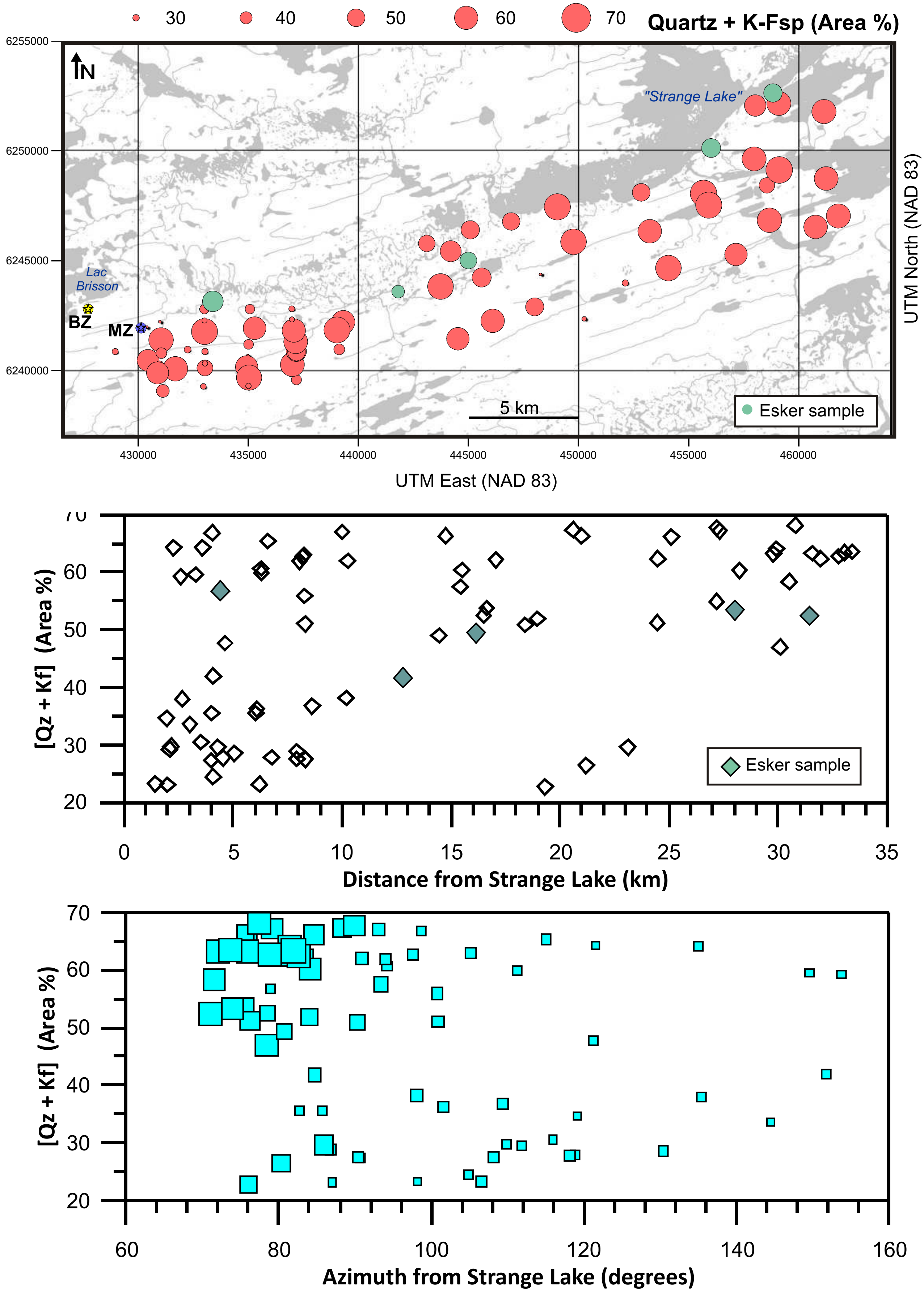

Figure 7.7. Geographic variation patterns for [quartz + K-feldspar] (area %). Upper Panel is a map view with proportional symbols. Lower panels show [Qz + Kf] abundances against distance and azimuth from Strange Lake. See text for discussion.

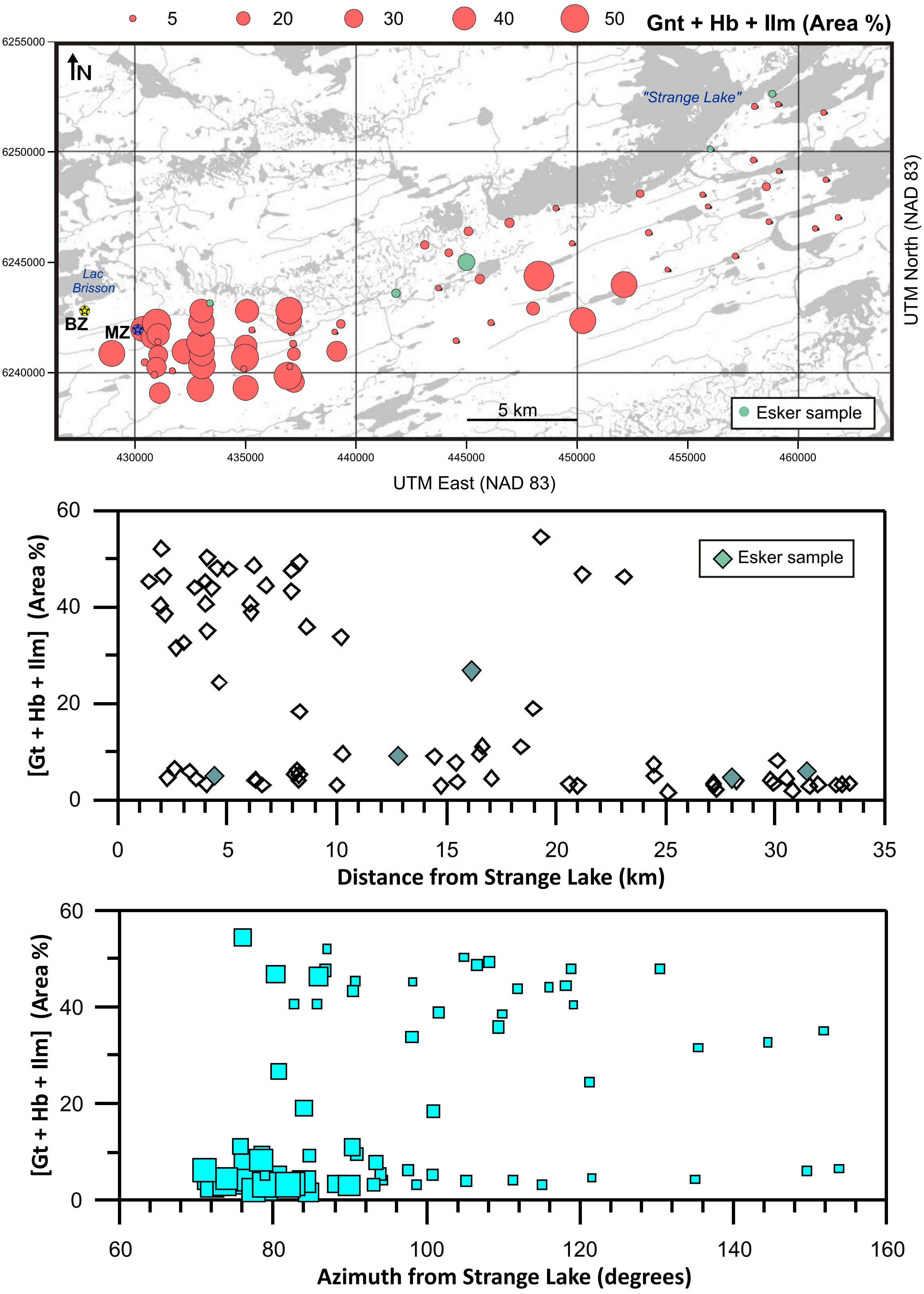

Figure 7.8. Geographic variation patterns for [garnet + hornblende + ilmenite] (area %). Upper Panel is a map view with proportional symbols. Lower panels show [gt + hb + ilm] abundances against distance and azimuth from Strange Lake. See text for discussion.

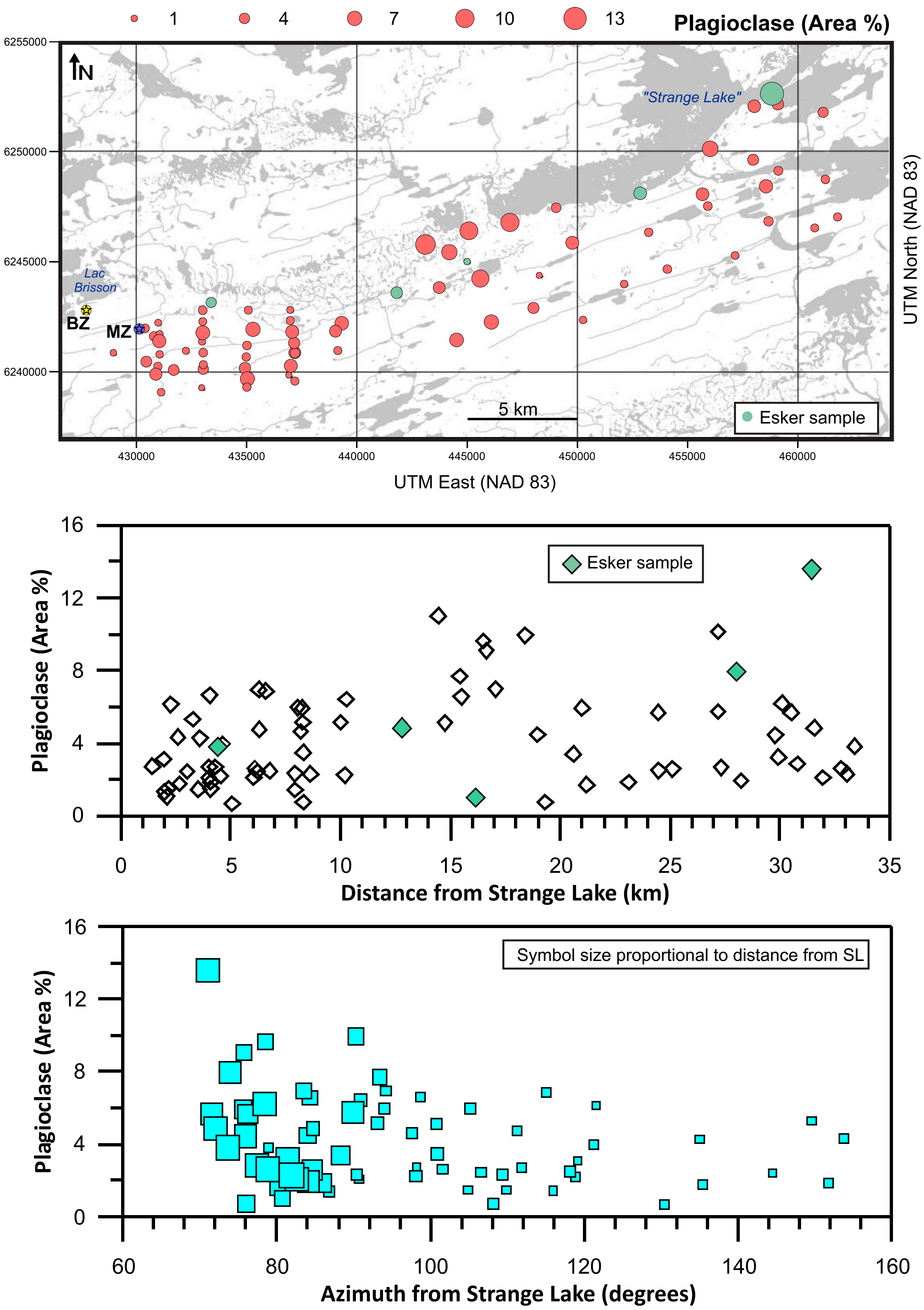

Figure 7.9. Geographic variation patterns for plagioclase (area %). Upper Panel is a map view with proportional symbols. Lower panels show plagioclase abundances against distance and azimuth from Strange Lake. See text for discussion.

Minor Minerals

Minor minerals are a diverse group dominated by silicates, but also include some oxides and phosphates. They include zircon and apatite, both of which are important at Strange Lake, but not diagnostic of it. As discussed in Chapter 6, statistical data suggest that at least some of these minerals show systematic geographic variations in abundance. Some of these minerals, such as nepheline and magnetite, show no obvious geographic patterns. Others, such as limonite (iron ... hydroxide) mimic the patterns of major iron-rich minerals such as garnet, ilmenite and hornblende. Thus, the pattern for limonite (Figure 7.10) is consistent with it forming as a weathering product of more abundant iron-rich minerals. Biotite and epidote show no strong geographic variation patterns, but both increase in abundance slightly with distance from Strange Lake, and chlorite has a similar pattern (Figure 7.11). For these minerals, there appears to be a 'transition' slightly west of the midpoint of the sample array, as noted previously for the major minerals and composite variables based upon them. Grunerite (an amphibole-group mineral enriched in Mg) shows a pattern very similar to that shown by [gt + hbl + Ilm] (Figure 7.12). This is an expected result, given the strong correlation revealed by statistical analysis (see Table 6.6). The pyroxene-group minerals augite and hypersthene both show increasing abundance with distance from Strange Lake, but the pattern for augite (Figure 7.13) is the most striking. This is also one of the few minerals for which samples collected from eskers (in the western part of the grid) diverge from trends shown by other samples.

Four minerals in this group (zircon, aegirine, titanite and apatite) may in part be controlled by dispersion from Strange Lake, as they are typically abundant in peralkaline igneous rocks. Aegirine (a Na-rich pyroxene) shows a peculiar pattern (Figure 7.14) that is distinct from that shown by other pyroxenes such as augite (compare to Figure 7.13). It is enriched in Grid 1, especially close to the Main Zone deposit, but is also enriched at the eastern end of the sample array, with generally low abundances between these extremes. Zircon has striking geographic variation in abundance, with strong enrichment in Grid 1, especially close to the Main Zone deposit, and diminishing abundance with distance from Strange Lake (Figure 7.15). However, moderate zircon enrichment is present in the southern part of Grid 2, where it corresponds with samples that are also enriched in garnet and hornblende (compare to Figure 7.8). Apatite was previously discussed in the introduction (see Figure 7.1), and is also relatively enriched in the Grid 1 area, close to Strange Lake, but not to the same extent as zircon. However, titanite shows no clear geographic variation pattern in abundance.

The similarities between geographic variation patterns shown by some of the minor minerals and those shown by major minerals suggests that for some minor minerals abundance variations are controlled by regional provenance, rather than by specific contributions from the Strange Lake area. However, the patterns shown by zircon and aegirine do not fit well with regional trends, suggesting that both may be influenced by contributions from Strange Lake. The rather strange pattern defined by aegirine, showing both proximal and distal enrichment, is something of a puzzle, but some less abundant accessory minerals mimic this pattern (see later discussion). Zircon is an important mineral locally at Strange Lake, but the core/till dilution factors for zircon are low (<5) and less than 1 with respect to some rock types (see Table 6.12 and Figure 6.15). Zircon is a common accessory mineral in many rock types, and is very durable, so other sources are likely also involved. The patterns shown by titanite and apatite are not as obvious and derivation of apatite entirely from Strange Lake is not likely, because it is more abundant in tills than in drill core. Apatite is present in many rocks, especially those of mafic igneous type. Titanite is even more widespread in many igneous and metamorphic rocks, so other sources are likely. In summary, none of these four minerals is fully diagnostic of Strange Lake, but the Strange Lake Intrusion and its mineral deposits probably contribute at least some material to nearby tills, especially for zircon and aegirine. Detailed maps showing the geographic patterns of zircon and aegirine in Grid 1 are illustrated in Figure 7.16, which shows the existence of two subparallel enrichment trends, one of which is spatially associated with the Main Zone deposit.

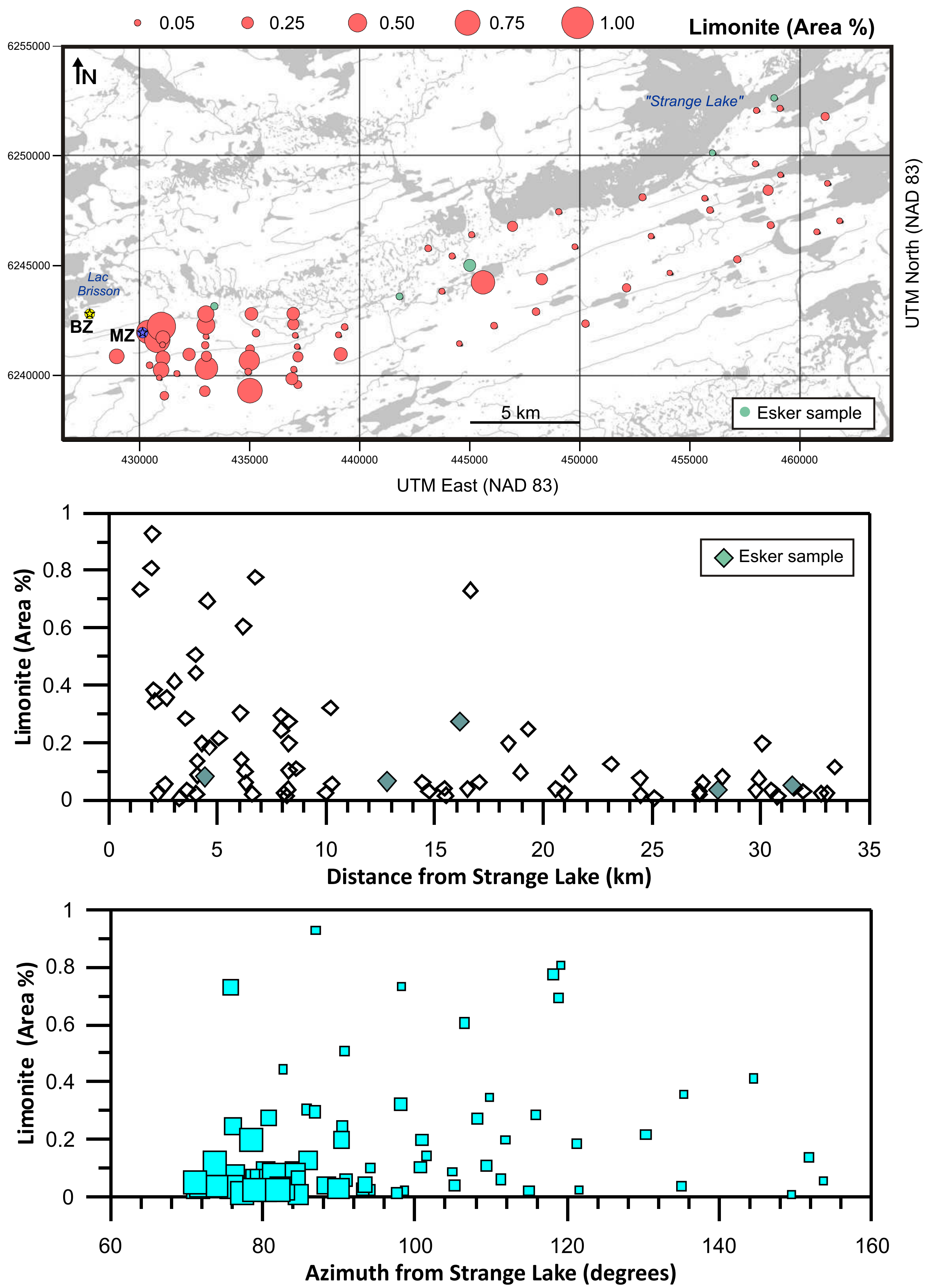

Figure 7.10. Geographic variation patterns for limonite (area %). Upper Panel is a map view with proportional symbols. Lower panels show limonite abundances against distance and azimuth from Strange Lake. See text for discussion.

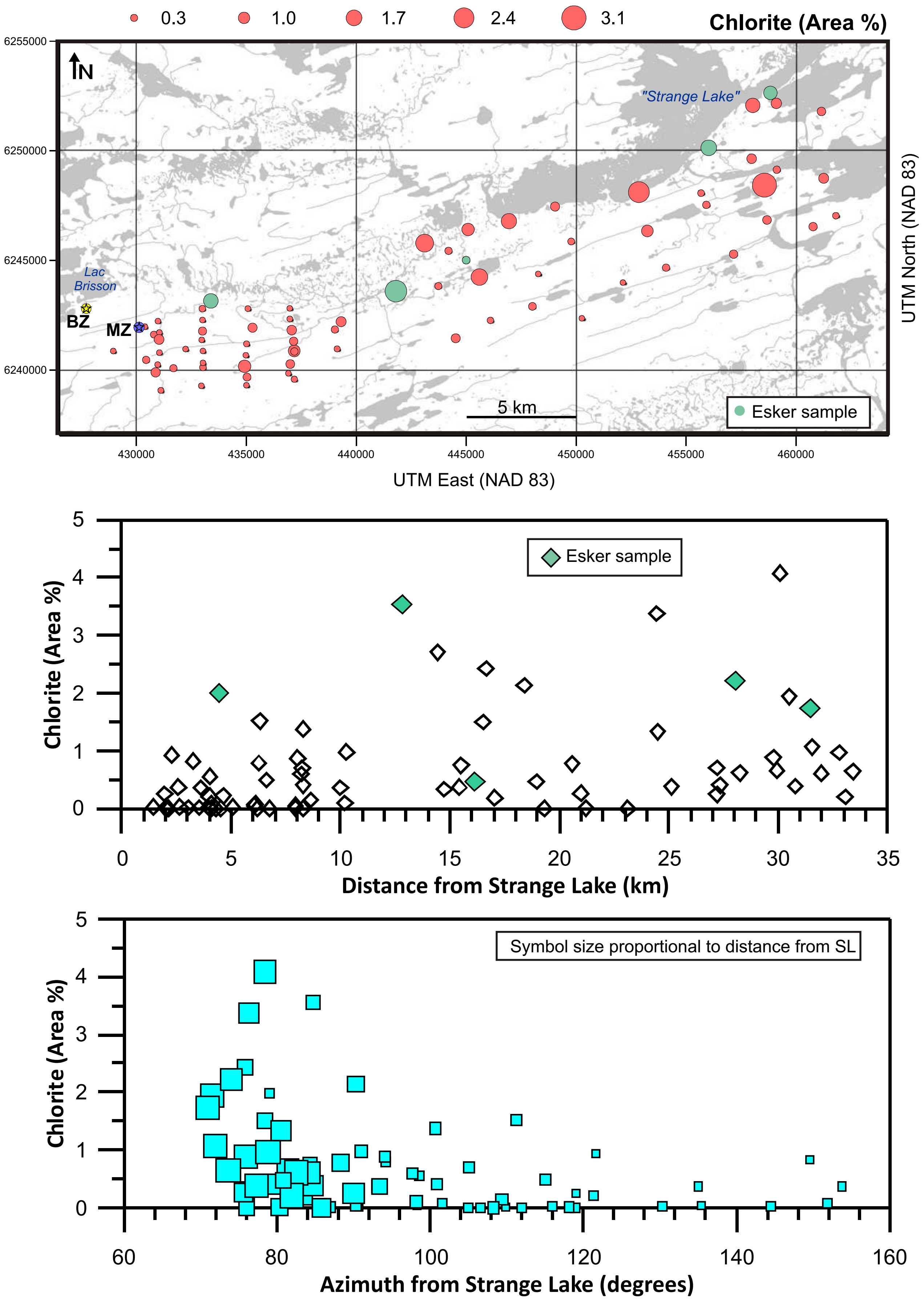

Figure 7.11. Geographic variation patterns for chlorite (area %). Upper Panel is a map view with proportional symbols. Lower panels show chlorite abundances against distance and azimuth from Strange Lake. See text for discussion.

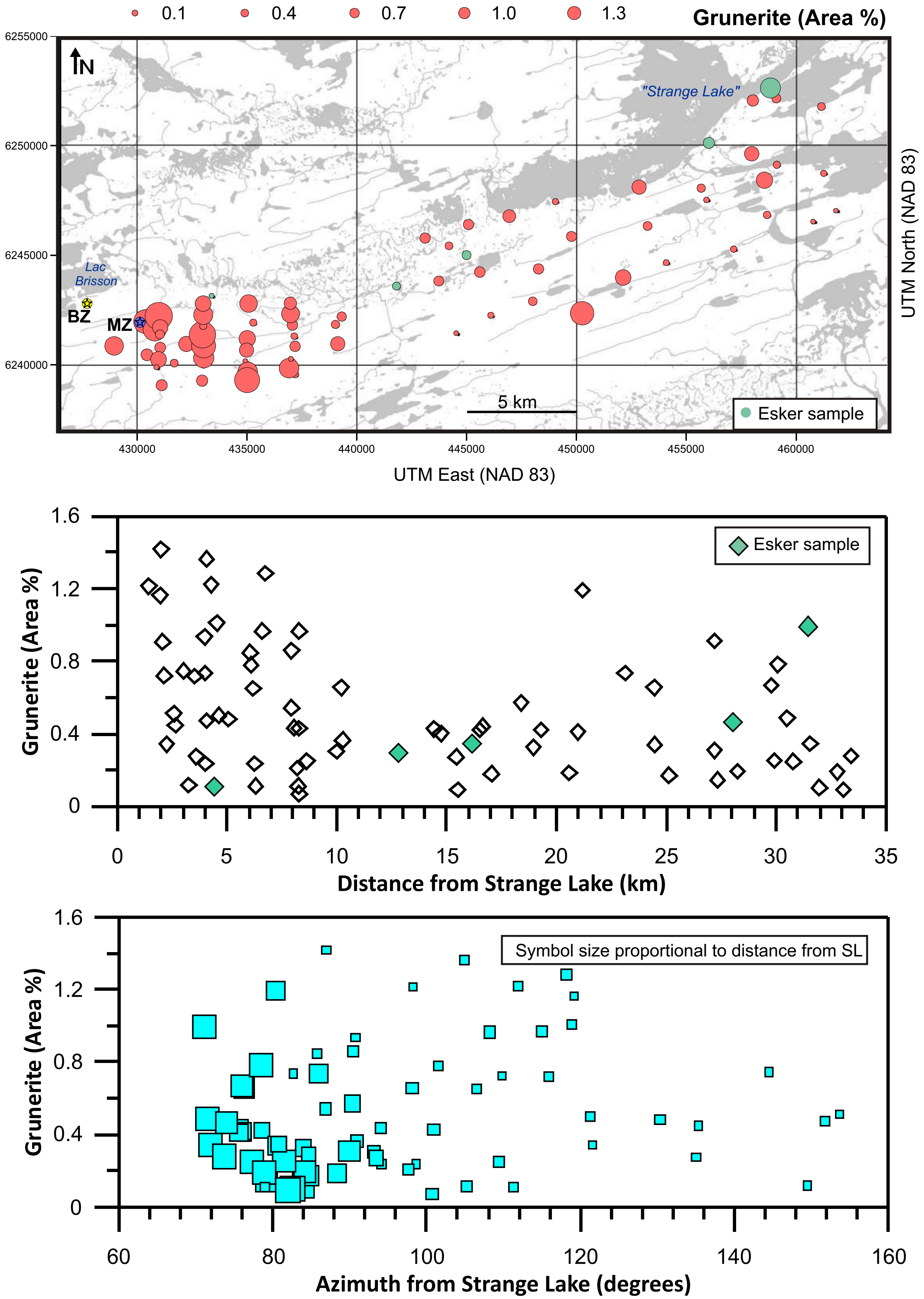

Figure 7.12. Geographic variation patterns for grunerite (area %). Upper Panel is a map view with proportional symbols. Lower panels show grunerite abundances against distance and azimuth from Strange Lake. See text for discussion.

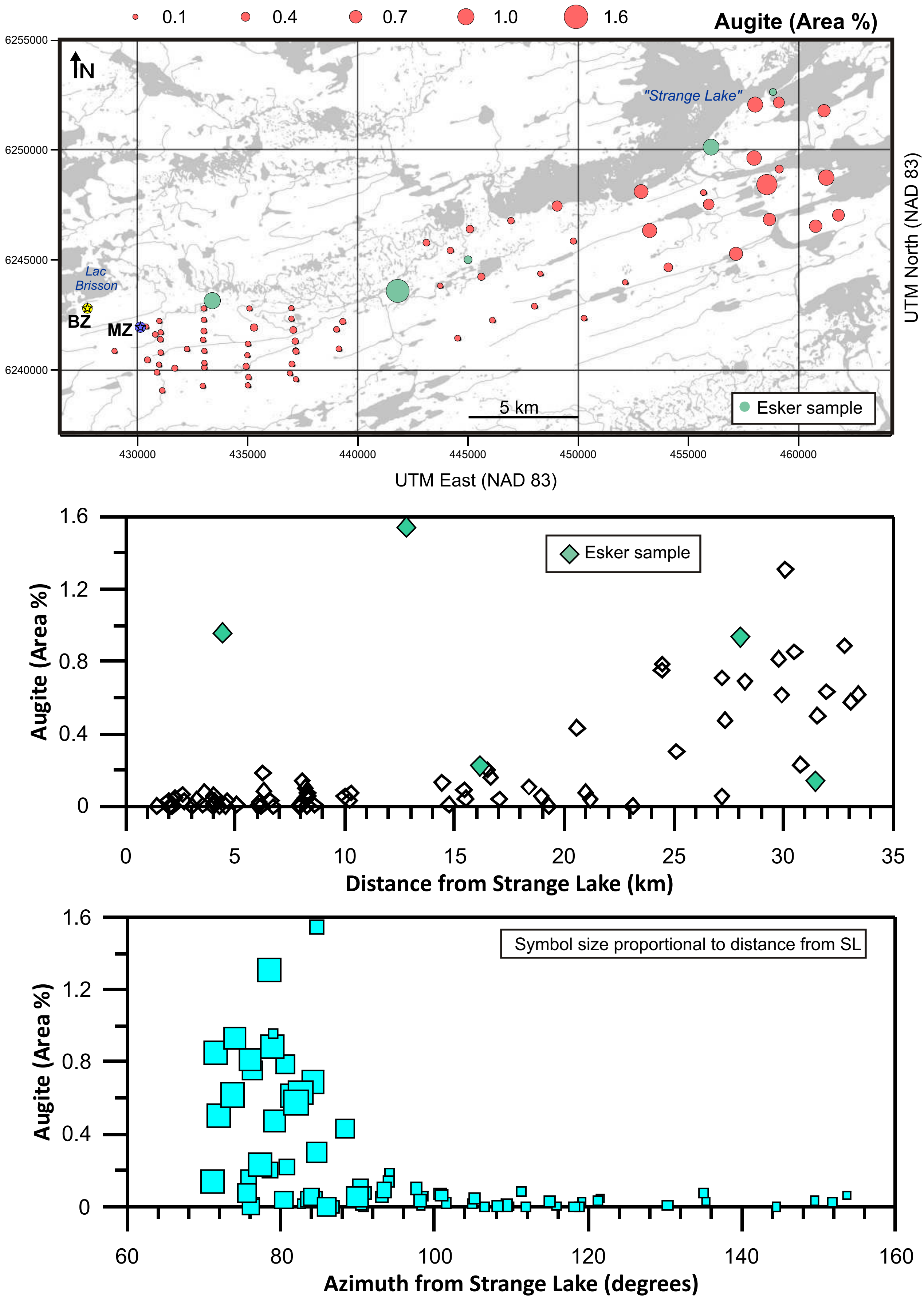

Figure 7.13. Geographic variation patterns for augite (area %). Upper Panel is a map view with proportional symbols. Lower panels show augite abundances against distance and azimuth from Strange Lake. See text for discussion.

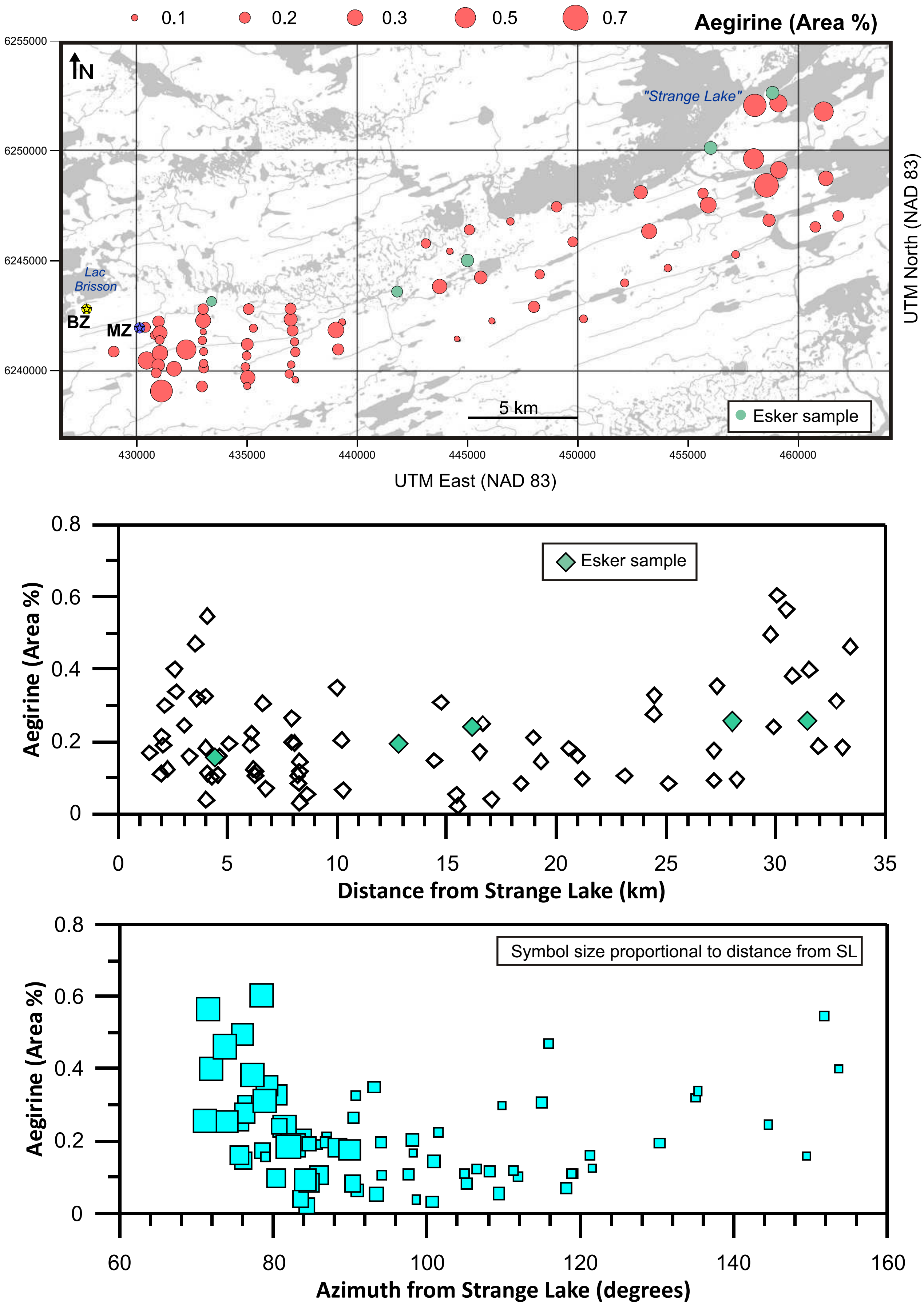

Figure 7.14. Geographic variation patterns for aegirine (area %). Upper Panel is a map view with proportional symbols. Lower panels show aegirine abundances against distance and azimuth from Strange Lake. See text for discussion.

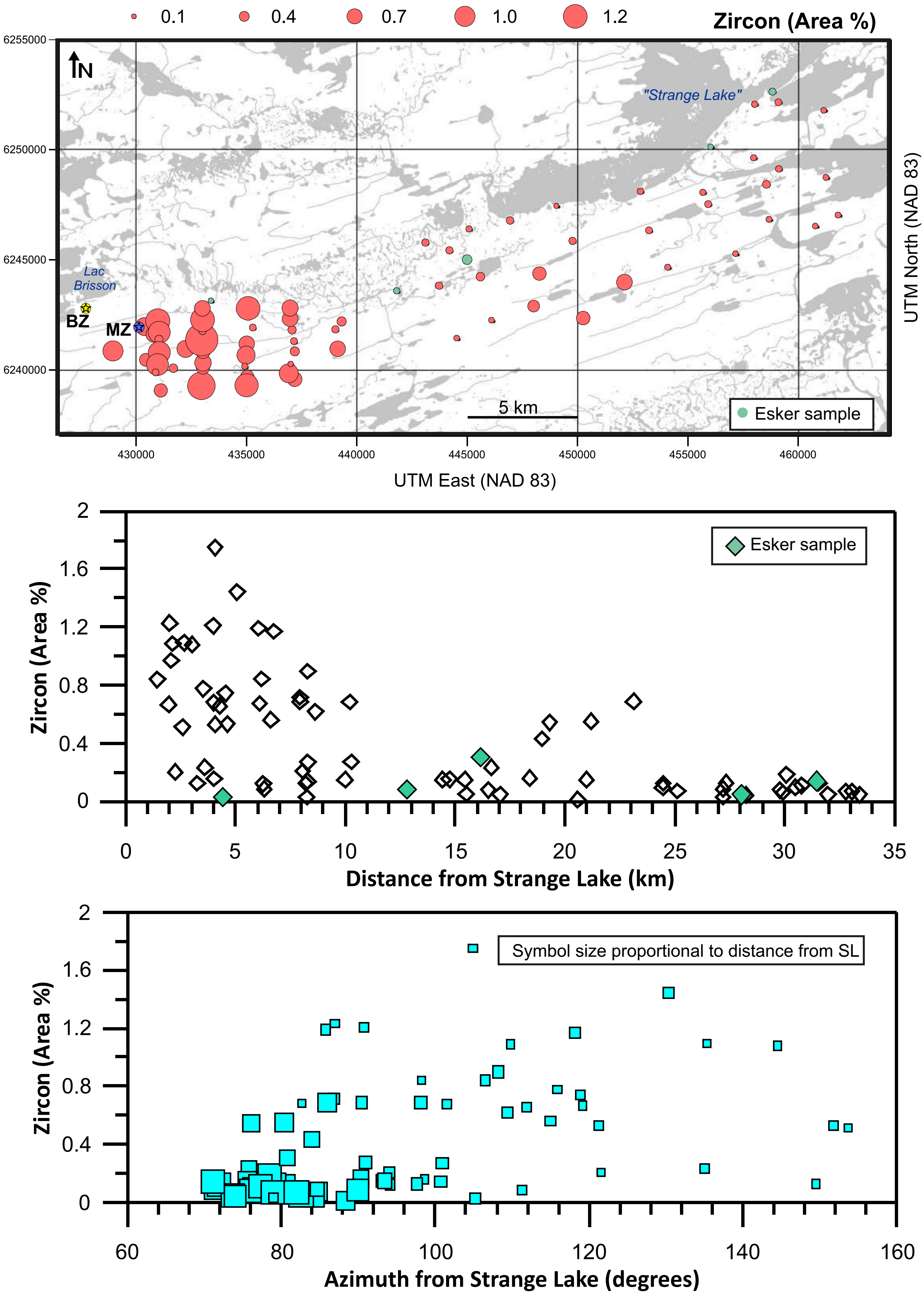

Figure 7.15. Geographic variation patterns for zircon (area %). Upper Panel is a map view with proportional symbols. Lower panels show zircon abundances against distance and azimuth from Strange Lake. See text for discussion.

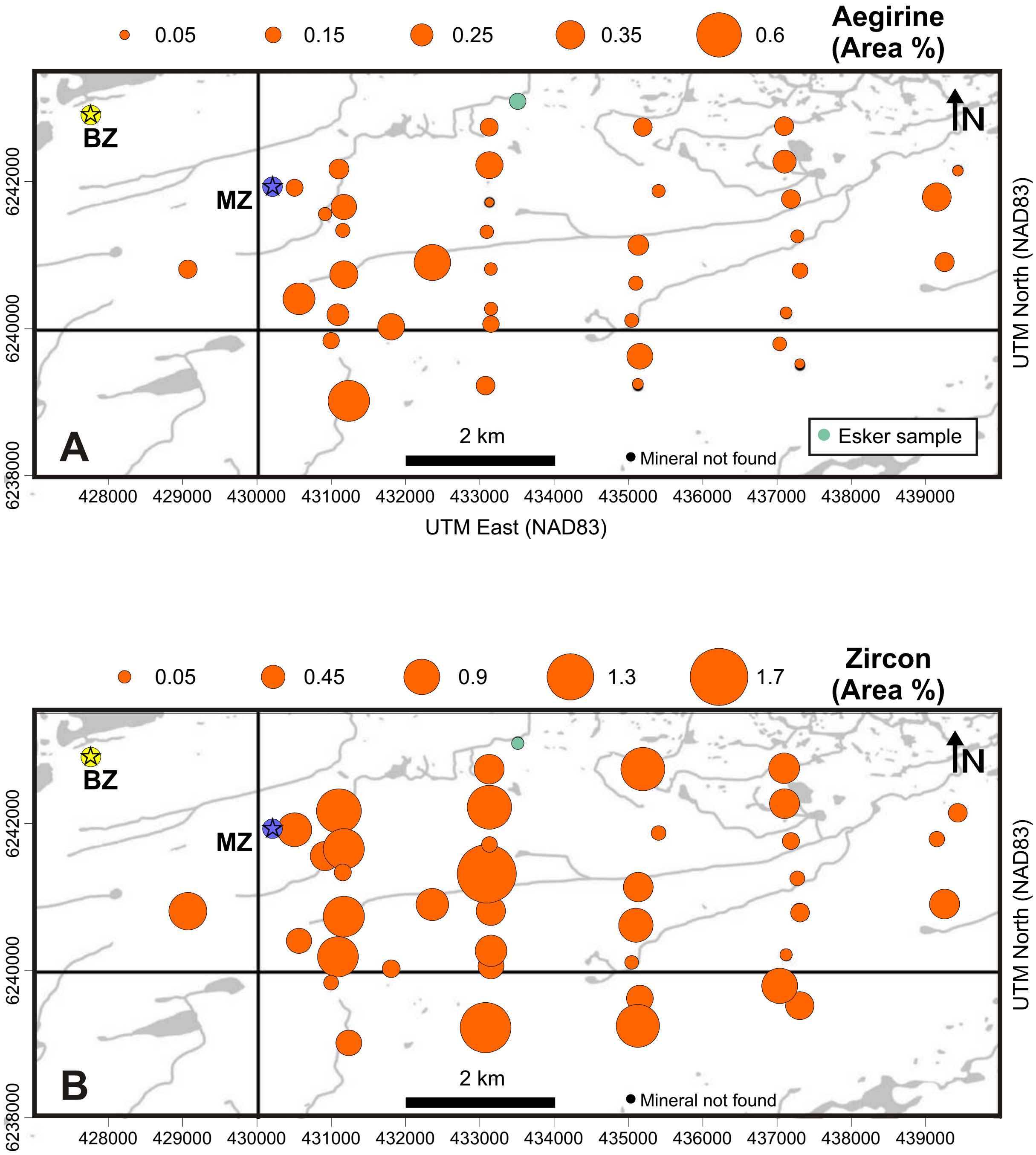

Figure 7.16. Geographic variation patterns for minerals in Grid 1, closest to the Strange Lake deposits. (A) Aegirine abundances. (B) Zircon abundances. See text for discussion.

Common Accessory Minerals

This group of minerals includes some that have some association with Strange Lake (gittinsite, possibly allanite and aenigmatite) and some that have far more diverse sources in igneous and metamorphic rocks. For ease of description and discussion, maps and profiles represent these minerals in area ppm, rather than in area %. Analysis of numerical data and statistical measures suggest that some of these minerals show systematic geographical variation (see Chapter 6).

Staurolite and Al-silicate (polymorph not discriminated) are common minerals in metamorphic rocks of sedimentary origin. Their patterns are generally uninformative, although both do seem to be more abundant, on average, in the eastern part of the sample array, distant from Strange Lake (e.g., Figure 7.17). Zoisite, also typically found in metamorphic rocks, has a similar geographic pattern, but seems to be anomalously abundant in esker samples from grids 1 and 2 (Figure 7.18). Among these three minerals, only staurolite displays any enrichment close to Strange Lake, but this is sporadic. For Al-silicate and zoisite, there appears to be a 'transition' in abundance patterns near the midpoint of the sample array, as noted previously for some major and minor minerals.

The rare zirconosilicate mineral gittinsite, which is highly characteristic of Strange Lake, has a curious pattern defined by enrichment in some parts of Grid 1, near Strange Lake, but also by enrichment within Grid 3, at the eastern end of the sample array (Figure 7.19). Overall, gittinsite abundances tend to *increase* with distance from Strange Lake, as illustrated by distance profiles, but some samples in the eastern part of the area retain low abundances. The pattern for gittinsite is similar in many respects to that shown by aegirine (compare to Figure 7.15). The uncommon mineral aenigmatite, known at Strange Lake but not unique to the deposit, also shows enrichment in areas closest to the Main Zone Deposit, but its pattern is not exactly the same as for gittinsite (Figure 7.20). Figure 7.21 shows detailed maps for gittinsite and aenigmatite in the Grid 1 area. Both minerals have localized enrichment in this area, and seem also to define two subparallel enrichment trends, one of which is spatially associated with the Main Zone deposit. Allanite patterns are illustrated in Figure 7.22, for comparison with the patterns for gittinsite and aenigmatite (Figures 7.19; 7.20). Allanite is certainly present at Strange Lake, and locally abundant, but is also common in many igneous and metamorphic rocks, so it is not as diagnostic as gittinsite, and there are no obvious geographic trends in its abundance pattern.

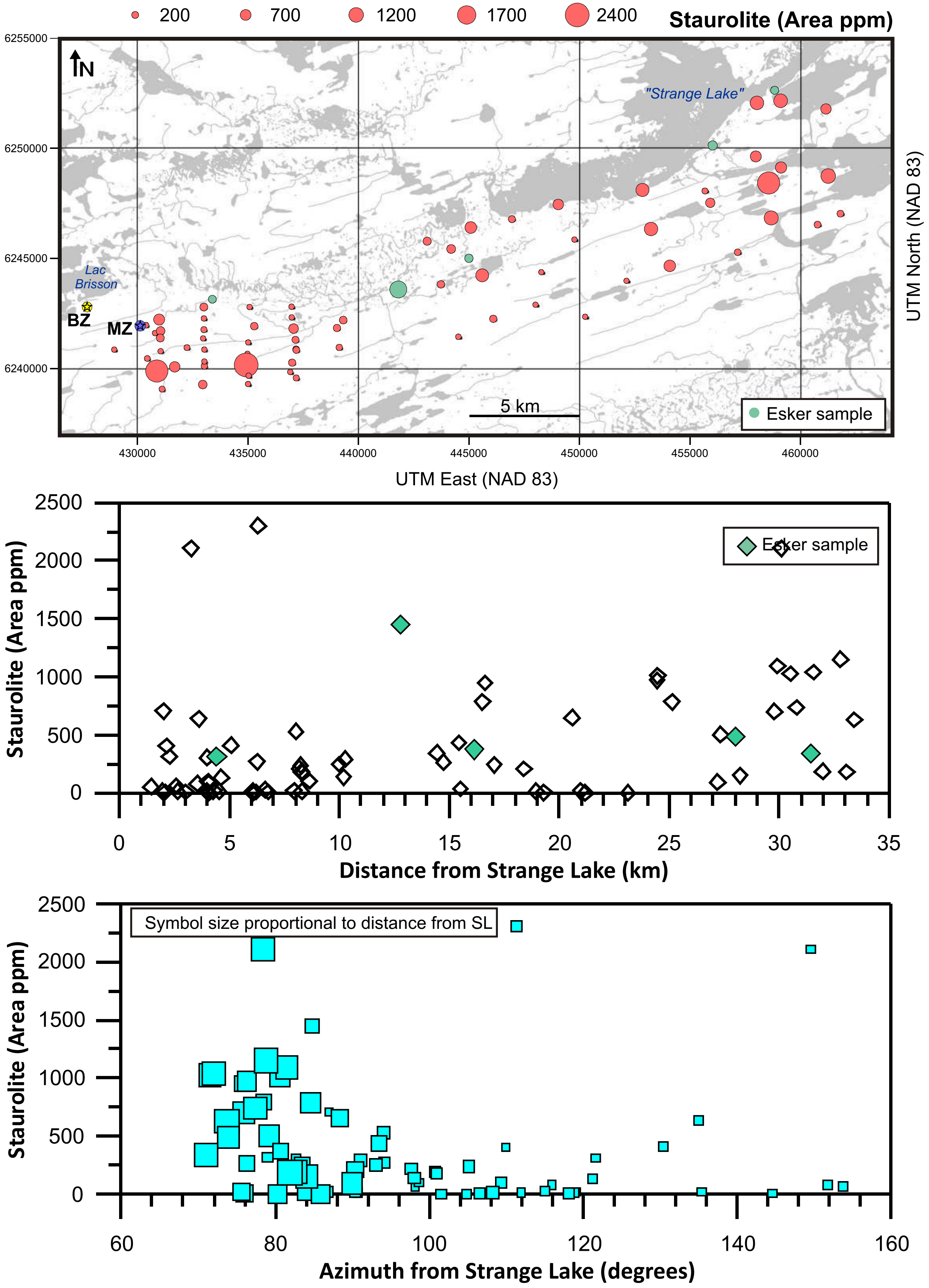

Figure 7.17. Geographic variation patterns for staurolite (area ppm). Upper Panel is a map view with proportional symbols. Lower panels show staurolite abundances against distance and azimuth from Strange Lake. See text for discussion.

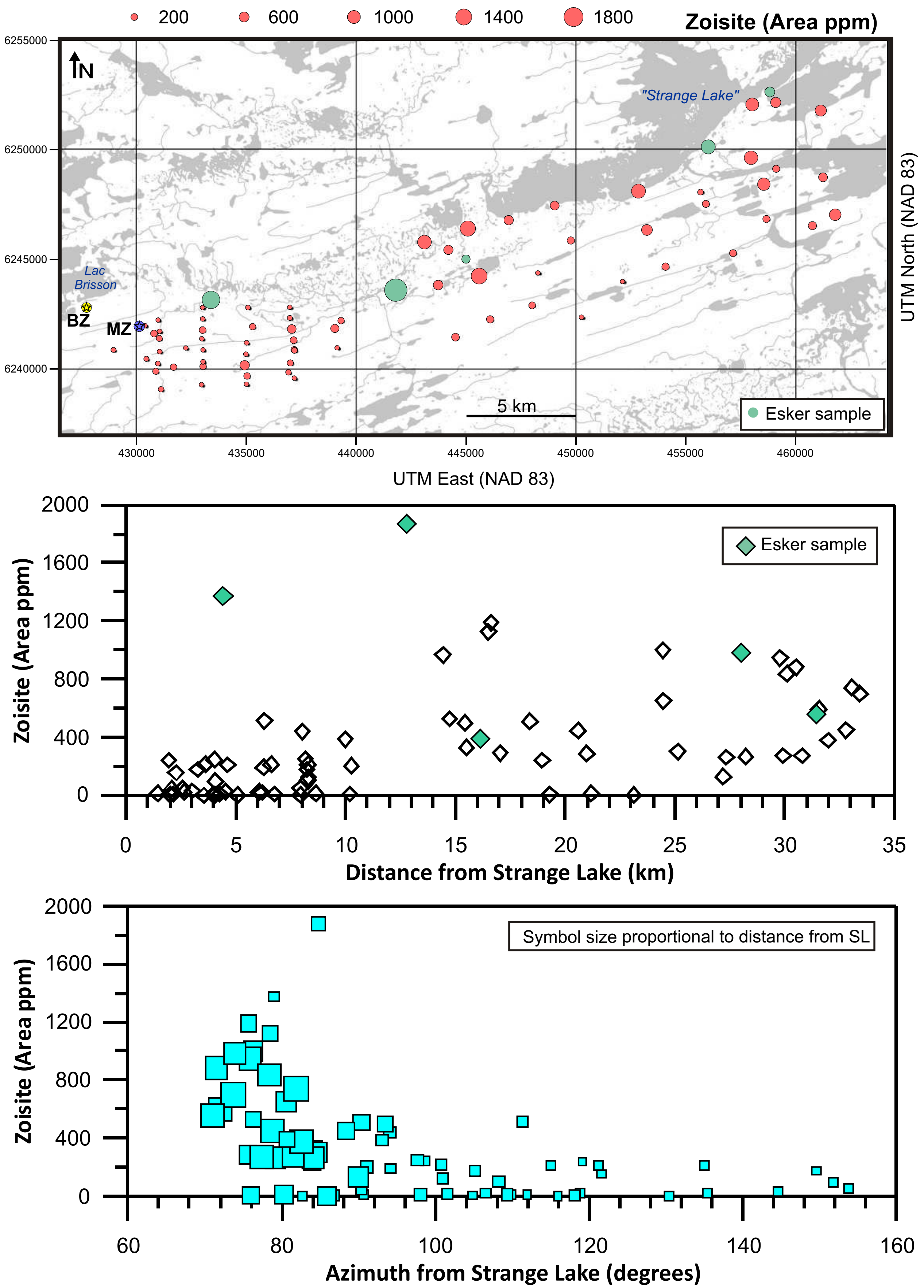

Figure 7.18. Geographic variation patterns for zoisite (area ppm). Upper Panel is a map view with proportional symbols. Lower panels show zoisite abundances against distance and azimuth from Strange Lake. See text for discussion.

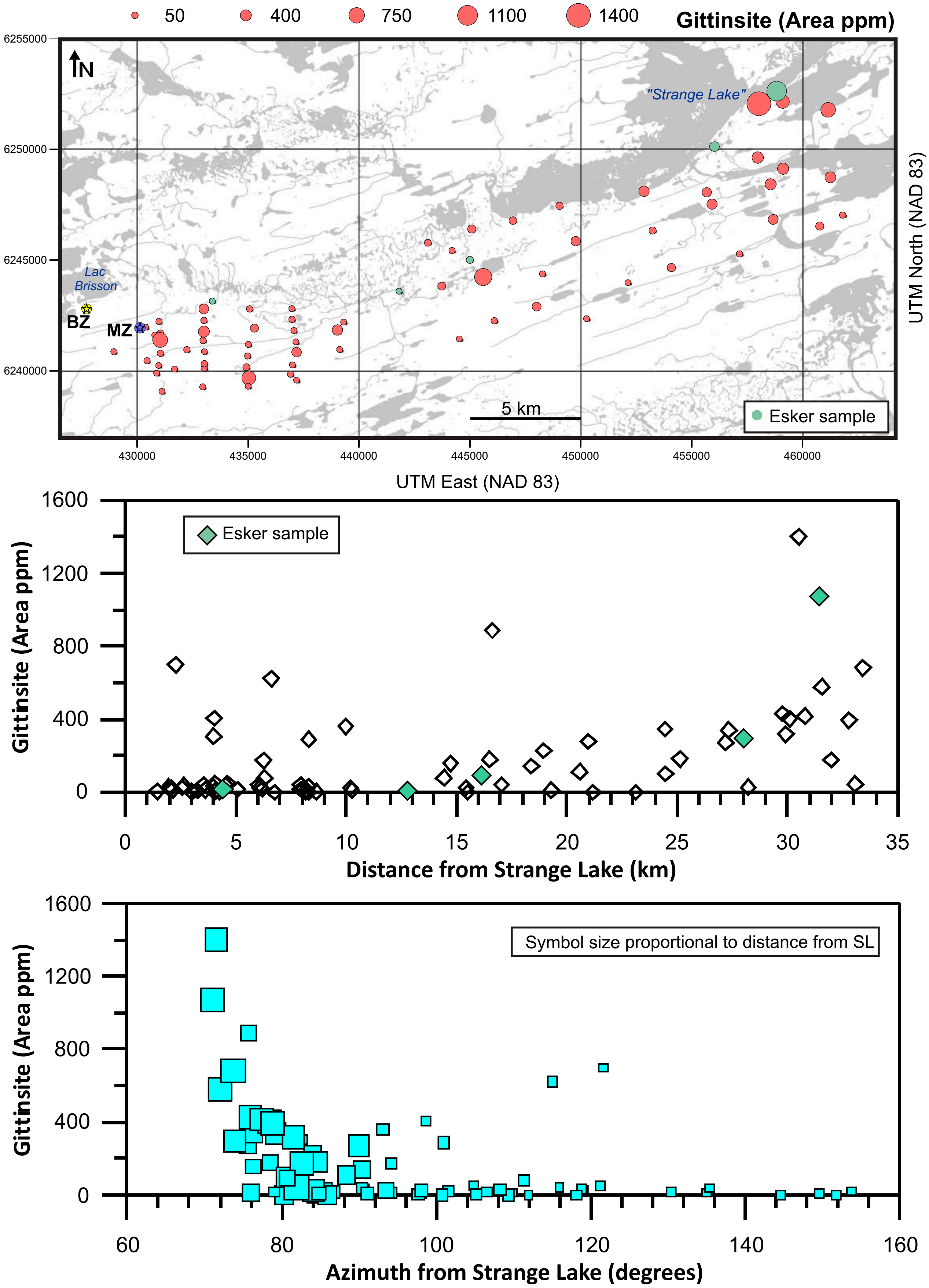

Figure 7.19. Geographic variation patterns for gittinsite (area ppm). Upper Panel is a map view with proportional symbols. Lower panels show gittinsite abundances against distance and azimuth from Strange Lake. See text for discussion.

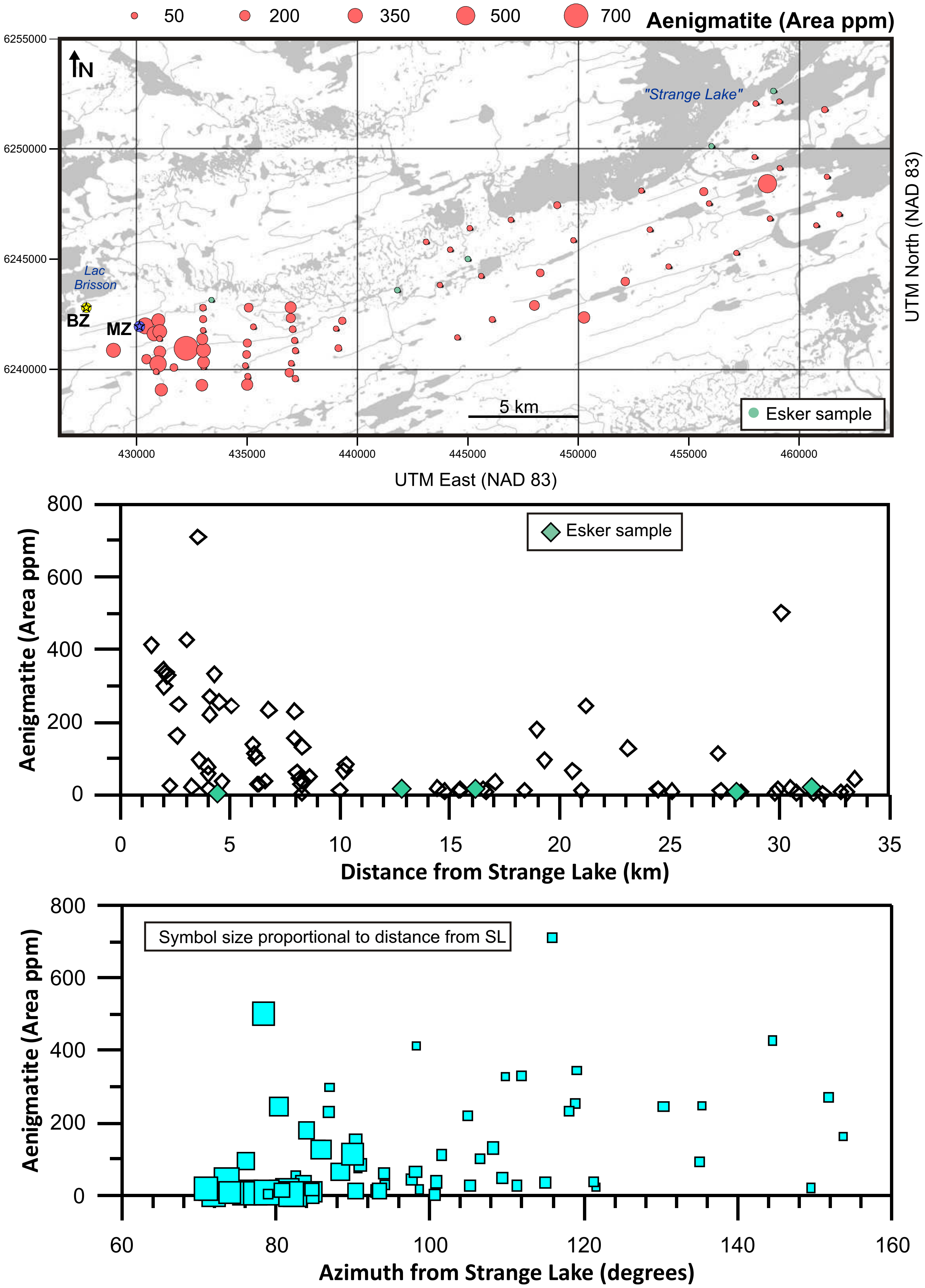

Figure 7.20. Geographic variation patterns for aenigmatite (area ppm). Upper Panel is a map view with proportional symbols. Lower panels show aenigmatite abundances against distance and azimuth from Strange Lake. See text for discussion.

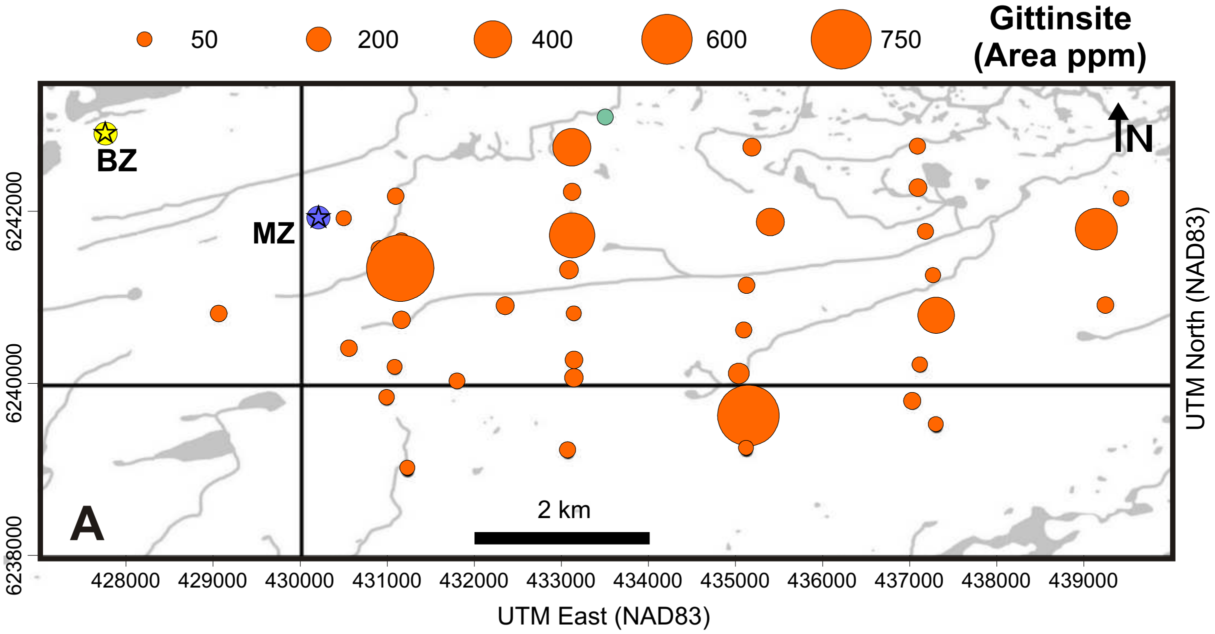

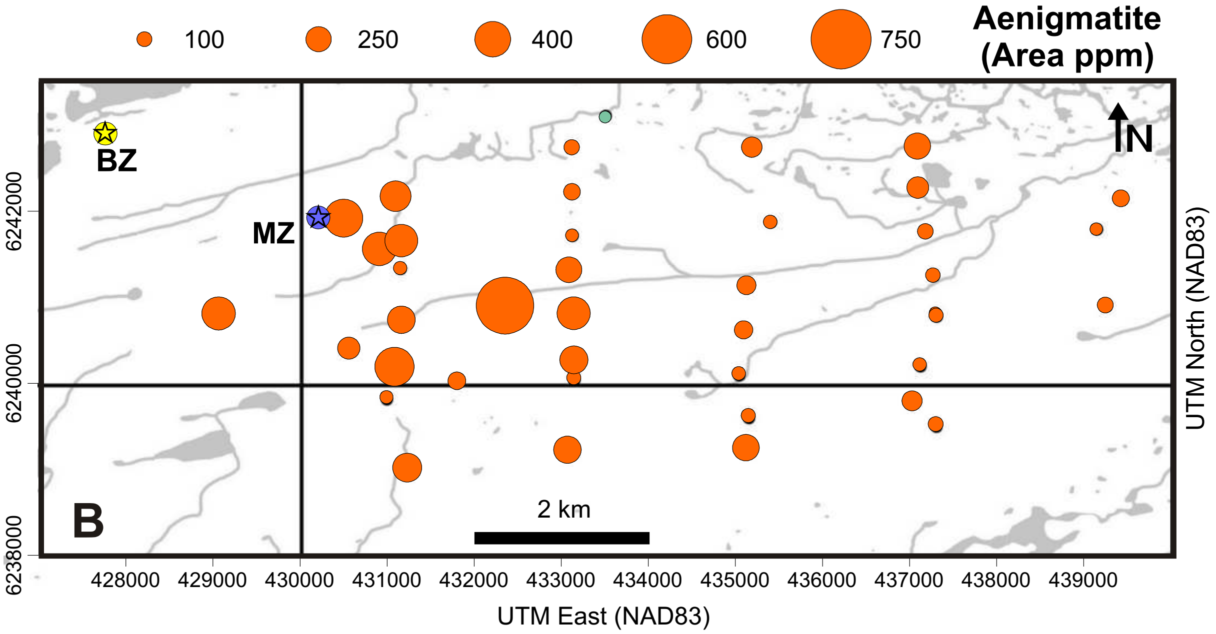

Figure 7.21. Geographic variation patterns for minerals in Grid 1, closest to the Strange Lake deposits. (A) Gittinsite abundances. (B) Aenigmatite abundances. See text for discussion.

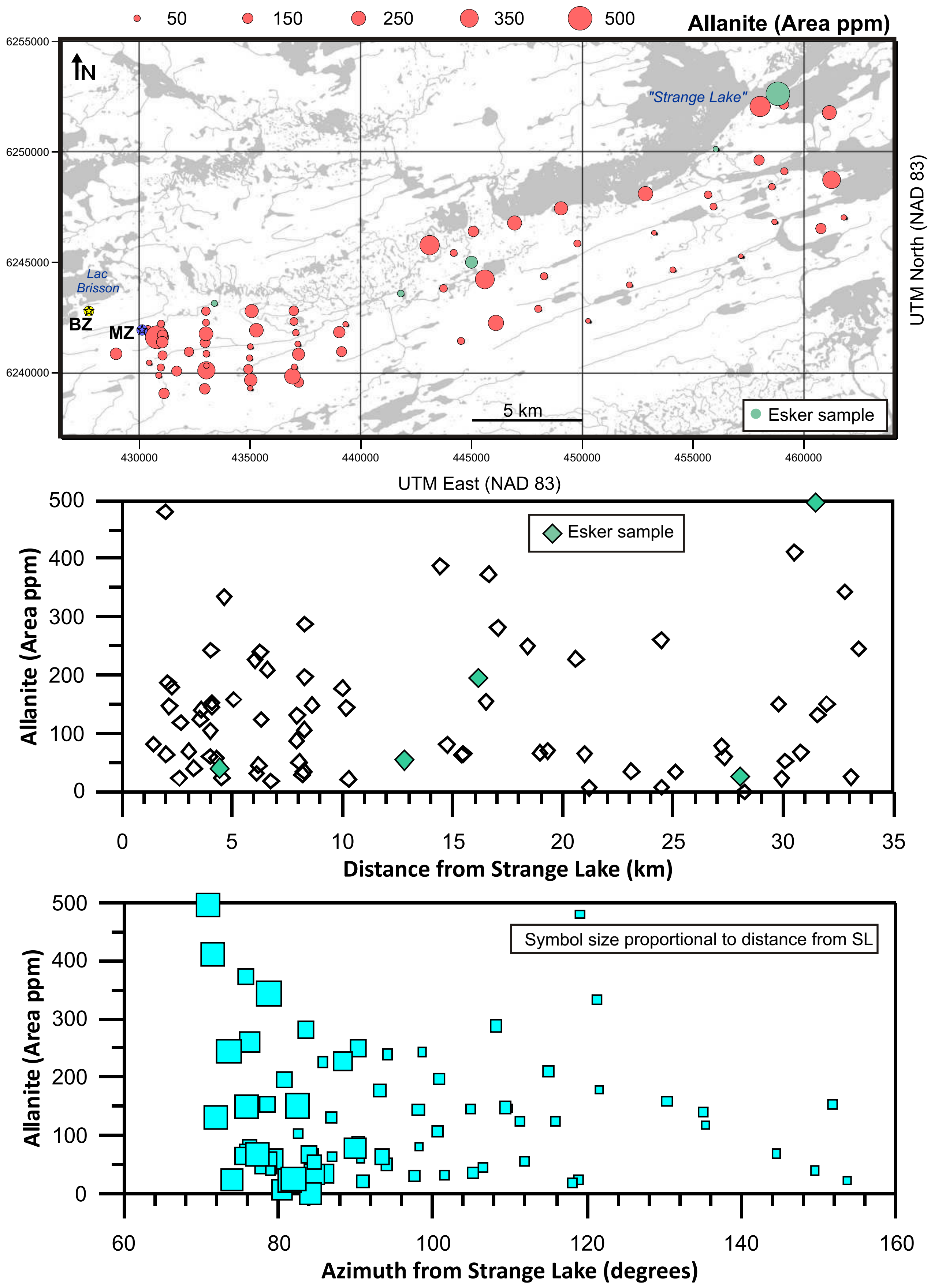

Figure 7.22. Geographic variation patterns for allanite (area ppm). Upper Panel is a map view with proportional symbols. Lower panels show allanite abundances against distance and azimuth from Strange Lake. See text for discussion.

Rare Accessory Minerals and Trace Minerals

General Information

Rare accessory and trace minerals are present only at low abundances (< 100 area ppm) and interpretation of their patterns is complicated by greater analytical uncertainties and also by the fact that they are missing from some or many samples. It is suspected that their local absence is in part due to the low probability that discrete particles of rare minerals would be present in small samples used for MLA-SEM analysis, even if they are present in the larger sample mass (see the discussion in Chapter 4). However, there is evidence that many of these minerals do not actually form entire particles, but rather occur as smaller grains within composite particles (see Chapter 6), which should mitigate these 'probability effects' to some extent. This suggests that the MLA-SEM data for at least some of them should be robust even if imprecise, and that comparisons of samples or sample groups are valid. Observations are partially consistent with this view, as some of these minerals do seem to show systematic geographic variation patterns. This would not be expected if their abundance in a given analyzed sample was entirely controlled by random probability effects. However, as discussed below, patterns for the least abundant members of this group become 'noisier' and more difficult to interpret.

This group includes most of the important Zr- REE- and Nb-bearing minerals that are characteristic of Strange Lake and, given their rarity, this is the only possible source location for them. These are accompanied by normally common minerals that are present only in trivial amounts (e.g., calcite, pyrite, barite and fluorite). These minerals and some other minerals present at extremely low abundances show no systematic geographic variation patterns and are not discussed further. Selected maps are presented to emphasize patterns possibly connected to Strange Lake, and additional maps are grouped in the Appendices.

Zirconosilicate and Titanosilicate Minerals

The most important zirconosilicate mineral associated with Strange Lake is gittinsite, which was discussed in the preceding section. Elpidite, which is similar in composition and structure to gittinsite, but Na-rich rather than Ca-rich, occurs in most samples, but it was also detected in the off-grid control sample (G2-15). Elpidite is well known at Strange Lake, but it may also have other regional sources. The optical properties of elpidite resemble those of quartz and feldspar, so it is difficult to identify in a thin section, and it may be more common in peralkaline igneous rocks than literature suggests (e.g., Currie and Zaleski, 1985). The geographic variation pattern for elpidite shows some enrichment in the area closest to Strange Lake, but it seems to persist at low abundances throughout all three sample grids (Figure 7.23). In this respect, it differs from the pattern noted for its Ca-rich counterpart gittinsite (Figure 7.19). The pattern for elpidite more closely resembles that of the titanosilicate mineral astrophyllite, which is also known from Strange Lake, but is not unique to it. Astrophyllite is is more common than elpidite, and is also found in peralkaline igneous rocks (Deer et al., 1992)

REE-bearing Minerals

Several uncommon REE-bearing minerals known from Strange Lake show systematic geographic patterns, even though they are present only in very small amounts and absent from some or many of the samples. These minerals include gerenite, perclevite, parisite, britholite, gadolinite, bastnaesite, stetindite and euxenite. The most informative patterns are for those minerals that have higher mean abundance, i.e., several tens of area ppm.

The Ca-Y-REE silicate mineral gerenite is essentially unique to Strange Lake and must be derived from this source. Gerenite shows obvious systematic geographic variation, with highest values (up to 500 area ppm) closest to the Main Zone, but its abundance declines to < 50 area ppm in more distant samples of Grid 3, with some local anomalies (Figure 7.24). The mineral is also present in almost every sample, and is missing only from a few locations in Grid 3 and control sample G2-15. This well-defined pattern is unlikely to be caused by probability effects, and particle/grain size data (Chapter 6) suggests that gerenite is widely dispersed as small grains within larger composite particles. The mineral perclevite shows a similar pattern of declining abundance from Grid 1 to Grid 3, but this is not as clear, and the mineral is missing from more samples. Parisite, which is a REE-rich carbonate, is mostly restricted to Grid 1, especially near to Strange Lake, and is virtually absent from Grid 3, aside from a single esker sample (Figure 7.25). Even within the Grid 1 area close to Strange Lake, parisite was absent in many of the samples. Britholite (a REE-silicate of varied composition) also follows this pattern, but is anomalously abundant in sample G1-6, located southwest of the Strange Lake Main Zone Deposit (Figure 7.26). It is also essentially absent from Grid 3. The increasingly ‘spotty’ geographic distribution of the less abundant REE minerals implies some influence from probability effects within Grid 1, but the virtually complete absence of parisite and britholite from more distant samples is probably significant. If these minerals were present widely in this region, it is reasonable to expect their presence in at least some samples.

The complex REE-silicate gadolinite is well known at Strange Lake, with an average abundance in drill core up to 700 area ppm (0.07 area %) (Baird, 2018). In the till samples, it is a trace mineral, with limited variation in abundance (where present) and seems to be enriched almost in the centre of the sample array, rather than at its western or eastern ends (Figure 7.27). One strongly enriched location (Sample G2-6) also has an anomalously high gerenite abundance, but is not enriched in any other REE-bearing minerals. Gadolinite is absent from many samples, even in areas close to Strange Lake, implying that it its pattern must be influenced by probability effects. Bastnaesite (another REE-bearing carbonate) shows a pattern similar to that of gadolinite, but is absent from sample G2-6, and instead strongly enriched in esker sample E-8 (Figure 7.28). Esker sample E-8 is also enriched in several other uncommon minerals (see below). Despite their rather 'spotty' pattern of occurrence, both gadolinite and bastnaesite do persist throughout the entire sample array, albeit at low levels and with more sporadic occurrence in Grid 3 compared to other grids. Thus, they do illustrate systematic patterns, even if these are noisy in their details. In contrast Stetindite, which is a Ce-rich member of the zircon family, shows geographic variation that resembles the pattern of gittinsite (Figure 7.19), with greatest abundance at the eastern end of the sample array, distant from Strange Lake (Figure 7.29). It shows some local enrichment close to Strange Lake, but is also missing from many Grid 1 samples. Euxenite, a rare polymetallic oxide mineral that also contains Nb, Ta and Ti, shows a restricted occurrence only within Grid 1, and is absent from most of the samples, although its highest abundance is in esker sample E-8, almost at the end of the sample array (Figure 7.30). On an individual sample level, the patterns for these rarer REE-bearing minerals are not consistent, but systematic trends can still be discerned. The increasingly noisy patterns for the least abundant minerals match expectations for increased disruption of 'real' variation by probability effects.

Nb-bearing Minerals

Although Nb is an important economic commodity at Strange Lake, only 3 Nb-bearing minerals (pyrochlore, fergusonite and changbaiite) were detected at average abundances greater than 1 area ppm, and these are absent from many of the samples. Despite very low abundances, the geographic variation patterns of these minerals appear to be systematic, and it is likely that they are derived from Strange Lake, even though they are not diagnostic of it. The pattern for pyrochlore resembles that shown by gittinsite, with anomalous samples located close to Strange Lake, but also at the eastern end of the sample array, about 35 km from the Main Zone deposit (Figure 7.31). The abundance of pyrochlore is very low, with a maximum value of 56 area ppm, and it is present in fewer than half the till samples. The Nb-Y-oxide fergusonite occurs more frequently (41 of 76 samples) and has a similarly wide distribution through the sample array, but it shows much more obvious enrichment in Grid 1, close to Strange Lake (Figure 7.32). The rare Nb-Pb-oxide mineral changbaiite (reported mostly from localities in China) shows a pattern broadly resembling that of pyrochlore, with some notable enrichment at the eastern end of Grid 3 (Figure 7.33). Patterns for all these minerals are very spotty or 'noisy', suggesting that they are influenced by probability effects, especially in the case of changbaiite, which is present only in 20 samples and has an 'average' abundance of only slightly more than 1 area ppm.

Radioactive Minerals

Thorite is significant in bulk samples and drill cores from Strange Lake, but it is a rare accessory mineral in till samples, with a mean abundance of only 14 area ppm, and is absent from many samples. It is present in most samples in Grid 1, but absent from about half of the samples in Grids 2 and 3 (Figure 7.34). Samples that are strongly enriched in thorite occur throughout the area, including esker sample E-8. Uraninite is absent from most samples in Grids 2 and 3, but more widely present in Grid 1 (Figure 7.35). However, its abundance does not vary much, aside from one very anomalous sample in Grid 1. Although uraninite was noted in bulk sample analyses (IOC, 1985), it was not specifically detected in Strange Lake drill cores by Baird (2018).

Geographic Variation Patterns Close to Strange Lake

Many of the Zr-, REE- and Nb-bearing minerals that are characteristic of the Strange Lake deposits occur mostly in the area of Grid 1, closest to the Main Zone Deposit and within the outcrop area of the Strange Lake Intrusion. This may also be the case for thorite and uraninite. As noted above, the geographic variation patterns seem to become noisier as the average abundances of the rare minerals diminish. This is illustrated in more detail for the Grid 1 area by a series of maps presented in Figures 7.36 to 7.41. Gittinsite and gerenite (Figure 7.36) show well-defined patterns, including subparallel 'enrichment trends' and both minerals are present in almost all samples (gittinsite was previously shown in Fig. 7.21, and is reproduced for comparison). Perclevite and elpidite (Figure 7.37) also show such patterns but not as clearly; some samples where perclevite is absent are enriched in elpidite, and vice-versa. Figures 7.38 and 7.39 illustrate parisite, britholite, gadolinite and bastnaesite. These patterns are harder to discern, and there is little consistency in the precise location of enriched samples. If the maps are examined quickly in sequence on a computer screen, it almost seems as if the samples are playing “hide and seek” – individual location seem to disappear and then reappear with variable symbol sizes. Figure 7.40 illustrates patterns for stetindite and euxenite, and Figure 7.41 illustrates pyrochlore and fergusonite, and both map pairs show these same inconsistencies. There are no sample locations that consistently show enrichment in several different minerals, and almost no sample locations for which all indicator minerals are missing. This behaviour is exactly what would be expected from an increasing disruption of ‘real’ variation by probability effects, but the disruption does not completely eradicate geographic trends.

The pattern of occurrence for potential indicator minerals from Strange Lake for all samples in the Grid 1 area is illustrated very well by a simplified table in which entries are reduced to ‘absent’, ‘present below mean value’ and ‘present above mean value’, and indicated by colour coding (Table 7.1). The indicator minerals are arranged in decreasing order of abundance from left to right, and samples are arranged by increasing distance from Strange Lake from top to bottom. Some minerals with uncertain (but possible) links to Strange Lake, such as “ericssonite”, are also included here. The table clearly shows that the number of ‘absent’ locations increases as abundance diminishes, but there are exceptions to this rule; for example, pyrochlore occurs much less frequently than fergusonite, even though their ‘mean’ abundance is nearly identical. For minerals with ‘mean’ abundances above ~ 15 area ppm, the majority of samples record their presence, even if the absolute abundances are low. Below this limit (with the exception of fergusonite) minerals are absent from the majority of the samples, and there is little consistency in their patterns. There are no samples that contain *all* indicator minerals with mean abundances below this limit (although G1-4 and G1-9 come close to this), and only one sample (G1-24) in which *all* of these minerals are missing. The best word to describe the occurrence of these minerals is ‘sporadic’; most samples contain some of them at low values, some of them at high values, and lack some of them entirely. A final important point to note is that there is very little indication from Table 7.1 that indicator minerals are more likely to be ‘absent’ than ‘present’ at greater distances from Strange Lake within Grid 1, although this is the case for some of them in Grids 2 and 3, as shown in simplified form in Table 7.2, which simply indicates presence or absence. The information in Tables 7.1 and 7.2 provides very strong evidence that variation patterns for the rarest minerals are variably disrupted, but it also gives a strong indication that observed variation for more abundant indicator minerals is both valid and systematic, albeit somewhat ‘noisy’.

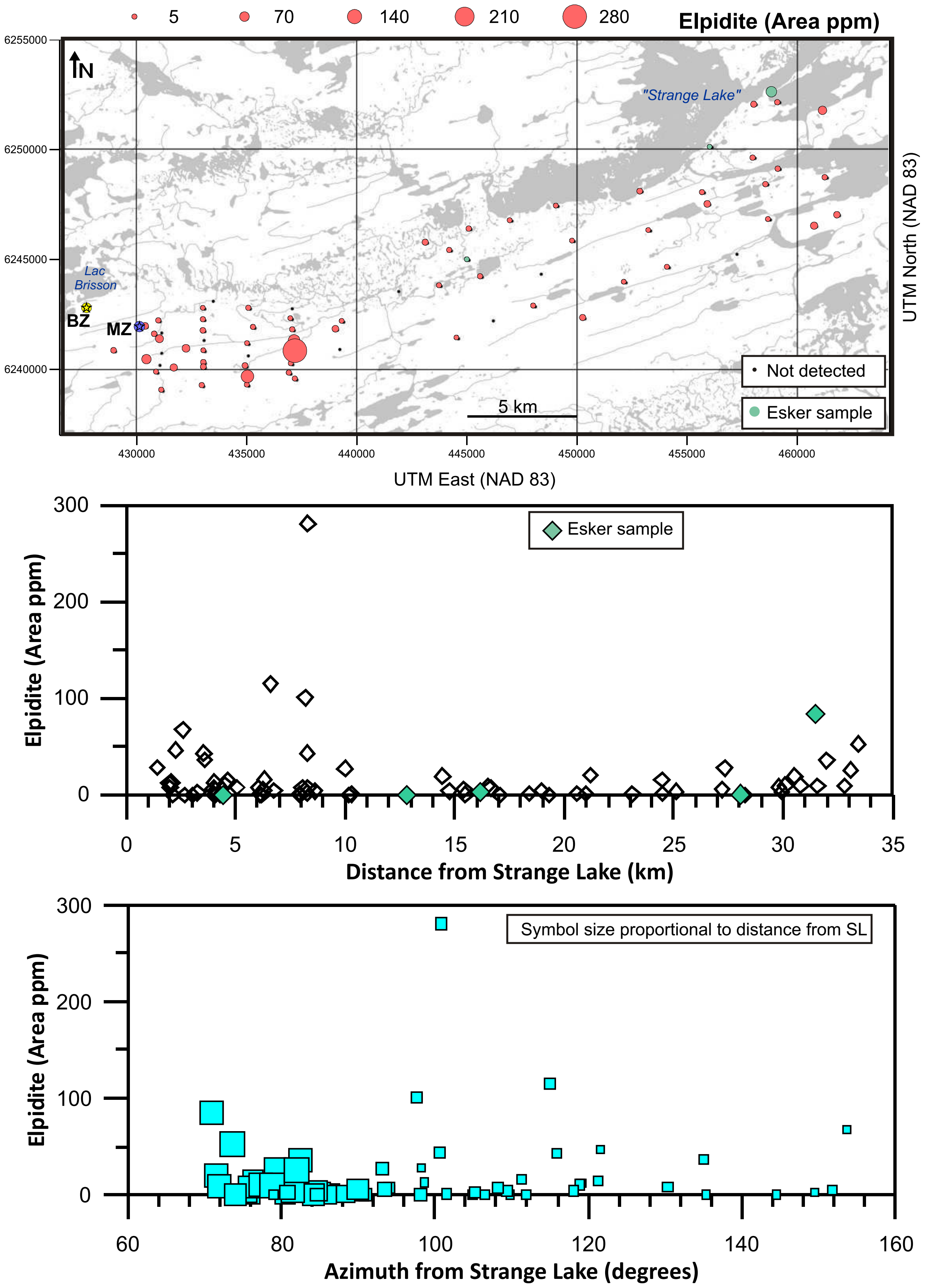

Figure 7.23. Geographic variation patterns for elpidite (area ppm). Upper Panel is a map view with proportional symbols. Lower panels show elpidite abundances against distance and azimuth from Strange Lake. See text for discussion.

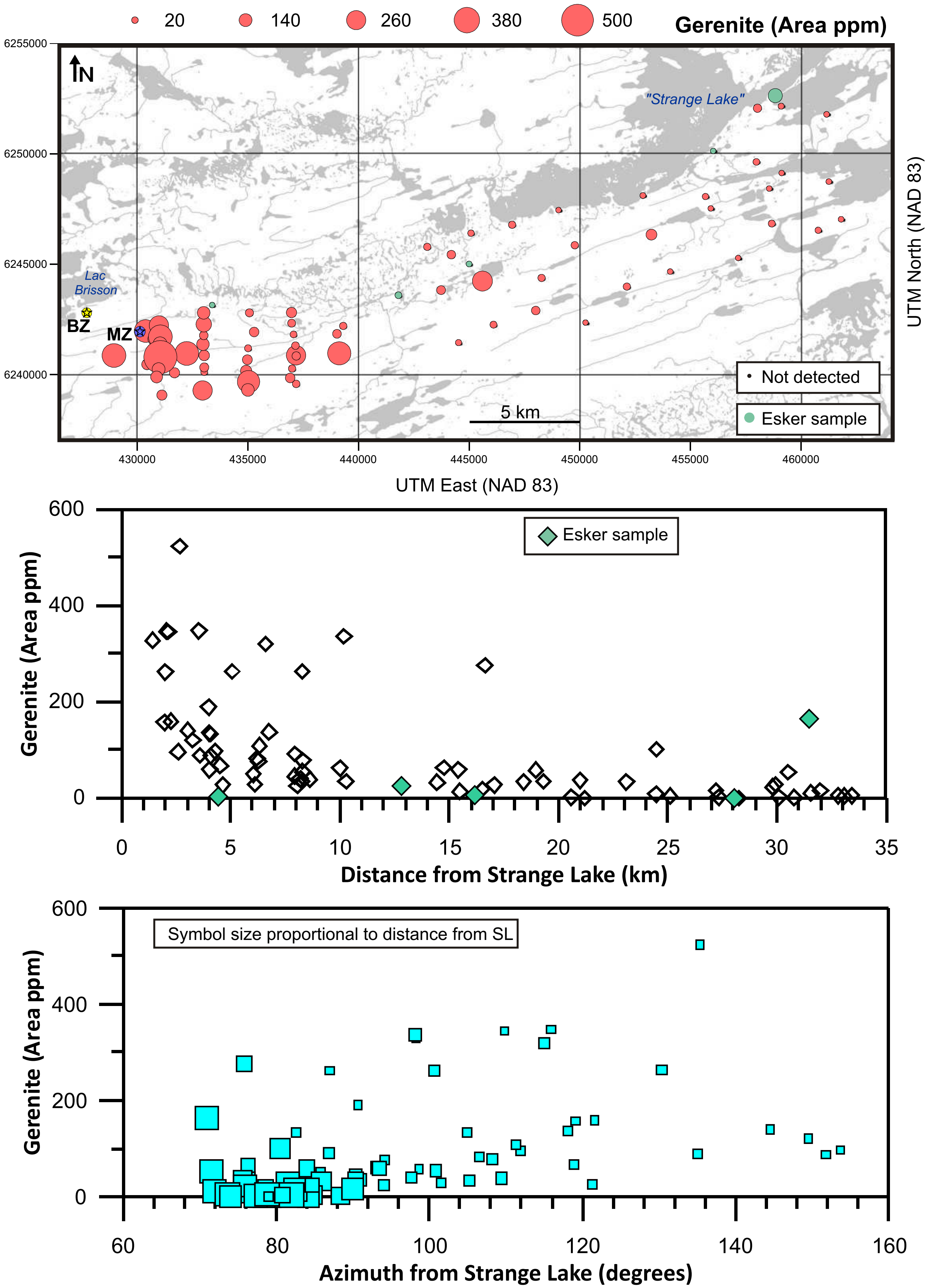

Figure 7.24. Geographic variation patterns for gerenite (area ppm). Upper Panel is a map view with proportional symbols. Lower panels show gerenite abundances against distance and azimuth from Strange Lake. See text for discussion.

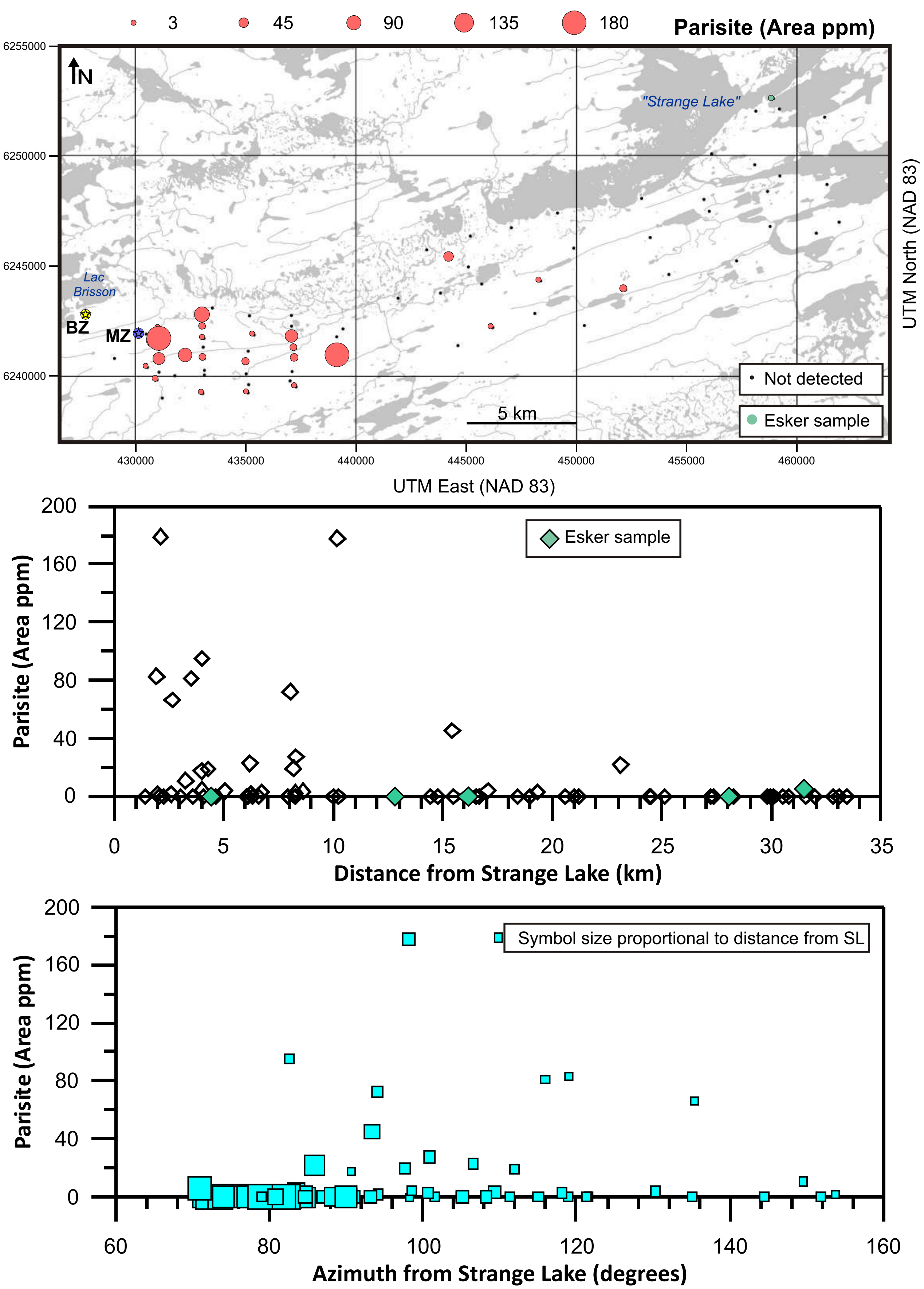

Figure 7.25. Geographic variation patterns for parisite (area ppm). Upper Panel is a map view with proportional symbols. Lower panels show parisite abundances against distance and azimuth from Strange Lake. See text for discussion.

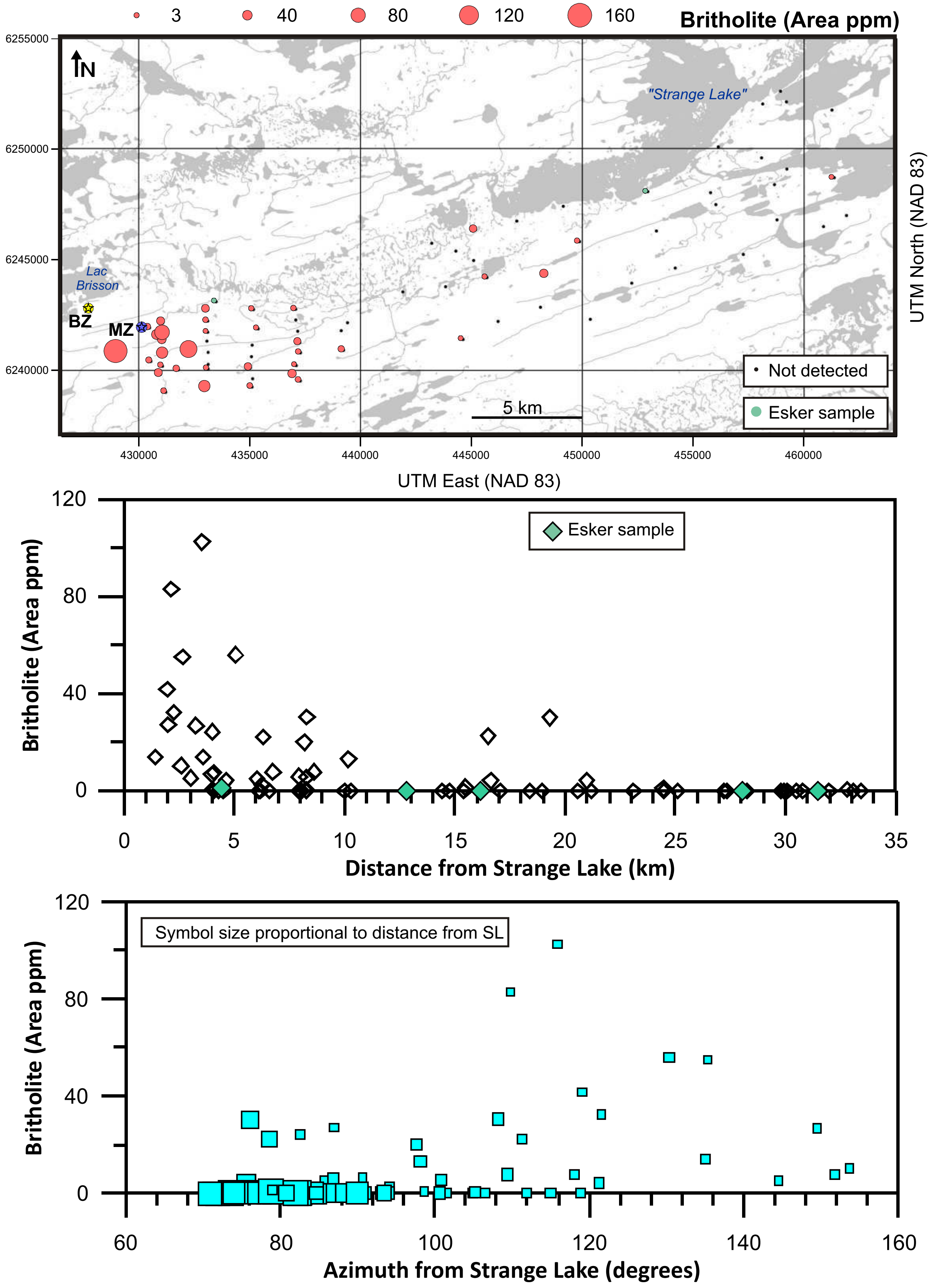

Figure 7.26. Geographic variation patterns for britholite (area ppm). Upper Panel is a map view with proportional symbols. Lower panels show britholite abundances against distance and azimuth from Strange Lake. See text for discussion.

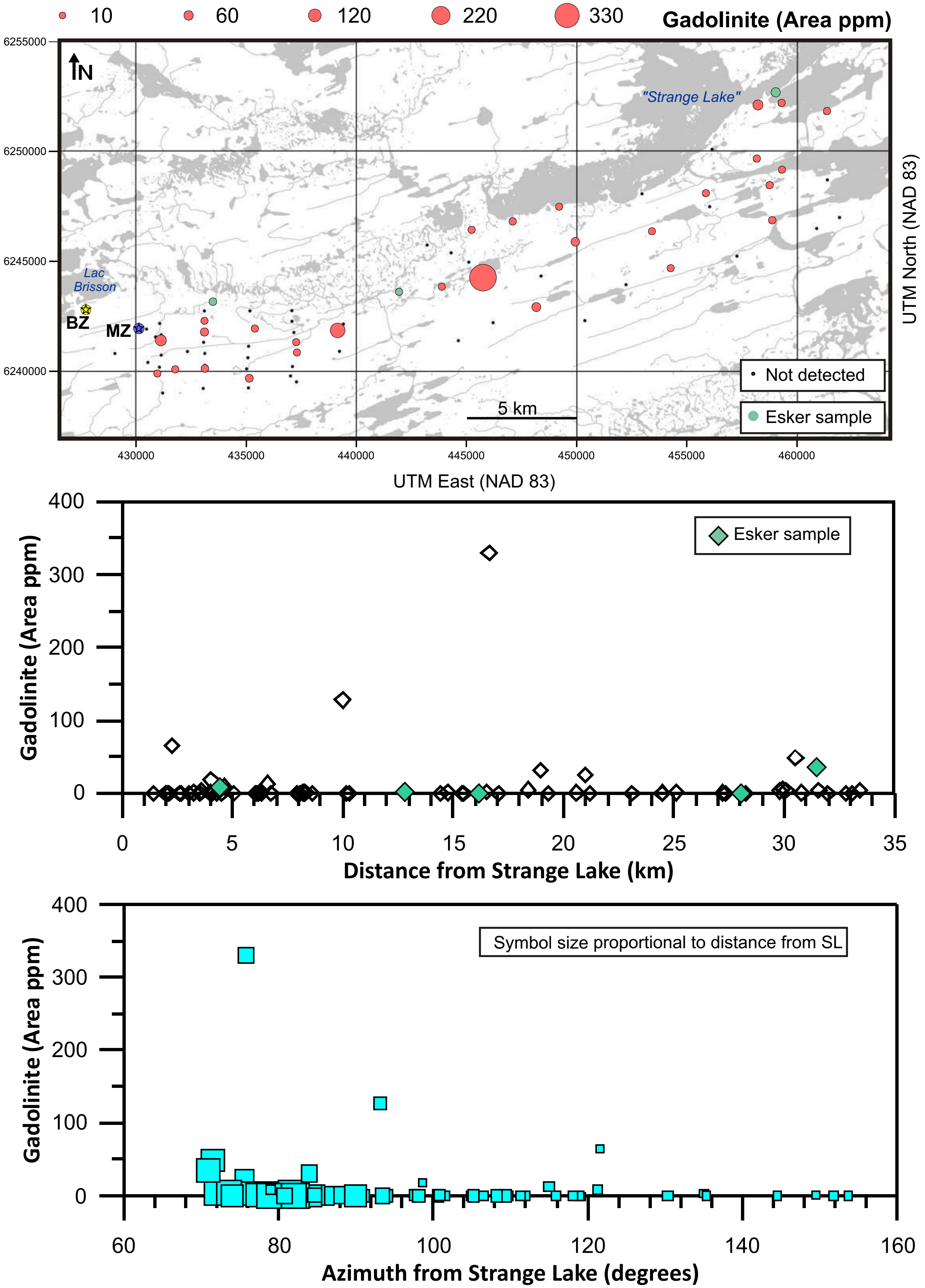

Figure 7.26. Geographic variation patterns for gadolinite (area ppm). Upper Panel is a map view with proportional symbols. Lower panels show gadolinite abundances against distance and azimuth from Strange Lake. See text for discussion.

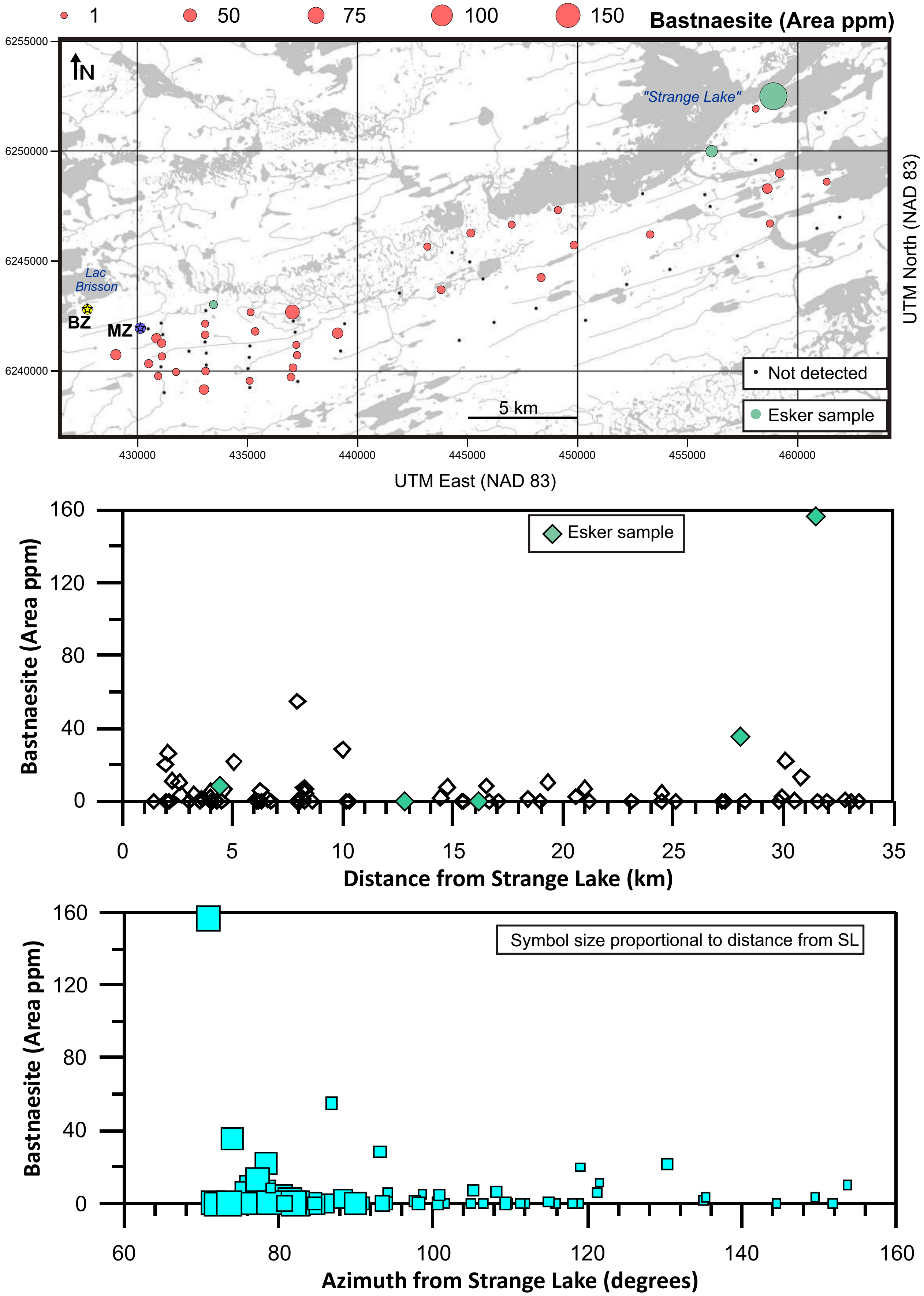

Figure 7.28. Geographic variation patterns for bastnaesite (area ppm). Upper Panel is a map view with proportional symbols. Lower panels show bastnaesite abundances against distance and azimuth from Strange Lake. See text for discussion.

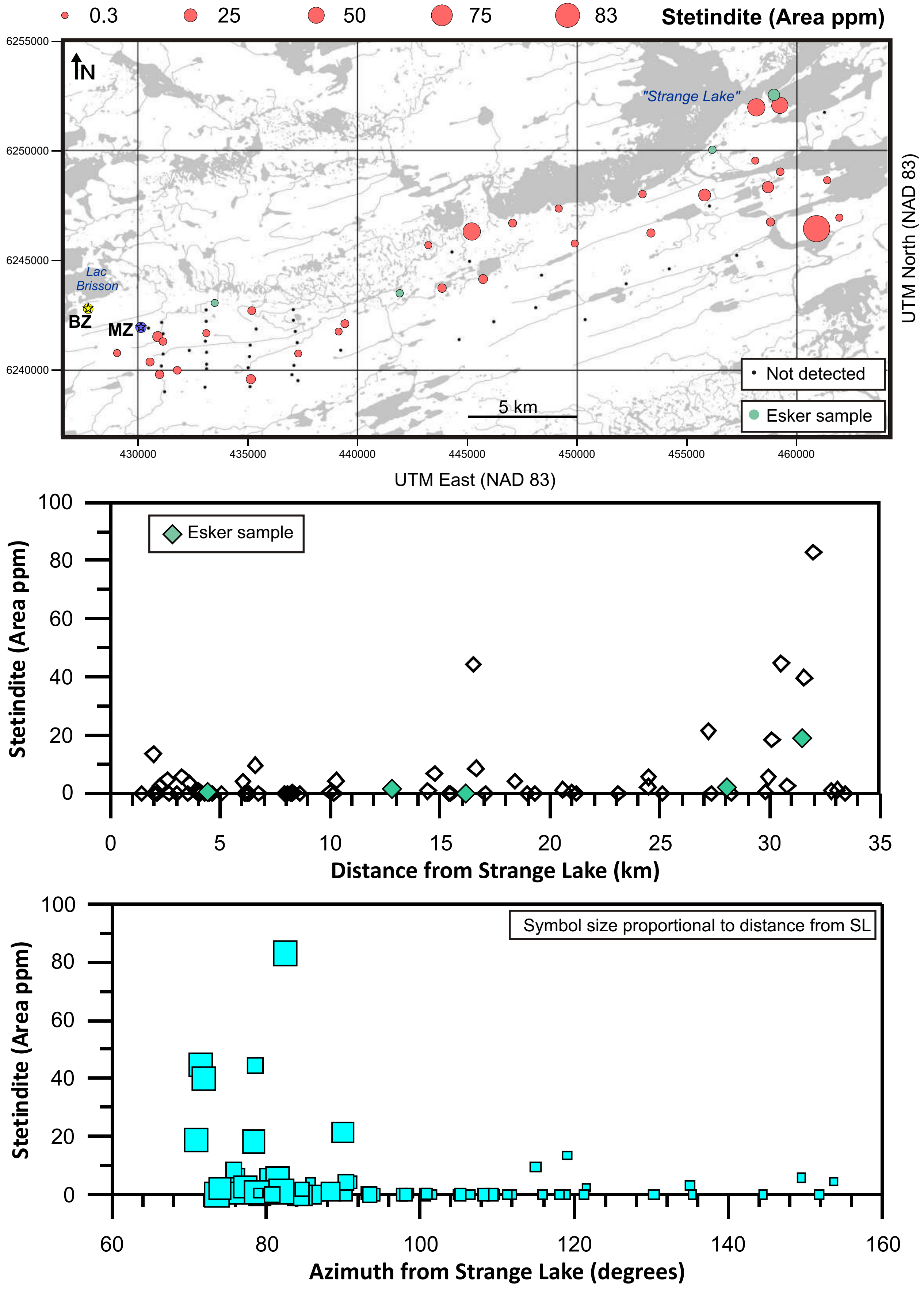

Figure 7.29. Geographic variation patterns for stetindite (area ppm). Upper Panel is a map view with proportional symbols. Lower panels show stetindite abundances against distance and azimuth from Strange Lake. See text for discussion.

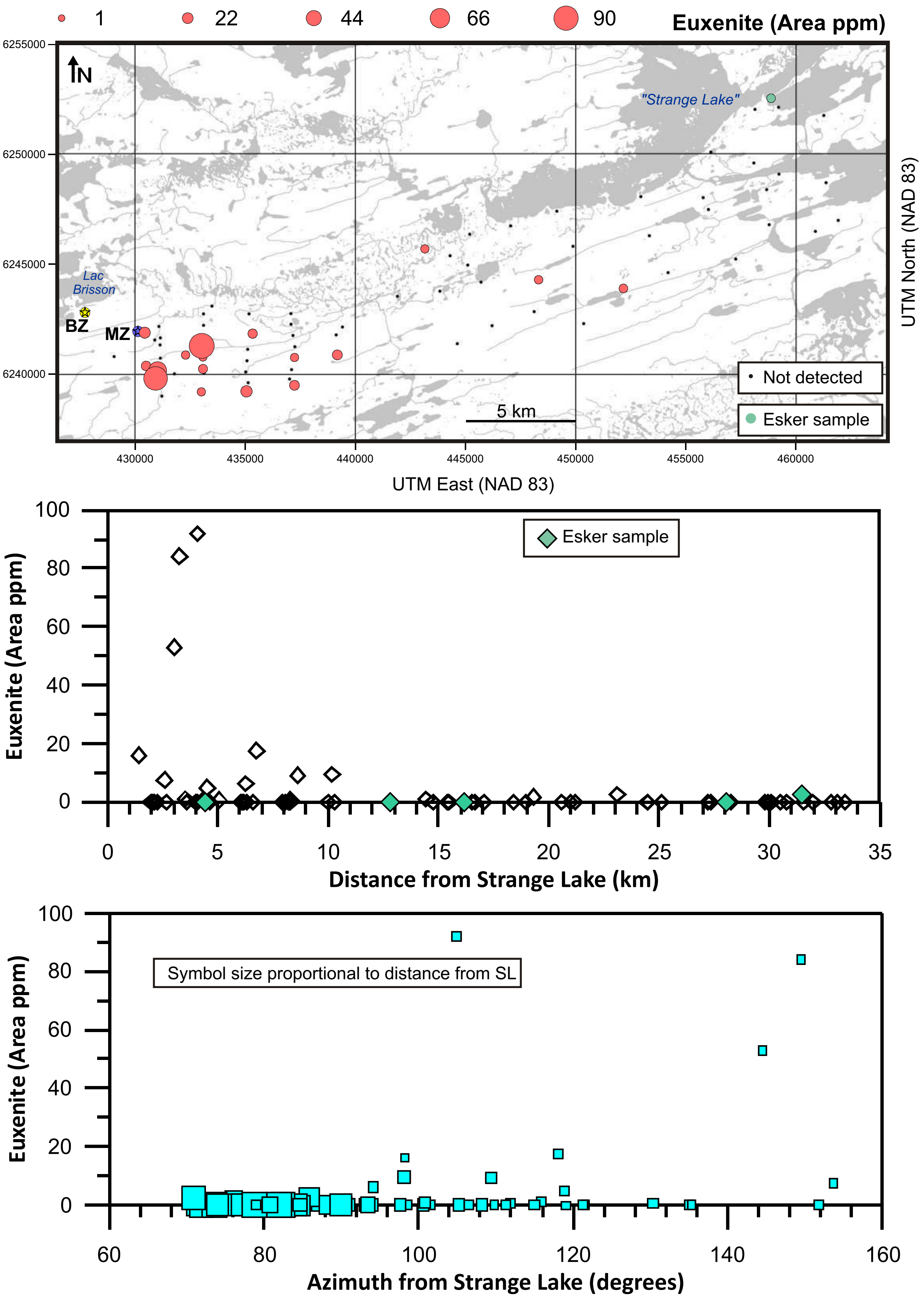

Figure 7.30. Geographic variation patterns for euxenite (area ppm). Upper Panel is a map view with proportional symbols. Lower panels show euxenite abundances against distance and azimuth from Strange Lake. See text for discussion.

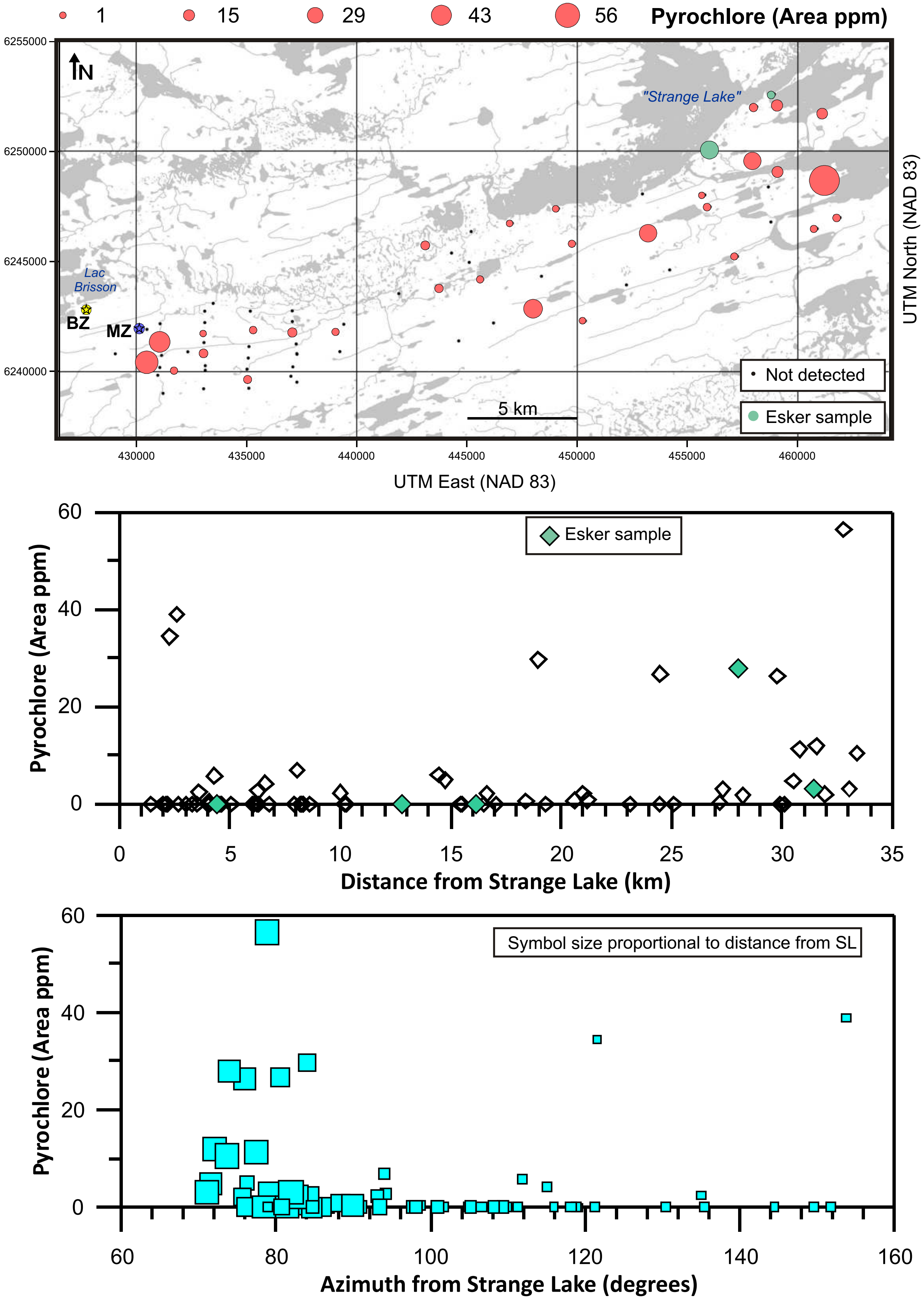

Figure 7.31. Geographic variation patterns for pyrochlore (area ppm). Upper Panel is a map view with proportional symbols. Lower panels show pyrochlore abundances against distance and azimuth from Strange Lake. See text for discussion.

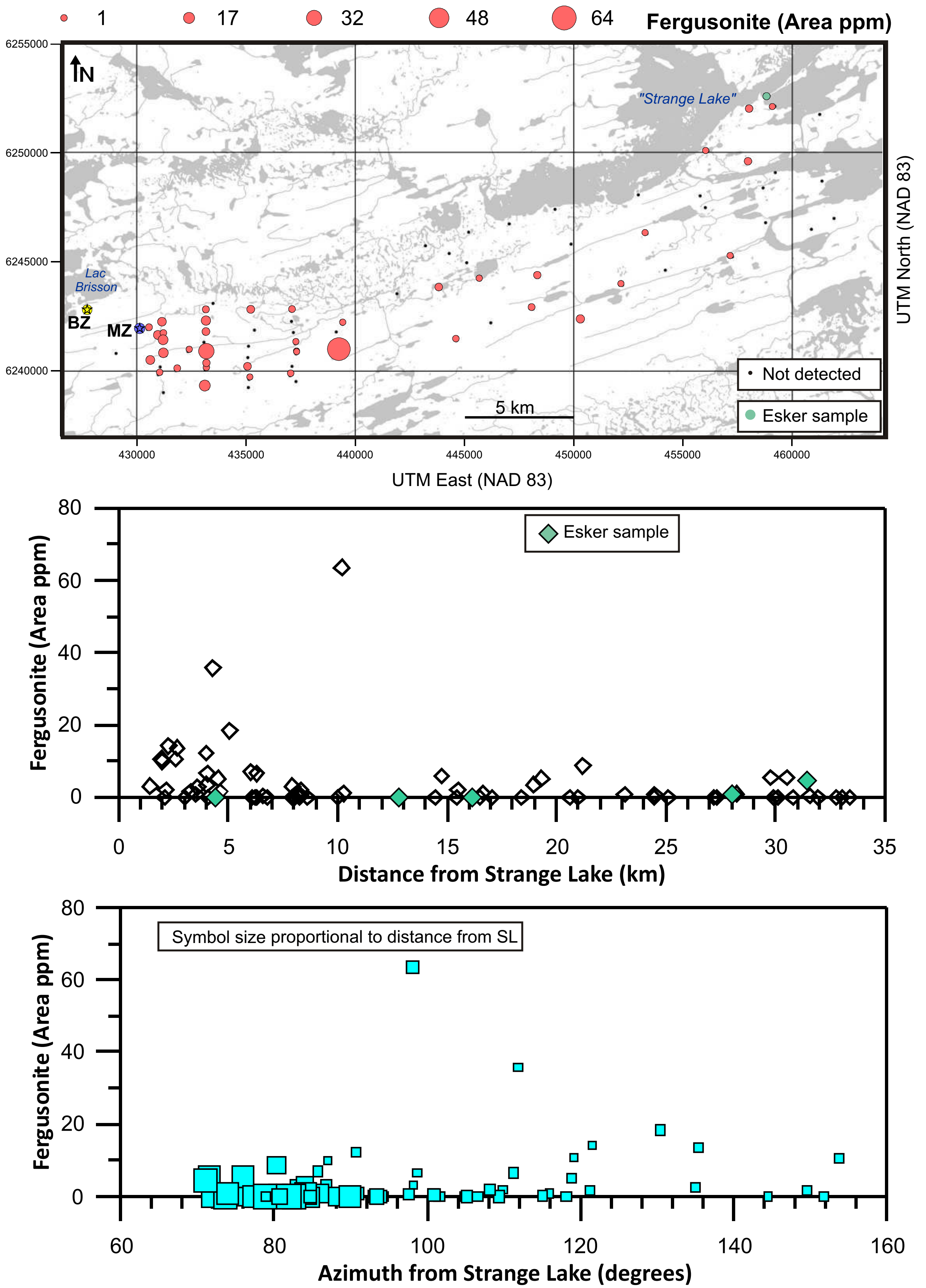

Figure 7.32. Geographic variation patterns for fergusonite (area ppm). Upper Panel is a map view with proportional symbols. Lower panels show fergusonite abundances against distance and azimuth from Strange Lake. See text for discussion.

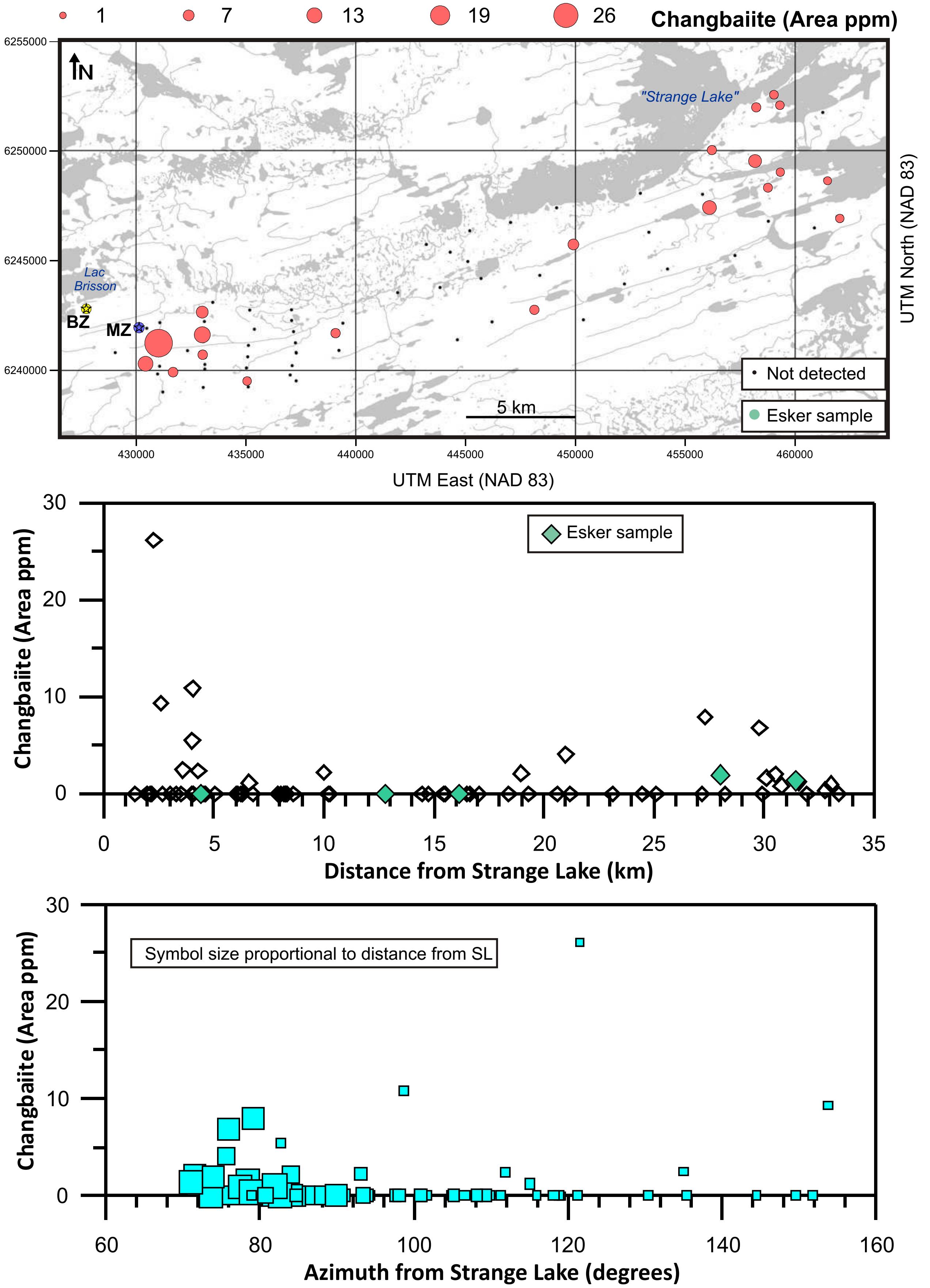

Figure 7.33. Geographic variation patterns for changbaiite (area ppm). Upper Panel is a map view with proportional symbols. Lower panels show changbaiite abundances against distance and azimuth from Strange Lake. See text for discussion.

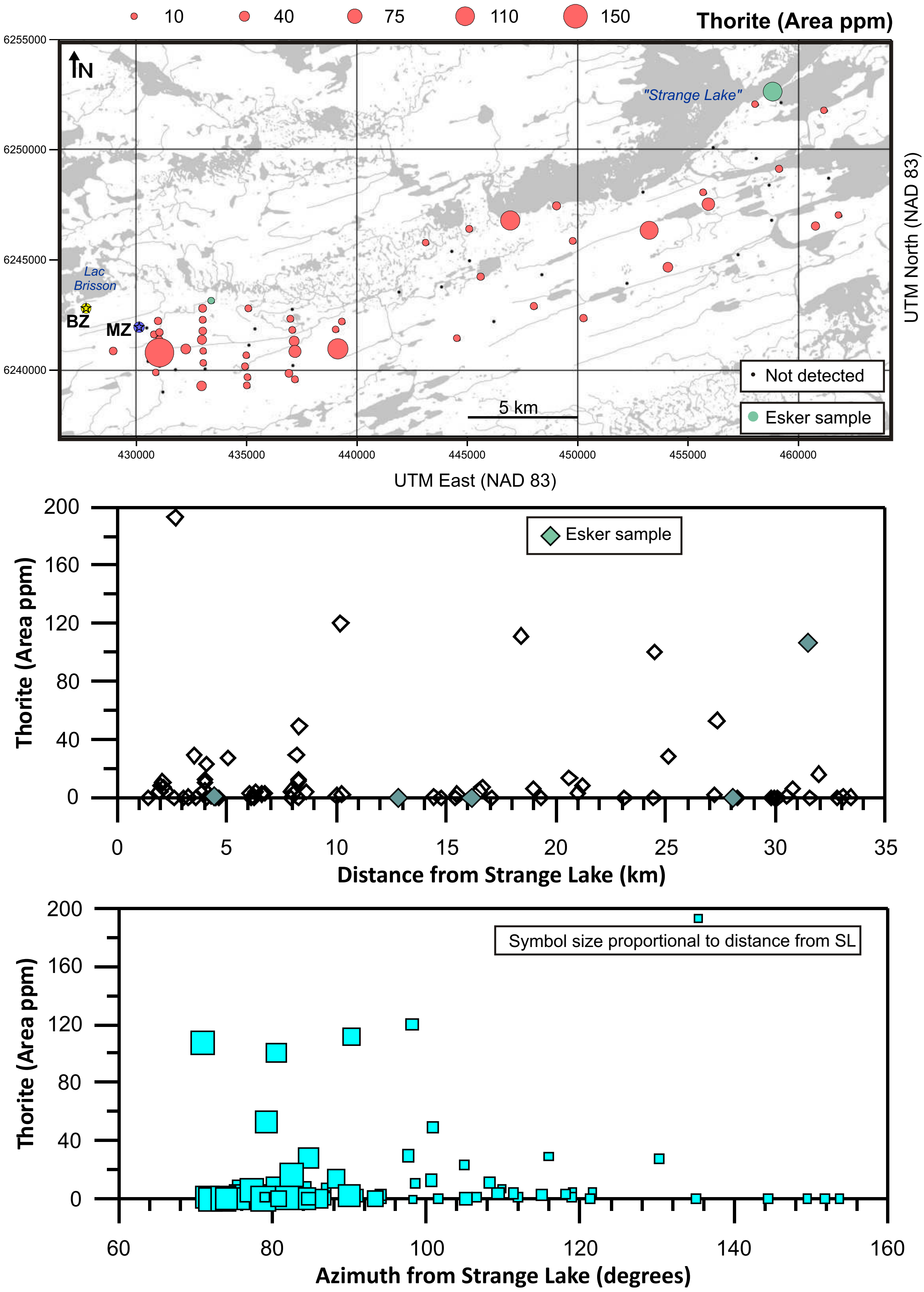

Figure 7.34. Geographic variation patterns for thorite (area ppm). Upper Panel is a map view with proportional symbols. Lower panels show thorite abundances against distance and azimuth from Strange Lake. See text for discussion.

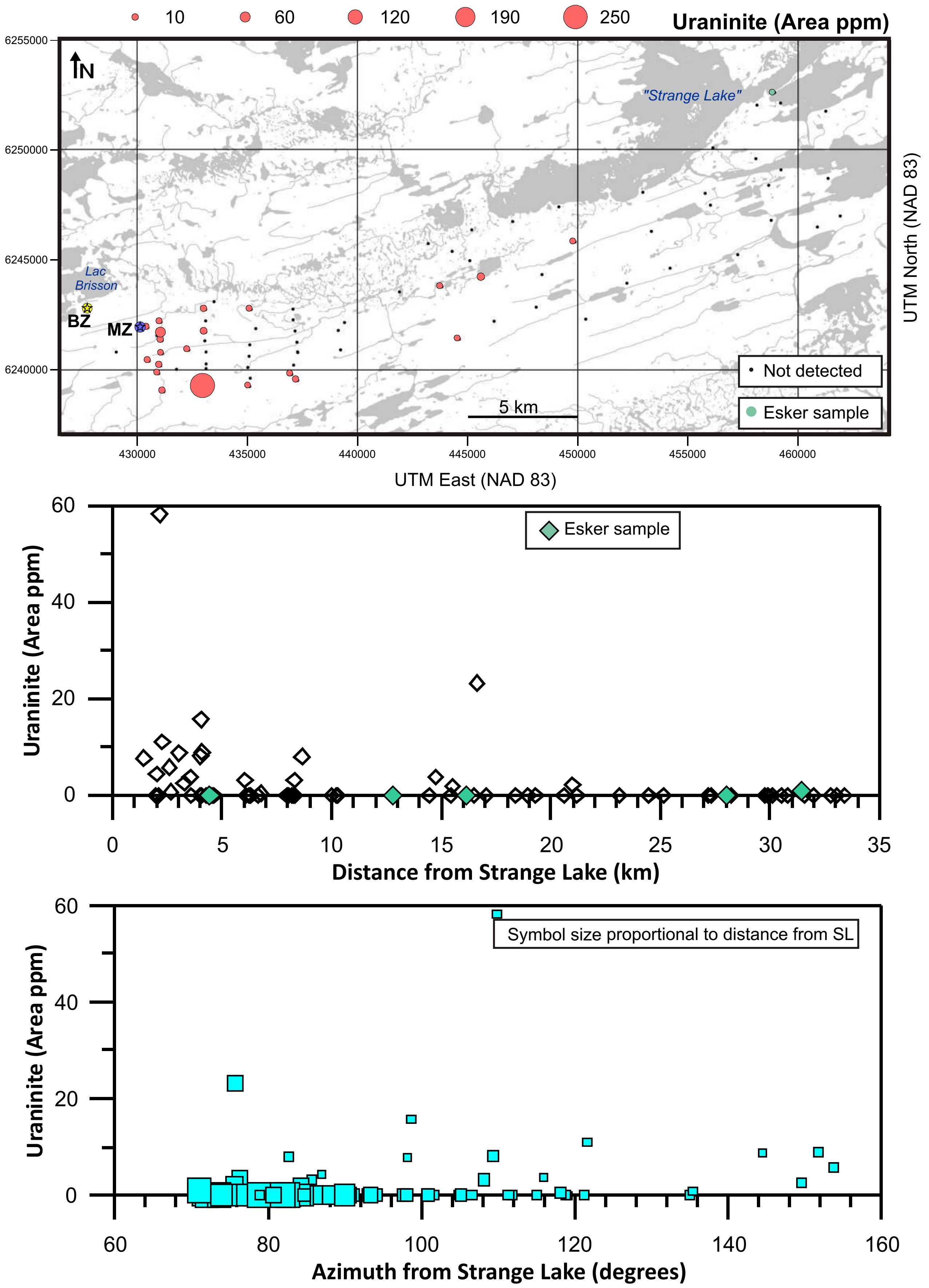

Figure 7.35. Geographic variation patterns for uraninite (area ppm). Upper Panel is a map view with proportional symbols. Lower panels show uraninite abundances against distance and azimuth from Strange Lake. See text for discussion.

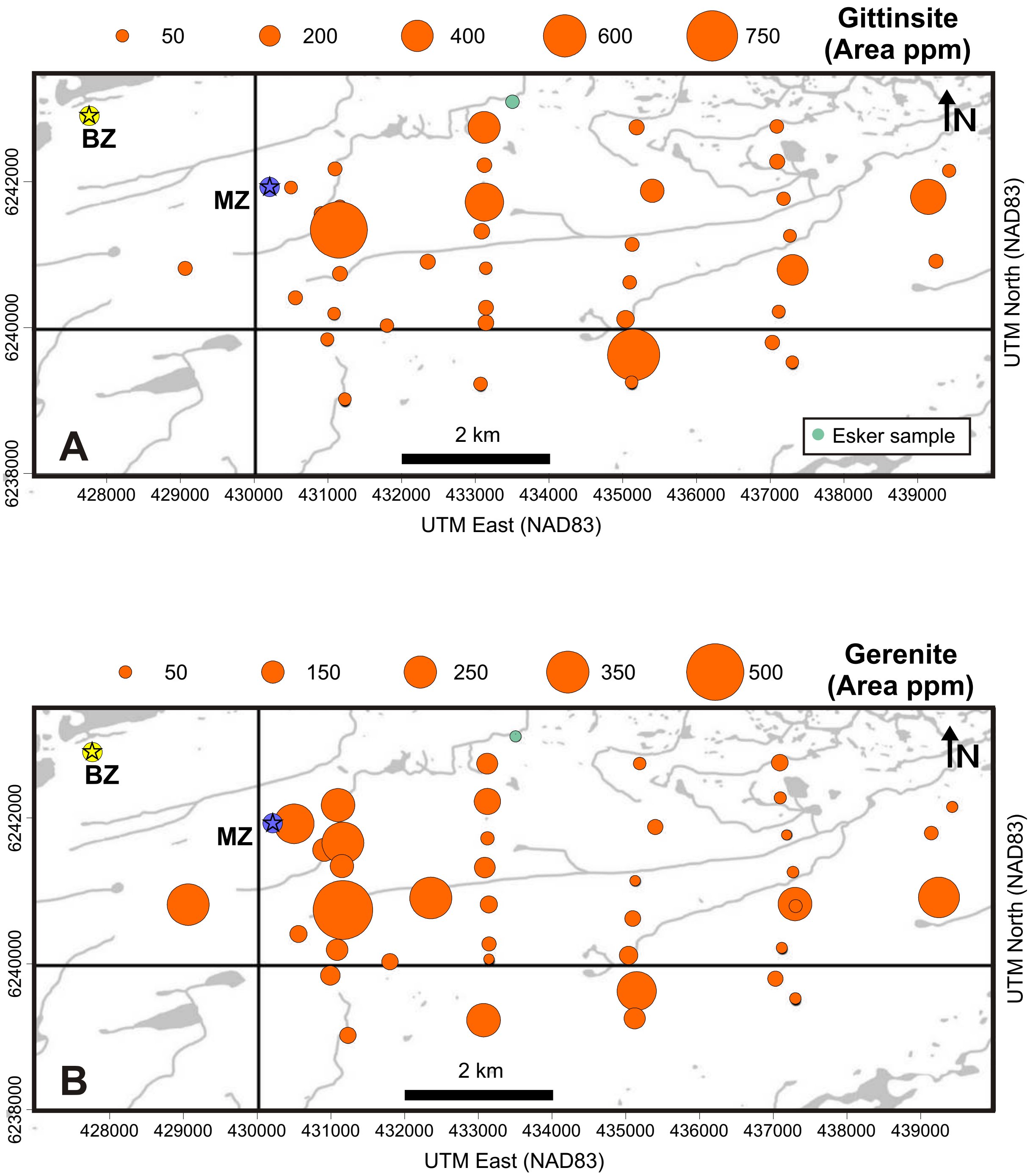

Figure 7.36. Geographic variation patterns for minerals in Grid 1, closest to the Strange Lake deposits. (A) Gittinsite abundances. (B) Gerenite abundances. See text for discussion.

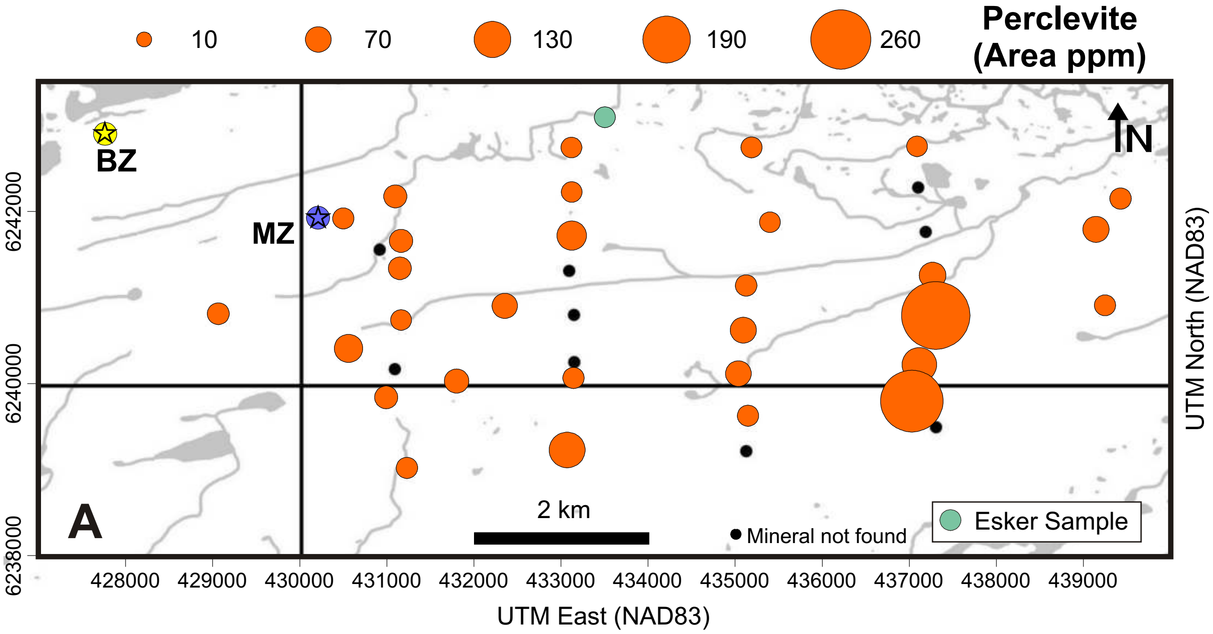

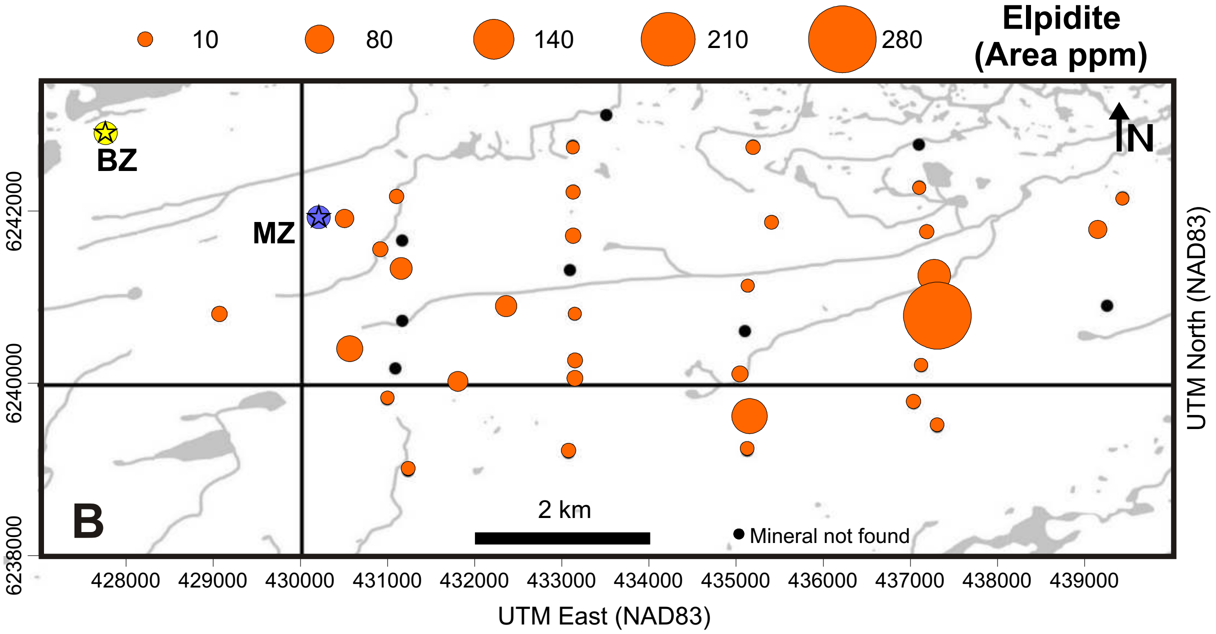

Figure 7.37. Geographic variation patterns for minerals in Grid 1, closest to the Strange Lake deposits. (A) Perclevite abundances. (B) Elpidite abundances. See text for discussion.

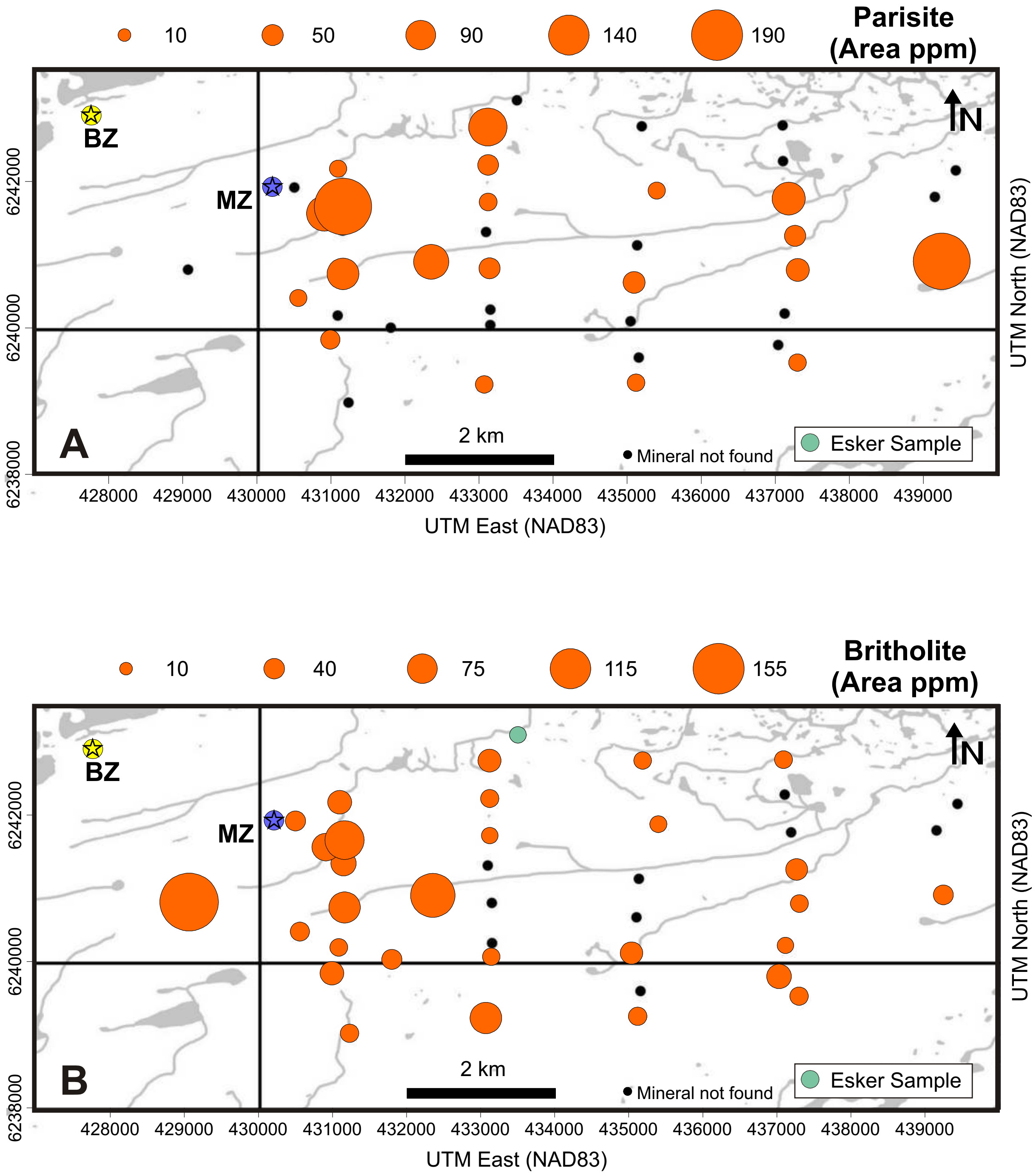

Figure 7.38. Geographic variation patterns for minerals in Grid 1, closest to the Strange Lake deposits. (A) Parisite abundances. (B) Britholite abundances. See text for discussion.

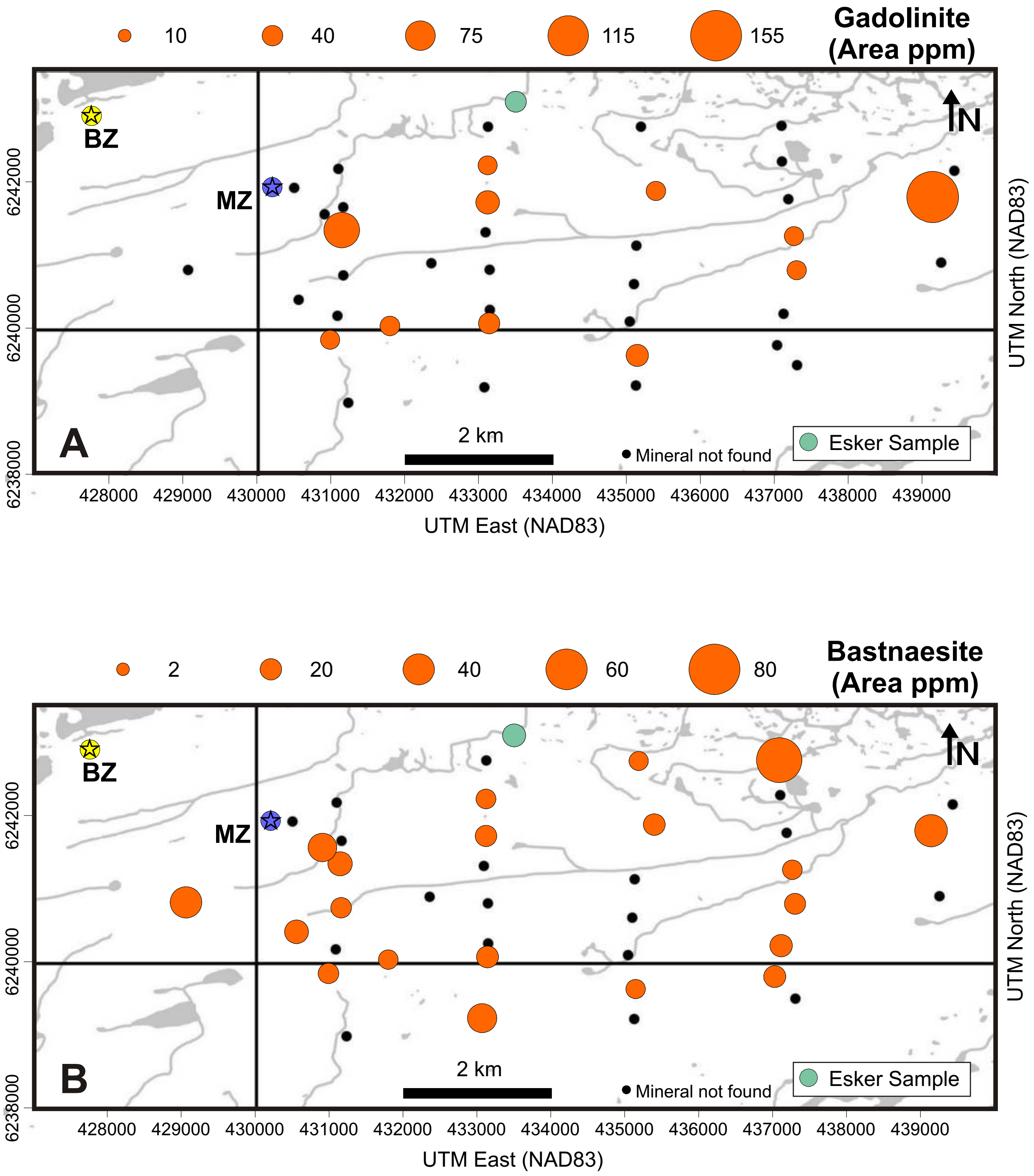

Figure 7.39. Geographic variation patterns for minerals in Grid 1, closest to the Strange Lake deposits. (A) Gadolinite abundances. (B) Bastnaesite abundances. See text for discussion.

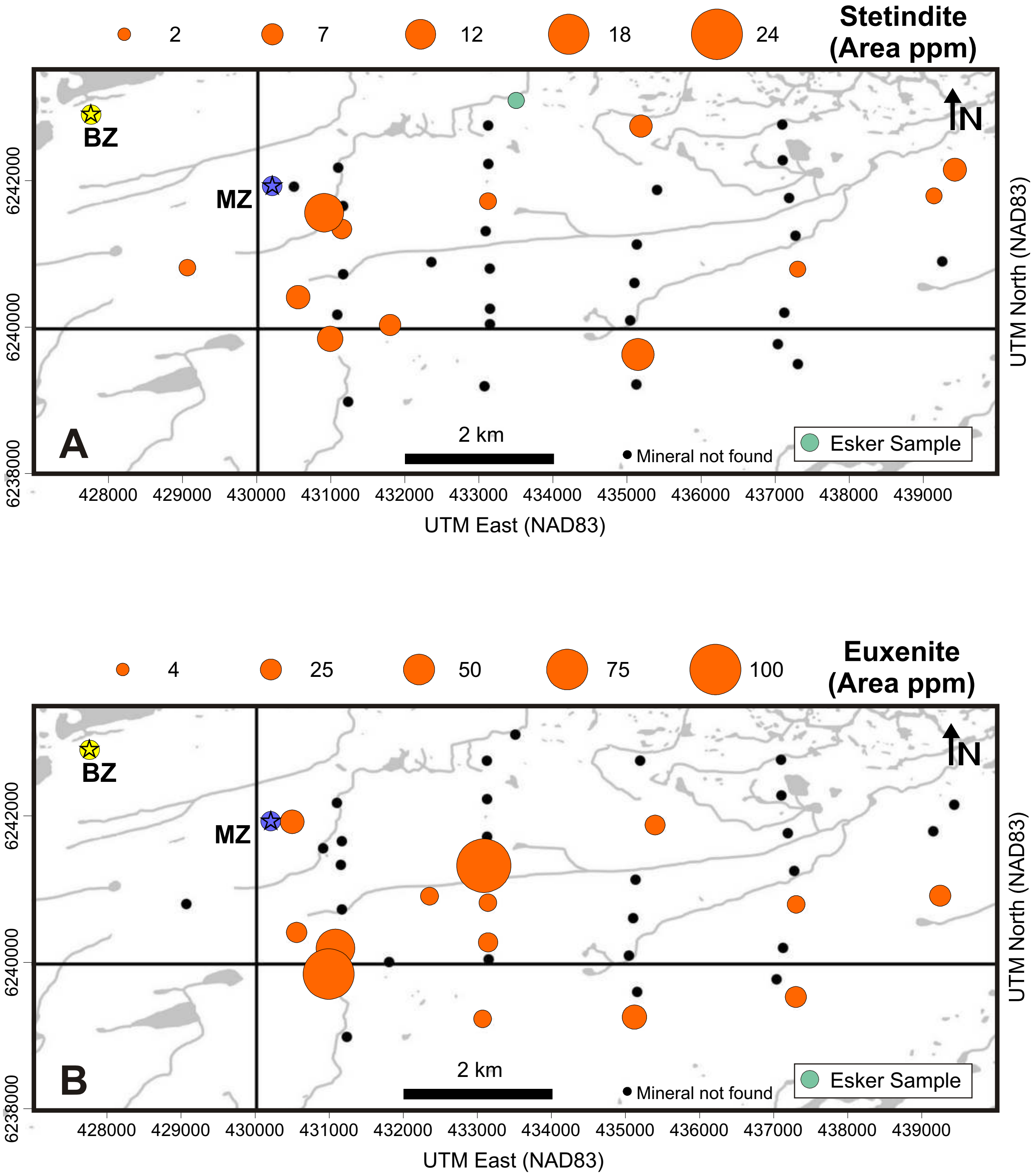

Figure 7.40. Geographic variation patterns for minerals in Grid 1, closest to the Strange Lake deposits. (A) Stetindite abundances. (B) Euxenite abundances. See text for discussion.

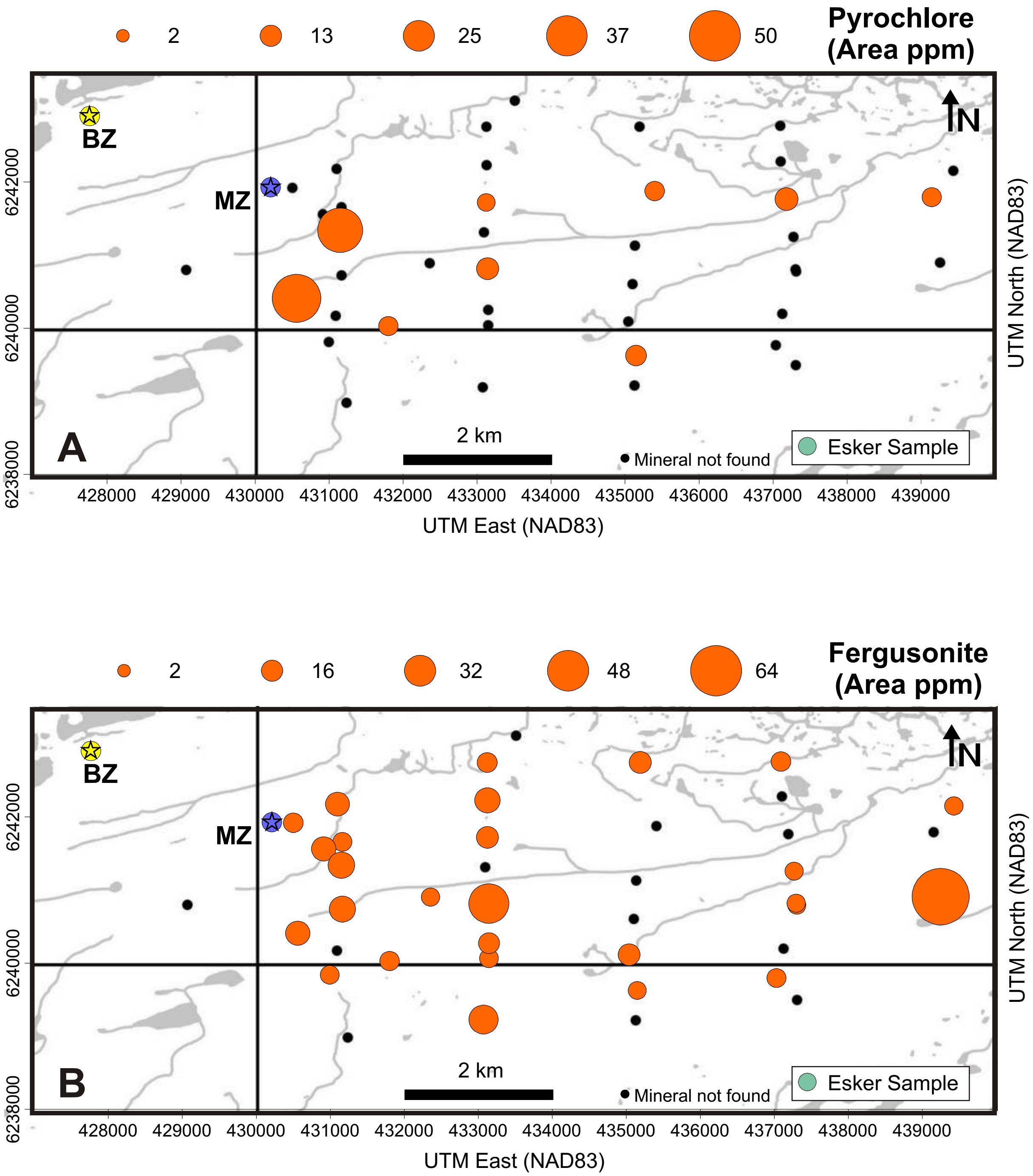

Figure 7.41. Geographic variation patterns for minerals in Grid 1, closest to the Strange Lake deposits. (A) Pyrochlore abundances. (B) Fergusonite abundances. See text for discussion.

Table 7.1. Graphical table showing the presence and absence of indicator minerals in Grid 1, close to Strange Lake

Sample	Distance (km)	Zircon*	Aegirine*	Apatite*	Gittinsite	Allanite*	Aenigmatite*	Gerenite	"Ericssonite"*	Percleveite	Elpidite	Astrophyllite*	Thorite	Parisite	Britholite	Gadolinite	Bastnaesite	Uraninite*	Rhodonite*	Stetindite	Pyrochlore	Fergusonite	Euxenite
G1-1	1.4	▨	□	□	□	□	▨	▨	▨	□	▨	▨	■	■	▨	■	■	▨	■	■	■	□	▨
G1-5	2.0	▨	□	▨	□	▨	▨	▨	▨	■	□	▨	□	▨	▨	■	▨	■	▨	▨	■	▨	■
G1-7	2.0	▨	▨	▨	□	□	▨	▨	▨	□	□	▨	□	□	▨	■	■	□	▨	■	■	▨	■
G1-6	2.1	▨	□	▨	□	▨	▨	▨	▨	□	□	▨	□	■	▨	■	▨	■	▨	□	■	■	■
G1-8	2.1	▨	▨	▨	□	▨	▨	▨	▨	□	■	□	□	▨	▨	■	■	▨	▨	■	■	□	■
G1-9	2.3	□	□	□	▨	▨	□	▨	□	□	▨	□	□	■	▨	▨	▨	▨	■	□	▨	▨	■
G1-4	2.6	▨	▨	□	□	□	▨	▨	▨	▨	▨	▨	■	□	□	■	▨	□	▨	□	▨	▨	▨
G1-10	2.7	▨	▨	▨	□	□	▨	▨	▨	□	■	□	▨	▨	▨	■	□	□	■	■	■	▨	■
G1-11	3.0	▨	▨	□	□	□	▨	▨	▨	□	■	▨	■	■	□	■	■	▨	□	■	■	■	▨
G1-12	3.3	□	□	▨	□	□	□	▨	□	□	□	□	□	□	▨	□	□	□	■	▨	■	□	▨
G1-2	3.5	▨	▨	▨	□	□	▨	▨	▨	▨	▨	▨	▨	▨	▨	■	■	□	■	■	■	□	□
G1-3	3.6	□	▨	□	□	▨	□	□	□	▨	▨	▨	■	■	▨	□	□	■	■	□	□	□	■
G1-20	4.0	▨	▨	▨	□	□	□	▨	▨	□	□	▨	□	▨	□	□	□	■	■	■	■	▨	■
G1-21	4.0	▨	□	▨	▨	□	□	▨	▨	□	□	□	□	▨	▨	■	■	▨	■	■	■	□	■
G1-19	4.0	□	□	□	▨	▨	□	□	□	▨	□	■	□	□	□	▨	□	▨	■	□	□	▨	■
G1-18	4.1	▨	□	▨	□	▨	▨	▨	▨	□	■	■	▨	■	■	■	■	■	■	■	■	■	▨
G1-13	4.1	▨	▨	▨	□	▨	▨	□	□	□	□	□	■	■	□	■	■	▨	■	■	■	■	■
G1-17	4.3	▨	□	▨	□	□	▨	▨	□	■	□	□	□	▨	■	■	■	■	■	■	▨	▨	□
E-1	4.4	□	□	▨	□	□	□	□	■	□	■	■	□	■	□	□	▨	■	■	□	■	■	■
G1-16	4.5	▨	□	▨	□	□	▨	□	▨	■	□	▨	□	■	■	■	■	■	■	■	■	▨	▨
G1-15	4.6	▨	□	□	□	▨	□	□	□	□	□	□	■	■	□	□	□	■	■	■	■	□	■
G1-14	5.1	▨	□	▨	□	▨	▨	▨	▨	▨	□	□	▨	□	▨	■	▨	▨	■	■	■	▨	□
G1-22	6.0	▨	□	▨	□	▨	▨	□	□	□	□	□	□	■	□	■	□	□	■	□	■	▨	■
G1-24	6.1	▨	▨	□	□	□	▨	□	▨	□	□	□	■	■	■	■	■	■	■	■	■	■	■
G1-25	6.2	▨	□	□	□	□	□	□	□	▨	■	□	□	▨	■	■	■	■	▨	■	■	■	■
G1-23	6.3	□	□	□	□	▨	□	□	□	□	□	□	■	□	□	□	□	■	■	■	□	■	▨
G1-26	6.3	□	□	□	□	□	□	▨	□	▨	□	▨	□	■	▨	■	■	■	■	■	■	▨	■
G1-27	6.6	▨	▨	□	▨	▨	□	▨	□	□	▨	□	□	■	■	▨	□	■	■	▨	□	□	■
G1-28	6.8	▨	□	▨	■	□	▨	▨	▨	■	□	□	□	□	□	■	■	□	■	■	■	■	▨
G1-36	7.9	▨	▨	□	□	□	▨	□	▨	■	□	▨	□	■	■	■	■	■	■	■	■	■	■
G1-37	7.9	▨	□	▨	□	□	▨	□	□	□	■	□	■	■	□	■	▨	■	■	■	■	□	■
G1-35	8.0	□	□	□	□	□	□	□	□	■	□	□	□	▨	■	■	■	■	■	■	▨	■	■
G1-34	8.2	□	□	□	□	□	□	□	□	▨	▨	■	▨	▨	▨	□	□	■	■	■	■	□	■
G1-31	8.2	□	□	▨	□	□	□	□	□	▨	□	□	■	■	□	■	▨	■	■	■	■	■	■
G1-32	8.3	□	□	□	■	□	□	▨	□	▨	▨	■	□	□	■	■	■	■	■	■	■	□	■
G1-30	8.3	▨	□	▨	□	▨	▨	□	□	▨	□	▨	□	■	▨	■	□	□	■	■	■	□	■
G1-33	8.3	□	□	□	▨	▨	□	□	▨	▨	▨	□	▨	▨	□	□	□	■	■	□	■	□	□
G1-29	8.6	▨	□	□	□	▨	□	□	▨	■	□	□	□	□	□	■	■	▨	■	■	■	■	▨
G1-39	10.0	□	▨	□	▨	▨	□	□	□	▨	▨	□	□	■	■	▨	▨	■	■	□	□	■	■
G1-40	10.2	▨	□	□	□	▨	□	▨	□	□	■	□	▨	▨	▨	■	■	■	■	■	■	▨	▨
G1-38	10.3	□	□	□	□	□	□	□	□	□	□	□	□	■	■	■	■	■	▨	□	■	□	■
Mean Value (area ppm)		4145	2114	1331	175	136	108	92	58	20	18	17	13	13	11	10	6.6	5.8	5.8	5.6	4.4	4.1	4.1

■ Mineral Absent □ Mineral < Mean Value ▨ Mineral > Mean Value

Notes: Distance is in kilometres measured from the midpoint between the Main Zone and B-Zone deposits
Mean abundance values include zero values and are unlikely to be representative for least abundant minerals. These are calculated for the entire database, rather than for Grid 1. * Mineral for which sources may not be restricted to Strange Lake

Table 7.2. Graphical table showing the presence and absence of indicator minerals throughout the area

		Sample	Distance (km)	Zircon*	Aegirine*	Apatite*	Gittinsite	Allanite*	Aenigmatite*	Gerenite	"Ericssonite"*	Percleveite	Elpidite	Astrophyllite*	Thorite	Parisite	Britholite	Gadolinite	Bastnaesite	Uraninite*	Rhodonite*	Stetindite	Pyrochlore	Fergusonite	Euxenite
GRID 1		G1-1	1.4	X	X	X	X	X	X	X	X	X	X	X	■	■	X	■	■	X	■	■	■	X	X
		G1-5	2.0	X	X	X	X	X	X	X	X	■	X	X	X	X	X	■	X	■	X	X	■	X	■
		G1-7	2.0	X	X	X	X	X	X	X	X	X	X	X	X	X	X	■	■	X	X	■	■	X	■
		G1-6	2.1	X	X	X	X	X	X	X	X	X	X	X	X	■	X	■	X	■	X	X	■	■	■
		G1-8	2.1	X	X	X	X	X	X	X	X	X	■	X	X	X	X	■	■	X	X	■	■	X	■
		G1-9	2.3	X	X	X	X	X	X	X	X	X	X	X	X	■	X	X	X	X	■	X	X	X	■
		G1-4	2.6	X	X	X	X	X	X	X	X	X	X	X	■	X	X	■	X	X	X	X	X	X	X
		G1-10	2.7	X	X	X	X	X	X	X	X	X	■	X	X	X	X	■	X	X	■	■	■	X	■
		G1-11	3.0	X	X	X	X	X	X	X	X	■	■	X	■	■	X	■	■	X	X	■	■	■	X
		G1-12	3.3	X	X	X	X	X	X	X	X	X	X	X	X	X	X	X	X	X	■	X	■	X	X
		G1-2	3.5	X	X	X	X	X	X	X	X	X	X	X	X	X	X	■	■	X	■	■	■	X	X
		G1-3	3.6	X	X	X	X	X	X	X	X	X	X	X	■	■	X	X	X	■	■	X	X	X	■
		G1-20	4.0	X	X	X	X	X	X	X	X	X	X	X	X	X	X	X	X	■	■	■	■	X	■
		G1-21	4.0	X	X	X	X	X	X	X	X	X	X	X	X	X	X	■	■	X	■	■	■	X	■
		G1-19	4.0	X	X	X	X	X	X	X	X	X	X	■	X	X	X	X	X	X	■	X	X	X	■
		G1-18	4.1	X	X	X	X	X	X	X	X	■	■	■	X	■	■	■	■	■	■	■	■	■	X
		G1-13	4.1	X	X	X	X	X	X	X	X	X	X	X	■	■	X	■	■	X	■	■	■	■	■
		G1-17	4.3	X	X	X	X	X	X	X	X	■	X	X	X	X	■	■	■	■	■	■	X	X	X
	ESKER	E-1	4.4	X	X	X	X	X	X	X	■	X	■	■	X	■	X	X	X	■	■	X	■	■	■
		G1-16	4.5	X	X	X	X	X	X	X	X	■	X	X	X	■	■	■	■	■	■	■	■	X	X
		G1-15	4.6	X	X	X	X	X	X	X	X	X	X	X	■	■	X	X	X	■	■	■	■	X	■
		G1-14	5.1	X	X	X	X	X	X	X	X	X	X	X	X	X	X	■	X	X	■	■	■	X	X
		G1-22	6.0	X	X	X	X	X	X	X	X	X	X	X	X	■	X	■	X	X	■	X	■	X	■
		G1-24	6.1	X	X	X	X	X	X	X	X	X	X	X	■	■	■	■	■	■	■	■	■	■	■
		G1-25	6.2	X	X	X	X	X	X	X	X	X	■	X	X	X	■	■	■	■	X	■	■	■	■
		G1-23	6.3	X	X	X	X	X	X	X	X	X	X	X	■	X	X	X	X	■	■	■	X	■	X
		G1-26	6.3	X	X	X	X	X	X	X	X	X	X	X	X	■	X	■	■	■	■	■	■	X	■
		G1-27	6.6	X	X	X	X	X	X	X	X	X	X	X	X	■	■	X	X	■	■	X	X	X	■
		G1-28	6.8	X	X	X	■	X	X	X	X	■	X	X	X	X	X	■	■	X	■	■	■	■	X
		G1-36	7.9	X	X	X	X	X	X	X	X	■	X	X	X	■	■	■	■	■	■	■	■	■	■
		G1-37	7.9	X	X	X	X	X	X	X	X	X	■	X	■	■	X	■	X	■	■	■	■	X	■
		G1-35	8.0	X	X	X	X	X	X	X	X	■	X	X	X	X	■	■	■	■	■	■	X	■	■
		G1-34	8.2	X	X	X	X	X	X	X	X	X	X	■	X	X	X	X	X	■	■	■	■	X	■
		G1-31	8.2	X	X	X	X	X	X	X	X	X	X	X	■	■	X	■	X	■	■	■	■	■	■
		G1-32	8.3	X	X	X	■	X	X	X	X	X	X	■	X	X	■	■	■	■	■	■	■	X	■
		G1-30	8.3	X	X	X	X	X	X	X	X	X	X	X	X	■	X	■	X	X	■	■	■	X	■
		G1-33	8.3	X	X	X	X	X	X	X	X	X	X	X	X	X	X	X	X	■	■	X	■	X	X
		G1-29	8.6	X	X	X	X	X	X	X	X	■	X	X	X	X	X	■	■	X	■	■	■	■	X
		G1-39	10.0	X	X	X	X	X	X	X	X	X	X	X	X	■	■	X	X	■	■	X	X	■	■
		G1-40	10.2	X	X	X	X	X	X	X	X	X	■	X	X	X	X	■	■	■	■	■	■	X	X
		G1-38	10.3	X	X	X	X	X	X	X	X	X	X	X	X	■	■	■	■	■	X	X	■	X	■
	ESKER	E-3	12.8	X	X	X	X	X	X	X	■	X	■	X	■	■	■	X	■	■	■	X	■	■	■
GRID 2		G2-1	14.4	X	X	X	X	X	X	X	X	X	X	X	X	■	■	■	X	■	■	X	X	■	X
		G2-2	14.7	X	X	X	X	X	X	X	X	X	X	X	■	X	■	X	X	X	■	X	X	X	■
		G2-4	15.4	X	X	X	X	X	X	X	X	X	X	X	■	X	■	■	■	■	■	■	■	■	■
		G2-3	15.5	X	X	X	■	X	X	X	X	X	X	■	X	■	X	■	■	X	■	■	■	X	■
	ESKER	E-4	16.1	X	X	X	X	X	X	X	■	■	X	X	■	■	■	■	■	■	X	■	■	■	■
		G2-5	16.5	X	X	X	X	X	X	X	X	X	X	X	X	■	X	X	X	■	X	X	■	■	■
		G2-6	16.6	X	X	X	X	X	X	X	X	X	X	X	X	■	X	X	■	X	■	X	X	X	■
		G2-7	17.0	X	X	X	X	X	X	X	X	■	■	■	■	X	■	■	■	■	■	■	■	■	■
		G2-8	18.4	X	X	X	X	X	X	X	X	X	X	X	X	■	■	X	X	■	X	X	X	■	■
		G2-10	19.0	X	X	X	X	X	X	X	X	X	X	X	X	■	■	X	■	■	X	■	X	X	■
		G2-9	19.3	X	X	X	X	X	X	X	X	■	■	X	■	X	X	■	X	■	X	■	■	X	X
		G2-11	20.6	X	X	X	X	X	X	X	■	X	X	■	X	■	■	X	X	■	■	X	X	■	■
		G2-12	21.0	X	X	X	X	X	X	X	X	X	X	X	X	■	X	X	X	X	X	X	X	■	■
		G2-13	21.2	X	X	X	■	X	X	■	X	X	X	X	X	■	■	■	■	■	■	■	X	X	■
		G2-16	23.1	X	X	X	■	X	X	X	X	■	X	■	■	X	■	■	■	■	■	■	■	X	X
		G2-17	24.5	X	X	X	X	X	X	X	■	X	X	■	■	■	X	■	■	■	■	X	■	■	■
		G2-18	24.5	X	X	X	X	X	X	X	X	X	X	■	X	■	■	X	X	■	X	X	X	X	■
		G2-19	25.1	X	X	X	X	X	X	X	■	X	X	X	X	■	■	X	■	■	■	■	■	■	■
	CONTROL	G2-15	27.2	X	X	X	■	X	X	■	■	■	X	■	■	■	■	■	■	■	X	■	■	X	■
		G2-14	27.2	X	X	X	X	X	X	X	X	X	X	X	X	■	■	X	■	■	■	X	X	■	■
GRID 3		G3-2	27.3	X	X	X	X	X	X	X	■	■	X	■	X	■	■	■	■	■	■	■	X	■	■
	ESKER	E-7	28.0	X	X	X	X	X	X	X	X	X	X	X	■	■	■	■	X	■	■	X	X	X	■
		G3-3	28.2	X	X	X	X	■	X	■	■	■	■	■	■	■	■	■	■	■	■	■	X	X	■
		G3-4	29.8	X	X	X	X	X	X	X	X	X	X	■	■	■	■	X	■	■	■	X	X	X	■
		G3-6	29.9	X	X	X	X	X	X	X	■	X	X	X	■	■	■	X	X	■	X	X	■	■	■
		G3-5	30.1	X	X	X	X	X	X	X	X	X	X	X	■	■	■	X	X	■	■	X	■	■	■
		G3-7	30.5	X	X	X	X	X	X	X	X	X	X	■	X	■	■	X	X	■	■	X	X	X	■
		G3-8	30.8	X	X	X	X	X	X	X	■	X	X	X	X	■	■	X	X	■	■	X	X	■	■
	ESKER	E-8	31.5	X	X	X	X	X	X	X	X	X	X	X	X	X	■	X	X	X	■	X	X	X	X
		G3-10	31.6	X	X	X	X	X	X	X	■	X	X	X	■	■	■	X	■	■	■	X	X	X	■
		G3-9	32.0	X	X	X	X	X	X	X	■	X	X	X	X	■	■	■	■	■	■	X	X	■	■
		G3-12	32.8	X	X	X	X	X	X	X	■	X	X	X	■	■	X	■	X	■	■	X	X	■	■
		G3-13	33.1	X	X	X	X	X	X	X	X	X	X	X	X	■	■	■	■	■	■	X	X	■	■
		G3-11	33.4	X	X	X	X	X	X	X	X	X	X	■	X	■	■	X	■	■	■	■	X	■	■

X	PRESENT
■	ABSENT

It is also possible to calculate correlation coefficients among potential indicator minerals for Strange Lake, in the same manner used in Chapter 6. However, this must be approached with caution because uncertainties are high and the actual amount of data that is assessed is small, because zero data values are excluded. Table 7.3 presents a correlation coefficient matrix for selected potential indicator minerals in Grid 1 samples only. The most obvious conclusion from these data is that there are few significant positive or negative correlations among these minerals. There are a few exceptions, but mostly between pairs of more abundant rare accessory minerals. There is little to be drawn from the very weak correlations indicated between the trace minerals.

Other Accessory and Trace Minerals

Some other rare accessory and trace minerals display geographic variation patterns that may be significant, but cannot be easily connected to dispersion from Strange Lake. The rare Ba-Mn-silicate “ericssonite” occurs in 62 of 76 samples, and its regional geographic pattern is similar to several of the REE-bearing minerals discussed above, including strong enrichment close to the Main Zone Deposit (Figure 7.42). At first sight, this might suggest a connection between “ericssonite” and Strange Lake, but Baird (2018) recorded this mineral only in a few drill-core samples, and then only in trivial amounts (< 8 area ppm). Thus, Strange Lake may not be a viable source. As noted in Chapter 6, there is also strong correlation between “ericssonite” and the composite variable [garnet + hornblende + ilmenite], which would suggest a regional control. However, this would imply that “ericssonite” is widespread, even though documented occurrences are only in Sweden and Japan (Sokolova et al., 2018; www.mindat.org). This is a puzzle, albeit a small one.

Additional information presented in Chapter 8 suggests that there might indeed be a connection between Strange Lake and “ericssonite”, but a more complex one, and also imply that this mineral identification might also need revision. The phosphate monazite does not show much sign of systematic geographic variations, and its average abundance in till samples is about ten times lower than in drill core samples from Strange Lake analyzed by Baird (2018). It is also widespread as an accessory mineral in other rock types. So, although monazite is present at Strange Lake, it is not likely that all monazite in till samples actually came from there. The patterns for calcite, fluorite, barite, “benitoite”, pyrite, wollastonite, and pectolite did not reveal any clear systematic geographic variations, but the Mn-rich pyroxene rhodonite seems mostly to be enriched in Grid 1, although missing from many samples (Figure 7.43). Maps and profiles for minerals not illustrated in this Chapter are provided in the Appendices.

Table 7.3. Spearman Correlation Matrix for minerals associated with the Strange Lake Intrusion and its mineral deposits, for till samples in the area of Grid 1, located in the area immediately east of and within the Strange Lake Intrusion (N=40)

	Zircon	Aegirine	Thorite	Gittinsite	Aenigmatite	Gerenite	Perclevite	Elpidite	Astrophyllite	Parisite	Britholite	Gadolinite	Bastnaesite	Stetindite	Fergusonite	Pyrochlore	Euxenite
Aegirine	0.30	.	.	.	.	.	.	.	.	.	.	.	.	.	.	.	.
Thorite	0.28	-0.08	.	.	.	.	.	.	.	.	.	.	.	.	.	.	.
Gittinsite	-0.05	0.18	0.26	.	.	.	.	.	.	.	.	.	.	.	.	.	.
Aenigmatite	0.72	0.33	0.00	-0.30	.	.	.	.	.	.	.	.	.	.	.	.	.
Gerenite	0.45	0.31	0.40	0.02	0.42	..	.	.	.	.	.	.	.	.	.	.	.
Perclevite	-0.34	0.00	0.19	0.09	-0.37	-0.01	.	.	.	.	.	.	.	.	.	.	.
Elpidite	-0.39	-0.01	0.08	0.29	-0.28	0.00	0.48	.	.	.	.	.	.	.	.	.	.
Astrophyllite	0.43	0.40	-0.03	-0.03	0.62	0.31	-0.08	0.07	.	.	.	.	.	.	.	.	.
Parisite	0.07	-0.01	0.54	-0.08	0.06	0.29	0.00	-0.15	-0.04	.	.	.	.	.	.	.	.
Britholite	0.24	0.23	0.39	0.01	0.32	0.58	0.22	0.14	0.47	0.32	.	.	.	.	.	.	.
Gadolinite	-0.48	0.01	-0.08	0.46	-0.62	-0.17	0.26	0.51	-0.38	-0.09	-0.10	.	.	.	.	.	.
Bastnaesite	-0.20	0.05	-0.03	0.34	-0.24	-0.03	0.34	0.34	-0.04	-0.15	0.27	0.47	.	.	.	.	.
Stetindite	-0.29	0.04	-0.10	0.28	-0.21	-0.01	0.19	0.43	0.01	-0.14	0.06	0.44	0.45	.	.	.	.
Fergusonite	0.17	0.06	0.27	0.18	0.12	0.40	0.06	0.11	0.36	0.28	0.42	0.00	0.19	0.16	.	.	.
Pyrochlore	-0.43	0.09	-0.28	0.25	-0.29	-0.11	0.03	0.34	-0.17	-0.05	-0.23	0.49	0.26	0.40	0.10	.	.
Euxenite	0.17	-0.13	-0.06	-0.21	0.23	0.19	-0.27	-0.12	0.03	0.11	0.02	-0.14	-0.22	-0.11	-0.05	-0.05	.
Changbaiite	-0.31	0.09	-0.11	0.34	-0.28	0.03	0.16	0.31	-0.10	-0.04	-0.06	0.48	0.24	0.47	0.29	0.76	-0.14

Classification	Colour Code	
"Strong" +	> 0.7	POSITIVE
"Moderate" +	0.5 to 0.7	CORRELATION
"Weak" +	0.3 to 0.5	
Not Significant	-0.3 to 0.3	
"Weak" -	-0.3 to -0.5	
"Moderate" -	-0.5 to -0.7	NEGATIVE (INVERSE)
"Strong" -	< -0.7	CORRELATION

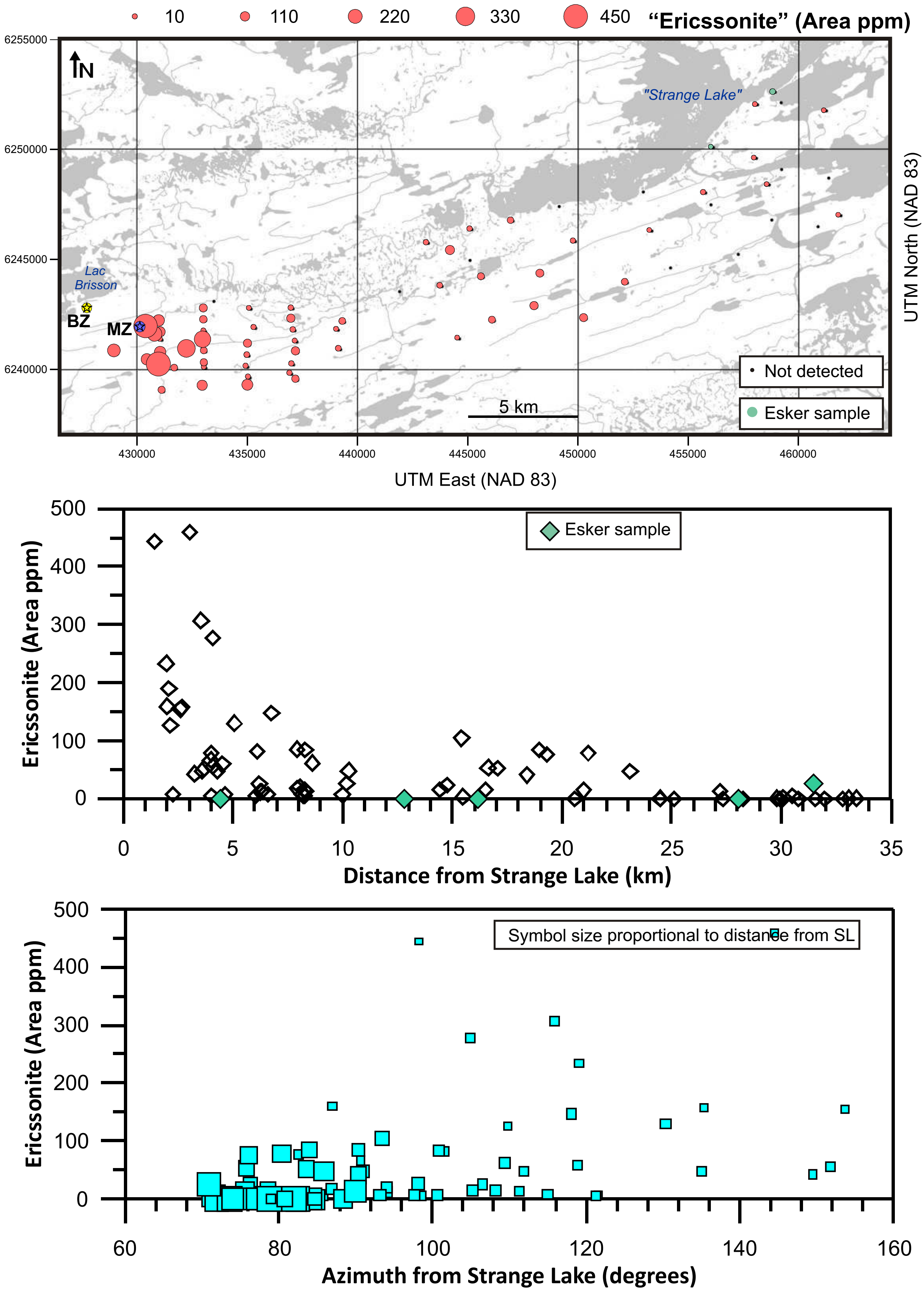

Figure 7.42. Geographic variation patterns for "ericssonite" (area ppm). Upper Panel is a map view with proportional symbols. Lower panels show "ericssonite" abundances against distance and azimuth from Strange Lake. See text for discussion.

SUMMARY OF OBSERVATIONS

Like many aspects of this project, assessing patterns of geographic variation in mineralogy involves processing and representing large amounts of information, and no method for this is perfect. However, proportional symbol maps (also known as ‘bubble maps’), in combination with profiles showing the relationships between mineral abundances and distance/azimuth from Strange Lake, provide useful insight into geographic variation. The inferences add to conclusions already drawn in Chapter 6 from analysis of numerical data. Many of the minerals detected in the till samples do indeed show systematic geographic abundance variations, but these patterns likely have more than one cause. Some reflect variations in the relative contributions of regional bedrock sources, whereas others must reflect very specific contributions from unusual source rocks of the Strange Lake area. In some cases, these regional and local patterns are superficially similar, which complicates their interpretation.

Variations in the abundance of major minerals (notably quartz, K-feldspar, garnet, hornblende and ilmenite) subdivide the samples into two distinct groups, which appear to be geographically discrete. These patterns are considered to be of a regional nature, because they are defined in part by minerals that are absent or rare at Strange Lake (e.g., garnet, ilmenite), and minerals that are not diagnostic of Strange Lake (e.g., quartz, K-feldspar). Minor minerals generally show geographic patterns that resemble those of these major minerals, suggesting that their abundance is also controlled to a large extent by similar regional provenance factors. A ‘transition’ in the abundances of many minerals around the midpoint of the study area corresponds generally with a marked change in bedrock geology (Figure 2.8; Ryan et al., 2003). However, zircon abundance variations likely include a significant contribution from Strange Lake, which is supported by its strong enrichment in Grid 1.

The diverse accessory and trace minerals display equally diverse geographic variation patterns, and some of these minerals show little or no systematic geographic variation. Systematic patterns for some accessory minerals (e.g., staurolite, zoisite and possibly “ericssonite”) broadly resemble those attributed to regional geological influences, but others show distinctive patterns that suggest derivation from the Strange Lake area. However, minerals that are known to be characteristic of Strange Lake show rather different styles of geographic variation. Some (e.g., zircon, parisite, britholite, stetindite and possibly also uraninite) are only abundant close to Strange Lake and decline rapidly in abundance with increasing distance, whereas others (e.g., gittinsite, gadolinite, gerenite and elpidite) persist throughout the entire sample array and may remain detectable beyond it. In some cases, notably for gittinsite, some of the highest abundances are in the distal regions of the sample array, rather than close to Strange

Lake. The gittinsite pattern contrasts with that shown by the Y-Ca-REE silicate gerenite, for which abundance clearly decreases with distance from Strange Lake. Nb-bearing minerals such as pyrochlore and fergusonite, despite being present at very low abundances, also reveal comparable geographic patterns that indicate derivation from Strange Lake. The interpretation of patterns for the rare accessory and trace minerals is complicated by the fact that these are absent from many till samples, even in locations close to the Strange Lake deposits. Detailed examination of patterns, especially in Grid 1, where the rarest minerals are generally most abundant, shows little or no consistent pattern of mineral enrichment at a sample level. Table 7.1 provides a visually striking illustration of the patterns of presence and absence for various indicator minerals, which is anything but systematic for the rarer minerals. Geographic variation patterns become progressive ‘noisier’ or ‘spottier’ as the overall abundance of minerals declines, but systematic trends can still be discerned in a general sense. The patterns observed are consistent with the idea that ‘real’ variation patterns are progressively disrupted by probability effects at low abundances. The relatively small size of the samples analyzed using MLA-SEM methods is an important but unavoidable factor in this, as discussed in Chapter 4. The impact of such effects on data reliability is not only determined by the abundance of minerals, as it will be mitigated in cases where the mineral in question forms smaller ‘grains’ within larger composite particles of a more abundant mineral. The contrast in patterns for pyrochlore and fergusonite (Table 7.1) may be an example of such an effect. The average GPS ratio for pyrochlore (6.1%) is only slightly higher than that for fergusonite (5.1%), but the standard deviation for pyrochore is double that of fergusonite (Table 6.10), implying that larger discrete grains of pyrochlore are more numerous. Similarly, the very high rate of absence for uraninite could be linked to its much higher average GPS ratio of 33% (see Table 6.10).

To summarize, systematic geographic patterns of abundance are present for most, but not all, minerals evaluated in this project, and are visible at a wide range of scales. The patterns related to dispersion of material from Strange Lake are of particular interest, but they are also very difficult to assess. This complexity reflects the wide ranges in source abundance for indicator minerals, differences in their physical properties and possibly mineral associations, and different behaviour in the glacial environment. For the least abundant of the indicator minerals, there are additional complications from probability effects, which themselves likely have complex controls related to grain/particle size distributions. These effects introduce additional uncertainties, manifested as increased scatter in the data, and partially obscure real variation patterns. This is a difficult issue to assess, and even more difficult to resolve, but it does not invalidate the observations of systematic geographic variation that *can* made from at least some of these unique data.

CHAPTER 8: DISCUSSION AND CONCLUSIONS

GENERAL SUMMARY

This final Chapter of the thesis provides some additional discussion on a wide range of topics from previous Chapters, and draws some general and specific conclusions. Initial topics include issues related to analytical precision and the reliability of data for low-abundance indicator minerals, followed by an assessment of the applicability of the MLA-SEM method to this specific project area and more widely for indicator-mineral studies. The patterns revealed by MLA-SEM data are discussed, as are their relationships to regional geology and to glacial dispersion of materials from the Strange Lake area. The results of the thesis study are compared to previous indicator-mineral studies in the Strange Lake area, and also to the information from regional till geochemistry projects. The latter supports many findings from this project, but also illuminates some potential problems that relate largely to the heterogeneity of sample materials. Some specific findings related to particular minerals and mineral associations are also reviewed and discussed. The Chapter concludes with a summary of the main findings, and some research recommendations that apply to future investigations using these methods.

INTRODUCTION

Like most research projects, this thesis did not closely follow the plan envisaged at its outset. Some objectives were successfully addressed, but results were not always exactly as anticipated. Some aspects did not provide useful insights, but may still be relevant for future work. Last, but not least, the data and evaluation of other related research work led to some unexpected conclusions, which have possible implications for future research. This final full chapter of the thesis selectively reviews key information presented in Chapters 5, 6 and 7, expands earlier discussions, and presents a closing summary of conclusions and suggestions for further research. In addition to the MLA-SEM data from it also discusses geochemical data from other recent exploration-related research. Components of figures and tables used in earlier Chapters are in places reused to emphasize similarities, contrasts or other aspects of importance. This approach is used for the convenience of readers, and the original figures are also referenced for additional information.

APPLICATION OF VISIBLE/INFRARED SPECTROSCOPY (VIRS) METHODS FOR RECOGNITION OF INDICATOR MINERALS

Chapter 5 reported on a pilot investigation using Visible/Infrared Reflectance Spectroscopy (VIRS) methods to examine fine-grained material from till samples. This was to see if such methods could detect unusual Zr- or REE-bearing minerals derived from the Strange Lake deposits. This is theoretically possible, as many of these minerals have distinctive spectral absorption features, notably in the visible and near-infrared (VNIR) regions. Kerr et al. (2011) successfully detected some minerals in coarse-grained, high-grade rock samples from Strange Lake. There are few available reference spectra for minerals from Strange Lake, but general information from Kerr et al. (2011), Turner et al. (2015 . ; 2018) and Jeanne Percival of the Geological Survey of Canada (unpublished data) was used for comparison.

Unfortunately, the absorption spectra from the till samples were completely uninformative. Closer examination of some spectra at expanded scale showed some subtle absorption features but these did not correspond with any features associated with the REE. The results do not indicate a lack of indicator minerals in the samples, because later MLA-SEM analysis demonstrated their presence, although their abundance was lower than anticipated. Other studies that characterize such minerals using VIRS used larger crystalline masses, or rocks containing percent-level concentrations of such minerals, rather than merely a few hundred area ppm (<0.1%). Zircon is the only possible indicator mineral that ever occurs at levels approaching or exceeding 1% in till samples, and it is not fully diagnostic of Strange Lake. In retrospect, the lack of any response to VIRS methods is not surprising. The results suggest that there is little possibility that such methods could detect glacially dispersed material from deposits like Strange Lake, unless there is an orders-of-magnitude increase in instrumental sensitivity.

EVALUATION OF MLA-SEM METHODS IN INDICATOR MINERAL STUDIES

General Information

Evaluation of the MLA-SEM method for indicator mineral studies was a prime objective of this research. The results were of research were generally positive, and support the views of Wilton et al. (2017) about the method’s long-term potential in mineral exploration. Indicator minerals were successfully identified in many samples, whereas earlier studies using conventional techniques found very few. However, the absolute abundance of diagnostic indicator minerals in till samples was less than anticipated from earlier information on source rocks at Strange Lake. The MLA-SEM data revealed systematic geographic variation patterns in mineral abundance, which are difficult to extract from the results of conventional surveys. The data for the rarest indicator minerals are difficult to assess, because these are missing from many samples. This observation prompted some consideration of problems related to analytical precision and the influence of 'probability effects' on low-level data. Many minerals detected at higher abundances are not diagnostic of Strange Lake, but their systematic variation patterns are also of interest in the context of regional geology. This aspect is reviewed in a later section.

Particles, Precision and Probability

MLA-SEM analysis produces vast amounts of data for even a relatively small project. The range of mineral abundance measured covers five orders of magnitude, from more than 60 area % (for quartz in some samples) to less than 10 area ppm (< 0.001 area %) for indicator minerals such as bastnaesite and pyrochlore. Previous accounts (e.g., Sylvester et al., 2012; Wilton et al., 2017) have generally not assessed the precision of analysis for such low-abundance minerals, but this is obviously important in interpretation.

The fundamental issue is quite simple, and was introduced in Chapter 4. In an analyzed sample containing 20,000 particles of roughly equal size, drawn from a much larger mass containing millions of such particles, a rare mineral that has an abundance of 50 area ppm would be represented by only one particle. Consequently, the presence of this particle (or a small number of particles) in the analyzed sample will be governed largely by probability effects. The probability that particles occur in proportion to their actual abundance is very small, but there is also an even smaller probability that they are over-represented. However, the most probable outcome is that they will be absent from the analyzed sample. This type of problem is intrinsic in the analysis of particulate materials (e.g., Davis, 2003), and is a perennial complication in the exploration of gold deposits, where it is dubbed 'the nugget effect'. The frequency distributions of the rarest minerals are strongly positively skewed, with many zero values and a few scattered highly anomalous values (see Chapter 6). This is a common signature of such 'probability effects' (e.g., Davis, 2003, Simmonds, 2009). If such effects dominate variation in the abundance of rare minerals, comparisons between samples and assessment of data 'trends', would have little real meaning. This prospect is rather discouraging, but it is not supported by empirical results for minerals that have mean abundances above a few tens of area ppm, including the key indicator minerals gittinsite and gerenite. As discussed in Chapter 6, these minerals are present in almost all samples, show systematic abundance variations, define geographic patterns, and have marked correlations with more abundant minerals. Some of the less abundant indicator minerals do seem to be absent from many samples in a rather random geographic pattern, but these still show generalized patterns of geographic variation (see Chapters 6 and 7). Thus, there is a contradiction between conceptual models and observations from MLA-SEM data, which needs to be explained if the latter are to be realistically interpreted.

Microscale textural information presented by Currie (2019) in her study of far-travelled gittinsite particles found near Voisey's Bay provides an important clue. Gittinsite in till samples *did not form* discrete larger particles, but instead occurred as much smaller subdomains ('grains') within composite particles generally dominated by quartz. Similar SEM imagery from this project (see Chapter 6) did find some larger monomineralic gittinsite particles, but in most cases gittinsite occurs as smaller-scale intergrowths within larger grains of common silicates. If rare indicator minerals from Strange Lake have the same mode of occurrence, degradation of low-level data by 'probability effects' will be mitigated, but likely not eliminated. If a rare mineral with an overall abundance of 50 area ppm is distributed through numerous particles of a common mineral, rather than forming discrete larger particles, the probability that an analyzed sample will contain the rare mineral is increased. Empirical data from replicate analyses, discussed in Chapter 4, suggest that analytical precision does degrade as abundance diminishes, but this is to be expected. Chapter 4 provides some additional discussion and a schematic diagram (Figure 4.11) that illustrates the reasoning.

The MLA-SEM data provide quantitative data that can be used to assess the mode of occurrence of rare minerals, and these were outlined and discussed in Chapter 6. Important information is available from calculation of the 'Grain/Particle Size Ratio' (GPS ratio) for minerals across the database. The GPS ratio, expressed here in %, compares the average size of 'grains' representing a given mineral compared to the average size of 'particles' in samples. The results show a generally inverse correlation between GPS ratio and mean abundance for minerals in the Strange Lake samples, with some exceptions. On this basis, it is concluded that less abundant minerals typically form small subdomains within larger composite particles, and that larger discrete particles of most indicator minerals are rare. The method is outlined in Chapter 6 and specifically illustrated in Figure 6.11, with summary data in Table 6.10. This provides an explanation for the presence of systematic (albeit noisy) geographic variation patterns for some minerals found only in trace amounts (< 10 area ppm), and perhaps also explains why some rare minerals do provide useful data. Some minerals (e.g., uraninite) have higher GPS ratios than minerals with similar mean abundances (e.g., fergusonite), suggesting that they are concentrated in fewer particles, and thus more vulnerable to probability effects. Symbolic tables used in Chapter 7 (specifically Tables 7.1 and 7.2) provide a good visual illustration, suggesting that probability effects (manifested by complete absence of a mineral in apparently random locations) become dominant below a threshold of about 30 area ppm, although vestiges of systematic patterns remain for some minerals.

These observations and interpretations presently apply only to Strange Lake, but may well apply to rare indicator minerals in other settings, especially where they tend to be fine-grained and/or occur in complex textural relationships. However, if indicator minerals typically form larger monomineralic particles (for example, if derived from diamondiferous kimberlites where they were originally in xenoliths) these 'probability effects' could provide obstacles for MLA-SEM methods. Some prior knowledge of these grain/particle size relationships is thus important for any planned MLA-SEM study of indicator minerals, although there are ways to gain such information from the data.

Comparisons with Results from Traditional Indicator Mineral Surveys

An earlier indicator mineral study in the Strange Lake area (McClenaghan et al., 2017; 2019; see Chapter 3) used traditional heavy-mineral concentration (HMC) methods followed by optical, physical and SEM methods for mineral identification. The original samples were much larger than those used in this project, because they were processed to concentrate higher-density minerals. The only indicator mineral widely detected in samples was gittinsite, and this was missing from many locations where it would reasonably have been expected.

In contrast, the MLA-SEM research found at least *some* indicator minerals in almost all samples, even though there are sporadic absences for the rarer minerals, likely due to probability effects discussed above. Given the much smaller sample size for the MLA-SEM study, the lack of prior processing, and its largely automated data acquisition, this outcome suggests advantages for the MLA-SEM method in future work. In addition to information on rare indicator minerals, the MLA-SEM method provides information on other major and minor minerals, which may be useful for other purposes linked to regional geology, geochemistry or environmental studies.

McClenaghan et al. (2019) commented on some of the challenges, and specifically discussed the absence of the characteristic Y-Ca-REE silicate gerenite. They noted earlier descriptions indicating that gerenite is commonly intergrown with other minerals, and suggested that particles of gerenite were simply not present in the 0.25 to 2 mm size fraction used for analysis. This highlights an important advantage of the MLA-SEM method; it allows subdomains in particles to be examined and counted, effectively looking *inside* the particles in a sample (e.g., Wilton et al., 2017). Direct imagery and data concerning grain and particle size distributions suggest that many of the indicator minerals from Strange Lake occur as subdomains within larger particles, and this may account for their absence in heavy mineral concentrates in previous investigations. Figure 8.1 shows calculated bulk densities for mixtures of quartz (density of 2.6 g/cc) and selected indicator minerals known from Strange Lake. Both gerenite and gittinsite have densities of about 3.5 g/cc, so they have much less impact on bulk density than some other REE-silicates, uraninite or thorite. Composite particles dominated by quartz and/or feldspars would retain bulk densities below 3.1 g/cc even if they include 35 to 50% volume percent of gittinsite or gerenite. Particles such as these would likely be rejected in density separation procedures, along with other ‘light’ minerals. If the host minerals were slightly denser silicates such as hornblende, the results would differ, but composite particles could still suffer rejection. Even if such particles are retained in heavy-mineral concentrates, it could be difficult to identify small subdomains of indicator minerals. The low average GPS ratios for most Strange Lake indicator minerals (< 10%; see Table 6.10) imply that they are by far subordinate in volume within most composite particles.

The absence of higher-density indicator minerals such as britholite or pyrochlore in previous indicator-mineral studies is harder to explain, but MLA-SEM data (which constrain their *original* abundance in till materials) show that they are very rare, even close to the Main Zone Deposit (see Chapter 6). Also, previous indicator mineral surveys used a coarser size fraction (0.25 to 2 mm) than the MLA-SEM analyses (0.125 to 0.18 mm), so results from the studies cannot be directly compared. There is also independent evidence suggesting that many indicator minerals continue to reside in coarser lithic material through much of the study area, rather than in finer-grained size fractions used for mineralogical and geochemical analysis. This issue is discussed in a later section.

The textural complexity and varied size distributions of indicator minerals in composite particles revealed by MLA-SEM methods also have implications for behaviour in natural processes. For example, Figure 8.1 implies that some will not behave as ‘heavy minerals’ in fluvial processes that could concentrate them in specific areas in watercourses. The persistence of composite particles in the

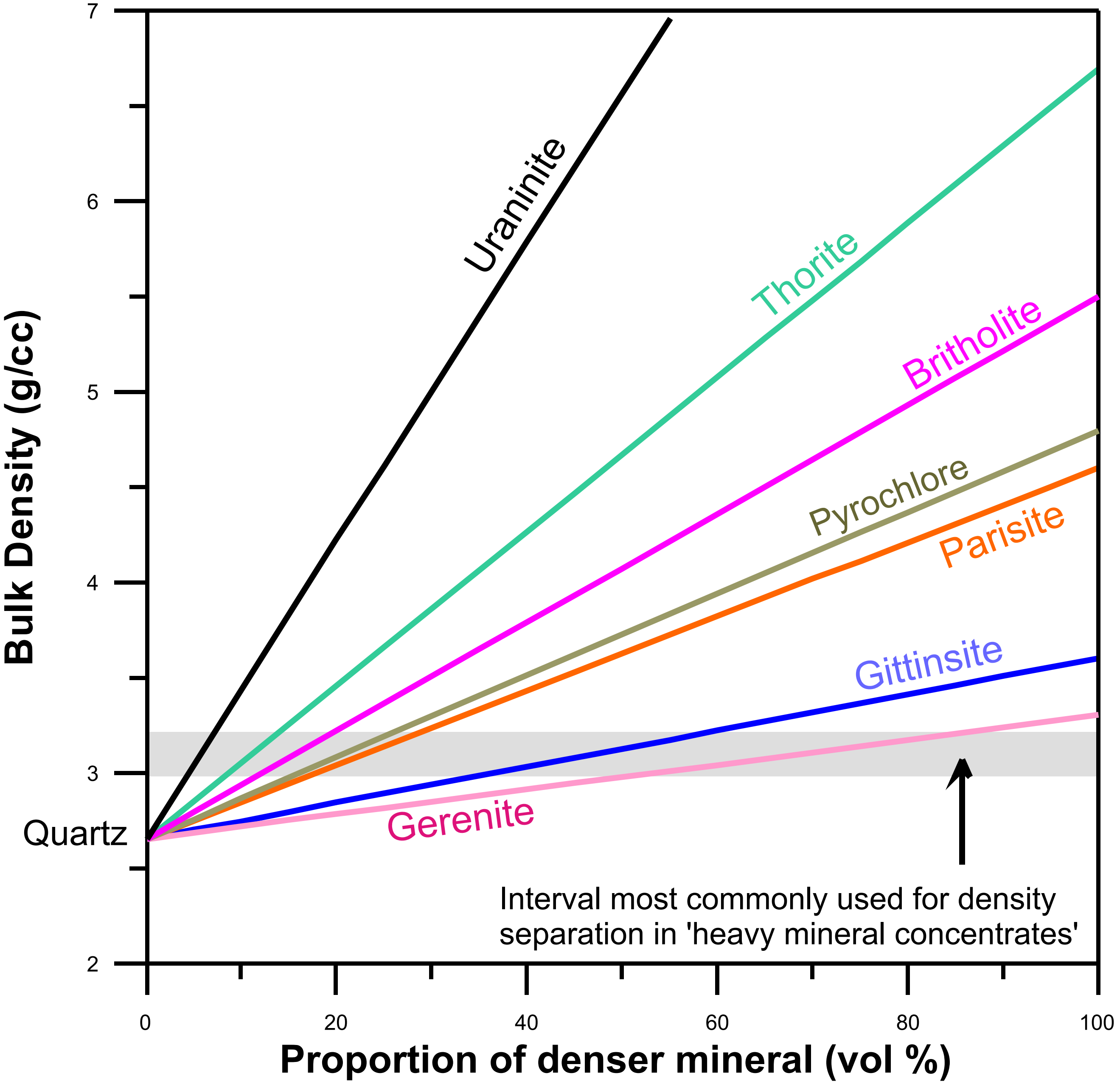

Figure 8.1. Mixing lines showing the bulk density of particles consisting of quartz (density of 2.6 g/cc) and various indicator minerals associated with Strange Lake. The chart indicates the volume % of an indicator mineral required for bulk density of the particle to exceed about 3.1 g/cc, which is the normal lower limit for density separation of 'heavy minerals' in sample processing. Note that this is indicative only as the densities of some minerals (e.g., Parisite, britholite) vary in nature. Replacing quartz with common feldspars as the associated mineral makes little difference, as their density is similar to that of quartz.

surficial environment will be controlled by properties of the host mineral, rather than by those of the indicator mineral. For example, gittinsite ‘grains’ in larger quartz ‘particles’ will benefit from the hardness and durability of the host mineral, which compensates for gittinsite’s relative softness and weakness. In effect, these indicator mineral grains are travelling within suits of armour, which may give them potential for long-distance travel. Mineral associations can be assessed from the MLA-SEM data, although this is very difficult to do for an entire database of 76 samples. Nevertheless, inferences based on a subset of samples enriched in indicator minerals suggest that the dominant host minerals associated with specific indicator minerals vary. These results were discussed briefly in Chapter 6, and it is suggested later that such ‘mineral associations’ may be an important control on the geographic variation patterns revealed by MLA-SEM data.

Advantages and Disadvantages of the MLA-SEM Method in Indicator Mineral Studies

Every method has its own advantages and its disadvantages, and some that excel in one situation may prove less effective in others; in some cases, the strengths of a method can also be its weaknesses in another context. Some of the issues around the MLA-SEM method were summarized in Chapter 4, and others are illustrated directly by results from this project.

The MLA-SEM method is a new and specialized technique with dedicated equipment and technology, and a relatively large price tag. It has yet to acquire a long usage record and the identification of problems and solutions is ongoing. This thesis project will hopefully contribute to that process. MLA-SEM methods can function with much smaller samples than traditional methods, and require little or no sample processing. However, the actual analyzed sample is very small (< 0.3 g) compared to the original mass, which is in turn a small aliquot from the natural source. This is a key issue in disturbance of low-abundance data by ‘probability effects’, as discussed above and in Chapter 4, but there is also a more fundamental question. How representative is the chosen size fraction of the original sample, and how representative is that sample is of the original glacial sediment The latter is a particular concern because tills are notorious for both compositional and textural heterogeneity (e.g., Benn and Evans, 2010). The MLA-SEM data do not address these questions, but examination of bulk till geochemical data acquired by Midland Exploration in the same area (Bourassa and Banville, 2012; 2013) suggests that the indicator-mineral content of various size fractions can differ significantly (see later discussion). It may thus be advantageous to collect larger field samples than are strictly necessary for MLA-SEM analysis, and also to geochemically analyze bulk material, and possibly different size fractions, as additional controls. In cases where sample collection requires helicopter support (as at Strange Lake) the actual analysis costs are small compared to the costs of transport and sample acquisition.

Automation of mineral identification and quantitative determination of mineral abundances are also cited as key advantages for MLA-SEM methods (e.g., Wilton et al., 2017). To acquire the large database for this project (76 samples and at least 50 minerals) through traditional visual and point-counting methods would be impossible. However, it is important to realize that although MLA-SEM methods can identify, characterize and enumerate millions of particles, there is still human involvement, as mineral identifications require assignment of mineral names on the basis of partially semi-quantitative data. Minerals can be misidentified or incorrectly grouped (or separated) via human error, but this issue is also important if using optical or physical properties, which may not be diagnostic. The MLA-SEM method also has the further advantage of *consistency* – if there is a misidentification, it is consistent, and the data are retained for later inspection. Such problems can be corrected, and proportions can be recalculated, without a need to repeat analyses or observations.

The reference database used for this project was developed over several years (D. Wilton, unpublished data) and is reliable, but it is not infallible. As discussed in a later section, minerals identified as ‘ericssonite’ and ‘benitoite’ (rare Ba-rich silicates) are more likely compositional variants of a more common Ba-(Fe)-Mn-Ti disilicate mineral named bafertisite. but this realization does not alter the numerical information recorded for each. The reassignment of these minerals in part comes from other information about titanosilicate minerals at Strange Lake, and the close compositional similarities between some members of this group. The example emphasizes the importance of remaining aware of possible misidentification or confusion, and seeking verification from other data. The true identity of “ericssonite” and “benitoite” is revealed and discussed in a later section of this Chapter.

COMPARISONS WITH OTHER SURFICIAL GEOCHEMISTRY PROJECTS IN THE STUDY AREA

General Information

In this section project results are compared to data from two projects that completed bulk geochemical analyses of tills within the same general area. Both projects were briefly summarized in Chapter 3, but are now discussed and interpreted in more detail. Particular attention is given to evidence for compositional and mineralogical heterogeneity in tills, and the presence of large mineralized ‘clasts’ (cobbles, boulders and even house-sized masses of rock) at considerable distances from the Main Zone Deposit.

Till Geochemical Data from the Local Area of the Strange Lake Deposits

Joanne Bell (1984) completed the very first research on till geochemistry and indicator minerals at Strange Lake, and made key observations close to the Main Zone Deposit, which was the only mineralization known at that time. She completed a geochemical study, looked for indicator minerals and conducted a ‘partitioning’ study on selected samples, by independently analyzing several size fractions.

The till samples contained particles of common rock-forming silicates, including those typical of the Strange Lake Intrusion, but also contained garnet, as noted in this investigation. Gittinsite and pyrochlore were recognized under the microscope as potential indicator minerals in tills. Trace elements associated with Strange Lake (e.g., Y, Nb, Zr) were enriched in tills directly east of the Main Zone Deposit, but Bell (1984) also found an unexpected subparallel zone of enrichment (oriented at ~ 075^{o}) about 1 km south of the main trend. No direct mineralized source was apparent for this second zone, and none has ever been found since. The contours for Y in tills (transcribed from Bell, 1984) are shown in Figure 8.2, which also shows gerenite abundances from MLA-SEM data (see also Figure 7.36). The geochemical and mineralogical data sets correspond fairly well, despite differences in scale, although the pattern for gerenite suggests the possible presence of a third subparallel enrichment trend in the south of Grid 1. The more recent data acquired by Midland Exploration also show such patterns, and they are also visible in some of the mineral abundance data from the MLA-SEM investigation (see Chapter 7). Unfortunately, the Midland Exploration survey did not cover the areas closest to the Main Zone Deposit (these are Exempt Mineral Lands) so they cannot be compared directly with earlier work by Bell (1984).

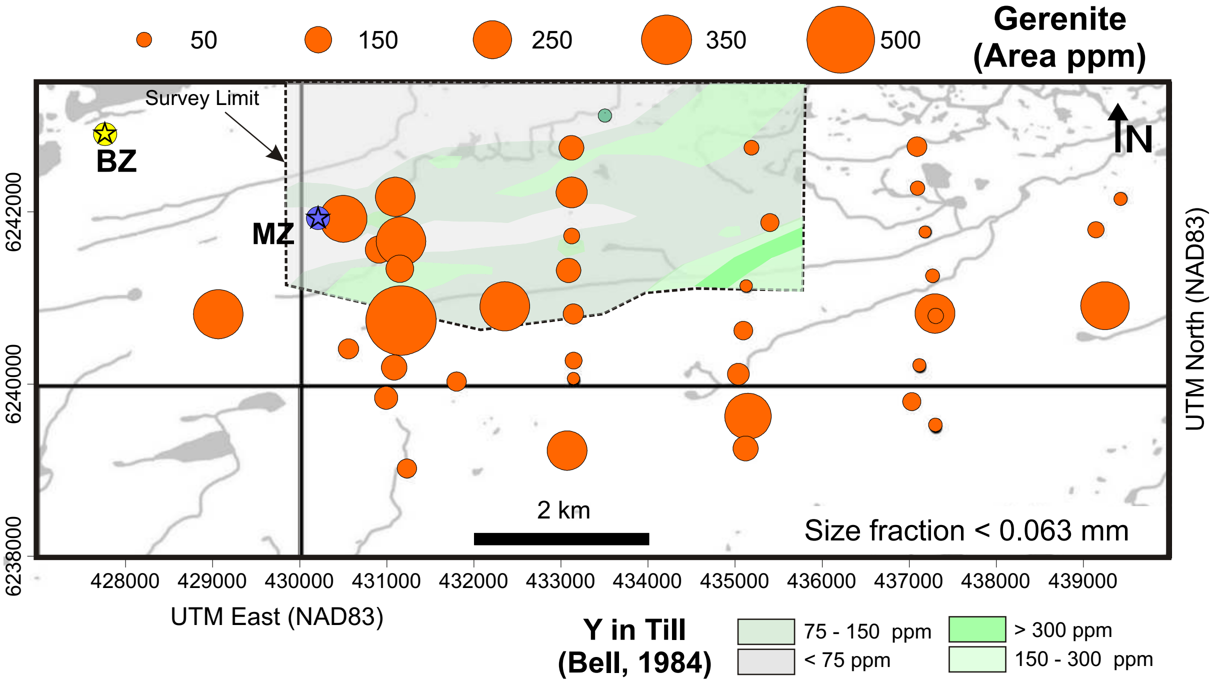

Figure 8.2. Till geochemistry data from Bell (1984) shown as contours, combined with the gerenite abundances (area %) derived from MLA-SEM analyses in this project in Grid 1.

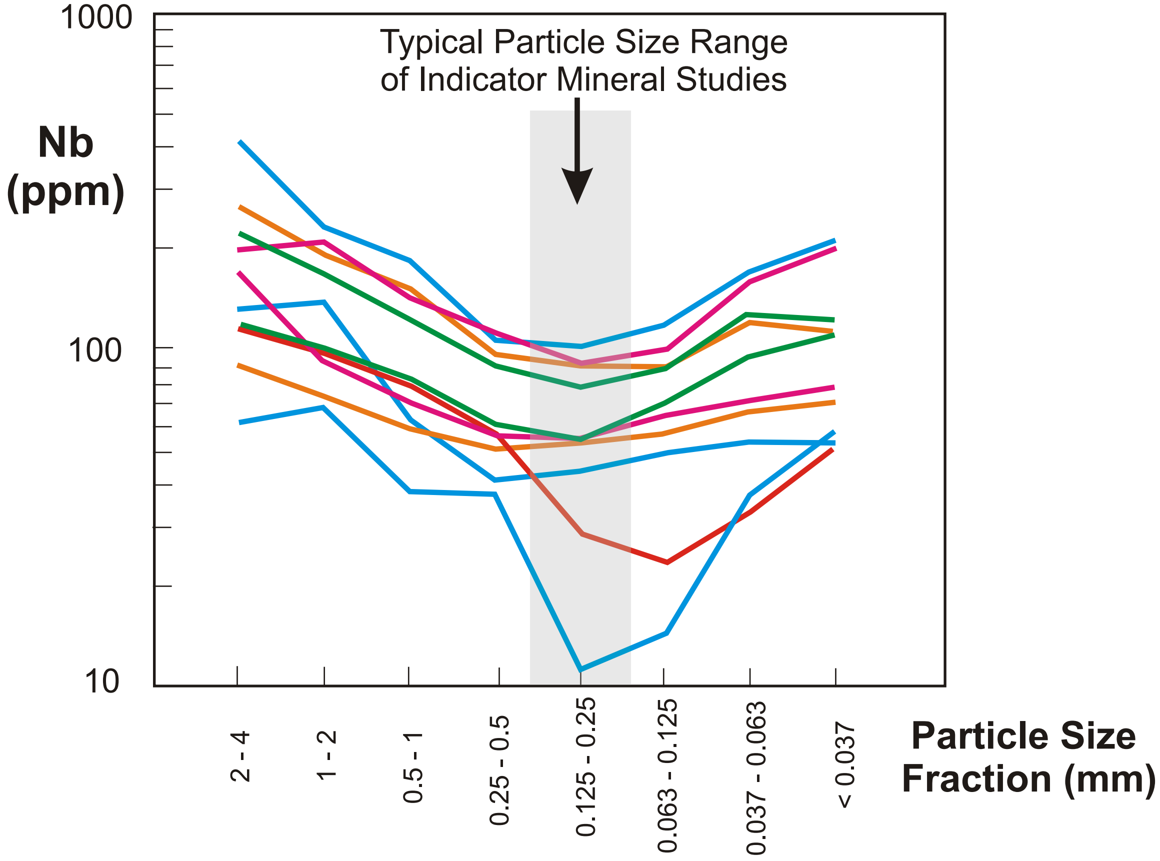

Figure 8.3. Abundance of Nb (ppm) in 10 samples analyzed by Bell (1984) for different size fractions of the till, showing significant variations from coarse material to fine material.

Results from the partitioning study of Bell (1984) are shown in Figure 8.3, which shows Nb contents for several size fractions from 10 samples. The Nb content of the till size fractions varies widely, but the greatest (but least consistent) enrichment is almost always in the coarsest-grained material. This suggests that till samples are also heterogeneous in terms of indicator mineral contents, at least for those containing Nb. Similar results were obtained for Y, Zr, Ce and Th across the size fractions, but a different style of geochemical divergence was noted for Li and U, which are not specifically associated with Strange Lake. The lowest concentrations of key trace elements recorded by Bell (1984) are from the size fractions most commonly used for both traditional and MLA-SEM indicator mineral surveys (i.e., from 0.1 mm to about 2.5 mm). Subsequent work (see below) confirmed the findings of Bell (1984), although the results of her thesis were never published.

Regional Till Geochemistry Surveys including Rare-Earth Elements

Work by Midland Exploration in 2011 and 2012 provides a broader perspective on the possible heterogeneity of till materials, and includes analytical data for all of the REE, rather than just Ce and Y (Bourassa and Banville, 2012; 2013; data archived through Geological Survey of Newfoundland and Labrador). As previously summarized in Chapter 3, the sampling area corresponds to the eastern section of Grid 1 and much of Grids 2 and 3 in this project, and has a high sampling density in the west, closest to the Strange Lake deposits (see Figure 3.6). Till samples came from depths of about 1 m, and were larger than those collected in this thesis project. Because the Midland Project was aimed at resource assessment (see Chapter 3) five separate size fractions were analyzed. The finest size fraction (< 0.25 mm) provides the closest analogue to material analyzed by MLA-SEM. The other fractions represented materials sized from 0.25 to 2 mm, 5 to 19 mm, 19 to 64 mm and > 64 mm, respectively. Material in the 2 to 5 mm size range was not analyzed, for reasons not explained. Nine sample locations in the area of Grid 1 from this project area sit close to sites sampled by Midland Exploration and so can be used for specific comparisons; information is provided in Table 8.1 for reference.

The geochemical data acquired by Midland Exploration define geochemical dispersion patterns very well in the general area of Grid 1, as indicated by ‘bubble maps’ for Y in two different size fractions (Figure 8.4). Strong enrichment is seen clearly, as are subparallel zones of enrichment, one of which is continuous with the Main Zone trend identified by Bell (1984). The maps in Figure 8.4 look very similar in terms of the general patterns that they define, but the Y contents of the samples are very different.

Table 8.1. Coordinates for sites where thesis samples and Midland Exploration samples are nearby.

Midland Site #	UTM East	UTM North	Thesis Sample	UTM East	UTM North
93	434993	6240297	G1-26	435024	6240115
94	434998	6240597	G1-25	435081	6240620
96	435059	6241133	G1-24	435113	6241139
103	435335	6241802	G1-23	435386	6241875
155	436951	6242348	G1-36	437081	6242275
158	437324	6241208	G1-34	437254	6241257
180	439199	6241056	G1-40	439234	6240910
182	439306	6241882	G1-39	439130	6241792
204	435065	6242604	G1-22	435175	6242745

Note: Coordinates are with reference to NAD 83 Datum

Table 8.2. Average trace element compositions of till samples from the Midland Exploration Project.

Fraction	<0.25 mm		0.25 to 2 mm		5.6 to 19 mm		19 to 64 mm		> 64 mm	
Element (ppm)	Mean	SD	Mean	SD	Mean	SD	Mean	SD	Mean	SD
V	26.6	32.7	30.5	8.4	33.9	10.5	39.7	22.8	20.5	25.4
Zn	88.4	91.7	78.8	31.9	167.1	102.8	233.7	160.3	561.7	310.5
Ga	18.2	2.6	17.1	3.2	25.1	4.8	27.9	8.0	44.0	12.6
Rb	144.7	43.6	124.5	42.8	235.7	70.7	272.4	131.7	534.8	234.5
Sr	221.5	25.9	235.4	30.3	184.5	37.8	185.7	71.0	127.8	116.6
Y	72.3	37.9	76.4	37.1	119.2	89.8	166.4	156.7	530.4	410.2
Zr	837.5	415.3	941.9	481.6	1527.1	1048.4	2151.8	1937.7	7239.2	6154.5
Nb	46.4	25.1	46.6	23.4	125.8	91.5	175.2	186.4	478.4	344.5
Sn	12.6	8.0	11.9	7.0	28.1	19.1	40.7	37.1	123.2	79.9
Ba	878.5	99.3	838.1	106.1	972.4	177.5	793.0	259.9	486.6	481.5
La	68.3	26.4	70.7	25.8	127.0	67.8	169.4	122.3	421.1	265.0
Ce	142.6	56.1	150.3	55.9	264.3	140.4	354.6	253.8	908.9	540.1
Pr	15.8	6.2	16.8	6.4	27.6	14.2	36.8	26.8	92.2	56.1
Nd	57.8	22.5	61.6	24.3	97.6	49.3	129.9	92.6	325.9	201.5
Sm	11.9	5.0	12.9	5.5	19.7	10.5	26.4	19.5	70.3	45.0
Eu	1.5	0.3	1.5	0.3	2.0	0.5	2.2	1.0	4.4	2.4
Gd	10.4	4.7	11.3	5.1	16.7	9.9	22.4	16.9	63.5	43.3
Tb	1.9	0.9	2.0	0.9	3.2	2.2	4.3	3.7	12.8	9.3
Dy	12.0	6.1	12.7	6.1	20.7	14.8	28.5	26.3	86.9	65.4
Ho	2.5	1.3	2.6	1.3	4.5	3.4	6.1	5.8	19.2	15.2
Er	7.8	4.1	8.1	3.9	14.6	11.2	20.3	19.8	64.7	53.5
Tm	1.2	0.7	1.3	0.6	2.5	1.9	3.4	3.3	11.0	9.3
Yb	8.4	4.4	8.7	4.1	16.7	12.6	23.2	22.0	72.7	63.0
Lu	1.3	0.7	1.3	0.6	2.6	1.9	3.6	3.4	11.1	9.6
Hf	21.9	11.5	23.4	11.8	42.4	29.7	60.2	55.1	205.9	179.5
Ta	3.3	1.7	3.3	1.6	8.3	6.2	11.7	12.5	32.2	23.3
Pb	39.2	16.1	40.1	14.7	56.5	28.3	70.5	72.5	142.8	99.0
Th	16.1	6.5	17.3	6.4	30.0	15.9	46.9	51.9	102.9	74.4
U	3.3	1.4	3.5	1.3	5.8	3.5	8.3	6.8	22.5	16.2

Notes: Original data from Bourassa and Banville (2012), archived by Geological Survey of NL (N=203)

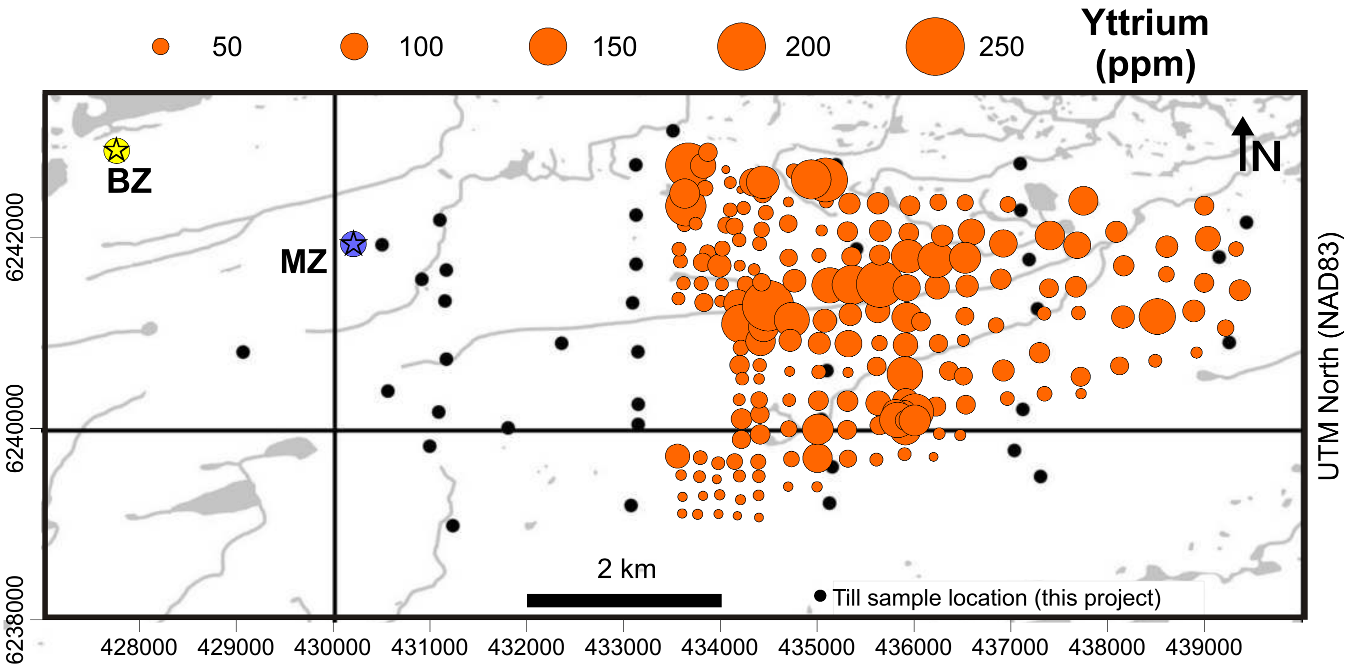

Fraction 1: size < 0.25 mm

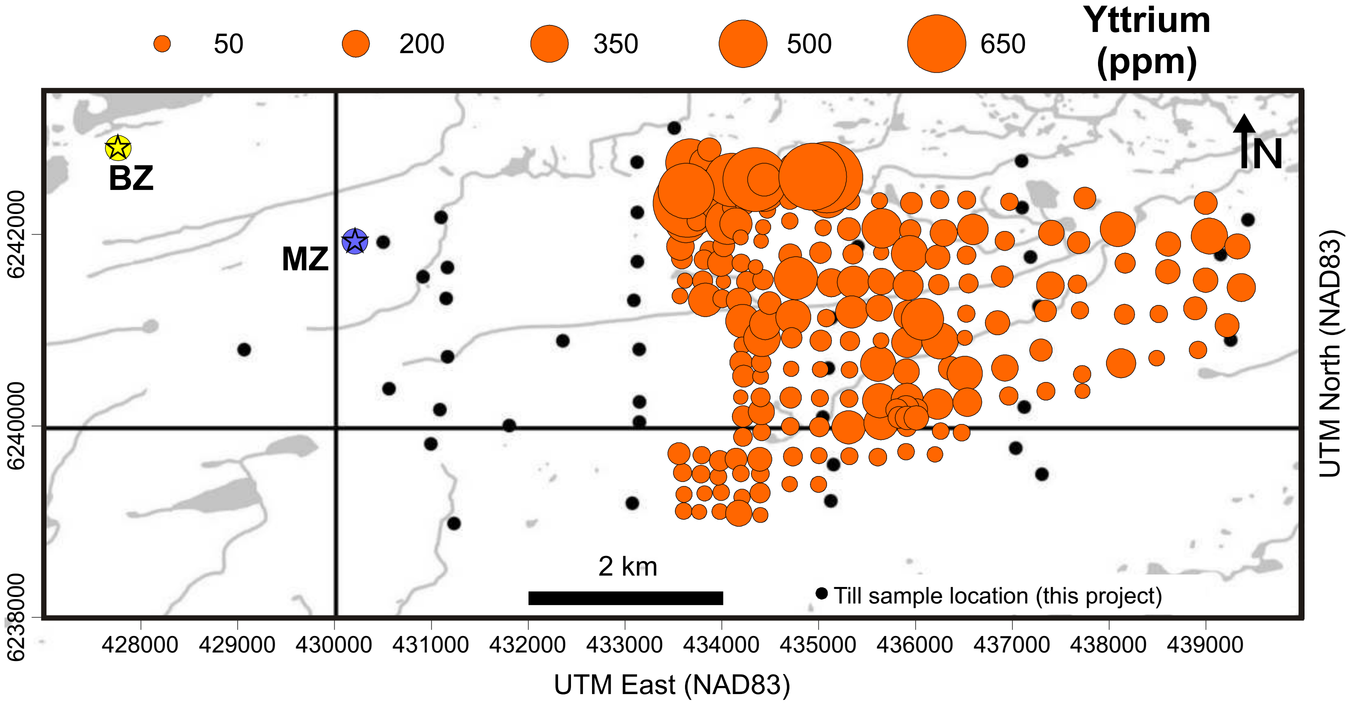

Fraction 4: size 19 to 63 mm

Figure 8.4. Proportional symbol maps showing the variation of yttrium (Y) in till samples analyzed by Midland Exploration in the eastern part of the area covered by Grid 1 in this project. Upper panel shows data for the < 0.25 mm size fraction broadly equivalent to MLA-SEM samples. Lower panel shows results from a coarser size fraction of till (19 to 64 mm). Although the patterns look similar, Y concentrations are much higher in the coarser fraction. Similar contrasts are shown for other trace elements associated with the Strange Lake deposits.

This is revealed by the reference symbols in the legend to the maps; samples representing the coarser fraction (19 to 64 mm) contain about three times as much Y as those from the < 0.25 mm size fraction. Equivalent maps for other REE, Zr, Nb and Th show closely similar patterns and strong relative enrichment in the coarsest size fractions. In the eastern part of the Midland project area, corresponding to Grid 3 of this project, the finer size fractions were not analyzed, but strong enrichment in key trace elements persists in coarse-grained till, contrasting with the low abundances of many Strange Lake indicator minerals in the MLA-SEM samples from Grid 3 (see later discussion).

The relationships between size fractions and geochemistry for different elements are further illustrated in Figure 8.5, which shows Y, Ce, Zr and Sr for the nine sample sites that are near to sample sites from this study. Coarser size fractions are typically enriched by a factor of 3 to 5 compared to the < 0.25 mm fraction for Y, Ce and Zr. Strontium shows an inverse pattern in which some coarse-grained fractions are depleted compared to finer-grained material. Other trace elements characteristically associated with Strange Lake (e.g., Nb, Th, Pb) show similar patterns to Y, Ce and Zr, as they are also preferentially enriched in coarser fractions. Univariate statistical data for the five size fractions throughout the western part of the Midland study area (equivalent to Grid 1) demonstrates the pattern for a wider selection of trace elements, including all of the REE (Table 8.2). The geochemical heterogeneity of the tills indicates that they must also be mineralogically heterogeneous, and that Zr-, Nb- and REE-bearing minerals are more abundant in coarser material. The size fractions closest in character to the material used in the MLA-SEM research, and also in other indicator-mineral studies such as McClenaghan et al. (2019) generally have the *lowest* concentrations of key trace elements, indicating that they are deficient in indicator minerals.

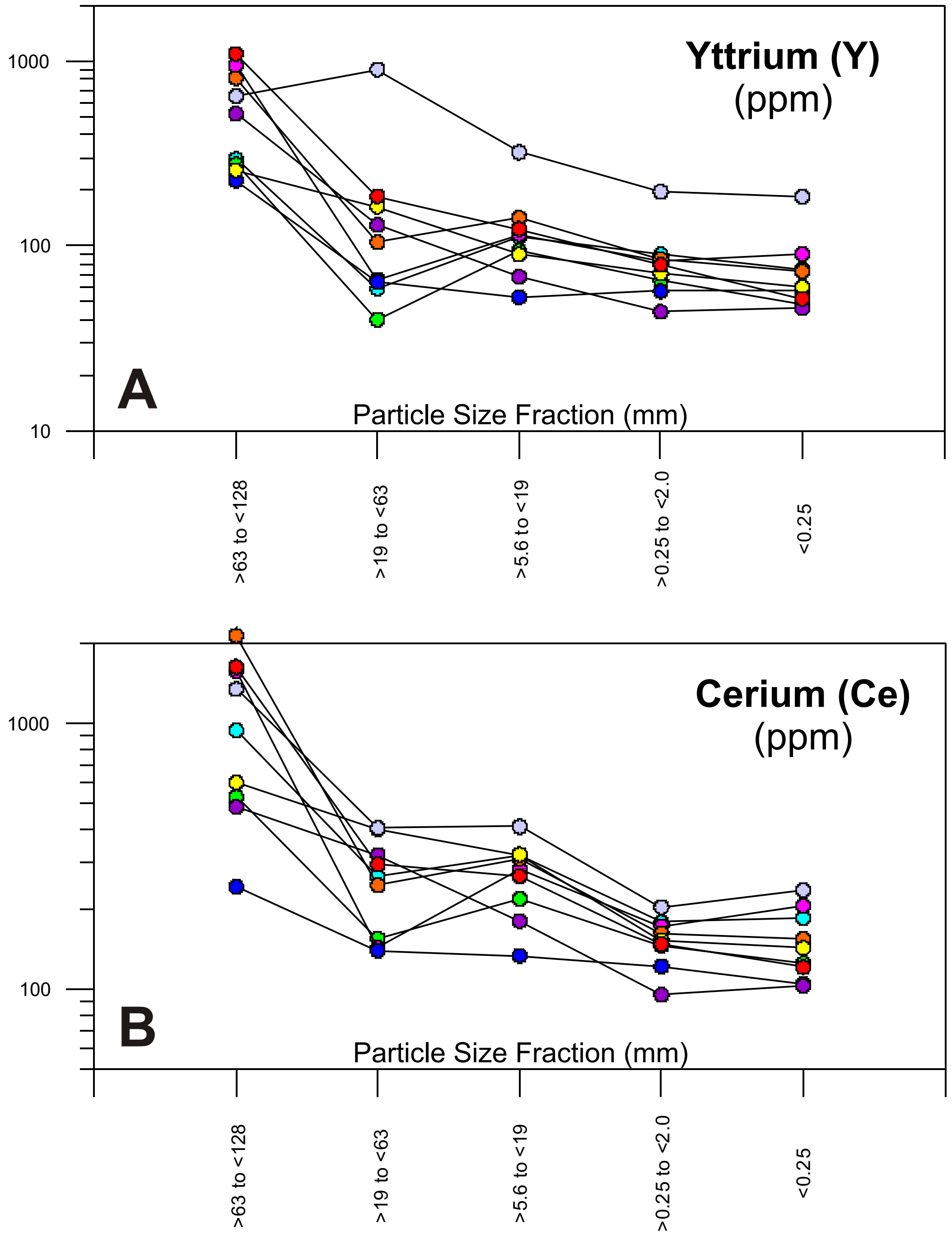

Figure 8.5 (Part 1). Trace element variations among different size fractions from Midland Exploration till samples collected at selected localities near to sample sites from this project. (A) Yttrium. (B) Cerium. See text for discussion..

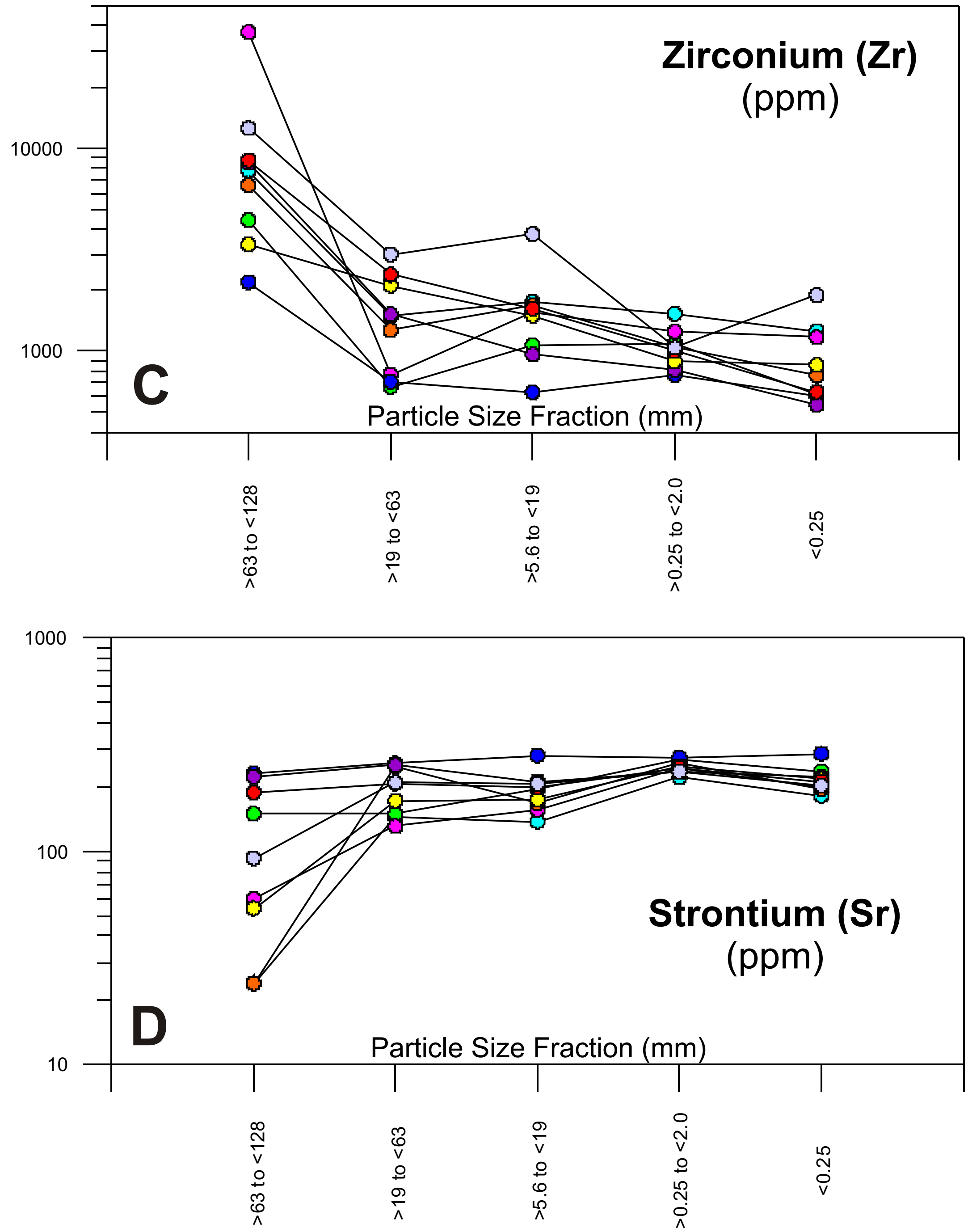

Figure 8.5 (Part 2). Trace element variations among different size fractions from Midland Exploration till samples collected at selected localities near to sample sites from this project. (C) Zirconium. (D) Strontium. See text for discussion..

Rare-Earth Patterns from Till Samples and their Significance

Given the strong evidence for geochemical and mineralogical heterogeneity in tills, another obvious question must be asked, i.e., do the proportions of indicator minerals also differ between till size fractions, and (if so) which minerals are preferentially found in finer or coarser material? This is an important issue for interpreting dispersion patterns and also in designing exploration projects. This can be assessed from the Midland Exploration program, because the data allow complete ‘REE profiles’ to be constructed. These are simple line charts that show the ratio between observed REE data and the accepted average values for the REE in chondritic meteorites. This approach removes the natural discrepancy between abundant REE (e.g., La, Ce, Dy, Er, Yb) and the rarer REE (e.g., Sm, Eu, Tb, Lu), and produces a smooth graph rather than a jagged saw-tooth profile. Also, because chondritic meteorites are viewed as the building blocks of terrestrial planets, they are representative of the Earth’s bulk composition, and REE profiles have geological significance. More commonly, REE profiles are used in a pragmatic way as ‘fingerprints’ of different types of rocks. For example, the Strange Lake Intrusion (and other similar rock types) have distinctive REE profiles that show relative enrichment in the ‘heavy’ REE (Gd to Yb) which are normally less abundant than the ‘light’ REE (e.g., Miller, 1986; Kerr, 2013).

Figure 8.6 illustrates REE profiles for different size fractions at four of the sites listed in Table 8.1, which are typical of other sample sites. The results show the change in overall REE (and Y) concentrations between finer and coarser size fractions, as noted from Figure 8.5. The REE profiles for material from Strange Lake are effectively mixtures between the light-REE-enriched minerals (e.g., bastnaesite, stetindite, monazite) and the heavy-REE-enriched minerals (e.g., gadolinite, gerenite) with lesser contributions from minerals such as zircon and gittinsite. The consistency of REE profiles from the Midland data argues against any significant variation in the relative abundance of light-REE- and heavy-REE-enriched minerals between till size fractions. This is encouraging, because it suggests that quantitative mineral abundance data from the finer size fractions, despite generally low abundances, are representative of the wider material and can be interpreted with confidence. Finally, Figure 8.7 compares average REE profiles for the two finest size fractions (< 0.25 mm and 0.25 mm to 2 mm) and a

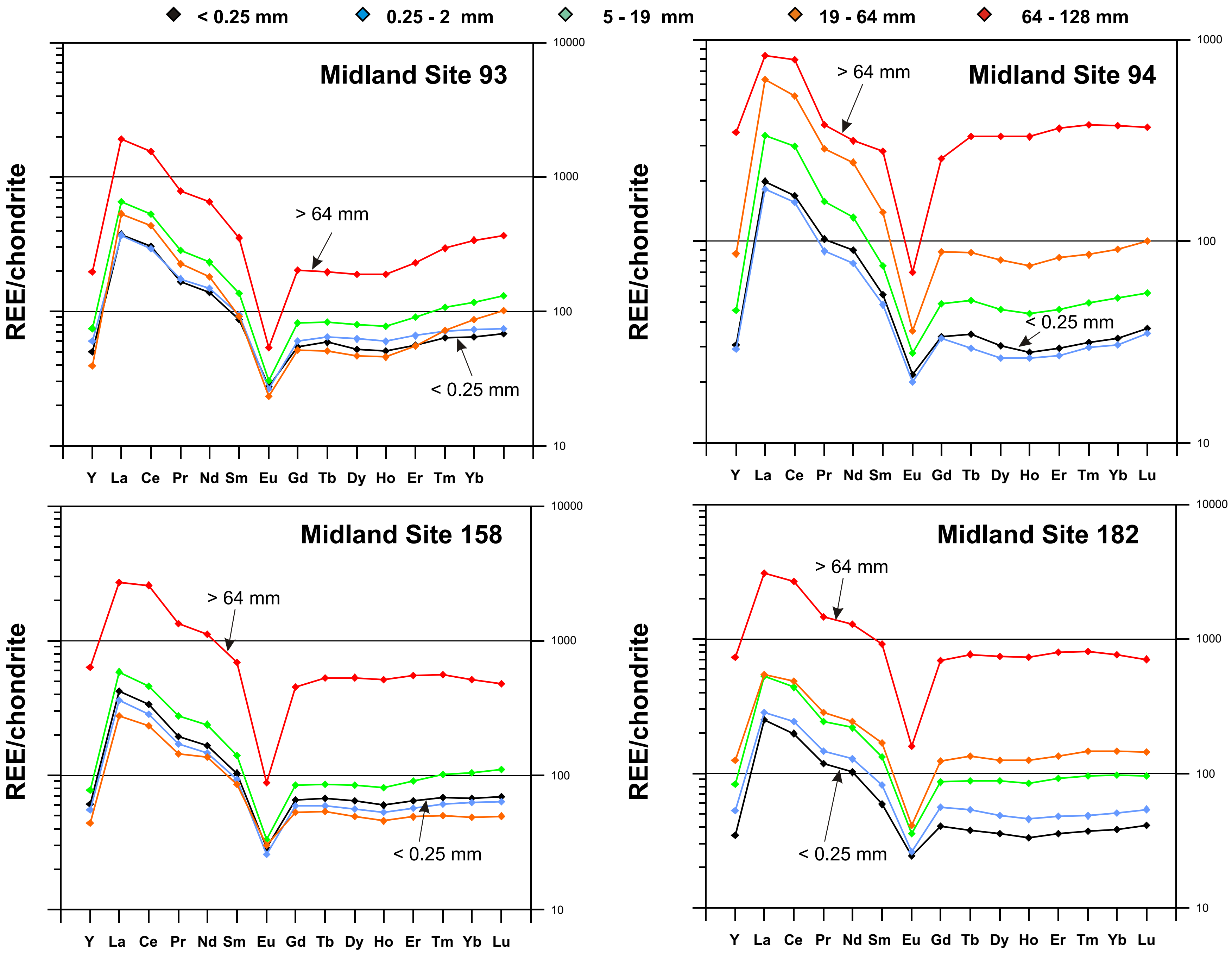

Figure 8.6. Rare-Earth Element (REE) profiles for different till size fractions from four selected Midland Exploration sites.

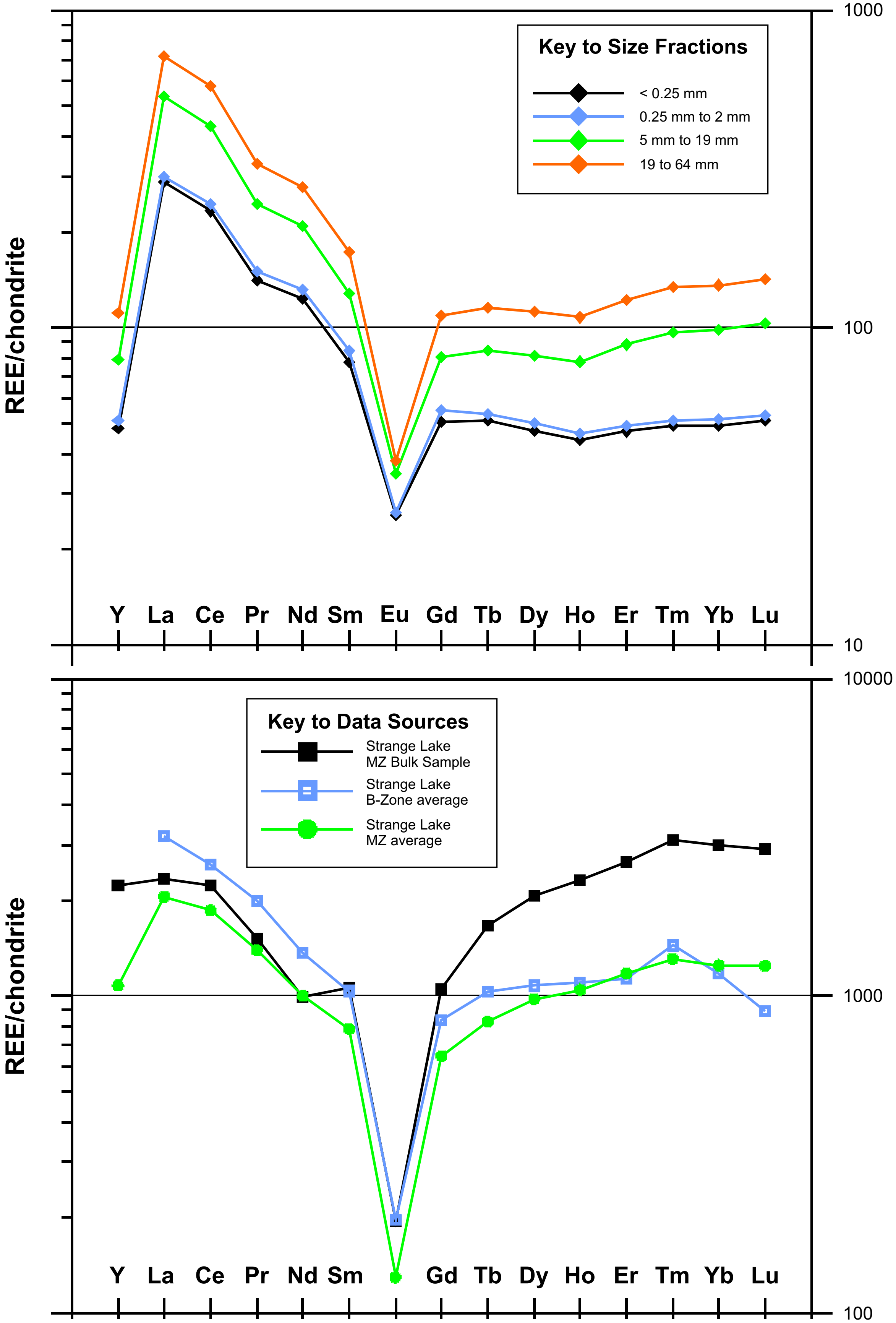

Figure 8.7. Average REE profiles for different till size fractions from Midland Exploration till samples (upper panel) compared to average REE profiles for the Main Zone bulk sample, Strange Lake Main Zone and B-Zone deposits (lower panel).

coarser fraction (19 to 64 mm) from all Midland data corresponding to Grid 1 of this project with some average REE profiles from the Strange Lake Main Zone and B-Zone deposits (from Kerr and Rafuse, 2012; Kerr, 2013). There is a general similarity, but some differences are apparent. The till-sample REE profiles show depletion in the heavy REE (Gd to Yb) compared to their likely bedrock sources, especially with respect to the REE profile for the bulk sample collected from the Main Zone (Zone 1 Lens) by IOC (analysis from Kerr and Rafuse, 2012). However, the high-grade material at the test site may not represent the Strange Lake Intrusion as a whole, which more closely matches the bulk estimate for the B-Zone Deposit or the Main Zone Deposit (compiled by Kerr and Rafuse, 2012). The till sample profiles provide a better fit to these data, although differences remain.

The differences between till-sample averages and bedrock source data may imply that some HREE-enriched minerals do not persist as well in the surficial environment as LREE-enriched minerals. In general terms, this is consistent with the ‘dilution factors’ calculated by comparing average mineral abundances in tills with those of the Strange Lake drill cores, as discussed in Chapter 6, and illustrated in Fig 6.15. With the exception of the Ce-rich mineral stetindite (present only in very small amounts) the dilution factors for light-REE-enriched minerals tend to be lower than those for minerals such as gerenite and gadolinite, which contain much of the Y and heavy REE at Strange Lake. Also, any non-diagnostic REE-bearing minerals (e.g., monazite, allanite, etc.) derived from sources other than Strange Lake (e.g., the Napeu Kainuit Intrusion) would likely be LREE-rich (Kerr and Hamilton, 2014; Kerr, 2015).

Quantity and Scale of Distribution for Materials Dispersed from Strange Lake

This project is focused on the smallest of scales represented by sand- and silt-sized particles. However, glacial dispersion of material from Strange Lake also includes ‘clasts’ that span the size range from pebbles to house-sized masses of rock. There is no better illustration of this than the stated rationale for the Midland Exploration project east of Strange Lake. The company was not interested in finding the source for indicator minerals in tills because this was already well known. Rather, they were interested in the possibility that heterogeneous till materials might be amenable to low-cost mining for REE. This illustrates the enormous amount of material that was removed from the Strange Lake area and dumped over tens of kilometres. Investigations of the surficial geology of the study area (e.g., Batterson, 1989) demonstrate that material derived from Strange Lake is not only present in the till materials, but that large ‘erratic’ masses, likely transported in glacial ice rather than at the base of the ice sheet, are abundant. The physical evidence and the geochemical evidence from bulk till analyses (Batterson and Taylor, 2009; Bourassa and Banville, 2012; 2013) are quite compelling. There is no shortage of material from Strange Lake even in the most distant portion of the study area; boulders and cobbles of mineralized granite and pegmatite exist, and the coarser fractions of the till blanket are highly anomalous in indicator trace elements, confirming that lithic and mineral debris is present there. Given these facts, the low abundances of indicator minerals in the silt- and sand-sized fractions analyzed by traditional methods and the MLA-SEM analyses remain something of a puzzle. Nevertheless, there are indications that such data are representative, and the patterns that are revealed by data are in the end more important than the actual numbers that define them.

OTHER Uncommon MINERALS FOUND IN TILL SAMPLES AND THEIR ORIGINS

Uncommon Minerals Associated with Regional Geological Units or Unknown Sources

In addition to the rare indicator minerals known to be associated with the Strange Lake deposits, some other unusual minerals were also detected in the till samples through MLA-SEM analysis. These findings are briefly discussed in this section.

Nepheline (mean abundance 0.34 area %) is widespread as a minor mineral. The geographic variation of nepheline (see Chapter 7) provides no indication that it is more abundant close to the Strange Lake deposits, so it likely has a regional source, perhaps in metamorphic rocks of calcareous sedimentary origin (Deer et al., 1992). This appears more likely than a source in undersaturated (silica-deficient) alkaline igneous rocks, as these are not known in the general area. Staurolite and Al-silicate (polymorph unknown) likely also originate in metamorphic rocks, as this is their normal habitat (Deer et al., 1992) and sources of suitable composition are present within the study area, especially in the east (see Chapter 7 and Ryan et al., 2003). Examination of ‘mineral associations’ for selected samples (see Chapter 6) shows that nepheline, staurolite and ‘Al-silicate’ occur together in composite particles, suggesting a common source. Wollastonite ($CaSiO_3$) is a pyroxene-like mineral, and is rare (mean of only 21 area ppm). It is also best known from metamorphic rocks that originally contained calcite. There is no evidence that any of these minerals are connected to Strange Lake.

Scheelite (calcium tungstate; $CaWO_4$) is a rare mineral that is in some cases an ore of tungsten, and its presence was unexpected. It occurs in only three samples, and was noted previously (see Chapter 4) as an extreme example of the 'nugget effect'. Particle and grain size data for G1-14, which has a scheelite abundance of 354 area ppm show that it contains only one scheelite particle that is several times larger than the average particle size for the entire sample. The three scheelite-bearing samples have no obvious geographic connection. The source of scheelite is unknown, but it is most common in pegmatites and hydrothermal vein deposits (www.mindat.org). There is no record of scheelite or tungsten mineralization anywhere in Labrador, but a few grains in remote tills are unlikely to spark widespread exploration activity.

Rhodonite (Mn-pyroxene; $MnSiO_3$) occurs in only 17 samples, and has a low mean abundance of 5.6 area ppm, with a maximum of 129 area ppm. It occurs mostly in metamorphic rocks and hydrothermal alteration zones, especially in association with iron-manganese deposits (Deer et al., 1992). However, Baird (2018) detected rhodonite in Strange Lake drill cores, with a maximum value of 426 area ppm. A link between rhodonite and Strange Lake is possible, especially considering the presence of other Ba-Mn silicates (see below) but the data are not compelling. The hydrated Na-Ca silicate mineral pectolite was also detected in Strange Lake drill cores, but its geographic distribution offers no clues as to a possible link.

"Ericssonite" and "Benitoite" Unmasked

The most puzzling of the uncommon minerals detected by in the results are "ericssonite" and "benitoite", which are extremely rare Ba-Mn and Ba-Ti silicates, respectively. Their known occurrences are essentially confined to southern Sweden (ericssonite; Sokolova et al., 2018) and San Benito County, California (benitoite; Laurs et al., 1997). Interest in these minerals increased when internet research revealed that benitoite was a valued gemstone, the mineral emblem of the State of California, and in some cases can be more valuable than diamonds on a carat-for-carat basis (Laurs et al., 1996). With a mean abundance below 10 area ppm, "benitoite" is a mere curiosity, but "ericssonite" has an average abundance of 58 area ppm (second after gerenite in the 'rare accessory' category; see Table 6.1) and is present in 62 of 76 samples. It requires consideration and explanation. The mineral also has a geographic pattern that *could* be interpreted in terms of derivation from Strange Lake, although there are problems with this model (see later discussion).

After mentioning them in several previous chapters, it is now time to discuss the true identity of these minerals. D. Grant (pers. comm., 2020) noted that compositions and spectral information for both were similar, that "benitoite' had evidence for minor Ce, and also that significant Fe and Ti were present in "ericssonite", in addition to Ba and Mn. He suggested that the two minerals might actually be a single mineral showing some compositional variation. Subsequently, G. Layne (pers. comm., 2020) speculated that a more common mineral known as "bafertisite", which he had encountered in an early student project connected to peralkaline igneous rocks in South Greenland, might be a better designation.

Bafertisite [$Ba(Fe^{2+}, Mn) TiSi_2O_7 (O,OH)_2$] is one of a surprisingly large number of Ba-Fe-Mn-bearing silicate minerals. Unlike ericssonite and benitoite, which are named for a person and a location, respectively, its name is derived from is chemical constituents: (*Ba*)rium (*Fer*)rous (*Ti*)tanium (*Si*)licon are joined to the suffix "*-ite*". It was originally recognized by Russian geologists in the 1950s and 1960s (information from www.mindat.org) and is described by Vrana et al. (1992) and Sokolova et al. (2018). It occurs far more widely than either ericssonite or benitoite, mostly in alkaline or peralkaline igneous rocks. The Bayan Obo REE deposit in China (one of the world's largest REE resources) is actually its type locality (Xu and Shen, 2005). Bafertisite has a Mn-rich analogue, named hejtmanite, and most natural examples contain both Fe and Mn (Vrana et al., 1992). Bafertisite is not exactly the most famous exotic mineral in the Strange Lake deposits, but it is mentioned briefly by Birkett et al. (1996) in a paper devoted to several obscure titanosilicate minerals. It occurs in very small amounts in granites at Strange Lake, typically forming rims around crystals of the Fe-Ti-oxide mineral ilmenite, which is itself a rare constituent. Birkett et al. (1996) noted compositional variation, including the presence of light REE elements, including Ce, and also noted a 'bafertisite-like phase' to include Ti-rich material that is enriched in Ce. No estimates were provided for the modal abundance of bafertisite in the granites, but judging by the brevity of the description it is probably the least abundant of the titanosilicate minerals discussed by Birkett et al. (1996).

On the basis of this information, "ericssonite" should probably be combined with generally trivial amounts of "benitoite" and relabelled as bafertisite. However, the recognition that bafertisite is present in the Strange Lake Intrusion granites creates a rather interesting puzzle, which is explored in the next section. However, the identification should be confirmed by future work.

Changbaiite – The Newest Member of the Strange Lake Exotic Mineral Club?

It seems to be a tradition that every research study connected to Strange Lake must detect a previously unreported mineral. The rarest of all the minerals considered in this project is Changbaiite ($PbNb_2O_6$; but with variable composition, including Fe, Ti and Ta). This mineral is described from potassium-rich granites in southeastern China, specifically in the Changbai Mountains along the border with North Korea (www.mindat.org). The identification of the mineral by MLA-SEM has not been fully assessed to confirm its accuracy or applicability. Aeschynite [(Ca, REE) $(Ti, Nb)_2(O, OH)_6$] is listed as a 'related mineral' (www.mindat.org) and this was listed in a table by McClenaghan et al. (2019) but the exact source of this information is unclear. There is strong correlation between "changbaiite" and fergusonite [(Y, REE)NbO_4], as listed in Table 7.3, suggesting that they occur together, and this is confirmed by MLA data for mineral associations in selected samples. Although changbaiite occurs in only 20 of the till samples and its geographic pattern is very noisy, it could be interpreted in terms of derivation from Strange Lake (see Figure 7.33).

If the identity of changbaiite is ultimately confirmed by future work, the first recognition from Strange Lake was by Baird (2018), who detected it in drill core samples at an average abundance of 228 area ppm. However, the mineral is not specifically mentioned in the text of her thesis, which was focused on REE-bearing minerals. The drill-core samples investigated by Baird (2018) would be the best place to further investigate the mineral. Again, this is an avenue for future research.

SPATIAL AND GEOGRAPHIC VARIATIONS IN MINERALOGY: PATTERNS, FEATURES AND POSSIBLE CAUSES

General Information

It is obvious from evaluation of numerical data that minerals in the till samples behave in 'groups', which are best defined from correlation patterns, discussed at length in Chapter 6. The most obvious example is provided by the composite variables [quartz + K-feldspar] and [garnet + hornblende + ilmenite], which are inversely correlated, and divide the till samples into two broad groups that must have geological significance (Chapter 6, specifically Figure 6.4). These two composite variables also show systematic geographic variation patterns, as do many minerals, which are illustrated by numerous maps in Chapter 7. These geographic variation patterns are at the very core of this thesis research, and prompt several questions. What types of patterns can be recognized among the various categories of minerals detected by MLA-SEM analysis? Are these patterns of regional or local extent, and can such differences be resolved? What are the ultimate causes for the different patterns, and what inferences about dispersion processes can be drawn from them? These answers are not always apparent, and further research is needed, but some initial interpretations are presented in this section.

Regional Variation Patterns and Their Links to Bedrock Geology

Most till samples are dominated by a small group of major minerals, namely quartz (11 to 52 area %), albite (15 to 33 area %), K-feldspar (9 to 20 area %), hornblende (1.3 to 33 area %), garnet (0.25% to 30 area %), plagioclase (0.7 to 14 area %) and ilmenite (0 to 3.7 area %). Collectively, these minerals make up > 95 area % of every sample in this project. Aside from garnet, these minerals are all present at Strange Lake and occur in many other rock types. These seven minerals account for almost all of the variance in the database and, aside from albite and plagioclase, they show systematic geographic variations in abundance, as documented in Chapter 7. Although some particles of these minerals (especially quartz and feldspars) *must* have been contributed by the Strange Lake Intrusion, this influence is likely small, and most of variation in major mineral abundance probably records contributions of material from regional geological units.

The unconsolidated glacial sediment termed "till" is poorly-sorted, and most material, especially in coarser size fractions, is of local derivation, but it will normally contain a smaller proportion from more distant sources (e.g., Sugden and John, 1976; Benn and Evans, 2010). The far-travelled component is mostly in finer size fractions, but visible fragments (clasts) of such rock types may also be present. The garnet found in sample sites underlain by the garnet-free rocks of the Strange Lake Intrusion could be derived from locations several kilometres to the southwest (i.e., up-ice), but visible clasts in those same tills are mostly local granite, although pieces of older gneiss are present (Batterson, 1989; A. Kerr, pers. comm., 2021). However, it is important to remember that the present land surface is *not* the same as the pre-glacial land surface. Thus, some material in tills may come from local sources that were once above the level of the present land surface, but which no longer exist. This complication may apply specifically to the area of the Strange Lake Intrusion, where the present land surface is considered to be very close to the original 'roof' of the intrusive body.

Although every till will contain material from different sources, and some well-travelled material, it is well established that most till materials originate within a few kilometres of its site of deposition. It is for this reason that till geochemistry and indicator mineral studies are considered valuable exploration techniques, because anomalies are usually fairly close to sources (e.g., McClenaghan and Paulen, 2017). This reasoning above suggests that geographic variations in major mineralogy should largely reflect contributions from local and regional bedrock sources and that point sources such as Strange Lake would have little influence on these patterns beyond their immediate vicinity.

The major minerals identified in the till samples, with the exception of garnet, could be derived from a wide variety of igneous, metamorphic or sedimentary rocks. The most obvious sources for quartz and K-feldspar are igneous rocks of granitic composition (including the Strange Lake Intrusion) but these minerals could also come from the metamorphic rocks in the east of the study area, which were derived from broadly granitic precursors (Ryan et al., 2003, Figure 2.8). On the other hand, Fe-Mg-rich silicates (e.g., hornblende) or Fe-Ti oxides (ilmenite, magnetite) are more abundant in igneous rocks of mafic to intermediate composition, which are commonly poorer in quartz and K-feldspar, or in their metamorphic derivatives, which can be strongly enriched in hornblende (these are sometimes called 'amphibolites' for this reason). However, garnet is much more restricted in terms of potential sources. It is very rarely found in granites (and is notably absent from any in the study area; Ryan et al., 2003) but is common in metamorphosed mafic igneous rocks, and also in some metamorphic rocks derived from Al-rich sedimentary rocks (originally siltstones, mudstones, etc.). This range of rock types exists mostly in the west of the study area (Figure 2.8; Ryan et al., 2003).

All of these potential source rocks exist within the area of till sampling, and at modest distances beyond it (Ryan et al., 2003; see also Figure 2.8). Although much of the sampling area is poorly exposed, regional north-south geological trends allow confident extrapolation from areas to the north and the south. As discussed in Chapter 2, the western part of the sampling area is underlain by metamorphic rocks of broadly mafic to intermediate composition, but includes rocks of metasedimentary origin. These are obvious sources for hornblende, ilmenite and garnet, as well as some quartz and plagioclase. The southwestern corner is underlain by the Strange Lake Intrusion, which is an unusual point-source for rare minerals, but otherwise will mostly contribute unremarkable quartz and alkali feldspars. As noted above, the Strange Lake Intrusion is thought to be exposed very close to its original roof zone, as shown by the presence of zones of metamorphic rocks within it (e.g., Miller, 1986; 199). Prior to the most recent glaciations, many of the granites around Strange Lake might have been *below* the paleosurface, under a lid of older metamorphic rocks. The eastern part of the sampling area, beneath Grids 2 and 3, is dominated by metamorphic rocks (gneisses) that were derived from igneous rocks of broadly granitic composition, more specifically tonalite (quartz and mostly plagioclase) and granodiorite (quartz and a mixture of feldspars). These rocks also contain some Fe-Mg-rich silicates but these are mostly pyroxenes (augite and hypersthene) rather than hornblende, because the metamorphic grade is higher (Ryan et al., 2003).

Viewed in the above perspective, geographic variations in the relative proportions of [quartz + K-feldspar], [garnet + hornblende + ilmenite] and other major and minor minerals are consistent with the local source rocks. This is illustrated in Figure 8.8, which combines two proportional-symbol maps used in Chapter 7 with a general representation of the boundary between major groups of geological units. The contrast in major mineral abundances from west to east corresponds roughly with the shift from mafic and intermediate bedrock units to dominantly granitic bedrock units, and is shown well by [garnet + hornblende + ilmenite] and by the minor mineral augite, (Figure 8.8) and also by other minerals. However, the transition point is locally displaced by about 2 km to the east of the inferred boundary. Closely similar patterns are shown by some minor and accessory minerals, and are also defined by moderate to strong (negative or positive) correlation coefficients against the two composite variables defined from major element data. The increasing occurrence of pyroxenes (augite, hypersthene) in the east is also consistent with information from the maps of Ryan et al. (2003). In previous investigations of bulk till geochemistry and its implications for glacial dispersion,

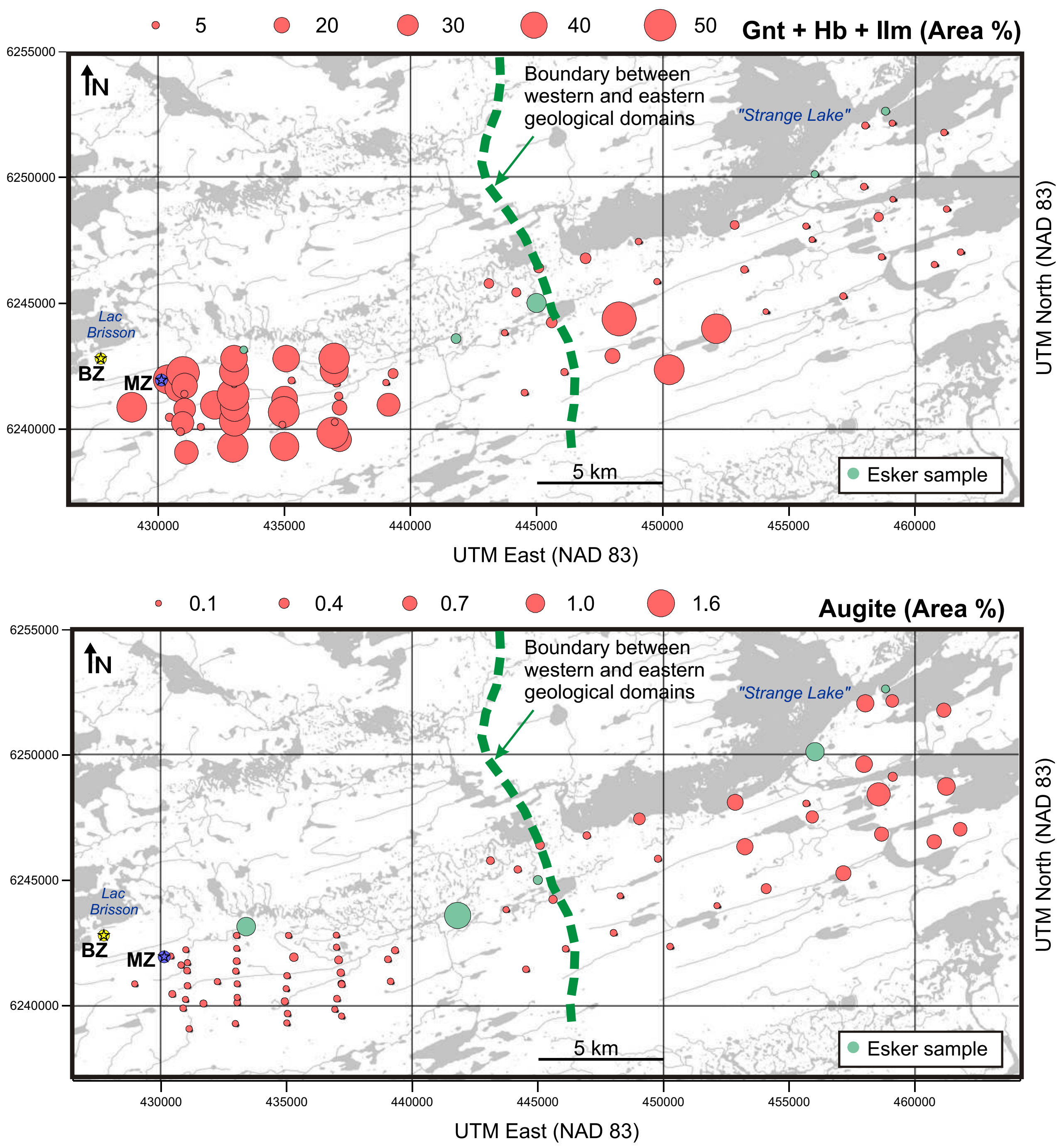

Figure 8.8. Examples of general correspondence between the two main geological domains in the study area and the patterns of mineral abundance. The western domain is dominated by metamorphic rocks of mafic to intermediate igneous origin and some of metasedimentary origin. The eastern domain is dominated by metamorphic rocks of broadly granitic origins (see Figure 2.8). Upper map shows variation in abundance for [garnet + hornblende + ilmenite]; lower map shows variation in abundance for augite (clinopyroxene). Boundary between geological domains is shown by green line.

Batterson (1989) and Batterson and Liverman (2000) noted signs of enrichment in Ni, Cu and other trace elements commonly associated with mafic igneous rocks, in the areas near the Strange Lake deposits. They also suggested that these patterns reflected the characteristics of local bedrock. These observations are consistent with the mineralogical data reported here.

At the western end of the sampling area, the immediate bedrock is defined by drilling, and consists of granites of the Strange Lake Intrusion and some areas of metamorphic rocks. Garnet is abundant in some (but not all) till samples, and quartz is depleted in some (but not all) till samples. This is shown in Figure 8.9, which shows patterns for garnet and quartz within the area of Grid 1, closest to Strange Lake. As one would expect, the garnet-rich samples are poorer in quartz, and vice-versa. Such a pattern could be interpreted to mean that some till samples are dominated by materials derived from the other side (west) of the Strange Lake Intrusion, whereas others more closely mirror the local bedrock, but this may not be so. The present land surface is likely close to the original roof zone of the Strange Lake intrusion but generally below it, which is why parts of the Main Zone and B-Zone deposits have been removed by glaciation. However, this land surface is not the same as the land surface that existed prior to or in early stages of glaciation. Also, the geological boundary that defined the roof of the intrusion is a three-dimensional surface rather than a plane, and it likely had its own topography. Thus, relatively quartz-rich tills could be derived from ‘high-points’ on the upper surface of the granite whereas quartz-poor, garnet-rich tills could come from remnants of metamorphic rocks at lower relative elevations. In other words, some of the possible sources for garnet- and amphibole-rich till materials may no longer exist because they have been removed by glaciation. As discussed in Chapter 7, patterns for some rare indicator minerals in the area of Grid 1 define subparallel zones of enrichment aligned with the inferred glacial transport direction, and these are confirmed by bulk geochemical data from tills (e.g., Figure 8.2; 8.4). These linear zones of enrichment could also come from preferential erosion of high points on the upper contact surface of the granite, perhaps including mineralized zones that were completely removed. As noted by Bell (1984), there are no known sources for some of the enriched zones identified by her detailed till sampling, but these may originally have been present near the roof of the granite body, in locations above the modern land surface. Figure 8.10 is a crude attempt to portray these suggestions using a three-dimensional sketch, but with full acknowledgement that such hypotheses are speculative and difficult to prove.

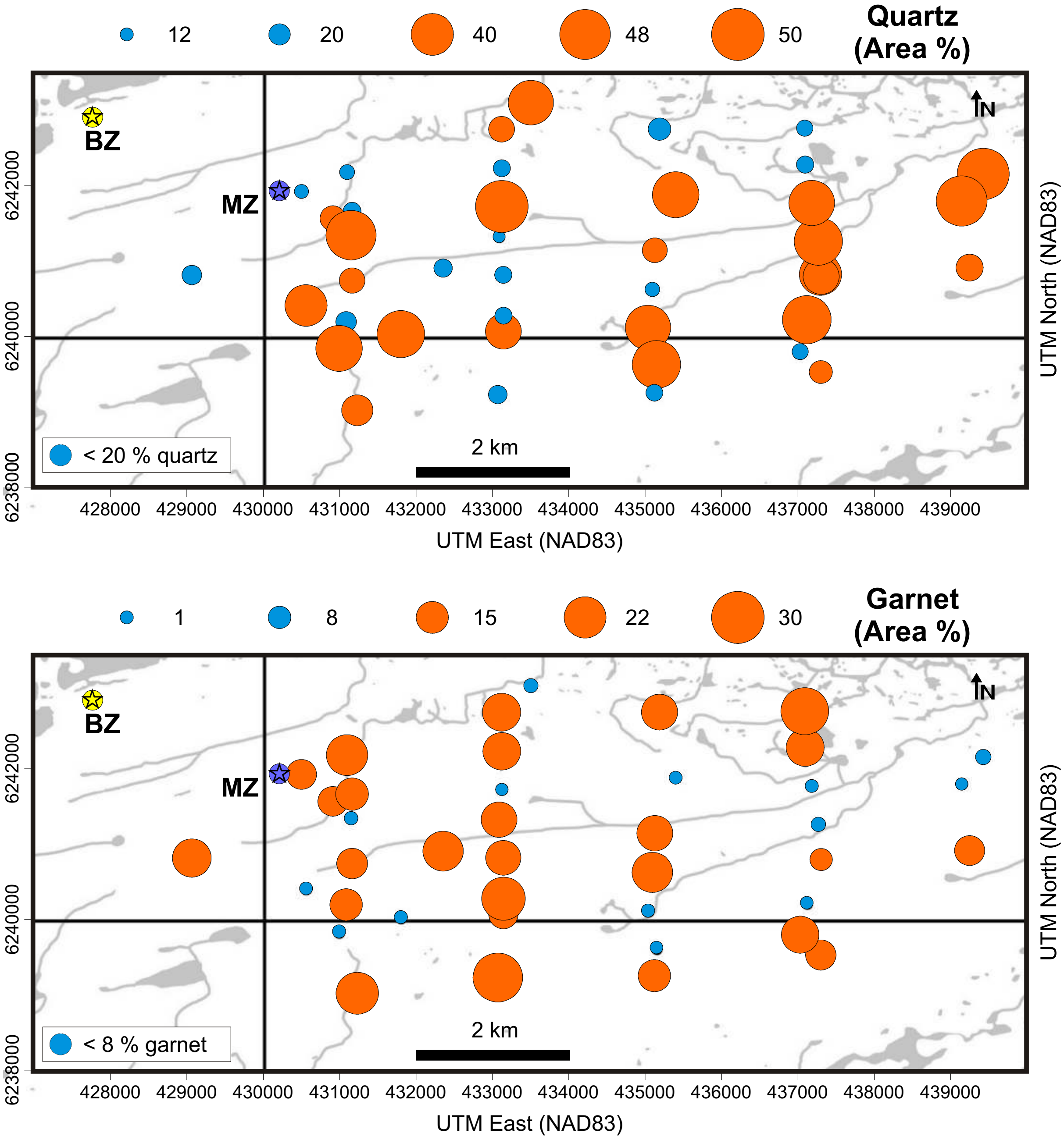

Figure 8.9. Detailed map showing abundance variations for quartz (upper panel) and garnet (lower panel) in the area of Grid 1, nearest to Strange Lake. For added clarity samples that have low abundances of each mineral are distinguished by colour, to illustrate that low-quartz samples are enriched in garnet and vice-versa. See text for additional discussion.

There appears to be a good case for concluding that large-scale patterns of regional geology, dominated by contrasting north-south striking units of metamorphic rocks (Ryan et al., 2003) control many mineralogical features of till samples, especially for major and minor minerals. However, the geographic variations exhibited by rare Zr-, Nb- and REE-bearing indicator minerals and also by bulk trace element patterns in tills (e.g., Batterson and Taylor, 2009; Bourassa and Banville, 2012) cannot be attributed to such regional controls, and must instead record dispersion from Strange Lake. These patterns are discussed in the next section.

Local Variation Patterns and their Links to the Strange Lake Deposits

Some General Considerations about Dispersion Processes

There is no doubt that some material from the Strange Lake Intrusion and its mineral deposits was removed and dispersed to the north-east by moving ice for at least 35 km, and possibly to much greater distances. Figure 8.10, outlined above, is merely a schematic cartoon, but it conveys possible complexities. The Strange Lake Intrusion was progressively 'unroofed' as older metamorphic rocks above it were removed by ice. The final erosion surface provides the present-day arrangement of geological units that we see on maps (e.g., Figures 2.3 and 2.8), but it is not the same as the original pattern near the deposits. The progressive erosion was sufficient to expose both the Main Zone and B-Zone deposits, but luckily it was insufficient to excavate the mineralization that remains in the shallow subsurface. The preservation of ore deposits in areas of glacial erosion (or, indeed any type of erosion) is always a matter of luck, and it is likely that other zones of mineralization originally situated *above* the present erosion surface were *completely* removed and transported by ice. The Main Zone and B-Zone deposits probably contributed some debris and mineral grains in tills through the study area, but the latter could also represent sources that no longer exist, as implied by Figure 8.10 and the related discussion. There are also different methods of transportation during glacial dispersion (Benn and Evans, 2010; McClenaghan and Paulen, 2017). Some bedrock material is ground down in size at or near the rock-ice interface, and then progressively moved away or deposited in local concentrations, but larger pieces may be removed to higher locations in the ice column and transported as 'englacial' debris, which may also be redeposited elsewhere, or left when residual ice disappears during deglaciation. Subglacial fluvial systems, which we now see as esker ridges, represent an additional mechanism to redistribute material initially removed by various processes. The Strange Lake area is inferred to have a relatively

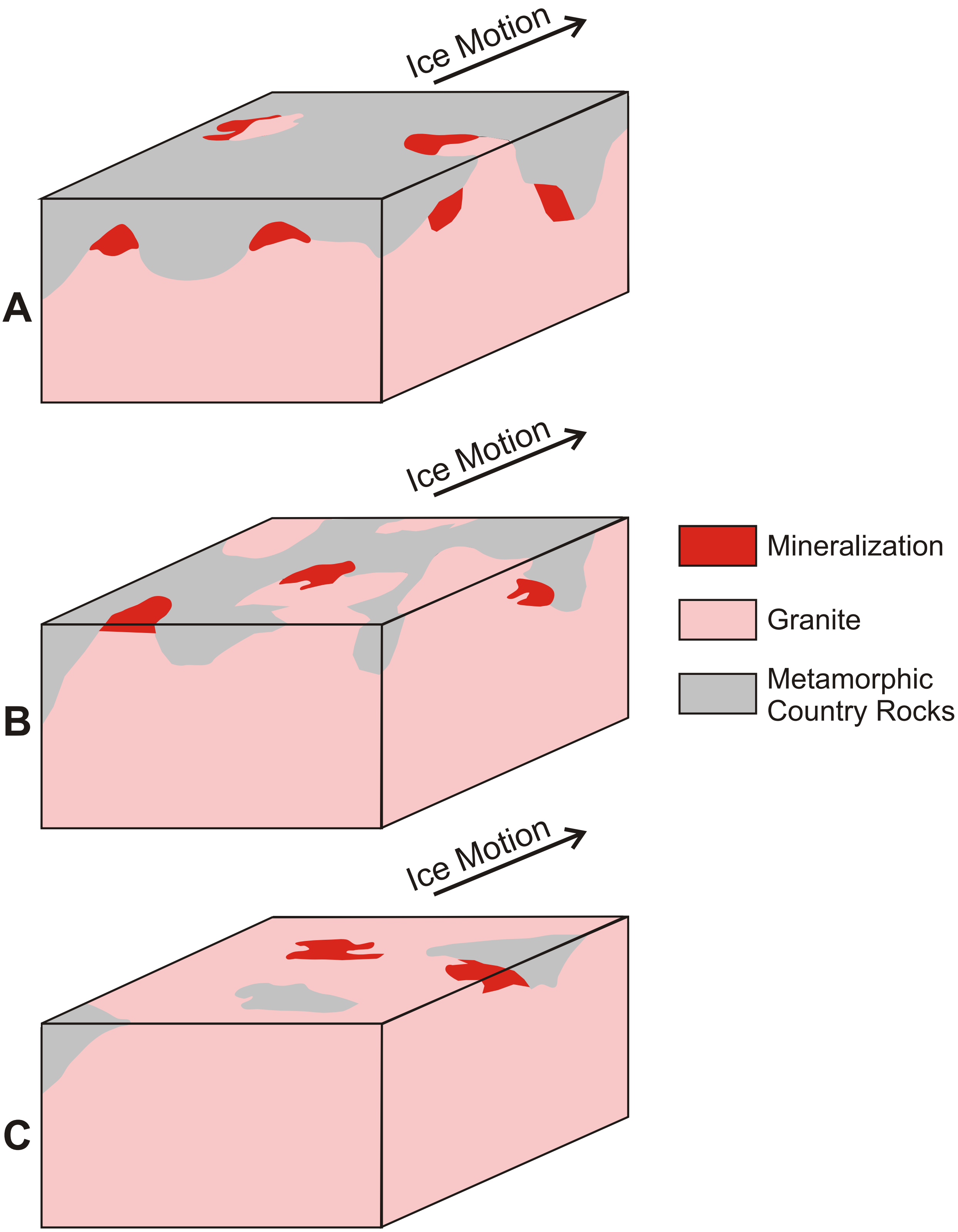

Figure 8.10. Schematic illustration of the gradual unroofing of the Strange Lake Intrusion by glaciation. (A) Early stage with metamorphic rocks in the roof of the body dominating erosion surface. (B) Intermediate stage with a mixture of metamorphic rocks and granite at the erosion surface, and erosion of some REE mineralization. (C) Later stage where granite dominates the erosion surface and some areas of REE mineralization remain, but others have been removed. See text for additional discussion.

simple glacial history, with fast-moving ice as part of an ice-stream and only a single phase of ice movement in a single direction, but there are many possible complexities. In their review of dispersion patterns observed in Newfoundland and Labrador, Batterson and Liverman (2000) note that till samples enriched in trace elements associated with Strange Lake (Zr, Nb, REE) are anomalous in certain parts of the dispersion train, notably on the up-ice sides of hilltops. They suggested that these topographic highs had acted to trap material derived from the Strange Lake deposits and concentrate it in relatively small areas. This may be an influence on local enrichments of indicator minerals (see Chapter 7) and is a further illustration of the complex nature of glacial dispersion in this area.

Any attempt to reconstruct the ice-age anatomy of Strange Lake and surrounding area, or the full details of erosion and dispersion processes, will inevitably be speculative. McClenaghan and Paulen (2017) discuss the possible complexities of glacial dispersion from the perspective of indicator mineral studies. In a wider context, much remains to be learned about the processes that occur beneath several kilometres of compressed ice over thousands of years, because modern examples in Greenland and Antarctica are totally inaccessible. Margold et al. (2015) and Storrer et al. (2013) suggest that spatial and map analysis of glacial landforms and features in northern latitudes provides an indirect approach to understanding the mysterious ancient land-ice interface. Similarly, spatial and map analyses provide the best approach to understanding finer details of glacial dispersion processes for indicator minerals, but there is no guarantee that they will give clear answers. The discussion in this section is focused mostly on the patterns shown by minerals derived from the Strange Lake Intrusion, and how they relate to information derived from the MLA-SEM study, rather than on trying to understand glacial and postglacial dispersion in detail, or attempting models for these processes. These are important aspects for future research, but they are beyond the scope of a largely laboratory-based project and need to be coordinated with investigations of the Quaternary stratigraphy of the study area and the physical characteristics of till units and esker systems.

Categories and Identities of Strange Lake Indicator Minerals

Not all the of the uncommon minerals that inhabit the Strange Lake deposits and occur in glacial sediments derived from them are fully diagnostic. Aenigmatite, allanite, astrophyllite, apatite and zircon are all present, but they also occur more widely as accessory minerals in igneous or metamorphic rocks (Deer et al., 1992). The zirconosilicate mineral elpidite, which is important at Strange Lake, is present in the off-grid control sample (G2-15) so it may also have other possible sources. Similarly, the Nb-bearing oxides pyrochlore and fergusonite are not unique to Strange Lake, although they are certainly rare. The most informative potential indicator minerals are those that occur *only* within the source, in the context of its regional setting. For Strange Lake, these include gerenite and gittinsite, and less abundant minerals such as bastnaesite, britholite, gadolinite, parisite, perclevite, stetindite and euxenite. The mineral initially named “ericssonite” and later identified as the similar Ba-Fe(Mn)-Ti silicate bafertisite may also be in this category, but interpretation is problematic, as discussed below. All of the diagnostic minerals show at least partially systematic spatial variation patterns, although these are less clear for the rarest minerals, likely due to the influence of probability effects. However, the presence of a geographic pattern that seems to change with the proximity of samples to the Strange Lake source (which is what would be expected) may not always indicate a causal link, as some minerals that have no association with Strange Lake can show abundance variations from west to east that are controlled by regional geology. A good example is provided by the Fe-Ti-oxide ilmenite, which is abundant in some of the metamorphic rocks but nearly absent in the Strange Lake Intrusion granites. At first sight, the ilmenite pattern could be interpreted as indicating derivation from Strange Lake, but the other information suggests that this is impossible.

Distinguishing Regional Patterns from Dispersion Patterns related to Strange Lake

As noted above, regional and local patterns can be difficult to distinguish. Ilmenite is a fairly obvious example, because the mineral is very rare at Strange Lake, but others are not as obvious. Both apatite and zircon show well-defined patterns in which their abundance is highest in areas close to Strange Lake (Grid 1), and diminishes eastward with distance through Grids 2 and 3. For complete reference, see the maps and profiles of Figures 7.1 and 7.2, and also Figure 7.15; for convenience of comparison, patterns are shown together in Figure 8.11. As discussed in Chapter 7, the pattern for apatite fits conventional expectations for an indicator mineral, but this is likely incorrect. Apatite abundance in Strange Lake drill cores (Baird, 2018) is generally lower than in the till samples, and the mineral is also known to be widespread in the regional metamorphic rocks in the west of the study area (Ryan et al., 2003). If there is an apatite contribution from Strange Lake, it is likely minor. The pattern for zircon is superficially similar to that of apatite, but zircon is far less common in the metamorphosed mafic and intermediate plutonic rocks in the west of the study area. Zircon is generally more abundant in granitic igneous rocks, whereas apatite is more widely associated with mafic and intermediate rocks

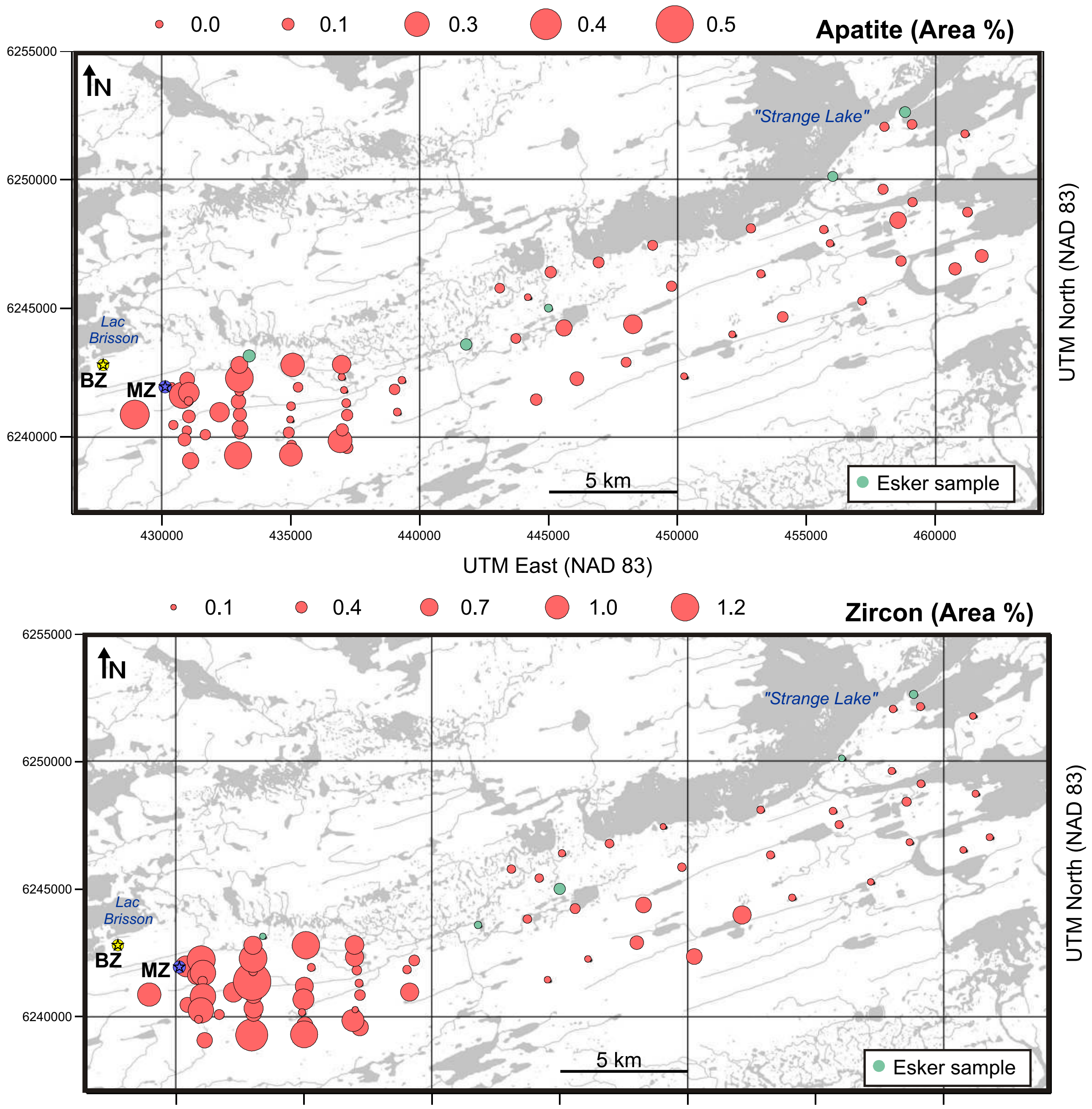

Figure 8.11. A comparison between the geographic variation in the abundance of apatite (upper panel) and the abundance of zircon (lower panel). Both of these minerals have potential sources at Strange Lake, but also potential sources in regional bedrock units of metamorphic origin. The patterns are superficially very similar, but apatite is interpreted to be of largely regional origin, because it is scarce at Strange Lake, but widespread in other bedrock sources in the west of the area, Zircon, on the other hand, is abundant at Strange Lake, but less common in the local metamorphic rocks. This illustrates the potential difficulty in separating regional versus local causes for mineralogical variations in cases where multiple sources are possible. See also discussion in Chapter 7.

(e.g., Deer et al., 1992), and zircon is also known to be important at Strange Lake. The declining abundance of zircon with distance from Strange Lake matches expectations for an indicator mineral that is fairly persistent in the surficial environment (e.g., McClenaghan and Paulen, 2017) and other evidence suggests that it is largely (but perhaps not entirely) derived from Strange Lake. The example of apatite and zircon illustrates that geographic patterns do not always allow simple interpretations; this same question – regional versus local control – also arises in the strange case of bafertisite (see below). Similarly, there are other minerals that *must* come from the Strange Lake deposits, but which do not show simple geographic patterns that conform to expectations.

Group 1: Dispersion Patterns with Exponential or Linear Decline with Distance

As discussed above, zircon provides a simple dispersion pattern, in which abundance diminishes with distance from the Strange Lake source. This same pattern is shown by the Y-Ca-REE silicate gerenite, which is the most abundant of the REE-bearing indicator minerals. The REE-bearing minerals britholite and parisite also follow this pattern, but diminish in abundance more rapidly, and are largely absent from samples in Grids 1 and 3, whereas gerenite persists. Maps for all three minerals are shown together for comparative purposes in Figure 8.12 (see also Figures 7.24, 7.25 and 7.26 for the associated profiles). The same pattern is shown by the fairly abundant titanosilicate mineral aenigmatite (see Figure 7.20) which is not diagnostic, but probably largely derived from the Strange Lake granites. It can also be seen for some other minerals, such as thorite (Figure 7.34) and fergusonite (Figure 7.32), and possibly also for uraninite (Figure 7.34) euxenite (Figure 7.30) and changbaiite (Figure 7.33). However, these latter patterns are much noisier, due to larger uncertainties caused by probability effects (see Chapter 4 and earlier discussion). If rhodonite is an indicator mineral from Strange Lake, as speculated in Chapter 7, it also belongs to this group, but its pattern is hardly convincing.

Patterns of this type conform to a general expectation, i.e., that they are most abundant closest to the source and then decline in both abundance and occurrence with distance. However, there are some differences between these minerals, most notably in the rate of decline. Gerenite persists throughout the sampling area, whereas all the others decline more rapidly. In the associated profiles (see Chapter 7), the decline of gerenite abundance with distance is more linear in appearance, whereas the other minerals show a more rapid initial type of abundance decay. The simplest interpretation is that contrasts are controlled by source abundance; gerenite is ten times more abundant in the source rocks at Strange Lake than other minerals, so there is a more abundant supply throughout the dispersion process as coarser lithic material is progressively reduced to small particles. However, the

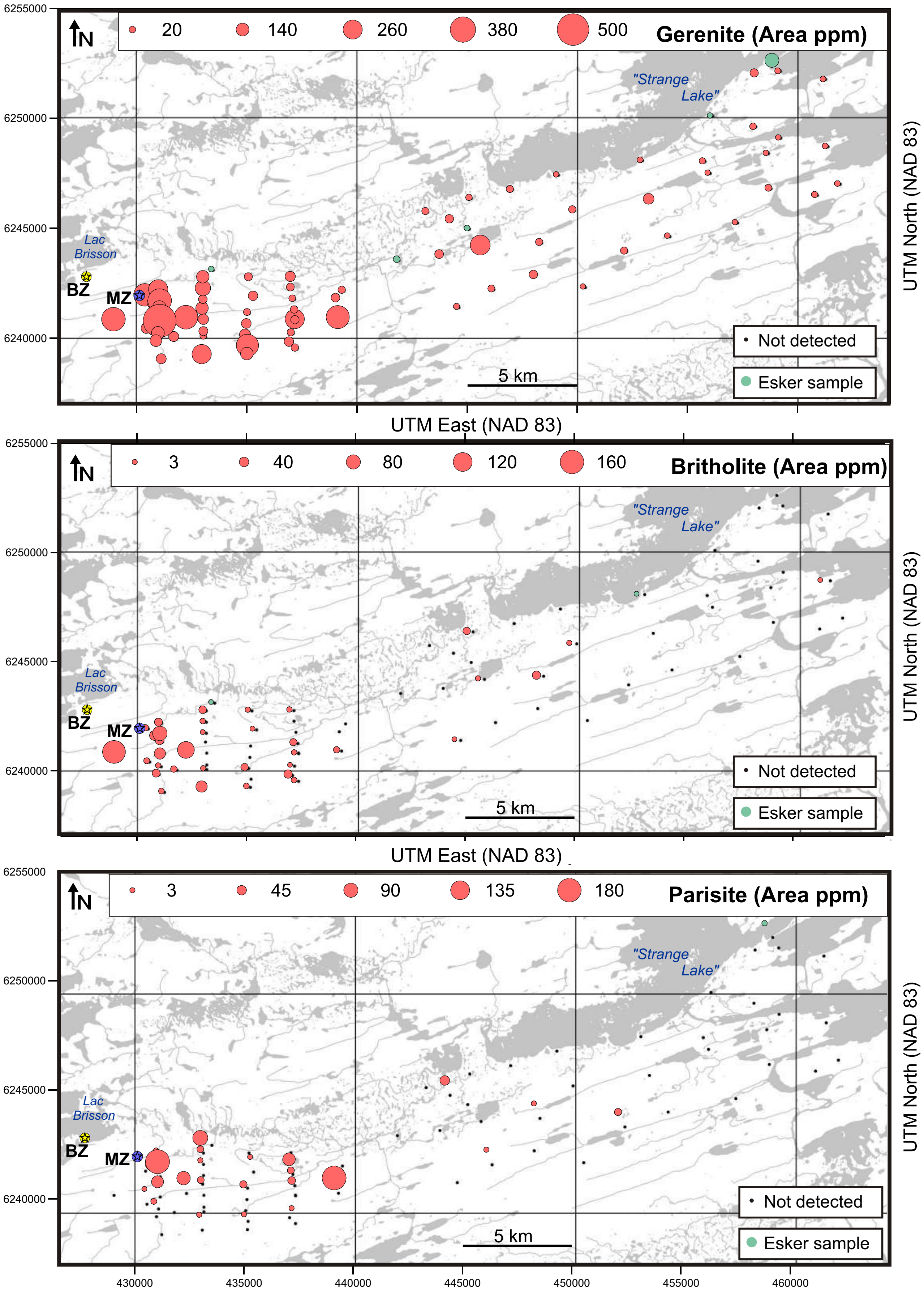

Figure 8.12. Comparison of geographic mineral abundance patterns for gerenite, britholite and parisite showing variable declines in abundance with distance from Strange Lake.

abundance of gerenite in till samples is also vastly reduced from its percent-level abundance in drill cores (see Figure 6.15) so its apparent persistence on maps is not necessarily an indication that the mineral is robust in the surficial environment. Other factors, notably the physical properties of minerals and mineral associations, should play a role in determining the rate at which the abundance of a given mineral declines. The pattern for thorite is another case in point. This mineral is not as abundant as gerenite in the source rocks but its abundance in tills is extremely low, especially considering the fact that there are radioactivity anomalies in the area east of Strange Lake, ascribed to thorium, its major constituent (see Chapter 3). The poor persistence of thorite as mineral grains could be related to its radioactive character; over geological time radioactive minerals will suffer damage from radioactive decay, which destroys their physical structure. Thorite is well known for developing so-called 'metamict textures' and, although it may survive well enough included as part of a lithic fragment in tills, it may disintegrate quickly when liberated as a smaller mineral grain.

Group 2: Dispersion Patterns with a Steady State, or a Slow Increase with Distance

Dispersion patterns showing exponential or linear decay were anticipated, as they are documented by many indicator mineral studies (e.g., McClenaghan and Paulen, 2017). However, a rather different type of dispersion pattern for some other Strange Lake indicator minerals is more difficult to interpret. Maps for three examples are shown for comparative purposes in Figure 8.13 (see also Figures 7.19, 7.23 and 7.29 for the associated profiles). The clearest example is for the zirconosilicate gittinsite, which is the most abundant diagnostic indicator mineral from Strange Lake. It shows some scattered high values in Grid 1, close to the deposit, but otherwise shows rather limited variation until the area of Grid 3, where it seems to increase in abundance at the eastern end of the sampling area. The pattern for pyrochlore is similar in many respects, although the overall abundance of the mineral is much less, and it is missing from many of the samples. The REE-silicate gadolinite shows a slightly different pattern in which there is little variation from west to east, but scattered anomalies of high abundance. Patterns for some other indicator minerals, such as perclevite (Figure 7.37) and bastnaesite (Figure 7.28) have similar patterns with limited variation as does the other common zirconosilicate mineral elpidite (Figure 7.23). Elpidite shows a fairly complete pattern, but the other minerals have noisier and less obvious trends due to the larger uncertainties caused by probability effects.

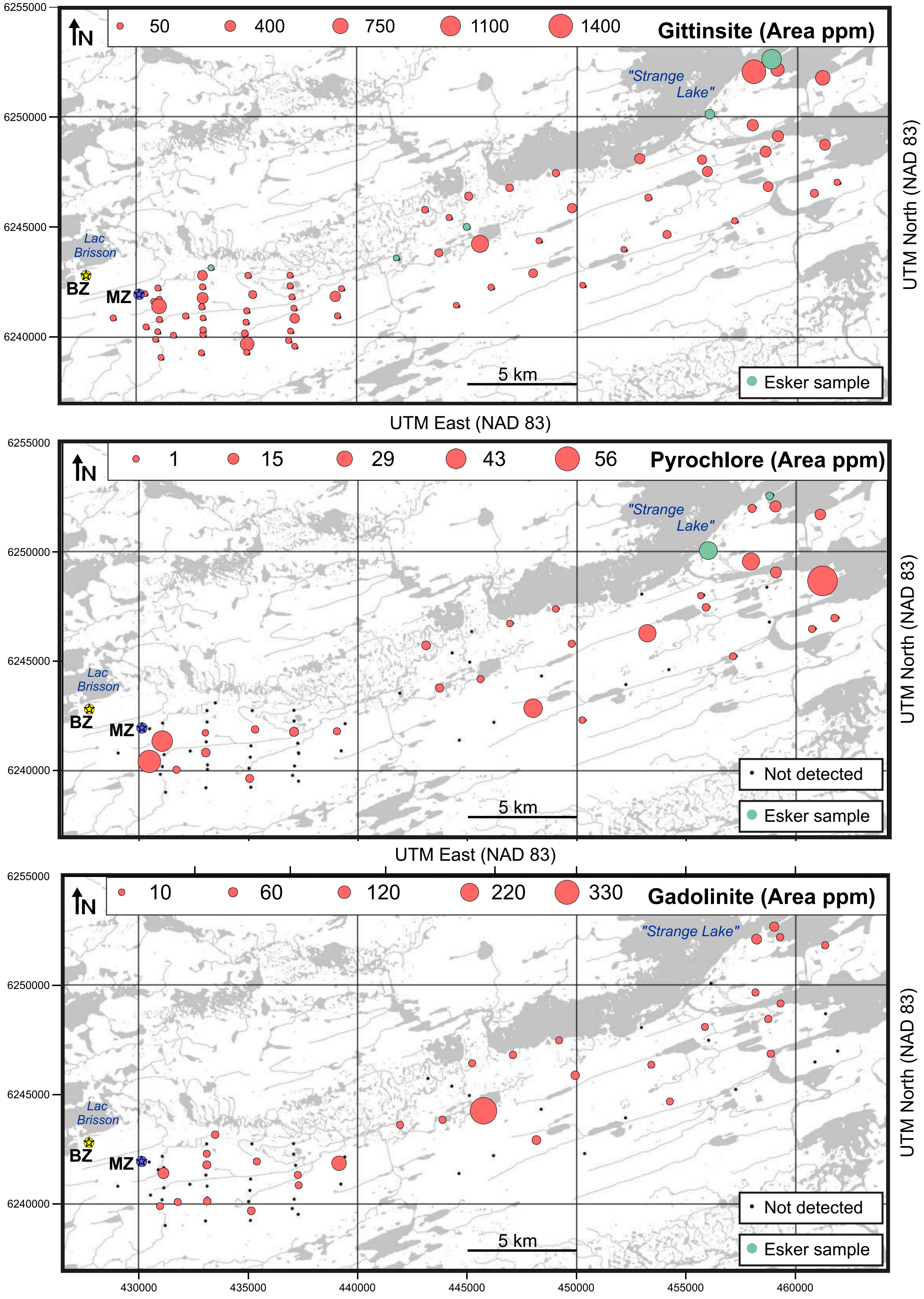

Figure 8.13. Comparison of geographic mineral abundance patterns for gittinsite, pyrochlore and gadolinite showing limited variation with distance from Strange Lake.

Patterns of this type do not fit conventional expectations for indicator minerals, and imply that some of the minerals derived from Strange Lake might persist for even greater distances to the east. The work of Currie (2019) on gittinsite near Voisey's Bay confirms this directly for one such mineral, but this new information implies that other indicator minerals might also be present at much greater distances. There is presently no information from any locations in the 70 km or so between the eastern end of Grid 3 and the Voisey's Bay area, but selective till sampling in this distance interval would be an obvious and interesting follow-up research project. The recognition of other diagnostic minerals would certainly strengthen the case for long-distance expression of Strange Lake through dispersion, but these would likely be present at very low abundances compared to gittinsite, which is more plentiful in the source location.

The area east of the Strange Lake deposits is interpreted to form part of an ancient ice-stream within the Laurentide ice-sheet (e.g., Margold et al., 2015; Stokes et al., 2016; Paulen et al., 2017). Indicator mineral studies from comparable settings, and theoretical treatments that assume relatively rapid ice movement and very efficient bedrock erosion in such settings, suggest that abundance trends for indicator minerals may differ from those seen more commonly in "normal" glacial settings. McClenaghan and Paulen (2017) and Paulen et al. (2017) suggest that ice-stream settings are characterized by slower, linear-style decay of indicator mineral abundances (or geochemical anomalies) with distance from the source, rather than the more rapid exponential decay described above for most of the Strange Lake indicator minerals. It seems reasonable to assume that the abundance of any indicator mineral must *ultimately* decline with distance from the source, but perhaps the rate of decline for some minerals from Strange Lake is low enough not to be apparent within the extent of the study area. Gittinsite is exceptionally abundant in drill cores from Strange Lake compared to the other minerals that show these types of trends, so it is likely that it has the greatest long-distance persistence. It would be very interesting to investigate the wider distribution of other minerals that show this type of geographic variation.

Group 3: Dispersion Patterns with Uncertain Characteristics

Most of the Strange Lake indicator minerals can be placed into the two categories discussed above. However, a few are harder to classify and interpret, such as stetindite, astrophyllite and pectolite, shown for comparison in Figure 8.14 (see Figure 7.29 for more information on stetindite; maps

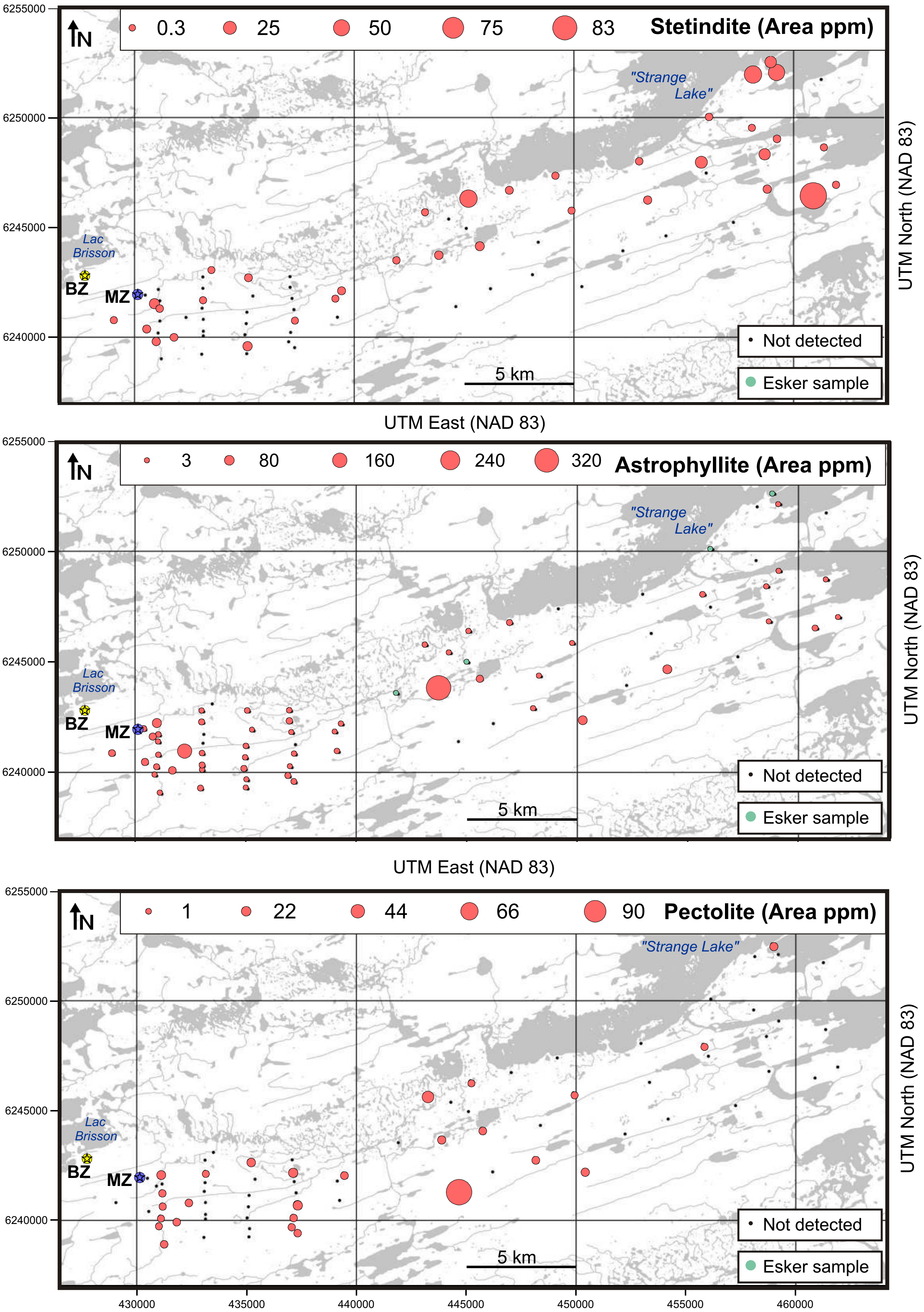

Figure 8.14. Comparison of geographic mineral abundance patterns for stetindite, astrophyllite and pectolite, which are more difficult to compare with other minerals.

and profiles for astrophyllite and pectolite are included in the Appendices). The most prominent enrichment for stetindite is at the eastern end of Grid 3, distant from Strange Lake, with least abundance in the centre of the area. Astrophyllite (a titanosilicate) and pectolite (a hydrated Ca-Na silicate) show rather disorganized patterns, with scattered anomalously high values associated with different samples. Pectolite seems largely to be confined to Grid 1, but has limited variation. These patterns cannot easily be interpreted, in part because stetindite and pectolite are missing from many samples due to probability effects. They are not readily assigned to Group 1 or Group 2 above.

The Strange Case of Bafertisite

Bafertisite (previously labelled as “ericssonite” by MLA-SEM analysis) should be considered as a possible Strange Lake indicator mineral, because it was noted and described there by Birkett et al. (1996). However, this creates an interesting puzzle. The MLA-SEM investigation of Baird (2018) also detected “ericssonite” in some drill cores, but only at very low abundances (< 8 area ppm), which is much less than its mean abundance in the till samples (58 area ppm). Birkett et al. (1996) indicate that bafertisite is generally associated with ilmenite at Strange Lake, but ilmenite is also very rare in the drill core samples, with an average abundance of only 26 area ppm. By contrast, ilmenite is a major mineral in till samples, averaging 1.13 area % (see Table 6.1). On this basis, as noted earlier in this section, ilmenite in till samples definitely cannot be explained by exclusive derivation from Strange Lake. The geographic variation pattern of bafertisite (see Figure 7.42) is very like that of ilmenite, but it also could be interpreted to resemble that of other indicator minerals for which abundance declines with distance from Strange Lake (e.g., zircon, gerenite). If this latter interpretation is favoured, there is a conflict, as the low abundance of bafertisite in the source rocks (Baird, 2018) seems inconsistent. How can this puzzle be resolved, if at all? How could bafertisite be derived from Strange Lake if it is nearly absent in drill cores extracted from the Main Zone Deposit? If bafertisite instead comes from regional bedrock sources and has nothing to do with Strange Lake, it must be widely distributed, which is inconsistent with its status as a rare mineral, and the reports of its occurrence by Birkett et al. (1996).

Birkett et al. (1996) proposed that bafertisite formed in granites at Strange Lake by reaction between early-formed ilmenite and pockets of fluid-rich residual magma or hydrothermal fluids exsolved from the magma. This was based largely on textural relationships that showed bafertisite to occur as rims around rare ilmenite crystals. The suggestion of a hydrothermal connection suggests a speculative interpretation that might resolve the puzzle. This hypothesis proposes is that bafertisite is *associated* with the Strange Lake deposits, but is actually rare *within* the deposits, because it is more widespread in older adjacent metamorphic country rocks that contain significant ilmenite. In other words, bafertisite was formed by local interaction of hydrothermal fluids with older metamorphic rocks that originally formed the roof zone to the Strange Lake Intrusion. This is consistent with the observations of Birkett et al. (1996), and provides a potential source that is physically discrete from the Strange Lake Intrusion or its mineral deposits. It is also consistent with the strong correlation between bafertisite (formerly known as "ericssonite") and ilmenite (see Chapter 6, and specifically Table 6.9) and the characteristic geographic distribution of the mineral (see Chapter 7, and specifically Figure 7.42). Investigation of mineral associations for selected samples that are enriched in the mineral (see Chapter 6) confirm that it is commonly present in ilmenite-dominated particles, which is also consistent with this idea.

If correct, the hypothesis indicates that bafertisite in the till samples came largely from erosion of metamorphic rocks that were originally in very close proximity to the Strange Lake deposits, perhaps situated above the present land surface. This idea could be tested through BSE imagery of ilmenite particles in the till samples, but would better be assessed through direct investigation of older metamorphic rocks close to the Strange Lake Intrusion. However, these country rocks are very poorly known because there are no local outcrops and very few drill holes actually encountered metamorphic rocks within the area of the intrusion and, if they did, they were quickly abandoned, so little drill core is available for study (Kerr, 2015).

Controls on Geographic Variation Patterns for Strange Lake Indicator Minerals

Understanding the different styles of geographic variation patterns defined by various indicator minerals from Strange Lake, and resolving their causes, was an important objective for this project, but remains very difficult.

The contrast between the Group 1 trends (fairly rapid declines in abundance) and Group 2 trends (little or no decline in abundance) within a single study area is not consistent with the idea that such patterns largely reflect the details of local glacial transport, as implied by other reviews (e.g., McClenaghan and Paulen, 2017). This research shows that patterns attributed elsewhere to "ice-stream" settings and "normal" glacial settings occur within a single environment that is presumably constant, at least at any one point in geological time. This probably indicates that other factors also influence the behaviour of individual indicator minerals, and may be the dominant influences.

The physical properties of minerals are one obvious possibility, although there is no obvious correlation between these patterns and hardness, or cleavage tendencies (see compilation table included in the Appendix). The original abundance of minerals in the source must also be an important influence, as it controls the availability of material. Gittinsite is roughly twice as abundant as gerenite in the till samples, which is similar to their abundance ratio in the drill core samples from Strange Lake, but both appear to be persistent over similar distances, although gerenite declines whereas gittinsite seems to increase. What other factors could influence such behaviour?

Given the evidence that many of the Strange Lake indicator minerals actually form smaller ‘grains’ within larger composite particles, it is likely that the scale of these intergrowths and the mineral associations play a role in determining persistence. This was discussed in part in Chapter 6, and there is good direct evidence from this project (and also from Baird, 2018 and Currie, 2019) for an association between gittinsite and quartz. Given the hardness and durability of quartz in the surficial environment, this may favour the survival of gittinsite through long-distance dispersion compared to other indicator minerals that may have more varied mineral associations. The assessment of this idea from the MLA mineral association data is difficult and time-consuming, as data from each sample must be processed individually, and then amalgamated to seek wider trends. However, investigation of a subset of samples (discussed in Chapter 6, and here illustrated as Figure 8.15; see also Table 6.11) shows that gittinsite and gerenite do have distinctly different mineral associations. Gittinsite shows a very strong association with quartz, whereas gerenite appears to be more widely distributed among quartz, feldspars and other minerals. The information on mineral associations compiled from selected samples suggests that REE-bearing indicator minerals that appear to be most persistent through the sampling area (gittinsite, elpidite and possibly stetindite) have stronger associations with quartz than minerals that diminish in abundance more rapidly with distance from Strange Lake (e.g., gerenite, perclevite and possibly bastnaesite). An association with quartz could also be a factor in the persistence of pyrochlore, despite its very low abundance in most samples. The information on mineral associations does not necessarily imply that such links are primary attributes of mineralization at Strange Lake (although this is possible). It is perhaps more likely that grains of pyrochlore that are associated with quartz are more likely to survive prolonged transportation than those associated with other less durable (tenacious) minerals.

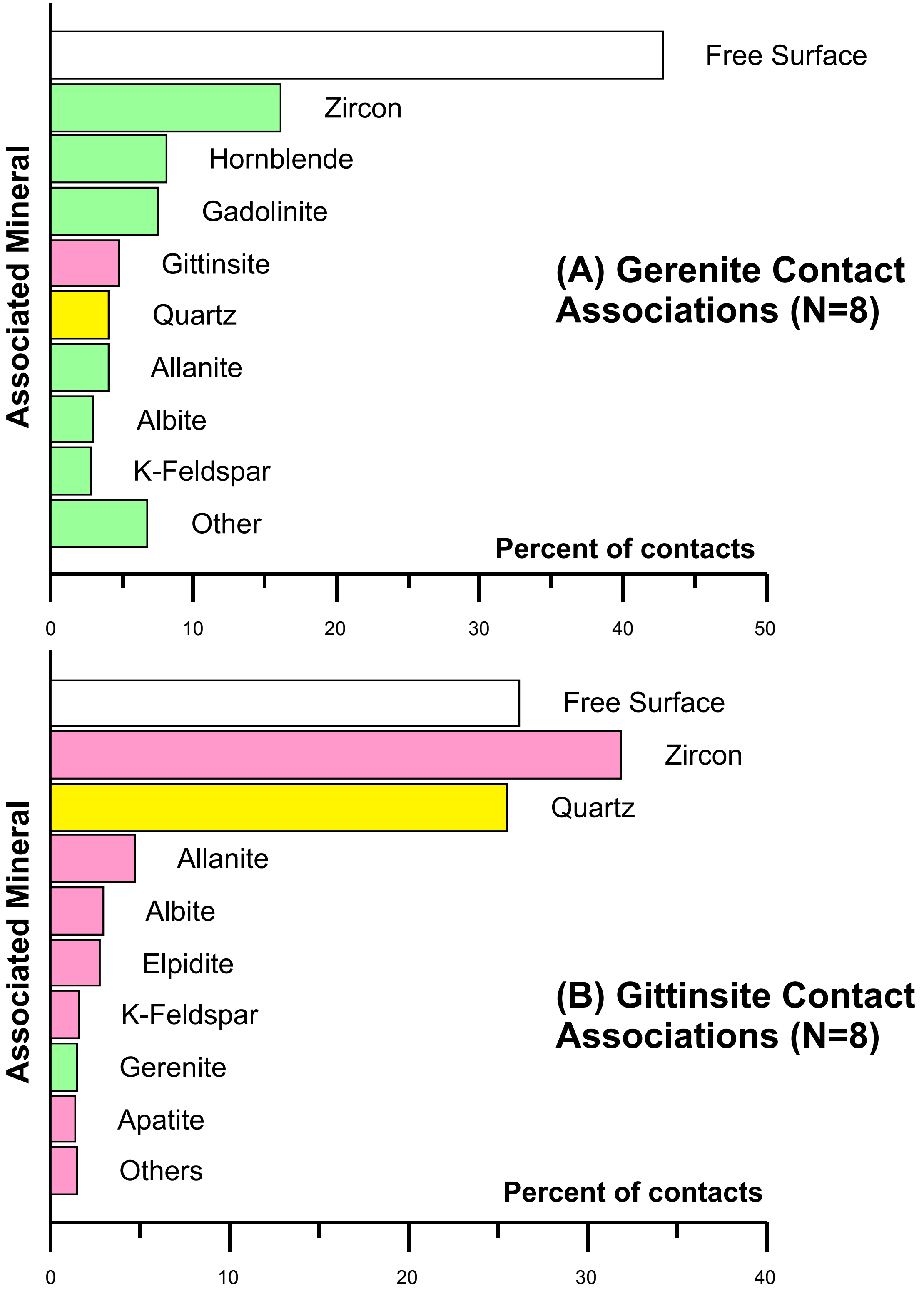

Figure 8.15. Bar charts illustrating the dominant mineral associations in composite particles for gerenite (upper panel) and gittinsite (lower panel). The charts indicate the percentage of contact surfaces for these minerals with the other minerals indicated, for a subset of 8 samples. The bar labelled 'free surface' refers to the natural external surfaces of particles, i.e., where grains of the mineral are not in contact with any other minerals. See text for additional discussion.

SUMMARY OF CONCLUSIONS

The main conclusions of this investigation are summarized below.

Visible/Infrared Reflectance Spectroscopy (VIRS) failed to produce useful results that might aid in initial initial screening of till samples for REE-bearing minerals. This is because the abundance of such indicator minerals is too low to be detectable by this method, and does not produce resolvable spectral absorption features. No further work using this method is recommended.

Evaluation of the MLA-SEM technique for quantitative mineralogical studies aimed at regional geology or indicator-mineral projects in mineral exploration shows that it is effective and could have wide application. A diverse suite of indicator minerals associated with the Strange Lake deposit was detected, and most till samples contained at least some indicator minerals. These data seem to be robust over distances of at least 35 km, although for some minerals abundances decline in areas distant from the Strange Lake source. The abundances of diagnostic minerals in the till samples were less than expected, so analytical precision and accuracy are potentially important issues. Despite low abundances (in some cases < 20 area ppm) many indicator minerals do show systematic geographic variation patterns, indirectly suggesting that these data are generally reliable. The possible impact of ‘probability effects’ linked to the small amounts of particulate material actually used for analysis needs to be considered for this method, but it may be mitigated if rare indicator minerals occur as smaller subdomains within larger particles of common minerals, rather than as discrete larger particles. Observations of particles using SEM imaging suggests that this is the case for gittinsite (a rare zirconosilicate mineral) and evaluation of grain and particle size patterns from MLA-SEM data suggests that this is the case for other indicator minerals. However, this may not always be the case for other geological settings, and if indicator minerals form discrete larger particles, they could be hard to detect reliably at low abundances.

The MLA-SEM results from the Strange Lake area were compared to results from till geochemistry surveys that analyzed bulk materials, and both methods illustrate similar patterns of dispersion. The geochemical data also provide information about the heterogeneity of sample materials, indicating that coarser size fractions are enriched in key trace elements, meaning that they must also be enriched in indicator minerals compared to the finer fractions used for MLA-SEM analysis. However, bulk REE profiles from contrasting size fractions are closely similar, suggesting that proportions of REE-bearing indicator minerals are similar in different size fractions. In future research of this type, the geochemical analysis of bulk sample materials (perhaps including different size fractions for some samples) should be considered, as it would help to constrain MLA-SEM results,

Many minerals detected by MLA-SEM analysis, over wide ranges in abundance, show systematic variation patterns that are revealed by statistical analysis and also by geographic analysis using maps. Variations in major and minor mineral abundances show a general correspondence to the inferred locations of two contrasting belts of metamorphic rocks within the study area. This suggests that variable contributions from these local bedrock sources control major mineralogy and that the tills have dominantly local sources. Many minor and some accessory minerals show similar patterns, suggesting that these may be controlled by similar factors. The accessory and trace minerals that are diagnostic of the Strange Lake deposits show more varied geographic patterns that are less easily connected to regional geology, although some are superficially similar to major mineral patterns. The most common pattern is one of rapid or steady decline in abundance with distance from Strange Lake, which fits with general expectations for indicator minerals. Other indicator minerals show less abundance variation with distance from the Strange Lake source, and some even seem to increase in abundance in the most distant parts of the study area. These two patterns conform to predictions for ‘normal glaciation’ and ‘ice-stream’ environments, respectively, but their presence in a single setting suggests that the glacial environment is only one of several controlling factors. The initial abundance of minerals in the source is an obvious control, but it is suspected that the mode of occurrence of indicator minerals and their mineral associations in composite particles also play important roles. The most persistent indicator mineral, gittinsite, shows a strong association with quartz, which is one of the hardest and most persistent common silicates, whereas other indicator minerals have more diverse mineral associations. The physical properties of indicator minerals may in the end be less important than those of the common silicates that they are associated with.

As always, major conclusions are accompanied by some lesser findings that are interesting in their own right. Two rare Ba-bearing minerals identified by MLA-SEM analysis were initially assigned false identities, but were later recognized tentatively as the slightly less rare Ba-Fe (Mn) Ti silicate mineral bafertisite. This is a possible indicator mineral for the Strange Lake deposits, as it is recorded there by earlier studies, but in amounts that cannot explain its abundance in till samples. This creates a contradiction, but there is a possible explanation if much bafertisite actually formed through hydrothermal processes in older metamorphic rocks adjacent to or originally above the Strange Lake

Intrusion. The rare Nb-Pb oxide mineral changbaiite may represent a new addition to the “Strange Lake exotic mineral club”, but more work is needed to confirm its identity.

RECOMMENDATIONS FOR RELATED RESEARCH

Several main recommendations for further research, which could assist in the wider application of MLA-SEM methods in geological and exploration programs, are listed below.

There is a need for more formal assessment of accuracy and precision for the method, with particular emphasis on evaluating natural variability in till samples, and uncertainties that may be introduced in sample preparation prior to analysis. This should include the collection of site duplicates during field work, and also the routine analysis of laboratory sample splits. These procedures were intended for this project, but the analysis of additional samples in the second phase of the project proved not to be possible. This work would give empirical information on the precision of analyses, especially at low abundances, and specific insights into the impact of ‘probability effects’. It could easily be undertaken using samples originally collected for this project. The latter could also be investigated experimentally by making artificial samples dominated by a common mineral (e.g., quartz) and ‘doping’ them with some unusual mineral at known abundances. It would be more difficult to investigate the impact of textural relationships where a rare mineral is included in particles of a more common mineral, but this is perhaps possible using computer simulations. In any event, a better understanding of these aspects would be useful in assessing variation patterns defined by rarer minerals, and also in comparing results from samples or groups of samples. Till samples originally collected as part of this project could probably be used to initiate such investigations.

The results of the research suggest that in this particular case, and perhaps in other situations, the mode of occurrence of indicator minerals and their ‘mineral associations’ represent important controls on their behaviour in the surficial environment, as well as affecting analytical integrity. Although the MLA-SEM method generates copious information on mineral associations at an individual sample level, it is very difficult and time-consuming to integrate and interpret this material. The same applies to information on grain and particle size distributions, although the total number of observations is far smaller in this case. The development of better software processing tools to integrate such data from a large number of samples would be a valuable step.

The variations in mineralogy determined by MLA-SEM analysis are just one aspect of the composition of samples, and the other aspect is provided by bulk geochemical analysis, The till geochemical data from the Midland Exploration program illuminate matters that cannot be determined from mineralogy, and vice-versa. The combination of the two methods is much more than their sum. It would have been extremely useful to have bulk geochemical analyses of the samples used for this project, and this should probably be standard procedure for future projects. The investigation of different size fractions would also be a useful procedure, for it is clear that indicator minerals are not distributed uniformly. In some cases it might be useful to selectively crush some coarser material to the right size range for MLA-SEM analysis. For projects in remote areas that require air support, the added cost of additional analyses is small compared to the costs of sample acquisition.

Finally, results from this project suggest that indicator minerals from Strange Lake remain detectable 35 km from the source, and the work of Currie (2019) shows that at least some composite quartz-gittinsite particles survived for an additional 65 km, at least. The Strange Lake area and Anaktalak Bay on the Labrador Coast are connected by a large and complex system of eskers that is clearly visible in satellite images and included in a recent compilation of such features across Canada (Storrer et al., 2013). It would be very interesting to analyze some samples spaced along this esker system to ascertain if gittinsite and other minerals from Strange Lake can be detected in the intervening area. In exploration for diamond deposits, regional sampling of esker systems has been used with considerable success, and the results from Labrador suggest that this might also be the case for Rare Earth Element deposits.

REFERENCES

Amhed, A, Cloutier, J., Walshe, J. L., 2012. ASD TerraSpec Workshop. Unpublished Report, CSIRO, Australia.

Amor, S., 2014. Geochemical quantification of the clastic component of Labrador lake sediments and its application to exploration. Newfoundland and Labrador Department of Natural Resources, Geological Survey, Open File LAB 1625.

Amor, S., McCurdy, M., and Garrett, R., 2019. Creation of an atlas of lake-sediment geochemistry for Labrador and northeastern Quebec. Geochemistry, Exploration, Environment, Analysis, v. 19, p. 369-393.

Baird, E. M., 2018. Mineralogy of the Main Zone, Strange Lake REE deposit as determined from SEM-MLA analysis. Unpublished B.Sc. Thesis, Memorial University of Newfoundland, St. John's, NL., 76 p.

Batterson, M. J., 1989. Quaternary geology and glacial dispersal in the Strange Lake area, Labrador. Newfoundland and Labrador Department of Natural Resources, Geological Survey, Report 89-3, 51 p.

Batterson, M. J., and Liverman, D., 2000. Contrasting styles of glacial dispersion in Newfoundland and Labrador: Methods and case studies. Newfoundland and Labrador Department of Natural Resources, Geological Survey, Report 2000-1, p. 1-31.

Batterson, M. J. and Taylor, D. D., 2009. Geochemical re-analysis of till samples from the Strange Lake area, Labrador (NTS map sheets 14D/5 and 24A/8). Newfoundland and Labrador Department of Natural Resources, Geological Survey, Open File LAB/1479, 116 p.

Bell, J. E., 1984. Mineralogy of till in a dispersal train derived from a peralkaline granite, Lac Brisson, Quebec-Newfoundland. Unpublished B.Sc. Thesis, Queen's University, Kingston, ON, 30 p.

Benn, D. I. and Evans, D. J. A., 2010. Glaciers and Glaciation. Second edition. Hodder Education, London.

Birkett, T. C., and Miller, R. R., 1991. Comment on "The role of hydrothermal processes in the granite-hosted Zr, Y, REE deposit at Strange Lake, Quebec/Labrador: Evidence from fluid inclusions" by S. Salvi and A. E. Williams-Jones. Geochimica et Cosmochimica Acta, v. 55, p. 3443-3445.

Birkett, T. C., Miller, R. R., Roberts, A. C., and Mariano, A. N., 1992. Zirconium-bearing minerals of the Strange Lake Intrusive Complex, Quebec-Labrador. Canadian Mineralogist, v. 30, p. 191-205.

Birkett, T. C., Trzcienski, W. E., and Stirling, J. A., 1996. Occurrence and compositions of some Ti-bearing minerals in the Strange Lake Intrusive complex, Quebec-Labrador boundary. Canadian Mineralogist, v. 34, p. 779-801.

Bourassa, S., and Banville, R., 2012. Third Year Assessment Report, Ytterby 1 Property, Licenses 19626M, 19981M, 20142M, 20143M, 20144M and 20145M, Labrador. Unpublished Report, Midland Exploration. Newfoundland and Labrador Department of Natural Resources, Geological Survey, File LAB 1699.

Bourassa, S., and Banville, R., 2013. Second Year Assessment Report, Ytterby 1 Property, Licenses 20841M and 20142M, NTS 14D/05, Labrador. Unpublished Report, Midland Exploration. Newfoundland and Labrador Department of Natural Resources, Geological Survey, File LAB 1719.

Corrigan, D., Wodicka, N., MacFarlane, C., LaFrance, I., van Rooyen, D., Bandyayera, D., and Bilodeau, C., 2018. Lithotectonic framework of the Core Zone, southeastern Churchill Province, Canada. Geoscience Canada, v. 45, p. 1-23.

CSIRO, 2015. The Spectral Geologist. Accessed: January 21, 2019. https://research.csiro.au/thespectralgeologist

Currie, K. L., 1985. An unusual peralkaline granite near Lac Brisson, Quebec-Labrador. Geological Survey of Canada Paper 85-1A, p. 73-80.

Currie, K. L., and Zaleski, E., 1985. The relative stability of elpidite and vlasovite: A P-T indicator for peralkaline rocks. Canadian Mineralogist, v. 23, p. 577-582.

Currie, V. C., 2019. Evaluation of hercynite and gittinsite as indicator minerals, Voisey's Bay area, Labrador. Unpublished B.Sc Thesis, Memorial University of Newfoundland, St. John's, NL, 60 p.

Daigle, P., Robinson, J., and Baughman, D., 2011. Strange Lake B-Zone: Resource model update. Consultant report by Wardrop and Associates for Quest Rare Minerals, 115 p. Available on Quest Rare Minerals Website or through www.sedar.com

Davis, J. C., 2003. Statistics and data analysis in geology, 3rd Edition. Wiley Interscience, 665 p.

Deer, W. A., Howie, R. A., and Zussman, J., 1992. An introduction to the rock-forming minerals, second edition. Longman Scientific and Technical Publishing, Harlow, UK, 696 pages.

Dominy, S. C., Johansen, G. F., and Annels, A. E., 2001. Bulk sampling as a tool for the grade evaluation of gold-quartz reefs. Transactions of the Institute of Mining and Metallurgy, Section B (Applied Earth Science), v. 100, p. B176-B191.

Dominy, S. C., Noppe, M. A., and Annels, A. E., 2002. Errors and uncertainty in mineral resource and ore reserve estimation: The importance of getting it right. Exploration and Mining Geology, v. 11, p. 77-98.

Dostal, J., 2016. Rare metal deposits associated with alkaline and peralkaline igneous rocks. Society of Economic Geologists, Reviews in Economic Geology, v. 18, p. 33-55.

Emslie, R. F., and Stirling, J. A. R., 1993. Rapakivi and related granitoids of the Nain Plutonic Suite; geochemistry, mineral assemblages and fluid equilibria. Canadian Mineralogist, v. 31, p. 821-847.

Emslie, R. F., Hamilton, W. A., and Theriault, R., 1994. Petrogenesis of a mid-Proterozoic anorthosite-mangerite-charnockite-granite (AMGC) complex: Isotopic and chemical evidence from the Nain Plutonic Suite. Journal of Geology, v. 102, p. 539-558.

Evans, D. J. A., Clark, C. D., and Rea, B. R., 2008. Landform and sediment imprints of fast glacial flow in the southwest Laurentide ice sheet. Journal of Quaternary Science, v. 23, p. 249–272.

FEI Company, 2007. Mineral Liberation Analyzer: Turning mineral analysis into profit. (accessed: February 5, 2019). http://www.microscop.ru/uploads/Oborudovanie/Analizatory/analizatory_materialov/C06FI68_1_MLA.pdf

FEI Company, 2011. MLA 650. (accessed: January 5, 2019) https://www.microscop.ru/uploads/Oborudovanie/Analizatory/analizatory_materialov/HR_DS_MLA650.pdf

Geological Survey of Canada, 1979. Regional lake sediment and water geochemical reconnaissance data, Labrador. Geological Survey of Canada, Open file 559.

Goldstein J. I., Newbury, D. E., Echlin, P., Joy, D. C., Romiger, A. D., Lyman, C. E., Fiori, C., and Lifshin, E., 1992. Scanning electron microscopy and X-Ray microanalysis. Plenum Press, New York.

Gowans, R. M., Lewis, W. J., Shoemaker, S., Spooner, J., and Zalnieriunas, R. V., 2014. Quest Rare Minerals Ltd. NI-43-101 Technical report on the preliminary economic assessment (PEA) for the Strange Lake Property, Quebec, Canada. Consultant Report by Micon International Limited, 244 p. Available from Quest Rare Minerals website or at www.sedar.com.

Gower, C. F., 1996. The evolution of the Grenville Province in eastern Labrador, Canada. Geological Society Special Publication 112, p. 197-218.

Grenier, A., Connell-Madore, S., McClenaghan, M. B., Wygergangs, M., and Moore, C. S., 2015. Study of cleaning methods for electro-welded sieves to reduce/eliminate carry over contamination between till samples. Geological Survey of Canada, Open File 7769.

Gu, Y., 2003. Automated scanning electron microscope based mineral liberation analysis. Journal of Minerals and Materials Characterization and Engineering, v. 2, p. 33-41.

Gysi, A. P., William-Jones, A. E., and Collins, P., 2016. Lithogeochemical vectors for hydrothermal processes in the Strange Lake peralkaline granite REE-Zr-Nb deposit. Economic Geology, v. 111, p. 1241-1276.

Haldar, S.K., 2013. Mineral exploration: principles and applications. Elsevier, 378 p.

Harris, J. R., Wickert, L., Lynds, T. Behnia, P., Rainbird, R., Grunsky, E., McGregor, R., and Schetselaar, E., 2011. Optical remote sensing: A review for remote predictive mapping in northern Canada. Geoscience Canada, v. 38, p. 49-83.

Hauff, P. L., 2008. An overview of VIS-NIR-SWIR field spectroscopy as applied to metals exploration. Spectral International Incorporated, technical report to accompany spectral libraries and indentification software, ASD Terraspec Reference Material, 71 p.

Hlava, M., and Krishnan, T.K., 1980. A report on the geological, geophysical and geochemical assessment work, Licenses 1368-1370 and 12128-12131, Strange Lake area, Newfoundland-Labrador, N.T.S. Sheet 24A/8. Unpublished report, Iron Ore Company of Canada. Newfoundland and Labrador Department of Natural Resources, Geological Survey File 024A/08/7.

Holtstam, D., Norrestam, R., and Andersson, U. B., 2003. Perclevite (Ce) – a new lanthanide disilicate from Bastmas, Skinnskattebarg, Sweden. European Journal of Mineralogy, v. 15, p. 725-731.

Hunt, J. A., and Berry, R. F., 2017. Geological contributions to geometallurgy: A review. Geoscience Canada, v. 44, p. 103-119.

Iron Ore Company of Canada (IOC), 1985. Preliminary feasibility study and related documents, Strange Lake Project. Unpublished Report, Iron Ore Company of Canada. Newfoundland and Labrador Department of Natural Resources, Geological Survey File 024A/08/0029.,

Iron Ore Company of Canada (IOC), 1986: Reports on metallurgical studies, and related documents, Strange Lake Project. Unpublished Report, Iron Ore Company of Canada. Newfoundland and Labrador Department of Natural Resources, Geological Survey File 024A/08/0028.

Jambor, J. L., Roberts, A. C., Grice, J. D., Birkett, T. C., Groat, L. A., and Zajac, S., 1998. Gerenite-(Y), $(Ca,Na)_2(Y,REE)_3Si_6O_{18}\cdot 2H_2O$, A new mineral species, and an associated Y-bearing gadolinite-group mineral, from the Strange Lake Peralkaline Complex, Quebec-Labrador. Canadian Mineralogist, v. 36, p. 793-800.

Kelley, D., Kelley, K., Coker, W., Caughlin, B., and Doherty, M., 2006. Beyond the obvious limits of ore deposits: The use of mineralogical, geochemical, and biological features for the remote detection of mineralization. Economic Geology, v. 101, p. 729-752.

Kerr, A., 2011. Rare-Earth Elements (REE) in Labrador: A review of known environments and the geological context of current exploration activity. Newfoundland and Labrador Department of Natural Resources, Geological Survey, Report 13-1, p. 109-145.

Kerr, A., 2013. Rare-Earth-Element (REE) behaviour in the Strange Lake Intrusion, Labrador: Resource estimation using predictive methods. Newfoundland and Labrador Department of Natural Resources, Geological Survey, Report 13-1, p. 117-136.

Kerr, A., 2015. Sm-Nd isotopic geochemistry of Rare-Earth-Element (REE) mineralization and associated peralkaline granites of the Strange Lake Intrusion, Labrador. Newfoundland and Labrador Department of Natural Resources, Geological Survey Branch, Report 12-1, p. 63-83.

Kerr, A., and Rafuse, H., 2010. The Strange Lake Zr-Y-Nb-Be-REE deposit, Labrador: A summary of geology, exploration and development proposals. Newfoundland and Labrador Department of Natural Resources, unpublished internal report.

Kerr, A., and Rafuse, H., 2012. Rare-Earth Element (REE) geochemistry of the Strange Lake deposits: Implications for resource estimation and metallogenic models. Newfoundland and Labrador Department of Natural Resources, Geological Survey, Report 12-1, p. 39-60.

Kerr, A., and Hamilton. M., 2014. Rare-Earth Element (REE) Mineralization in the Mistastin Lake and Smallwood Reservoir areas, Labrador: field relationships and preliminary U-Pb zircon ages from host granitoid rocks. Newfoundland and Labrador Department of Natural Resources, Geological Survey, Report 14-1, p. 45-62.

Kerr, A., Ryan, A. B., Gower, C. F., and Wardle, R. J., 1996. The Makkovik Province: Extension of the Ketilidian Mobile Belt in mainland North America. Geological Society Special Publication 112, p. 155-177.

Kerr, A., Rafuse, A., Sparkes, G., Hinchey, J., and Sandeman, H., 2011. Visible/Infrared Spectroscopy (VIRS) as a research tool in economic geology: Background and pilot studies from Newfoundland and Labrador. Newfoundland and Labrador Department of Natural Resources, Geological Survey, Report 11-1, p. 145-166.

Laurs, B. M., Rohtert, W. R., and Gray, M., 1997. Benitoite from the New Idria district, San Benito county, California. Gems and Gemology, v. 33, p. 166-188.

Layton-Matthews, D., Hamilton, C., and McClenaghan, M. B., 2014. Mineral chemistry: modern techniques and applications to exploration. Geological Survey of Canada, 26th International Applied Geochemistry Symposium, Short Course SC07, p. 9-18.

Lougheed, H. D., McClenaghan, M. B., Layton-Matthews, D., Leybourne, M. I., 2019. Evaluation of single-use nylon-screened sieves for use with fine-grained sediment samples. Geological Survey of Canada, Open File 8613.

Margold, M., Stokes, C. R., and Clark, C. D., 2015. Ice Streams in the Laurentide Ice Sheet: Identification, characteristics and comparison to modern ice sheets. Earth Science Reviews, v. 143, p. 117-146.

Mateo, S., 2010. MLA v.3.0. Regional Training Manual. Unpublished Report, FEI Ltd.

McClenaghan, M. B., Thorleifson, L. S., Dilabio, R. N. W., 2000. Till geochemical and indicator mineral methods in mineral exploration. Ore Geology Reviews, v. 16, p. 145-166.

McClenaghan, M. B. and Paulen, R., 2017. Application of till mineralogy and geochemistry to mineral exploration. In: Menzies, J., van der Meer, J.J.M. (eds), Past Glacial Environments, 2nd Edition, p. 685-791. Elsevier.

McClenaghan, M. B., Paulen, R. C., Kjarsgaard, I. M., and Fortin, R., 2017. Rare earth element indicator minerals: an example from the Strange Lake deposit, Quebec and Labrador, eastern Canada. Geological Survey of Canada, Open File 8345.

McClenaghan, M. B., Paulen, R. C., and Kjarsgaard, I. M., 2019. Rare metal indicator minerals in bedrock and till at the Strange Lake peralkaline complex, Quebec and Labrador, Canada. Canadian Journal of Earth Sciences, v. 56, p. 857-869.

McConnell, J. W., and Batterson, M. J., 1987. The Strange Lake Zr-Y-Nb-Be-REE deposit, Labrador: a geochemical profile in till, lake and stream sediment, and water. Journal of Geochemical Exploration, v. 29, p. 105-127.

Miller, R. R., 1986. Geology of the Strange Lake Alkalic Complex and the associated Zr-Y-Nb-Be-REE mineralization. Newfoundland Department of Mines and Energy, Mineral Development Division, Report 86-1, p. 11-19.

Miller, R.R., 1990. The Strange Lake pegmatite-aplite-hosted rare metal deposit, Labrador Newfoundland Department of Mines and Energy, Mineral Development Division, Report 90-1, p. 171-182.

Miller, R. R., 1996. Structural and textural evolution of the Strange Lake peralkaline rare-element granitic pegmatite, Quebec-Labrador. Canadian Mineralogist, v. 34, p. 349-371.

Miller, R. R., Heaman, L. M., and Birkett, T. C., 1997: U-Pb zircon age of the Strange Lake peralkaline complex: implications for Mesoproterozoic peralkaline magmatism in north-central Labrador. Precambrian Research, v. 81, p. 67-82.

Pietersen, K. Phan, V. H., Chen, W., Lam, A., Donaldson A., Lasker, R., 2009. Dataview 2009 Beta 2: Release notes for Build 2. Unpublished Report and Software Manual. JKTech Ltd.

Paulen, R. C., Stokes, C. R., Fortin, R., Rice, J. M., Dubé-Loubert, H., and McClenaghan, M. B., 2017. Dispersal trains produced by ice streams: An Example from Strange Lake, Labrador, Canada, In: Exploration 17 - Proceedings of the Sixth Decennial International Conference on Mineral Exploration, Toronto, Canada, p. 871-875.

Rafuse, H., and Kerr, A., 2009. Rare metals. Newfoundland and Labrador Department of Natural Resources, Geological Survey, Commodity Series, Report 7.

Reed, S. J. B., 2005. Electron microprobe analysis and scanning electron microscopy in geology. Cambridge University Press.

Richardson, D. G. and Birkett, T. C., 1995. Peralkaline rock-associated rare metals. In: Eckstrand, O. R., Sinclair, W. D., and Thorpe, R. I. (eds) Geology of Canadian Mineral Deposit Types. Geological Survey of Canada, Geology of Canada, No. 8., p. 523–540.

Rowan, L. C., Kingston, M. J., and Crowley, J. K., 1986. Spectral reflectance of carbonatites and related alkalic igneous rocks: Selected samples from four North American localities. Economic Geology, v. 81, p. 857-871.

Ryan, A. B., 1998. The Mesoproterozoic Nain Plutonic Suite in eastern Canada, and the setting of the Voisey's Bay Ni-Cu-Co deposit. Geoscience Canada, v. 24, p. 173-188.

Ryan, A. B., Lee, D., and Dunphy, D., 2003. Geology of the unnamed map sheet (NTS 14D/5) and the eastern part of the Lac Dihourse map sheet (24A/08), Labrador. Newfoundland and Labrador Department of Natural Resources, Geological Survey, Map 2003-09. Open File LAB 1376.

Salvi, S., and Williams-Jones, A. E., 1990. The Role of Hydrothermal Processes in the Granite-hosted Zr, Y, REE deposit at Strange Lake, Quebec/Labrador. Geochimica et Cosmochimica Acta, v. 54, p. 2403-2418.

Salvi, S., and Williams-Jones, A. E., 1992. Reduced orthomagmatic C-O-H-N-NaCl fluids in the Strange Lake rare-metal granitic complex, Quebec/Labrador, Canada. European Journal of Mineralogy, v. 4, p. 1155-1174.

Schluter, J., Malcherek, T., and Husdal, T., 2009. The new mineral Stetindite, CeSiO4, a cerium end-member of the zircon group. Neues Jahrbuch fur Mineralogie, v. 186, p. 195-200.

Scott, D. S., 2014. Geochemistry in Mineral Deposits. In: Holland, H. D., and Turekian, K. K. (eds), Treatise on Geochemistry, 2nd Edition, v. 1, Chapter 16. Elsevier.

Simmonds, S. J., 2009. The nugget effect in describing the variability of an ore deposit. Unpublished M.Sc. Thesis, Rhodes University, Grahamstown, South Africa, 104 p.

Sokolova, E., Hawthorne, F. C., Camara, F., and Back, M. E., 2018. The Ericssonite group of Fe^{3+} disilicate minerals. Canadian Mineralogist, v. 56, p. 95-99.

Stokes, C. R. and Clark, C. D., 2001. Palaeo-ice streams. Quaternary Science Reviews, v. 20, p. 1437-1457.

Stokes, C. R., Margold, M., Clark, C. D., and Tarasov, L., 2016. Ice stream activity scaled to ice sheet volume during Laurentide ice sheet deglaciation. Nature, v. 530, p. 322-326.

Storrer, R. D., Stokes, C. R., and Evans, D. J., 2013. A map of large Canadian eskers from Landsat satellite imagery. Journal of Maps, v. 9, p. 456-473.

Sugden, D. E., and John, B. E., 1976. Glaciers and landscape: A geomorphological approach. Edward Arnold, 376 p.

Swapp, Susan, 2017. Scanning Electron Microscopy (SEM). (accessed: February 18, 2019). https://serc.carleton.edu/research_education/geochemsheets/techniques/SEM.html

Swinden, H. S., Wardle, R, J., Davenport, P. H., Gower, C. F., Kerr, A., Meyer, J. R., Miller, R. R., Nolan, L., Ryan, A. B., and Wilton, D. H., 1991. Mineral exploration opportunities in Labrador: A perspective for the 1990s. Newfoundland Department of Mines and Energy, Mineral Development Division, Report 91-1, p. 349-390.

Sylvester, P. J., 2012. Use of the Mineral Liberation Analyzer (MLA) for mineralogical studies of sediments and sedimentary rocks. In: Sylvester, P.J. (ed.) Quantitative Mineralogy and Microanalysis of Sediments and Sedimentary Rocks. Mineralogical Association of Canada, Short Course Series, v. 42, p. 1-16.

Turner, D. J., Rivard, B., and Groat, L. A., 2015a Visible and short-wave infrared relectance spectroscopy of REE fluorocarbonates. American Mineralogist, v. 99, p. 1335-1346.

Turner, C., Rivard, B., and Groat, L., 2015b. Visible to short-wave infrared reflectance spectroscopy of Rare Earth Element minerals. In: Simandl, G. J. and Neetz, M., (eds.), Symposium on Strategic and Critical Materials Proceedings, November 13-14, 2015, Victoria, British Columbia. British Columbia Ministry of Energy and Mines, British Columbia Geological Survey Report 2015-3, p. 219-229.

Turner, D. J., Rivard, B., and Groat, L. A., 2018. Visible and short-wave infrared reflectance spectroscopy of selected REE-bearing silicate minerals. American Mineralogist, v. 103, p. 927-943.

Vasyukova, O., and Williams-Jones, A. E., 2014. Fluoridesilicate melt Immiscibility and its role in REE ore formation: Evidence from the Strange Lake rare metal deposit, Quebec–Labrador, Canada. Geochimica et Cosmochimica Acta. v. 139, p. 110–130.

Venkatswaran, G. P., 1983. A report of the geological, geophysical and geochemical assessment work, Licences 1368-1370 and 12128-12131, Strange Lake area, Newfoundland-Labrador, NTS Sheet 24A/8. Unpublished report, Iron Ore Company of Canada. Newfoundland and Labrador Department of Natural Resources, Geological Survey File 024A/08 (7).

Verplanck, P., and Hitzman, M. W., 2016. Rare Earth and critical elements in ore deposits. Society of Economic Geologists, Reviews in Economic Geology, v. 18, p. 1-5.

Vrana, S., Reider, M., and Gunter, M. E., 1992. Hejtmanite, a Mn-dominant analogue of bafertisite: a new mineral. European Journal of Mineralogy, v. 4, p. 35-43.

Wardle, R. J., Gower, C. F., Ryan, A. B., Nunn, G. A. G., James, D. T. and Kerr, A., 1997. Geological map of Labrador, 1:1 million scale. Newfoundland and Labrador Department of Mines and Energy, Geological Survey, Map 97-07.

Wilton, D. H. C., 1996. A metallogenic overview of the Nain Province, northern Labrador. Canadian Institute of Mining and Metallurgy Bulletin, v. 89, Issue 997.

Wilton, D. H. C., 2016. A potential regional mineral exploration tool for Labrador: Correlating mineralogical and geochemical signatures of indicator minerals of the Strange Lake REE deposits with remote spectral data. Unpublished application to Newfoundland and Labrador Research Development Corporation, 17 p.

Wilton, D. H. C. and Winter, L. S., 2012. SEM-MLA (Scanning Electron Microprobe – Mineral Liberation Analyser) research on indicator minerals in glacial till and stream sediments – An example from the exploration for awaruite in Newfoundland and Labrador. In: Sylvester, P.J. (ed.) Quantitative Mineralogy and Microanalysis of Sediments and Sedimentary Rocks. Mineralogical Association of Canada, Short Course Series 42, p. 265-283.

Wilton, D. H. C., Thompson, G., M., Grant, D., C., 2017. The Use of automated indicator mineral analysis in the search for mineralization – A next generation drift prospecting tool. Explore, v. 174, 2-28.

Xu, J., and Shen, G., 2005. Acta Mineralogical Sinica, v. 25, 213-216 (Chinese, with English Abstract).

Zajac, I.S., 2015. John Jambor's contributions to the mineralogy of the Strange Lake Peralkaline Complex, Quebec–Labrador, Canada. Canadian Mineralogist, v. 53, p. 885-894.

Zajac, I. S., Miller, R., Birkett, T., & Nantel, S., 1984. The Strange Lake deposit, Quebec–Labrador. Transcript of paper presented at Canadian Institute of Mining and Metallurgy, Annual Meeting, Ottawa.

APPENDIX A
MLA-SEM DATA

This Appendix to the Thesis Document contains a tabular listing of the Mineral Liberation Analyzer – Scanning Electron Microscope (MLA-SEM) data for the till samples from the Strange Lake area. The data are provided in column format for each sample, as this is the easiest arrangement that allows all to be listed in a fashion that is easily read.

Location data (latitude, longitude and other geographic information) for all samples are listed in the text of the thesis in Table 4.1. The Mineralogical data are reported in area % for major and minor minerals (mean abundance > 0.1%) and in area ppm for all accessory and trace minerals. For reference, 1% = 10,000 ppm.

The data are also provided in digital format, suitable for processing and import, in Microsoft Excel (*.xls; readable by all versions of the software). The digital data consists of two separate files, as follows:

Miller_2021_MSC_MLASEM_Data.xls: Contains all information from the printed table in this Appendix.

Miller_2021_MSC_Locations.xls: Contains all information listed in Table 4.1

Appendix A1. Tabular listing of MLA-SEM data for all samples

Sample	UNIT	G1-1	G1-2	G1-3	G1-4	G1-5	G1-6	G1-7	G1-8	G1-9	G1-10
	(area)										
Quartz	%	12.937	17.054	45.196	39.869	23.905	18.309	13.865	16.524	47.528	24.000
Albite	%	24.507	19.505	22.666	23.929	16.578	19.373	18.052	25.357	19.831	24.012
K-Feldspar	%	10.359	13.514	19.038	19.357	10.782	11.007	9.301	13.297	16.733	14.001
Hornblende	%	28.277	20.281	3.151	5.309	24.143	24.464	26.648	20.835	3.111	14.844
Garnet	%	13.529	20.941	1.050	0.887	13.346	19.770	21.692	15.336	1.377	13.968
Ilmenite	%	3.520	2.842	0.134	0.321	2.884	2.194	3.693	2.396	0.145	2.709
Plagioclase	%	2.730	1.466	4.274	4.325	3.101	1.063	1.315	1.496	6.119	1.774
Biotite	%	0.194	0.240	0.971	1.902	0.407	0.102	0.145	0.241	1.572	0.509
Chlorite	%	0.031	0.020	0.367	0.376	0.261	0.015	0.014	0.008	0.930	0.033
Epidote	%	0.010	0.015	0.621	0.924	0.307	0.003	0.001	0.011	0.452	0.138
Grunerite	%	1.213	0.717	0.275	0.513	1.163	0.907	1.417	0.721	0.342	0.447
Nepheline	%	0.132	0.099	0.662	0.517	0.120	0.067	0.063	0.122	0.783	0.185
Zircon	%	0.839	0.778	0.235	0.511	0.667	0.972	1.228	1.088	0.204	1.093
Augite	%	0.002	0.006	0.077	0.066	0.033	0.001	0.000	0.002	0.046	0.031
Aegirine	%	0.168	0.470	0.319	0.400	0.110	0.190	0.214	0.299	0.124	0.338
Limonite	%	0.734	0.284	0.037	0.056	0.807	0.384	0.928	0.345	0.023	0.357
Magnetite	%	0.371	0.122	0.145	0.127	0.190	0.174	0.305	0.175	0.048	0.251
Hypersthene	%	0.001	0.000	0.254	0.054	0.001	0.000	0.001	0.000	0.079	0.008
Titanite	%	0.007	0.014	0.166	0.212	0.039	0.010	0.006	0.017	0.170	0.075
Apatite	%	0.009	0.303	0.088	0.059	0.465	0.529	0.191	0.333	0.045	0.141
Staurolite	ppm	55.3	83.0	639.2	65.1	16.4	9.1	707.5	408.5	315.8	17.4
Zoisite	ppm	13.3	0.5	212.3	51.8	243.2	42.9	5.0	10.6	154.9	22.6
Goethite	ppm	193.0	384.1	343.6	194.3	403.5	189.8	439.7	343.5	39.0	140.8
Al Silicate	ppm	24.9	72.0	210.5	446.2	864.4	45.7	32.1	137.4	70.6	54.1
Rutile	ppm	62.7	0.5	157.2	477.7	11.0	34.8	0.4	0.0	57.5	124.5
Gittinsite	ppm	4.4	41.4	13.5	24.1	26.4	24.5	22.7	13.6	696.8	36.5
Allanite	ppm	81.2	124.9	140.8	22.9	480.9	186.8	63.7	146.4	179.3	118.4
Aenigmatite	ppm	412.4	710.4	94.5	162.9	343.2	337.2	298.7	328.0	24.7	248.4
Gerenite	ppm	327.0	347.6	88.4	96.1	157.1	346.7	261.7	345.1	159.1	523.1
"Ericssonite"	ppm	444.0	306.8	48.1	154.8	233.4	189.9	159.4	126.2	7.7	157.3
Serpentine	ppm	0.0	0.0	2.4	0.0	0.0	0.0	0.0	0.0	0.0	3.5
Monazite	ppm	0.0	0.0	4.4	164.7	1.2	0.0	0.0	0.0	130.1	0.0
Calcite	ppm	13.6	75.7	36.7	20.1	10.1	33.8	16.7	32.2	3.1	5.3
Wollastonite	ppm	132.6	39.3	37.7	0.0	13.6	32.1	9.5	10.3	58.5	7.5
Perclevite	ppm	3.2	26.1	20.7	42.9	0.0	6.8	13.7	14.6	12.3	0.7
Elpidite	ppm	28.1	43.1	36.4	67.5	11.7	13.1	7.5	0.0	46.3	0.0
Astrophyllite	ppm	19.6	157.0	43.4	37.5	36.2	32.3	68.6	10.5	5.1	7.0
Thorite	ppm	0.0	29.0	0.0	0.0	4.6	10.9	8.3	7.3	4.4	192.9
Parisite	ppm	0.0	81.1	0.0	1.6	82.6	0.0	1.9	178.8	0.0	66.4
Britholite	ppm	13.7	102.5	13.9	10.2	41.8	153.8	27.2	82.9	32.4	55.0
"Benitoite"	ppm	0.0	9.1	0.0	7.6	0.7	10.3	0.0	0.0	1.2	9.9
Pyrite	ppm	0.0	0.8	0.0	0.0	13.5	1.8	0.0	0.0	0.0	0.0
Barite	ppm	0.0	2.0	5.5	0.0	12.6	0.0	0.0	0.0	0.6	0.0
Gadolinite	ppm	0.0	0.0	3.0	0.0	0.0	0.0	0.0	0.0	65.4	0.0
Bastnaesite	ppm	0.0	0.0	1.5	10.2	20.3	26.4	0.0	0.0	11.2	3.5
Uraninite	ppm	7.7	3.7	0.0	5.7	0.0	0.0	4.4	58.2	11.0	0.7
Rhodonite	ppm	0.0	0.0	0.0	12.5	49.8	14.1	127.4	51.3	0.0	0.0
Scheelite	ppm	0.0	0.0	0.0	0.0	0.0	0.0	0.0	0.0	0.0	0.0
Stetindite	ppm	0.0	0.0	3.4	4.7	13.4	0.6	0.0	0.0	2.5	0.0
Pyrochlore	ppm	0.0	0.0	2.4	38.9	0.0	0.0	0.0	0.0	34.5	0.0
Fergusonite	ppm	3.1	0.8	2.7	10.6	10.6	0.0	9.9	2.0	14.1	13.6
Euxenite	ppm	16.0	1.1	0.0	7.4	0.0	0.0	0.0	0.0	0.0	0.0
Pectolite	ppm	0.0	3.4	3.4	0.0	0.0	0.0	9.4	0.0	2.2	1.5
Fluorite	ppm	0.0	1.9	0.9	2.1	0.3	0.0	0.0	0.0	0.9	0.0
Changbaiite	ppm	0.0	0.0	2.5	9.3	0.0	0.0	0.0	0.0	26.1	0.0

Appendix A1. Tabular listing of MLA-SEM data for all samples (continued)

Sample	**UNIT**	**G1-11**	**G1-12**	**G1-13**	**G1-14**	**G1-15**	**G1-16**	**G1-17**	**G1-18**	**G1-19**	**G1-20**
	(area)										
Quartz	**%**	19.110	44.045	29.424	17.298	33.898	15.829	15.852	11.071	50.081	15.907
Albite	**%**	27.446	24.282	17.410	18.525	20.060	18.115	20.241	18.979	19.722	20.330
K-Feldspar	**%**	14.491	15.526	12.529	11.286	13.822	11.994	13.760	13.483	16.756	11.457
Hornblende	**%**	15.457	4.499	11.132	17.835	10.301	22.882	24.888	30.307	2.673	22.750
Garnet	**%**	15.143	1.098	22.478	27.726	12.819	23.368	17.158	17.643	0.510	19.143
Ilmenite	**%**	2.051	0.421	1.434	2.242	1.240	1.749	1.870	2.341	0.124	3.436
Plagioclase	**%**	2.431	5.308	1.860	0.679	3.945	2.178	2.684	1.489	6.626	2.078
Biotite	**%**	0.284	1.106	0.456	0.229	0.600	0.263	0.095	0.301	0.818	0.200
Chlorite	**%**	0.022	0.828	0.082	0.028	0.223	0.008	0.002	0.004	0.560	0.023
Epidote	**%**	0.047	0.825	0.281	0.032	0.356	0.004	0.010	0.041	0.557	0.046
Grunerite	**%**	0.745	0.118	0.473	0.479	0.500	1.009	1.221	1.362	0.237	0.935
Nepheline	**%**	0.211	0.652	0.341	0.145	0.316	0.011	0.074	0.095	0.505	0.129
Zircon	**%**	1.080	0.126	0.532	1.444	0.534	0.745	0.658	1.750	0.157	1.210
Augite	**%**	0.003	0.036	0.027	0.009	0.034	0.004	0.002	0.018	0.062	0.000
Aegirine	**%**	0.245	0.158	0.546	0.194	0.160	0.108	0.100	0.112	0.040	0.325
Limonite	**%**	0.414	0.007	0.137	0.216	0.183	0.693	0.198	0.088	0.022	0.506
Magnetite	**%**	0.195	0.165	0.126	0.139	0.194	0.078	0.255	0.280	0.070	0.426
Hypersthene	**%**	0.000	0.071	0.064	0.006	0.090	0.001	0.001	0.004	0.048	0.000
Titanite	**%**	0.033	0.210	0.039	0.022	0.120	0.050	0.002	0.032	0.111	0.010
Apatite	**%**	0.061	0.144	0.228	0.487	0.095	0.216	0.153	0.185	0.058	0.500
Staurolite	**ppm**	9.8	2109.2	85.2	411.5	134.8	15.0	18.4	4.2	99.5	17.6
Zoisite	**ppm**	30.3	176.8	98.5	3.0	208.4	25.3	7.5	6.0	245.9	10.2
Goethite	**ppm**	182.4	99.0	153.4	162.7	103.8	90.8	88.8	181.7	28.5	423.8
Al Silicate	**ppm**	2.8	323.0	0.0	233.7	274.1	201.6	4.3	25.2	59.9	268.9
Rutile	**ppm**	457.7	151.0	291.9	2.2	499.1	105.0	76.7	58.0	67.1	0.0
Gittinsite	**ppm**	0.9	7.9	1.8	16.9	48.6	37.1	0.5	49.9	406.0	34.0
Allanite	**ppm**	69.3	40.2	152.9	158.5	334.3	24.0	56.6	145.6	242.5	60.0
Aenigmatite	**ppm**	426.3	22.1	270.2	244.9	36.4	254.2	331.6	220.1	16.6	77.5
Gerenite	**ppm**	140.2	120.0	87.4	263.1	26.8	67.1	96.7	132.1	58.4	189.1
"Ericssonite"	**ppm**	458.9	43.0	56.4	129.9	6.6	59.2	48.3	276.9	4.7	66.4
Serpentine	**ppm**	0.0	2.4	124.5	0.0	0.0	0.0	0.0	0.0	55.9	0.0
Monazite	**ppm**	1.8	76.5	10.7	12.0	4.2	0.0	1.6	0.0	5.7	0.0
Calcite	**ppm**	0.0	10.8	2.0	156.0	1.8	11.7	3.8	6.9	12.1	10.1
Wollastonite	**ppm**	2.3	9.7	14.2	16.1	0.5	4.3	14.8	0.0	23.6	2.0
Perclevite	**ppm**	0.0	13.1	3.9	84.9	3.4	0.0	0.0	0.0	49.1	0.4
Elpidite	**ppm**	0.0	2.3	5.0	7.6	14.9	10.4	0.4	0.0	13.1	6.4
Astrophyllite	**ppm**	16.9	4.6	4.8	16.1	6.5	16.8	9.7	0.0	0.0	18.7
Thorite	**ppm**	0.0	0.2	0.0	27.4	0.0	0.6	0.7	23.1	10.5	4.6
Parisite	**ppm**	0.0	10.8	0.0	3.7	0.0	0.0	18.9	0.0	4.3	17.6
Britholite	**ppm**	5.2	26.7	7.5	55.9	4.2	0.0	0.0	0.0	0.6	6.6
"Benitoite"	**ppm**	0.0	0.0	10.2	0.0	0.0	0.0	0.0	0.0	114.7	0.0
Pyrite	**ppm**	0.0	0.0	7.7	0.9	33.3	3.7	1.6	0.0	0.0	0.4
Barite	**ppm**	8.6	0.3	0.0	0.0	1.6	0.0	0.5	5.1	0.0	8.2
Gadolinite	**ppm**	0.0	0.8	0.0	0.0	9.0	0.0	0.0	0.0	18.1	0.4
Bastnaesite	**ppm**	0.0	3.5	0.0	21.6	6.4	0.0	0.0	0.0	5.2	1.8
Uraninite	**ppm**	8.7	2.5	8.9	259.0	0.0	0.0	0.0	0.0	15.7	0.0
Rhodonite	**ppm**	3.3	0.0	0.0	0.0	0.0	0.0	0.0	0.0	0.0	0.0
Scheelite	**ppm**	0.0	0.0	0.0	354.1	0.0	0.0	0.0	0.0	0.0	0.0
Stetindite	**ppm**	0.0	5.7	0.0	0.0	0.0	0.0	0.0	0.0	0.8	0.0
Pyrochlore	**ppm**	0.0	0.0	0.0	0.0	0.0	0.0	5.7	0.0	0.4	0.0
Fergusonite	**ppm**	0.0	1.6	0.0	18.5	1.5	5.1	35.8	0.0	6.6	12.3
Euxenite	**ppm**	53.0	84.1	0.0	0.6	0.0	4.8	0.4	91.9	0.0	0.0
Pectolite	**ppm**	0.5	0.6	2.8	0.0	0.0	0.0	0.0	0.0	0.0	0.5
Fluorite	**ppm**	0.0	3.7	0.0	0.0	6.0	0.0	0.0	0.0	9.0	0.0
Changbaiite	**ppm**	0.0	0.0	0.0	0.0	0.0	0.0	2.4	0.0	10.8	0.0

Appendix A1. Tabular listing of MLA-SEM data for all samples (continued)

Sample	UNIT	G1-21	G1-22	G1-23	G1-24	G1-25	G1-26	G1-27	G1-28	G1-29	G1-30
	(area)										
Quartz	%	24.339	21.060	44.053	23.362	13.397	42.915	45.864	15.608	21.583	14.924
Albite	%	16.956	17.131	23.279	19.268	22.153	25.086	20.249	20.386	22.204	18.657
K-Feldspar	%	11.249	14.535	16.605	12.865	9.858	17.018	19.563	12.284	15.202	12.598
Hornblende	%	19.120	19.147	2.974	19.126	25.407	2.868	2.355	26.186	20.462	27.327
Garnet	%	19.441	17.952	0.953	17.686	21.119	1.149	0.681	15.141	13.733	18.847
Ilmenite	%	2.131	3.509	0.255	2.041	2.095	0.089	0.149	3.095	1.700	3.179
Plagioclase	%	2.699	2.106	6.954	2.625	2.451	4.753	6.867	2.477	2.312	0.732
Biotite	%	0.460	0.376	1.283	0.236	0.257	1.518	0.389	0.123	0.406	0.087
Chlorite	%	0.215	0.061	0.794	0.084	0.005	1.519	0.498	0.008	0.153	0.005
Epidote	%	0.087	0.060	0.799	0.179	0.016	0.840	0.344	0.005	0.189	0.005
Grunerite	%	0.734	0.848	0.236	0.779	0.650	0.112	0.966	1.283	0.249	0.964
Nepheline	%	0.248	0.138	0.619	0.169	0.036	0.883	0.519	0.063	0.249	0.072
Zircon	%	0.683	1.191	0.122	0.675	0.843	0.087	0.562	1.171	0.620	0.898
Augite	%	0.018	0.004	0.186	0.023	0.001	0.085	0.033	0.000	0.009	0.005
Aegirine	%	0.182	0.191	0.106	0.224	0.124	0.118	0.306	0.070	0.055	0.116
Limonite	%	0.443	0.304	0.102	0.142	0.606	0.060	0.022	0.775	0.110	0.274
Magnetite	%	0.120	0.365	0.130	0.193	0.182	0.036	0.060	0.292	0.106	0.316
Hypersthene	%	0.015	0.030	0.023	0.006	0.001	0.084	0.103	0.000	0.002	0.013
Titanite	%	0.091	0.028	0.220	0.012	0.020	0.215	0.123	0.034	0.119	0.038
Apatite	%	0.242	0.400	0.069	0.044	0.003	0.102	0.074	0.383	0.120	0.408
Staurolite	ppm	307.9	16.5	270.9	0.4	10.4	2303.4	27.4	9.9	102.9	16.0
Zoisite	ppm	0.0	23.2	192.0	18.9	19.8	511.4	213.5	9.1	11.3	100.5
Goethite	ppm	120.3	260.0	131.3	105.2	226.3	146.0	24.5	165.8	153.5	209.0
Al Silicate	ppm	447.0	460.3	401.1	31.4	32.0	219.4	375.1	5.3	32.9	19.0
Rutile	ppm	268.1	3.3	279.3	100.1	12.7	10.7	179.6	10.2	39.9	2.6
Gittinsite	ppm	306.9	41.4	173.2	22.6	16.8	78.7	620.7	0.0	1.2	30.1
Allanite	ppm	104.0	226.3	239.2	31.3	45.1	124.0	209.5	18.5	148.3	287.9
Aenigmatite	ppm	56.9	137.7	29.3	113.3	102.5	28.4	37.4	232.8	49.4	131.4
Gerenite	ppm	134.6	49.3	76.8	28.3	82.1	108.6	319.5	137.0	38.3	77.3
"Ericssonite"	ppm	77.9	5.2	11.9	81.5	25.2	12.9	7.9	147.4	61.6	14.1
Serpentine	ppm	0.0	0.0	0.0	0.0	0.0	0.0	0.0	0.0	0.0	0.0
Monazite	ppm	242.3	1.3	1.6	18.1	0.5	4.2	14.4	0.0	2.9	0.4
Calcite	ppm	45.2	10.7	4.8	9.2	16.3	61.3	191.5	0.0	65.7	14.3
Wollastonite	ppm	280.3	12.9	0.0	6.4	0.0	4.2	2.2	0.0	68.1	29.4
Perclevite	ppm	1.0	2.5	0.8	5.0	30.4	28.4	3.3	0.0	0.0	231.5
Elpidite	ppm	0.5	7.2	5.1	0.6	0.0	16.3	115.0	4.4	4.2	7.4
Astrophyllite	ppm	4.9	10.8	0.6	8.6	8.4	21.0	1.7	1.8	15.1	18.9
Thorite	ppm	12.1	3.2	0.0	0.0	1.3	3.9	2.7	3.2	3.9	11.2
Parisite	ppm	95.1	0.0	1.7	0.0	22.7	0.0	0.0	3.1	3.4	0.0
Britholite	ppm	24.3	4.7	2.3	0.0	0.0	22.2	0.0	7.7	7.7	30.5
"Benitoite"	ppm	0.0	3.7	0.0	0.0	0.0	0.0	0.0	0.0	6.3	4.6
Pyrite	ppm	4.3	0.0	2.0	0.0	2.1	5.5	0.0	0.0	2.9	0.0
Barite	ppm	4.1	22.2	2.2	1.1	2.9	0.0	0.0	0.0	92.2	35.2
Gadolinite	ppm	0.0	0.0	1.7	0.0	0.0	0.0	12.9	0.0	0.0	0.0
Bastnaesite	ppm	0.0	0.6	5.9	0.0	0.0	0.0	1.0	0.0	0.0	6.5
Uraninite	ppm	8.0	3.2	0.0	0.0	0.0	0.0	0.0	0.4	8.0	3.2
Rhodonite	ppm	0.0	0.0	0.0	0.0	129.5	0.0	0.0	0.0	0.0	0.0
Scheelite	ppm	0.0	0.0	0.0	0.0	0.0	0.0	0.0	0.0	0.0	0.7
Stetindite	ppm	0.0	4.0	0.0	0.0	0.0	0.0	9.6	0.0	0.0	0.0
Pyrochlore	ppm	0.0	0.0	2.7	0.0	0.0	0.0	4.1	0.0	0.0	0.0
Fergusonite	ppm	3.5	6.9	0.0	0.0	0.0	6.5	0.3	0.0	0.0	2.0
Euxenite	ppm	0.0	0.0	6.2	0.0	0.0	0.0	0.0	17.5	9.1	0.0
Pectolite	ppm	0.0	7.8	0.0	0.0	0.0	0.0	0.0	0.0	2.9	1.9
Fluorite	ppm	23.8	0.0	0.0	0.0	0.0	0.0	0.0	0.0	1.5	0.5
Changbaiite	ppm	5.5	0.0	0.0	0.0	0.0	0.0	1.2	0.0	0.0	0.0

Appendix A1. Tabular listing of MLA-SEM data for all samples (continued)

Sample	UNIT	G1-31	G1-32	G1-33	G1-34	G1-35	G1-36	G1-37	G1-38	G1-39	G1-40
	(area)										
Quartz	%	46.249	39.960	33.983	45.746	43.323	16.044	15.134	49.462	48.155	25.534
Albite	%	23.209	27.056	23.426	21.996	19.601	23.625	18.810	15.239	21.169	22.160
K-Feldspar	%	16.702	15.985	17.051	16.963	18.569	11.595	13.774	12.525	18.805	12.611
Hornblende	%	3.075	3.811	9.716	3.733	4.194	22.220	18.977	6.035	2.419	18.164
Garnet	%	0.766	1.334	7.778	2.057	1.012	19.230	26.348	2.718	0.519	13.527
Ilmenite	%	0.215	0.117	0.890	0.417	0.230	1.867	2.235	0.840	0.152	2.124
Plagioclase	%	5.947	5.143	3.478	4.628	5.953	2.314	1.425	6.429	5.145	2.250
Biotite	%	0.906	2.332	0.673	1.101	2.395	0.258	0.149	2.399	0.623	0.325
Chlorite	%	0.700	1.376	0.411	0.601	0.881	0.055	0.011	0.985	0.369	0.099
Epidote	%	0.531	0.835	0.320	0.865	0.937	0.057	0.018	0.628	0.399	0.102
Grunerite	%	0.113	0.069	0.429	0.209	0.433	0.859	0.542	0.364	0.303	0.656
Nepheline	%	0.699	1.063	0.584	0.533	1.080	0.282	0.107	0.674	0.546	0.259
Zircon	%	0.029	0.139	0.269	0.127	0.210	0.688	0.715	0.275	0.151	0.684
Augite	%	0.050	0.074	0.062	0.103	0.141	0.011	0.000	0.075	0.055	0.032
Aegirine	%	0.084	0.031	0.144	0.107	0.196	0.264	0.199	0.065	0.349	0.204
Limonite	%	0.039	0.102	0.198	0.016	0.024	0.245	0.296	0.058	0.026	0.322
Magnetite	%	0.124	0.041	0.056	0.165	0.266	0.075	0.175	0.583	0.220	0.231
Hypersthene	%	0.086	0.030	0.041	0.132	0.100	0.002	0.023	0.246	0.046	0.007
Titanite	%	0.181	0.227	0.041	0.201	0.121	0.021	0.043	0.070	0.188	0.044
Apatite	%	0.131	0.020	0.109	0.048	0.002	0.010	0.280	0.017	0.091	0.024
Staurolite	ppm	238.8	189.3	176.0	213.8	529.9	20.0	20.8	293.6	249.3	140.3
Zoisite	ppm	179.2	214.2	122.9	246.9	438.1	48.7	1.9	202.5	387.3	8.3
Goethite	ppm	103.0	27.8	22.1	110.5	143.9	147.1	525.9	421.8	167.1	198.9
Al Silicate	ppm	351.5	151.9	253.8	243.3	775.6	0.0	0.0	692.3	330.4	128.4
Rutile	ppm	65.3	444.9	32.9	440.0	621.5	47.1	1.5	57.7	29.2	125.2
Gittinsite	ppm	5.9	0.0	288.3	4.3	15.3	39.2	17.3	10.3	360.2	24.3
Allanite	ppm	34.9	106.6	196.5	29.5	50.4	87.5	130.9	21.7	177.9	144.1
Aenigmatite	ppm	27.1	3.7	39.0	44.0	60.9	156.2	229.0	82.8	11.9	65.7
Gerenite	ppm	34.0	263.0	54.6	39.8	24.5	45.2	91.2	34.8	61.5	336.2
"Ericssonite"	ppm	15.4	6.0	83.9	6.4	20.3	84.9	17.3	48.4	6.7	26.0
Serpentine	ppm	0.5	0.0	0.0	0.0	0.0	0.0	0.0	0.0	0.0	0.0
Monazite	ppm	29.6	0.0	38.5	2.1	3.4	2.7	0.0	251.8	107.6	0.0
Calcite	ppm	0.0	0.6	24.5	9.2	103.9	32.0	13.4	3.5	1.5	12.1
Wollastonite	ppm	32.3	4.4	10.9	1.3	19.2	14.2	0.0	8.0	173.3	4.1
Perclevite	ppm	77.2	108.1	264.9	33.2	0.0	0.0	0.4	4.4	30.8	2.5
Elpidite	ppm	1.8	43.1	281.0	100.7	7.1	1.3	0.0	0.9	27.2	0.0
Astrophyllite	ppm	0.9	0.0	6.2	0.0	2.7	23.8	9.5	4.8	0.8	9.2
Thorite	ppm	0.0	12.7	49.2	29.6	2.9	4.5	0.0	2.2	1.4	120.0
Parisite	ppm	0.0	2.4	27.5	19.4	72.2	0.0	0.0	0.0	0.0	177.8
Britholite	ppm	0.3	0.0	5.6	19.9	0.0	0.0	5.8	0.0	0.0	13.1
"Benitoite"	ppm	4.0	0.0	0.7	9.8	7.1	3.6	0.6	0.0	0.0	0.0
Pyrite	ppm	0.9	0.0	7.2	0.0	0.0	2.9	1.8	0.0	3.7	0.0
Barite	ppm	25.3	6.1	23.8	32.6	52.1	28.7	16.3	70.1	13.8	6.5
Gadolinite	ppm	0.0	0.0	1.1	1.1	0.0	0.0	0.0	0.0	127.8	0.0
Bastnaesite	ppm	7.5	0.0	4.5	1.5	0.0	0.0	55.0	0.0	28.5	0.0
Uraninite	ppm	0.0	0.0	0.0	0.0	0.0	0.0	0.0	0.0	0.0	0.0
Rhodonite	ppm	0.0	0.0	0.0	0.0	0.0	0.0	0.0	12.4	0.0	0.0
Scheelite	ppm	0.0	0.0	0.0	0.0	0.0	0.0	0.0	0.0	0.0	0.0
Stetindite	ppm	0.0	0.0	0.3	0.0	0.0	0.0	0.0	4.4	0.4	0.0
Pyrochlore	ppm	0.0	0.0	0.0	0.0	6.9	0.0	0.0	0.0	2.3	0.0
Fergusonite	ppm	0.0	0.7	0.4	0.6	0.0	0.0	3.0	1.1	0.0	63.6
Euxenite	ppm	0.0	0.0	0.7	0.0	0.0	0.0	0.0	0.0	0.0	9.5
Pectolite	ppm	3.0	7.8	11.4	0.0	0.0	11.2	0.0	4.1	0.0	0.0
Fluorite	ppm	0.6	2.6	0.0	0.6	0.0	0.0	0.0	0.0	0.0	0.0
Changbaiite	ppm	0.0	0.0	0.0	0.0	0.0	0.0	0.0	0.0	2.2	0.0

Appendix A1. Tabular listing of MLA-SEM data for all samples (continued)

Sample	UNIT (area)	G2-1	G2-2	G2-3	G2-4	G2-5	G2-6	G2-7	G2-8	G2-9	G2-10
Quartz	%	35.235	48.472	43.800	41.694	39.112	43.189	45.027	36.197	13.710	38.502
Albite	%	20.862	22.156	25.112	20.420	20.166	16.674	22.543	19.667	19.702	20.543
K-Feldspar	%	13.845	17.829	16.549	15.814	13.419	10.644	17.127	14.695	9.084	13.448
Hornblende	%	6.108	2.064	2.827	6.049	6.644	6.045	3.734	6.540	23.124	10.734
Garnet	%	2.332	0.650	0.764	1.120	2.247	4.028	0.531	3.752	29.511	7.667
Ilmenite	%	0.632	0.252	0.196	0.646	0.706	1.084	0.225	0.719	1.859	0.631
Plagioclase	%	11.016	5.112	6.555	7.689	9.619	9.086	6.968	9.942	0.737	4.483
Biotite	%	2.493	0.394	1.076	1.828	2.210	2.180	0.804	2.154	0.104	0.910
Chlorite	%	2.712	0.337	0.753	0.373	1.500	2.424	0.193	2.139	0.006	0.472
Epidote	%	1.047	0.614	0.691	1.351	1.288	0.668	0.829	1.024	0.008	0.446
Grunerite	%	0.427	0.402	0.092	0.272	0.421	0.441	0.179	0.571	0.423	0.326
Nepheline	%	0.940	0.537	0.709	1.044	0.661	0.521	0.601	0.754	0.135	0.347
Zircon	%	0.150	0.153	0.051	0.151	0.080	0.234	0.047	0.161	0.545	0.433
Augite	%	0.130	0.011	0.045	0.093	0.201	0.163	0.042	0.107	0.001	0.055
Aegirine	%	0.147	0.308	0.022	0.053	0.172	0.250	0.041	0.084	0.145	0.210
Limonite	%	0.062	0.032	0.017	0.041	0.039	0.731	0.062	0.198	0.247	0.095
Magnetite	%	0.934	0.134	0.103	0.652	0.539	0.069	0.206	0.399	0.073	0.134
Hypersthene	%	0.301	0.144	0.122	0.228	0.265	0.168	0.200	0.343	0.001	0.116
Titanite	%	0.137	0.120	0.214	0.122	0.166	0.319	0.253	0.105	0.051	0.091
Apatite	%	0.069	0.072	0.113	0.000	0.110	0.226	0.167	0.099	0.285	0.074
Staurolite	ppm	346.5	265.1	35.7	433.1	787.7	947.5	245.9	210.1	5.6	15.3
Zoisite	ppm	967.3	528.8	330.7	497.8	1124.7	1189.3	289.8	508.6	5.0	240.9
Goethite	ppm	308.6	64.3	161.1	307.0	283.6	19.0	221.6	387.3	249.6	287.0
Al Silicate	ppm	1087.1	284.4	224.7	716.0	216.9	721.7	432.3	437.7	19.0	29.7
Rutile	ppm	558.2	67.4	682.0	469.6	439.7	963.1	150.6	516.8	41.8	72.1
Gittinsite	ppm	76.8	156.1	0.0	24.3	178.1	885.0	40.8	142.5	9.4	228.2
Allanite	ppm	386.8	80.6	65.0	63.0	154.7	373.1	281.6	249.4	70.3	66.9
Aenigmatite	ppm	17.7	9.4	13.0	11.9	15.8	7.4	35.2	12.2	95.6	179.7
Gerenite	ppm	32.7	63.1	13.6	58.3	18.3	275.4	27.1	33.1	34.5	57.7
"Ericssonite"	ppm	15.5	23.8	2.9	104.3	15.7	53.2	52.0	41.2	76.3	84.6
Serpentine	ppm	0.0	0.0	1.1	180.9	8.0	0.0	40.0	264.0	0.0	17.1
Monazite	ppm	15.8	4.9	14.6	51.9	454.9	39.9	4.8	8.2	1.5	0.4
Calcite	ppm	1.2	18.0	9.0	9.2	3.3	13.5	5.4	16.2	11.5	20.1
Wollastonite	ppm	6.8	13.9	0.0	0.0	14.2	26.0	0.0	8.3	2.1	0.3
Perclevite	ppm	5.9	4.4	0.6	1.1	12.6	8.2	0.0	4.1	0.0	95.0
Elpidite	ppm	19.6	3.8	0.3	5.4	9.5	7.2	0.0	1.6	0.0	4.3
Astrophyllite	ppm	7.1	332.4	0.0	3.6	5.0	37.4	0.0	17.6	3.4	5.3
Thorite	ppm	0.4	0.0	2.3	0.0	4.6	7.0	0.0	111.3	0.0	6.3
Parisite	ppm	0.0	0.0	0.0	45.1	0.0	0.0	3.9	0.0	3.1	0.0
Britholite	ppm	0.0	0.0	1.3	0.0	22.4	4.2	0.0	0.0	30.2	0.0
"Benitoite"	ppm	0.6	3.0	3.0	0.0	1.7	24.3	3.3	6.8	17.7	0.0
Pyrite	ppm	5.2	12.1	47.4	0.0	0.6	4.9	0.0	7.9	4.6	2.0
Barite	ppm	19.2	8.7	13.9	0.0	7.2	80.2	0.8	8.9	26.0	2.4
Gadolinite	ppm	0.0	1.1	0.0	0.0	2.0	329.8	0.0	4.7	0.0	31.4
Bastnaesite	ppm	1.8	7.7	0.0	0.0	8.4	0.0	0.0	1.3	10.3	0.0
Uraninite	ppm	0.0	3.7	1.9	0.0	0.0	23.2	0.0	0.0	0.0	0.0
Rhodonite	ppm	0.0	0.0	0.0	0.0	1.6	0.0	0.0	10.8	3.7	1.3
Scheelite	ppm	24.8	0.0	0.0	0.0	0.0	0.0	0.0	0.0	0.0	0.0
Stetindite	ppm	0.8	6.7	0.0	0.0	44.4	8.6	0.0	4.2	0.0	0.0
Pyrochlore	ppm	6.0	4.9	0.0	0.0	0.0	2.1	0.0	0.6	0.0	29.7
Fergusonite	ppm	0.0	5.9	2.0	0.0	0.0	1.1	0.0	0.0	5.1	3.4
Euxenite	ppm	0.9	0.0	0.0	0.0	0.0	0.0	0.0	0.0	1.7	0.0
Pectolite	ppm	22.1	6.0	89.0	0.0	0.4	3.8	0.0	0.0	0.0	4.5
Fluorite	ppm	0.0	0.0	1.0	0.0	0.0	0.8	0.0	0.0	2.2	3.3
Changbaiite	ppm	0.0	0.0	0.0	0.0	0.0	0.0	0.0	0.0	0.0	2.1

Appendix A1. Tabular listing of MLA-SEM data for all samples (continued)

Sample	UNIT	G2-11	G2-12	G2-13	G2-14	G2-15	G2-16	G2-17	G2-18	G2-19
	(area)									
Quartz	%	51.543	49.023	15.701	50.080	41.477	16.353	35.590	45.910	49.038
Albite	%	22.032	21.546	22.411	20.554	25.548	20.048	26.095	24.379	27.226
K-Feldspar	%	15.821	17.259	10.776	17.647	13.488	13.316	15.639	16.442	17.105
Hornblende	%	2.254	2.140	29.960	2.145	2.559	25.311	4.647	3.119	1.315
Garnet	%	0.945	0.526	14.505	0.656	0.772	18.296	2.016	1.262	0.243
Ilmenite	%	0.118	0.354	2.269	0.191	0.248	2.604	0.824	0.585	0.044
Plagioclase	%	3.389	5.935	1.719	5.741	10.149	1.838	5.673	2.495	2.572
Biotite	%	1.246	0.350	0.084	0.477	1.149	0.097	1.368	0.927	0.261
Chlorite	%	0.777	0.270	0.017	0.252	0.710	0.002	3.375	1.337	0.382
Epidote	%	0.410	0.364	0.087	0.406	0.385	0.008	1.223	0.703	0.526
Grunerite	%	0.185	0.411	1.192	0.308	0.911	0.735	0.655	0.339	0.170
Nepheline	%	0.082	0.543	0.044	0.572	0.103	0.119	0.173	0.196	0.122
Zircon	%	0.012	0.152	0.552	0.086	0.030	0.690	0.098	0.124	0.074
Augite	%	0.432	0.079	0.037	0.054	0.707	0.003	0.752	0.786	0.302
Aegirine	%	0.182	0.161	0.097	0.176	0.093	0.106	0.276	0.328	0.085
Limonite	%	0.039	0.023	0.091	0.030	0.023	0.127	0.076	0.019	0.008
Magnetite	%	0.052	0.211	0.126	0.092	0.194	0.224	0.459	0.257	0.059
Hypersthene	%	0.089	0.235	0.003	0.215	0.687	0.002	0.374	0.212	0.057
Titanite	%	0.072	0.115	0.023	0.114	0.185	0.004	0.117	0.149	0.130
Apatite	%	0.075	0.084	0.000	0.039	0.192	0.002	0.060	0.033	0.093
Staurolite	ppm	651.7	19.1	3.1	96.4	469.1	3.4	972.5	1011.5	785.9
Zoisite	ppm	447.4	287.5	13.7	130.4	1279.4	0.7	999.5	650.6	299.9
Goethite	ppm	229.7	93.1	198.5	182.0	281.4	101.8	1065.4	617.9	160.1
Al Silicate	ppm	234.3	399.9	46.0	241.1	1208.3	3.0	634.2	1002.3	208.1
Rutile	ppm	94.3	10.3	4.0	105.0	211.6	0.0	99.7	15.7	51.6
Gittinsite	ppm	110.4	277.4	0.0	271.2	0.0	0.0	345.9	99.0	180.9
Allanite	ppm	227.9	64.4	6.9	78.0	98.7	34.5	260.3	7.3	34.2
Aenigmatite	ppm	64.9	10.3	244.5	113.4	3.6	127.2	14.9	16.3	9.6
Gerenite	ppm	1.6	36.1	0.0	16.0	0.0	33.0	7.8	100.8	3.4
"Ericssonite"	ppm	0.0	14.3	78.4	13.2	0.0	47.6	0.0	0.6	0.0
Serpentine	ppm	189.6	138.0	0.0	0.0	66.8	0.0	216.3	62.7	0.0
Monazite	ppm	4.0	3.9	0.0	99.9	0.0	0.0	277.2	151.9	0.8
Calcite	ppm	1.2	451.1	4.1	62.2	18.2	31.9	0.0	2.9	0.0
Wollastonite	ppm	13.4	11.0	6.9	11.8	39.7	16.5	3.8	0.0	26.8
Perclevite	ppm	19.5	37.9	21.7	31.7	0.0	0.0	2.5	4.5	0.8
Elpidite	ppm	1.3	1.3	20.1	5.7	21.0	0.6	15.6	1.2	3.6
Astrophyllite	ppm	0.0	1.9	65.6	13.2	0.0	0.0	0.0	0.0	65.8
Thorite	ppm	13.7	3.5	8.2	2.1	0.0	0.0	0.0	100.4	28.4
Parisite	ppm	0.0	0.0	0.0	0.0	0.0	21.7	0.0	0.0	0.0
Britholite	ppm	0.0	4.1	0.0	0.0	0.0	0.0	1.0	0.0	0.0
"Benitoite"	ppm	0.0	0.4	0.0	0.0	0.0	0.0	0.0	0.0	0.0
Pyrite	ppm	22.0	75.3	13.0	17.5	84.1	0.7	93.4	5.1	2.0
Barite	ppm	0.7	6.2	5.2	2.9	1.8	2.9	0.0	1.8	3.2
Gadolinite	ppm	0.6	24.7	0.0	0.4	0.0	0.0	0.0	0.6	0.8
Bastnaesite	ppm	2.5	7.0	0.0	0.0	0.0	0.0	0.0	4.5	0.0
Uraninite	ppm	0.0	2.1	0.0	0.0	0.0	0.0	0.0	0.0	0.0
Rhodonite	ppm	0.0	2.5	0.0	0.0	0.7	0.0	0.0	0.8	0.0
Scheelite	ppm	0.0	0.0	0.0	0.0	0.0	0.0	0.0	0.0	0.0
Stetindite	ppm	1.2	0.4	0.0	21.5	0.0	0.0	2.3	5.5	0.0
Pyrochlore	ppm	0.7	2.1	0.8	0.3	0.0	0.0	0.0	26.7	0.0
Fergusonite	ppm	0.0	0.0	8.7	0.0	30.3	0.8	0.0	0.8	0.0
Euxenite	ppm	0.0	0.0	0.0	0.0	0.0	2.7	0.0	0.0	0.0
Pectolite	ppm	0.0	1.0	6.6	1.3	0.0	0.0	0.0	0.0	0.0
Fluorite	ppm	0.6	0.0	2.6	0.0	0.0	8.1	0.0	0.0	0.0
Changbaiite	ppm	0.0	4.0	0.0	0.0	0.0	0.0	0.0	0.0	0.0

Appendix A1. Tabular listing of MLA-SEM data for all samples (continued)

Sample	UNIT	G3-2	G3-3	G3-4	G3-5	G3-6	G3-7	G3-8	G3-9	G3-10	G3-11
	(area)										
Quartz	%	50.575	44.081	46.706	34.041	47.558	42.120	51.073	45.867	49.113	48.884
Albite	%	24.974	29.006	23.171	25.175	25.181	24.411	24.309	28.790	23.992	24.799
K-Feldspar	%	16.610	16.213	16.500	12.955	16.499	16.216	17.048	16.496	14.205	14.634
Hornblende	%	1.518	2.915	2.735	4.308	2.140	2.987	1.525	2.540	2.114	2.217
Garnet	%	0.396	0.754	1.026	2.446	1.068	1.204	0.272	0.544	0.626	0.965
Ilmenite	%	0.290	0.279	0.396	1.499	0.274	0.295	0.156	0.138	0.152	0.307
Plagioclase	%	2.668	1.939	4.442	6.201	3.238	5.674	2.847	2.091	4.846	3.810
Biotite	%	0.196	0.994	0.365	1.334	0.548	0.844	0.236	0.396	0.537	0.544
Chlorite	%	0.407	0.619	0.887	4.078	0.668	1.942	0.394	0.609	1.071	0.648
Epidote	%	0.447	1.019	0.470	1.236	0.425	0.558	0.426	0.646	0.590	0.546
Grunerite	%	0.144	0.193	0.668	0.781	0.253	0.487	0.247	0.103	0.345	0.279
Nepheline	%	0.094	0.131	0.131	0.234	0.102	0.196	0.129	0.187	0.204	0.204
Zircon	%	0.130	0.045	0.081	0.186	0.063	0.098	0.110	0.048	0.127	0.049
Augite	%	0.474	0.690	0.813	1.306	0.614	0.852	0.230	0.633	0.500	0.618
Aegirine	%	0.353	0.095	0.496	0.604	0.240	0.564	0.381	0.187	0.398	0.462
Limonite	%	0.060	0.082	0.034	0.197	0.076	0.035	0.013	0.031	0.043	0.116
Magnetite	%	0.120	0.289	0.200	1.237	0.182	0.202	0.102	0.044	0.211	0.072
Hypersthene	%	0.136	0.132	0.293	0.746	0.246	0.445	0.101	0.079	0.328	0.361
Titanite	%	0.150	0.226	0.157	0.336	0.202	0.183	0.082	0.234	0.088	0.122
Apatite	%	0.015	0.034	0.079	0.232	0.086	0.058	0.058	0.133	0.070	0.030
Staurolite	ppm	503.1	152.6	703.0	2105.7	1093.1	1026.3	739.8	187.9	1043.2	629.9
Zoisite	ppm	264.0	266.8	946.4	836.2	274.1	881.7	272.0	379.0	594.2	700.0
Goethite	ppm	310.9	593.0	459.4	3406.8	258.8	783.4	263.6	330.9	458.5	290.0
Al Silicate	ppm	583.4	48.8	184.1	424.0	1111.6	286.8	458.5	77.4	941.2	184.8
Rutile	ppm	48.4	338.8	61.1	115.4	97.6	471.4	92.0	103.0	292.9	293.5
Gittinsite	ppm	340.4	28.2	429.0	401.9	317.3	1400.8	415.1	176.3	576.1	680.4
Allanite	ppm	59.3	0.0	150.2	52.4	22.2	411.2	67.1	150.8	131.8	245.0
Aenigmatite	ppm	10.3	8.5	5.7	500.9	14.2	17.3	5.1	2.1	4.0	42.8
Gerenite	ppm	1.2	0.0	22.8	1.9	27.7	52.9	0.5	15.5	10.4	5.1
"Ericssonite"	ppm	0.0	0.0	0.7	1.0	0.0	5.1	0.0	0.0	0.0	0.7
Serpentine	ppm	0.0	1042.4	283.5	0.0	72.2	468.9	0.0	30.1	192.8	73.8
Monazite	ppm	0.0	6.3	11.8	228.6	4.3	17.0	0.0	76.7	7.2	15.9
Calcite	ppm	3.7	0.0	0.0	0.0	0.0	40.5	0.2	66.0	1.8	0.0
Wollastonite	ppm	1.2	45.2	1.1	1.3	0.0	14.2	1.0	4.5	19.2	0.2
Perclevite	ppm	0.0	0.0	1.1	10.3	7.3	36.6	10.7	5.1	3.3	6.4
Elpidite	ppm	27.7	0.0	8.3	9.6	3.4	19.5	9.8	35.6	9.2	52.6
Astrophyllite	ppm	0.0	0.0	0.0	4.2	1.1	0.0	3.8	17.0	1.3	0.0
Thorite	ppm	52.9	0.0	0.0	0.0	0.0	1.0	6.1	16.0	0.0	0.4
Parisite	ppm	0.0	0.0	0.0	0.0	0.0	0.0	0.0	0.0	0.0	0.0
Britholite	ppm	0.0	0.0	0.0	0.0	0.0	0.0	0.0	0.0	0.0	0.0
"Benitoite"	ppm	0.0	0.0	0.0	0.0	0.0	163.2	145.2	0.0	0.0	0.0
Pyrite	ppm	70.6	4.9	12.0	91.3	3.4	1.8	20.0	1.9	0.0	0.0
Barite	ppm	1.8	0.0	23.2	0.0	1.8	0.0	0.0	0.0	0.0	0.0
Gadolinite	ppm	0.0	0.0	3.3	3.5	5.5	48.7	0.7	0.0	3.8	4.1
Bastnaesite	ppm	0.0	0.0	0.0	22.2	2.5	0.3	13.1	0.0	0.0	0.0
Uraninite	ppm	0.0	0.0	0.0	0.0	0.0	0.0	0.0	0.0	0.0	0.0
Rhodonite	ppm	0.0	0.0	0.0	0.0	1.1	0.0	0.0	0.0	0.0	0.0
Scheelite	ppm	0.0	0.0	0.0	0.0	0.0	0.0	0.0	0.0	0.0	0.0
Stetindite	ppm	0.0	0.0	0.4	18.3	5.5	44.6	2.6	83.0	39.8	0.0
Pyrochlore	ppm	3.0	1.8	26.3	0.0	0.0	4.8	11.2	2.0	11.9	10.5
Fergusonite	ppm	0.0	0.9	5.5	0.0	0.0	5.5	0.0	0.0	0.3	0.0
Euxenite	ppm	0.0	0.0	0.0	0.0	0.0	0.0	0.0	0.0	0.0	0.0
Pectolite	ppm	0.0	0.0	0.0	0.0	0.0	0.0	0.0	0.0	0.0	0.0
Fluorite	ppm	31.3	0.0	0.0	0.0	0.0	0.0	0.8	0.0	0.0	0.0
Changbaiite	ppm	7.9	0.0	6.8	1.6	0.0	2.0	0.8	0.0	1.2	0.0

Appendix A1. Tabular listing of MLA-SEM data for all samples (continued)

Sample	**UNIT**	**G3-12**	**G3-13**	**E-1**	**E-3**	**E-4**	**E-7**	**E-8**
	(area)							
Quartz	**%**	46.419	46.434	42.746	26.066	36.919	36.699	36.722
Albite	**%**	27.097	28.112	25.883	33.182	19.301	26.840	19.578
K-Feldspar	**%**	16.303	16.966	14.068	15.676	12.520	16.704	15.780
Hornblende	**%**	2.531	2.296	3.009	6.019	12.525	3.069	4.380
Garnet	**%**	0.446	0.701	1.887	2.658	13.440	1.156	1.124
Ilmenite	**%**	0.195	0.217	0.200	0.561	0.808	0.346	0.543
Plagioclase	**%**	2.607	2.295	3.819	4.844	0.995	7.961	13.566
Biotite	**%**	0.456	0.314	2.594	1.701	0.537	0.732	1.668
Chlorite	**%**	0.973	0.212	1.995	3.546	0.478	2.218	1.740
Epidote	**%**	0.667	0.612	0.911	1.430	0.229	0.824	0.800
Grunerite	**%**	0.190	0.092	0.108	0.292	0.345	0.466	0.992
Nepheline	**%**	0.164	0.158	0.170	0.286	0.033	0.360	0.897
Zircon	**%**	0.069	0.068	0.033	0.087	0.307	0.046	0.141
Augite	**%**	0.886	0.576	0.958	1.542	0.224	0.934	0.139
Aegirine	**%**	0.311	0.184	0.157	0.194	0.241	0.256	0.257
Limonite	**%**	0.024	0.024	0.081	0.066	0.273	0.037	0.052
Magnetite	**%**	0.026	0.047	0.361	0.623	0.301	0.229	0.334
Hypersthene	**%**	0.064	0.136	0.181	0.185	0.052	0.602	0.439
Titanite	**%**	0.156	0.204	0.261	0.268	0.017	0.117	0.155
Apatite	**%**	0.071	0.148	0.128	0.110	0.028	0.077	0.099
Staurolite	**ppm**	1151.2	184.5	318.2	1449.1	375.7	490.1	343.8
Zoisite	**ppm**	449.2	742.4	1373.4	1873.4	391.7	984.3	556.1
Goethite	**ppm**	151.9	152.2	1181.9	1549.7	632.2	750.5	240.7
Al Silicate	**ppm**	631.2	549.7	661.7	442.2	177.8	287.3	211.4
Rutile	**ppm**	89.3	67.6	461.0	813.7	7.7	127.9	767.9
Gittinsite	**ppm**	392.3	43.6	14.6	8.5	93.2	293.6	1073.7
Allanite	**ppm**	343.1	24.9	40.5	54.0	194.9	25.0	496.6
Aenigmatite	**ppm**	8.6	5.8	3.2	17.4	15.1	6.9	21.1
Gerenite	**ppm**	4.9	4.2	1.6	24.0	4.7	0.2	164.9
"Ericssonite"	**ppm**	0.0	0.3	0.0	0.0	0.0	0.3	26.1
Serpentine	**ppm**	57.9	46.7	17.6	211.8	17.4	74.2	194.4
Monazite	**ppm**	16.4	19.6	189.6	4.2	11.5	22.2	1.1
Calcite	**ppm**	7.6	0.0	0.0	0.0	2.7	0.0	61.6
Wollastonite	**ppm**	46.2	36.9	39.5	29.3	0.9	0.9	21.6
Perclevite	**ppm**	6.1	1.2	1.7	0.6	0.0	16.3	19.6
Elpidite	**ppm**	9.4	25.5	0.0	0.0	2.5	0.5	84.3
Astrophyllite	**ppm**	0.8	0.5	0.0	0.6	0.9	0.8	3.4
Thorite	**ppm**	0.0	0.5	1.2	0.0	0.0	0.0	106.9
Parisite	**ppm**	0.0	0.0	0.0	0.0	0.0	0.0	5.5
Britholite	**ppm**	0.7	0.0	1.0	0.0	0.0	0.0	0.0
"Benitoite"	**ppm**	0.0	8.8	155.5	0.0	0.5	0.0	11.4
Pyrite	**ppm**	0.0	0.5	2.6	42.4	0.0	0.0	0.7
Barite	**ppm**	0.0	0.0	0.6	0.0	0.9	0.0	44.6
Gadolinite	**ppm**	0.0	0.0	8.4	1.1	0.0	0.0	35.7
Bastnaesite	**ppm**	0.7	0.0	8.5	0.0	0.0	35.7	156.5
Uraninite	**ppm**	0.0	0.0	0.0	0.0	0.0	0.0	1.0
Rhodonite	**ppm**	0.0	0.0	0.0	0.0	0.9	0.0	0.0
Scheelite	**ppm**	0.0	0.0	0.0	0.0	0.0	0.0	0.0
Stetindite	**ppm**	0.8	1.1	0.4	1.7	0.0	2.1	19.0
Pyrochlore	**ppm**	56.4	3.1	0.0	0.0	0.0	27.9	3.2
Fergusonite	**ppm**	0.0	0.0	0.0	0.0	0.0	0.9	4.6
Euxenite	**ppm**	0.0	0.0	0.0	0.0	0.0	0.0	2.6
Pectolite	**ppm**	0.0	0.6	0.0	0.0	0.0	0.0	5.7
Fluorite	**ppm**	0.0	0.0	0.0	0.0	0.0	0.0	0.0
Changbaiite	**ppm**	0.3	1.0	0.0	0.0	0.0	2.0	1.3

Table A2. Location and Geographic Information for Samples (also provided in Table 4.1)

Sample Number	Latitude (dd.dddd) (North)	Longitude (dd.dddd) (West)	NTS Map (1:50K Sheet)	UTM EAST (NAD 83) (metres)	UTM NORTH (NAD 83) (metres)	Distance from Strange Lake (Main Zone, km)	Distance from Strange Lake (B- Zone, km)	Azimuth (degrees) (Main Zone)	Azimuth (degrees) (B- Zone)	Distance Average (km)	Azimuth Average (degrees)
G1-1	56.3168	-64.1247	24A/08	430487	6241919	0.13	2.74	83.2	113.2	1.44	98.2
G1-2	56.3079	-64.0944	24A/08	432341	6240902	2.22	4.85	116.4	115.4	3.54	115.9
G1-3	56.3000	-64.1031	24A/08	431788	6240028	2.36	4.85	142.3	127.7	3.60	135.0
G1-4	56.3032	-64.1233	24A/08	430547	6240408	1.51	3.67	172.5	135.0	2.59	153.7
G1-5	56.3137	-64.1179	24A/08	430898	6241562	0.64	3.27	122.1	116.1	1.95	119.1
G1-6	56.3066	-64.1476	24A/08	429052	6240811	1.71	2.46	229.5	205.5	2.08	217.5
G1-7	56.3192	-64.1151	24A/08	431084	6242175	0.77	3.22	69.2	104.7	2.00	87.0
G1-8	56.3146	-64.1139	24A/08	431150	6241658	0.83	3.46	107.0	112.8	2.14	109.9
G1-9	56.3117	-64.1140	24A/08	431137	6241339	0.96	3.58	125.7	117.5	2.27	121.6
G1-10	56.3063	-64.1136	24A/08	431151	6240738	1.41	3.91	145.5	125.3	2.66	135.4
G1-11	56.3014	-64.1148	24A/08	431072	6240192	1.86	4.19	157.0	132.0	3.02	144.5
G1-12	56.2982	-64.1162	24A/08	430979	6239839	2.16	4.37	162.9	136.2	3.27	149.6
G1-13	56.2909	-64.1121	24A/08	431218	6239018	3.01	5.15	163.1	140.5	4.08	151.8
G1-14	56.2930	-64.0824	24A/08	433058	6239227	3.80	6.34	134.4	126.3	5.07	130.3
G1-15	56.3005	-64.0815	24A/08	433131	6240064	3.33	5.94	123.2	119.4	4.63	121.3
G1-16	56.3024	-64.0815	24A/08	433132	6240272	3.22	5.84	120.1	117.6	4.53	118.9
G1-17	56.3073	-64.0817	24A/08	433129	6240814	2.98	5.61	111.1	112.7	4.29	111.9
G1-18	56.3118	-64.0827	24A/08	433074	6241319	2.78	5.38	101.8	108.0	4.08	104.9
G1-19	56.3154	-64.0822	24A/08	433110	6241719	2.76	5.30	93.5	103.8	4.03	98.6
G1-20	56.3199	-64.0823	24A/08	433110	6242226	2.77	5.20	82.9	98.4	3.98	90.6
G1-21	56.3246	-64.0825	24A/08	433107	6242744	2.87	5.14	72.6	92.6	4.01	82.6
G1-22	56.3249	-64.0491	24A/08	435175	6242745	4.89	7.21	79.7	91.8	6.05	85.7
G1-23	56.3171	-64.0455	24A/08	435386	6241875	5.03	7.50	89.9	98.4	6.26	94.1
G1-24	56.3105	-64.0497	24A/08	435113	6241139	4.81	7.38	98.8	104.3	6.10	101.5
G1-25	56.3058	-64.0501	24A/08	435081	6240620	4.89	7.50	104.8	108.2	6.20	106.5
G1-26	56.3012	-64.0509	24A/08	435024	6240115	5.00	7.63	110.6	112.0	6.31	111.3
G1-27	56.2969	-64.0490	24A/08	435135	6239625	5.29	7.92	115.1	114.9	6.61	115.0
G1-28	56.2935	-64.0493	24A/08	435107	6239251	5.44	8.07	118.8	117.4	6.75	118.1
G1-29	56.2963	-64.0142	24A/08	437286	6239526	7.32	9.95	108.6	110.1	8.63	109.4
G1-30	56.2986	-64.0186	24A/08	437016	6239795	6.98	9.60	107.2	109.2	8.29	108.2
G1-31	56.3025	-64.0173	24A/08	437103	6240219	6.95	9.55	103.6	106.6	8.25	105.1
G1-32	56.3079	-64.0146	24A/08	437282	6240819	7.01	9.56	98.5	102.9	8.29	100.7
G1-33	56.3076	-64.0144	24A/08	437290	6240791	7.02	9.58	98.7	103.0	8.30	100.9
G1-34	56.3118	-64.0151	24A/08	437254	6241257	6.92	9.45	95.0	100.3	8.19	97.7
G1-35	56.3165	-64.0158	24A/08	437168	6241766	6.81	9.28	90.8	97.3	8.04	94.1
G1-36	56.3209	-64.0182	24A/08	437081	6242275	6.73	9.14	86.4	94.3	7.94	90.4
G1-37	56.3253	-64.0184	24A/08	437076	6242757	6.77	9.11	82.4	91.2	7.94	86.8
G1-38	56.3201	-63.9804	14D/05	439413	6242150	9.06	11.47	88.0	93.9	10.26	91.0
G1-39	56.3169	-63.9849	14D/05	439130	6241792	8.77	11.22	90.3	95.9	10.00	93.1
G1-40	56.3089	-63.9830	14D/05	439234	6240910	8.93	11.46	96.0	100.2	10.19	98.1

Table A2. Location and Geographic Information for Samples (continued): (also provided in Table 4.1)

Sample Number	Latitude (dd.dddd) (North)	Longitude (dd.dddd) (West)	NTS Map (1:50K Sheet)	UTM EAST (NAD 83) (metres)	UTM NORTH (NAD 83) (metres)	Distance from Strange Lake (Main Zone, km)	Distance from Strange Lake (B- Zone, km)	Azimuth (degrees) (Main Zone)	Azimuth (degrees) (B- Zone)	Distance Average (km)	Azimuth Average (degrees)
G2-1	56.3527	-63.9198	14D/05	443210	6245730	13.41	15.48	73.0	79.5	14.44	76.3
G2-2	56.3352	-63.9093	14D/05	443836	6243772	13.60	15.88	81.7	86.9	14.74	84.3
G2-3	56.3140	-63.8960	14D/05	444624	6241395	14.27	16.73	91.6	95.2	15.50	93.4
G2-4	56.3497	-63.9022	14D/05	444298	6245378	14.36	16.49	75.6	81.4	15.43	78.5
G2-5	56.3586	-63.8880	14D/05	445186	6246352	15.48	17.53	72.9	78.6	16.51	75.8
G2-6	56.3391	-63.8792	14D/05	445702	6244182	15.51	17.77	81.2	85.8	16.64	83.5
G2-7	56.3215	-63.8707	14D/05	446203	6242209	15.85	18.25	88.5	92.1	17.05	90.3
G2-8	56.3622	-63.8580	14D/05	447045	6246733	17.37	19.43	73.5	78.6	18.40	76.0
G2-9	56.3407	-63.8360	14D/05	448376	6244325	18.18	20.44	81.9	85.9	19.31	83.9
G2-10	56.3274	-63.8399	14D/05	448113	6242848	17.78	20.14	86.6	90.1	18.96	88.3
G2-11	56.3684	-63.8242	14D/05	449142	6247397	19.57	21.62	73.3	77.9	20.59	75.6
G2-12	56.3542	-63.8120	14D/05	449876	6245806	19.90	22.08	78.3	82.3	20.99	80.3
G2-13	56.3228	-63.8035	14D/05	450361	6242303	20.00	22.40	88.5	91.4	21.20	89.9
G2-14	56.3746	-63.7168	14D/05	455782	6248011	26.15	28.25	76.1	79.4	27.20	77.8
G2-15	56.4631	-63.7876	14D/05	451523	6257909	26.53	27.86	52.9	57.3	27.20	55.1
G2-16	56.3376	-63.7736	14D/05	452229	6243933	21.96	24.27	84.3	87.4	23.12	85.9
G2-17	56.3747	-63.7626	14D/05	452954	6248057	23.42	25.48	74.4	78.2	24.45	76.3
G2-18	56.3588	-63.7560	14D/05	453341	6246286	23.39	25.58	78.8	82.3	24.49	80.5
G2-19	56.3439	-63.7420	14D/05	454189	6244613	23.98	26.26	83.1	86.1	25.12	84.6
G3-2	56.3698	-63.7128	14D/05	456022	6247475	26.26	28.40	77.8	80.6	27.33	79.2
G3-3	56.3497	-63.6924	14D/05	457260	6245228	27.10	29.37	83.0	85.3	28.24	84.1
G3-4	56.3889	-63.6798	14D/05	458083	6249580	28.77	30.82	74.5	77.3	29.79	75.9
G3-5	56.3781	-63.6702	14D/05	458664	6248374	29.03	31.15	77.1	79.7	30.09	78.4
G3-6	56.3638	-63.6681	14D/05	458779	6246786	28.84	31.04	80.3	82.6	29.94	81.4
G3-7	56.4107	-63.6794	14D/05	458134	6252010	29.55	31.47	70.0	73.0	30.51	71.5
G3-8	56.3845	-63.6612	14D/05	459224	6249077	29.74	31.83	76.0	78.6	30.79	77.3
G3-9	56.3613	-63.6341	14D/05	460876	6246483	30.86	33.09	81.5	83.6	31.97	82.5
G3-10	56.4116	-63.6620	14D/05	459204	6252103	30.59	32.53	70.5	73.4	31.56	72.0
G3-11	56.4085	-63.6287	14D/05	461257	6251733	32.42	34.41	72.4	74.9	33.41	73.6
G3-12	56.3811	-63.6266	14D/05	461359	6248688	31.73	33.86	77.7	80.0	32.80	78.8
G3-13	56.3659	-63.6174	14D/05	461912	6246982	31.96	34.17	80.9	82.9	33.06	81.9
E-1	56.3278	-64.0764	24A/08	433491	6243096	3.35	5.52	69.2	88.8	4.43	79.0
E-3	56.3329	-63.9404	14D/05	441907	6243540	11.66	13.94	81.9	87.4	12.80	84.7
E-4	56.3460	-63.8891	14D/05	445100	6244956	15.05	17.24	78.3	83.1	16.14	80.7
E-7	56.3932	-63.7115	14D/05	456131	6250076	27.04	29.03	72.4	75.5	28.03	74.0
E-8	56.4159	-63.6665	14D/05	458936	6252581	30.51	32.41	69.5	72.4	31.46	71.0

APPENDIX B
ADDITIONAL MAPS/PROFILES SHOWING GEOGRAPHIC VARIATION PATTERNS

This Appendix to the Thesis Document contains proportional symbol maps for minerals that were not specifically illustrated in Chapters 6 and 7. No figure is provided for scheelite, as it is present in only 3 samples. The figures are presented in alphabetical order, as follows.

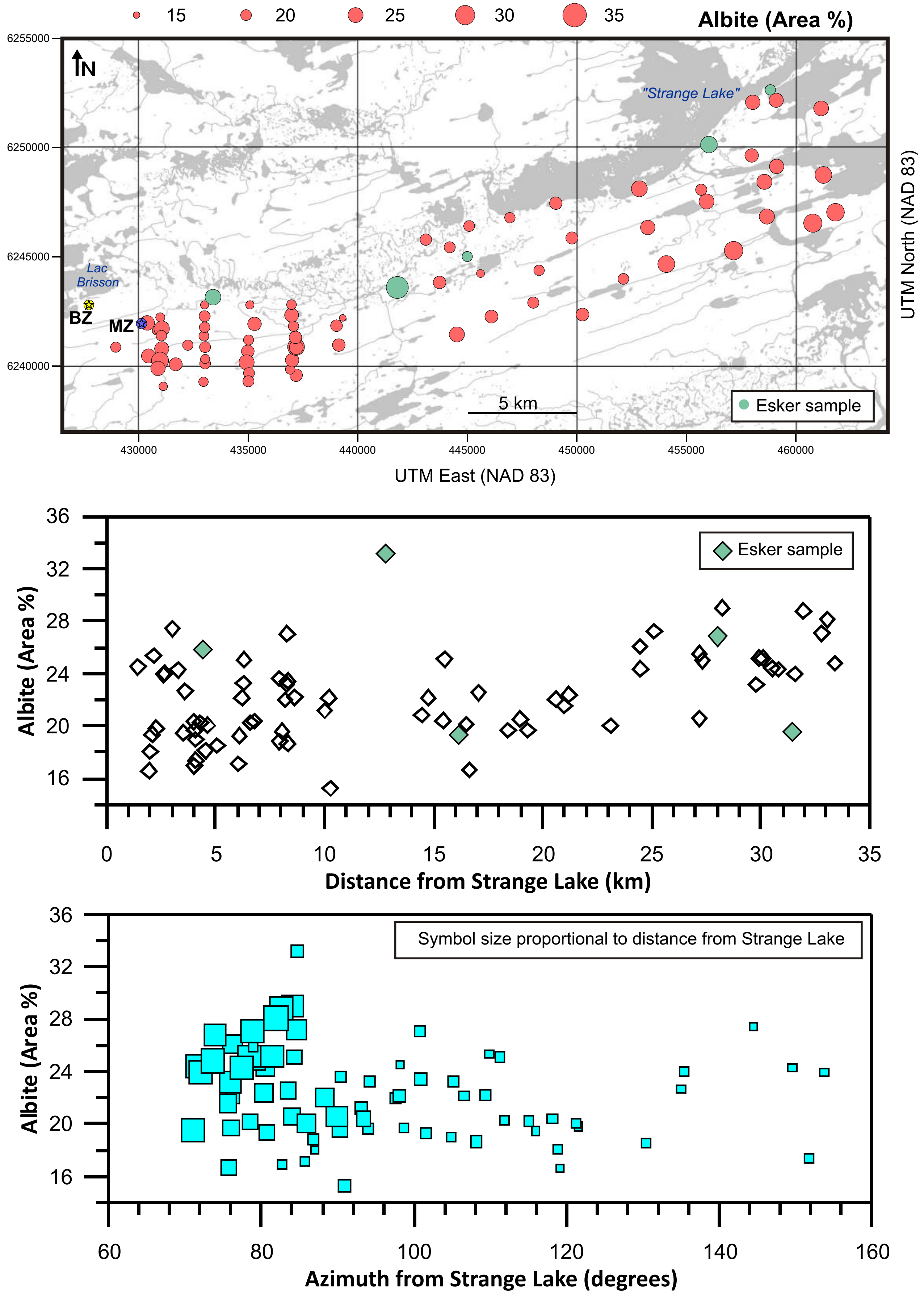

Figure B.1. Geographic variation patterns for albite (area %). Upper Panel is a map view with proportional symbols. Lower panels show abundances against distance and azimuth from Strange Lake.

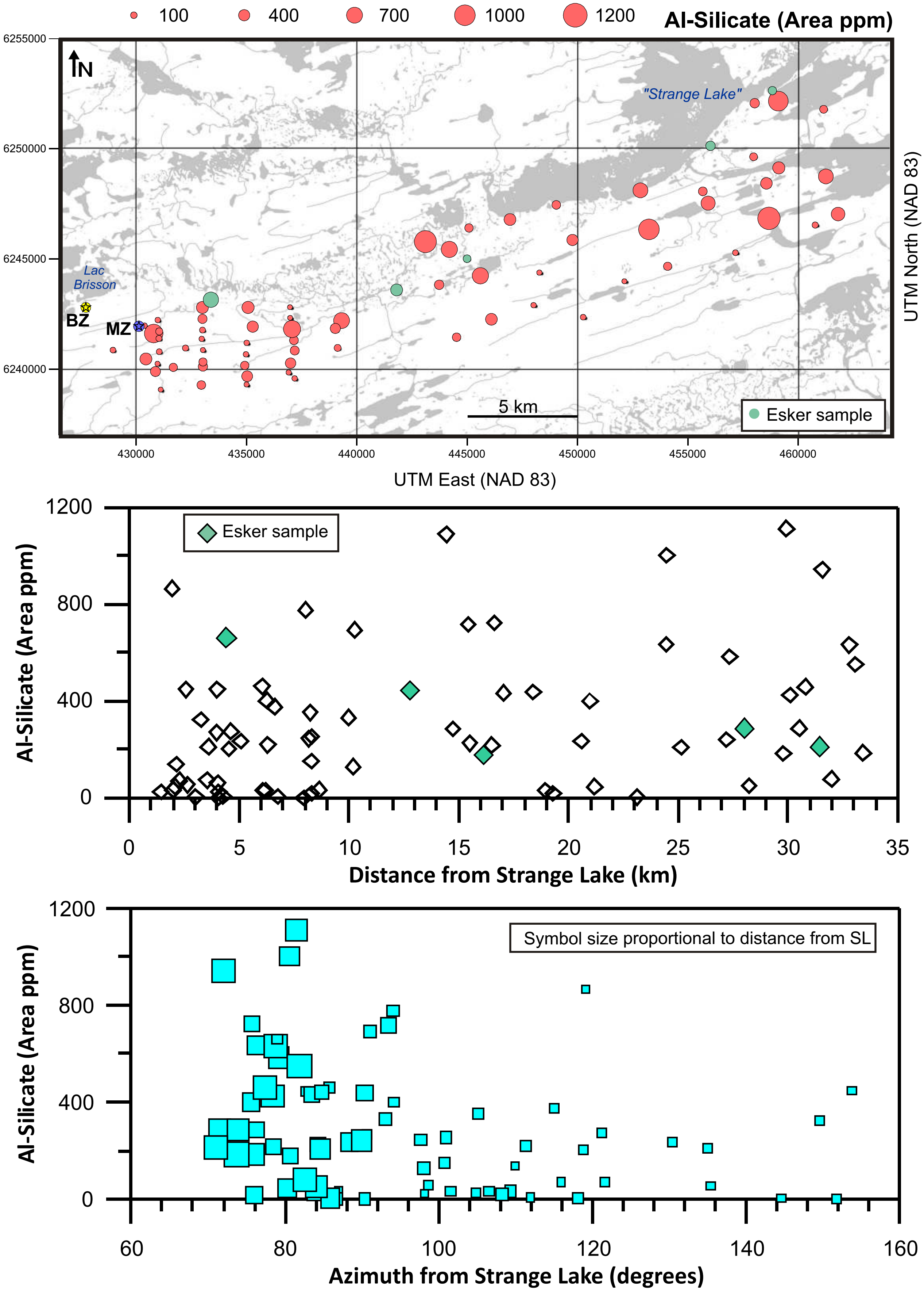

Figure B.2. Geographic variation patterns for Al-Silicate (area ppm). Upper Panel is a map view with proportional symbols. Lower panels show abundances against distance and azimuth from Strange Lake.

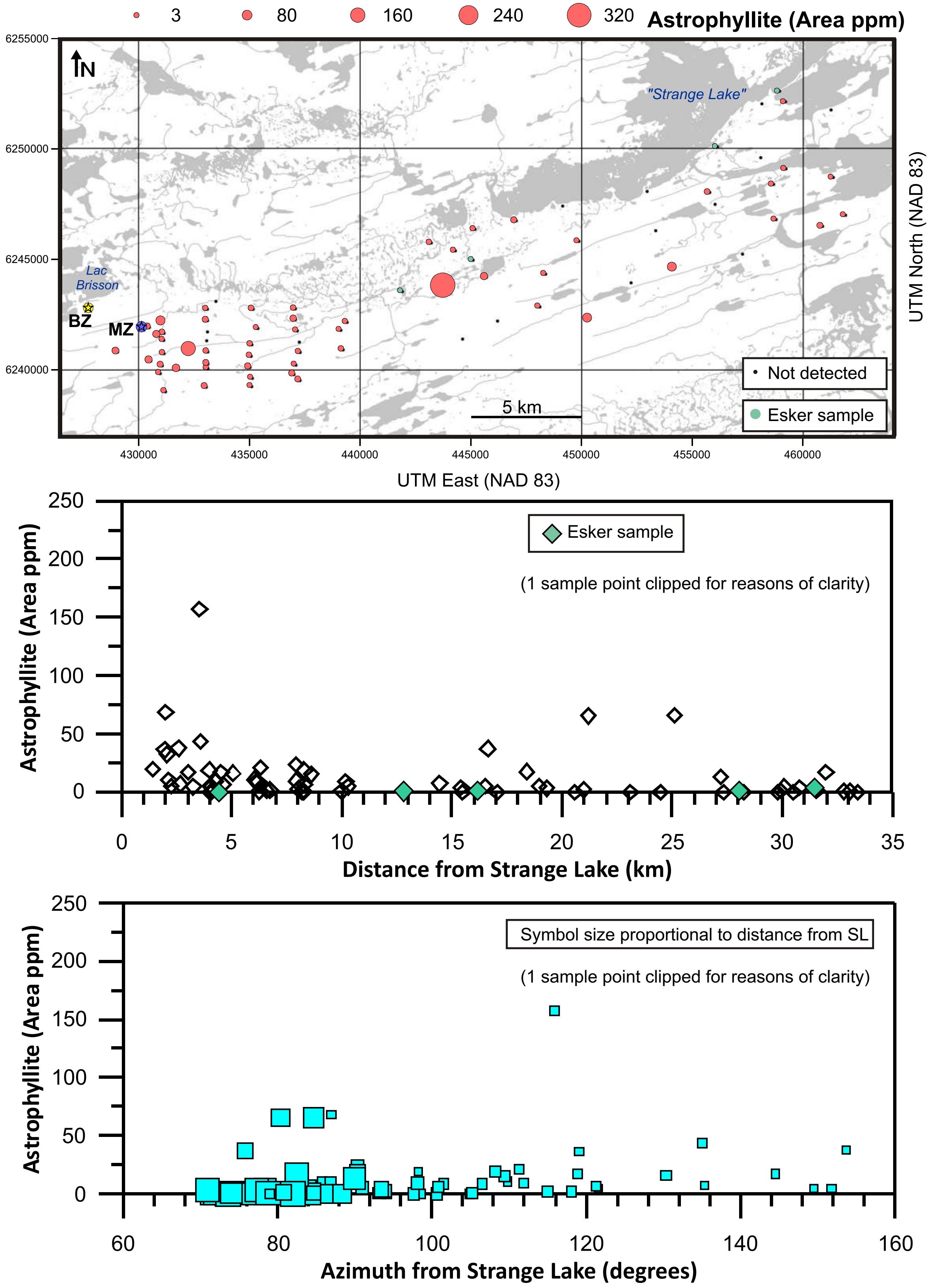

Figure B.3. Geographic variation patterns for astrophyllite (area ppm). Upper Panel is a map view with proportional symbols. Lower panels show abundances against distance and azimuth from Strange Lake.

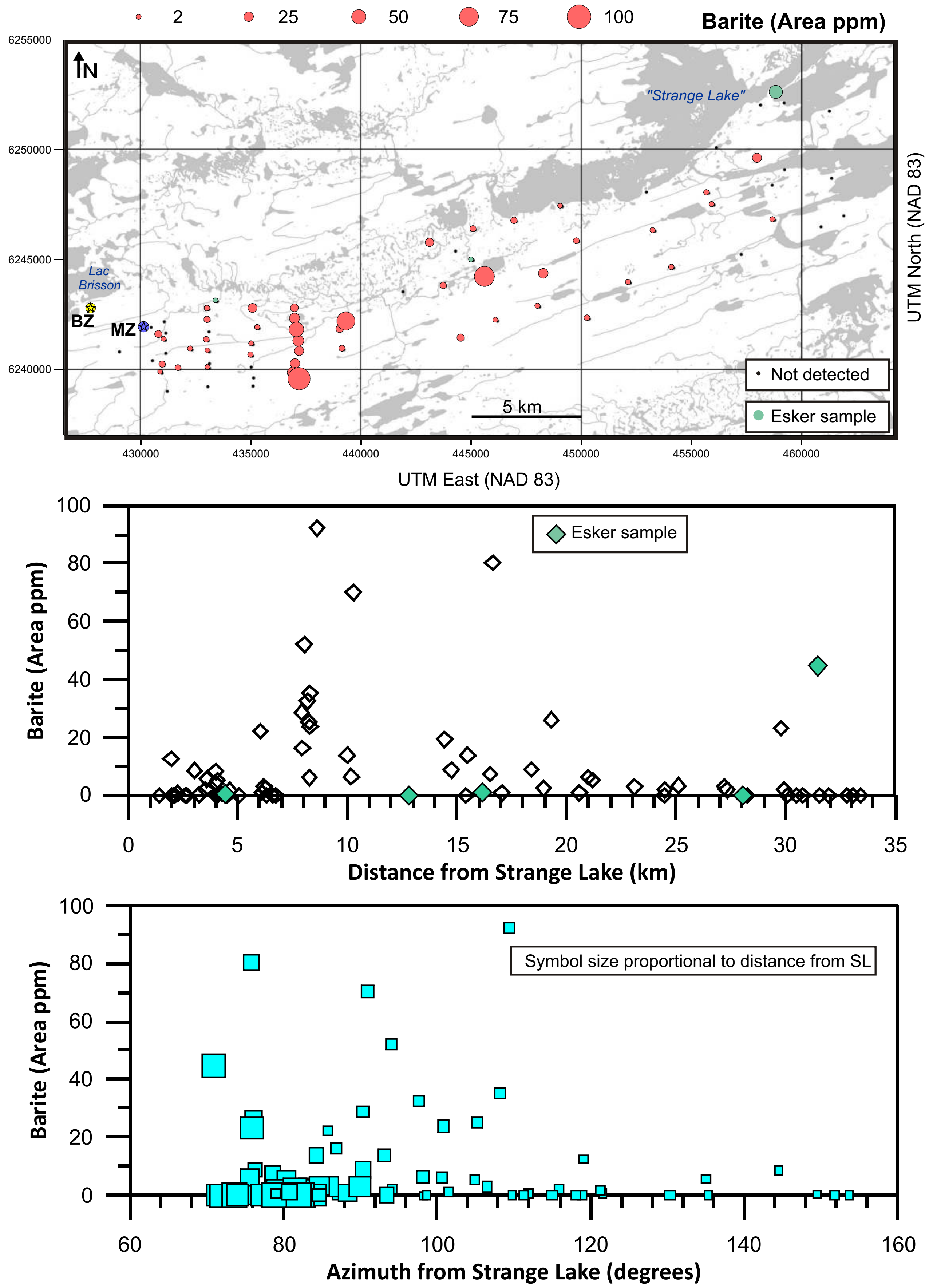

Figure B.4. Geographic variation patterns for barite (area ppm). Upper Panel is a map view with proportional symbols. Lower panels show abundances against distance and azimuth from Strange Lake.

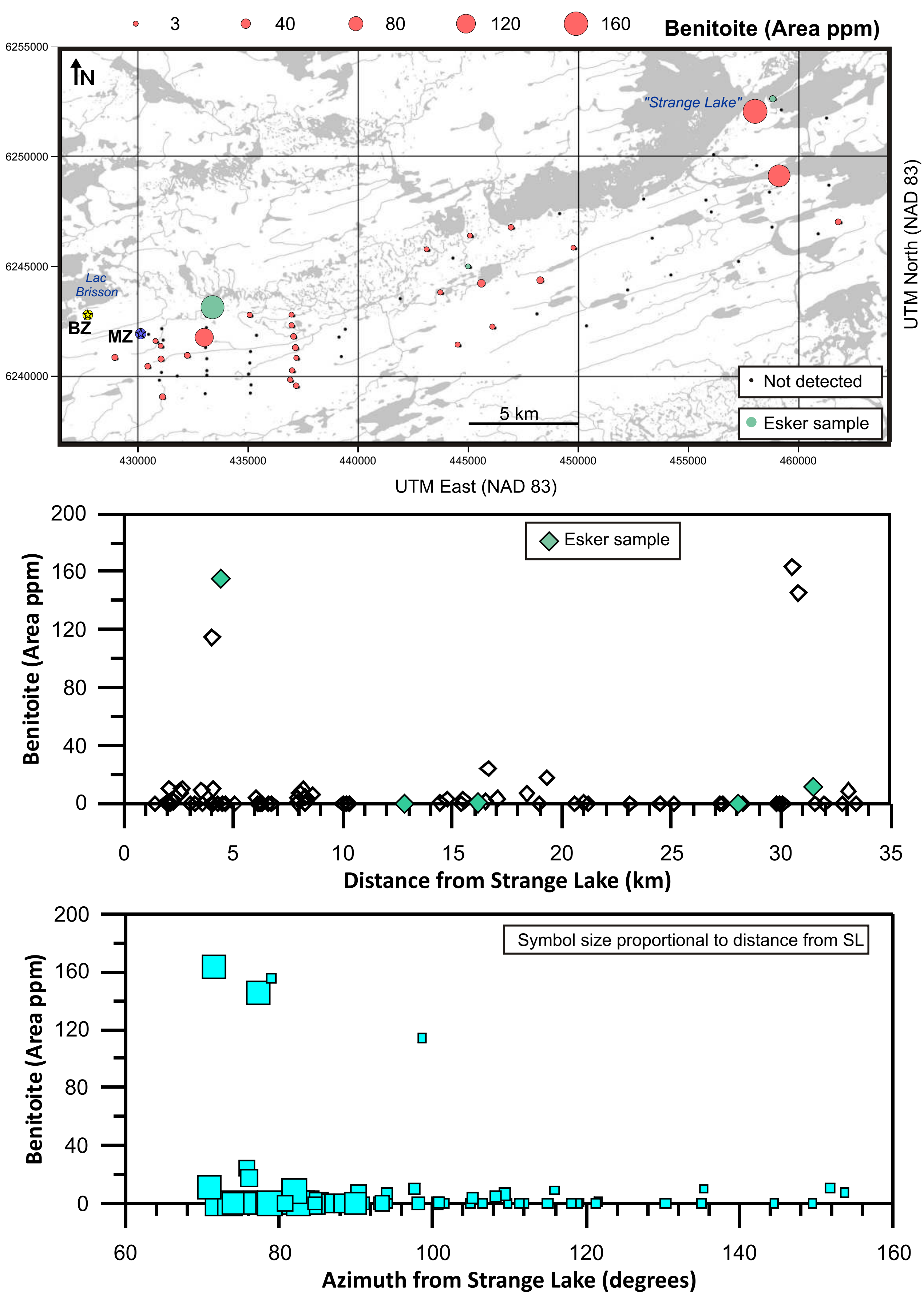

Figure B.5. Geographic variation patterns for benitoite (area ppm). Upper Panel is a map view with proportional symbols. Lower panels show abundances against distance and azimuth from Strange Lake.

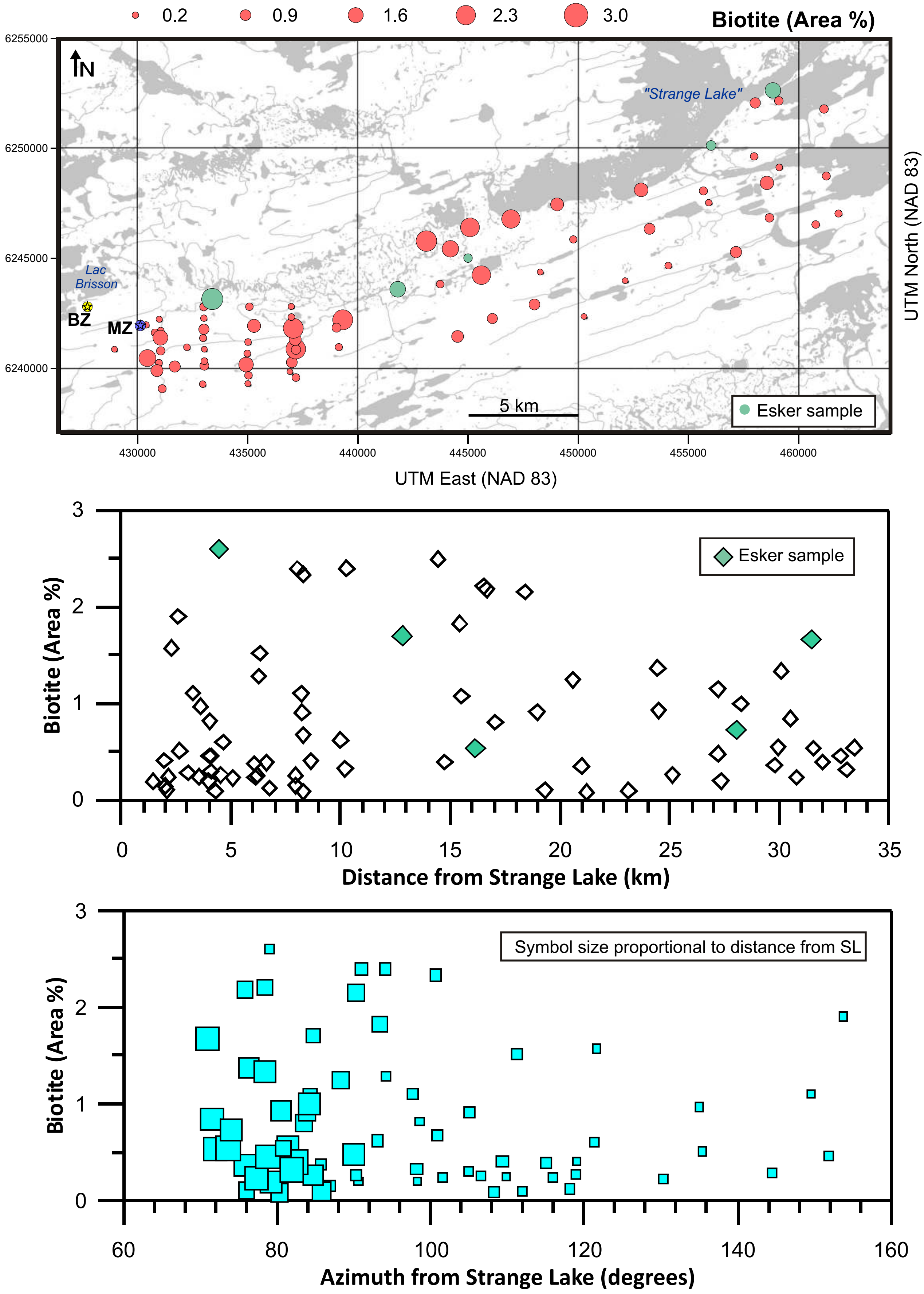

Figure B.6. Geographic variation patterns for biotite (area %). Upper Panel is a map view with proportional symbols. Lower panels show abundances against distance and azimuth from Strange Lake.

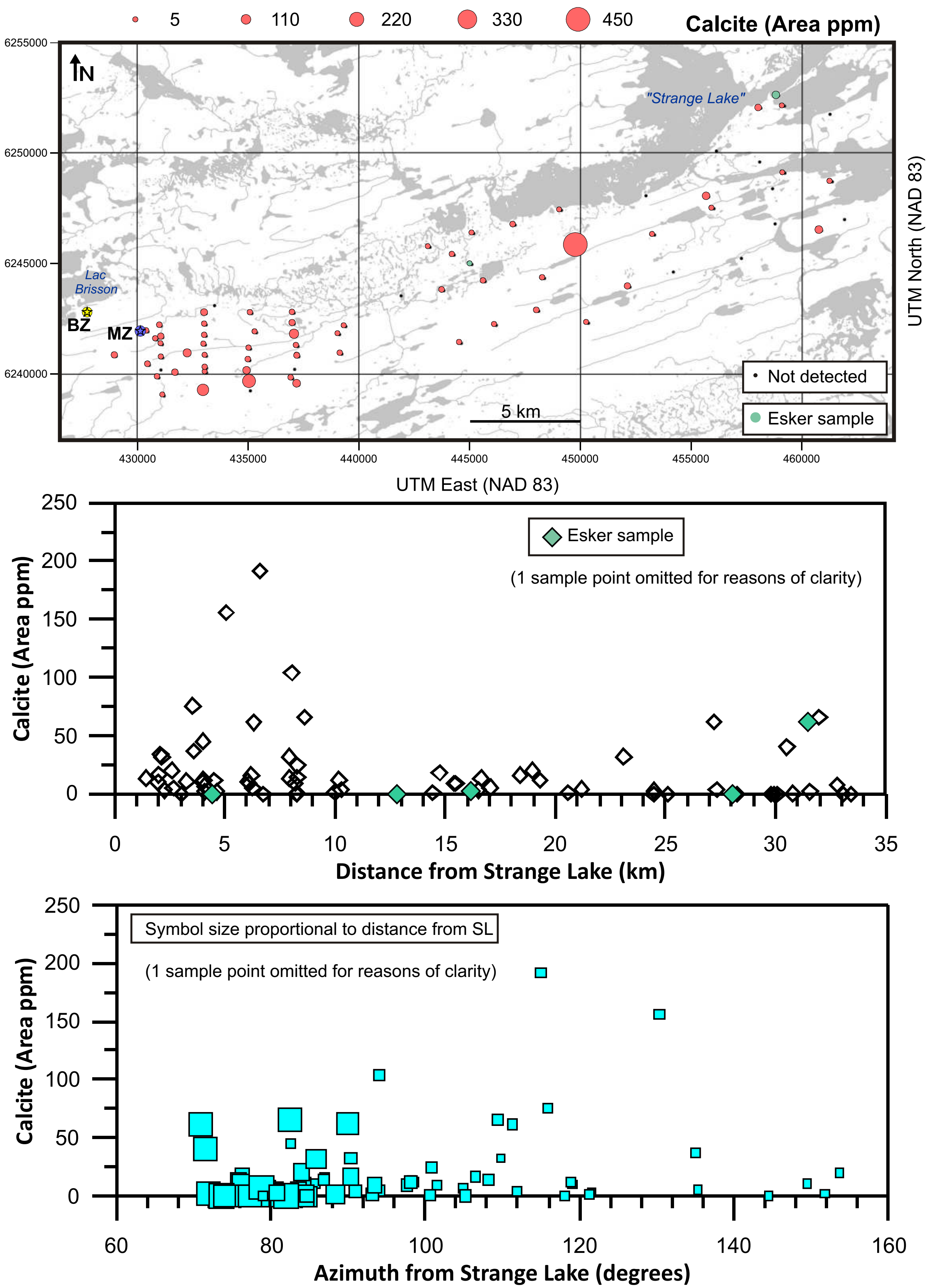

Figure B.7. Geographic variation patterns for calcite (area ppm). Upper Panel is a map view with proportional symbols. Lower panels show abundances against distance and azimuth from Strange Lake.

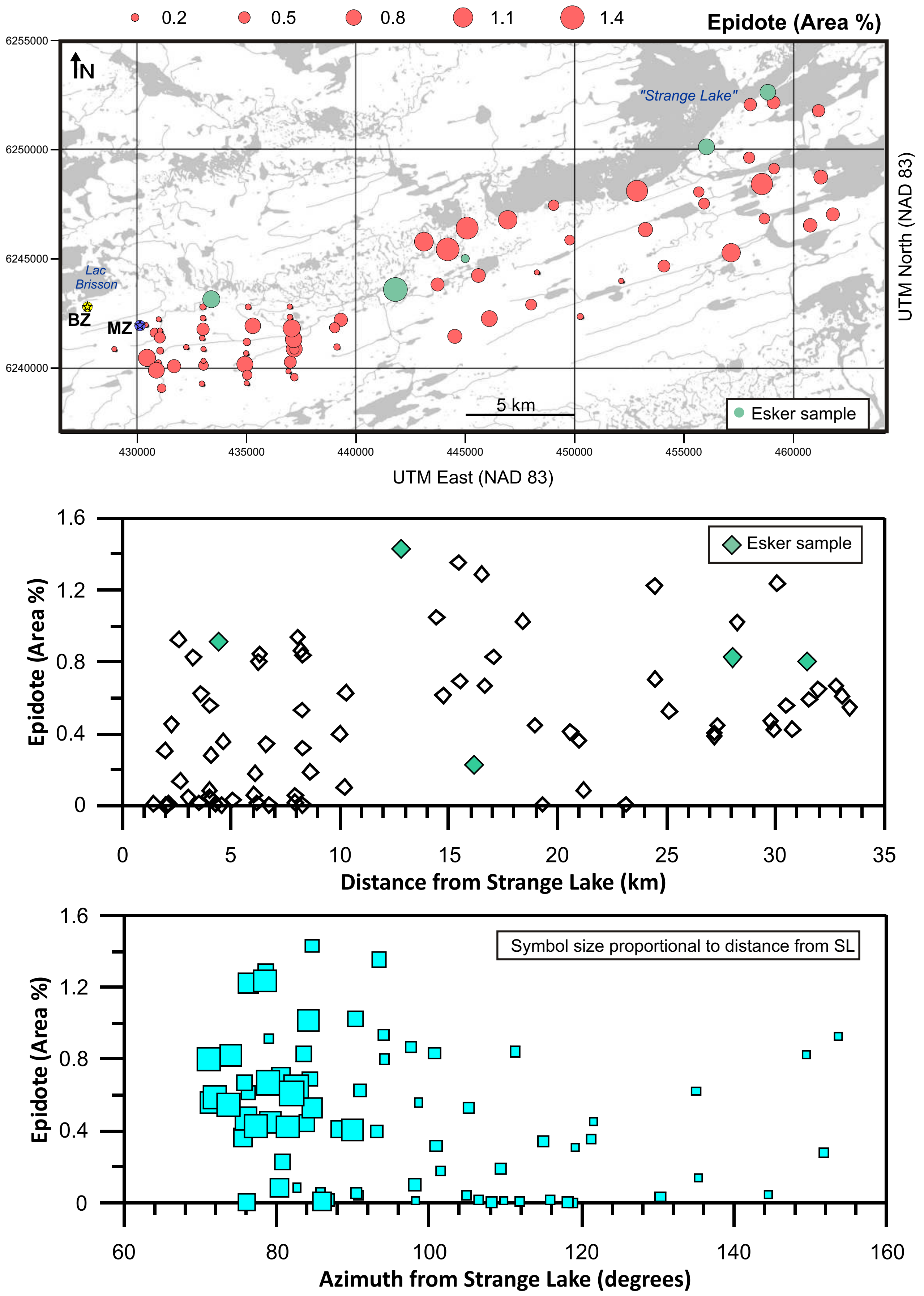

Figure B.8. Geographic variation patterns for epidote (area %). Upper Panel is a map view with proportional symbols. Lower panels show abundances against distance and azimuth from Strange Lake.

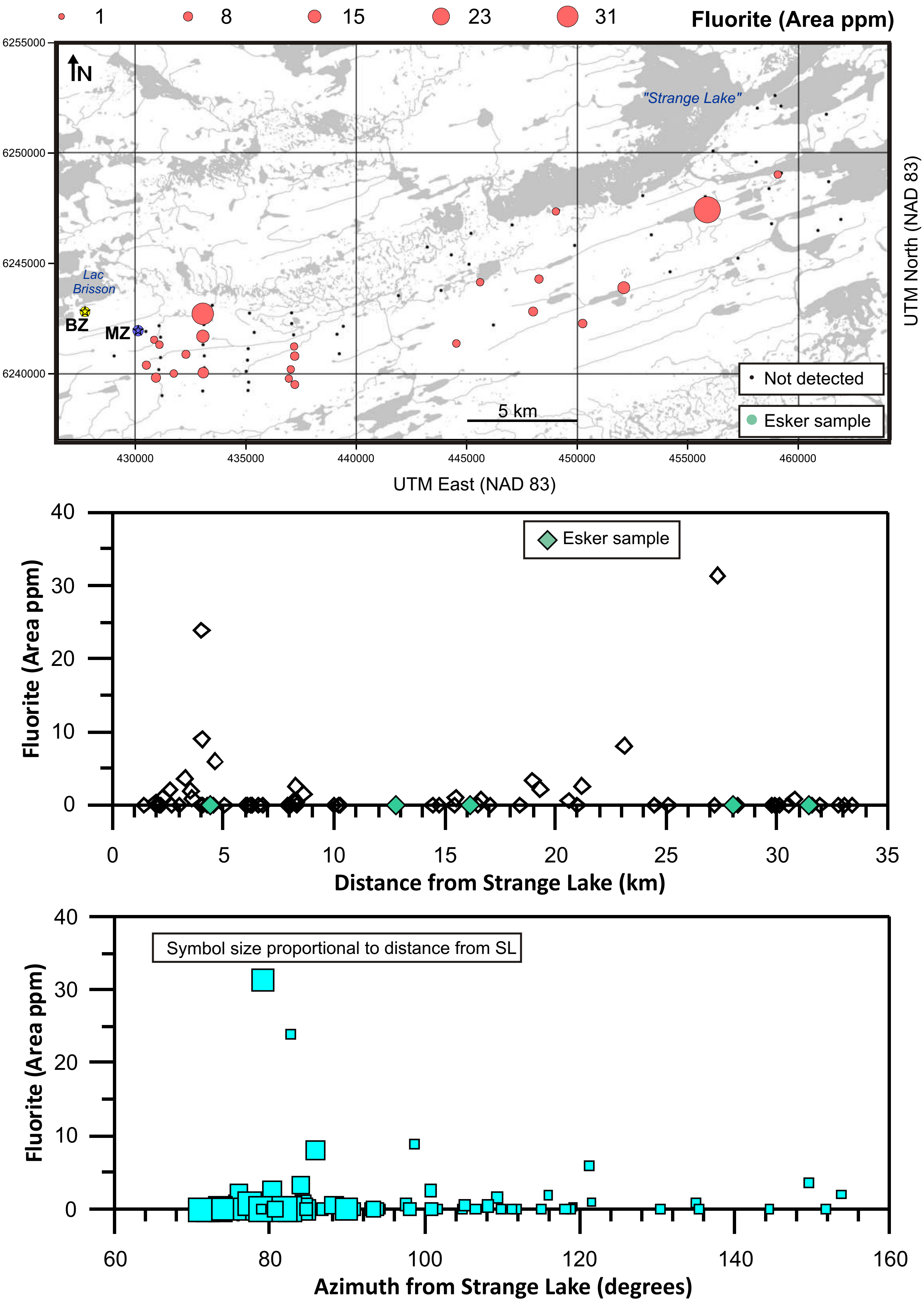

Figure B.9. Geographic variation patterns for fluorite (area ppm). Upper Panel is a map view with proportional symbols. Lower panels show abundances against distance and azimuth from Strange Lake.

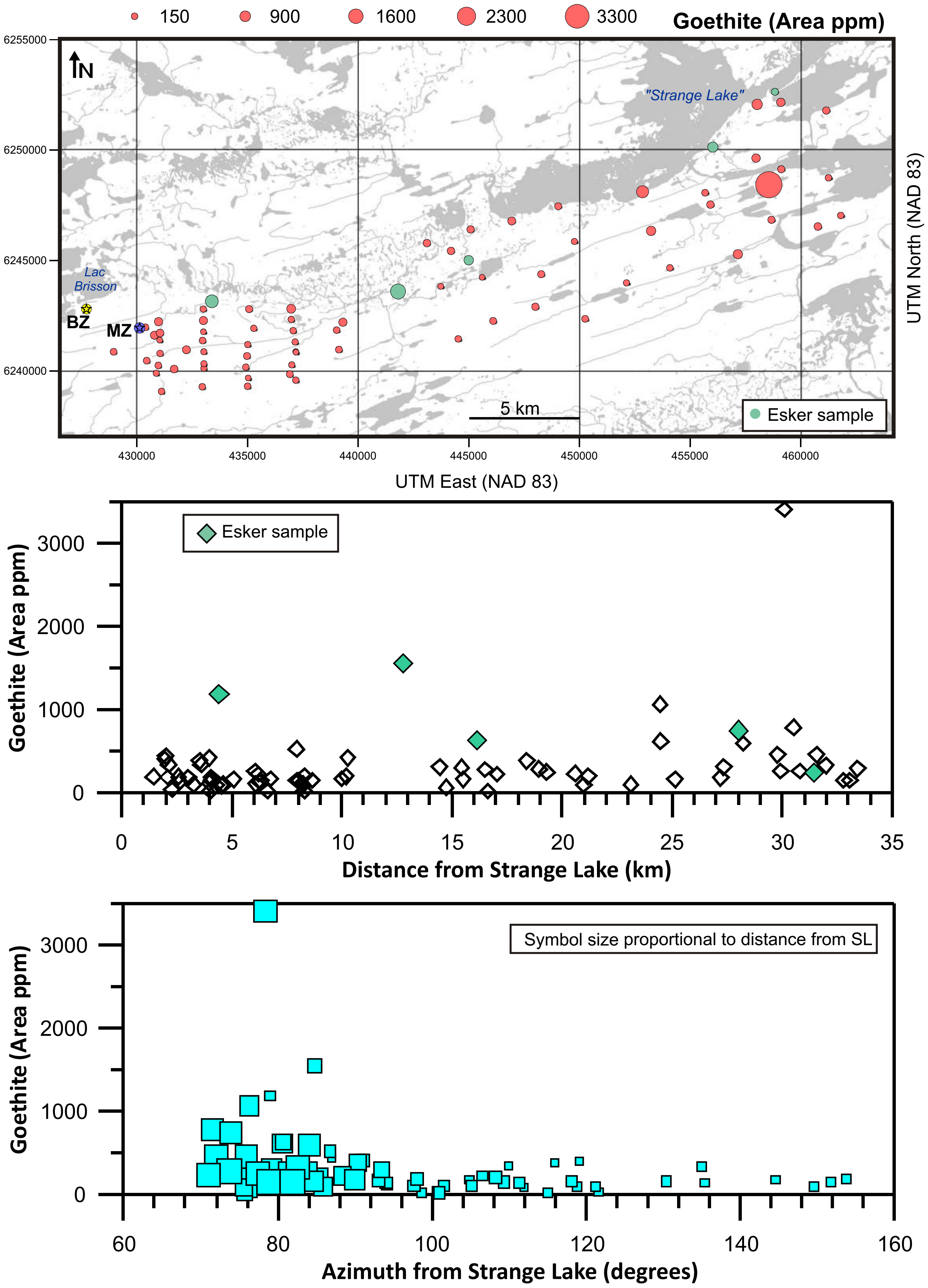

Figure B.10. Geographic variation patterns for goethite (area ppm). Upper Panel is a map view with proportional symbols. Lower panels show abundances against distance and azimuth from Strange Lake.

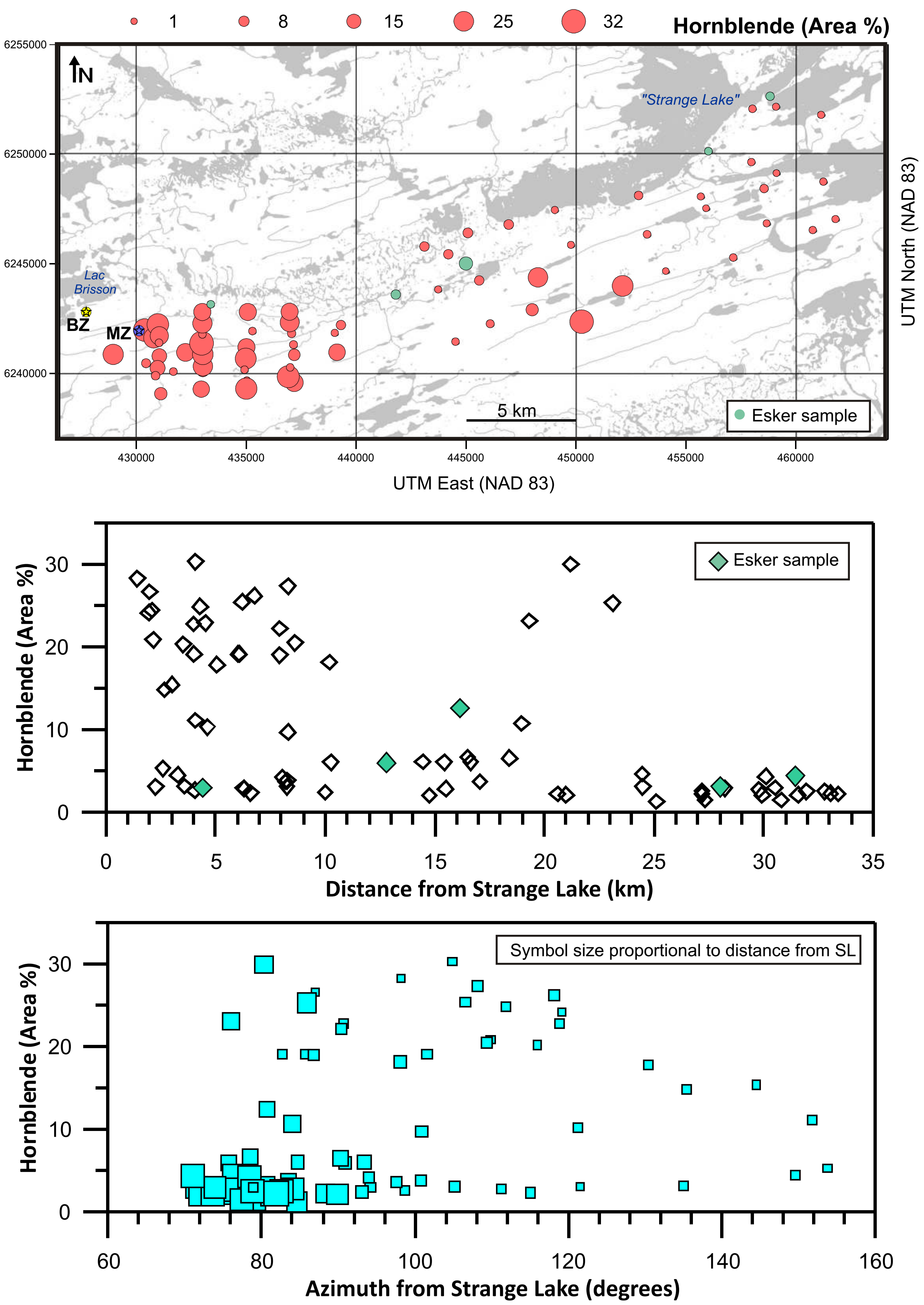

Figure B.11. Geographic variation patterns for hornblende (area %). Upper Panel is a map view with proportional symbols. Lower panels show abundances against distance and azimuth from Strange Lake.

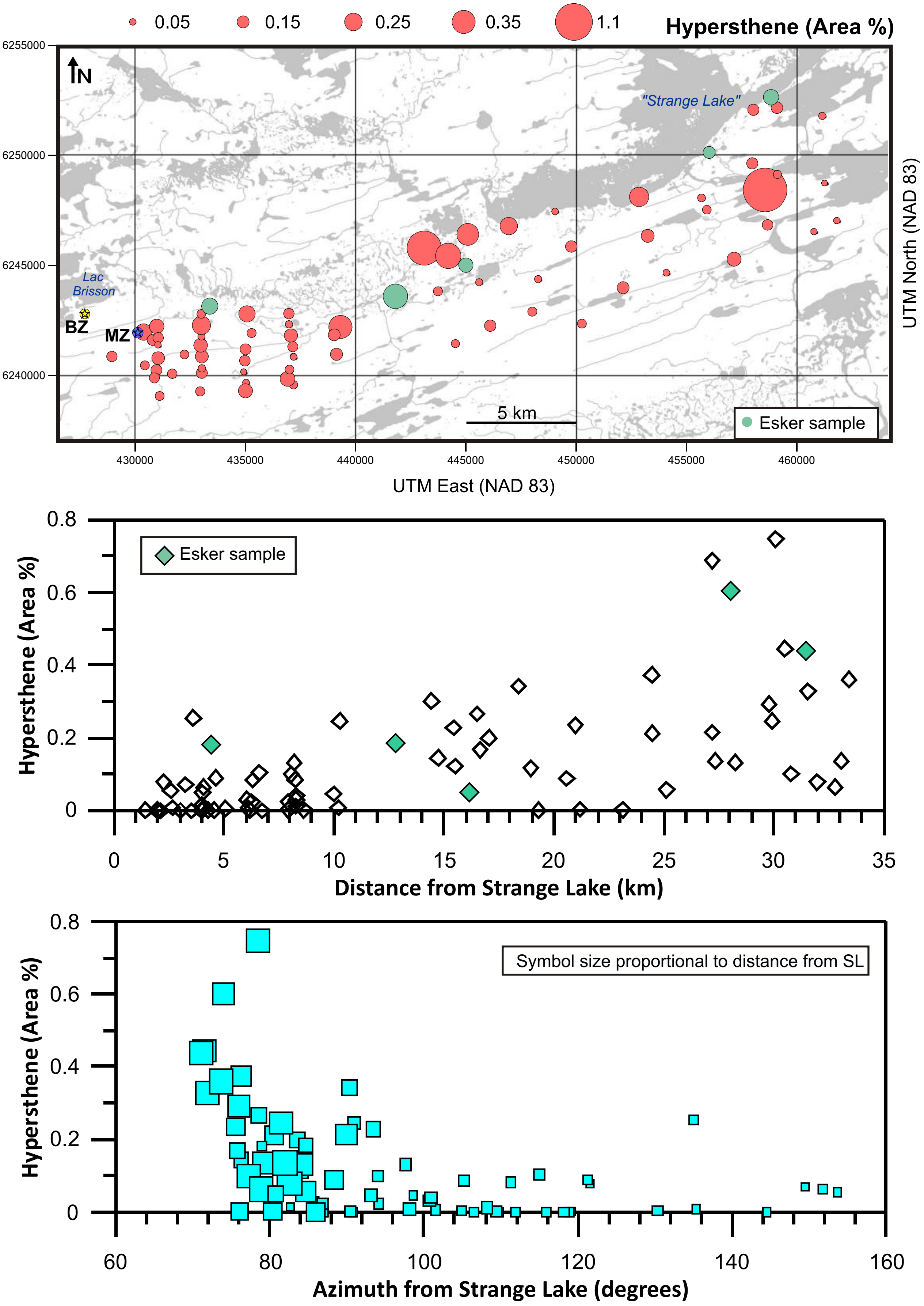

Figure B.12. Geographic variation patterns for hypersthene (area %). Upper Panel is a map view with proportional symbols. Lower panels show abundances against distance and azimuth from Strange Lake.

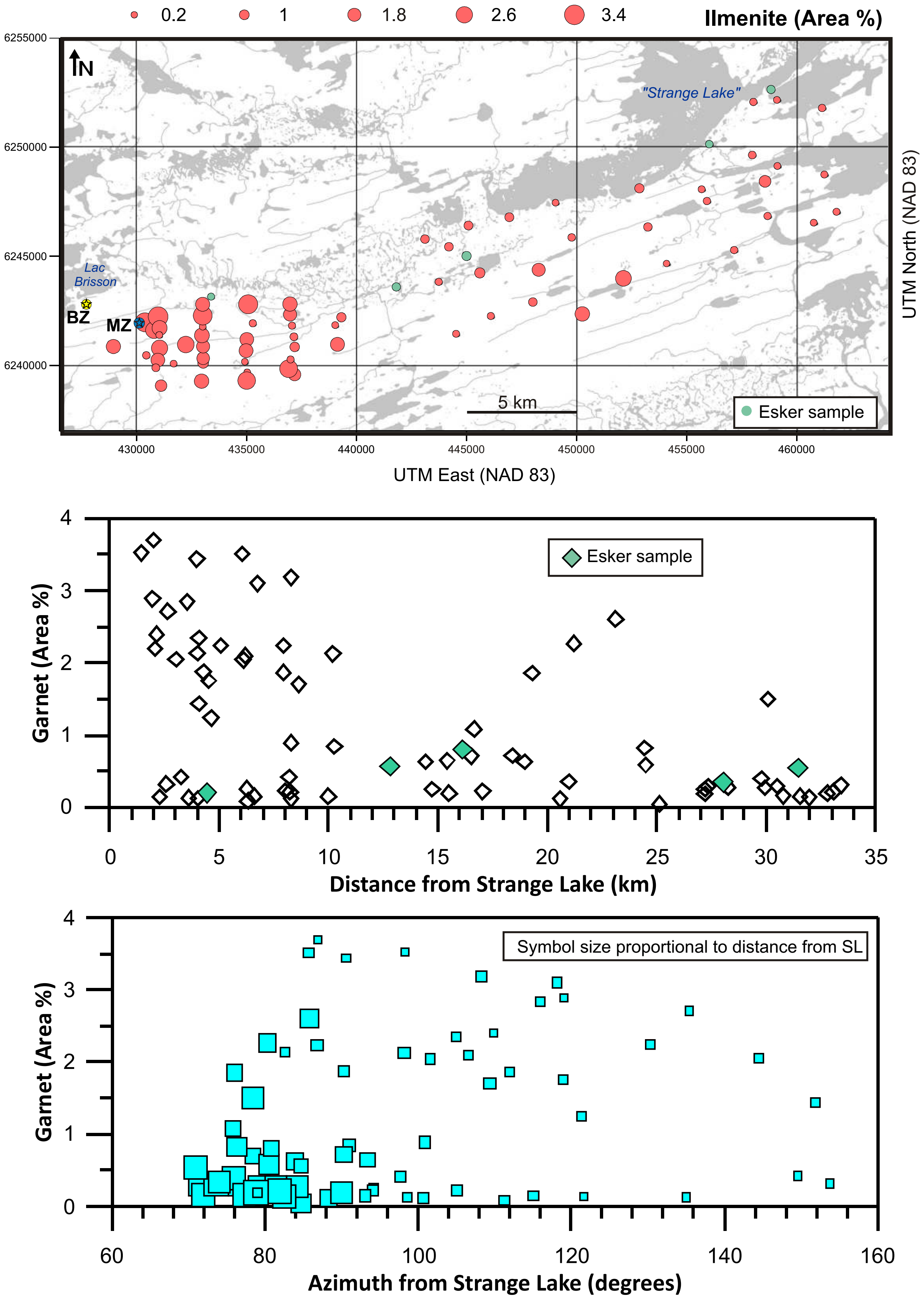

Figure B.13. Geographic variation patterns for ilmenite (area %). Upper Panel is a map view with proportional symbols. Lower panels show abundances against distance and azimuth from Strange Lake.

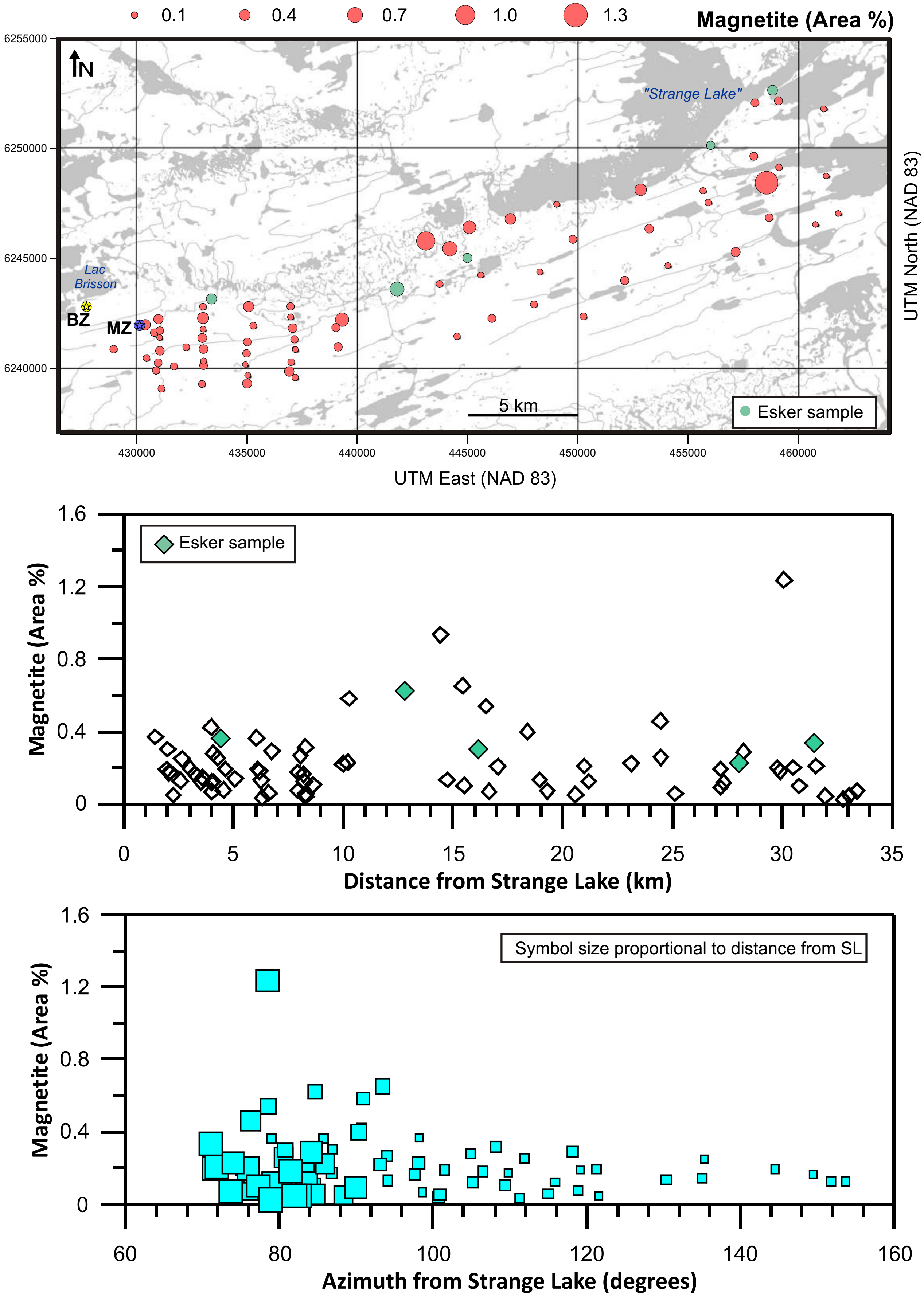

Figure B.14. Geographic variation patterns for magnetite (area %). Upper Panel is a map view with proportional symbols. Lower panels show abundances against distance and azimuth from Strange Lake.

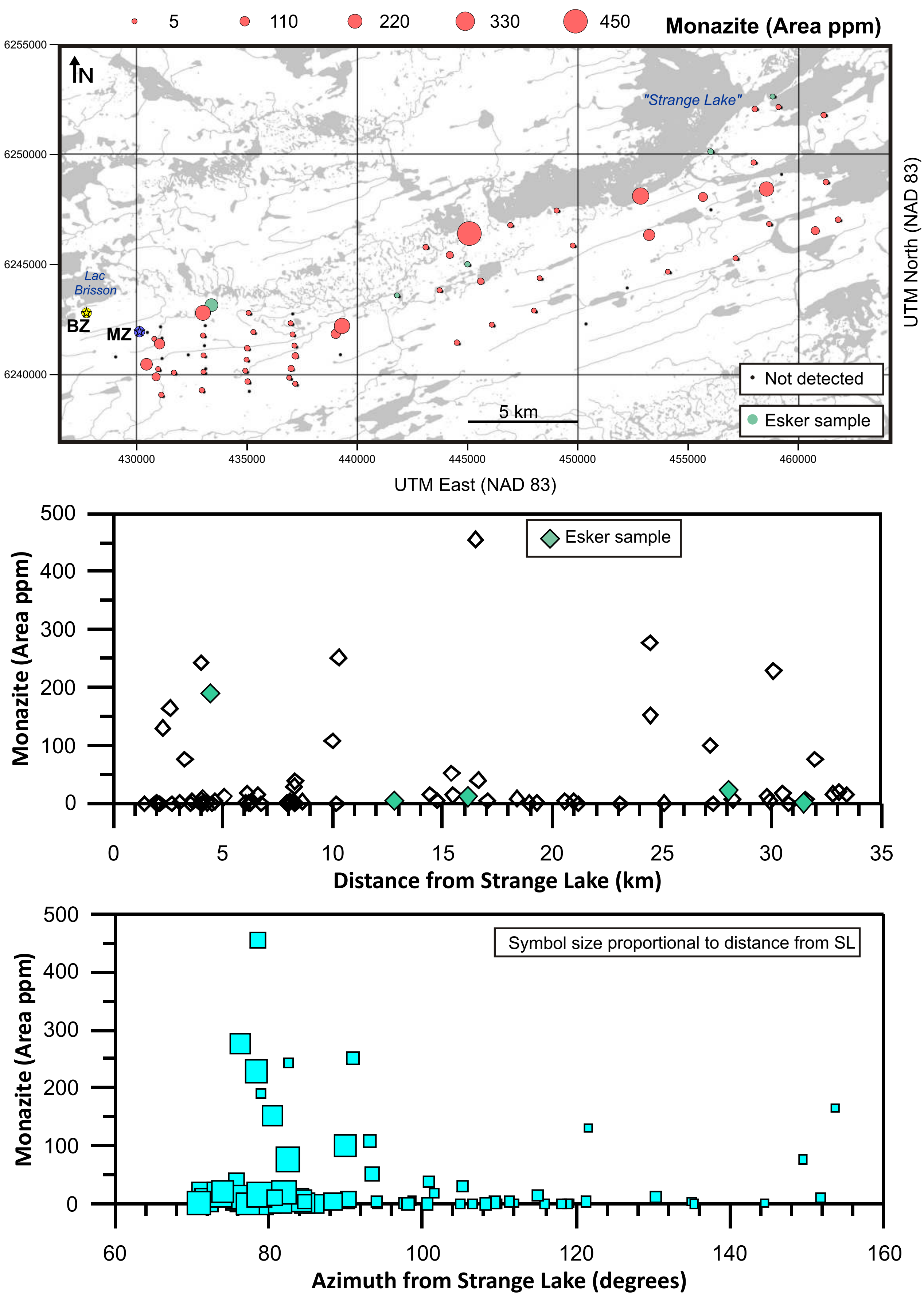

Figure B.15. Geographic variation patterns for monazite (area ppm). Upper Panel is a map view with proportional symbols. Lower panels show abundances against distance and azimuth from Strange Lake.

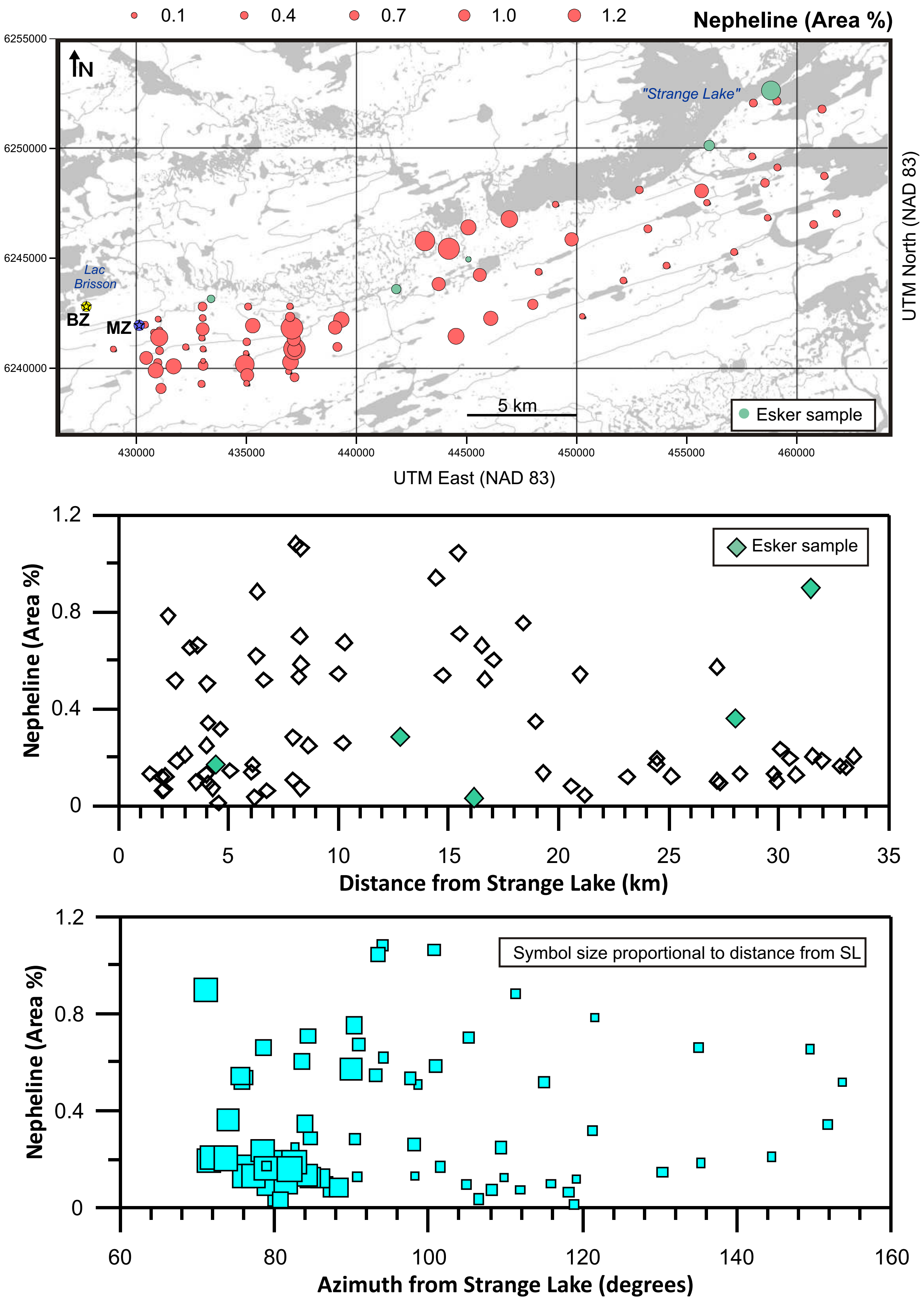

Figure B.16. Geographic variation patterns for nepheline (area %). Upper Panel is a map view with proportional symbols. Lower panels show abundances against distance and azimuth from Strange Lake.

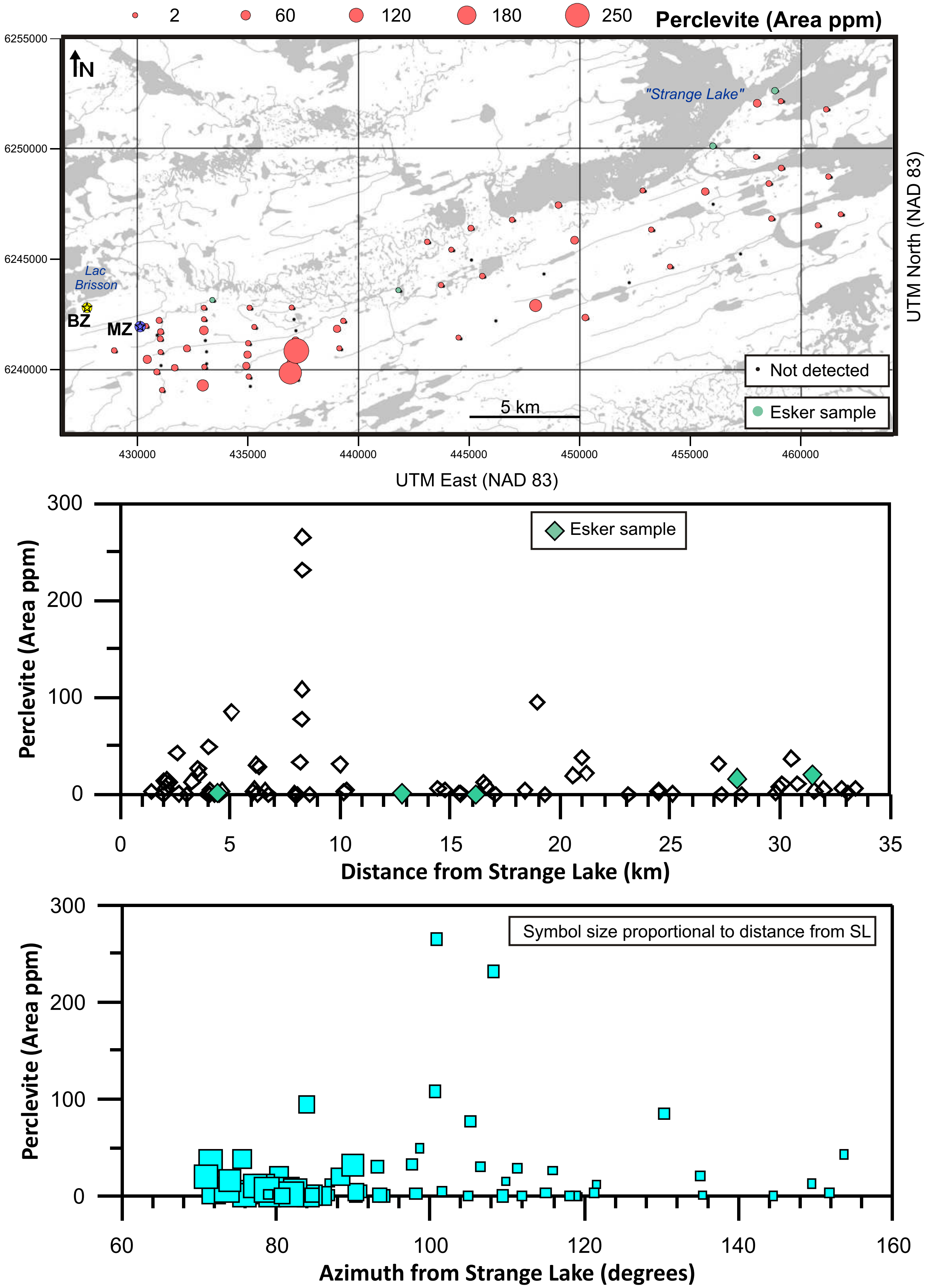

Figure B.17. Geographic variation patterns for perclevite (area ppm). Upper Panel is a map view with proportional symbols. Lower panels show abundances against distance and azimuth from Strange Lake.

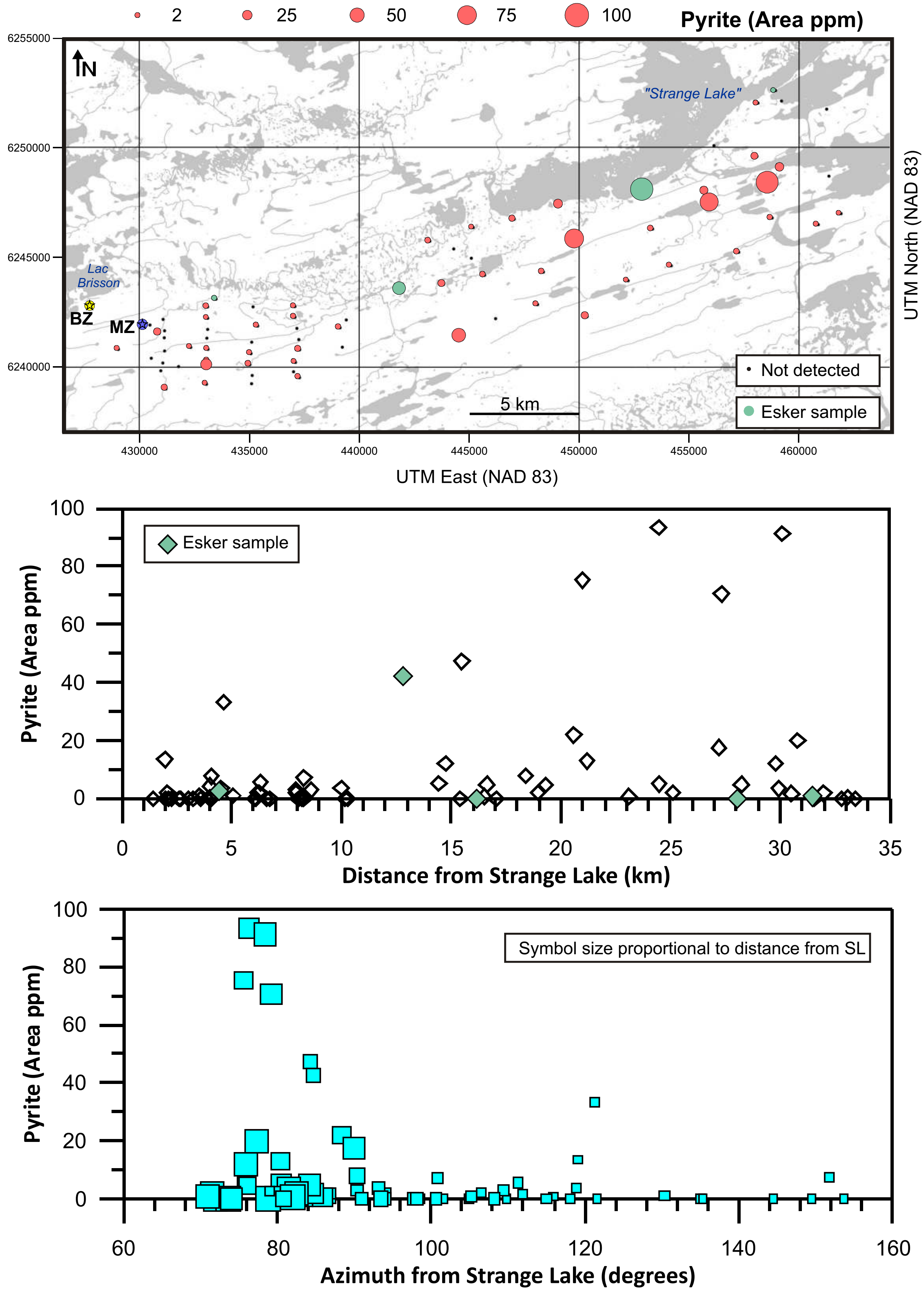

Figure B.18. Geographic variation patterns for pyrite (area ppm). Upper Panel is a map view with proportional symbols. Lower panels show abundances against distance and azimuth from Strange Lake.

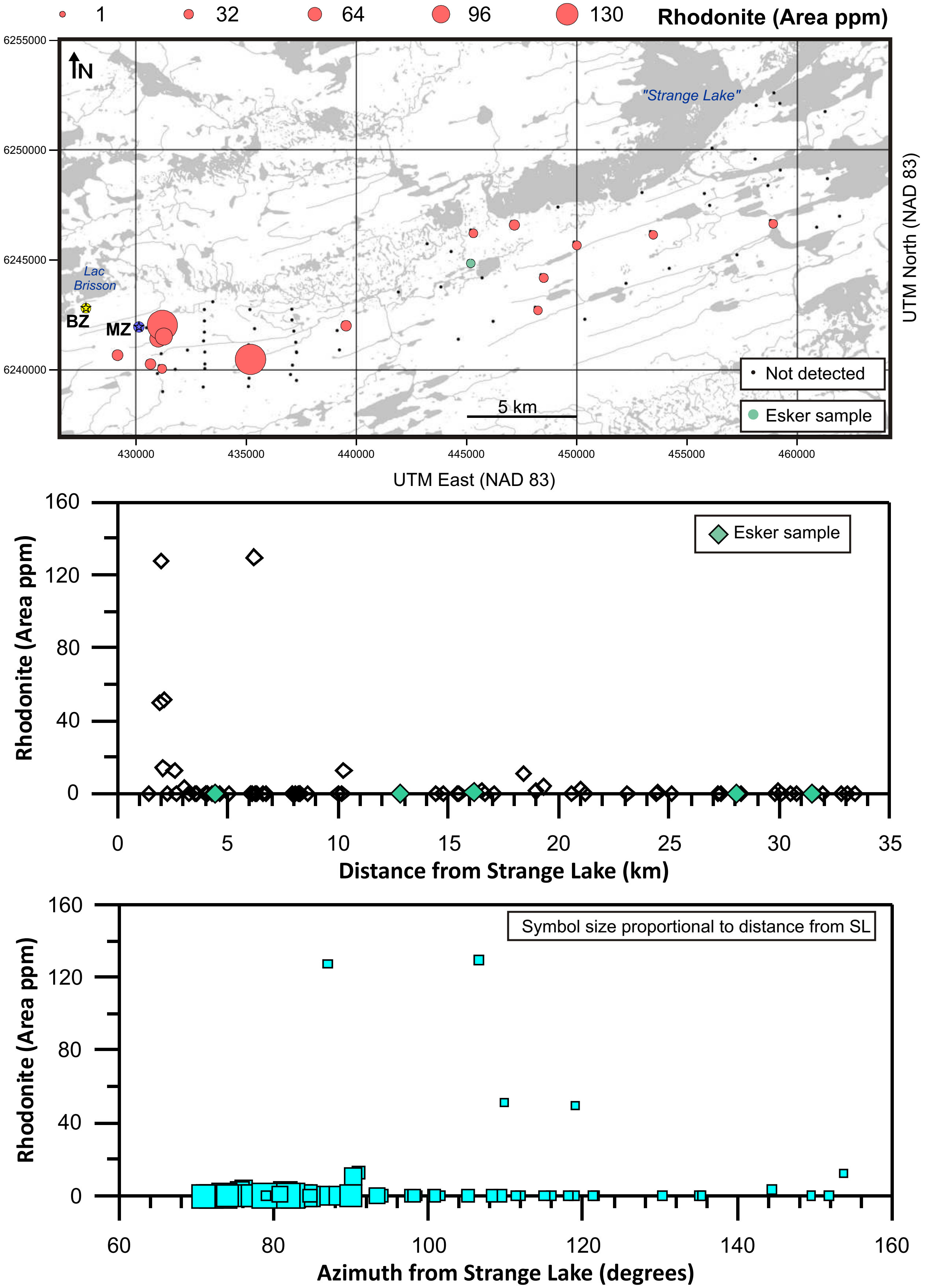

Figure B.19. Geographic variation patterns for rhodonite (area ppm). Upper Panel is a map view with proportional symbols. Lower panels show abundances against distance and azimuth from Strange Lake.

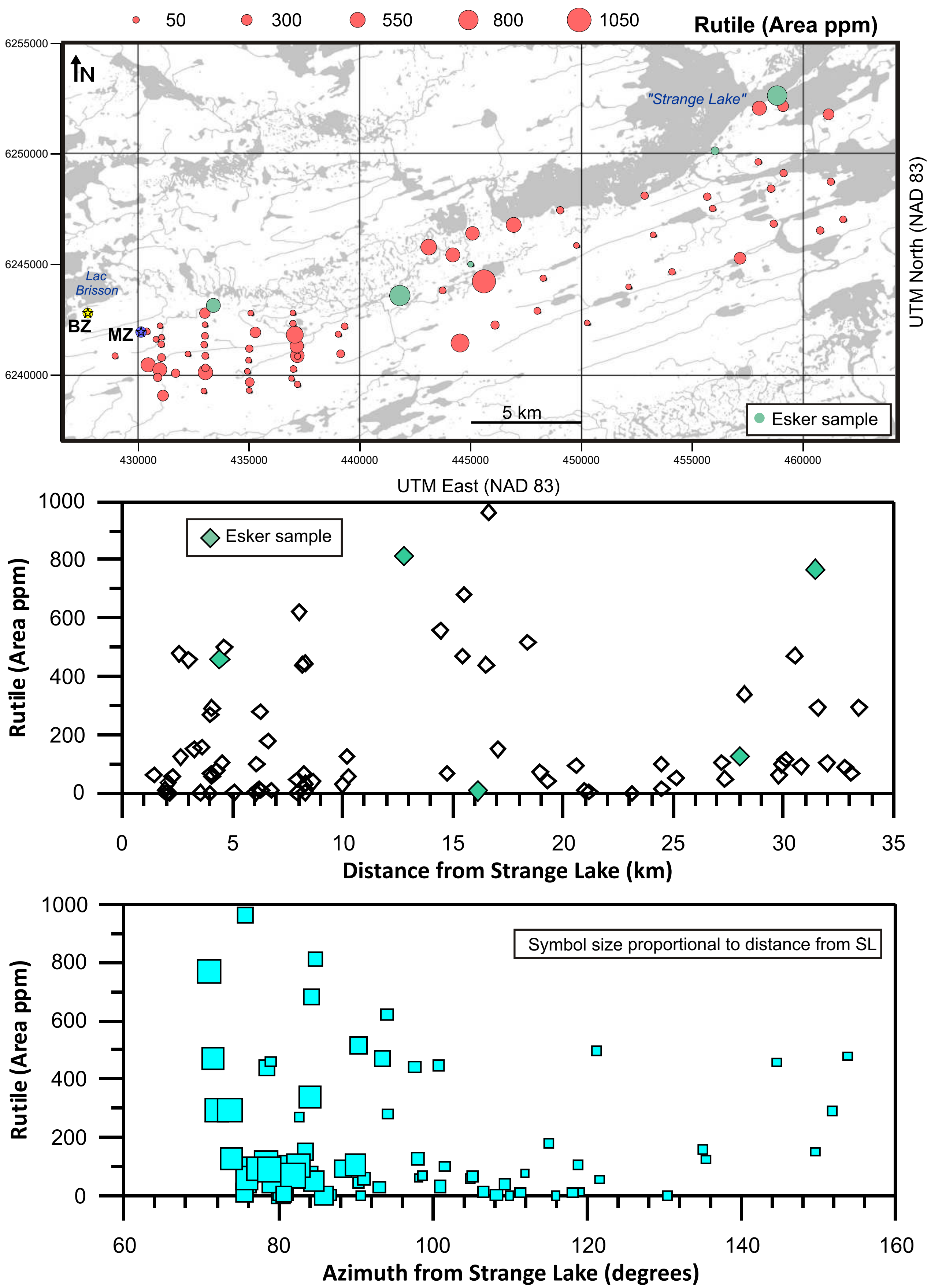

Figure B.20. Geographic variation patterns for rutile (area ppm). Upper Panel is a map view with proportional symbols. Lower panels show abundances against distance and azimuth from Strange Lake.

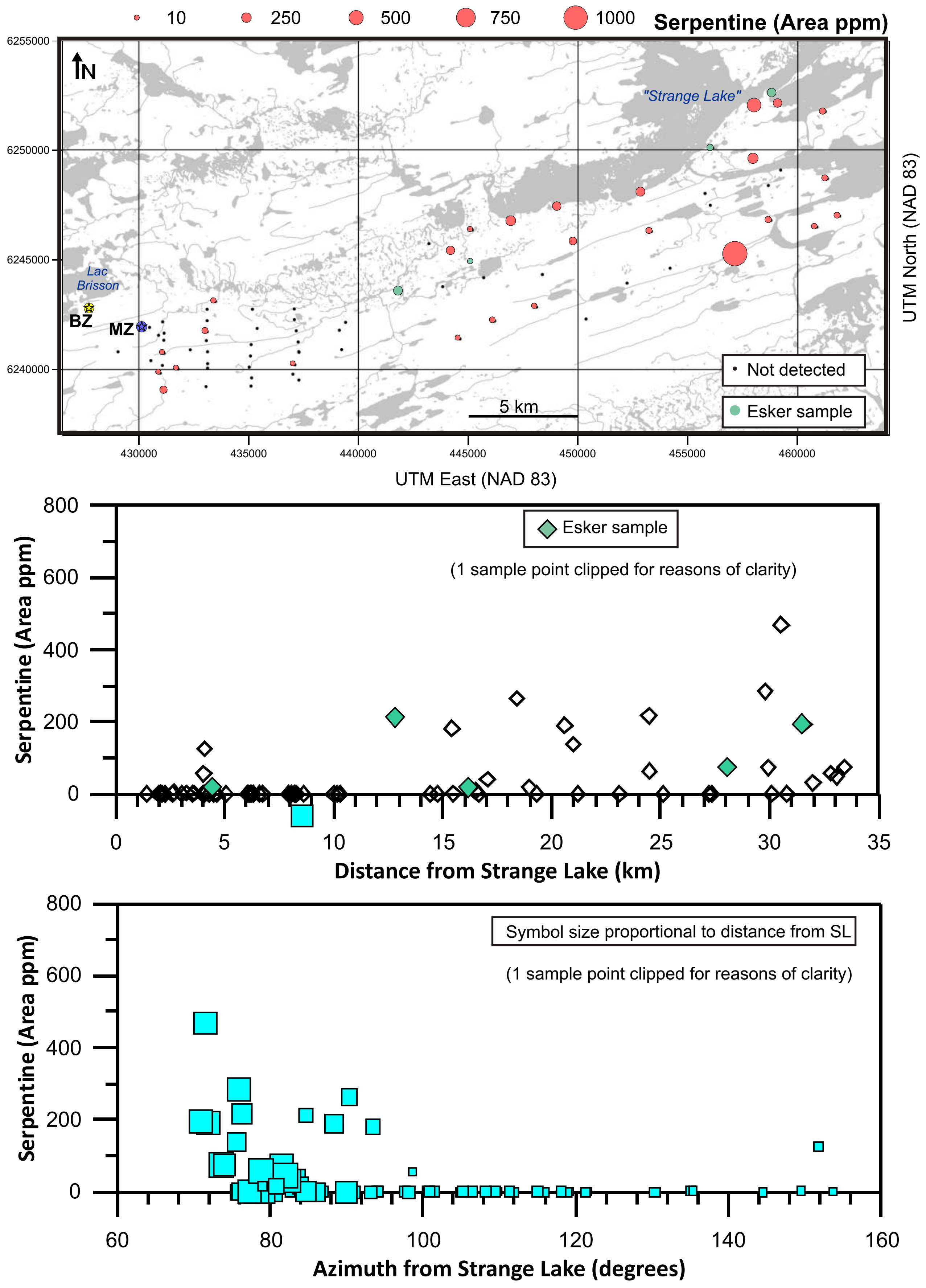

Figure B.21. Geographic variation patterns for serpentine (area ppm). Upper Panel is a map view with proportional symbols. Lower panels show abundances against distance and azimuth from Strange Lake.

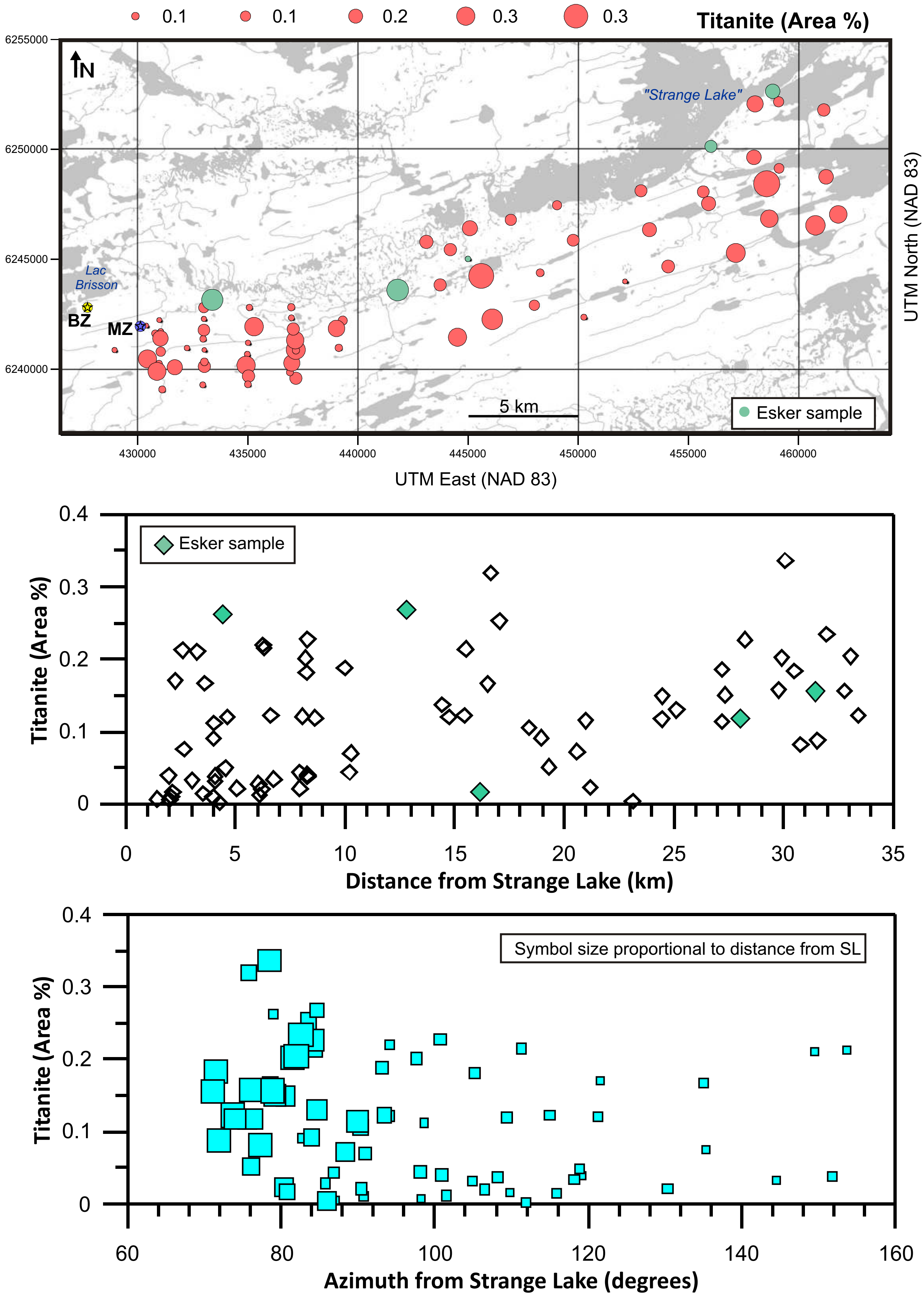

Figure B.22. Geographic variation patterns for titanite (area %). Upper Panel is a map view with proportional symbols. Lower panels show abundances against distance and azimuth from Strange Lake.

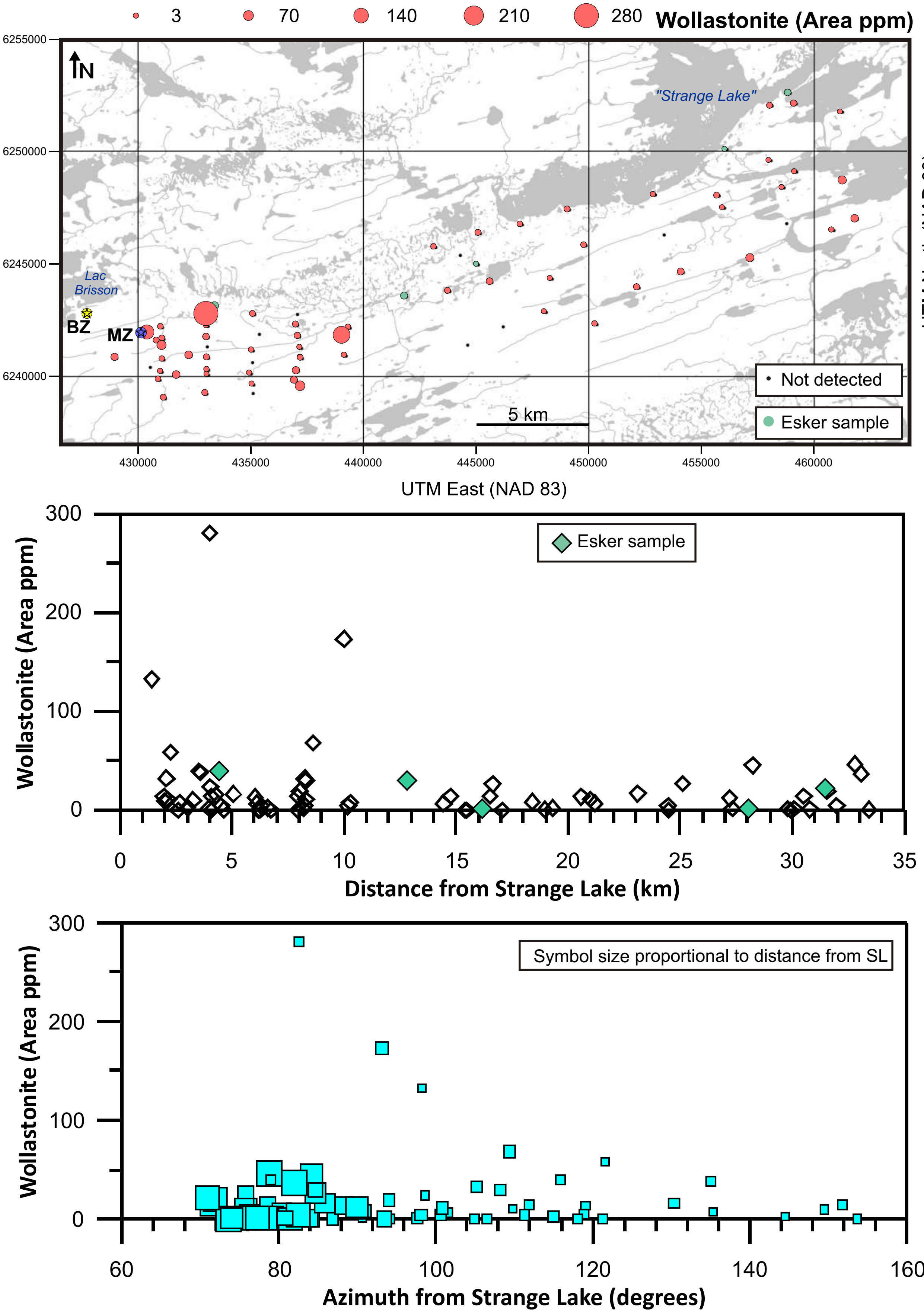

Figure B.23. Geographic variation patterns for wollastonite (area ppm). Upper Panel is a map view with proportional symbols. Lower panels show abundances against distance and azimuth from Strange Lake.

Table 1. List of potential indicator minerals in the Strange Lake deposit compiled from Birkett et al. (1992), Miller (1996), Jambor et al. (1998), and Gowans et al. (2014). Indicator minerals that were recovered from bedrock and till samples in this study are indicated.

Mineral	Formula	Hardness*	Density*	Reported by others	Seen in bedrock PTS in this study	Seen in bedrock HMC in this study	Seen in till HMC in this study	Element source in glacial dispersal train
U, Th minerals								
cerianite	$(Ce,Th)O_2$	not determined	7.2	no	no	yes	no	Ce, Th
thorite	$Th(SiO_4)$	5.0	4–6.7	Miller (1996)	no	yes	yes	Th
thorianite	ThO_2	6.0	10.0	no	yes	yes	yes	Th
uraninite	UO_2	5–6	6.5–10.95	no	yes	yes	no	U
Zr minerals								
elpidite	$Na_2ZrSi_6O_{15}\cdot 3(H_2O)$	7	2.54	Birkett et al. (1992)	yes	no	yes	Zr
hilairite	$Na_2ZrSiO_3O_9\cdot 3H_2O$	4.5	2.72	Roelofson and Veblen (1999)	no	no	no	Zr
dalyite	$K_2ZrSi_6O_{15}$	7.5	2.84	Birkett et al. (1992)	no	no	no	Zr
vlasovite	$Na_2ZrSi_4O_{11}$	6	2.97	Birkett et al. (1992)	no	no	no	Zr
zircon	$ZrSiO_4$	7.5	4.6–4.7	Birkett et al. (1992)	yes	yes	yes	Zr
armstrongite	$CaZrSi_6O_{15}\cdot 3(H_2O)$	4.5	2.7	Birkett et al. (1992)	no	no	no	Zr
catapleiite	$NaZrS_33O_9\cdot 2(H_2O)$	4.5–5	2.8	Birkett et al. (1992)	yes	yes	no	Zr
Ca-catapleiite	$CaZrSi_3O_9\cdot 2(H_2O)$	4.5–5	2.8	Birkett et al. (1992)	yes	yes	no	Zr
calciohilairite	$CaZrSi_3O_9\cdot 3(H_2O)$	4	2.68	Birkett et al. (1992)	no	no	no	Zr
gittinsite	$CaZrSi_2O_7$	3.5-4	3.6	Birkett et al. (1992)	yes	yes	yes	Zr
Ti minerals								
aeschynite	$(Y,Ca,Fe)(Ti,Nb)_2(O,OH)_6$	5–6	4.9–9.1	no	yes	no	no	Y
ilmenite	$FeTiO_3$	5–5.5	4.7	Birkett et al. (1996)	no	yes	no	
narsarsukite	$Na_2(Ti,Fe)Si_4(O,F)_{11}$	7	2.7	Miller (1996)	no	no	no	
bafertisite	$Ba(Fe,Mn)_2TiSi_2O_7(O,OH)_2$	5	3.96–4.25	Birkett et al. (1996)	no	no	no	
neptunite	$KNa_2Li(Fe,Mn)_2Ti_2Si_8O_{24}$	5–6	3.23	Birkett et al. (1996)	no	no	no	
aenigmatite	$(Na,Ca)_4(Fe,Ti,Mg)_{12}Si_{12}O_{40}$	5–6	3.7–3.9	Birkett et al. (1996)	no	yes	yes	
astrophyllite	$K_2Na(Fe,Mn)_7Ti_2Si_8O_{26}(OH)_4$	3-3.5	3.3–3.4	Birkett et al. (1996)	yes	no	no	
titanite	$CaTiSiO_5$	5–5.5	3.4–3.56	Miller (1996)	yes	yes	yes	
komarovite	$(Ca,Mn)_2(Nb,Ti)_2Si_2O_7(O,F)_2\cdot 3.5(H_2O)$	4	3.61–3.76	no	no	no	yes	Nb
chevkinite	$(Ce,La,Ca,Th)_4(Fe,Mg)_2(Ti,Fe)_3Si_4O_{22}$	5–5.5	4.5	no	no	no	yes	Ce, La, Th
Phosphate minerals								
xenotime	YPO_4	4–5	4.4–5.1	no	no	no	yes	Y
monazite	$(La,Ce,Y,Th)PO_4$	5–5.5	4.8–5.5	Miller (1996)	yes	yes	yes	Ce, La, Y, Th
fluorapatite	$Ca_5(PO_4)_3F$	5.0	3.1–3.2	no	no	yes	no	
apatite	$Ca_5(PO_4)_3(OH,F,Cl)$	5.0	3.2	Gowans et al. (2014)	yes	yes	yes	
britholite	$(Ce,Ca,Th,La,Nd)_5(SiO_4,PO_4)_3(OH,F)$		4.2–4.7	no	yes	no	no	Ce, La, Th
rhabdophane	$(Ce,La)PO_4\cdot(H_2O)$	3.5	4.0	no	no	yes	yes	Ce, La
Other minerals								
gadolinite group	$Be_2(Ca,REE,Fe)_3Si_2O_{10}$	6.5–7	4.2	Miller (1996)	no	no	no	Be, Ce, La, Y
arfvedsonite	$Na_3Fe_4Fe(Si_8O_{22})(OH)_2$	5.5–6	3.44–3.45	Miller (1996)	yes	yes	yes	
aegerine	$NaFe(Si_2O_6)$	6.0	3.5–3.6	Miller (1996)	yes	yes	yes	
pyrochlore	$(Na,Ca)_2Nb_2O_6(OH,F)$	5–5.5	4.2–6.4	Miller (1996)	yes	yes	yes	Nb
bastnaesite	$Ce(CO_3)F$	4-5	4.95–5	Miller (1996)	no	no	yes	Ce
parisite	$Ca(Ce,La)_2(CO_3)_3F_2$	4.5	4.4	no	no	yes	yes	Ce, La
kainosite	$Ca_2(Y,Ce)_2Si_4O_{12}(CO_3)\cdot H_2Oleif$	5–6	3.4–3.6	Miller (1996)	no	no	yes	Ce, Y
anthophyllite	$Mg_7(Si_8O_{22})(OH)_2$	5–6	2.9–3.6	no	no	no	yes	
allanite	$(Ce,Ca,Y)_2(Al,Fe)_3(SiO_4)_3(OH)$	5.5	3.3–4.2	Birkett et al. (1992)	yes	no	yes	Ce, Y
milarite	$K_2Ca_4Al_2Be_4Si_{24}O_{60}\cdot(H_2O)$	6	2.52	Gowans et al. (2014)	no	no	no	Be
gerenite	$(Ca,Na)_2(Y,REE)_3Si_6O_{18}\cdot 2(H_2O)$	5	3.3–3.52	Jambor et al. (1998)	no	no	no	Ce, La, Nd, Y
leifite	$Na_2(Si,Al,Be)_7(O,OH,F)_{14}$	6	2.57	Sinclair et al. (1992)	no	no	no	Be
danburite	$CaB_2Si_2O_8$	7.0	3.0	no	no	yes	no	
zajacite-(Ce)	$Na(REE_xCa_{1-x})(REE_yCa_{1-y})F_6$ where $(x \neq y)$	3.5	4.4–4.6	Jambor et al. (1996)	no	no	no	Ce, La, Nd
gagarinite-(Y)	$NaCaY(F,Cl)_6$	4.5	4.2	Jambor et al. (1996)	yes	no	no	Y
sphalerlite	$(Zn,Fe)S$	3.5–4	3.9–4.2	Miller (1996)	no	no	no	
molybdenite	MoS_2	1.0	5.5	no	no	yes	no	
galena	PbS	2.5	7.2–7.6	Miller (1996)	no	no	no	
fluorite	CaF_2	4.0	3.0–3.3	Miller (1996)	yes	yes	yes	